

**Antimicrobial Efficacies for Metal Ions and Graphene-  
based Compounds Against *Klebsiella pneumoniae*,  
*Acinetobacter baumannii* and *Enterococcus faecium* in  
the Absence and Presence of Conditioning Films**

**Misha Y Vaidya**

**Department of Life Sciences**

**Manchester Metropolitan University**

**A Thesis submitted in partial fulfilment of the  
requirements of Manchester Metropolitan  
University for the degree of Doctor of Philosophy**

**2019**

## **Declaration**

This is a declaration to certify that the material contained in this thesis has not been accepted in substance for any other degree and it is not currently submitted in candidature for any other academic award.

**Misha Y Vaidya**

## **Acknowledgement**

I would like to express my genuine gratitude to my director of studies Dr Kathryn Whitehead for her constant advice, support and patience. She has been a very motivating and positive factor throughout this research. I would also like to thank my supervisory team Prof Andrew McBain and Prof Craig Banks for their guidance. Also, I would like to acknowledge Prof. Craig Banks for providing the graphene-based compounds. My sincere thanks to Dr Paul Benson for being a wonderful laboratory technician. I would like to thank Hayley Andrews for the humble support as laboratory technician and teaching me the SEM, EDAX and RAMAN equipment. A special thanks to Dr Christopher Liauw for guiding me through the Raman analysis. I would also like to thank Dr Nina Dempsey-Hibbert for guiding me through the cell toxicity assays. I would like to dedicate this thesis to my loving husband Hasim Nakhuda for his trust, patience, support and financial help and without whom this thesis would have not been possible. I would like to thank my parents for their positive thoughts and constant prayers and my siblings for their love and care.

## Abstract

The occurrence and transmission of antimicrobial resistant (AMR) bacteria in the health-care and community settings is rising. With the lack of newer antibiotics in the pipeline and increasing resistance for the existing antibiotics and biocides that are available, it is estimated that the mortality rate due to non-treatable infections might rise to 10 million by 2050. This AMR related problem can be in part controlled by the discovery of novel antimicrobial sources. This study investigated the use of metal ions and graphene-based compounds (GBCs) singularly and in combination as potential antimicrobial agents against three medically related pathogens (*Klebsiella pneumoniae*, *Acinetobacter baumannii* and *Enterococcus faecium*). In order to determine the compounds efficacy in conditions that resembled those more found *in vivo*, the antimicrobials were also tested in the presence of 10 % bovine plasma conditioning films (CF). Moreover, the antimicrobial efficacies of the compounds were evaluated against two bacterial phenotypes, planktonic and biofilm.

The preliminary antimicrobial efficacy screening was performed for fifteen metal ions and fourteen graphene based compounds (GBCs) using zone of inhibition, minimum inhibitory concentration and minimum bactericidal concentration assays in the absence and presence of 10 % plasma CF. Five metal ions (Ag, Cu, Pt, Au and Pd) and four GBCs (GO, AgGO, AuGO and PdGO) were selected for physical, chemical and elemental analysis using scanning electron, Raman and electron dispersive X-ray microscopy respectively. The antimicrobial agents were combined to determine synergistic effects using fractional inhibitory and bactericidal concentration assays. A crystal violet biofilm assay was used to analyse the antibiofilm efficacies. A biotoxicity evaluation using skin fibroblast cell lines was tested using an MTT assay.



The results demonstrated that overall, the most active antimicrobial agents were Ag, Pt, Pd and Au ions amongst tested metal ions and AgGO amongst tested GBCs, but their antimicrobial activity was dependent on whether the form of the bacteria was planktonic or biofilm. In some cases, the presence of a CF had an adjuvant effect on the antimicrobial activity of the metal ions or GBCs. Palladium ions amongst the metal ions and PdGO amongst the GBCs demonstrated the least cell toxicity. *Enterococcus faecium* was the most resistant bacteria in all the tests. These results suggest that metal ions, and metal ion combinations with GO, or other metal ions possess the potential to be used as biocides or in topical applications as antimicrobials, however the effect of tested samples on cell toxicity is a significant concern.

## Table of contents

<b>Declaration</b>	i
<b>Acknowledgement</b>	ii
<b>Abstract</b>	iii-iv
<b>Table of Contents</b>	v-xiii
<b>List of Figures</b>	xiv-xvii
<b>List of Tables</b>	xix-xxii
<b>Abbreviations</b>	xxiii-xxiv
<b>1. Introduction</b>	1-50
1.1. Antibiotics	1
1.2. Increasing antibiotics resistance	2
1.2.1. General causes of antibiotic resistance	5
1.3. Antibiotics bacterial toxicity mechanism	7
1.4. Bacterial resistance mechanism to antibiotics	9
1.4.1. Intrinsic antibiotic resistance	11
1.4.2. Acquired antibiotic resistance	11
1.5. Biocides and biocide resistance	13
1.6. AMR and MDR bacterial species and their burden	14
1.7. AMR, MDR and XDR infections in general	15
1.8. Bacterial species tested in the study	16
1.8.1. <i>Klebsiella pneumoniae</i>	16
1.8.2. <i>Acinetobacter baumannii</i>	18
1.8.3. <i>Enterococcus faecium</i>	20
1.9. Bacterial biofilms	21
1.9.1. <i>K. pneumoniae</i> biofilms	23

1.9.2. <i>A. baumannii</i> biofilms	24
1.9.3. <i>E. faecium</i> biofilms	25
1.10. Bovine plasma as conditioning films of bacteria	26
1.11. Difference in Gram-positive and Gram-negative bacterial structure and their effect on resistance	27
1.12. Bacteria macromolecules	29
1.13. Need for alternative antimicrobials	31
1.14. Metal ions as alternative antimicrobials	31
1.15. General metal antimicrobial mechanism	31
1.16. Antimicrobial efficacy of the metal tested in this study	36
1.16.1. Silver	36
1.16.2. Copper	37
1.16.3. Platinum	38
1.16.4. Gold	38
1.16.5. Palladium	39
1.16.6. Rhodium and ruthenium	39
1.16.7. Titanium and tantalum	40
1.16.8. Zinc and gallium	40
1.16.9. Yttrium, niobium, molybdenum and indium	41
1.17. Graphene oxide and metal-GO as alternative antimicrobial	42
1.18. Combination of antimicrobial efficacy against planktonic bacterial form	47
1.19. Antimicrobial efficacy on bacterial biofilm phenotypes	48
1.20. Potential cytotoxicity of metal ions and GBCs	49
Aim	50

<b>2. Methods and Materials</b>	<b>51-70</b>
2.1. Synthesis of graphene-based compounds	51
2.2. Metal ions preparation	52
2.3. Bacterial strains and growth conditions	55
2.4. Bacterial preparation	55
2.5. Bacterial conditioning film (CF) preparation	56
2.6. Zone of inhibition (ZoI) assay in the absence and presence of 10 % CF	56
2.7. Minimum inhibitory concentration (MIC) assay in the absence and presence of 10 % CF	57
2.8. Minimum bactericidal concentration (MBC) assay in the absence and presence of 10 % CF	59
2.9. Time kill assay in the absence and presence of 10 % CF	59
2.10. Scanning electron microscopy (SEM) in the absence and presence of 10 % CF	60-61
2.10.1. Sample preparation	60
2.10.2. Fixation	60
2.10.3. Dehydration	60
2.10.4. Sputter coating	60
2.10.5. Sample microscopy	61
2.11. Energy dispersive X-ray spectroscopy (EDAX) in the absence and presence of 10 % CF	61
2.12. Raman spectroscopy in the absence and presence of 10 % CF	61
2.13. ZoI for combined samples assay in the absence and presence of 10 % CF	63

2.14. Fractional inhibitory concentration (FIC) assay in 2:1, 1:1 and 1:2 ratios in the absence and presence of 10 % CF	65
2.15. Fractional bactericidal concentration (FBC) assay in 2:1, 1:1 and 1:2 ratios in the absence and presence of 10 % CF	66
2.16. Crystal Violet biofilm assay (CVBA) for single sample antimicrobial effects in the absence and presence of 10 % CF	68
2.16.1. Preparation of stainless-steel coupons	68
2.16.2. Biofilm formation and CVBA assay	68
2.17. CVBA for combined samples in ratios and absence and presence of 10 % CF	69
2.18. Cytotoxicity assay	70
2.19. Statistical analysis	70
<b>3. Results for metal ions</b>	71-172
<b>3.0. Introduction and objective</b>	71-72
<b>3.1. Antimicrobial efficacies screening for single metal ions</b>	73-88
3.1.1. ZoI assay results of 15 metal ions in the absence and presence of CF	73-78
3.1.2. MIC assay results of 15 metal ions in the absence and presence of CF	79-83
3.1.3. MBC assay results of 15 metal ions in the absence and presence of CF	84-88
3.1.4. Antimicrobial efficacies using time kill assay for 5 metal ions	89-97

3.4.1.1. Antimicrobial efficacy against <i>K. pneumoniae</i> with and without 10 % bovine plasma CF	89-91
3.4.1.2. Antimicrobial efficacy against <i>A. baumannii</i> with and without 10 % bovine plasma CF	92-94
3.4.1.3. Antimicrobial efficacy against <i>E. faecium</i> with and without 10 % bovine plasma CF	95-97
3.1. Discussion	98-102
<b>3.2. Morphological changes after 5 metal ions treatment using SEM</b>	
3.2.1. SEM analysis results for five metal ions at 0 h and 24 h treatment against <i>K. pneumoniae</i> , <i>A. baumannii</i> and <i>E. faecium</i> in the absence of CF	103-106
3.2.2. SEM analysis results for five metal ions at 0 h and 24 h treatment against <i>K. pneumoniae</i> , <i>A. baumannii</i> and <i>E. faecium</i> in the presence of CF	107-110
3.2. Discussion	111-112
<b>3.3. Elemental changes after 5 metal ions treatment using EDAX</b>	113-122
3.3.1. EDAX analysis results for five metal ions at 24 h treatment against <i>K. pneumoniae</i> , <i>A. baumannii</i> and <i>E. faecium</i> in the absence of CF	113-117
3.3.2. EDAX analysis results for five metal ions at 24 h treatment against <i>K. pneumoniae</i> , <i>A. baumannii</i> and <i>E. faecium</i> in the presence of CF	118-122
3.3. Discussion	123-124

<b>3.4. Chemical changes after 5 metal ions treatment using RAMAN</b>	125-134
3.4.1. Raman analysis results for five metal ions at 24 h treatment against <i>K. pneumoniae</i> , <i>A. baumannii</i> and <i>E. faecium</i> in the absence of CF	125-129
3.4.2. Raman analysis results for five metal ions at 24 h treatment against <i>K. pneumoniae</i> , <i>A. baumannii</i> and <i>E. faecium</i> in the presence of CF	130-134
3.4. Discussion	135-137
<b>3.5. Combined metal ions antimicrobial efficacies</b>	138-152
3.5.1. ZoI combinations antimicrobial efficacies for interaction type and inhibition grade against <i>K. pneumoniae</i> , <i>A. baumannii</i> and <i>E. faecium</i> in the absence and presence of CF	138-140
3.5.2. FIC results in 2:1, 1:1 and 1:2 ratio against <i>K. pneumoniae</i> , <i>A. baumannii</i> and <i>E. faecium</i> in the absence and presence of CF	141-146
3.5.3. FBC results in 2:1, 1;1 and 1:2 ratio against <i>K. pneumoniae</i> , <i>A. baumannii</i> and <i>E. faecium</i> in the absence and presence of CF	147-152
3.5. Discussion	153-156
<b>3.6. Antibiofilm efficacies using CVBA</b>	157-169
3.6.1. Antibiofilm assay for 5 single metal ions against <i>K. pneumoniae</i> , <i>A. baumannii</i> and <i>E. faecium</i> in the presence and absence of CF	157-160
3.6.2. Antibiofilm assay for ten combined ions against <i>K. pneumoniae</i> , <i>A. baumannii</i> and <i>E. faecium</i> in the absence of CF	161-164

3.6.3. Antibiofilm assay for ten combined ions against <i>K. pneumoniae</i> , <i>A. baumannii</i> and <i>E. faecium</i> in the presence of CF	165-169
3.6. Discussion	170
<b>3.7. Cytotoxicity for five metal ions</b>	171-172
<b>4. Results for graphene-based compounds (GBCs)</b>	173-247
<b>4.0. Introduction and objective</b>	173
<b>4.1. Initial antimicrobial efficacies screening for single GBCs</b>	174-185
4.1.1. ZoI assay results of 14 GBCs in the absence and presence of CF	174-176
4.1.2. MIC assay results of 14 GBCs in the absence and presence of CF	177-179
4.1.3. MBC assay results of 14 GBCs in the absence and presence of CF	180-182
4.1.4. Antimicrobial efficacies using time kill assay for 4 GBCs in the absence and presence of CF	183-185
4.1. Discussion	186-189
<b>4.2. Morphological changes after 4 GBCs treatment using SEM</b>	190-197
4.2.1. SEM analysis results 4 GBCs ions at 0 h and 24 h treatment against <i>K. pneumoniae</i> , <i>A. baumannii</i> and <i>E. faecium</i> in the absence of CF	190-193
4.2.2. SEM analysis results 4 GBCs at 0 h and 24 h treatment against <i>K. pneumoniae</i> , <i>A. baumannii</i> and <i>E. faecium</i> in the presence of CF	194-197
4.2. Discussion	198
<b>4.3. Elemental changes after 4 GBCs treatment using EDAX</b>	199-208



4.3.1. EDAX analysis results for 4 GBCs at 24 h treatment against <i>K. pneumoniae</i> , <i>A. baumannii</i> and <i>E. faecium</i> in the absence of CF	199-203
4.3.2. EDAX analysis results for 4 GBCs at 24 h treatment against <i>K. pneumoniae</i> , <i>A. baumannii</i> and <i>E. faecium</i> in the presence of CF	204-208
<b>4.4. Chemical changes after 4 GBCs treatment using RAMAN</b>	209-218
4.4.1. Raman analysis results for 4 GBCs at 24 h treatment against <i>K. pneumoniae</i> , <i>A. baumannii</i> and <i>E. faecium</i> in the absence of CF	209-213
4.4.2. Raman analysis results for 4 GBCs at 24 h treatment against <i>K. pneumoniae</i> , <i>A. baumannii</i> and <i>E. faecium</i> in the presence of CF	214-218
4.4. Discussion	219
<b>4.5. Combined GBCs antimicrobial efficacies</b>	220-233
4.5.1. ZoI combinations antimicrobial efficacies for interaction type and inhibition grade against <i>K. pneumoniae</i> , <i>A. baumannii</i> and <i>E. faecium</i> in the absence and presence of CF	220-221
4.5.2. FIC results in 2:1, 1:1 and 1:2 ratio against <i>K. pneumoniae</i> , <i>A. baumannii</i> and <i>E. faecium</i> in the absence and presence of CF	221-227
4.5.3. FBC results in 2:1, 1;1 and 1:2 ratio against <i>K. pneumoniae</i> , <i>A. baumannii</i> and <i>E. faecium</i> in the absence and presence of CF	228-233
4.5. Discussion	234-236
<b>4.6. Antibiofilm efficacies using CVBA</b>	237-243
4.6.1. Antibiofilm assay single GBCs against <i>K. pneumoniae</i> , <i>A. baumannii</i> and <i>E. faecium</i> in the presence and absence of CF	237-239
4.6.2. Antibiofilm assay for combined GBCs against <i>K. pneumoniae</i> , <i>A. baumannii</i> and <i>E. faecium</i> in the absence of CF	240-241

4.6.3. Antibiofilm assay for combined GBCs against <i>K. pneumoniae</i> , <i>A baumannii</i> and <i>E. faecium</i> in the presence of CF	242-243
4.6. Discussion	244-245
4.7. Cytotoxicity for GBCs	246-247
5. Discussion	248-255
6. Conclusion and future work	256-258
Presentations	259
Publications	260
Appendix	261-268
References	269

## List of Figures

<b>Figure 1.1.</b>	Antibiotic discover and resistance timeline	4
<b>Figure 1.2.</b>	Schematic representation of bacterial resistance	10
<b>Figure 1.3.</b>	Antimicrobial activity mechanism of metal ions	33
<b>Figure 1.4.</b>	Antimicrobial mechanism of iron, copper and arsenic	34
<b>Figure 1.5.</b>	Antimicrobial mechanism of copper, gallium and cadmium	34
<b>Figure 1.6.</b>	Structure of graphene and graphene oxide	43
<b>Figure 1.7.</b>	Antimicrobial mechanism of Metal-GO hybrids	46
<b>Figure 2.1.</b>	Dilution of antimicrobial agents in the MIC test	58
<b>Figure 3.1.</b>	ZoI for 15 metal ions in the absence of plasma CF	77
<b>Figure 3.2.</b>	ZoI for 15 metal ions in the presence of plasma CF	78
<b>Figure 3.3.</b>	Time kill assay results for 5 metal ions against <i>K. pneumoniae</i> in the absence of plasma CF	90
<b>Figure 3.4.</b>	Time kill assay results for 5 metal ions against <i>K. pneumoniae</i> in the presence of plasma CF	91
<b>Figure 3.5.</b>	Time kill assay results for 5 metal ions against <i>A. baumannii</i> in the absence of plasma CF	93
<b>Figure 3.6.</b>	Time kill assay results for 5 metal ions against <i>A. baumannii</i> in the presence of plasma CF	94
<b>Figure 3.7.</b>	Time kill assay results for 5 metal ions against <i>E. faecium</i> in the absence of plasma CF	96

<b>Figure 3.8.</b>	Time kill assay results for 5 metal ions against <i>E. faecium</i> in the presence of plasma CF	97
<b>Figure 3.9.</b>	The EDAX results for 5 metal ions against <i>K. pneumoniae</i> in the absence of CF signifying elemental changes	115
<b>Figure 3.10.</b>	The EDAX results for 5 metal ions against <i>A. baumannii</i> in the absence of CF signifying elemental changes	116
<b>Figure 3.11.</b>	The EDAX results for 5 metal ions against <i>E. faecium</i> in the absence of CF signifying elemental changes	117
<b>Figure 3.12.</b>	The EDAX results for 5 metal ions against <i>K. pneumoniae</i> in the presence of CF signifying elemental changes	120
<b>Figure 3.13.</b>	The EDAX results for 5 metal ions against <i>A. baumannii</i> in the presence of CF signifying elemental changes	121
<b>Figure 3.14.</b>	The EDAX results for 5 metal ions against <i>E. faecium</i> in the presence of CF signifying elemental changes	122
<b>Figure 3.15.</b>	The Raman results for 5 metal ions against <i>K. pneumoniae</i> in the absence of CF signifying chemical changes	127
<b>Figure 3.16.</b>	The Raman results for 5 metal ions against <i>A. baumannii</i> in the absence of CF signifying chemical changes	128
<b>Figure 3.17.</b>	The Raman results for 5 metal ions against <i>E. faecium</i> in the absence of CF signifying chemical changes	129
<b>Figure 3.18.</b>	The Raman results for 5 metal ions against <i>K. pneumoniae</i> in the presence of CF signifying chemical changes	132
<b>Figure 3.19.</b>	The Raman results for 5 metal ions against <i>A. baumannii</i> in the presence of CF signifying chemical changes	133

<b>Figure 3.20.</b>	The Raman results for 5 metal ions against <i>E. faecium</i> in the presence of CF signifying chemical changes	134
<b>Figure 3.21.</b>	ZoI interaction examples for combined metal ions	140
<b>Figure 3.22.</b>	Antibiofilm efficacies for single metal ions in the absence of plasma CF	159
<b>Figure 3.23.</b>	Antibiofilm efficacies for single metal ions in the presence of plasma CF	160
<b>Figure 3.24.</b>	Antibiofilm efficacies for combined metal ions against <i>K. pneumoniae</i> in 2:1, 1:1 and 1:2 ratios in the absence of plasma CF	162
<b>Figure 3.25.</b>	Antibiofilm efficacies for combined metal ions against <i>A. baumannii</i> in 2:1, 1:1 and 1:2 ratios in the absence of plasma CF	163
<b>Figure 3.26.</b>	Antibiofilm efficacies for combined metal ions against <i>E. faecium</i> in 2:1, 1:1 and 1:2 ratios in the absence of plasma CF	164
<b>Figure 3.27.</b>	Antibiofilm efficacies for combined metal ions against <i>K. pneumoniae</i> in 2:1, 1:1 and 1:2 ratios in the presence of plasma CF	167
<b>Figure 3.28.</b>	Antibiofilm efficacies for combined metal ions against <i>A. baumannii</i> in 2:1, 1:1 and 1:2 ratios in the presence of plasma CF	168
<b>Figure 3.29.</b>	Antibiofilm efficacies for combined metal ions against <i>E. faecium</i> in 2:1, 1:1 and 1:2 ratios in the presence of plasma CF	169
<b>Figure 3.30.</b>	Cytotoxicity results for metal ions	172
<b>Figure 4.1.</b>	ZoI for 14 GBCs in the absence of plasma CF	175
<b>Figure 4.2.</b>	ZoI for 14 GBCs in the presence of plasma CF	176
<b>Figure 4.3.</b>	Time kill assay results for GO and metal-GO hybrids against <i>K. pneumoniae</i> , <i>A. baumannii</i> and <i>E. faecium</i> in the absence of plasma CF	184

<b>Figure 4.4.</b>	Time kill assay results for GO and metal-GO hybrids against <i>K. pneumoniae</i> , <i>A. baumannii</i> and <i>E. faecium</i> in the presence of plasma CF	185
<b>Figure 4.5.</b>	The EDAX results for GO and metal-GO hybrids against <i>K. pneumoniae</i> in the absence of CF signifying elemental changes	201
<b>Figure 4.6.</b>	The EDAX results for GO and metal-GO hybrids against <i>A. baumannii</i> in the absence of CF signifying elemental changes	202
<b>Figure 4.7.</b>	The EDAX results for GO and metal-GO hybrids against <i>E. faecium</i> in the absence of CF signifying elemental changes	203
<b>Figure 4.8.</b>	The EDAX results for GO and metal-GO hybrids against <i>K. pneumoniae</i> in the presence of CF signifying elemental changes	206
<b>Figure 4.9.</b>	The EDAX for GO and metal-GO hybrids results against <i>A. baumannii</i> in the presence of CF signifying elemental changes	207
<b>Figure 4.10.</b>	The EDAX results for GO and metal-GO hybrids against <i>E. faecium</i> in the presence of CF signifying elemental changes	208
<b>Figure 4.11.</b>	The Raman results against <i>K. pneumoniae</i> in the absence of CF signifying chemical changes	211
<b>Figure 4.12.</b>	The Raman results for GO and metal-GO hybrids against <i>A. baumannii</i> in the absence of CF signifying chemical changes	212
<b>Figure 4.13.</b>	The Raman results for GO and metal-GO hybrids against <i>E. faecium</i> in the absence of CF signifying chemical changes	213
<b>Figure 4.14.</b>	The Raman results for GO and metal-GO hybrids against <i>K. pneumoniae</i> in the presence of CF signifying chemical changes	216
<b>Figure 4.15.</b>	The Raman results for GO and metal-GO hybrids against <i>A. baumannii</i> in the presence of CF signifying chemical changes	217

<b>Figure 4.16.</b>	The Raman results for GO and metal-GO hybrids against <i>E. faecium</i> in the presence of CF signifying chemical changes	218
<b>Figure 4.17.</b>	Antibiofilm efficacies for single GO and metal-GO hybrids in the absence of plasma CF	238
<b>Figure 4.18.</b>	Antibiofilm efficacies for single GO and metal-GO hybrids in the presence of plasma CF	239
<b>Figure 4.19.</b>	Antibiofilm efficacies for combined GO and metal-GO hybrids against <i>K. pneumoniae</i> , <i>A. baumannii</i> , <i>E. faecium</i> in 2:1, 1:1 and 1:2 rations in the absence of plasma CF	241
<b>Figure 4.20.</b>	Antibiofilm efficacies for combined GO and metal-GO hybrids against <i>K. pneumoniae</i> , <i>A. baumannii</i> in 2:1, 1:1 and 1:2 rations in the presence of plasma CF	243
<b>Figure 4.21.</b>	Cytotoxicity results for metal ions	247

## **List of Tables**

<b>Table 1.1.</b>	Summary of mechanistic action and bacterial target of antibiotics	8
<b>Table 1.2.</b>	Composition of biofilms	22
<b>Table 1.3.</b>	General differentiative features of Gram-negative and Gram-positive bacterial cell-wall	28
<b>Table 1.4.</b>	The macromolecules in the bacterial cell and their subunits and location	30
<b>Table 1.5.</b>	The antimicrobial properties of the tested metal ions in this study	35
<b>Table 2.1.</b>	Chemistry of metal ions tested in this study	54
<b>Table 2.2.</b>	Raman experimental set up	62
<b>Table 2.3.</b>	Four possible interactions for antimicrobial combinations	64
<b>Table 2.4.</b>	Volumes for individual metal ions in combined metal ions and GBCs in combination in the FIC test	65
<b>Table 2.5.</b>	Individual metal ion / GBCs concentrations in a combination in respective ratios in the FICs and FBCs tests	67
<b>Table 2.6.</b>	Volumes added of individual metal ions in combined metal ions and GBCs in combined GBCs in the CVBA assay	69
<b>Table 3.1.</b>	MIC for 15 metal ions in the absence of plasma CF	82



<b>Table 3.2.</b>	MIC for 15 metal ions in the presence of plasma CF	83
<b>Table 3.3.</b>	MBC for 15 metal ions in the absence of plasma CF	87
<b>Table 3.4.</b>	MBC for 15 metal ions in the presence of plasma CF	88
<b>Table 3.5.</b>	Physical damage observed using SEM for 5 metal ions against <i>K. pneumoniae</i> in the absence of plasma CF	104
<b>Table 3.6.</b>	Physical damage observed using SEM for 5 metal ions against <i>A. baumannii</i> in the absence of plasma CF	105
<b>Table 3.7.</b>	Physical damage observed using SEM for 5 metal ions against <i>E. faecium</i> in the absence of plasma CF	106
<b>Table 3.8.</b>	Physical damage observed using SEM for 5 metal ions against <i>K. pneumoniae</i> in the presence of plasma CF	108
<b>Table 3.9.</b>	Physical damage observed using SEM for 5 metal ions against <i>A. baumannii</i> in the presence of plasma CF	109
<b>Table 3.10.</b>	Physical damage observed using SEM for 5 metal ions against <i>E. faecium</i> in the presence of plasma CF	110
<b>Table 3.11.</b>	The ZoI combination results for interactions type and inhibition grade of combined metal ions against <i>K. pneumoniae</i> , <i>A. baumannii</i> and <i>E. faecium</i> in the absence and presence plasma CF	139
<b>Table 3.12.</b>	The FIC results for combined metal ions in 2:1. 1:1 and 1:2 ratios in the absence and presence of CF against <i>K. pneumoniae</i>	144
<b>Table 3.13.</b>	The FIC results for combined metal ions in 2:1. 1:1 and 1:2 ratios in the absence and presence of CF against <i>A. baumannii</i>	145
<b>Table 3.14.</b>	The FIC results for combined metal ions in 2:1. 1:1 and 1:2 ratios in the absence and presence of CF against <i>E. faecium</i>	146

<b>Table 3.15.</b>	The FBC results for combined metal ions in 2:1. 1:1 and 1:2 ratios in the absence and presence of CF against <i>K. pneumoniae</i>	150
<b>Table 3.16.</b>	The FBC results for combined metal ions in 2:1. 1:1 and 1:2 ratios in the absence and presence of CF against <i>A. baumannii</i>	151
<b>Table 3.17.</b>	The FBC results for combined metal ions in 2:1. 1:1 and 1:2 ratios in the absence and presence of CF against <i>E. faecium</i>	152
<b>Table 4.1.</b>	MIC for 14 GBCs in the absence of plasma CF	178
<b>Table 4.2.</b>	MIC for 14 GBCs in the presence of plasma CF	179
<b>Table 4.3.</b>	MBC for 14 GBCs in the absence of plasma CF	181
<b>Table 4.4.</b>	MBC for 14 GBCs in the presence of plasma CF	182
<b>Table 4.5.</b>	Physical damage observed using SEM for GO and metal-GO hybrids against <i>K. pneumoniae</i> in the absence of plasma CF	191
<b>Table 4.6.</b>	Physical damage observed using SEM for GO and metal-GO hybrids against <i>A. baumannii</i> in the absence of plasma CF	192
<b>Table 4.7.</b>	Physical damage observed using SEM for GO and metal-GO hybrids against <i>E. faecium</i> in the absence of plasma CF	193
<b>Table 4.8.</b>	Physical damage observed using SEM for GO and metal-GO hybrids against <i>K. pneumoniae</i> in the presence of plasma CF	195
<b>Table 4.9.</b>	Physical damage observed using SEM for GO and metal-GO hybrids against <i>A. baumannii</i> in the presence of plasma CF	196
<b>Table 4.10.</b>	Physical damage observed using SEM for GO and metal-GO hybrids against <i>E. faecium</i> in the presence of plasma CF	197
<b>Table 4.11.</b>	The ZoI combination results for interactions type and inhibition grade of combined GO and metal-GO hybrids against <i>K.</i>	221

*pneumoniae*, *A. baumannii* and *E. faecium* in the absence and presence plasma CF

<b>Table 4.12.</b>	The FIC results for combined GO and metal-GO hybrids in 2:1. 1:1 and 1:2 ratios in the absence and presence of CF against <i>K. pneumoniae</i>	225
<b>Table 4.13.</b>	The FIC results for combined GO and metal-GO hybrids in 2:1. 1:1 and 1:2 ratios in the absence and presence of CF against <i>A. baumannii</i>	226
<b>Table 4.14.</b>	The FIC results for combined GO and metal-GO hybrids in 2:1. 1:1 and 1:2 ratios in the absence and presence of CF against <i>E. faecium</i>	227
<b>Table 4.15.</b>	The FBC results for combined GO and metal-GO hybrids in 2:1. 1:1 and 1:2 ratios in the absence and presence of CF against <i>K. pneumoniae</i>	231
<b>Table 4.16.</b>	The FBC results for combined GO and metal-GO hybrids in 2:1. 1:1 and 1:2 ratios in the absence and presence of CF against <i>A. baumannii</i>	232
<b>Table 4.17.</b>	The FBC results for combined GO and metal-GO hybrids in 2:1. 1:1 and 1:2 ratios in the absence and presence of CF against <i>E. faecium</i>	233

### **Abbreviations**

AMR	Antimicrobial resistant
MDR	Multidrug resistant
XDR	Extensively drug resistant
Ag	Silver
Cu	Copper
Au	Gold
Pt	Platinum
Pd	Palladium
Rh	Rhodium
Ru	Ruthenium
Mo	Molybdenum
Y	Yttrium
Ti	Titanium
Ta	Tantalum
In	Indium
Ga	Gallium
Nb	Niobium
Zn	Zinc

Cd	Cadmium
GO	Graphene oxide
CF	Conditioning films
GBCs	Graphene-based compounds
ZoI	Zone of inhibition
MIC	Minimum inhibitory concentration
MBC	Minimum bactericidal concentration
CFU $\text{mL}^{-1}$	Colony forming units per mL
SEM	Scanning electron microscopy
EDAX	Energy dispersive analysis X-ray
FIC	Fractional inhibitory concentration
FBC	Fractional bactericidal concentration
CVBA	Crystal violet biofilm assay
MTP	Microtitre plate
DNA	Deoxyribonucleic acid
ROS	Reactive oxygen species

# Chapter 1

## 1. Introduction

### 1.1. Antibiotics

Antibiotics were believed to be used for the longest time before the beginning of modern medicine. For example, ancient Egyptians used filamentous fungi growth on bread to cure infected wounds and burns. In the Middle Ages, Chinese and Greek therapists, used mouldy surfaces to cure several illnesses (Davies and Davies, 2010; Sommer and Dantas, 2011). In the 19<sup>th</sup> century, while studying the growth of *Bacillus anthracis* in a urine sample, Louis Pasteur with his colleague Jules François Joubert in 1877 noticed that a few bacteria could inhibit others (Chast, 2008). It was in 1928, when the first antibiotic was inadvertently discovered by Alexander Fleming in his elapsed *Staphylococcus aureus* colonies that a fungus (*Penicillium notatum*) was shown to prevent the growth of bacteria (Bennett and Chung, 2001; Demain, 2006). However, it was in 1940 that the industrial manufacture of this antibiotic using *Penicillium chrysogenum* was performed by Howard Florey and colleagues (Ligon, 2004). Selman Waksman was the first to perform systematic research on soil samples and highlighted the antagonistic effects between different bacteria species (Ligon, 2004; Muniz et al, 2007; Kardos and Demain, 2011). This work by Selman Waksman discovered several antibiotics, such as actinomycin, streptomycin and neomycin as antibacterials and fumigacin and clavacin as antifungals (Kingston, 2004; Kresge et al., 2004). Waksman research encouraged the pharmaceutical companies for novel antibiotics investigations which directed most of the current antibiotic discovery. Between the 1940s and the 1970s is considered the golden era of antibiotics (Muniz et al., 2007; Kresge et al., 2004).

The definition of an antibiotic, first proposed following the discovery of streptomycin by Selman Waksman, is any class of organic substance that prevents or kills micro-organisms by targeting bacteria through a specific interaction without consideration of the compound source

of origin. However, medically, antibiotics are now considered to be compounds produced or obtained from microorganisms that control or treat infections by either inhibiting or destroying the pathogens (Davies and Davies, 2010; Sommer and Dantas, 2011). Antibiotics discovery was a turning step in the history of medicine as countless lives have been saved. The ability of these compounds to selectively target the pathogen, without critically damaging human cellular processes further increased the popularity of antibiotics usage. For example, antibiotics such as tetracycline and chloramphenicol target and denature the bacterial ribosome. However, these antibiotics have no effect on the eukaryotic ribosome, thus showing selective toxicity against prokaryotic bacterial cells (Stefanović et al., 2012).

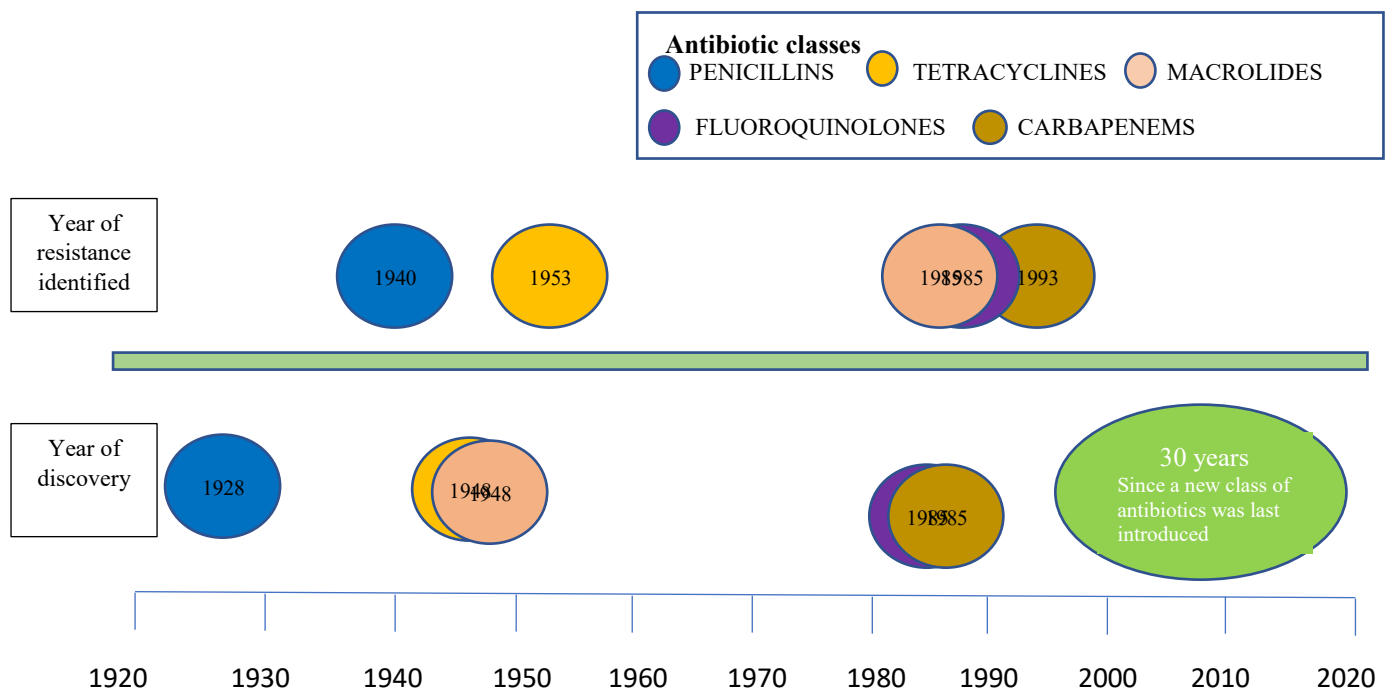
Antibiotics not only saved life of people from life threatening infectious diseases, but also played a major part in healthcare and surgical areas (Mccord and Chowdhury, 2003). For example, antibiotics aided the treatment and prevention of infections that might occur during and post surgeries, particularly in immunocompromised patients. Moreover, the use of antibiotics extended life expectancy worldwide by decreasing morbidity and mortality (Sasso and Garrido, 2008; Khan et al., 2017).

## **1.2. Increasing antibiotic resistance**

Several years before the therapeutic use of penicillin, bacterial penicillinase was identified (Davies and Davies, 2010). Sulphonamide resistance was first reported in the late 1930s and similar resistance mechanisms towards a range of antibiotics were also reported 70 years later (Livermore, 2012) (Figure 1.1). Thus, since the introduction of the first effective antibiotics, resistance has been observed because their therapeutic use. For instance, resistant strains of *Mycobacterium tuberculosis* were identified to therapeutic concentrations of streptomycin, during its application in 1940s to cure tuberculosis patients (Aminov, 2010; Davies and Davies, 2010). As other antibiotics have been discovered and introduced into clinical practice, a similar course of events has ensued (Unemo and Shafer, 2014). Moreover, after the wide use of

antibiotics, resistant strains that can inactivate the efficacy of drugs increased eventually (Shahid et al., 2009; Davies and Davies, 2010; Frère et al., 2016).





**Figure 1.1.** Antibiotic discovery and resistance timeline (Aminov, 2010; Davis and Davies, 2010; Ventola, 2015)

### **1.2.1. General causes of antibiotic resistance**

Antibiotics are the therapeutic tools used to prevent and treat several infectious diseases. However, today a large number of antibiotics have become less effective and this resistance is found to increase gradually over a period of time (Kollef and Fraser, 2001). Direct or indirect factors that might influence the bacterial resistance are listed below (Ventola, 2015).

#### **1.2.1.1. Antibiotics overuse**

The misuse of antibiotics initiates the development of bacterial resistance. Epidemiological research has confirmed that there is a direct correlation between antibiotic overuse and the development and propagation of resistant pathogens (Zaman et al., 2017). For example, among the bloodstream of infectious patients in different countries, there was found to be a 0 to 82 % incidence of bacterial resistance to at least one of the most commonly used antibiotics (Ventola, 2015; Zaman et al., 2017). Penicillin resistance has been shown to range between 0 to 51 % worldwide, which was common to treat pneumonia (Okeke et al., 2005; Prestinaci et al., 2015). Urinary tract infections caused by Gram-negative species such as *Escherichia coli* and *Klebsiella pneumoniae* showed up to 8 % to 65 % increased resistance for commonly used ciprofloxacin (Paterson, 2006; Kaye and Pogue, 2015). Thus, it has been proposed that over prescription of antibiotics world-wide might directly affect increased in bacterial resistance (Ventola, 2004).

#### **1.2.1.2. Inappropriate prescription**

Various studies demonstrated that the first line of treatment, selection and duration of antibiotic therapy was incorrect in nearly 30 – 50 % of cases (Bartlett et al., 2013). For instance, according to a US report on antibiotics resistance, pathogen identification was reported only in 7.6 % of 17,435 hospitalised patients. Even in the intensive care units, nearly 30% to 60% of the prescribed antibiotics have been found to be needless, inappropriate, or suboptimal (Bartlett et al., 2013; Luyt et al., 2014).

#### 1.2.1.3. Extensive agricultural use

Antibiotics are widely used worldwide as supplements in livestock and as pesticides on plants. It is estimated that 80% of antibiotics sold in the US are used in animals to prevent infection and as growth promoters. This is alarming because it creates a vicious cycle of resistance transfer into the environment, animals and humans (Gross, 2013; Spellberg and Gilbert, 2014; Ventola, 2015).

#### 1.2.1.4. Availability of fewer antibiotics

The number of new antibiotics in the market is reducing, for example, between 1983 and 1987, sixteen new antibiotics were approved, while only seven were permitted between 1998 – 2002 (Bush et al., 2011). Recently, only new two classes of antibiotics namely daptomycin and oxazolidinone, have been reported to treat Gram-positive bacterial infections, whilst, novel antibiotics against Gram-negative infections are still proving to be a struggle (Miller et al., 2014). Moreover, antibiotics with novel modes of action are also less in number. One of the major problems with the development of novel classes of drugs is that pharmaceutical companies no longer consider their production to be an economically wise investment due to the relatively short periods that antibiotics are used for. However, big companies are interested in development of drugs that can be used to treat long term chronic diseases such as asthma and diabetes, which can bring a greater financial reward (Bush et al., 2011; Whang et al., 2013; Miller et al., 2014).

#### 1.2.1.5. Regulatory bodies

Regulatory bodies such as the Food and Drug Administration and European Medicines Agency are the regulatory bodies responsible for the approval of antibiotics (Gould and Bal, 2013). Bureaucracy, differences in clinical trial requirements among countries, absence of clarity, changes in regulatory and licensing rules, and ineffective channels of communication are

considered some of the difficulties in pursuing regulatory approval (Piddock, 2012; Michael et al., 2014).

### **1.3. Antibiotics bacterial toxicity mechanisms**

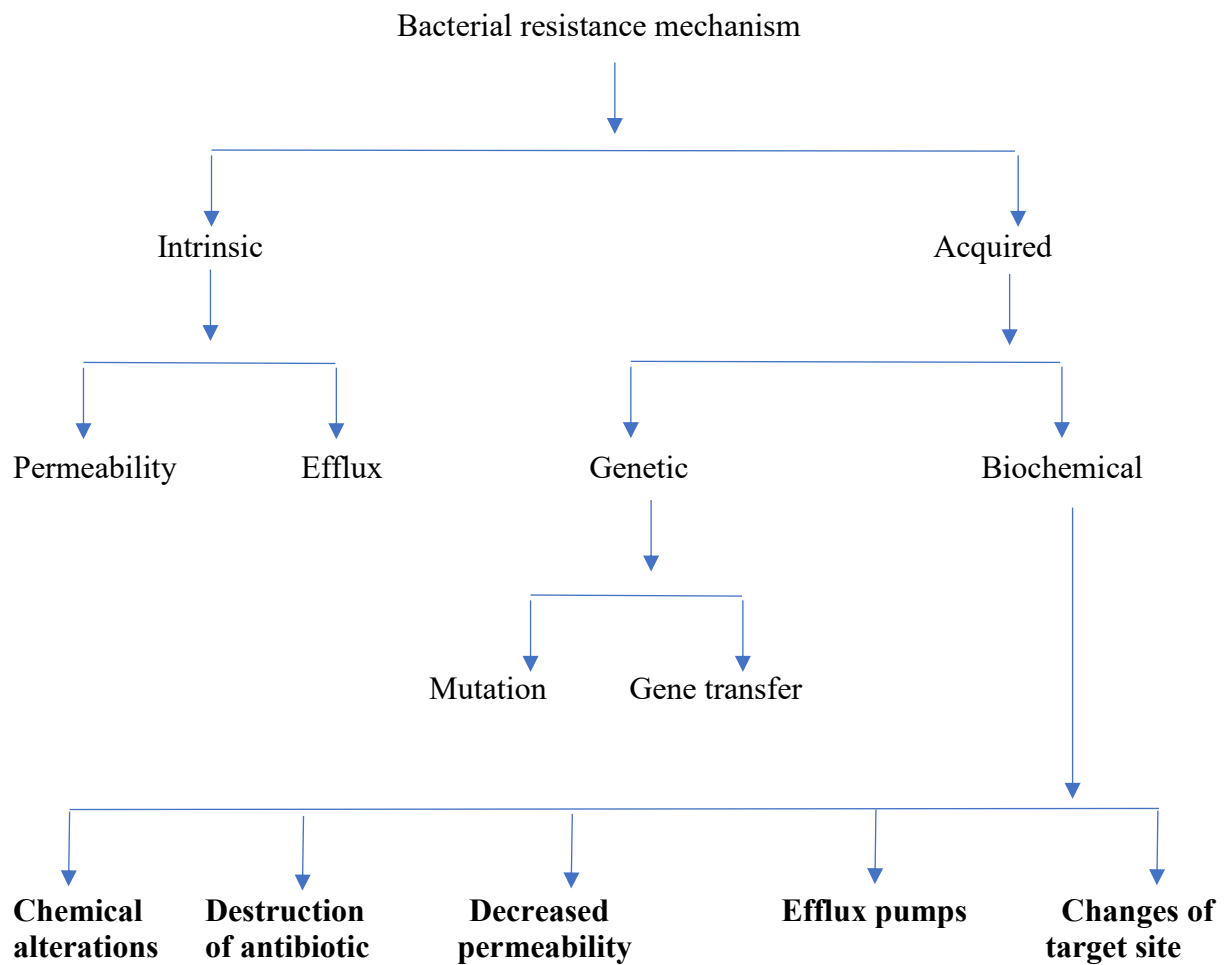
Antibiotics are widely known to damage vital bacterial cellular processes without substantially hindering or affecting the host cells (Guilhelmelli et al., 2013). Different classes of antibiotics (Table 1.1) inhibit or destruct the bacterial cell in different ways. An understanding of the mode of action of the molecules on bacteria can enhance the development of novel approaches for antimicrobial development (Kaufmann and Hung, 2010; Kohanski et al., 2010).

**Table 1.1.** Summary of mechanistic action and bacterial target of different classes of antibiotics  
(adapted from Brötz-Oesterhelt and Brunner, 2008).

Antibiotic classes	Mode of action	Target bacterial structure
<b>Beta-lactams (Penicillin, Carbapenems, Monobactam, Cephalosporins); Cyclic lipopeptides (Daptomycin); Glycopeptides</b>	Inhibition of cell wall synthesis	Blocking the transpeptidation process by inhibiting penicillin binding proteins making peptidoglycan crosslink weak, terminating D-ananyl-D-alanine amino acid in the peptidoglycan polysaccharide
<b>Aminoglycosides; Tetracycline; Macrolides; Oxazolidonones (Linezolid); Chloramphenicol (lincosamides, streptogramin)</b>	Inhibition of protein synthesis	Binding 30s and 50s subunits of ribosome, blockage of t-ribonucleic acid (tRNA) to 30s subunit of ribosome
<b>Fluoroquinolones (Ciprofloxacin)</b>	Inhibition of deoxyribonucleic acid (DNA) synthesis	Act on DNA gyrase enzyme responsible for the replication of DNA
<b>Rifampin</b>	Inhibition of RNA synthesis	Act on RNA polymerase responsible for the replication of RNA
<b>Sulphonamides</b>	Inhibition of folic acid pathway	Competitively inhibit dihydropteroate synthetase responsible for folic acid synthesis
<b>Polymyxins (Polymyxin-B, Colistin)</b>	Cell membrane permeability	Increase permeability and leakage of cell membrane, target lipopolysaccharide (LPS) of the outer membrane

#### **1.4. Bacterial resistance mechanisms to antibiotics**

Antibiotic resistance can be described in a biochemical term, as incapability of the chosen antibiotic to reach the targeted microbial site and inhibit the bacterial vital processes (Kashef and Hamblin, 2017). There are several mechanisms by which bacteria can demonstrate resistance to antibiotics (Figure 1.2).



**Figure 1.2.** Schematic representation of bacterial resistance (adapted from Cox and Wright, 2013; Munita and Arias, 2016).

#### **1.4.1. Intrinsic antibiotic resistance**

This type of resistance is developed naturally in the absence of any selected antimicrobial pressure (D'Costa et al., 2011; Bhullar et al., 2012). The intrinsic mechanisms of resistance are the permeability of the bacterial cell wall, whereby the peptidoglycan and outer membrane are selective barriers against toxic substances and the ability of the bacteria to transport one or more toxic components from the bacterial cell (Van Bambeke et al., 2000; Pagès et al., 2005; Liu et al., 2010; Cox and Wright, 2013; Randall et al., 2013). Apart from the two main mechanisms described above, the genetics of the bacteria also plays a vital role in the intrinsic resistance mechanism (Shakil et al., 2008; Cox and Wright, 2013).

#### **1.4.2. Acquired antibiotic resistance**

This type of resistance happens when any specific microbe possesses the capability to resist previously active antibiotics. Acquired resistance occurs through molecular or genetic means (Munita and Arias, 2016).

##### **i) Genetic basis**

Two main genetic strategies can be used by bacteria to resist the action of antibiotics and include;

- a) mutations in a gene or genes that result in bacterial resistance through a reduction in the affinity for the drug, drug uptake reduction and stimulation of efflux mechanisms to extrude the toxic substances (Manson et al., 2010; Gupta and Birdi, 2017; Yilmaz and Özcengiz et al., 2017).

- b) foreign DNA acquisition that codes for resistance traits through horizontal or vertical gene transfer (Munita and Arias, 2016). In the vertical gene transfer, mutation of one gene trait can lead to alteration in the various amino acids of the bacterial DNA. This might result in the development of resistant cell structure or enzyme that can bypass toxic compounds (Nielsen et al., 2014; Munita and Arias,



2016). In horizontal gene transfer, the resistant genes that might be present on the plasmids, transposons or integrons may be transferred to bacteria of same or entirely different genus or species (Giedraitienė et al., 2011; Domingues et al., 2012; Gandon and Vale, 2014; Brown-Jaque et al., 2015; Sharma et al., 2016). This might occur through conjugation (direct bacterial cell contact), transformation (part of a died or lysed bacterial DNA is picked up from environment) or transduction (viruses transferring DNA between two closely connected bacteria) (Huddleston, 2014; Sharma et al., 2016)

## **ii) Molecular basis**

Complex mechanisms of antimicrobial resistance might be evolved by bacteria over years. Multiple biochemical pathways can normally lead to evolve a cadre of resistance mechanisms that aid in the survival from the attack of a drug. The following are the various categories of the biochemical development of resistance (Munita and Arias, 2016).

- a) chemical alteration of the antibiotic occurs through the production of bacterial enzymes at the ribosomal level in both Gram-negative and Gram-positive bacteria (Wilson, 2014). The modifications are mostly found to occur in enzyme production, for example acetyltransferase and adenyltransferase alter biochemical processes and induce biochemical changes to the antibiotic molecule (Ramirez and Tolmasky, 2010; Hollenbeck and Rice, 2012). The most frequent biochemical reactions catalysed by these enzymes include adenylation (aminoglycosides, lincosamides), acetylation (aminoglycosides, chloramphenicol, streptogramins) and phosphorylation (aminoglycosides, chloramphenicol) (Ramirez and Tolmasky, 2010).
- b) Destruction of the antibiotic molecule; for example, the principle mechanism of the beta-lactamase enzyme is the destruction of beta-lactam family of antibiotics

by damaging the amide bond of the beta-lactam ring making the drug ineffective (D'Costa et al, 2011, Malloy and Campos, 2011; Karen Bush, 2013).

- c) Decreased permeability can be induced since porins present in the outer membranes selectively prevent the influx of the antibiotics. For example, Gram negative *Acinetobacter baumannii* and *Pseudomonas* possess an innate lower susceptibility to  $\beta$ -lactams than *Enterobacteriaceae* owing to lowered porin expression (Hancock and Brinkman, 2002; Pagès et al., 2005; Pagès et al., 2008).
- d) Efflux pumps result in bacterial resistance when the bacterial cell can pump out antimicrobial compounds. *Enterobacteriaceae* and *P. aeruginosa* have shown tetracycline resistance as a part of multidrug resistant species by extruding the drug using efflux pumps using protons as a source of energy (McMurry et al., 1980; Singh et al., 2002; Poole, 2005).
- e) Changes in the target site can be achieved by the bacteria not allowing antimicrobials to reach their binding site or by altering the target site that might reduce drug affinity. This can be achieved through various mechanisms such as changes / modifications / mutation in the target site and enzymatic alteration or complete replacement or bypassing of the target site (Campbell et al., 2001; Floss and Yu, 2005).

### **1.5. Biocides and biocide resistance**

Owing to the increasing bacterial resistance mechanism properties, much focus has been made in utilising antimicrobials as biocides. According to the European Parliament and Council Directive 98/8/EC, biocidal are product that have one or more active substances, that are intended to damage, avoid the action, render harmless, or otherwise exert a regulatory effect on any harmful organism either biologically or chemically (Kogan, 2005). The global elevation

in bacterial antimicrobial resistance that has led to a greater mortality and morbidity rate underlines the importance of the development of biocides to reduce bacterial transmission and infection in medical systems (Chen and Cooper, 2002). Biocides are utilised as antiseptics in hand disinfection, thus, preventing pathogen transmission (Silver et al., 2006). Biocides are also used for the sterilization or disinfection of heat sensitive devices where vapour high pressure decontamination is not possible. Sterilization is an important step to reduce infection risks, for medical devices that are used for skin penetration, like surgical instruments, implants and urinary catheters (Russell, 2003). Biocides are also used as disinfectants of non-critical devices, for instance, stethoscopes. However, extensive biocides usage has led to concerns that of bacterial emergence with decreased biocidal susceptibility and potentially antimicrobial resistance development (Fraise, 2002). Further, the introduction of the Biocide Directive has reduced the number of substances that can be used. Thus, novel antimicrobials such as metal ions and graphene based compounds (GBCs) can be considered as biocides to decrease the bacterial transmission and infections risks.

#### **1.6. Antimicrobially resistant and multidrug resistant bacterial species and their burden**

One or combinations of the antimicrobial mechanisms mentioned in Figure 1.2 used by bacteria may result in the development of clinical susceptibility breakpoints of isolates (susceptible, intermediate and resistant). Emergence of resistance to one antibiotic (AMR) or multiple antibiotics (MDR) is a great concern for the treatment of infections in the healthcare system (Stefanović et al., 2012). Moreover, some bacteria are found to be extensively drug resistant (XDR) meaning resistant to all approved therapeutic drugs (Magiorakos et al., 2012). The development of resistance in pathogenic bacteria compromises the treatment of invasive procedures such as transplantations, that require antibiotics for both pre- and post operations. It is predicted that between 38.7% and 50.9% of surgical infections are resistant to the usual prophylactic antibiotics in the U.S (Santajit and Indrawattana, 2016). Since the antibiotic

resistance evolution, treatment of patients infected by MDR and XDR pathogens is becoming difficult thus increasing risks, reducing numbers of positive clinical outcomes and increasing the number of deaths. For example, around a two-fold elevation has been reported in patient mortality and treatment cost when infected with resistant *Enterobacter species* versus susceptible patient culture infections (Reddy et al., 2009). Another study stated that nearly a two-fold greater death risk was attributed to infections produced by carbapenem-resistant *Klebsiella pneumoniae* versus susceptible strains in adult patients with *K. pneumoniae* (Shorr et al., 2009). Antibiotic resistant bacterial infections are thought to cause approximately 2 million infections and 23,000 deaths a year in the U.S. alone. In Europe, nearly 25,000 people die annually due to MDR bacterial infections (Santajit and Indrawattana, 2016). The AMR, MDR and XDR burden is not only limited to the healthcare sector but poses a significant pressure on the economy worldwide. Accordingly, an extra \$10,000–40,000 is spent on average for the patient's treatment when infected with resistant bacteria compared to susceptible strains (Santajit and Indrawattana, 2016). In Europe, it is estimated that the annual healthcare expenses associated with resistant infections are as high as €9 billion, which equates to £20,000 per patient episode in hospital (Oxford and Kozlov, 2013; Llor and Bjerrum, 2014).

### **1.7. AMR, MDR and XDR infections in general**

Owing to the transmission and resistance risks, it is estimated that 9% of in-patients in England and Wales suffer from hospital-acquired infections, resulting around 5000 mortalities with an economic burden related to extra care of more than £1 billion per year (Vaidya et al., 2018). Mostly MDR bacterial infections are transmitted through direct or indirect contact through contaminated surfaces. Owing to bacterial persistence or resistance to prescribed antibiotics and transmission risks, there is an increased risk of acquiring AMR, MDR and XDR bacterial infections during the usage of such medical devices, as catheters, bone implants and biomedical material implants (Joyanes et al., 2000; Kreisler et al., 2003; Smith and Hunter, 2008).

According to the Infectious Disease Society of America, the three tested pathogens used in this research namely *K. pneumoniae*, *A. baumannii* and *Enterococcus faecium* are considered among the ESKAPE pathogens. ESKAPE pathogens possess not only tendency to escape the antimicrobial action of broad range of antibiotics but simultaneously represent new methods of pathogenesis (Pendleton et al., 2013).

## **1.8. Bacterial species tested in this study**

### **1.8.1. *Klebsiella pneumoniae***

In 1882, Carl Friedlander first isolated *Klebsiella pneumoniae* from the lungs of patients that had died of pneumonia and describe them as an encapsulated *Bacillus* (Jondle et al., 2018). *Klebsiella pneumoniae* is a Gram-negative, non-motile and encapsulated bacterium, which belongs to the *Enterobacteriaceae* family. *Klebsiella pneumoniae* characteristically inhabits the surfaces of the human mucosal of the oropharynx and gastrointestinal tract. This bacterium can display high level of virulence and antibiotic resistance once it enters the body (Ashurst and Dawson, 2018).

*K. pneumoniae* causes community-acquired, hospital associated and nosocomial infections. Moreover, several other miscellaneous infections such as septicaemia, meningitis purulent abscesses, and pneumonia are caused by this bacteria (Doorduyn et al., 2016). All these infections are responsible for the high mortality and morbidity rate that occurs with this infection (Vuotto et al., 2014; Kondratyeva et al., 2017). Over the years, resistance in *K. pneumoniae* has occurred against four major antibiotic classes: aminoglycosides, cephalosporins, carbapenems and fluoroquinolones, and this has been steadily increasing (Doorduyn et al., 2016). There is a prevalence of extended spectrum beta-lactamase (ESBL) producing strains of *K. pneumoniae* in the USA and in some European countries. Moreover, Mediterranean countries and Eastern and South-Western Europe are endemic to MDR *K. pneumoniae* because of ESBL production (Kondratyeva et al., 2017).

The acquisition of antibiotic genes and intrinsic resistance to various classes of antibiotics limits treatment options, further worsening the situation. The proposed resistance mechanisms against different classes of antibiotics of *K. pneumoniae* comprise of i) the alteration of metabolic pathways, ii) changes in membrane permeability, iii) activation of efflux pump systems, iv) modification of antibiotic target sites, and v) release of antibiotic-inactivating enzymes. Among these mechanisms, the enzymatic degradations have played a vital role in the development of MDR and extensive drug resistance in *K. pneumoniae* (Lee et al 2017a). Currently, *K. pneumoniae* species producing carbapenemases and ESBLs enzymes have spread worldwide (Shahid et al., 2009).

Apart from showing resistance, bacteria have also developed several lines of evasion strategies and counter attacks to survive within the host (Kim et al., 2016). However, the genes that are responsible for the *K. pneumoniae* colonization and infections have not been completely elucidated (Martin et al., 2016). The bacterial capsule is considered as one of the most common defensive structures in *K. pneumoniae*, which protects it against antimicrobial agents, lysis and phagocytosis (Paczosa and Mecsas, 2016). The *K. pneumoniae* capsule is a thick, ~160 nanometer dense layer of polysaccharide that efficiently guards the bacterium from antagonistic surroundings by providing stability and protection to the organism (Schembri et al., 2005). Polysaccharides are high molecular weight structures formed of single or branched repeating components of two to seven monosaccharides (Cain et al., 2018). The outer membrane proteins of *K. pneumoniae* are also a major line of defence to protect the bacteria from toxic chemicals (Cain et al., 2018). The complex structure of the lipopolysaccharide and proteins controls the efflux and influx pumps that regulate the bacterial homeostatic mechanism (Zanzen et al., 2018).

Pneumonia has been identified by the World Health Organization and the Centre for Disease Control as an urgent threat to human health which is only curable with a trickle of last-line

antibiotics, such as colistin (Nation et al., 2014). Colistin was discovered in 1947 and first used as an antimicrobial in the late 1950s for Gram-negative infection treatment. However, its usage decreased in the 1970s owing to nephrotoxicity and the use of colistin was largely replaced by aminoglycosides (Velkov et al., 2014). Lately, colistin was reintroduced into the clinical setting because it remains largely effective against MDR *K. pneumoniae*. However, worldwide colistin resistance rates are around 1.5% for *K. pneumoniae*, and in some high-use countries this is thought to have reached up to 40% (Cain et al., 2018).

### **1.8.2. *Acinetobacter baumannii***

*Acinetobacter baumannii* was first isolated by the Dutch microbiologist Beijerinck in 1911 from soil using minimal media enriched with calcium acetate. *Acinetobacter baumannii* is a Gram-negative coccobacillus that is aerobic, non-fermentative and non-motile (Howard et al., 2012). *Acinetobacter baumannii* is commonly found to occur within aquatic environments, on skin and in high numbers from the respiratory and oropharynx secretions of infected patients. It has been categorised as a “red alert” human pathogen, causing alarm among the medical association, owing to its broad antibiotic resistance spectrum (Gootz and Marra, 2008; Howard et al., 2012).

It is considered as an opportunistic pathogen and has been found to cause a high incidence of nosocomial infections among immunocompromised individuals with a prolonged hospital stay in intensive care units worldwide (Gootz and Marra, 2008). The most common *A. baumannii* infections are pneumoniae, bacteraemia, wound and urinary tract infections. A mortality rate of nearly 26 % in the hospital setting and as high as 43 % in intensive care units are owing to *A. baumannii* infections (Manchanda et al., 2010). Among the inpatients of ventilator-associated pneumonia, nearly 15% of all hospital-acquired infections are caused by *A. baumannii*. This causes the maximum morbidity and mortality in healthcare units, with over 50 % reported cases

for resistant species to already effective and prescribed drugs (Perez et al., 2007; Manchanda et al., 2010).

*Acinetobacter baumannii* infections were treated preferably during the early 1970s with ampicillin, nalidixic acid, minocycline, carbenicillin or gentamicin, singly or in a combination therapy (Montefour et al., 2008). Since 1975, the organism was found to show resistance in almost all sets of therapy including the first and second generation cephalosporins. Moreover, a gradual increase in the resistance was found against the third and fourth generation cephalosporins, fluoroquinolones, semi synthetic aminoglycosides, and carbapenems (Manchanda et al., 2010). In contrast, imipenem was a drug of choice with almost 100% *A. baumannii* susceptibility. Nevertheless, a global emergence and spread of resistant to imipenem further limited the choice of antibiotics. Thus, carbapenems were the only useful agents remaining that could combat many severe *A. baumannii* infections. Furthermore, due to the emergence of carbapenem resistance of *A. baumannii*, largely through clonal spread, the therapeutic options are decreasing (Villers et al., 1998; Canduela et al., 2006; Manchanda et al., 2010).

Antibiotic resistance mechanisms shown by *A. baumannii* fall into three broad categories: i) enzymes that inactivate the broad spectrum of antibiotics such as  $\beta$ -lactamases and carbapenemases ii) outer membrane protection by selective permeability through porins and efflux pumps and iii) mutations altering the target sites or cellular functions like penicillin-binding proteins (Thomson and Bonomo, 2005; Rice, 2006; Eliopoulos et al., 2008). In *A. baumannii*, single or combination use of these mechanisms may occur in the pathogen resulting in resistance. The virulence factors showed by *A. baumannii* further increase its survival and pathogenicity making them an extensively resistant species (Lee et al., 2017b). Some of the prominent invasive strategies shown by this bacterium include production of capsular polysaccharide, which in turn shows intrinsic resistance to range of antibiotics. Further, *A.*



*baumannii* lipopolysaccharide consists of endotoxin that adds to their virulence by releasing O-antigen. Lastly, proteins present in the outer membrane possess strong adhesive properties towards epithelia cells, which aids in making it easier for the bacteria to localise and invade the host (Lin and Lan, 2014; Lee et al., 2017). Thus, virulence factors coupled with antibiotic resistance has made *A. baumannii* a global threat for infections (Manchanda et al., 2010).

### **1.8.3. *Enterococcus faecium***

*Enterococci* are one of the earliest members of the animal microbiome, which are believed to have existed in the early Devonian period around million years ago (Van Tyne and Gilmore, 2014). An oxygen-depleted environment which was rich in nutrients enabled the growth of these bacteria. *Enterococcus faecium* is commonly found in the gastrointestinal tract as a commensal in various organisms including humans (Miller et al., 2014; Tyne and Gilmore, 2014). *E. faecium* are Gram-positive cocci, facultative anaerobes, which are non-sporulating. *E. faecium* is considered one of the most prevalent multidrug resistant organisms in the hospital setting worldwide (Van Tyne et al., 2013). It is the third most commonly prevalent pathogen in the health-care settings responsible to cause several infections such as sepsis, surgical wounds, urinary tract infections and endocarditis (Van Tyne et al., 2013; Miller et al., 2014).

Hospital acquired *E. faecium* infections began to emerge in the late 1990s in the United States, alongside with the acquisition of vancomycin resistance. Vancomycin resistant *E. faecium* now occurs in most of the European countries such as Germany, Cyprus, Italy, Portugal and the UK and prevalence rates have risen above 10%. In some regions (e.g., Ireland and Greece) rates have exceeded 30% (Arias and Murray, 2012; Faron et al., 2016).

*Enterococcus faecium* has shown a gradual resistance to range of antibiotics such as ampicillin, imipenem, gentamicin, vancomycin and streptomycin (Arias and Murray, 2012). Various mechanisms that cause antibiotic resistance in *E. faecium* are i) the cell wall acting

as a protective barrier which inactivates drug binding proteins by altering the target sites or by causing drug inactivation, ii) the cell membrane increases bacterial resistance by altering the target and iii) changes in the ribosome decreases drug uptake, causes antibiotic inactivation and changes in cell signalling through efflux pump alteration (Hollenbeck and Rice, 2012). The last line of therapeutic drugs, daptomycin has been shown to fail and there have been an increased number of resistant isolates demonstrated (Rosa et al., 2014). It is thought that bacteria developed resistance gradually due to multiple mutations involving genes that control cell envelop homeostasis (Palmer et al., 2011).

### **1.9. Bacterial biofilms**

A biofilm is a one or more microbial species in a complex association within which cells stick to each other on abiotic or biotic surfaces, enclosed within milieu of extracellular polymeric substance (EPS) secreted by the bacteria themselves (Jarm, 2014; Vos, 2015) (table1.2). The substrate characteristics, for instance hydrophobicity / hydrophilicity, roughness and chemistry highly influence biofilm formation (Song et al., 2015).

**Table 1.2.** Composition of biofilms (Jamal et al., 2015)

<b>Composition</b>	<b>Percentage of matrix</b>
<b>Microbial cells</b>	2 – 5 %
<b>DNA and RNA</b>	< 1 – 2 %
<b>Polysaccharide</b>	1 – 2 %
<b>Protein</b>	< 1 – 2 % (including enzymes)
<b>Water</b>	Up to 97 %

It is generally considered that biofilms shield microorganisms from opsonization, not only from the antibiotics but also from innate immune responses of antibodies, the ciliary action of epithelial cells and phagocytosis (Song et al., 2015). In addition, the bacterial inhabitants of biofilms are significantly more resistant than planktonic phenotype cells to antimicrobial substances. Thus, after biofilm formation the treatment of an infection is generally more difficult (Römling et al., 2014). Bacteria that form biofilms are often found on the surfaces of tissues and on biomaterials in areas of persistent infection (Costerton et al., 1999). Medical devices, implants and catheters are specifically susceptible to biofilm development. In fact, biofilm development is a major concern of implant failure and frequently restricts the lifespan of many indwelling medical components (Dror et al., 2009; McConoughey et al., 2014; Percival et al., 2015).

The mechanisms of the antimicrobial resistance of biofilms are categorized into four categories which comprise of a) direct inactivation of antimicrobially active molecules b) modifications in target action sensitivity c) drug concentration reduction before reaching to the target area and (d) efflux schemes. However, it should be noted that the levels of antibiotic resistance in biofilms can differ among diverse settings and the crucial aspects responsible for this resistance may also vary (Xu et al., 2000; Mah and O'Toole, 2001; Høiby et al., 2010).

#### **1.9.1. *Klebsiella pneumoniae* biofilms**

*Klebsiella pneumoniae* can produce biofilms in which bacterial cell aggregates are embedded inside an EPS which stick to one other and / or to a substrate. Polysaccharides and DNA are the main constituents of complex EPS (Di Martino et al., 2003). The most clinically noteworthy biofilms of *K. pneumoniae* are those developed on the internal surfaces of catheters and other indwelling devices (Niveditha et al., 2012). Biofilms of *K. pneumoniae* can be a significant reason for the colonization of the respiratory, gastrointestinal and urinary tracts, that ultimately

lead to the development of aggressive infections particularly in immunocompromised patients (Nicolle, 2014).

Formation of biofilms of *K. pneumoniae* on abiotic / biotic substrata begin with the adherence of cells which progresses to microcolony development, maturation of the colonies and lastly dispersal of planktonic cells. The vital *K. pneumoniae* bacterial structures responsible in the biofilm development process are the fimbriae and the capsular polysaccharides (CPs) (Wang et al., 2016). Fimbriae facilitate adherence, whilst the CPs supports cell-to-cell communication and biofilm structure. Given the dynamic process of biofilm production and the variability of environmental stimuli, embedded cells must be capable of swift and extensive changes in gene expression (Vuotto et al., 2014). The bacterial cell cycles are vital processes controlled by quorum sensing, which is a system of responses responsible for the co-ordination of genetic factors in a microorganism community. In *K. pneumoniae*, regulators and autoinducers of a putative quorum sensing system have been designated, however data is still incomplete (Schroll et al., 2010; Vuotto et al., 2014). *Klebsiella pneumoniae* biofilms are partly protected from immune defences. The milieu of the complex biofilms blocks the contact of antibodies and other antimicrobial substances, thus decreasing their efficacy (Nicolle, 2014).

### **1.9.2. *Acinetobacter baumannii* biofilms**

As major infections are acquired in healthcare surroundings, an improved understanding of microorganism survival and their persistence in this environment is important. It is hypothesized that the capability of clinical isolates to survive dehydration, therapeutic options and the stress of nutrient availability direct the microbes to form biofilms on medically used materials. Bacterial functions such as cell to cell communication, substrate-controlled attachments, and excretion of biomolecules are vital aspects for biofilm development (Dufour et al., 2010). *Acinetobacter baumannii* can form biofilms on abiotic surfaces such as polystyrene and glass (Longo et al., 2014).

For *A. baumannii* biofilm formation, pili production is essential. Using the pili, the bacterial cells can attach to the substrate and form microcolonies which ultimately lead to full biofilm development (Cerqueira and Peleg, 2011; Longo et al., 2014). Biofilm related proteins are responsible for cell adhesion and cell to cell communication of biofilms (Weber et al., 2016). In addition, the production of capsular polysaccharide, surface antigen protein, the protection system of iron acquisition and outer membrane porins, when taken together increases bacterial resistance to most antibiotics, making *A. baumannii* an increasingly important resistant pathogen (Lee et al., 2017b). Though this species of bacteria is generally described as being ubiquitous in nature, strains belonging to *A. baumannii* are emerging as difficult opportunistic pathogens owing to the rapid increase in multidrug resistance. These infections can cause diseases particularly in compromised human and lately in the worst cases of necrotizing fasciitis (Longo et al., 2014; Lee et al., 2017b).

### **1.9.3. *Enterococcus faecium* biofilms**

*Enterococcus faecium* is considered a significant nosocomial pathogen which can develop biofilms on implanted biomaterials. It is responsible for the cause of several infections that are linked with wounds, burns and the urinary tract. This pathogen is a cause of concern in pyogenic infections, pelvic infections, endocarditis, blood stream and intra-abdominal infections owing to its rapid ability to form a biofilm matrix (Paganelli et al., 2013; Almohamad et al., 2014).

Pili expression is the first step of *E. faecium* cell adhesion on the substrate. Moreover, pili and EPS are considered to form a complex milieu that aid the bacterial cell to adhere to each other as well as to the surfaces (Hendrickx et al., 2013). The subsequent steps that lead to the *E. faecium* biofilm maturation is still not clearly described. However, various genes that lead to the formation of microcolonies after bacterial adhesion are autolysins, glycolipids and cell wall associated proteins. After the adhesion phase, components such as polysaccharides,

lipoteichoic acid, extracellular DNA, and proteases can contribute to maturation of the biofilms (Dunny et al., 2014; Farahani, 2016).

Apart from the bacterial existence in a planktonic form or as a sessile aggregation, the presence of nutrient rich conditioning films such as plasma or blood further increases the resistance capacity of pathogens. The next section describes details about bovine plasma which was used as conditioning film in this research.

#### **1.10. Bovine plasma as conditioning films of bacteria**

Conditioning films (CF) are formed on either surfaces or surrounding the cells and occur in the presence of organic biomolecules, especially proteins. The microbial host is a complex system comprising of a range of different types of organic load. According to various studies, CFs composed of proteinaceous and polysaccharide components from blood, plasma, tears, urine, and saliva respiratory secretions may affect the attachment of bacteria to biomaterials (Dunne, 2002; Lorite et al., 2011; Quintana et al., 2017).

Pathogens are surrounded in the *in vivo* conditions with a variety of organic materials such as plasma, blood and toxins that can affect the efficacy of an antimicrobial agents (Lourenço et al., 2018). In this study, plasma from bovine was used as one such substance to determine its effect on the antimicrobial efficacy of the compounds. The common proteins comprised in bovine plasma are albumin and prealbumin, transferrin, immunoglobulins, glycoprotein, lipoproteins, complement proteins, and coagulation proteins (for example plasminogen, thrombin, and fibrinogen). The presence of a CF provides a nutrient rich milieu that can enhance planktonic bacterial growth and might also decrease their susceptibility to antimicrobial agents. Moreover, the presence of CF on any substrate (biotic / abiotic) alters the adhesion conditions for the bacteria to this surface (Dunne, 2002; Gnanadhas et al., 2013).

Metals coatings such as titanium nitrate and zirconium nitride silver surfaces have been described as a potential material for use in bone fixation implants. These coatings were shown

to have a reduction in the retention of *Staphylococcus epidermis* and *S. aureus* when tested in presence of bovine serum albumin and blood conditioning films (Saubade et al., 2018 and Slate et al., 2019). However, studies related to the impact of conditioning films on bacteria growth pattern and antimicrobial efficacy in liquid medium conditions have not been widely explored.

### **1.11. Difference in Gram-positive and Gram-negative bacterial structures and their effect on resistance**

Broadly, owing to the majorly different cell-wall structure between two types of bacteria (Table 1.3), the resistance mechanisms are varied for each targeting antibacterial molecule between Gram-negative and Gram-positive bacteria (Hans et al., 2014). In Gram-negative bacteria, the penetration of various toxic substances is prevented by the outer membrane (Munita and Arias, 2016). Beta-lactams, some fluoroquinolones and tetracyclines are hydrophilic in nature and are particularly affected by any modification in the outer membrane, as they often target water-filled diffusion channels (porins) to cross the cell wall. A major example of this is vancomycin, which is found to be majorly inactive against Gram-negative bacteria owing to its outer membrane protection mechanism (Pagès et al., 2008). Gram-negative and Gram-positive bacteria also demonstrate differences in their susceptibility towards therapeutic agents. Similarly, low susceptibility of *Acinetobacter baumannii* and *Pseudomonas* to beta lactams compared to *Enterobacteriaceae* is in part owing to the reduced number of differential porin expression (Hancock and Brinkman, 2002).



**Table 1.3.** General differentiative features of Gram-negative and Gram-positive bacterial cell-wall (Sondi and Salopek-Sondi, 2004; Schäffer and Messner, 2005 and Weidenmaier and Peschel, 2008).

<b>Gram-positive Cell wall</b>	<b>Gram-negative cell wall</b>
Single layer and majorly made of peptidoglycan	Double layer with a peptidoglycan inside outer membrane
Thicker peptidoglycan layer (20 to 80 nanometer (nm))	Thinner peptidoglycan (5 to 10 nm)
Periplasmic space is absent	Periplasmic space is present
Outer membrane is absent	Outer membrane is present (7 to 10 nm thick)
Teichoic acid is present	Teichoic acid is absent
Porins are absent	Porins are present
Low lipid content (2 – 5 %)	High lipid content (15 – 20 %)
Generally, lipopolysaccharide is absent	Lipopolysaccharide is present
Example <i>E. faecium</i>	Example <i>K. pneumoniae</i> and <i>A. baumannii</i>

### **1.12. Bacteria macromolecules**

Some bacteria have flagella and pili on to the outer surface (Ferris and Beveridge, 1985). The cell envelope contains a capsule, cell wall, and cell membrane. The cytoplasm consists of enzymes, plasmid (DNA), the ribosomes (RNA and protein), and some inclusions that store nutrients and waste (Madigan, 2015). A living bacterial cell is composed of 70 % water and 30 % of ‘dry’ composition which includes macromolecules and small quantity of monomers and inorganic ions (Beveridge, 1999; Huang et al., 2008). Macromolecules (proteins, polysaccharides, lipids) which represent 96% of the cell dry biomass are small monomers (Madigan, 2015). These monomers are sugars, nucleotides, amino acids, fatty acids and their precursors, which represent 3% of the dry cell weight while inorganic ions of the cell comprise the remaining 1% (Kaiser, 2007; Madigan, 2015) (Table 1.6)

**Table 1.4.** The macromolecules in the bacterial cell and their subunits and location (Kaiser et al., 2007; Madigan, 2015).

Macromolecule	Primary subunit (monomer)	Location in the cell
<b>Proteins</b>	Amino acids	Cell wall, cell membrane, pili, flagella, ribosomes, as enzymes in the cytoplasm
<b>Lipids</b>	Fatty acids	Membranes, storage depots
<b>Polysaccharides</b>	Sugars (carbohydrates molecules)	Cell wall, capsule, inclusions (energy and carbon storage)
<b>Lipopolysaccharides</b>	Sugars and fatty acids	Membranes
<b>DNA</b>	Nucleotides	Ribosomes
<b>RNA</b>	Nucleotides	Nucleoid, plasmid

### **1.13. Need for an alternative antimicrobial**

All the above-mentioned factors such as bacterial resistance to existing antibiotics, the lack of new antibiotic discovery, increase in the AMR, MDR and XDR, morbidity and mortality due to bacterial infections, formation of bacterial biofilms and interaction of the organic biomolecules have produced a plethora of complex interactions leading to antimicrobial resistance that require novel interventions. This study tested a range of metal ions and graphene-based compounds (GBCs) as antimicrobials. In this work, these materials have been considered for use as biocides for cleaning solutions or for use in topical interventions to prevent the transmission and subsequent infection of infection.

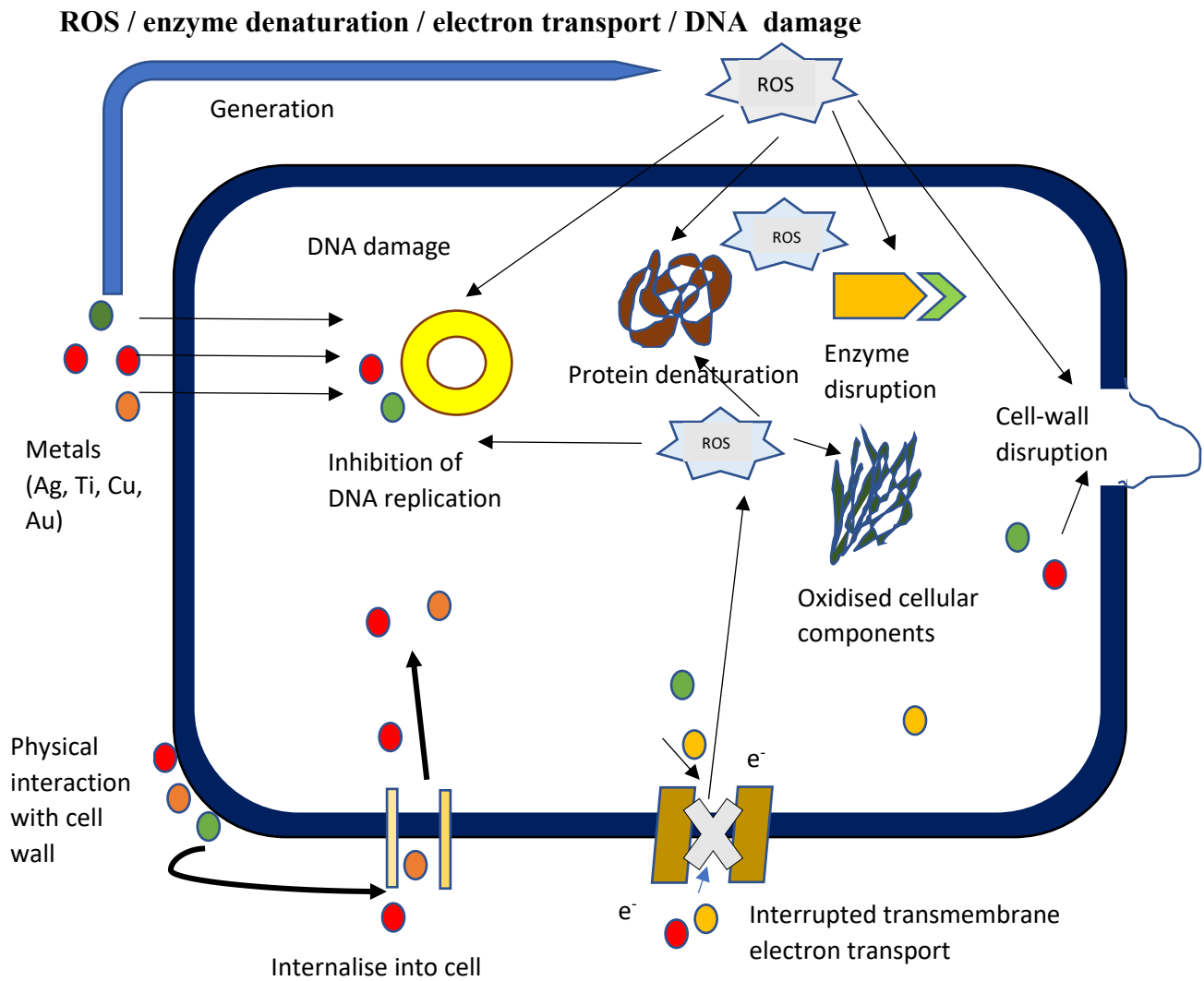
### **1.14. Metal ions as antimicrobials**

The antimicrobial properties of metals have been recognised throughout the history of medicine and healthcare (Elsome et al., 1996). For example, silver salts were used to control eye and wound infections and copper/mercury salts were used to prevent leprosy, gonorrhoea, tuberculosis and syphilis (Lemire et al., 2013). The wide application of metals in medicine was predominant until the discovery of antibiotics after which the use of metals as antimicrobials began to diminish. However, at the commencement of the twenty-first century, a rapid increase in antimicrobial resistance (AMR) threats and a lack of new available antibiotic drugs was observed (Habiba et al., 2015). Due to the development of pathogens in counteracting biocidal action of the antimicrobials, metals and their derivatives (for example, ions, nanoparticles and complex) may provide a solution to reduce the transmission of AMR bacteria.

### **1.15. General metal antimicrobial mechanism**

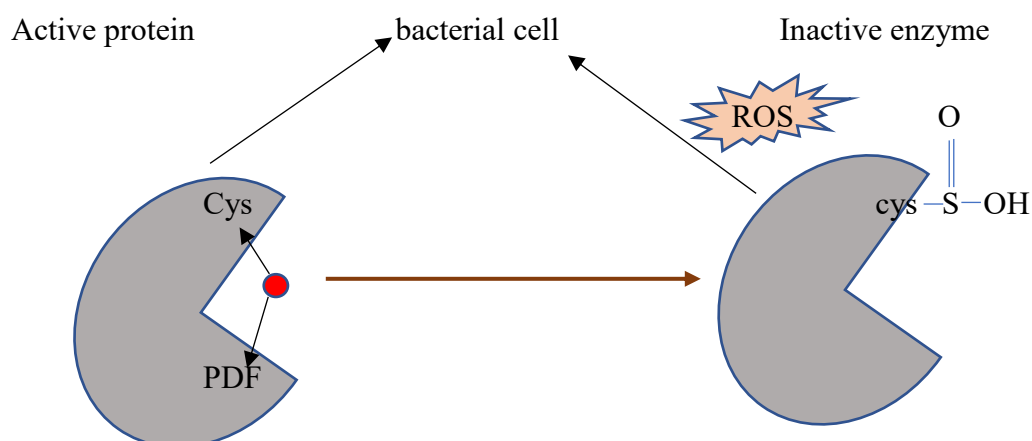
Despite the historic documented utilisation of metals as antimicrobials, the details of the toxicity of the metals is not clear. However, there is some chemical effect of metals that determines their antimicrobial efficacies on the cells (Hobman and Crossman, 2014). The antimicrobial action of metals begins with the metal ions affinity for varied cellular components

and biomolecules, which might form stable complexes leading to damaging vital bacterial cell processes (Nies et al., 1999; Hobman and Crossman, 2014). Metals demonstrate toxological effects in several ways, such as displacement / damage of essential enzymes, blocking vital biomolecule functional groups and participating in cellular chemical reactions (Lemire et al., 2013). One or more of these processes may damage proteins, denature DNA, induce oxidative stress and effect the biological walls / membranes (Lemire et al., 2013; Hobman and Crossman, 2014) (Figure 1.3 – 1.5). Usually metals demonstrate more than one type of antimicrobial mode of action (Table 1.5).



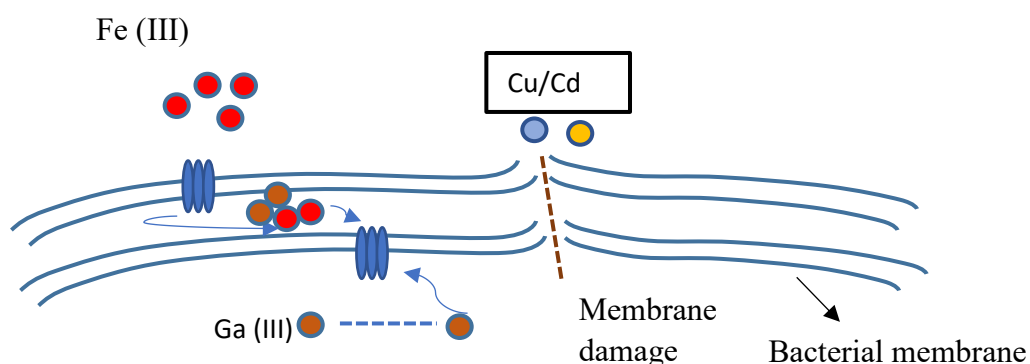
**Figure 1.3.** Antimicrobial activity mechanisms associated with metal nanoparticles that release metal ions (Adapted from Dizaj et al., 2014; Kolmas et al., 2014).

## Protein dysfunction



**Figure 1.4.** Antimicrobial mechanism showing metals such as iron, copper and arsenic increase intracellular ROS, which lead to DNA or vital enzymes (cysteine and peptide deformylase) degradation which are required for cell growth (Adapted from Lemire et al. 2013).

## Interference with nutrient uptake / membrane damage



**Figure 1.5.** Antimicrobial mechanism showing that the content of the bacterial membrane is highly electronegative, it attracts metal cations (such as copper (Cu), Cadmium (Cd) or Gallium (Ga) (III)), which assimilate leading to cell lysis (Adapted from Lemire et al. 2013).

**Table 1.5.** The antimicrobial properties of the metal ions tested in this study.

Metals in ionic form	Bacteria	Antimicrobial properties	References
Silver	<i>S. aureus</i> , <i>E. coli</i>	Precipitation of electron-dense particles, cell membrane damage, binding to protein and enzymes in the cell wall and membrane.	Sondi & Salopek-Sondi, 2004; Pal et al., 2007; Feng et al., 2000
Copper	<i>E. coli</i> , <i>Salmonella</i> species	Reactive oxygen species generation (ROS), Cu-bacterial protein binding, DNA damage, enzyme degeneration.	Stevenson et al., 2013
Rhodium / Ruthenium	<i>A. baumannii</i> , <i>E. faecium</i> , <i>K. pneumoniae</i>	Interruption of translation and transcription process, damage to ribosomal unit.	Bien et al., 1999; Beloglazkina et al., 2016; Vaidya et al., 2018
Zinc	<i>S. aureus</i> , <i>S. pyogenes</i> , <i>P. aeruginosa</i>	Oxidative stress, ROS production, structural changes in cell wall.	Ann et al., 2014; Sirelkhatim et al., 2015
Gold	<i>P. aeruginosa</i> , <i>E. coli</i>	Disrupt bacterial cell membrane, destruction of intracellular structures, and interaction with bacterial DNA.	Zhao et al., 2010
Platinum / Palladium	<i>E. coli</i> , <i>B. subtilis</i> , <i>B. cereus</i> , <i>S. aureus</i>	Bacterial protein and DNA damage, cellular protein-metal binding and exchange.	Kovala-Demertzi et al., 2003
Gallium / Indium / Niobium	<i>P. aeruginosa</i> , <i>E. coli</i>	Interference with cellular Fe metabolism, Fe irreversible mechanism.	Rogers et al., 1982; Olakanmi et al., 2010
Molybdenum	<i>E. coli</i> , <i>B. subtilis</i>	DNA lesions, disturbance in iron haemostasis	Lemire et al., 2013
Titanium / Tantalum	<i>S. aureus</i> , <i>E. coli</i>	ROS generation through production of hydroxyl radicals	Wang et al., 2016
Yttrium	<i>S. aureus</i> , <i>E. coli</i>	Disrupt membrane potential, reduce internal pH, increase lipoperoxidation	Lellouche et al., 2012



## 1.16. Antimicrobial potency of metal tested in this study

### 1.16.1. Silver

Biomaterial implants in tissue, bone and organ replacement therapy have been extensively used. Bacterial transmission risks and colonisation on biomaterial surfaces are significant post-implantation problems. The bacterial risks can be reduced with antibiotic impregnation. However, increased AMR species pose a challenge in controlling bacterial infections. Silver and its compounds have been used in medical devices because of their antimicrobial potency (Samani et al., 2013). Though the metallic form of Ag is inert, ionised Ag exhibits high reactivity as it can readily bind to nuclear membranes, microbial cell walls, and tissue proteins. This can lead to cell distortion and death (Krishnani et al., 2012). An *in vitro* study by Feng et al. (2000), demonstrated that Ag ions successively inhibited Gram negative (*E. coli*) and Gram positive (*S. aureus*) cells by entering inside the cytoplasm and damaging the DNA. Two studies confirmed that Ag in an ionic form successively inhibited AMR pathogens including *Enterococcus* species and *A. baumannii*, thus demonstrating the use of Ag as potential medical implant antimicrobial (Hrenovic et al., 2013; Ahmad and Viljoen, 2015).

Wounds may be colonised with pathogenic bacteria, which are responsible for localised and systemic infections, and therefore delayed wound healing. To reduce bacterial infections risks, Ag is used in wound dressings to control tissue damage at the wound site owing to bacterial colonisation (Jones et al., 2004; Thomas et al., 2011). The disk diffusion antimicrobial susceptibility test for silver alginate has been demonstrated to produce an enlarged zone of inhibition (ZoI) against bacterial species isolated from burn wounds including *A. baumannii*, *K. pneumoniae* and *E. faecium* (Thomas et al., 2011). The Ag dressing showed up to 30 mm (millimetre) ZoI against *E. coli*, *S. aureus* and *Streptococcus faecalis* (Castellano et al., 2007). Another study found that the Ag containing Hydrofibre demonstrated a greater ZoI against aerobic, anaerobic and antibiotic-resistant bacteria. Silver Hydrofibre were found to kill all

these challenging microbes after a 30 minutes exposure period, which was tested through the depth of penetration assays (Jones et al., 2004). Such work demonstrates the potential of Ag for use as an antimicrobial including for its use in dressings.

#### **1.16.2. Copper as an antimicrobial**

Surfaces in hospitals such as door handles, touch plates, call buttons, bed rails and toilet seats can be highly contaminated with pathogenic bacteria (Grass et al., 2011). Recently, the antimicrobial properties of Cu have gained significant attention to reduce the microbial load and thus, the transmission risks (Casey et al., 2010). Copper ions (0.4 and 0.8 mg/L concentrations) showed a significant potential application to disinfect water at hospital site, by reducing *P. aeruginosa* and *A. baumannii* by 99.99% after 1.5 and 24 hours respectively (Huang et al., 2008). Copper and its alloys are thought to possess medical and health care applications owing to their ability to kill bacteria by contact (Hans et al., 2014). However, the antimicrobial potency of Cu ions has been shown to vary according to the Cu content, time exposure and moisture content (Elguindi et al., 2011). This is supported by the work of Espirito et al. (2011), which concluded that a dry surface and 99.99 % pure Cu demonstrated a broad-spectrum and greater antimicrobial activity in laboratory and hospital settings compared to a lower content of Cu coupons. In addition, an Austrian study confirmed that the antimicrobial efficacy of the Cu coupons elevated with exposure of time (Steindl et al., 2012). Copper metal when in complex form has also showed a greater and specific toxicity against pathogens (Szymbański et al., 2012). Schiff base complexes chelated with Cu metal have gained significant attention for their antimicrobial abilities (Rosu et al., 2006). The release of the hydroxyl group of Cu ions from such complexes blocks the functional group on bacterial proteins and enzymes, inhibits or alters nucleic acids synthesis and/or changes bacterial cell wall synthesis (Amachawadi et al., 2015). Thus, Cu possesses a bacteria contact killing potency, which can be utilised on hospital surfaces and in water disinfection services in hospitals.

### **1.16.3. Platinum**

Platinum is low in abundance in the earth crust (0.003 parts per million (ppm) – 5 ppm) making it an extremely valuable and an expensive metal. After Rh, it is the second most expensive metal costing £37.66/gram on the London Platinum and Palladium Market (Capeness et al., 2015). Despite its cost, Pt possess the potential application to be utilised in high end medical implants (such as cardiovascular defibrillators, hip and knee implants) and catheters, to treat antimicrobially persistent infections (Cowley and Woodward, 2011; Saygun et al., 2006). Although platinum possesses antimicrobial properties, platinum complexes are already known to have low human cell toxicity (Mishra et al., 2006). The cisplatin Pt (II) and Pt (IV) complexes have been shown to have potential as anticancer sources with high action and low toxicity. However, in the Gaballa (2010) study, it was reported that the Pt co-ordination charge changes the complex antimicrobial action on bacterial cell permeability, with ionic form demonstrating a greater antimicrobial efficacy than neutral co-ordination forms.

### **1.16.4. Gold**

The antimicrobial property of Au and its compounds have been documented since earliest civilization by medical specialists to treat infections caused by bacterial. Recently, rising attention in the antimicrobial efficacy of Au against resistant pathogens (especially against Gram-positives) have been studied for use in the medical field (Sim et al., 2014). Work by others has demonstrated that Au ions and complexes (sulfanylcarboxylates and phosphane-gold (I) dithiocarbamates) possess greater antimicrobial efficacy against Gram-positive species (*S. aureus* and *B. subtilis*) compared to Gram-negative species (*K. pneumoniae*, *E. coli* and *P. aeruginosa*) (Barreiro et al., 2012; Nazari et al., 2012; Sim et al., 2014).

### **1.16.5. Palladium**

For over 20 years, palladium based alloys has been utilised in the dental restorative materials (dental crown implants and bridge alloys). Palladium based dental biomaterials are considered

biocompatible for oral environments and are thought to control oral pathogenic infections (Woodward, 2012). Recently, Pd alloys were considered as a potential catheter guidewire as a temporary implant, since as this material is antimicrobial, it can prevent cardiovascular disease infections (Woodward, 2012). Much attention has been carried out on screening the antimicrobial efficacy of the Pd complexes in medical implants to control bacterial transmissions (Juribašić et al., 2011). This is because Pd complexes possess a similar antimicrobial activity to antibiotics, which can be used as therapeutic sources to prevent AMR species infections (Sharma et al., 2011). Results demonstrating greater antimicrobial inhibitory effects were found for Pd complexes (with o-toluidinethiosemicarbazone and tetradentate macrocyclic) than antibiotics (amoxicillin and penicillin) against *Bacillus cereus*, *K. pneumoniae* and *E. coli* (Khan and Yusuf, 2009; Anacona et al., 1999).

#### **1.16.6 Rhodium and ruthenium**

Rhodium and Ru possesses a potential to be used as organometallic antimicrobials, in photodynamic antimicrobial chemotherapy and as photosensitisers or as topical applications to control bacterial infections. Both these complexes possess a greater toxicity against bacterial cells than eukaryotic cells (Bien et al., 1999; Ernst et al., 2011; Gorle et al 2014; Mukherjee et al., 2014; Li et al., 2015). This was confirmed with two studies using Human Colorectal Carcinoma cell lines to test for the cytotoxicity of Rh metalloinsertors against Human monocytic THP-1 cells and red blood cells to test oligonuclear polypyridylruthenium (II) complexes (Ernest et al., 2011; Li et al., 2011). The mononuclear methyl Rh complex showed excellent antimicrobial properties against range of Gram-positive and Gram-negative bacteria (Li et al., 2015). The polypyridylruthenium (II) demonstrated good antimicrobial activity (MIC = 12.5  $\mu\text{gml}^{-1}$  against *S. aureus*) (Li et al., 2011). Rhodium complexes with tetraaza macrocyclic and Ru (II) carbonyl thiosemicarbazone complexes have also been shown to possess an effective antimicrobial efficacy against range of bacteria (Bien et al., 1999; Jayabalakrishnan and Natarajan, 2002; Kannan et al., 2008).

#### **1.16.7. Titanium and tantalum**

Orthopaedic implants are generally introduced into joints of the spine, knee and shoulder. Moreover, metal plates are often implanted as adjacent bone in case of fracture repair and re-alignment of spine (Zhao et al 2009; Chang et al., 2014). Bacterial adhesion and infections are the major risk associated with implants, which are unsuceptible to most therapeutic options (Chang et al., 2014). Titanium / Ta is naturally selected for such implantation owing to combination of characteristics such as corrosion resistivity, bio-compatibility, mechanical strength, cost, capability to connect with bone and other tissues and primarily owing to their antibacterial potency (Zhao et al., 2009; Wu et al., 2018). Titanium / Ta has found extensive usage as orthopaedic implants for joint replacement, fracture healing and bone regeneration and as dental restoration materials (Silva et al., 2002; Del Curto et al., 2005; Zhao et al., 2009; Ferraris and Spriano, 2016; Ijaz et al., 2018). Both these metals-based materials are often found to be used in surgical instruments (Zhao et al., 2009). According to two studies, the antimicrobial efficacy of Ti coated surfaces demonstrated bacterial control. Titanium coated film releases Ti ions, which demonstrated no viable bacterial counts after 40 h of incubation against *S. aureus* and *E. coli* (Chung et al., 2008). However, titanium surfaces showed *E. coli* reduction (bacterial adhesion test) and bacterial accumulation (scanning electron microscopy (SEM) (Seddiki et al., 2014). Two studies by Huang et al. (2010) and Zhang et al. (2015) demonstrated that Ta-nitride and Ta oxide based coatings demonstrated antibacterial effects against both *S. aureus* and *Actinobacillus actinomycetemcomitans*.

#### **1.16.8. Zinc and gallium**

In burn / invasive wound infections are at a greater risk for the pathogen infections and transmission risks (Yang et al., 2017). Zinc (Zn) / gallium (Ga) is widely applied to treat burn / wounds owing the release of enzymes that are needed for microbial elimination in the infected area. In addition, owing to its anticancer and antibacterial properties Zn and Ga in nanoparticle

and ions forms were found to have drug delivery applications (Zhou et al., 2007; Zhu et al., 2015). Moreover, Zn is relatively inexpensive, relatively less toxic and biocompatible (Kumar et al., 2013). Owing to antimicrobial and ultraviolet absorption properties, Zn is also found an application in cosmetics and sunscreen (Kumar et al., 2013; Lu et al., 2015). The use of zinc oxide nanoparticles showed a 90 % and 48 % growth reduction against *B. subtilis* and *E. coli* respectively (Adam et al., 2014). A study by Ghule et al. (2006) demonstrated < 20 colonies after treatment with Zn-nitride against *S. aureus*. Yang et al. (2017) showed that Ga ions had an effective inhibitory concentration against *E. coli* and *E. faecalis* ( $256 \mu\text{g mL}^{-1}$ ) and  $512 \mu\text{g mL}^{-1}$  against *S. aureus*, *K. pneumoniae*, *A. baumannii*, *S. epidermis*, *P. aeruginosa*, *E. cloacae*, and *S. maltophilia*, which are all microbes commonly associated with burn infections.

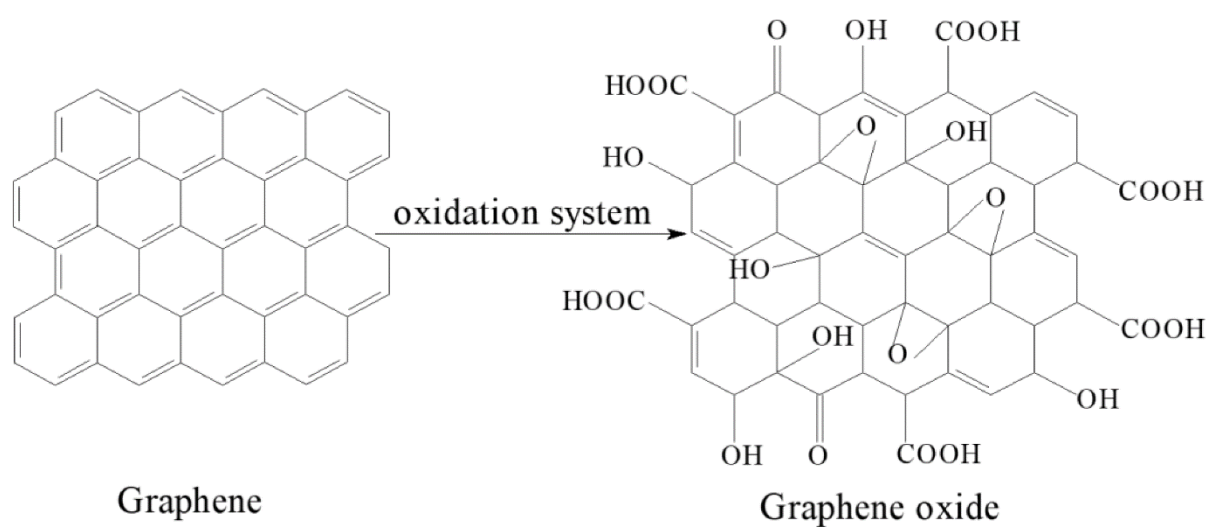
#### **1.16.9. Yttrium, indium, molybdenum and niobium**

With the increasing risk of pathogenic dissemination in the healthcare setting, novel metals such as Y, Mo and Nb usage as material coatings or as biomaterials have been investigated and have been found to decrease bacterial load (Baena et al., 2006; Gordon et al., 2007; Krishnamoorthy et al., 2013). Various studies have demonstrated the use of yttrium-based lasers to remove microbial load on dentures and dental implants (Kreisler et al., 2003; Gordon et al., 2007; Kamel et al., 2014). Yttrium-based lasers have been shown to produce up to 99 % bacterial reduction including the reduction of *Enterococcus faecalis* (Kreisler et al., 2003; Gordon et al., 2007). Yttrium complexes have demonstrated effective antibacterial activity against several Gram-negative and Gram-positive bacteria. Yttrium (III) complex with pyridinedicarboxylate demonstrated an inhibitory concentration of  $600 \mu\text{g mL}^{-1}$  -  $900 \mu\text{g mL}^{-1}$  against *E. coli* and *S. aureus* (Cai et al., 2010). Molybdenum trioxide ( $\text{MoO}_3$ ) was found to inhibit (100 %) pathogens such as *P. aeruginosa* and *S. aureus* (Zollfrank et al., 2012) after 6 h of incubation. This study claimed that a Mo based coating could be used as an innovative approach to prevent pathogen dissemination. Another study investigated the antibacterial

efficiency of MoO<sub>3</sub> nanoplates against *E. coli*, *Salmonella typhimurium* and *Enterococcus faecalis*, and *Bacillus subtilis* (MIC = 8 µgmL<sup>-1</sup> – 16 µgmL<sup>-1</sup>). The study demonstrated that MoO<sub>3</sub> had antimicrobial efficacy equivalent with the standard antibiotic kanamycin (Krishnamoorthy et al., 2013). Tests of the antimicrobial activity against *E. coli* were performed using a Mo coating and it was demonstrated that there was a complete kill of bacterial colonies (Mardare and Hassel, 2014). Moreover, Mo disulphide nanostructures inhibited *P. aeruginosa* biofilm up to 60 % at 150 µgmL<sup>-1</sup> (Qureshi et al., 2015). Binuclear Niobium(V)Tartrate complexes have been shown to display an effective antimicrobial inhibition (8 mm – 16 mm) at 60 µg against range of pathogens (Revanasiddappa et al., 2012). Also, Nb coating were found to reduce 95 % of *E. coli* biofilms (Baena et al., 2006). Indium (III) is an electron emitter, which allows its complexes to be possible dual imaging-therapeutic agents (Wang et al., 2017). An In (III) complex with semicarbazone demonstrated an antimicrobial inhibitory zone of 8 mm – 16 mm and MIC of 62.5 µgmL<sup>-1</sup> – 1000 µgmL<sup>-1</sup> against range of Gram-positive and Gram-negative bacteria (Wang et al., 2017). Indium coated nanoparticles demonstrated *P. aeruginosa* and *S. epidermis* inhibition of up to 20 mm (Pradeev Raj et al., 2017).

### **1.17. Graphene oxide (GO) and metal-GO as alternative antimicrobial**

Graphene is a single atom thick, two-dimensional sheet of carbon arranged hexagonally which was first isolated in 2004 by Geim and Novoselov (Chen et al., 2014). Graphene based compounds are recognised as a promising antibacterial material for application in the biological and medical fields (Szunerits and Boukherroub, 2016). Graphene oxide (GO) is a derivative of graphene that is modified by a various oxygen containing groups like carboxyl, epoxy and carbonyl. These groups provide chemical stability and solubility in water to GO (He et al., 2015).

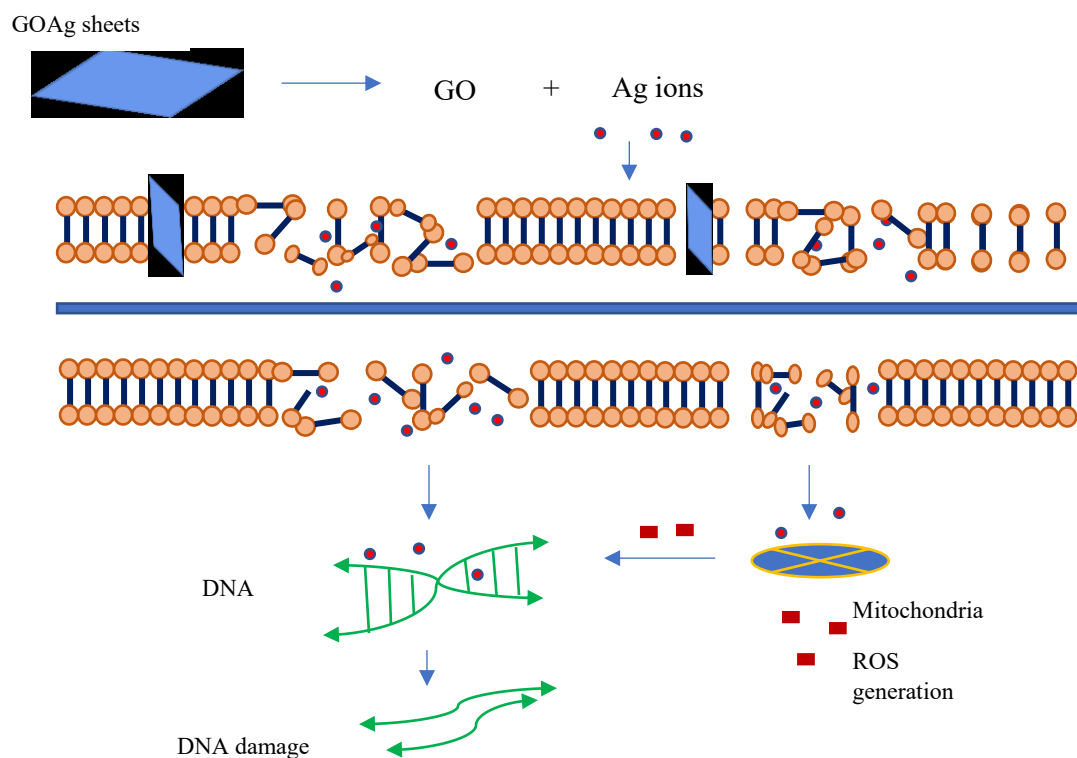


**Figure 1.6.** Structure of graphene and graphene oxide (Li et al., 2018).



The antimicrobial activity of graphene materials is dependent on both physical and chemical effects. Physical damage is brought about by the direct contact of sharp edges with bacterial membranes, which has been suggested to lead to destructive extraction of lipid molecules. Chemically, the generation of oxidative stress owing to release of intracellular ROS species is the major mechanism of bacterial destruction for graphene-based compounds (Figure 1.6) (Zou et al., 2016; Prasad et al., 2017). According to Adlhart et al. (2018), GO possess the potential to be used as a coated biocide in hospital settings to reduce / control the transmission risk associated with bacterial infections. This is owing to the morphological structure of GO with sharp edges. According to a study by Hu et al. (2010) and Hui et al. (2014), GO, rGO and graphene demonstrated inhibitory activity against the growth of a range of Gram-positive and Gram-negative bacteria including *A. baumannii* and *E. faecium*. Furthermore, graphene-based compounds have been used to disperse and stabilize various materials, such as polymers, metals and metalloids (Zou et al., 2016; Al-Jumaili et al., 2017). The use of graphene compounds not only provide a platform for the metal's stabilization and delivery but also prevents their aggregation. This is because the use of the graphene compounds provides the advantage of increased surface area of the particle, and thus, potentially elevated antimicrobial efficacy (Whitehead et al., 2017). Moreover, metals possess a range of transition states and GO possess a high capacity of storing and transporting electrons (Yang et al., 2013). Such a hybrid can provide an excellent photocatalytic material to control an aquatic bacterial load (Yang and Xu, 2013). In addition, such metal-graphene materials have shown to control medical pathogens. The graphenes have shown potential antimicrobial activities that can be used in commercial product packing, biomedical application, medical infection control and crop diseases (Chen et al., 2014; Nanda et al., 2016). Bacterial cell viability assays were shown to provide nearly a 90 % reduction for *Pseudomonas syringae* and *Xanthomonas campestris* when tested with GO (Chen et al., 2014). An AgGO composite was also shown to demonstrate strong antibacterial activity

with no viable *E. coli* cells after 10 mins of AgGO contact in a slurry reactor (Ma et al., 2011). Graphene oxide and rGO were also found to display lower numbers of viable bacterial counts compared to control against *E. coli* (Hu et al., 2010).



**Figure 1.7.** Antimicrobial mechanism of metal-GO hybrids on the bacterial cell membrane leading to death of the bacteria owing to physical damage of membrane by GO and internalisation of metal ions leading to cellular process damage producing ROS which can damage / lyse DNA (Adapted from Chowdhuri et al., 2015; Jin et al., 2017).

### 1.18. Efficacy of antimicrobials in combination

Combination therapy might be advantageous over monotherapy owing to several reasons: i) tackling development of bacteria resistance, ii) achieve broad spectrum target to inhibit bacteria iii) combinations might act additively or synergistically and iv) have broad antimicrobial activity and v) decrease the risk of inappropriate treatments (Pletz et al., 2017; Rhodes et al., 2017).

There is growing interest for the use of metal ion applications as organometallics therapy in combination with antibiotics for the treatment of arthritis and cancer tumors a part of which is to control the problem of transmission or colonization of AMR bacteria as an alternative strategy (Nazari et al., 2012; Ahmad et al., 2014). A study revealed that  $\text{Au}^{+3}$  ions increased the antimicrobial potency of several antibiotics such as cephalexin, tetracycline, amikacin, clindamycin, vancomycin and nitrofurantoin against *E. coli* and *P. aeruginosa* (Nazari et al., 2012). Due to an increasing failure of antibiotics towards resistant bacterial species, the clinical efficacy of various metal combined with medicinal plant extracts has also been screened. A study concluded that Zn ions combined with methanol and ethanol plant extracts of aloe vera and coriander enhanced the ZoI by up to 30 mm against *S. aureus*, *P. aeruginosa* and *E. coli* (Pandey and Shrivastava, 2013). Another study revealed a synergistic type of antimicrobial effect between Ag ion and *Mentha piperita* essential oil (Ahmad et al., 2014).

Metal coatings are extensively used as an implant device to control bacterial infections. A study aimed to test the combined antimicrobial effect of Ag and Zn ions coated onto hydroxyapatite (HAp). This study concluded that Ag and Zn ion incorporation onto a HAp structure improved its antimicrobial potency (Samani et al., 2013). A study by Huang et al. (2008) confirmed the synergistic effects of Ag and Cu ions against *A. baumannii*. This study found that combined Ag and Cu metals led to a greater inhibition compared to Ag and Cu metals in isolation. A bacterial (*Staphylococcus epidermis* and *S. aureus*) colony count method also demonstrated a

significantly lowered (66 %) bacterial load on Au-Pd combination coated prosthetic graft (60 % Au and 40 % Pd) after 12 hours of incubation compared to a control graft (Saygun et al., 2006). Thus, metal combinations seem to be a positive approach to find alternative antimicrobial sources because of their synergistic antimicrobial efficacy (Harrison et al., 2008). Silver and zinc coated zeolites were found to demonstrate 6 log and 3.5 log reduction in the bacterial count of *S. aureus* and *E. coli* respectively after 6 h (Cowan et al., 2003). An 8-fold of antimicrobial efficacy enhancement was achieved in a combinatorial treatment of Zn, Cu, nickel, cadmium and Ag against *E. coli* and *B. subtilis*. These combinations demonstrated synergistic efficacy and showed lower minimum inhibitory concentration (MIC) compared to the individual efficacy (Garza-Cervantes et al., 2017). Further Ravichandran et al. (2016) confirmed that combination of Zn, Cu and graphene produced a strong antimicrobial activity with inhibition of 16 mm against *E. coli* and *S. aureus*.

These findings suggest the use of metals may provide a positive approach to reducing AMR transmission and colonisation in some areas. Further, a synergistic effect of metal combinations with medicinal plants, antibiotics and with each other may also enhance antimicrobial efficacies. These properties thus possess a potential application not only to control AMR bacteria, but also to control them using lower antimicrobial concentrations.

### **1.19. Antimicrobial efficacy on bacterial biofilm phenotype**

A biofilm is difficult to treat owing to its complex polymeric structure and innate resistance. Once formed on a medical device, such as implants, or contaminated surfaces lead to infections risks. Thus, there is a need to design biomaterials that can restrict bacterial increased survival and hence biofilm development. Metals and GO alone or in combination with other antimicrobial agents can be an effective disinfectant (on hospital equipment or surfaces) or antisepsis (as biomaterials) to control bacterial biofilms (Ma et al., 2011; Ma et al., 2013; Zou et al., 2016). Gallium coated modified medical devices have demonstrated antimicrobial efficacy in *P.*

*aeruginosa* biofilm control (Ma et al., 2013). Moreover, these antimicrobials also showed an effective control on pathogens found in wound infected areas. The sol-gel dressing made of Ag metal showed an effective reduction in the adhesion and formation of *S. epidermis* biofilm over period of 10 days (Stobie et al. 2008). Biofilm evaluation techniques using microtiter plates revealed that newly formed and mature biofilms of *S. aureus* and *P. aeruginosa* was effectively reduced by GO after 24 h of treatment. According to this study GO can be an effective antiseptic in controlling chronic wounds bacterial infections (Di Giulio et al., 2018). Oral pathogen biofilms are responsible for the etiopathogenesis causing periodontal disease. The conventional anti-biofilm approaches are usually focused on developing dental adhesives that can to control attachment and colonization of pathogens (Yang et al., 2012; Sadekuzzaman et al., 2015). Lately, graphene-based materials such as GO have been tested against oral pathogens signifying an option to use them in dental materials (He et al., 2015; Rago et al., 2015). Bregnocchi et al. (2017) demonstrated only 28 % *Streptococcus mutans* biofilm survival after 24 h of incubation with GO based dental adhesives using a crystal violet biofilm assay. Combinations of antimicrobials further enhances the antimicrobial efficacy to prevent bacterial colonisation. Javeen Kim et al. (2008) found that Ag and tobramycin sequential treatments demonstrated an enhanced antimicrobial potency of 200% on biofilm of *P. aeruginosa*. Gallium-Ti coated surfaces after 28 days of incubation, showed an effective *E. coli* biofilms control (Zhu et al., 2015). The addition of 0.1 % Nb to Cu was also shown to reduce 99.9 % of *E. coli* biofilms after 24 h of treatment (Baena et al., 2006).

#### **1.20. Potential cytotoxicity of metal ions and GBCs**

The effect of the metal on the human cell in terms of toxicity also needs consideration. A study by Heidenau et al. (2005), demonstrated that higher concentrations ( $2.5 \times 10^{-3} \text{ molL}^{-1}$ ) of Cu were tolerable by tissue cells (surrounding the abdominal wall). However, the histopathology evaluation for Au and Pd coatings of a polypropylene graft (a graft used in abdominal wall

defects and inguinal hernia) demonstrated a tolerable fibroblastic proliferation and tissue denaturation (Saygun et al., 2006). Silver dressings have also been found to exhibit tissue and cell toxicity. To extend this, multiple daily application of Ag topical creams and solutions in wound dressing showed astringent effects on surrounding tissues leading to its discolouration (Saygun et al., 2006). Silver ions released from silver nitrate solution higher than  $50 \times 10^{-4} \%$  to prevent wound bacterial infections were found to show toxic effects on keratinocyte monolayer and fibroblastic cell lines after 3 hours of incubation (Poon and Burd, 2004). Metal combinations (silver, mercury and zinc) on titanium coatings (used in fracture implantation) increased the coatings antimicrobial efficacy against *S. aureus*. However, these metals exhibited strong cytotoxicity. More than 50 percent (%) fibroblastic cells were reduced at concentrations  $3.5 \times 10^{-3}$ ,  $3.6 \times 10^{-3}$  and  $4.2 \times 10^{-3}$  M/L of Ag, Zn and Hg respectively. It is important to adjust confounding factors such as test parameters (temperature, pH, moisture content) for culture conditions of cell lines and bacteria to enable a more direct *in vitro* metal toxicity comparison (Heidenau et al., 2005).

## **Aim**

Evaluate the antimicrobial efficacies for metal ions and GBCs against *K. pneumoniae*, *A. baumannii* and *E. faecium* in the absence and presence of bovine plasma as conditioning films.

## Chapter 2

### 2. Methods and materials

#### 2.1. Synthesis of graphene-based compounds

The GO, AgGO, CuGO, AuGO and PdGO were prepared in the laboratories of Prof. Craig Banks by his research students at Manchester Metropolitan University. For the synthesis of the compounds, all chemicals (analytical grade or higher) were used as received from Sigma-Aldrich (UK) without any further purification and all solutions were prepared with deionised water of a resistivity not less than 18.2 MU cm. Synthetic graphite powder was commercially obtained from Gwent Group (Pontypool, UK).

Graphene oxide (GO) was synthesized by using the Hummers method via the oxidation of synthetic graphite (Hummers Jr. and Offeman, 1958). Graphite flakes (5 g) and  $\text{NaNO}_3$  (2.5 g) were combined in 115 mL of concentrated  $\text{H}_2\text{SO}_4$  and stirred for 30 min.  $\text{KMnO}_4$  (15.0 g) was gradually added to the suspension, whilst kept in an ice bath ( $<5^\circ\text{C}$ ), and the rate of addition was controlled to keep the reaction temperature below  $15^\circ\text{C}$ . The mixture was heated to  $35^\circ\text{C}$  for a 30 min period and underwent continuous stirring producing a brown paste. A further dilution was made by adding 250 mL of water to the mixture and the temperature was increased to  $70^\circ\text{C}$  for 15 min. The resultant mixture was diluted by adding  $\text{H}_2\text{O}$  until a final volume of 1 L was obtained. Finally, the solution was treated with 15 mL of  $\text{H}_2\text{O}_2$  (30% w/w) to terminate the reaction, at which stage the solution became yellow in appearance. For purification, the mixture was filtrated and the obtained solid was washed thoroughly with Milli Q water several times in order to remove sulphate contamination.

The powder was dried at  $60^\circ\text{C}$  during 48 h. In the preparation of the AgGO, a sonochemical reduction method was utilised (Anandan and Muthukumaran, 2015). Following preparation of the GO, 0.5 g was added to 150 mL of ethylene glycol and sonicated for 30 min. In a separate vesicle, 1.0 g of silver nitrate was added to 20 mL of ethylene glycol and sonicated for 30 min.



The silver nitrate dispersion was added drop-wise to the GO solution whilst undergoing sonication for 30 min to produce a homogeneous mixture. Finally, 50 mL of 0.1 M NaBH<sub>4</sub> was added to the resultant AgGO mixture and a further 30 min of sonication was performed. The product was purified with repeated steps of H<sub>2</sub>O and ethanol washing, after which the solution was dried at 50 °C.

The ZnOGO was fabricated by dissolving 5.0 g GO in 200 mL of N, N, -dimethylformamide (DMF), along with 20 mL of 1M zinc acetate dihydrate (pH of 6.5). The homogeneous solution was heated to 60 °C and was stirred continuously for 120 min, after which the solution was heated to 250 °C. Following solvent evaporation, partial ZnO/ZnOHGO was produced. The resulting dried product was collected and ground in an agate mortar prior to being annealed at 450 °C for 120 min within atmospheric conditions to obtain the final ZnOGO product (Liu et al., 2012).

The graphene oxide solution, graphene, graphene carboxyl, graphene fluorocarbons, graphene nanoplatelets, graphene oxygen, graphene argon, graphene ammonia and graphene nitrogen were purchased from Graphene Supermarket (USA). Except for the graphene oxide solution, all GBCs were ground to fine particles using a mortar and pestle. Two milligrams of ground GBCs were suspended in 2 mL of sterile water and using a vortex mixer a homogenous mix was obtained. Each time before use the suspension was vortex.

## **2.2. Metal ions preparation**

Standard ionic solutions of 1 mgmL<sup>-1</sup> of yttrium (Y), titanium (Ti), tantalum (Ta), indium (In), niobium (Nb), rhodium (Rh), ruthenium (Ru), molybdenum (Mo), zinc (Zn), gallium (Ga), silver (Ag), copper (Cu), platinum (Pt), gold (Au) and palladium (Pd) (Sigma-Aldrich, UK) were used (Table 2.1). These were diluted with a sterile water to obtain 0.5 mgmL<sup>-1</sup>, 0.1 mgmL<sup>-1</sup> and 0.05 mgmL<sup>-1</sup> metal concentrations respectively. As the metals were dissolved in acids,

four acid control solutions were used; 5 % hydrochloric acid (HCl) 10 % HCl, 5 % nitric acid (HNO<sub>3</sub>) and 2 % (HNO<sub>3</sub>), which corresponded to the ion diluents (Fisher Scientific, UK).

**Table 2.1.** Metal ions, acid diluents, atomic number, electronic configuration, subshell electronic configuration, electronegativity (Pauling scale), charge on ions and counter ions in solution for the metal ions used in this study (Lenntech, 2017; Science notes, 2015; The catalyst, no year).

Please note that as the metals were dissolved in acid solutions it is difficult to find the exact metal charges, hence all the possible metal charges are mentioned with the most common in bold. \* EN = electronegativity

Metals	Acids controls	Atomic number	Electronic configuration	EN**	Possible charge on Ion in solution	Counter ion in solution
Y	2 % HNO <sub>3</sub>	39	[Kr]4d <sup>1</sup> 5s <sup>2</sup>	1.22	<b>+3</b> , +2, +1	Nitrate
Ti	2 % HNO <sub>3</sub>	22	[Ar]3d <sup>3</sup> 4s <sup>2</sup>	1.54	<b>+4</b> , +3, +2, +1, -1, -2	Nitrate
Ta	2 % HNO <sub>3</sub>	73	[Xe]4f <sup>14</sup> 5d <sup>3</sup> 6s <sup>2</sup>	1.50	<b>+5</b> , +4, +3, +2, +1, -1, -3	Nitrate
In	2 % HNO <sub>3</sub>	49	[Kr]4d <sup>10</sup> 5s <sup>2</sup> 5p <sup>1</sup>	1.78	<b>+3</b> , +2, +1, -1, -2, -5	Nitrate
Nb	2 % HNO <sub>3</sub>	41	[Kr]4d <sup>4</sup> 5s <sup>1</sup>	1.60	<b>+5</b> , +4, +3, +2, -2, -1, -3	Nitrate
Zn	2 % HNO <sub>3</sub>	30	[Ar]3d <sup>10</sup> 4s <sup>2</sup>	1.65	0, +1, <b>+2</b> , -2	Nitrate
Ag	2 % HNO <sub>3</sub>	47	[Kr]4d <sup>10</sup> 5s <sup>1</sup>	1.93	<b>+1</b> , +2, +3, +4, -2, -1	Nitrate
Cu	2 % HNO <sub>3</sub>	29	[Ar]3d <sup>10</sup> 4s <sup>1</sup>	1.90	<b>+1</b> , +2, +3, +4, -2	Nitrate
Ga	5 % HNO <sub>3</sub>	31	[Ar]3d <sup>10</sup> 4s <sup>2</sup> 4p <sup>1</sup>	1.81	<b>+3</b> , +2, +1, -1, -2, -4	Nitrate
Rh	5 % HCl	45	[Kr]4d <sup>8</sup> 5s <sup>1</sup>	2.28	+6, +5, +4, +3, +2, <b>+1</b> , -1, -3	Chloride
Ru	5 % HCl	44	[Kr]4d <sup>7</sup> 5s <sup>1</sup>	2.20	<b>+1</b> , +2, +3, +4, +5, +6, +7, +8, -4, -2	Chloride
Pt	5 % HCl	78	[Xe]4f <sup>14</sup> 5d <sup>9</sup> 6s <sup>1</sup>	2.28	<b>+6</b> , <b>+5</b> , <b>+4</b> , <b>+3</b> , <b>+2</b> , <b>+1</b> , -1, -2, -3	Chloride
Au	5 % HCl	79	[Xe]4f <sup>14</sup> 5d <sup>10</sup> 6s <sup>1</sup>	2.54	+5, +3, +2, <b>+1</b> , -1, -2, -3	Chloride
Pd	5 % HCl	46	[Kr]4d <sup>10</sup>	2.20	<b>0</b> , <b>+1</b> , <b>+2</b> , <b>+3</b> , <b>+5</b> , <b>+4</b> , <b>+6</b>	Chloride
Mo	10 % HCl	42	[Kr]4d <sup>5</sup> 5s <sup>1</sup>	2.16	+6, +5, +4, +3, +2, <b>+1</b> , -1, -2, -4	Chloride

### 2.3. Bacterial strains and growth conditions

Pure cultures of *K. pneumoniae* NCTC 9633, *A. baumannii* NCTC 12156 and *E. faecium* NCTC 7171 were used and stored at -80°C. *K. pneumoniae* and *A. baumannii* were sub-cultured every 3 weeks onto a nutrient agar and incubated at 37°C in aerobic conditions for 24 h. Brain heart infusion agar was used to subculture *E. faecium* every 3 weeks and was grown in a 5 % CO<sub>2</sub> incubator for 24 h at 37 °C. Nutrient agar and broth for *K. pneumoniae* and *A. baumannii* and brain heart infusion agar and broths for *E. faecium* were used for all the tests.

### 2.4. Bacterial preparation

From overnight growth of the bacterial cultures, 10 mL of appropriate broth were put into a sterile universal for Zone of inhibition (ZOI) assays. One hundred and fifty millilitres of appropriate broth were put into a conical flask for minimum inhibitory concentrations (MICs) assays and crystal violet biofilm assays (CVBAs). These were inoculated with a single colony of bacteria and incubated overnight according to the above conditions. Following incubation, the cells were harvested at  $1721 \times g$  for 10 min and washed once using sterile distilled water and vortexed until formation of homogenous mixture. The washed bacterial suspension was re-harvested by centrifuging again  $1721 \times g$  for 10 min and re-suspended in sterile water. The inocula were measured in a spectrophotometer at 540 nanometres and compared against a blank of sterile distilled water to determine their optical density (OD). To determine the cell concentrations, the OD adjusted inocula were serially diluted. Hundred microliters (µL) of the OD adjusted inoculums were spread onto the respective agars using sterile spreaders and incubated for 24 h in the appropriate conditions. After incubation, the colonies were counted and quantified using following formula.

$$\text{Number of colonies} \times \text{dilution factor} / \text{conversion of dilution factor to mL}$$

The cell concentrations corresponded to *K. pneumoniae*  $2.82 \times 10^8$ , *A. baumannii*  $1.85 \times 10^8$  and *E. faecium*  $3.95 \times 10^8$  colony forming units per mL (CFU/mL).

## **2.5. Bacterial conditioning film (CF) preparation**

Powdered bovine plasma (P4639 Sigma Aldrich, UK) was used to form the conditioning films. One gram of plasma was dissolved in 10 mL of sterile water. Using a 10 mL sterile syringe, the plasma suspension was filter sterilised through 0.2  $\mu\text{m}$  filters into a sterile universal. The sterile plasma suspension was stored at  $-4\text{ }^{\circ}\text{C}$  for future use.

To prepare the bacteria with a conditioning film, 1 mL of sterilised plasma was mixed into 9 mL of  $\text{OD} = 1 \pm 0.1$  adjusted bacterial suspension. These plasma and bacterial mix suspension (10 %) were directly used to perform the microbiology tests.



All the following assays are performed in the absence and presence of 10 % bovine plasma condition films.

## **2.6. Zone of inhibition (ZoI) to test single samples in the absence and presence of 10 % CF**

The ZoI was measured using the different metal ion solution concentrations,  $0.05\text{ mgmL}^{-1}$ ,  $0.1\text{ mgmL}^{-1}$ ,  $0.5\text{ mgmL}^{-1}$  and  $1\text{ mgmL}^{-1}$ . Hundred microliters of cell suspension or cell suspension and 10 % plasma CF was pipetted and spread across the entire area of the agar. Three equal wells (8 mm diameter) were cut out of each agar plate using a sterile cork borer and a stainless-steel needle, which were sterilised in 70 % ethanol and flamed before use. To each of the wells, 100  $\mu\text{L}$  of the metal ions or GBCs was added. The plates were incubated in the appropriate incubating condition for 24 h. The ZoI was measured in mm to determine an average mean value ( $n = 24$ ). The tested metal ions were categorised based on inhibition zones demonstration into i) 0 mm = no effect, ii) 0 mm – 4 mm = weak effect, iii) 4 mm – 9 mm = moderate effect and iv)  $> 9\text{ mm}$  = strong effect.

## **2.7. Minimum inhibitory concentration test (MIC) in the absence and presence of 10 % CF**

The minimal inhibitory concentration (MIC) is defined as the lowest concentration of antimicrobial to prevent bacterial growth (Russel and Chopra, 1990). One millilitre of Triphenyl tetrazolium chloride (TTC) blue metabolic dye (Sigma-Aldrich, UK), was added into 9 mL of the cell suspension so that the working concentration of the dye was 0.15 % w/v. To determine the MIC, 100  $\mu$ L of the test samples / acid controls were added to a 96 well flat-bottomed micro titre plate (MTP). One hundred microliters of bacterial suspension or bacterial suspension and 10 % plasma CF with the TTC dye was then added using a multi-channel pipette; the first column of cell/metal ion suspension was mixed, then 100  $\mu$ L of the sample/bacterial mix was transferred to the column 2 wells. The dilution method was repeated until column 10 upon which 100  $\mu$ L of the mixture was disposed of. To column 11, 100  $\mu$ L of bacterial suspension without a metal (positive control) was added and to column 12 and 100  $\mu$ L of un-inoculated broth was added (negative control). After incubation, the MIC was taken as lowest concentration that inhibited the visible growth of the bacteria by comparison with the controls. Growth was indicated by a change of colour in the well to dark blue/purple ( $n = 4$ ).

	1	2	3	4	5	6	7	8	9	10	11	12
A												
B												
C												
D												
E												
F												
G												
H												

**Figure 2.1.** The dilution of metals ions or GBCs and bacterial suspension with and without plasma CF across the 96 wells of the MTP. The red and blue lines indicate the dilution of the content across the plate.

## **2.8. Minimum bactericidal concentration test (MBC) in the absence and presence of 10 % CF**

The MBC is defined as the lowest concentration required to completely inactivate the inoculum in a given time (Humphreys et al., 2011). Twenty-five microliters of culture were taken from the first well that showed no growth and the last well that demonstrated growth and was pipetted onto agar plates using Miles and Misra methodology. These plates were incubated overnight for 24 h at 37 °C in a 5 % CO<sub>2</sub> incubator. After incubation, the lowest concentration well sample that showed no bacterial growth on the agar plate was determined to be the MBC for that test sample (n = 4).

## **2.9. Time kill assay in the absence and presence of 10 % CF**

Time kill assays were performed to investigate the viable cell count over period in presence of antimicrobial agents using 100 µL of 0.01 mgmL<sup>-1</sup>, 0.1 mgmL<sup>-1</sup> and 1 mgmL<sup>-1</sup> of metal ions and 1 mg and 10 mg of GBCs over a period of 0 h, 2 h, 4 h and 24 h. To evaluate the effect of metal ions and GBCs on bacteria; t = 0 is considered after addition of the test samples and OD adjusted bacteria into media broth. As metals were dissolved into acids. 2 % HNO<sub>3</sub> and 5 % HCl acid controls antimicrobial effects were also tested against each isolate. A negative control without any antimicrobial agents were also performed. In a sterile universal, 15 mL of sterile respective broth was taken. One hundred microliters of OD = 1.0 ± 0.1 adjusted bacterial suspension or bacterial suspension and 10 % plasma CF was added to the 15 mL of the broth. At each time point, 100 µL of sample was taken and serially diluted to 10<sup>-8</sup>. One hundred microliters were taken from each dilution and poured onto sterile agar plates, which were incubated for 24 h. The plates were used to quantify for viable bacterial cells using below formula,

$$\text{Colony forming unit per mL (CFUmL}^{-1}\text{)} = \frac{(\text{no. of colonies} \times \text{dilution factor})}{\text{volume of culture}}$$



## **2.10. Scanning electron microscopy (SEM) in the absence and presence of 10 % CF**

### **2.10.1 Sample preparation**

Polished silicon wafers (Montco Technologies, USA) were cut into 1 cm × 1 cm size pieces using a ruler and diamond scribe pen. In a conical flask, 30 mL of sterile broth was prepared. Into the broth, 1 mL of OD adjusted bacterial suspension or bacterial suspension and 10 % plasma CF were added. One hundred microliters of metal ions and 20 mg of GBCs were added to test against both the Gram-negative species. Against Gram-positive *E. faecium* 200 µL of metal ion solutions and 40 mg of GBCs were added. Five millilitres of treated bacterial suspension or bacterial suspension and 10 % plasma CF from conical flask were taken at 0 h and 24 h into a sterile universal and centrifuged at 1727 g for 15 min. The supernatant was poured off and the treated bacterial pellet was re-suspended in 0.5 mL of sterile water. Twenty-five microliters of the treated bacterial suspension were pipetted onto a silicon wafer and dried at room temperature for 2 h before the fixation and dehydration process.

### **2.10.2. Fixation**

The air-dried treated cells were then fixed using 4 % glutaraldehyde solution made from a 25 % glutaraldehyde (Agar Scientific, UK) stock solution. The samples were kept in the fridge overnight.

### **2.10.3. Dehydration**

The silicon wafers with the fixed treated cells were dehydrated in 10 %, 30 %, 50 %, 70 %, 90 % and absolute graded ethanol solutions for 10 min at each concentration and air dried.

### **2.10.4. Sputter coating**

The dehydrated cells were put on carbon tabs and were coated with Au-Pd film using Polaron sputter SC7640 for 2 min with 200 voltage and 20 mA current.

#### **2.10.5. Sample microscopy**

The samples were analysed for any change in the morphology by means of Carl Zeiss Ltd. scanning electron microscopy (Supra 40VP) using SmartSEM software.

### **2.11. Energy dispersive analysis (EDAX) in the absence and presence of 10 % CF**

#### **2.11.1. Sample preparation**

The samples for EDAX analysis were prepared in a similar way as described in 2.10.1 – 2.10.4 following all the steps of fixation, dehydration, and sputter coating.

#### **2.11.2. Sample microscopy**

The coated samples were analysed for any change in the composition of carbon, nitrogen, oxygen, potassium and phosphorous over 0 h and 24 h of metal ions / GBCs treatment. The EDAX Inc. manufacturer and Apollo 40 SDD model of microscope was used. The software used to analyse the samples was Genesis. Point analysis was used at magnification of 25x (n = 3).

### **2.12. Raman spectroscopy in the absence and presence of 10 % CF**

#### **2.12.1. Sample preparation**

The bacterial control and metal ions / GBCs treated samples for Raman analysis were prepared in the same way as described in 2.10.1. The only difference was that glass slides were used instead of silicon wafers to prepare the bacterial samples for Raman analysis (n = 3).

#### **2.12.2. Sample microscopy**

The samples were analysed using DXR Raman microscope model of Thermo Scientific manufacturer and OMNIC software. The following experimental conditions were used (Table 2.2). The sample was focussed with the help of the laser on the target using the microscope adjustment knobs to get the clearest image on the screen.


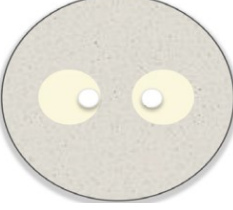
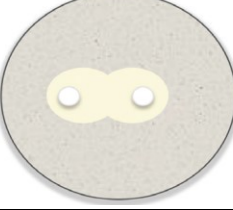
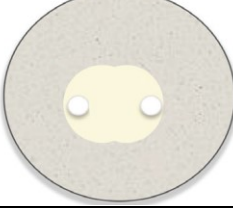
**Table 2.2.** Raman experimental set up

<b>Parameters</b>	<b>Selected set up</b>
<b>Collection exposure time</b>	5 sec
<b>Preview exposure time</b>	1 sec
<b>Sample exposure</b>	20
<b>Cosmic ray threshold</b>	Medium
<b>Photo bleach time</b>	1 min
<b>Laser wavelength</b>	532 nano-metre
<b>Laser power</b>	10 mega watt
<b>Spectrograph aperture</b>	25 micrometre pinhole
<b>Minimum and maximum range</b>	100 $\text{cm}^{-1}$ and 3000 $\text{cm}^{-1}$
<b>Estimated resolution</b>	2.7 $\text{cm}^{-1}$ – 4.2 $\text{cm}^{-1}$
<b>Estimated spot size</b>	0.7 micrometre
<b>Objective of microscope</b>	50x
<b>Grating</b>	900 line / millimetre

### **2.13. Zone of inhibition assay to test combined samples in the absence and presence of 10 % CF**

All the steps of ZoI synergy assay were performed as was the single metal test. The only difference was that only two wells of same size (8 mm diameter) were cut out of the agar plate to test metal combinations efficacy ( $n = 8$ ). ZoI results looked for the type (synergy, additivity, antagonism and autonomy) (Table 2.1) and grade (I-IV) of inhibition results for different metal ions combination at four ( $0.05 \text{ mgmL}^{-1}$ ,  $0.1 \text{ mgmL}^{-1}$ ,  $0.5 \text{ mgmL}^{-1}$  and  $1 \text{ mgmL}^{-1}$ ) concentrations (Table 2.4).

**Table 2.3.** Four possible interaction outcomes for the antimicrobial combinations (autonomy, antagonism, additivity and synergism) using ZoI tests (Davidson et al., 2005; Kalan and Wright, 2011).

Type of interactions	Interpretation	
<b>Autonomy</b>	The independent efficacy of the combined antimicrobials with no enhancement or reduction impact of the individual metals.	
<b>Antagonism</b>	The reduced the efficiency of the combined antimicrobials compared to their additive response.	
<b>Additivity</b>	The equivalent efficiency of the combined antimicrobials compared to the additive response of each antimicrobial acting independently.	
<b>Synergism</b>	The increased efficiency of the combined antimicrobials compared to their additive response.	

#### 2.14. Fractional inhibitory concentration (FIC) test in 1:2, 1:1 and 2:1 in the absence and presence of 10 % CF

The bacterial suspension or bacterial suspension and 10 % plasma CF and test samples for the FIC test were prepared as described for the MIC test (sub section 2.4). The FIC was determined using a 96 well flat-bottomed MTPs. The metal ions / GBCs were added as described in Table 2.5. The bacterial suspension with 0.15% (w/v) TTC (100  $\mu$ L) was added into each well of the MTP in rows A-F, working backwards from column 12 using a multi-channel pipette. The inoculation and metals mixture were mixed in column 1 and then 150  $\mu$ L was transferred to column 2. This was repeated across all the wells to column 12, where once mixed, 150  $\mu$ L was removed and disposed of. The MTP were then incubated overnight at 37 °C. After incubation, the FIC was taken as lowest concentration that inhibited the visible growth of the bacteria (Table 2.6). Growth was indicated by a change of colour in the well from clear/cloudy/metal colour to that of a dark blue/purple (n = 4).

**Table 2.4.** Volumes for individual metal ions in combined metal ions and GBCs in combined GBCs.

Ratios	Samples	Volume
2:1	Sample 1	100 $\mu$ L
	Sample 2	50 $\mu$ L
1:1	Sample 1	75 $\mu$ L
	Sample 2	75 $\mu$ L
1:2	Sample 1	50 $\mu$ L
	Sample 2	100 $\mu$ L

### **2.15. The fractional bactericidal concentration in 1:2, 1:1 and 2:1 in the absence and presence of 10 % CF**

The FBC assays were performed using a 50-dropper pipette, to take an aliquot of the bacteria and metal / GBCs mix sample from the MIC well that showed no growth. Twenty five microliters were pipetted as a drop onto an agar plate. The first well that showed growth was served as a control. These plates were incubated overnight at 37 °C. After incubation, the lowest concentration well sample that showed no bacterial growth on the agar plate was determined to be the MBC for that test sample (n = 4).

The mean well numbers were used to represent the results for the FIC and the FBC for metal ions / GBCs combinations values. The corresponding concentrations according to the three ratios 2:1, 1:1 and 1: 2 of metal combinations are demonstrated (Table 2.6).

The FIC / FBC values were calculated as

$$[ \sum \text{FIC} / \text{FBC} = \text{FIC} / \text{FBC of agent A} + \text{FIC} / \text{FBC of agent B} ]$$

Where

$$[ \text{FIC/FBC of agent A} = \frac{\text{MIC of agent A in combination}}{\text{MIC of agent A alone}} ]$$

And

$$[ \text{FIC/FBC of agent B} = \frac{\text{MIC of agent B in combination}}{\text{MIC of agent B alone}} ]$$

Following which, the compounds investigated (A and B) were synergistic if  $\text{FIC} \leq 0.5$ , additive if  $\text{FIC} > 0.5 \leq 1.0$ , indifferent if  $\text{FIC} > 1.0 \leq 4$  and antagonistic if  $\text{FIC} > 4$  (Perwaiz et al., 2007).

**Table 2.5.** Individual metal ion / GBCs concentrations in a combination in respective ratios in the FICs and FBCs tests across the wells 1-12 in mgmL<sup>-1</sup>. MC- metal combination, M<sub>1</sub>- metal 1 and M<sub>2</sub> – metal 2.

MC	Volumes	Ratio	1	2	3	4	5	6	7	8	9	10	11	12
M <sub>1</sub>	100	2:1	0.333	0.166	0.083	0.041	0.020	0.010	0.005	0.002	0.001	0.0006	0.0003	0.0001
M <sub>2</sub>	50		0.166	0.083	0.041	0.020	0.010	0.005	0.002	0.001	0.0006	0.0003	0.0001	0.00008
M <sub>1</sub>	75	1:1	0.250	0.125	0.062	0.031	0.015	0.007	0.003	0.001	0.0009	0.0004	0.0002	0.0001
M <sub>2</sub>	75		0.250	0.125	0.062	0.031	0.015	0.007	0.003	0.001	0.0009	0.0004	0.0002	0.0001
M <sub>1</sub>	50	1:2	0.166	0.083	0.041	0.020	0.010	0.005	0.002	0.001	0.0006	0.0003	0.0001	0.00008
M <sub>2</sub>	100		0.333	0.166	0.083	0.041	0.020	0.010	0.005	0.002	0.0013	0.0006	0.0003	0.0001



## **2.16. Crystal violet biofilm assay (CVBA) to test single sample effects in the absence and presence of 10 % CF**

### **2.16.1. Preparation of stainless steel coupons**

Fine polished (FP) 304 grade stainless steel coupons (10 mm × 10 mm) were used in the assays to grow the biofilms on. The coupons were washed thoroughly by sequentially soaking the coupons into beakers each containing either acetone, methanol or ethanol (BDH, UK) for 10 min with a sterile water wash in between each step. The washed coupons were air dried and stored for use at room temperature.

### **2.16.2. Biofilm formation and crystal violet biofilm assay**

The cell suspension or cell suspension and 10 % plasma CF were prepared in the same manner as described in section 2.4 and 2.5. Twelve well culture plates were used to grow the biofilms. The cleaned coupons were placed in the centre of the well with the fine polished side facing upward. One millilitre of adjusted cell suspension was added to each well and incubated for 7 days at 37 °C to produce a biofilm. A parafilm cover was used on the outer side of the plate to prevent against moisture loss and air contaminants over the incubation time. After incubation, the stainless-steel coupons were carefully washed with 2 mL of sterile distilled water using a pipette to remove any loose planktonic cells whilst avoiding damaging the biofilms. These coupons were air dried at room temperature for 2 h. One millilitre of test samples at different concentrations (50 mg/L, 100 mg/L, 250 mg/L or 500 mg/L) was added into each respective well. The plates were incubated for 24 h at 37 °C. Respective broths were also added into one of the wells to serve as a negative control. Following incubation, the metal ion solutions were removed using a pipette and disposed of. The coupons were washed gently with 1 mL of sterile distilled using a pipette and air dried at room temperature for 2 h. One millilitre of 0.03 % crystal violet solution (Oxoid, UK) was added into each well with a coupon and left for 30 min. The coupons were gently washed with 2 mL sterile distilled water using a pipette

to remove any excess stain. The coupons were placed into new 12 well plates and air dried at room temperature for 1 h. One millilitre of 33 % glacial acetic acid (BDH, UK) was added to each well and left for 30 min to solubilise any stained biofilm. The solution was removed using a pipette and the absorbance was measured at OD<sub>590</sub>.

### **2.17. Crystal violet biofilm assay for combined samples antimicrobial effects in 1:2, 1:1 and 2:1 in the absence and presence of 10 % CF**

All the steps were followed in a similar manner as described for single CVBA assay (sub section 2.16). The only difference was the individual samples were added as described in Table 2.7.

**Table 2.6.** Volumes added of individual metal ions in combined metal ions and GBCs in combined GBCs in the CVBA assay.

Ratios	Samples	Volume
<b>2:1</b>	Sample 1	75 µL
	Sample 2	25 µL
<b>1:1</b>	Sample 1	50 µL
	Sample 2	50 µL
<b>1:2</b>	Sample 1	25 µL
	Sample 2	75 µL

### 2.18. Cytotoxicity assay

The *in vitro* cytotoxicity of different metal ions (Ag, Cu, Au, Pd and Au) and GBCs (GO, AgGO, AuGO and PdGO) were assessed using a 3-(4,5-dimethyl-2-thiazolyl)-2,5-diphenyl-2H-tetrazolium bromide (96992, Sigma-Aldrich, UK) (MTS) assay in skin fibroblast cell lines (American Type Culture Type). All cell lines were maintained in Dulbecco's modified Eagle's medium (DMEM) (D5030; Sigma-Aldrich, UK) supplemented with 10% foetal calf serum (F0804, Sigma-Aldrich, UK) at 37°C and 5% CO<sub>2</sub>. Cells were counted with a haemocytometer and  $3 \times 10^4$  cells per well were seeded in 96-well plates and incubated for 24 h at 37°C and 5% CO<sub>2</sub>. The cells were incubated with metal ions (Ag, Cu, Pt, Au and Pd) and GBCs (GO, AgGO, AuGO and PdGO) at 1 mgmL<sup>-1</sup>. After incubation at 37°C and 5% CO<sub>2</sub>, the cells were washed using Roswell Park Memorial Institute (RPMI) medium (1640, Sigma-Aldrich, UK). One hundred microliters of RPMI media and 20 µL of MTS solution were added to the culture plate and incubated for 1 h – 6 h at 37°C and 5% CO<sub>2</sub>. The percentage of cell viability was determined at 490 nm. Untreated cells were used as negative control and cells treated with ethanol, 2 % HNO<sub>3</sub> and 5 % HCl were used as positive controls.

### 2.19. Statistical analysis

Mean values were used to compare the antimicrobial efficacy results of the metal ions / GBCs samples at varying concentrations. Standard error was used to analyse the distributions of the data from the mean value, and confidence intervals of 95% were calculated for the ZoI, MIC, MBC, time kill assay and CVBAs and were used to plot the error bars. Data were analysed for normal distribution using Shapiro-Wilk test. The data that were normally distributed were analysed using two-tailed independent student's t-test. Whilst, the data that were not normally distributed were analysed using Mann-Whitney U-test. Microsoft Excel and SPSS were used for the data analysis.

## Chapter 3

### **3. Metal ions antimicrobial efficacies against *K. pneumoniae*, *A. baumannii* and *E. faecium* in the presence and absence of 10 % bovine plasma conditioning film**

#### **3.0. Introduction**

This chapter investigated fifteen metal ion solutions antimicrobial efficacies using preliminary tests such as zone of inhibition, minimum inhibitory concentration and minimum bactericidal concentration. These methods were feasible and easy to use. The metal ions solutions that demonstrated the greatest antimicrobial efficacies were further tested against selected pathogens using following methods.

*a) time kill assay:* this assay was used to study the activity of an antimicrobial agent against a bacterial strain to determine the bactericidal or bacteriostatic activity of an antimicrobial agent over time.

*b) scanning electron microscopy:* this method was used to analysed morphological changes to bacteria after antimicrobial agent treatment.

*c) energy dispersive x-ray microscopy:* this method was used to analyse the elemental changes (carbon, oxygen, phosphorous, nitrogen and potassium) into the bacteria after antimicrobial agent treatment.

*d) Raman spectroscopy:* Raman spectroscopy is a label-free analytical technique that can provide detailed molecular information of a sample in a non-destructive way. Raman spectroscopy measure the transitions between vibrational levels of the molecules. The most important feature of the Raman spectroscopy is the ability to measure molecular properties of live cells in a culture medium. This method was used to analysed chemical changes (polysaccharide, protein, lipid and amide) into bacteria after antimicrobial agents treatment.

e) *combination assays*: to analyse the antimicrobial efficacies of antimicrobial agents in combinations; zone of inhibition, fractional inhibitory concentration and fractional bactericidal concentration assays were used. These assays measured the possible interactions between the tested antimicrobial agents.

f) *crystal violet biofilm assay*: this assay was used to analyse the antimicrobial agents efficacy against the biofilm phenotype of bacteria.

g) *MTT assay*: this assay was used to analyse the potential cell toxicity of antimicrobial agents for skin fibroblast cells.

### *Objective*

- Evaluate the antimicrobial efficacies of the metal ions using ZoI, MIC, MBC and time kill assays against three selected pathogens in the absence and presence of 10 % bovine plasma.
- Demonstrate the morphological, elemental and chemical changes for Ag, Cu, Pt, Au and Pd ions in the absence and presence of 10 % bovine plasma.
- Determine the antimicrobial efficacies of Ag, Cu, Pt, Au and Pd against selected bacterial biofilms in the absence and presence of 10 % bovine plasma.
- Determine antimicrobial efficacies of metal ions combinations (AgCu, AgPt, AgAu, AgPd, CuPt, CuAu, CuPd, AuPt, AuPd, PtPd) in the absence and presence of 10 % bovine plasma.

### **3.1 Antimicrobial efficacies for fifteen tested single metal ions in the absence and presence of 10 % bovine plasma conditioning films**

#### **3.1.1 Zone of inhibition**

Zone of inhibition assays were carried out using fifteen different single metal ions in the absence and presence of 10 % bovine plasma to determine the antimicrobial efficacy of the metal ions in a semi-solid matrix (agar). The results demonstrated that generally, an increasing antimicrobial efficacy was found with increasing concentrations of metal ions, from 0.05 mgmL<sup>-1</sup> to 1 mgmL<sup>-1</sup> ( $p < 0.001$ ) (Figure 3.1 and 3.2, a-c) against the three tested pathogens. The antimicrobial samples were categorised based on inhibition zones demonstration into i) 0 mm = no effect, ii) 0 mm – 4 mm = weak effect, iii) 4 mm – 9 mm = moderate effect and iv) > 9 mm = strong effect.

#### **3.1.1.1. Antimicrobial efficacies for *K. pneumoniae*, *A. baumannii* and *E. faecium* in the absence of 10 % bovine plasma conditioning film**

##### *K. pneumoniae*

Against *K. pneumoniae*, at 1 mgmL<sup>-1</sup>, the Rh ions (11.5 mm) demonstrated the strongest antimicrobial efficacies. At 1 mgmL<sup>-1</sup>, Ru ions (10.7 mm), Pt ions (10.3 mm), Au and Pd ions (up to 10.0 mm) demonstrated strong antimicrobial efficacy. The Ti and Ta ions demonstrated moderate antimicrobial efficacies at all tested concentrations (1.0 mm – 9.0 mm). The Pt ions (3.5 mm – 6.0 mm) followed with the Au, Pd and Rh ions (1.5 mm – 4.0 mm) demonstrated the strongest antimicrobial efficacies at 0.05 mgmL<sup>-1</sup> and 0.1 mgmL<sup>-1</sup> concentrations. The Mo ions demonstrated a weak antimicrobial activity at 0.1 mgmL<sup>-1</sup>, 0.5 mgmL<sup>-1</sup> and 1 mgmL<sup>-1</sup> (> 2.5 mm) (Figure 3.1, a). Against *K. pneumoniae*, Y and Zn ions demonstrated no inhibition at 0.05 mgmL<sup>-1</sup> and 0.1 mgmL<sup>-1</sup>. Niobium Ga and Cu ion demonstrated no inhibition at 0.05 mgmL<sup>-1</sup>.

#### *A. baumannii*

Against *A. baumannii*, the strongest antimicrobial efficacies at 1 mgmL<sup>-1</sup> was found for the Rh ions (12.5 mm), followed with the Pt ions (9.7 mm), then Au (8.7 mm), Ru (8.0 mm) and Pd (7.2 mm) ions. The Mo ions (1.0 mm, 3.0 mm and 2.0 mm) and the Cu ions (1.0 mm, 2.9 mm and 2.8 mm) demonstrated weak antimicrobial efficacies at 0.1 mgmL<sup>-1</sup>, 0.5 mgmL<sup>-1</sup>, 1 mgmL<sup>-1</sup> respectively (Figure 3.1, b). Yttrium, Mo, Zn and Cu ions demonstrated no inhibitory zones at 0.05 mgmL<sup>-1</sup>.

#### *E. faecium*

Against *E. faecium*, the strongest antimicrobial efficacies at 0.5 mgmL<sup>-1</sup> and 1 mgmL<sup>-1</sup> were demonstrated for Rh ions (6.0 mm and 7.0 mm respectively). The Pt, Au, Pd, Ag, Ti and Ta ions demonstrated moderate efficacies at 0.5 mgmL<sup>-1</sup> and 1 mgmL<sup>-1</sup> (3.0 mm – 5.5 mm) (Figure 3.1, c). At concentration of 0.05 mgmL<sup>-1</sup> and 0.1 mgmL<sup>-1</sup> only Ag (3.1 mm and 3.7 mm) and Au ions (1 mm and 1.4 mm) and at 0.1 mgmL<sup>-1</sup> Ti ions (0.5 mm) demonstrated inhibitory zones. The remaining ions displayed no inhibitions at 0.05 mgmL<sup>-1</sup> and 0.1 mgmL<sup>-1</sup> concentrations.

### **3.1.1.2. Antimicrobial efficacies for *K. pneumoniae*, *A. baumannii* and *E. faecium* in the presence of 10 % bovine plasma conditioning film**

#### *K. pneumoniae*

Against *K. pneumoniae*, at 1 mgmL<sup>-1</sup>, Rh ions (11 mm) demonstrated the strongest efficacies, followed with Ru ions (10.5 mm) and Pt ions (10 mm). The Zn, Ti, Au and Pd ions (6.0 mm – 9.0 mm) demonstrated a moderate antimicrobial efficacy at 0.5 mgmL<sup>-1</sup> and 1 mgmL<sup>-1</sup>. The Mo ions demonstrated lower antimicrobial efficacies at all tested concentrations (0.1 mm – 1.5 mm) (Figure 3.2, a). Yttrium and Zn ions demonstrated no inhibition at 0.05 mgmL<sup>-1</sup> and 0.1 mgmL<sup>-1</sup>. Moreover, Nb, Ga and Cu ion demonstrated no inhibition at 0.05 mgmL<sup>-1</sup>.

### *A. baumannii*

Against *A. baumannii*, The Rh ions demonstrated the strongest efficacies at 1 mgmL<sup>-1</sup> (11 mm) and Pd ions demonstrated the strongest efficacies at 0.05 mgmL<sup>-1</sup>, 0.1 mgmL<sup>-1</sup> and 0.5 mgmL<sup>-1</sup> (5.5 mm, 4 mm and 8 mm respectively). Moreover, Pt (9 mm), Au (8 mm) and Pd (7.5 mm) ions demonstrated good antimicrobial efficacies at 1 mgmL<sup>-1</sup>. The Mo ions (1.3 mm, 2 mm and 2 mm) and Cu ions (0.2 mm, 0.5 mm and 2 mm) demonstrated weak antimicrobial efficacies at 0.1 mgmL<sup>-1</sup>, 0.5 mgmL<sup>-1</sup>, 1 mgmL<sup>-1</sup> respectively (Figure 3.2, b). The Zn and Ga ions demonstrated no inhibitory zones at 0.05 mgmL<sup>-1</sup> and 0.1 mgmL<sup>-1</sup>. Moreover, Y, Ti and In at 0.05 mgmL<sup>-1</sup> displayed no inhibition.

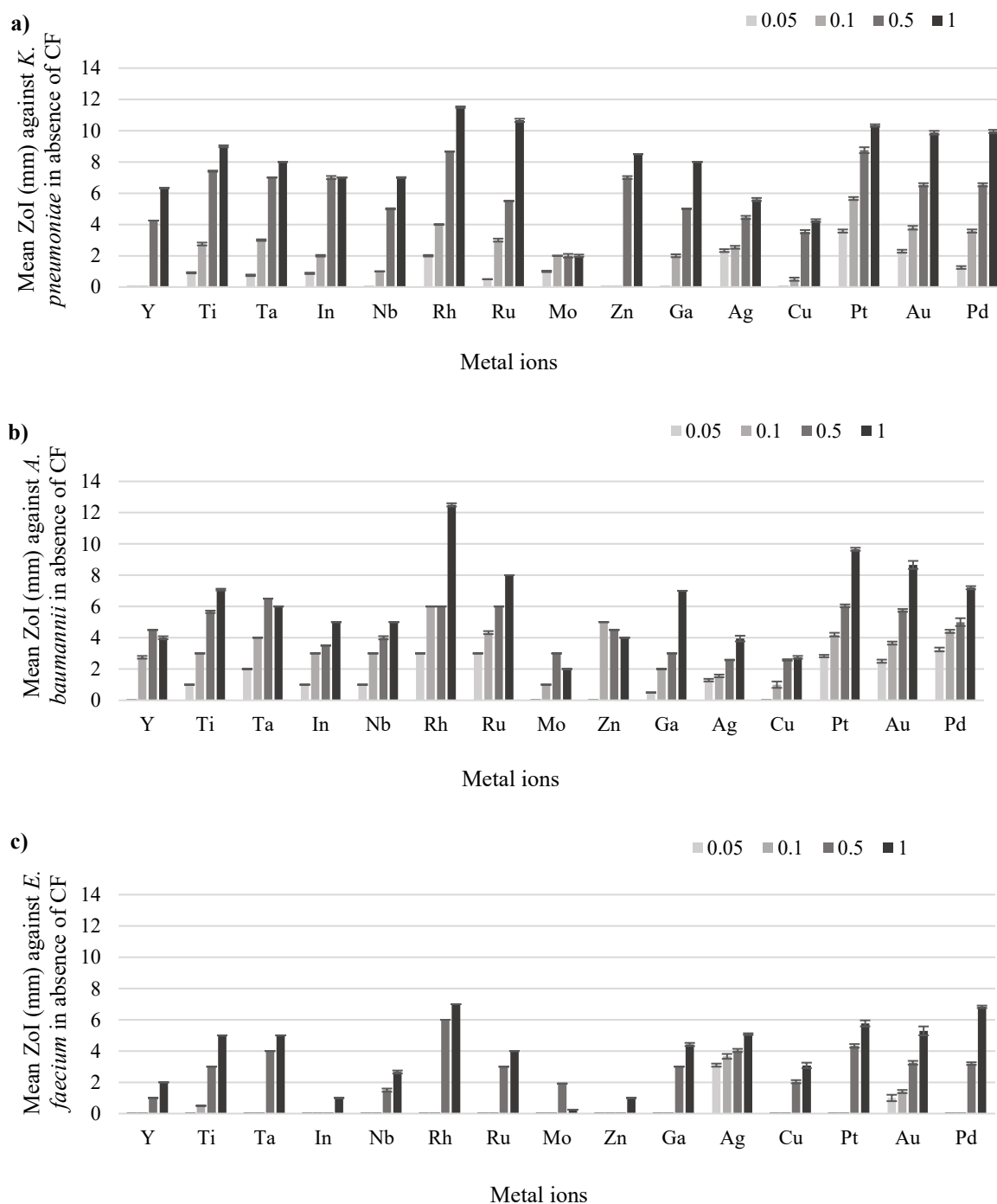
### *E. faecium*

Against *E. faecium*, the strongest antimicrobial efficacies at 0.5 mgmL<sup>-1</sup> and 1 mgmL<sup>-1</sup> were demonstrated for the Rh ions (5.0 mm and 6.5 mm respectively), followed with Au and Pd ions (4.0 mm and 6.0 mm respectively). The Pt, Ag, Ti and Ta ions demonstrated moderate efficacies at 0.5 mgmL<sup>-1</sup> and 1 mgmL<sup>-1</sup> (3.0 mm – 5.5 mm) (Figure 3.2, c). At 0.05 mgmL<sup>-1</sup> and 0.1 mgmL<sup>-1</sup> only Ag ions (1.6 mm and 1.9 mm respectively) and Au ions (1 mm) at 0.1 mgmL<sup>-1</sup> demonstrated inhibition. The remaining metal ions displayed no inhibitions at 0.05 mgmL<sup>-1</sup> and 0.1 mgmL<sup>-1</sup> concentrations.

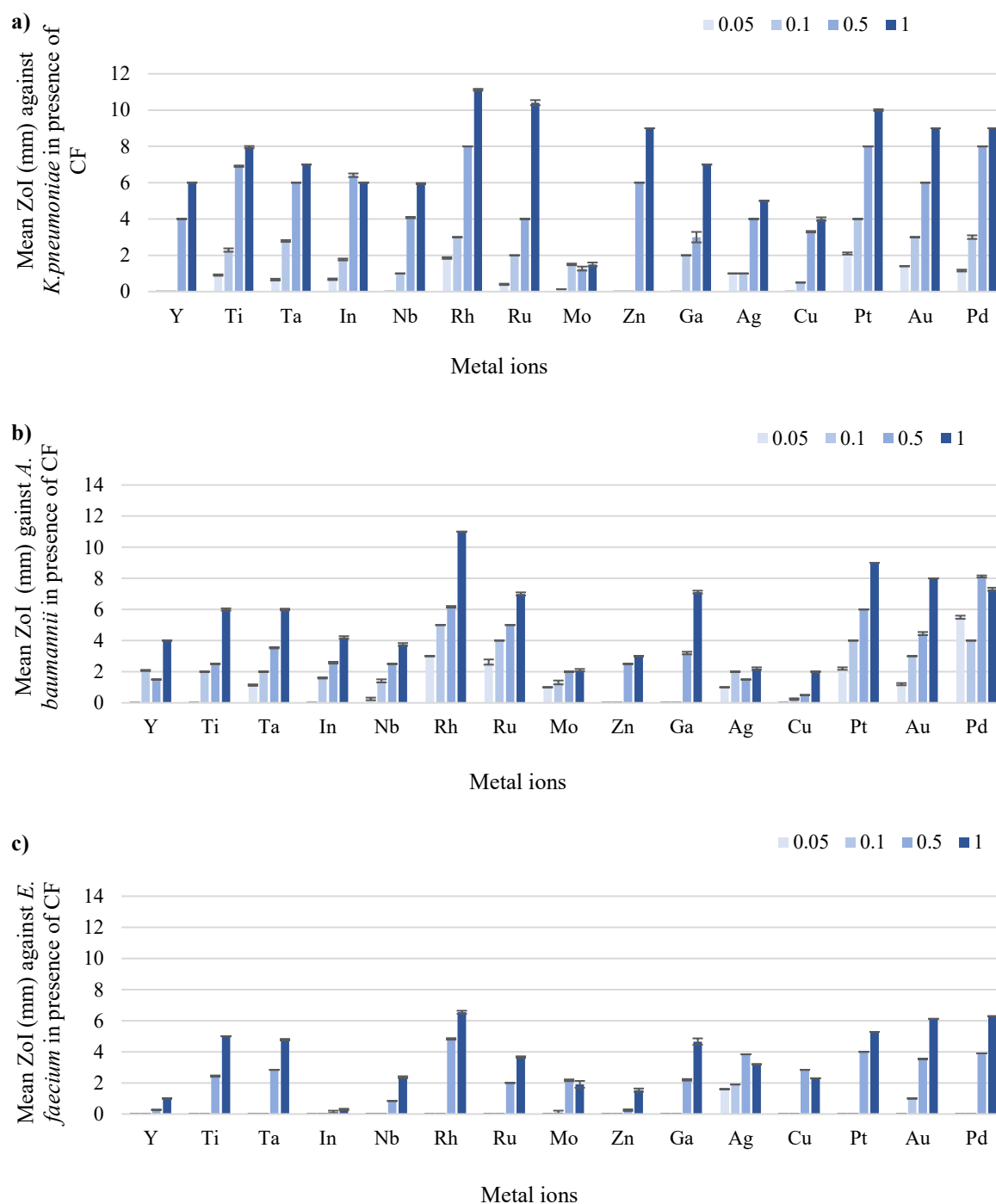
Overall, the Rh ions demonstrated the strongest antimicrobial efficacy, followed with Pt ions and Pd ions against all the tested pathogens. At 0.05 mgmL<sup>-1</sup> and 0.1 mgmL<sup>-1</sup>, the weakest antimicrobial metal ions were Y and Zn and Mo at 0.5 mgmL<sup>-1</sup> and 1 mgmL<sup>-1</sup> against *K. pneumoniae*. Against *A. baumannii*, Mo ions in the absence of CF and Zn and Ga ions in the presence of CF at 0.05 mgmL<sup>-1</sup> and 0.1 mgmL<sup>-1</sup> and Cu ions at 0.5 mgmL<sup>-1</sup> and 1 mgmL<sup>-1</sup> showed the weakest antimicrobial activity. Against *E. faecium*, Y, Zn and In ions demonstrated the weakest antimicrobial activity. The presence of 10 % conditioning film (CF) resulted



inhibitory zones reduction of up to 1.0 mm to 1.5 mm against all the tested pathogens at all the tested concentrations.



**Figure 3.1.** Inhibitory effects for fifteen metal ions at 0.05 mgmL<sup>-1</sup>, 0.1 mgmL<sup>-1</sup>, 0.5 mgmL<sup>-1</sup> and 1 mgmL<sup>-1</sup> against a) *K. pneumoniae*, b) *A. baumannii* and c) *E. faecium* in the absence of 10 % plasma conditioning film (n = 24).



**Figure 3.2.** Inhibitory effects for fifteen metal ions at 0.05 mgmL<sup>-1</sup>, 0.1 mgmL<sup>-1</sup>, 0.5 mgmL<sup>-1</sup> and 1 mgmL<sup>-1</sup> against a) *K. pneumoniae*, b) *A. baumannii* and c) *E. faecium* in the presence of 10 % plasma conditioning film (n = 24).

### 3.1.2. Minimum inhibitory concentrations (MICs)

The MIC effects were evaluated by comparing the metal ions inhibitory concentrations with their respective acid control inhibitory concentrations.

#### 3.1.2.1. MICs against *K. pneumoniae*, *A. baumannii* and *E. faecium* in the absence of 10 % bovine plasma conditioning film

##### *K. pneumoniae*

Against *K. pneumoniae*, Pt ions ( $0.003 \text{ mgmL}^{-1}$ ) demonstrated the strongest efficacies compared to its respective acid control (5 % HCl,  $0.015 \text{ mgmL}^{-1}$ ). The Ag ( $0.01 \text{ mgmL}^{-1}$ ) and Au and Pd ions ( $0.05 \text{ mgmL}^{-1}$ ) displayed the second strongest antimicrobial inhibitory effects (2 % HNO<sub>3</sub> ( $0.03 \text{ mgmL}^{-1}$ ) and 5 % HCl ( $0.015 \text{ mgmL}^{-1}$ )). The Mo ions ( $0.03 \text{ mgmL}^{-1}$ ), Zn ( $0.03 \text{ mgmL}^{-1}$ ), Ru ( $0.015 \text{ mgmL}^{-1}$ ) and Ga ions ( $0.015 \text{ mgmL}^{-1}$ ) demonstrated with the same inhibitory values as their respective controls, hence the weakest inhibitory efficacies ( $0.03 \text{ mgmL}^{-1}$ ) (Table 3.1).

##### *A. baumannii*

Against *A. baumannii*, the Ag ions ( $0.003 \text{ mgmL}^{-1}$ ) demonstrated the strongest efficacies, followed with the Ta ions ( $0.007 \text{ mgmL}^{-1}$ ) compared with 2 % HNO<sub>3</sub> control ( $0.062 \text{ mgmL}^{-1}$ ). Weak antimicrobial efficacies were found with Ga ( $0.011 \text{ mgmL}^{-1}$ ), Zn ( $0.031 \text{ mgmL}^{-1}$ ) and Y ions ( $0.031 \text{ mgmL}^{-1}$ ) compared to their respective controls ( $0.015 \text{ mgmL}^{-1}$  and  $0.062 \text{ mgmL}^{-1}$ ) (Table 3.1). The weakest efficacy was demonstrated for Mo ions ( $0.003$ ), with similar as control inhibitory concentration.

##### *E. faecium*

Against *E. faecium*, the strongest efficacy was demonstrated for Ag ions ( $0.015 \text{ mgmL}^{-1}$ ) compared to 2 % HNO<sub>3</sub> control ( $0.125 \text{ mgmL}^{-1}$ ). The Ta and Ti ions displayed the second strong inhibitory antimicrobial efficacy ( $0.031 \text{ mgmL}^{-1}$ ). The Mo ( $0.015 \text{ mgmL}^{-1}$ ), Y ( $0.125$

mgmL<sup>-1</sup>) and Ga (0.062 mgmL<sup>-1</sup>) ions displayed the weakest efficacies with same inhibitory values as their respective controls (10 % HCl, 2 % HNO<sub>3</sub> and 5 % HNO<sub>3</sub>). The Pt (0.011 mgmL<sup>-1</sup>), Pd (0.015 mgmL<sup>-1</sup>) and Au (0.011 mgmL<sup>-1</sup>) ions displayed strong efficacies when compared with 5 % HCl control (0.062 mgmL<sup>-1</sup>) (Table 3.1).

### **3.1.2.1. The MICs against *K. pneumoniae*, *A. baumannii* and *E. faecium* in the presence of 10 % bovine plasma conditioning films**

#### *K. pneumoniae*

Against *K. pneumoniae*, the Pt ions, Au ions and Pd ions (0.007 mgmL<sup>-1</sup>) demonstrated the strongest efficacies compared with 5 % HCl control (0.031 mgmL<sup>-1</sup>). The Ag ions (0.013 mgmL<sup>-1</sup>) demonstrated the second strong antimicrobial efficacy compared with 2 % HNO<sub>3</sub> (0.039 mgmL<sup>-1</sup>). The Ti (0.023 mgmL<sup>-1</sup>), Ta (0.015 mgmL<sup>-1</sup>), Rh (0.011 mgmL<sup>-1</sup>) and Ru (0.015 mgmL<sup>-1</sup>) displayed moderate efficacies compared with respective controls (2 % HNO<sub>3</sub> and 5 % HCl). The Mo (0.003 mgmL<sup>-1</sup>) and Zn ions (0.039 mgmL<sup>-1</sup>) displayed the same inhibitory values as their respective controls and hence the weakest efficacies (10 % HCl (0.003 mgmL<sup>-1</sup>) and 5 % HNO<sub>3</sub> (0.039 mgmL<sup>-1</sup>)). (Table 3.2).

#### *A. baumannii*

Against *A. baumannii*, the Ag ions (0.004 mgmL<sup>-1</sup>) demonstrated the strongest antimicrobial activity compared with 2 % HNO<sub>3</sub> control (0.062 mgmL<sup>-1</sup>). Tantalum (0.015 mgmL<sup>-1</sup>) and Rh (0.009 mgmL<sup>-1</sup>) ions displayed moderate inhibition compared with 2 % HNO<sub>3</sub> (0.062 mgmL<sup>-1</sup>) and 5 % HCl (0.031 mgmL<sup>-1</sup>) controls respectively. Zn (0.039 mgmL<sup>-1</sup>) and Y (0.046 mgmL<sup>-1</sup>) ions displayed a weak inhibition (2 % HNO<sub>3</sub> control (0.062 mgmL<sup>-1</sup>)). The Mo (0.003 mgmL<sup>-1</sup>) displayed same inhibitory values as their respective controls (10 % HCl (0.003 mgmL<sup>-1</sup>)) and thus, the weakest efficacies. (Table 3.2).

### *E. faecium*

Against *E. faecium*, the Ag ions ( $0.015 \text{ mgmL}^{-1}$ ) displayed the strongest efficacy (2 %  $\text{HNO}_3$  ( $0.125 \text{ mgmL}^{-1}$ )). Platinum, Au and Pt ions ( $0.015 \text{ mgmL}^{-1} - 0.019 \text{ mgmL}^{-1}$ ) and Ti and Ta ions ( $0.031 \text{ mgmL}^{-1}$ ) displayed a moderate compared with their controls 5 % HCl ( $0.078 \text{ mgmL}^{-1}$ ) and 2 %  $\text{HNO}_3$  ( $0.125 \text{ mgmL}^{-1}$ ) respectively. The Y ( $0.125 \text{ mgmL}^{-1}$ ), Zn ( $0.125 \text{ mgmL}^{-1}$ ) and Mo ( $0.015 \text{ mgmL}^{-1}$ ) ions demonstrated the weakest inhibition with same concentrations as their respective controls (2 %  $\text{HNO}_3$  and 10 % HCl respectively) (Table 3.2).

Thus, in summary, the best antimicrobial inhibitory efficacy was demonstrated for the Pt ions against *K. pneumoniae*. Whilst, the Pt ions, Pd ions and Au ions demonstrated the best antimicrobial efficacies in the presence of plasma against *K. pneumoniae*. Against *A. baumannii* and *E. faecium*, the Ag ions demonstrated the best MICs. The Mo ions against Gram negative species and the Mo, Y and Zn ions against *E. faecium* demonstrated with the weakest MICs. All the tested metal ions demonstrated a lower antimicrobial activity against all the three bacterial isolates in the presence of 10 % bovine plasma CF. The most resistant bacteria were *E. faecium*.

**Table 3.1.** Minimum inhibitory concentration for fifteen metal ions and four acid carrier solutions against *K. pneumoniae*, *A. baumannii* and *E. faecium* in the absence of 10 % plasma conditioning films (n = 4). The highlighted blue colour represents the greatest antimicrobial efficacy compared to their respective acid controls.

Metal ions/acid controls	<i>K. pneumoniae</i>	<i>A. baumannii</i>	<i>E. faecium</i>
Y (2 % HNO <sub>3</sub> )	0.015 ± 0	0.031 ± 0	0.125 ± 0
Ti (2 % HNO <sub>3</sub> )	0.015 ± 0	0.015 ± 0	0.031 ± 0
Ta (2 % HNO <sub>3</sub> )	0.007 ± 0	0.007 ± 0	0.031 ± 0
In (2 % HNO <sub>3</sub> )	0.015 ± 0	0.015 ± 0	0.062 ± 0
Nb (2 % HNO <sub>3</sub> )	0.015 ± 0	0.015 ± 0	0.062 ± 0
Rh (5 % HCl)	0.007 ± 0	0.007 ± 0	0.031 ± 0
Ru (5 % HCl)	0.015 ± 0	0.007 ± 0	0.031 ± 0
Mo (10 % HCl)	0.003 ± 0	0.003 ± 0	0.015 ± 0
Zn (2 % HNO <sub>3</sub> )	0.031 ± 0	0.031 ± 0	0.125 ± 0
Ga (5 % HNO <sub>3</sub> )	0.015 ± 0	0.011 ± 0.002	0.062 ± 0
Ag (2 % HNO <sub>3</sub> )	0.011 ± 0.002	0.003 ± 0	0.015 ± 0
Cu (2 % HNO <sub>3</sub> )	0.015 ± 0	0.015 ± 0	0.062 ± 0
Pt (5 % HCl)	0.003 ± 0	0.005 ± 0.001	0.011 ± 0.002
Au (5 % HCl)	0.005 ± 0.001	0.003 ± 0	0.011 ± 0.002
Pd (5 % HCl)	0.005 ± 0.001	0.007 ± 0	0.015 ± 0
2 % HNO <sub>3</sub>	0.031 ± 0	0.062 ± 0	0.125 ± 0
5 % HNO <sub>3</sub>	0.015 ± 0	0.015 ± 0	0.062 ± 0
5 % HCl	0.015 ± 0	0.015 ± 0	0.062 ± 0
10 % HCl	0.003 ± 0	0.003 ± 0	0.015 ± 0

**Table 3.2.** Minimum inhibitory concentration for fifteen metal ions and four acid carrier solutions against *K. pneumoniae*, *A. baumannii* and *E. faecium* in the presence of 10 % plasma conditioning films (n = 4). The highlighted blue colour represents the greatest antimicrobial efficacy compared to their respective acid controls.

Metal ions/acid controls	<i>K. pneumoniae</i>	<i>A. baumannii</i>	<i>E. faecium</i>
Y (2 % HNO <sub>3</sub> )	0.031 ± 0	0.046 ± 0.007	0.125 ± 0
Ti (2 % HNO <sub>3</sub> )	0.023 ± 0.003	0.031 ± 0	0.031 ± 0
Ta (2 % HNO <sub>3</sub> )	0.015 ± 0	0.015 ± 0	0.031 ± 0
In (2 % HNO <sub>3</sub> )	0.031 ± 0	0.031 ± 0	0.109 ± 0.013
Nb (2 % HNO <sub>3</sub> )	0.031 ± 0	0.031 ± 0	0.125 ± 0
Rh (5 % HCl)	0.011 ± 0.002	0.009 ± 0.001	0.031 ± 0
Ru (5 % HCl)	0.015 ± 0	0.015 ± 0	0.031 ± 0
Mo (10 % HCl)	0.003 ± 0	0.003 ± 0	0.015 ± 0
Zn (2 % HNO <sub>3</sub> )	0.039 ± 0.006	0.039 ± 0.006	0.125 ± 0
Ga (5 % HNO <sub>3</sub> )	0.031 ± 0	0.015 ± 0	0.062 ± 0
Ag (2 % HNO <sub>3</sub> )	0.013 ± 0.00	0.004 ± 0.0008	0.015 ± 0
Cu (2 % HNO <sub>3</sub> )	0.031 ± 0	0.031 ± 0	0.062 ± 0
Pt (5 % HCl)	0.007 ± 0	0.007 ± 0	0.015 ± 0
Au (5 % HCl)	0.007 ± 0	0.007 ± 0	0.015 ± 0
Pd (5 % HCl)	0.007 ± 0	0.007 ± 0	0.019 ± 0.003
2 % HNO <sub>3</sub>	0.039 ± 0.006	0.062 ± 0	0.125 ± 0
5 % HNO <sub>3</sub>	0.039 ± 0.006	0.031 ± 0	0.093 ± 0.015
5 % HCl	0.031 ± 0	0.031 ± 0	0.078 ± 0.013
10 % HCl	0.003 ± 0	0.003 ± 0	0.015 ± 0



### 3.1.3. Minimum bactericidal concentrations (MBCs)

The MBCs antimicrobial effects were evaluated by comparing with their respective acid control values.

#### 3.1.3.1. The MBCs against *K. pneumoniae*, *A. baumannii* and *E. faecium* in the absence of 10 % bovine plasma conditioning film

##### *K. pneumoniae*

Against *K. pneumoniae*, the Ag ions ( $0.011 \text{ mgmL}^{-1}$ ) demonstrated the strongest antimicrobial activity compared to 2 %  $\text{HNO}_3$  control concentration ( $0.062 \text{ mgmL}^{-1}$ ). The Pt, Au and Pd ( $0.003 \text{ mgmL}^{-1}$ ) ions demonstrated the second strong bactericidal activity (5 % HCl control ( $0.015 \text{ mgmL}^{-1}$ )). In addition, the Cu, Ti and Ta ions ( $0.015 \text{ mgmL}^{-1}$ ) displayed moderate efficacies compared with 2 %  $\text{HNO}_3$  ( $0.062 \text{ mgmL}^{-1}$ ) control concentration. The Nb ions ( $0.046 \text{ mgmL}^{-1}$ ), followed with the Zn and In ( $0.031 \text{ mgmL}^{-1}$ ) ions displayed weak bactericidal efficacies compared with 2 %  $\text{HNO}_3$  control ( $0.062 \text{ mgmL}^{-1}$ ). The Mo ions displayed similar bactericidal concentration as the acid control ( $0.003 \text{ mgmL}^{-1}$ ) and hence the weakest bactericidal efficacy (Table 3.3).

##### *A. baumannii*

Against *A. baumannii*, the Ag ions ( $0.007 \text{ mgmL}^{-1}$ ) demonstrated the strongest bactericidal efficacy compared to 2 %  $\text{HNO}_3$  control concentration ( $0.062 \text{ mgmL}^{-1}$ ). Moderate bactericidal efficacies were demonstrated for the Ti, Ta, Cu ( $0.015 \text{ mgmL}^{-1}$ ) compared with 2 %  $\text{HNO}_3$  control ( $0.062 \text{ mgmL}^{-1}$ ) and Pt, Au and Pd ions ( $0.005 \text{ mgmL}^{-1} - 0.007 \text{ mgmL}^{-1}$ ) compared with 5 % HCl control ( $0.015 \text{ mgmL}^{-1}$ ). The weakest bactericidal efficacy was demonstrated for the Mo ( $0.007 \text{ mgmL}^{-1}$ ) and Rh ( $0.015 \text{ mgmL}^{-1}$ ) ions with same bactericidal concentrations as their respective controls (Table 3.3).

### *E. faecium*

Against *E. faecium*, the strongest bactericidal activity was demonstrated for the Ta and Ag (0.062 mgmL<sup>-1</sup>) ions compared to 2 % HNO<sub>3</sub> (0.250 mgmL<sup>-1</sup>) concentration and Pt, Au and Pd ions (0.031 mgmL<sup>-1</sup>) compared with 5 % HCl (0.125 mgmL<sup>-1</sup>) concentration. The Mo (0.015 mgmL<sup>-1</sup>) and Zn (0.250 mgmL<sup>-1</sup>) ions demonstrated the weakest bactericidal efficacies with same bactericidal concentrations as their respective controls (Table 3.3).

### **3.1.3.2. The MBCs against *K. pneumoniae*, *A. baumannii* and *E. faecium* in the presence of 10 % bovine plasma conditioning films**

#### *K. pneumoniae*

Against *K. pneumoniae*, Ag ions (0.015 mgmL<sup>-1</sup>) demonstrated the strongest efficacies compared with the 2 % HNO<sub>3</sub> control value (0.078 mgmL<sup>-1</sup>). In addition, the Pt, Au and Pd ions (0.015 mgmL<sup>-1</sup>) displayed a significant bactericidal activity compared with 5 % HCl (0.062 mgmL<sup>-1</sup>). The Ti (0.039 mgmL<sup>-1</sup>) and Ta (0.031 mgmL<sup>-1</sup>) ions compared with 2 % HNO<sub>3</sub> (0.078 mgmL<sup>-1</sup>) displayed moderate efficacies. Moreover, Y, In, Nb, Cu (0.062 mgmL<sup>-1</sup>) (2 % HNO<sub>3</sub> control) and Ga ions (0.062 mgmL<sup>-1</sup>) (5 % HNO<sub>3</sub> (0.078 mgmL<sup>-1</sup>)) demonstrated weak antimicrobial efficacy compared with respective controls. The Mo (0.007 mgmL<sup>-1</sup>) and Zn (0.078 mgmL<sup>-1</sup>) demonstrated the weakest antimicrobial effects with similar bactericidal concentration as 10 % HCl and 2 % HNO<sub>3</sub> respectively (Table 3.4).

#### *A. baumannii*

Against *A. baumannii*, the Ag ions (0.007 mgmL<sup>-1</sup>) demonstrated the strongest bactericidal efficacy compared to the 2 % HNO<sub>3</sub> control concentration (0.125 mgmL<sup>-1</sup>). Moderate bactericidal efficacies were demonstrated for the Ti (0.039 mgmL<sup>-1</sup>) and Ta (0.031 mgmL<sup>-1</sup>) compared with 2 % HNO<sub>3</sub> control (0.125 mgmL<sup>-1</sup>) and Pt, Au and Pd ions (0.015 mgmL<sup>-1</sup>) compared with 5 % HCl control (0.062 mgmL<sup>-1</sup>). The least bactericidal efficacy was

demonstrated for the Mo ions ( $0.007 \text{ mgmL}^{-1}$ ) with same bactericidal concentrations as their respective controls (Table 3.4).

#### *E. faecium*

Against *E. faecium*, the strongest bactericidal activity was demonstrated for the Ag ( $0.031 \text{ mgmL}^{-1}$ ) ions compared to 2 %  $\text{HNO}_3$  ( $0.250 \text{ mgmL}^{-1}$ ) concentration and Pt, Au and Pd ions ( $0.031 \text{ mgmL}^{-1}$ ) compared with 5 % HCl ( $0.125 \text{ mgmL}^{-1}$ ) concentration. Whilst, the weakest bactericidal activity was demonstrated for the Y (2 %  $\text{HNO}_3$  ( $0.250 \text{ mgmL}^{-1}$ )), Zn 2 % ( $\text{HNO}_3$  ( $0.250 \text{ mgmL}^{-1}$ )) and Mo (2 % HCl ( $0.015 \text{ mgmL}^{-1}$ )) ions with similar values as their acid controls (Table 3.4).

In summary the bactericidal efficacies demonstrated that the Ag ions against both the Gram-negative pathogens and Ag, Pt, Au and Pd ions against *E. faecium* demonstrated the strongest bactericidal concentrations in the presence and absence of plasma CF. The weakest bactericidal efficacy was demonstrated for the Mo ions against all the tested pathogens in the presence or absence of plasma. Moreover, Zn and Y ions demonstrated the least efficacies against *E. faecium*. Interestingly, Ag ions were found to demonstrate a greater antimicrobial activity in presence of 10 % plasma CF ( $0.031 \text{ mgmL}^{-1}$ ) than without plasma ( $0.062 \text{ mgmL}^{-1}$ ) against *E. faecium*. All the tested metal ions demonstrated a lower bactericidal activity against all the three bacterial isolates in the presence of 10 % bovine plasma CF. Gram-positive *E. faecium* was the most resistant bacteria.

**Table 3.3.** Minimum bactericidal concentrations for fifteen metal ions and four acid carrier solutions against *K. pneumoniae*, *A. baumannii* and *E. faecium* in the absence of 10 % plasma conditioning film (n = 4). The highlighted blue colour represents the greatest antimicrobial efficacy compared to their respective acid controls.

Metal ions/acid controls	<i>K. pneumoniae</i>	<i>A. baumannii</i>	<i>E. faecium</i>
Y (2 % HNO <sub>3</sub> )	0.023 ± 0.005	0.031 ± 0	0.125 ± 0
Ti (2 % HNO <sub>3</sub> )	0.015 ± 0	0.015 ± 0	0.125 ± 0
Ta (2 % HNO <sub>3</sub> )	0.015 ± 0	0.015 ± 0	0.062 ± 0
In (2 % HNO <sub>3</sub> )	0.031 ± 0	0.031 ± 0	0.125 ± 0
Nb (2 % HNO <sub>3</sub> )	0.046 ± 0.011	0.015 ± 0	0.125 ± 0
Rh (5 % HCl)	0.015 ± 0	0.007 ± 0	0.062 ± 0
Ru (5 % HCl)	0.015 ± 0	0.015 ± 0	0.062 ± 0
Mo (10 % HCl)	0.003 ± 0	0.007 ± 0	0.015 ± 0
Zn (2 % HNO <sub>3</sub> )	0.031 ± 0	0.031 ± 0	0.250 ± 0
Ga (5 % HNO <sub>3</sub> )	0.015 ± 0	0.015 ± 0	0.062 ± 0
Ag (2 % HNO <sub>3</sub> )	0.011 ± 0.002	0.007 ± 0	0.062 ± 0
Cu (2 % HNO <sub>3</sub> )	0.015 ± 0	0.015 ± 0	0.125 ± 0
Pt (5 % HCl)	0.003 ± 0	0.007 ± 0	0.031 ± 0
Au (5 % HCl)	0.003 ± 0	0.005 ± 0.001	0.031 ± 0
Pd (5 % HCl)	0.003 ± 0	0.007 ± 0	0.031 ± 0
2 % HNO <sub>3</sub>	0.062 ± 0	0.062 ± 0	0.250 ± 0
5 % HNO <sub>3</sub>	0.031 ± 0	0.031 ± 0	0.125 ± 0
5 % HCl	0.015 ± 0	0.015 ± 0	0.125 ± 0
10 % HCl	0.003 ± 0	0.007 ± 0	0.015 ± 0

**Table 3.4.** Minimum bactericidal concentrations for fifteen metal ions and four acid carrier solutions against *K. pneumoniae*, *A. baumannii* and *E. faecium* in the presence of 10 % plasma conditioning film (n = 4). The highlighted blue colour represents the greatest antimicrobial efficacy compared to their respective acid controls.

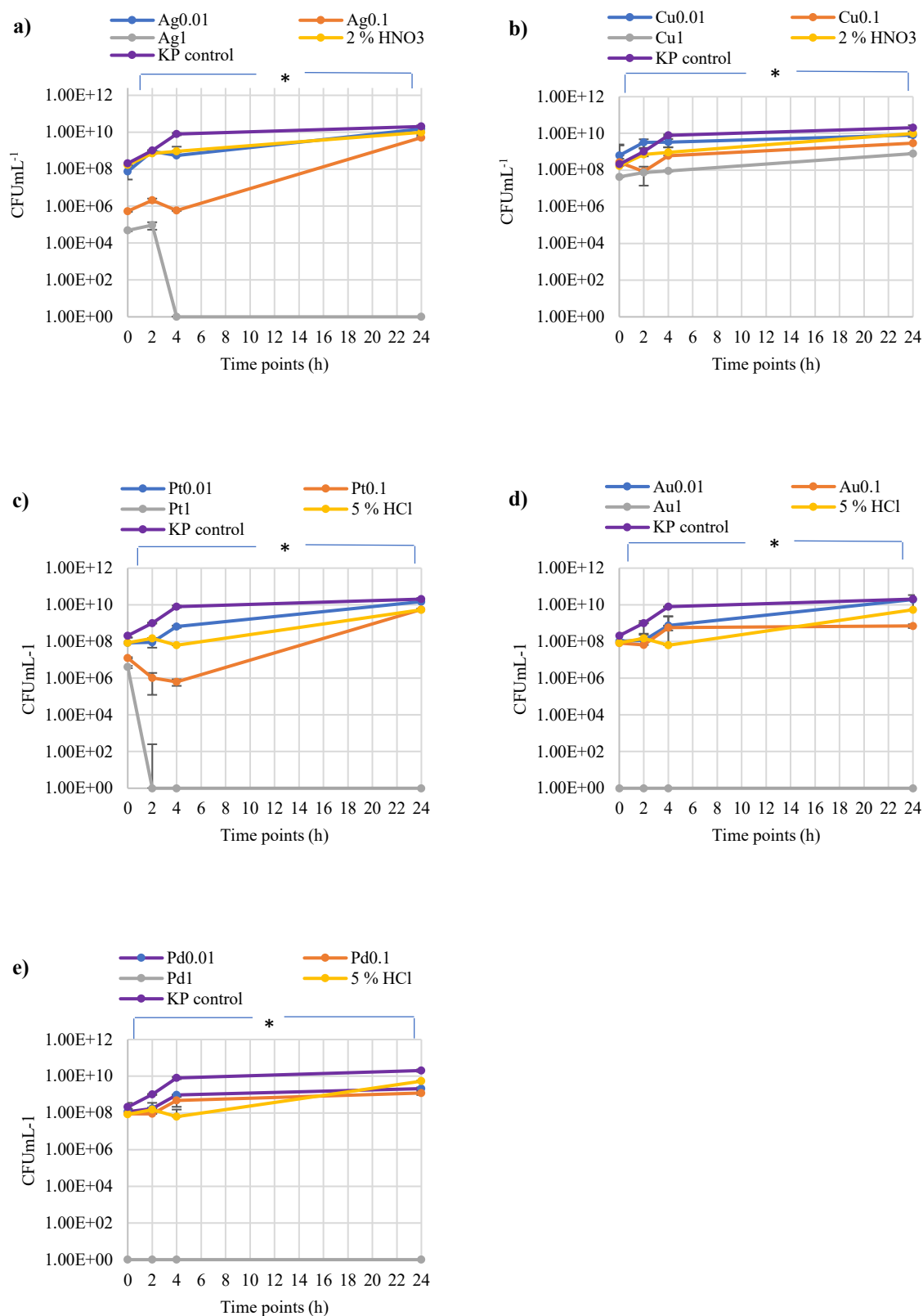
Metal ions/acid controls	<i>K. pneumoniae</i>	<i>A. baumannii</i>	<i>E. faecium</i>
Y (2 % HNO <sub>3</sub> )	0.062 ± 0	0.062 ± 0	0.250 ± 0
Ti (2 % HNO <sub>3</sub> )	0.039 ± 0.006	0.039 ± 0.006	0.062 ± 0
Ta (2 % HNO <sub>3</sub> )	0.031 ± 0	0.031 ± 0	0.062 ± 0
In (2 % HNO <sub>3</sub> )	0.062 ± 0	0.062 ± 0	0.125 ± 0
Nb (2 % HNO <sub>3</sub> )	0.062 ± 0	0.062 ± 0	0.125 ± 0
Rh (5 % HCl)	0.031 ± 0	0.015 ± 0	0.062 ± 0
Ru (5 % HCl)	0.031 ± 0	0.031 ± 0	0.062 ± 0
Mo (10 % HCl)	0.007 ± 0	0.007 ± 0	0.015 ± 0
Zn (2 % HNO <sub>3</sub> )	0.078 ± 0.027	0.062 ± 0	0.250 ± 0
Ga (5 % HNO <sub>3</sub> )	0.062 ± 0	0.031 ± 0	0.125 ± 0
Ag (2 % HNO <sub>3</sub> )	0.015 ± 0	0.007 ± 0	0.031 ± 0
Cu (2 % HNO <sub>3</sub> )	0.062 ± 0	0.062 ± 0	0.125 ± 0
Pt (5 % HCl)	0.015 ± 0	0.015 ± 0	0.031 ± 0
Au (5 % HCl)	0.015 ± 0	0.015 ± 0	0.031 ± 0
Pd (5 % HCl)	0.015 ± 0	0.015 ± 0	0.031 ± 0
2 % HNO <sub>3</sub>	0.078 ± 0.017	0.125 ± 0	0.250 ± 0
5 % HNO <sub>3</sub>	0.078 ± 0.017	0.062 ± 0	0.208 ± 0.027
5 % HCl	0.062 ± 0	0.062 ± 0	0.166 ± 0.027
10 % HCl	0.007 ± 0	0.007 ± 0	0.015 ± 0

### 3.1.4. Time kill assay for five selected metal ions (Ag, Cu, Pt, Au and Pd ions)

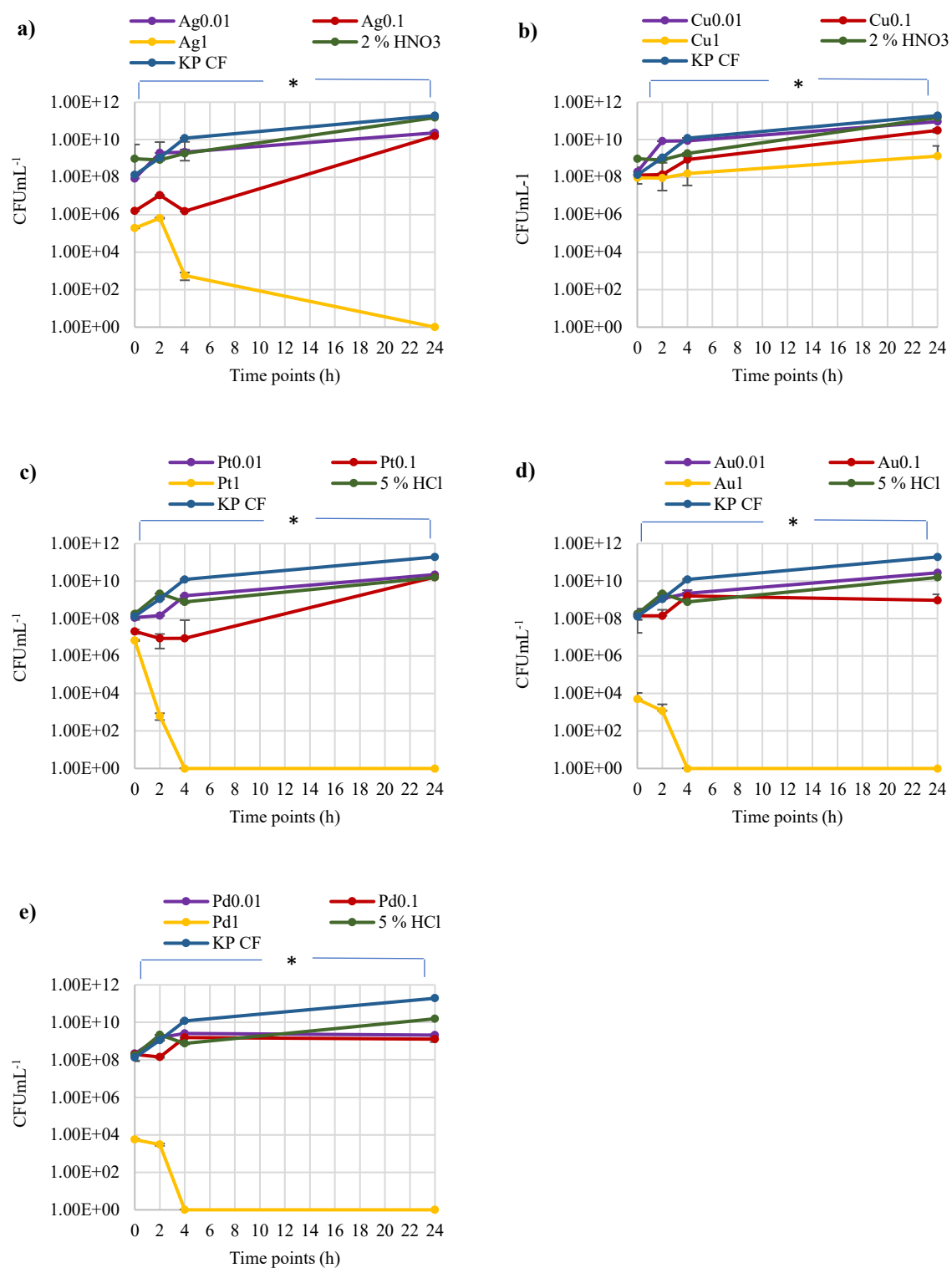
#### 3.1.4.1. Antimicrobial efficacy against *K. pneumoniae* with and without 10 % bovine plasma conditioning film

The antimicrobial effects of five metal ions Ag, Cu, Pt, Au and Pd were tested at 0 h, 2 h, 4 h and 24 h time points. These metals were tested in the presence and absence of 10 % bovine plasma against *K. pneumoniae* (Figure 3.3 and 3.4, a-e). The bacterial growth pattern was also analysed in the presence 2 % HNO<sub>3</sub> and 5 % HCl acid controls. With and without CF, 1 to 2 log reductions in bacterial viable count were demonstrated for all tested metal ions when compared with acid controls (2 % HNO<sub>3</sub> and 5 % HCl) and negative control (from 10<sup>11</sup> to 10<sup>9</sup>) ( $p < 0.05$ ). With and without CF, the tested bacteria time kill profile for Ag, Pt, Au and Pd ions (0.01 mgmL<sup>-1</sup> and 0.1 mgmL<sup>-1</sup>) and Cu ions (0.01 mgmL<sup>-1</sup>, 0.1 mgmL<sup>-1</sup> and 1 mgmL<sup>-1</sup>) showed a gradual rise in the viable cells over a period of 24 h (from 10<sup>7</sup> to 10<sup>9</sup>) ( $p > 0.05$ ). At 1 mgmL<sup>-1</sup>, Ag ions at 4 h, Pt ions at 2 h and Au and Pd ions at 0 h time points demonstrated 100 % bacterial reduction in the absence of plasma CF. At 1 mgmL<sup>-1</sup>, Ag ions at 24 h and Pt, Au and Pd ions at 4 h ( $p < 0.001$ ) demonstrated 100 % bacterial reduction in the presence of plasma CF. The bacterial control growth pattern showed a log increase in viable count when allowed to grow in presence of 10 % bovine plasma (Figure 3.3 and 3.4, a-e).

Overall, without plasma CF, Au and Pd ions and with plasma CF, Pt ions, Au ions and Pd ions demonstrated the best antimicrobial efficacies whilst, Cu ions showed the least antimicrobial efficacy.



**Figure 3.3.** Time kill assay results for a) Ag, b) Cu, c) Pt, d) Au and e) Pd ions at 0.01 mgmL<sup>-1</sup>, 0.1 mgmL<sup>-1</sup> and 1 mgmL<sup>-1</sup> concentrations against *K. pneumoniae* in the absence of 10 % plasma conditioning film ( $p < 0.001$ ) (n = 3).



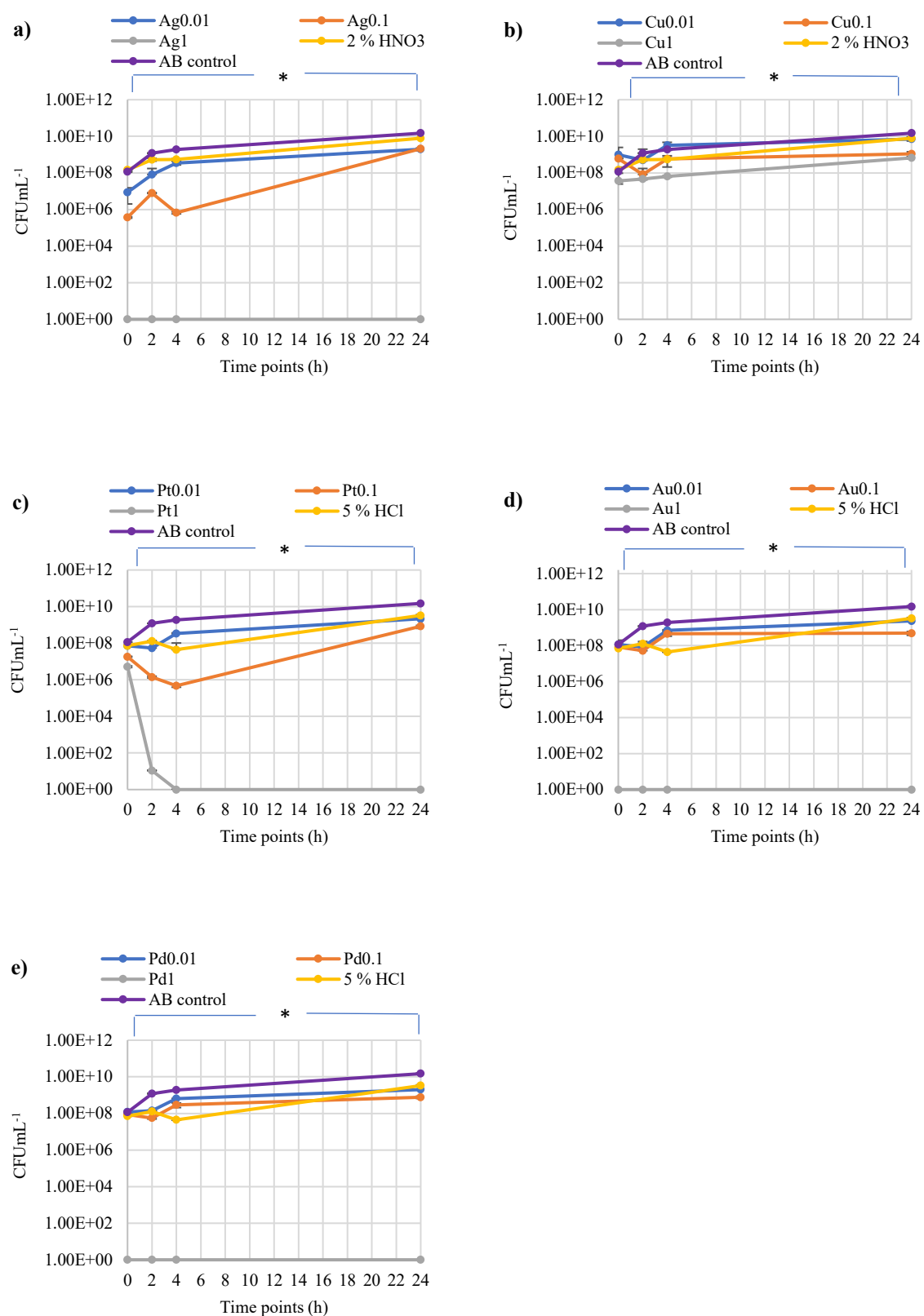
**Figure 3.4.** Time kill assay results for a) Ag, b) Cu, c) Pt, d) Au and e) Pd ions at 0.01 mgmL<sup>-1</sup>, 0.1 mgmL<sup>-1</sup> and 1 mgmL<sup>-1</sup> concentrations against *K. pneumoniae* in the presence of 10 % plasma conditioning film ( $p < 0.001$ ) (n = 3).



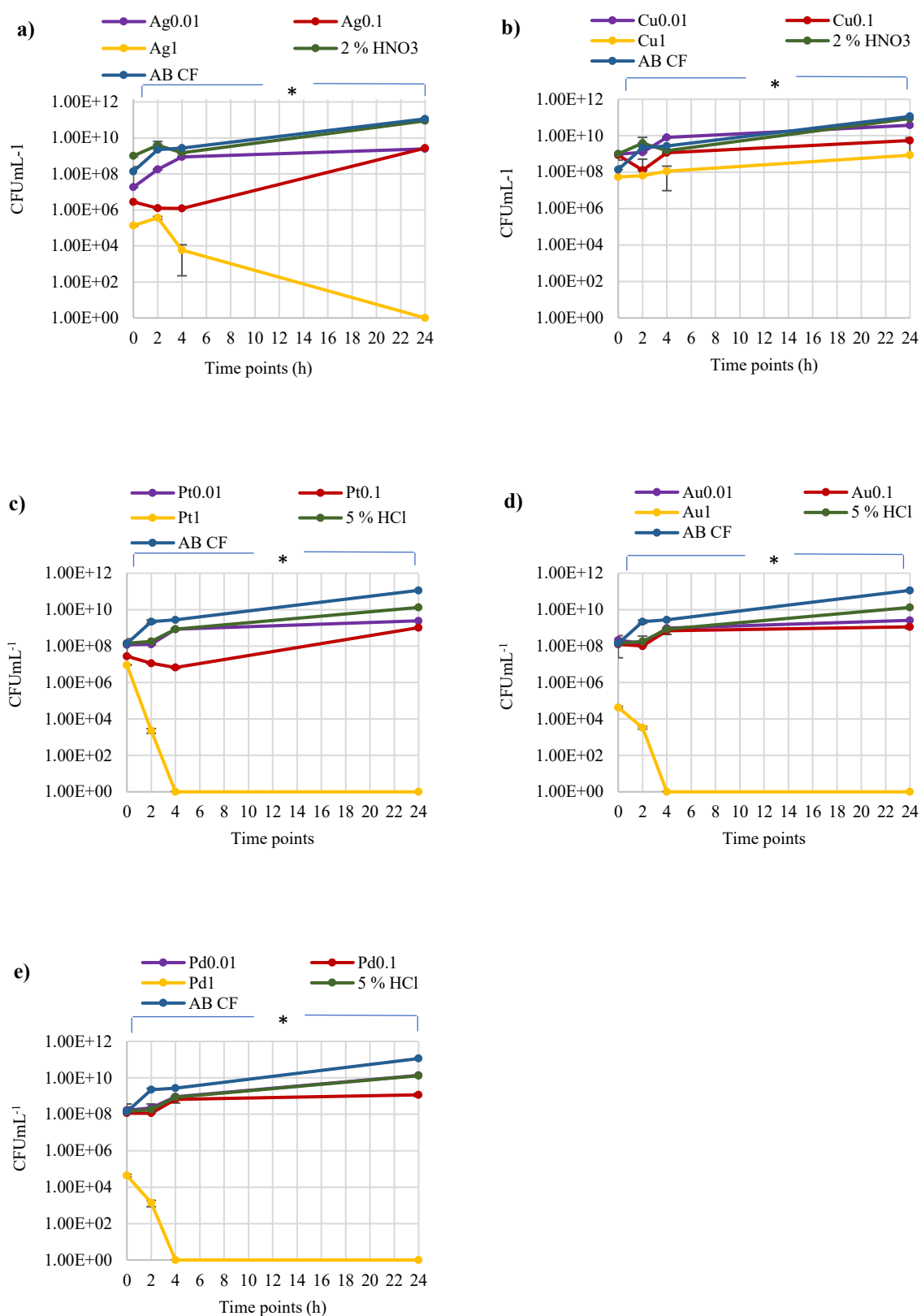
### **3.1.4.2. Antimicrobial efficacy against *A. baumannii* with and without 10 % bovine plasma conditioning films**

The antimicrobial effects of five metal ions Ag, Cu, Pt, Au and Pd were tested at 0 h, 2 h, 4 h and 24 h time points. These metal ions were tested in the presence and absence of 10 % bovine plasma against *A. baumannii* (Figure 3.5 and 3.6, a-e). The bacterial growth pattern was also analysed for 2 % HNO<sub>3</sub> and 5 % HCl acid controls. With and without CF, 1 to 2 log reductions in bacterial viable count were demonstrated for all tested metal ions when compared with acid controls (2 % HNO<sub>3</sub> and 5 % HCl) and negative control (from 10<sup>11</sup> to 10<sup>9</sup>) ( $p < 0.05$ ). With and without CF, the tested bacteria time kill profile for Ag, Pt, Au and Pd ions (0.01 mgmL<sup>-1</sup> and 0.1 mgmL<sup>-1</sup>) and Cu ions (0.01 mgmL<sup>-1</sup>, 0.1 mgmL<sup>-1</sup> and 1 mgmL<sup>-1</sup>) showed a gradual rise in the viable cells over a period of 24 h (from 10<sup>7</sup> to 10<sup>9</sup>) ( $p > 0.05$ ). At 1 mgmL<sup>-1</sup>, Ag ions at 24 h, Pt ions at 2 h and Au and Pd ions at 0 h time points demonstrated 100 % bacterial reduction in the absence of plasma CF. At 1 mgmL<sup>-1</sup>, Ag ions at 24 h and Pt ions, Au and Pd ions at 4 h ( $p < 0.001$ ) demonstrated 100 % bacterial reduction in the presence of plasma CF. The bacterial control growth pattern showed a log increase in viable count when allowed to grow in presence of 10 % bovine plasma (Figure 3.5 and 3.6, a-e).

Overall, without plasma CF, Au and Pd ions and with plasma CF, Pt, Au and Pd ions demonstrated the best antimicrobial efficacies, whilst, Cu ions showed the least antimicrobial efficacy.



**Figure 3.5.** Time kill assay results for a) Ag, b) Cu, c) Pt, d) Au and e) Pd ions at 0.01 mgmL<sup>-1</sup>, 0.1 mgmL<sup>-1</sup> and 1 mgmL<sup>-1</sup> concentrations against *A. baumannii* in the absence of 10 % plasma conditioning film ( $p < 0.001$ ) (n = 3).

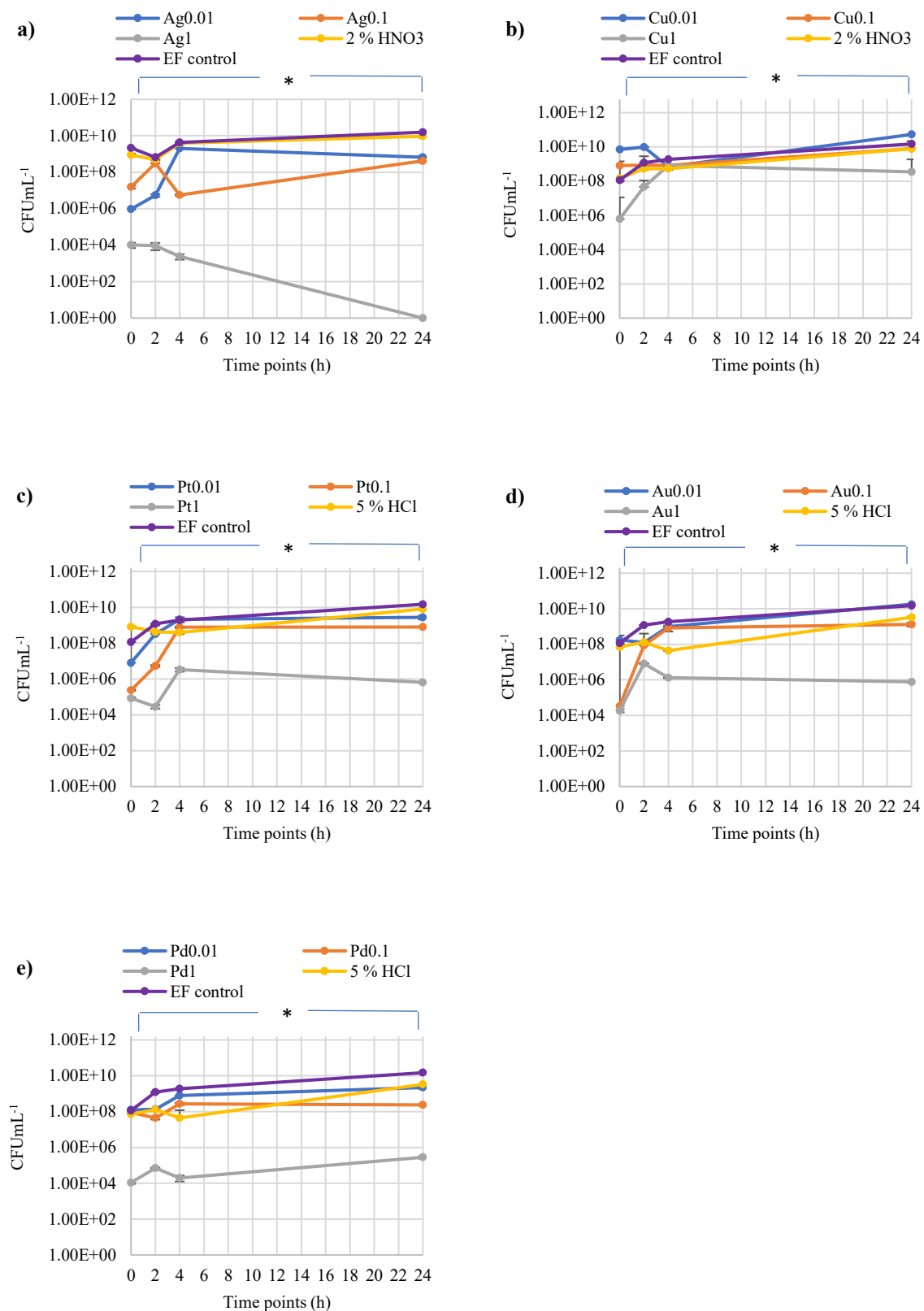


**Figure 3.6.** Time kill assay results for a) Ag, b) Cu, c) Pt, d) Au and e) Pd ions at 0.01 mgmL<sup>-1</sup>, 0.1 mgmL<sup>-1</sup> and 1 mgmL<sup>-1</sup> concentrations against *A. baumannii* in the presence of 10 % plasma conditioning film ( $p < 0.001$ ) (n = 3).

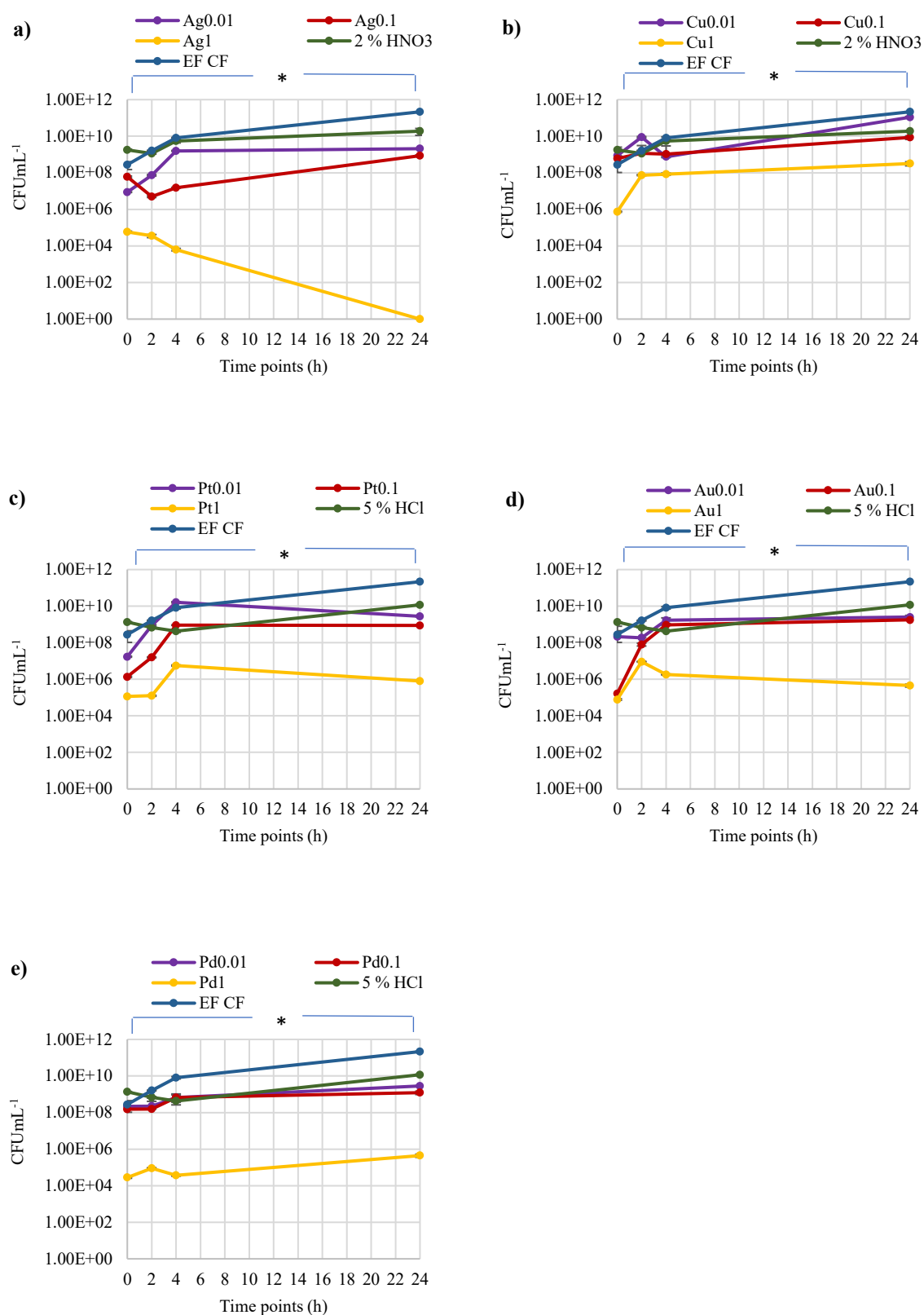
### 3.1.4.3 Antimicrobial efficacy against *E. faecium* with and without 10 % bovine plasma conditioning films

The antimicrobial effects of five metal ions Ag, Cu, Pt, Au and Pd were tested at 0 h, 2 h, 4 h and 24 h time points. These metals were tested in the presence and absence of 10 % bovine plasma against *E. faecium* (Figure 3.7 and 3.8, a-e). The bacterial growth pattern was also analysed for 2 % HNO<sub>3</sub> and 5 % HCl acid controls. With and without CF, 1 to 2 log reductions in bacterial viable count were demonstrated for all tested metal ions when compared with acid controls (2 % HNO<sub>3</sub> and 5 % HCl) and negative control (from 10<sup>11</sup> to 10<sup>9</sup>) ( $p < 0.05$ ). With and without CF, the tested bacteria time kill profile for Ag, Pt, Au and Pd ions (0.01 mgmL<sup>-1</sup> and 0.1 mgmL<sup>-1</sup>) and Cu ions (0.01 mgmL<sup>-1</sup>, 0.1 mgmL<sup>-1</sup> and 1 mgmL<sup>-1</sup>) showed a gradual rise in the viable cells over a period of 24 h (from 10<sup>7</sup> to 10<sup>9</sup>) ( $p > 0.05$ ). Silver ions demonstrated the best antimicrobial effects with zero viable bacterial at 24 h when tested in the presence or absence of CF plasma at 1 mgmL<sup>-1</sup> ( $p < 0.001$ ). Platinum, Au and Pd ions showed a 5-log reduction in bacterial viable count when compared with *E. faecium* negative control at 1 mgmL<sup>-1</sup> ( $p < 0.05$ ) (Figure 3.7 and 3.8, a-e).

Overall, with and without plasma CF, Ag ions demonstrated the best antimicrobial efficacy and Cu ions demonstrated the least antimicrobial activity. *E. faecium* was found to be the most resistant against all the tested metals.



**Figure 3.7.** Time kill assay results for a) Ag, b) Cu, c) Pt, d) Au and e) Pd ions at 0.01 mgmL<sup>-1</sup>, 0.1 mgmL<sup>-1</sup> and 1 mgmL<sup>-1</sup> concentrations against *E. faecium* in the absence of 10 % plasma conditioning film ( $p < 0.05$ ) (n = 3).



**Figure 3.8.** Time kill assay results of a) Ag, b) Cu, c) Pt, d) Au and e) Pd ions at 0.01 mgmL<sup>-1</sup>, 0.1 mgmL<sup>-1</sup> and 1 mgmL<sup>-1</sup> concentrations against *E. faecium* in the presence of 10 % plasma conditioning film ( $p < 0.05$ ) (n = 3).

### 3.1. Discussion

#### *Antimicrobial efficacies in the absence conditioning film*

Various antimicrobial applications of metals to reduce bacterial infection and transmission risks have been explored, for instance, silver in wound dressings, silver and copper to disinfect water at hospital sites and gold and palladium coatings on catheters (Huang et al., 2008; Chandra et al., 2011; Thomas et al., 2011). Recently, graphene based compound have been suggested a potential material for the development of antimicrobial surfaces owing to their contact-based antimicrobial efficacy (Perreault et al., 2015).

From this work, the Rh, Pt and Pd ions demonstrated the best antimicrobial efficacies in the ZoI results. Silver, Pt, Pd and Au ions demonstrated strong antimicrobial efficacies in the MIC, MBC and time kill assay.

#### *Metal ions suggested antimicrobial mechanisms*

##### *Platinum, palladium and rhodium*

The target of Pt in the form of primary cis-platin is DNA but it also has an affinity for the sulphur and selenium donors present in many proteins (Lippard, 1989; Roberts and Thomson, 1979). A palladium complex with 1,6-bis(benzimidazol-2-yl)-3,4-dithiahexane was thought to exhibit bacterial toxicity mechanisms due to metal protein binding leading to DNA damage, causing cell death. Rhodium ions were suggested to target protein synthesis and enzyme disruption (Vaidya et al., 2018). Aslan et al. (2011) used salicylaldehyde benzenesulfonylhydrazone Pd complexes (12 mm) and demonstrated a greater ZoI compared to Pt (10 mm) when used at a  $140 \mu\text{g disk}^{-1}$  against *K. pneumoniae*. Further, in agreement with our results, the tetraaza macrocyclic complexes of metals (Pt, Pd and iridium (Ir)) demonstrated antimicrobial activity in order of  $\text{Pd} > \text{Pt} > \text{Ir}$  against *S. aureus* and *E. coli* (Chandra et al., 2011). Platinum nanoparticles have demonstrated antimicrobial efficacies against *Bacillus subtilis*, *S. aureus*, *P. aeruginosa* and *E. coli* (Ayaz Ahmed et al., 2016) whereas other studies

have found no effect (Wernicki et al., 2014). A study tested the antibacterial properties of nine different metal surfaces against *S. aureus* and *E. coli* and found that Pd demonstrated a greater antimicrobial efficacy than other metals tested (Yasuyuki et al., 2010). Another study also looked at the antimicrobial efficacy of number of metals including platinum and palladium and it was found that they were effective against *E. coli* (Kawakami et al., 2008). Similar to our results, Pt cisplatin ionic co-ordinated complexes have demonstrated an effective ZoI (19 mm, 21 mm and 25 mm) at 200  $\mu\text{MmL}^{-1}$  and MIC of 75  $\mu\text{MmL}^{-1}$  against *B. subtilis*, *S. aureus* and *E. coli* respectively (Gaballa, 2010). The Rh (III) complex with tetradentate macrocyclic demonstrated an antimicrobial inhibitory zone of 25 mm against *E. coli* and 28 mm against *S. aureus* (Chandra et al., 2011).

### Gold

The mechanistic action of gold has been suggested to be due to strong cationic attractions to the negatively charged plasma membrane of microbes which lead to cell membrane disruption, ROS accumulation and consequent cell death (Huh and Kwon, 2011; Casey et al., 2010). A study found that gold demonstrated little effect against *Escherichia coli* or *S. aureus* (Kawakami et al., 2008). However, gold in nanoparticle and ionic form has been suggested to have antimicrobial activity (Zhang et al., 2015). Few studies have demonstrated the antimicrobial efficacy of Au in their ionic forms; however, Au complexes (tetradentate macrocyclic, etc.) have been shown to demonstrate inhibition against bacterial pathogens (Saygun et al., 2006; Mishra et al., 2006; Nazari et al., 2012). In agreement to our results, Au complex of phosphanegold (I) dithiocarbamates has been shown to demonstrate lower MICs and MBCs (7.81 to 125  $\mu\text{g mL}^{-1}$ ) against *S. aureus* and *B. subtilis* (Sim et al., 2014).

### Silver

Silver alginate has displayed antimicrobial efficacy against bacterial species including *A. baumannii*, *K. pneumoniae* and *E. faecium* (Castellano et al., 2007; Thomas et al., 2011).



Another study stated that nano-silver particles inhibited 99 % of *E. coli* within 30 mins of exposure at 0.5 g (Xia et al., 2017). The antimicrobial efficacies of Ag have been a combination of mechanisms. Firstly, Ag ions might bind and destabilise the bacterial cell membrane phospholipids (Jung et al., 2008). This would lead to disruption in the electron transport chain and loss of potassium ions and decreased adenosine triphosphate (Sutterlin et al., 2012). Secondly, Ag ions can interact with cytoplasmic molecules such as nucleic acids and enzymes. Thirdly, intracellular Ag ion accumulation might generate ROS. Furthermore, Ag ions impact on the process of cell division by interacting with the nitrogen bases of the deoxyribonucleic acid chains (Jung et al., 2008; Dakal et al., 2016). These processes might lead to cell destruction. Silver ions have also been shown to demonstrate low MIC values (0.004 to 0.64 mgL<sup>-1</sup>) against the tested pathogens including *Enterococcus* species (Ahmad and Viljoen, 2015).

### *Copper*

Though Cu is a known antimicrobial and possess some of the above-mentioned chemical antimicrobial modes of action against bacterial cells in this study. Copper ions demonstrated weak antimicrobial efficacies against the tested bacteria. In agreement with our results, Ag ions demonstrated a greater antimicrobial efficacy than Cu ions in the bacterial viability tests against *Listeria monocytogenes* (Tamayo et al., 2014). The lower antimicrobial efficacy of Cu has been suggested to be due to the hemostasis mechanisms (Slavin et al., 2017). It has also been suggested that Cu<sup>+2</sup> is reduced to Cu<sup>+</sup>, once Cu<sup>+2</sup> binds with the bacterial protein thiol group. This is followed with a dismutation of the displaced Cu<sup>+</sup> to regenerate Cu<sup>+2</sup> (Berthon et al., 1995; Slavin et al., 2017). The reversible bonding of Cu and bacterial thiol group might form oxidized variable of amino acids (e.g. cystine an oxidized variable of cysteine). These oxidized amino acids can participation in the vital bacterial cellular process (Berthon et al., 1995; Rigo et al., 2004). However, Ag<sup>+</sup> binds to amino acids in an irreversible bonding forming

amino acid precipitation leaving no residue to participate in vital cellular process (Scarpa et al., 1996; Rigo et al., 2004). In contrast to our results, Cu (II) complexes with ethylenediamine were found to be the most antimicrobial with inhibitory concentrations of  $4\ \mu\text{g mL}^{-1}$  –  $6\ \mu\text{g mL}^{-1}$  compared to nickel (II) and zinc (II) complex ( $6\ \mu\text{g mL}^{-1}$  –  $8\ \mu\text{g mL}^{-1}$ ) against *E. coli*, *S. aureus* and *P. aeruginosa* (Raman et al., 2011). Copper ions released from copper alloys have been suggested to target bacteria by increasing ROS production and thus inducing DNA damage. However, this concept has been contested and it has further been demonstrated that the cell envelope is the first part of the attack when bacteria are in contact with the dry copper surface (Santo et al., 2011). In terms of the results of this study, this concept holds true and would in part explain the low antimicrobial results when the copper was used in solution. Further, there are significant differences that exist between the exposure of bacteria to copper ions and exposure to metallic copper surfaces, since the cells on dry metallic copper surfaces are not in an environment that promotes growth. Therefore, these cells face challenges that are different from those in a wet environment (Casey et al., 2010; Santo et al., 2011). It has also been suggested that the antibacterial property of copper is attributed mainly to the adhesion of the bacteria to the copper because of their opposite electrical charges, resulting in a reduction reaction at the bacterial cell wall; this has led to suggestions that copper ions do not act like some other metals ions such as silver (Zanzen et al., 2013). Thus, it may be that when the bacteria are in direct contact with copper surfaces, an enhanced antimicrobial effect is achieved.

### ***Effect of conditioning films***

The metal ions were also tested in the presence of 10 % bovine plasma, to replicate *in vivo* like conditions. It should also be noted that in presence of 10 % plasma CF, a decrease in the antimicrobial efficacies of all the metals were found in all the tests when used against the metal ions alone. Bovine plasma is a mixture of variety of proteins such as albumin, pre-albumin, glycoprotein, immunoglobins etc. (Farrell et al., 2013). This can be explained in part metal ions

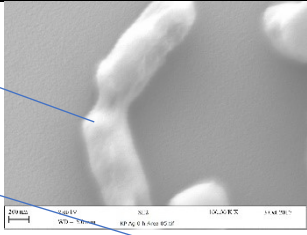
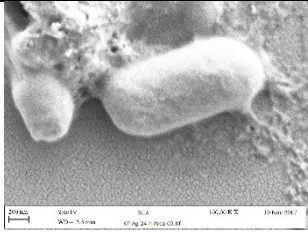
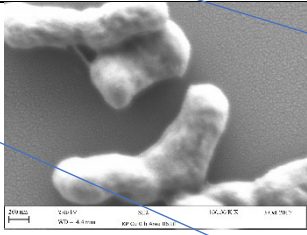
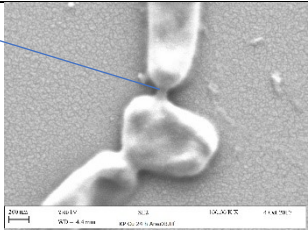
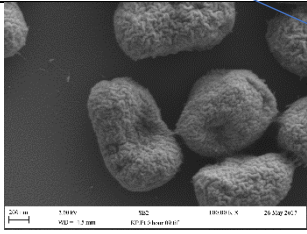
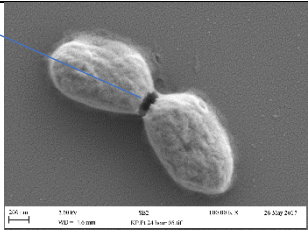
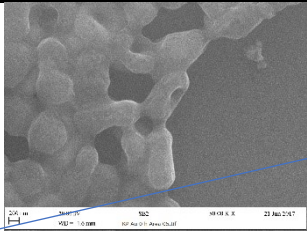
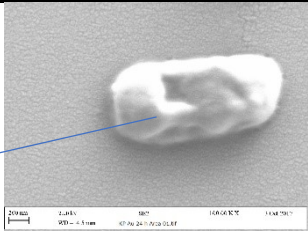
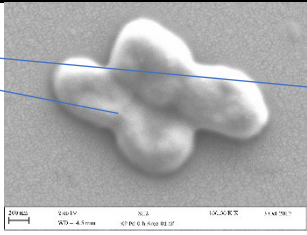
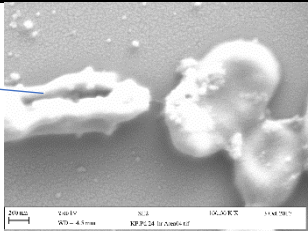
in a liquid phase undergo immediate hydrolysis, when in the presence of the plasma proteins. The hydrolysis process makes metal ions a weak component to bind with the bacterial components owing to formation of a multiple oxidation state. This might increase the overall time of the redox reaction between metal ions and bacterial components (Iqbal et al., 2009; Benedetti et al., 2011; Bal et al., 2013). In agreement with our finding, Lourenco et al. (2018) demonstrated that Au nanoparticles demonstrated a 3.8 log *S. aureus* reduction in absence of bovine serum albumin (BSA); whilst only 0.5 log bacterial reduction in the presence of BSA. Similarly, titanium nitride silver coated surfaces showed no inhibition in presence of blood and BSA condition films and 0.06 to 0.1 mm of inhibitory zones were found against *S. aureus* in absence of CFs (Saubade et al., 2018).

### 3.2. Morphological changes observed using scanning electron microscopy (SEM)

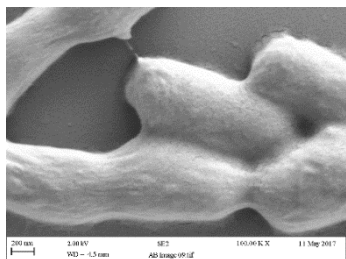
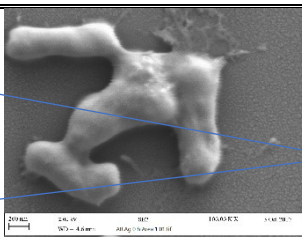
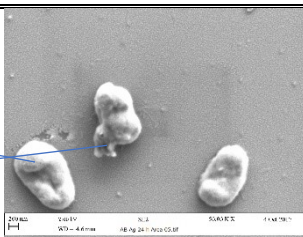
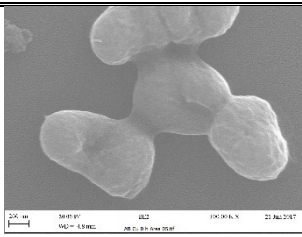
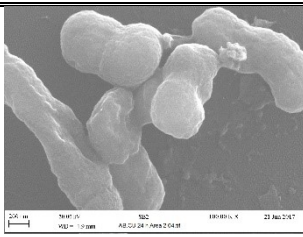
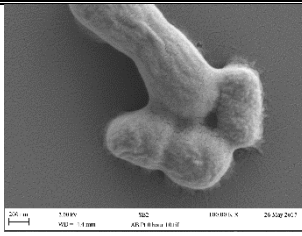
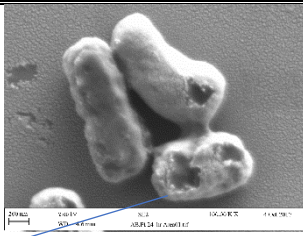
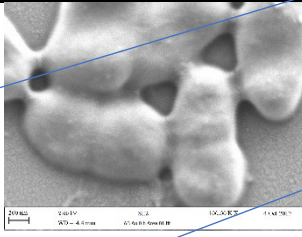
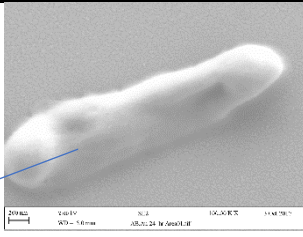
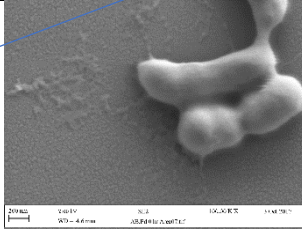
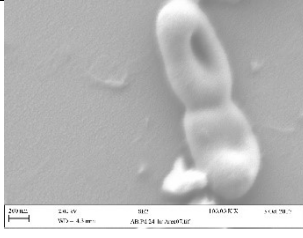
#### 3.2.1. *Klebsiella pneumoniae*, *A. baumannii* and *E. faecium* structural changes after treatment with metal ions (Ag, Cu, Pt, Au and Pd) at 0 h and 24 h in the absence of 10 % bovine plasma conditioning film

The changes in the bacterial cell morphology after the metal ions treatment was analysed using SEM. The untreated cells were found to have normal and smooth surface and intact shape (Table 3.5 - 3.7, a). Different characteristics of morphological changes were observed after metal ion treatment at 0 h and 24 h. It was also evident that all the bacterial cells were found with greater deformities after 24 h metal ion treatment than 0 h treatment. The prominent changes after Ag and Cu ions treatment against *A. baumannii* and *E. faecium* were cell seepage and hence lysis (Table 3.6 and 3.7 – i c and ii c). The significant morphological changes observed after Pt, Au and Pd ions treatment were numerous pits / holes formation on the surfaces, cell surface grooves, cell shape changes (deformed or elongation) when compared with the control (Table 3.5 – 3.7, iii – iv - b, c). The noticeable deformed feature in the *K. pneumoniae* cells was the breakage of cell junction after 24 h Pt ion treatment (Table 3.5, iii – c). Against *E. faecium* in the presence Pt, Au and Pd ions stressed environment, a blanket of cell seepage content appearance was observed (Table 3.7 – iii – v, c).

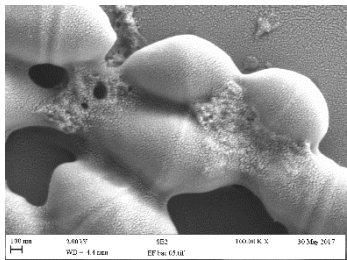
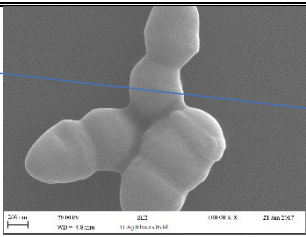
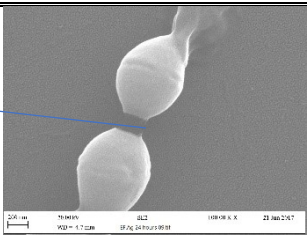
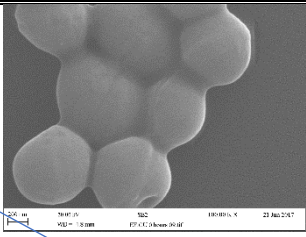
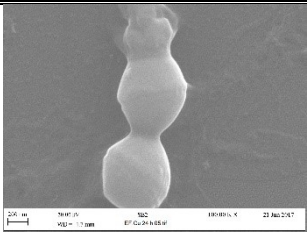
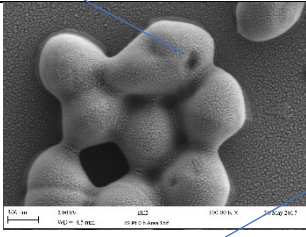
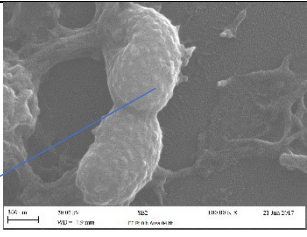
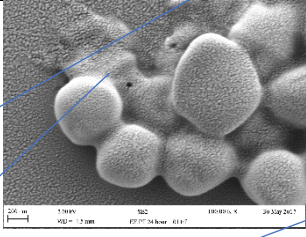
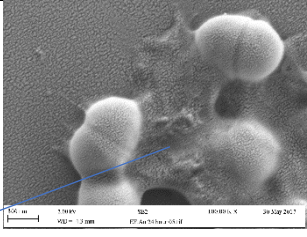
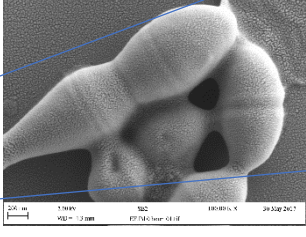
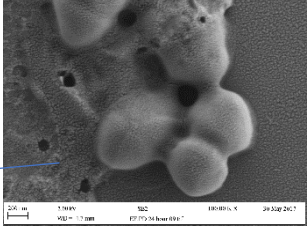
**Table 3.5.** Morphological changes of *K. pneumoniae* in the absence of 10 % plasma conditioning film after metal ions treatment at 0 h and 24 h. Ag = silver, Cu = copper, Pt = platinum, Au = gold and Pd = palladium.

Control	Metal ion solutions	<i>K. pneumoniae</i> after 0 h metal treatment in the absence of CF	<i>K. pneumoniae</i> after 24 h metal treatment in the absence of CF
Elongation		b)	c)
Deformation	Ag i)		
Cell junction breakage	Cu ii)		
a)	Pt iii)		
	Au iv)		
Grove formation	Pd v)		

**Table 3.6.** Morphological changes of *A. baumannii* in the absence of 10 % plasma conditioning film after metal ions treatment at 0 h and 24 h. Ag = silver, Cu = copper, Pt = platinum, Au = gold and Pd = palladium.

Control	Metal ion solutions	<i>A. baumannii</i> after 0 h metal treatment in the absence of CF	<i>A. baumannii</i> after 24 h metal treatment in the absence of CF
		b)	c)
<p>a)</p> 	Ag i)		
	Cu ii)		
	Pt iii)		
	Au iv)		
	Pd v)		
Deformed cell			
Seepage			
Holes			
Cell elongation			

**Table 3.7.** Morphological changes of *E. faecium* in the absence of 10 % plasma conditioning film after metal ions treatment at 0 h and 24 h. Ag = silver, Cu = copper, Pt = platinum, Au = gold and Pd = palladium.

Control	Metal ion solutions	<i>E. faecium</i> after 0 h metal treatment in the absence of CF	<i>E. faecium</i> after 24 h metal treatment in the absence of CF
		b)	c)
<p>Cell junction breakage</p> <p>Pits</p> <p>a)</p>  <p>Rough surface</p> <p>Cell seepage blanket</p>	Ag i)		
	Cu ii)		
	Pt iii)		
	Au iv)		
	Pd v)		

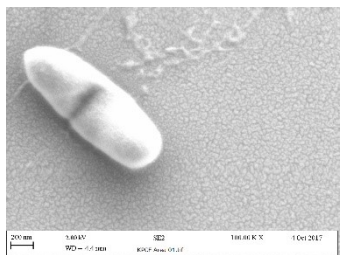
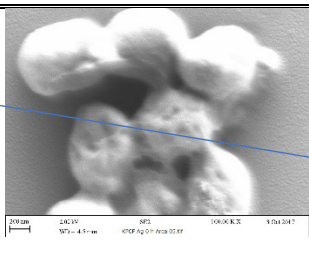
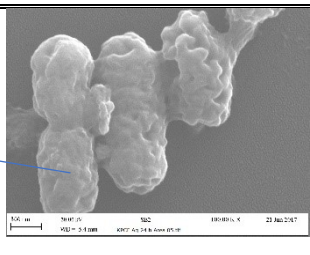
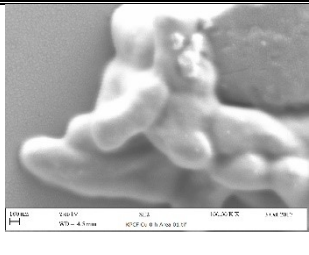
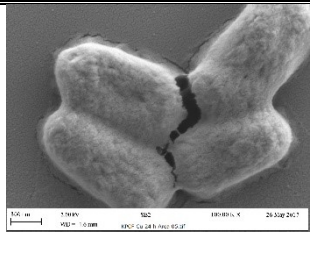
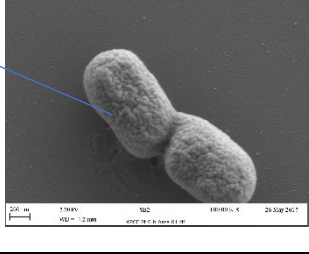
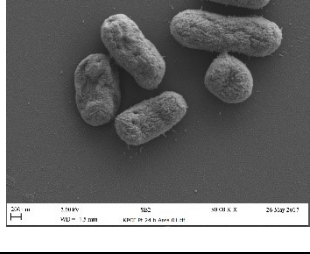
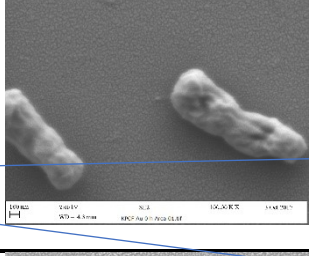
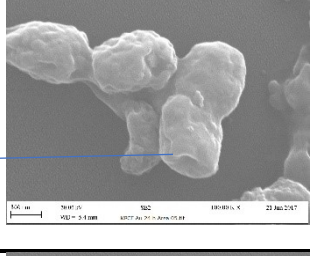
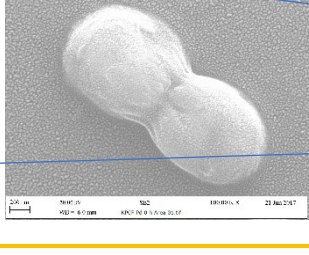
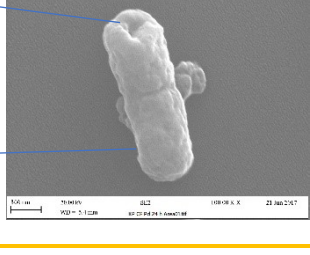


### **3.2.2. *Klebsiella pneumoniae*, *A. baumannii* and *E. faecium* structural changes after metal ions (Ag, Cu, Pt, Au and Pd) treatment at 0 h and 24 h in the presence of 10 % bovine plasma conditioning film**

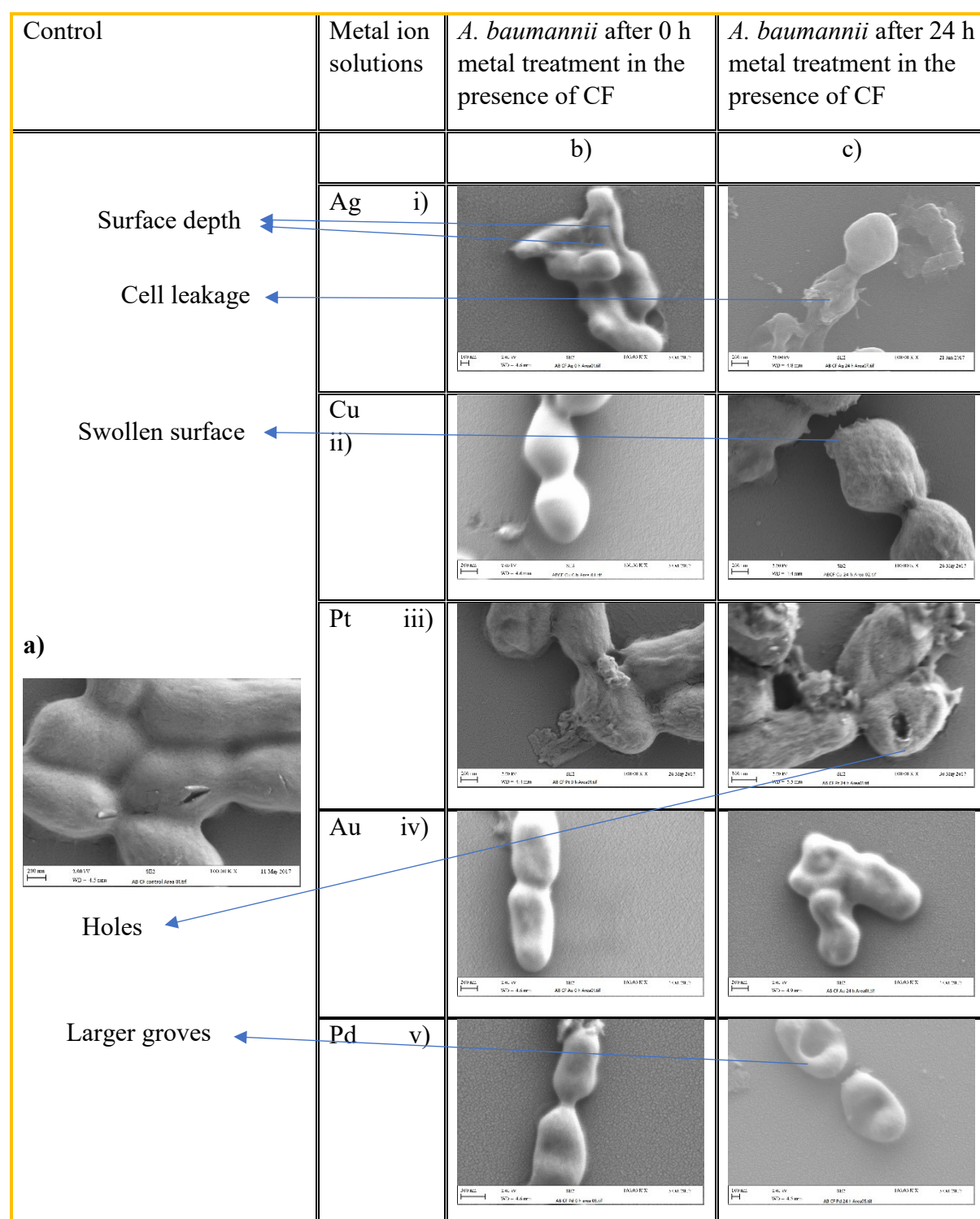
The changes in the bacterial cell morphology after the metal ions treatment in the presence of conditioning film was analysed using SEM. The untreated cells remained intact and plump (Table 3.8 – 3.10; a). Different characteristics of morphological changes were observed after metal ions treatment at 0 h and 24 h. It is also apparent that all the bacterial cells were found with severe irregularities after 24 h metal ions treatment than 0 h treatment. After Pt, Au and Pd ions treatment at 0 h, cells were found to become flattened with pits on surfaces of Gram-negative bacteria (Table 3.8 and 3.9, iii – v (b)). It was observed that the cells of *E. faecium* become spongy looking in structure and shorter in shape with visible pits on the surface (Table 3.10, iii – v (b)). When treated with Ag and Cu ions at 0 h, the *K. pneumoniae* cells morphology transformed to abnormal shape with a rough surface (Table 3.8, i - ii (b)), *E. faecium* became more elongated and flattened with deep holes (Table 3.10, i - ii (b)) and *A. baumannii* cells were lysed (Ag ions) and swollen with pits (Cu ions) (Table 3.9, i - ii (b)) compared with the untreated cells. Platinum and Ag ions were found to be the most aggressive of all tested ionic solutions on all the tested cells with total distortion of cells, larger and numerous pits and even cell lysis (Table 3.8 - 3.10 i and iii – c). Platinum, Au and Pd ions demonstrated numerous grooves and what looked to be deeper holes against *K. pneumoniae*; flattened surface, large depths and swollen edges in most of the cell area when the metal ions were treated against *A. baumannii* and cell lysis with small pits (Au / Pd ions) and a narrowed width with large holes (Pt ions) against *E. faecium*. Specifically, the *K. pneumoniae* cell wall after 24 h treatment in Pd ion solution were found to have deep folds and distortion of the cell so that is appeared cylindrical in shape was observed (Table 3.8 v-c).



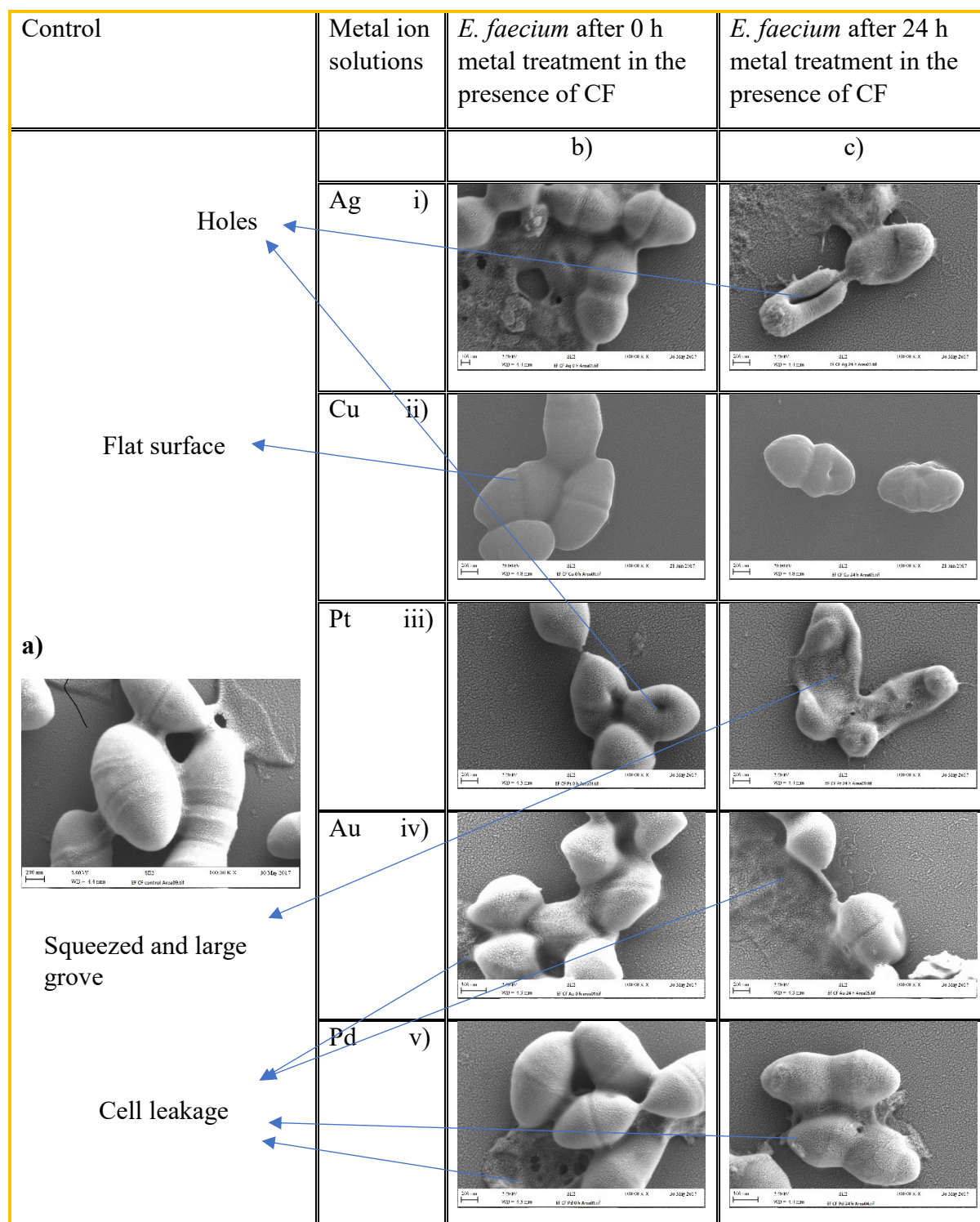
**Table 3.8.** Morphological changes of *K. pneumoniae* in the presence of 10 % plasma conditioning film after metal ions treatment at 0 h and 24 h. Ag = silver, Cu = copper, Pt = platinum, Au = gold and Pd = palladium.

Control	Metal ion solutions	<i>K. pneumoniae</i> after 0 h metal treatment in the presence of CF	<i>K. pneumoniae</i> after 24 h metal treatment in the presence of CF
		b)	c)
<p>Rough surface</p> <p>Swollen surface</p> <p>a)</p>  <p>Holes</p> <p>Deep folds</p>	Ag i)		
	Cu ii)		
	Pt iii)		
	Au iv)		
	Pd v)		

**Table 3.9.** Morphological changes of *A. baumannii* in the presence of 10 % plasma conditioning film after metal ions treatment at 0 h and 24 h. Ag = silver, Cu = copper, Pt = platinum, Au = gold and Pd = palladium.



**Table 3.10.** Morphological changes of *E. faecium* in the presence of 10 % plasma conditioning film after metal ions treatment at 0 h and 24 h. Ag = silver, Cu = copper, Pt = platinum, Au = gold and Pd = palladium.



## 3.2. Discussion

### *In the absence of conditioning films*

All the tested bacterial cells demonstrated physical abnormalities after metal ions treatment compared to the untreated cells in this study. Several studies demonstrated similar bacterial physical damage results, where untreated cells were intact and normal (Klaus-Joerger et al., 2001; Sondi et al., 2004; Khan et al., 2005). Bacterial cells were found to appear shorter than control after the Pd and Pt ions treatment in our study. Similarly, *Campylobacter jejuni* cells appeared shorter and compact with craters on the surface following treatment with magnesium oxide nanoparticles treatment at 1 mgmL<sup>-1</sup>. The mechanism suggested that resulted in the shorter cell length was leakage of the cellular contents leading to cell size reduction (He et al., 2016). In this study, bacterial cells treated with Pt ions were swollen with numerous grooves on the surface, and some of the bacteria treated with metal ions also displayed cell elongation. Similar morphological changes were demonstrated in the studies of Santos et al. (2014) and Huang et al. (2017), where the underlining mechanism was cell wall extraction or disorganisation leading to internalisation of the metal ions and alteration in the cytoplasm content after Ag, Cu and Ga ions treatment.

### *In the presence of conditioning films*

It has been suggested that the presence of organic proteins surrounds the bacteria in *in vivo* conditions (Sotogaku et al., 1999; Cardile et al., 2014; Franca and Cerca et al., 2016). Bacterial adhesion to such proteins might boost their growth and thus increase pathogenicity (Cardile et al., 2014). All the tested metal ions demonstrated morphological abnormalities after Ag, Cu, Pt, Au and Pd ions treatment in the presence of plasma CF as similar grade to when tested in the absence of plasma CF. However, a study confirmed *S. aureus* cells were less damaged in the 10 % human plasma after vancomycin treatment owing a formation of additional protective layer that surrounded the bacteria (Cardile et al., 2014). According to Tedjo et al. (2007),

protein adsorption might decrease the negative charge on the bacterial surface and thus reduce bacterial affinity for the antimicrobial cations. It has further been demonstrated that citrate capped Ag nanoparticles, polyvinylpyrrolidone coated Ag nanoparticles and uncapped Ag nanoparticles demonstrated severe damage to *S. typhimurium* cells without organic load. However, only uncapped Ag nanoparticles at  $6 \mu\text{g mL}^{-1}$  –  $8 \mu\text{g mL}^{-1}$  demonstrated membrane damage to bacteria in the presence of 3 % bovine serum albumin (Gnanadhas et al., 2013). Such results demonstrate that several factors such as metal chelation with proteins and hydrophobic forces between bacterial surface and proteins affects the antimicrobial and cell interactions and thus the extent of the bacterial morphological damage (Gnanadhas et al., 2013; Tuson and Weibel, 2013). It is clear that the effect of the presence of conditioning films and their influence on the antimicrobial action of molecules is complex, and further investigation is warranted.

### 3.3. Elemental changes observed using energy dispersive X-ray analysis

#### 3.3.1. Elemental changes for *Klebsiella pneumoniae*, *A. baumannii* and *E. faecium* after treatment with metal ions (Ag, Cu, Pt, Au and Pd) at 24 h in the absence of 10 % bovine plasma conditioning film (n = 3)

The EDAX analysis results were presented for an average of three atomic percentage (At %) analysis for untreated cells and cells treated with Ag, Cu, Pt, Au and Pd ions after 24 h.

##### *K. pneumoniae*

Against *K. pneumoniae* in the absence of plasma CF, the control elemental At % was 51.33 % for carbon, 20 % for nitrogen, 28 % for oxygen, 0.41 % for phosphorous and 0.15 % for potassium. Treatment of the bacteria with the Pd ions demonstrated the greatest changes in all the bacterial elements, with the strongest changes seen for the carbon (36.83 %), oxygen (48.44 %) and nitrogen (0.99 %) content. Platinum ions demonstrated At % changes in nitrogen (15 %), carbon (56 %), phosphorous (0.65 %) and potassium (0.03 %) content. Gold ions demonstrated At % changes for oxygen (23 %), phosphorous (0.08 %) and potassium (0.65 %) content. Silver ions demonstrated an effect on phosphorous content (0.25) of the cells. Copper ions demonstrated the least effects on the elemental composition of the cell wall (Figure 3.9, a-e).

##### *A. baumannii*

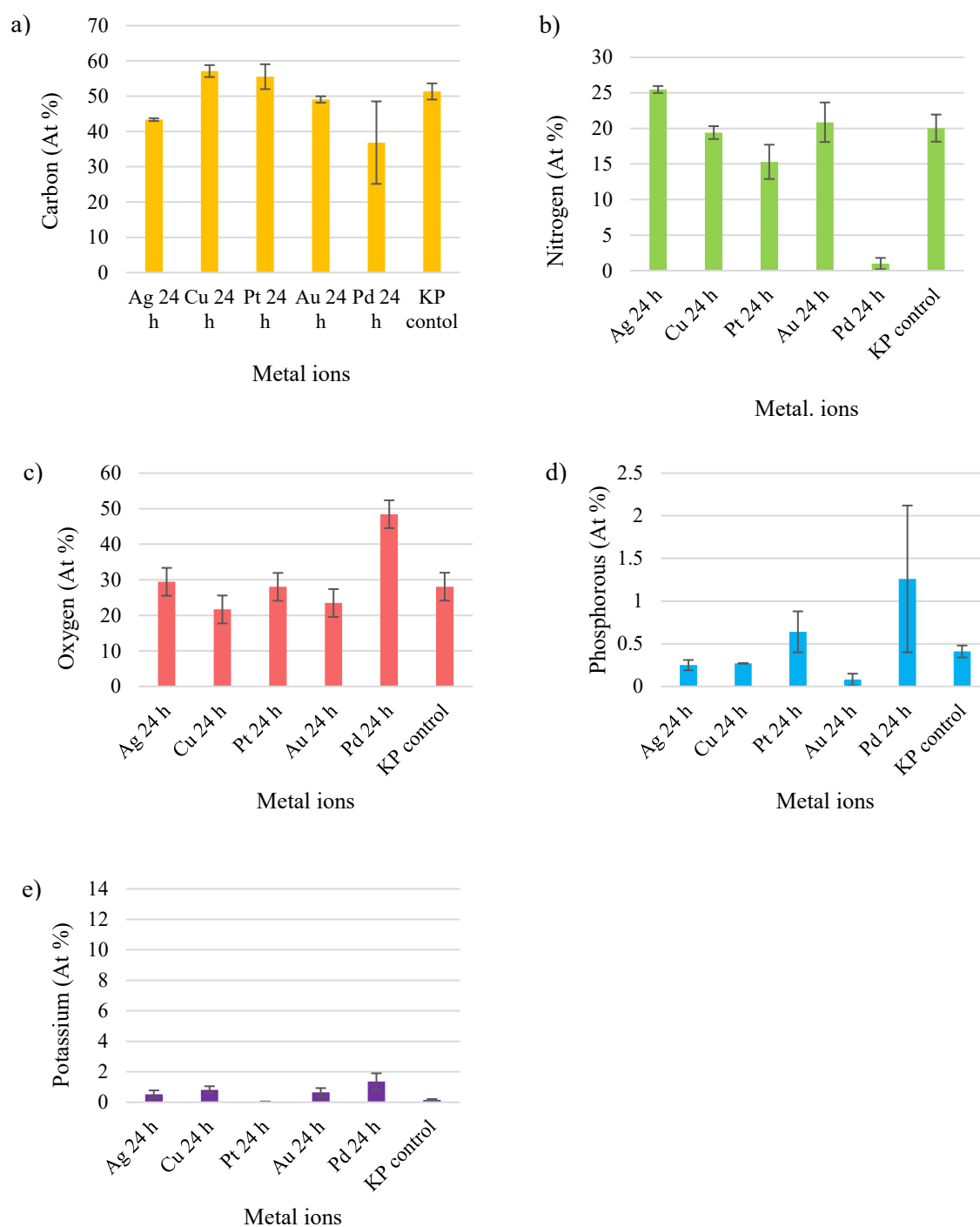
Against *A. baumannii* in the absence of plasma CF, the control elemental At % was 49 % for carbon, 23 % for nitrogen, 26 % for oxygen, 0.86 % for phosphorous and 0.51 % for potassium. A strong elemental change was demonstrated for Ag and Pt ions (carbon = 59 % and 56 %, nitrogen = 18 % and 13 %, oxygen = 21 % and 25 %, phosphorous = 0.15 % and 1.37 % and potassium = 0.45 % and 2.77 % respectively). Copper ions demonstrated a weak effect on At % of carbon (53 %) and oxygen (25 %). Gold ions demonstrated the least effects on At % of nitrogen (20 %) and phosphorous (0.64 %) (Figure 3.10, a-e).

### *E. faecium*

Against *E. faecium* in the absence of plasma CF, the control elemental At % were 46 % for carbon, 24 % for nitrogen, 30 % for oxygen, 0.29 % for phosphorous and 0.4 % for potassium. A strong change in the At % of carbon (59 %), nitrogen (16 %) and oxygen (23 %) was demonstrated against bacteria treated with Au ions. The maximum At % change for phosphorous (0.03 %) and potassium (0.87 %) was demonstrated with Pt ions and Ag ions respectively. Moreover, Ag ions demonstrated a significant change on the At % of nitrogen (14 %). Treatment of *E. faecium* with Pd ions showed the least elemental changes in the cell walls (Figure 3.11, a-e).

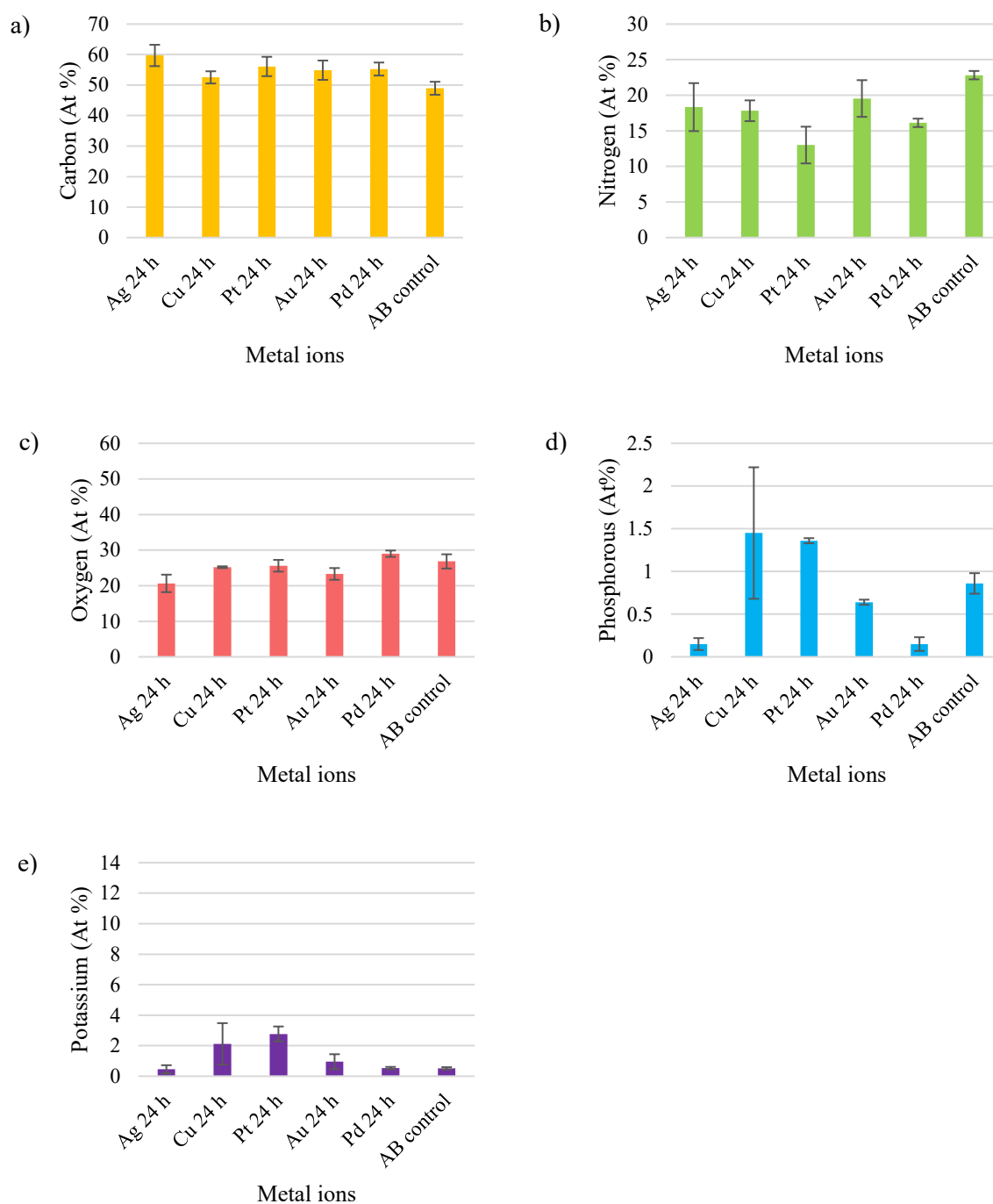
Overall, the most active ions were Pd ions against *K. pneumoniae*, Ag and Pt ions against *A. baumannii* and Au ions against *E. faecium*. The least active ions were Cu against *K. pneumoniae*, Cu and Au against *A. baumannii* and Pd against *E. faecium*.



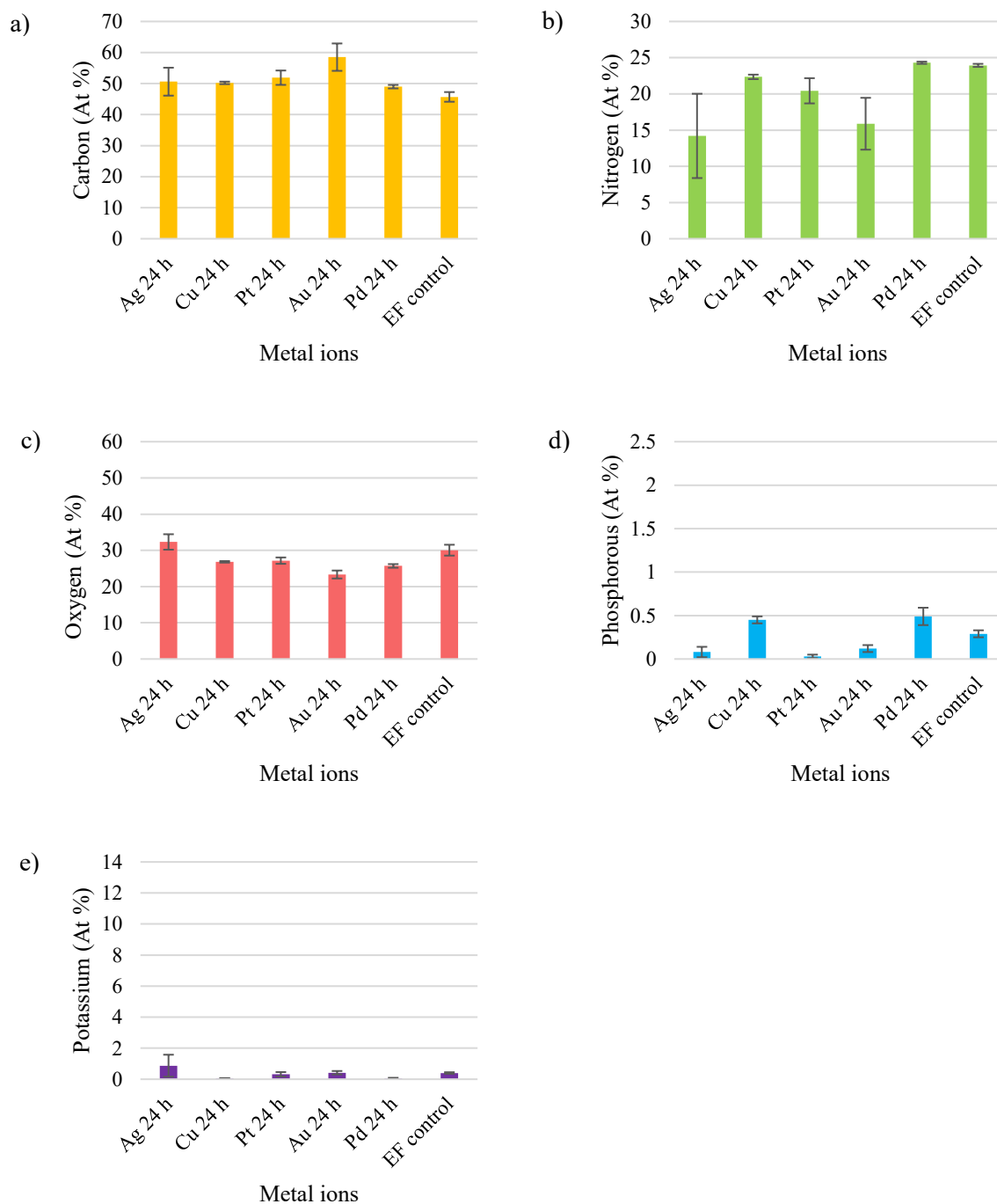


**Figure 3.9.** The EDAX results against *K. pneumoniae* in the absence of 10 % plasma conditioning film signifying elemental changes after metal ions treatment at 24 h. a) At % of carbon, b) At % of nitrogen, c) At % of oxygen, d) At % of phosphorous; e) At % of potassium. Ag = silver, Cu = copper, Pt = platinum, Au = gold and Pd = palladium (n = 3).





**Figure 3.10.** The EDAX results against *A. baumannii* in the absence of 10 % plasma conditioning film signifying elemental changes after silver, copper, platinum, gold and palladium ions treatment at 24 h. a) At % of carbon, b) At % of nitrogen, c) At % of oxygen, d) At % of phosphorous; e) At % of potassium. Ag = silver, Cu = copper, Pt = platinum, Au = gold and Pd = palladium (n = 3).



**Figure 3.11.** The EDAX results against *E. faecium* in the absence of 10 % plasma conditioning film signifying elemental changes after silver, copper, platinum, gold and palladium ions treatment at 24 h. a) At % of carbon, b) At % of nitrogen, c) At % of oxygen, d) At % of phosphorous; e) At % of potassium. Ag = silver, Cu = copper, Pt = platinum, Au = gold and Pd = palladium (n = 3).

### **3.3.2. Elemental changes for *Klebsiella pneumoniae*, *A. baumannii* and *E. faecium* after metal ions (Ag, Cu, Pt, Au and Pd) 24 h treatment in the presence of 10 % bovine plasma conditioning film**

The EDAX analysis results were taken at the atomic percentage (At %) for cells treated with Ag, Cu, Pt, Au and Pd ions at 24 h in the presence of CF.

#### *K. pneumoniae*

Against *K. pneumoniae* in the presence of CF, the control elemental At % was 55 % for carbon, 16 % for nitrogen, 28 % for oxygen, 0.32 % for phosphorous and 0.85 % for potassium. Compared with the control, Pd ions demonstrated the strongest effects in the At % of carbon (29 %), nitrogen (6.3 %), oxygen (51 %) phosphorous (1.3 %) and potassium (9.23 %). Moreover, Au ions demonstrated an effect on the elemental composition of the bacteria At % of carbon (60 %), nitrogen (21 %) and phosphorous (0.22 %). The Cu ions on At % of carbon (55 %) and phosphorous (0.37 %) and Au ions on At % of nitrogen (18 %) and potassium (0.86 %) were the least affected (Figure 3.12, a-e).

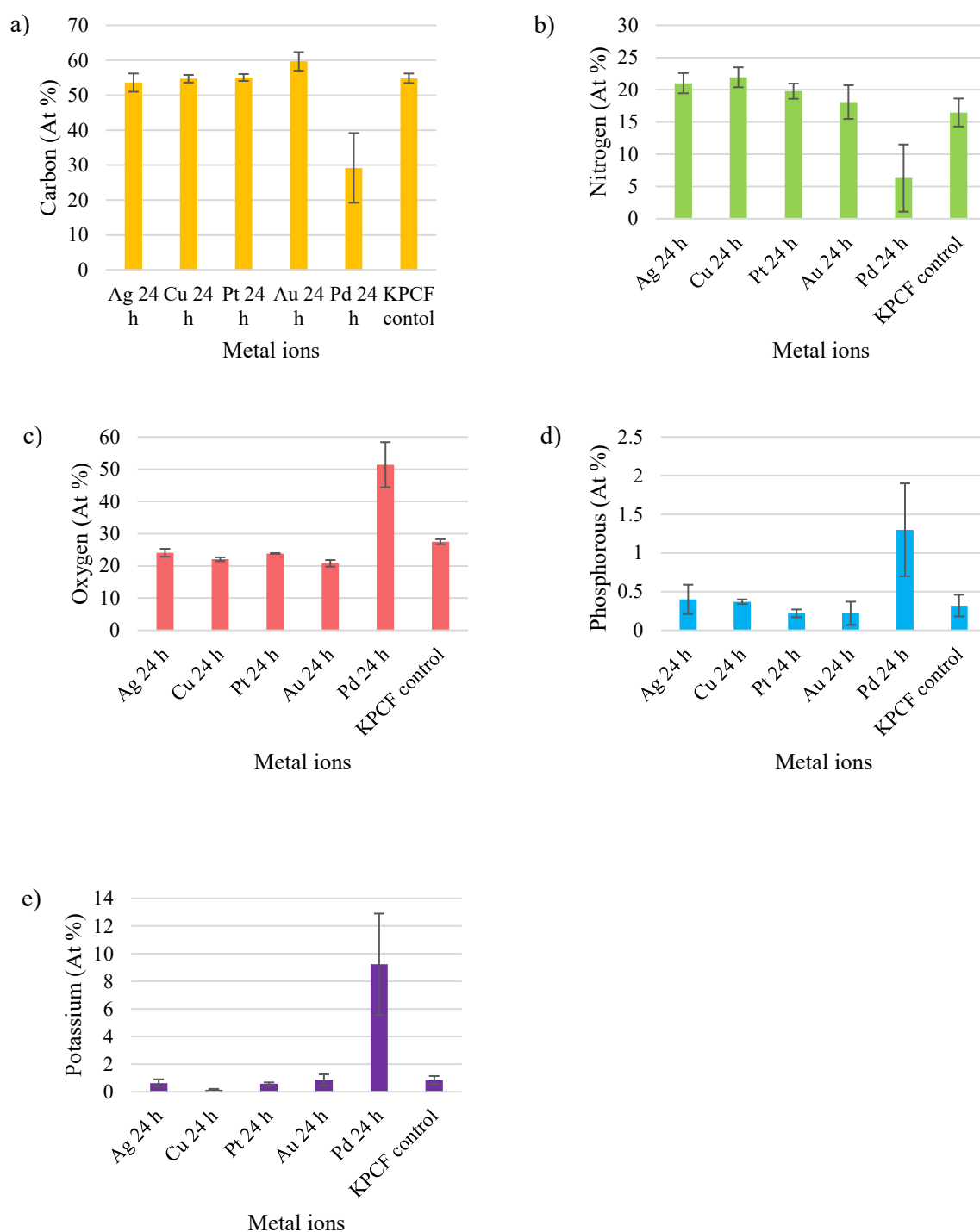
#### *A. baumannii*

Against *A. baumannii* in the presence of plasma CF, the control elemental At % was 54 % for carbon, 17 % for nitrogen, 28 % for oxygen, 0.09 % for phosphorous and 0.52 % for potassium. The maximum effects were demonstrated for Pd ions treated bacterial cells with At % for carbon = 49 %, nitrogen = 24 %, oxygen = 26 %, phosphorous = 0.3 % and potassium = 0 % compared with control. A noteworthy change was demonstrated in At % of potassium with Pt (2.85 %), Cu (1.15 %) and Au (1.07 %) ions. A weak effect was demonstrated with Au ions on At % of carbon (54 %), nitrogen (18 %) and oxygen (26 %). Moreover, a weak effect was also demonstrated with Cu ions on At % of carbon (54 %) and phosphorous (0.09 %) (Figure 3.13, a-e).

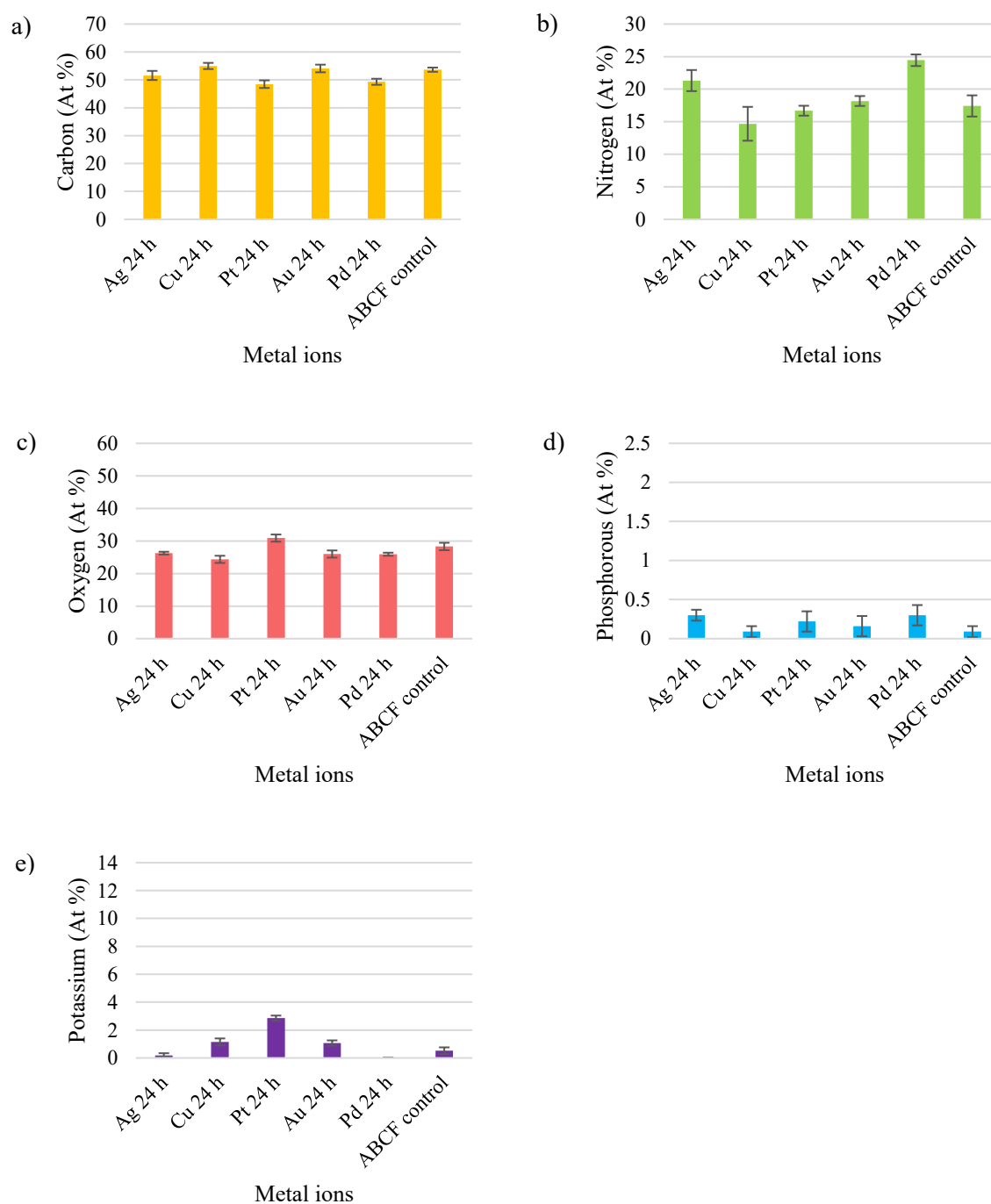
### *E. faecium*

Against *E. faecium* in the presence of plasma CF, the control elemental At % was 52 % for carbon, 20 % for nitrogen, 27 % for oxygen, 0.75 % for phosphorous and 0.17 % for potassium. The Cu ions demonstrated a strong effect on At % of carbon (55 %), nitrogen (17 %), oxygen (26 %) and potassium (0.3 %) compared with the control. Moreover, Pt ions also demonstrated a good effect on At % of carbon (49 %), nitrogen (22 %), phosphorous (0.03 %) and potassium (0.09 %). A weak At % effect was demonstrated for Pd ions on carbon (51 %), nitrogen (20 %), oxygen (27 %) and phosphorous (0.75 %) with Pd ions (Figure 3.14, a-e).

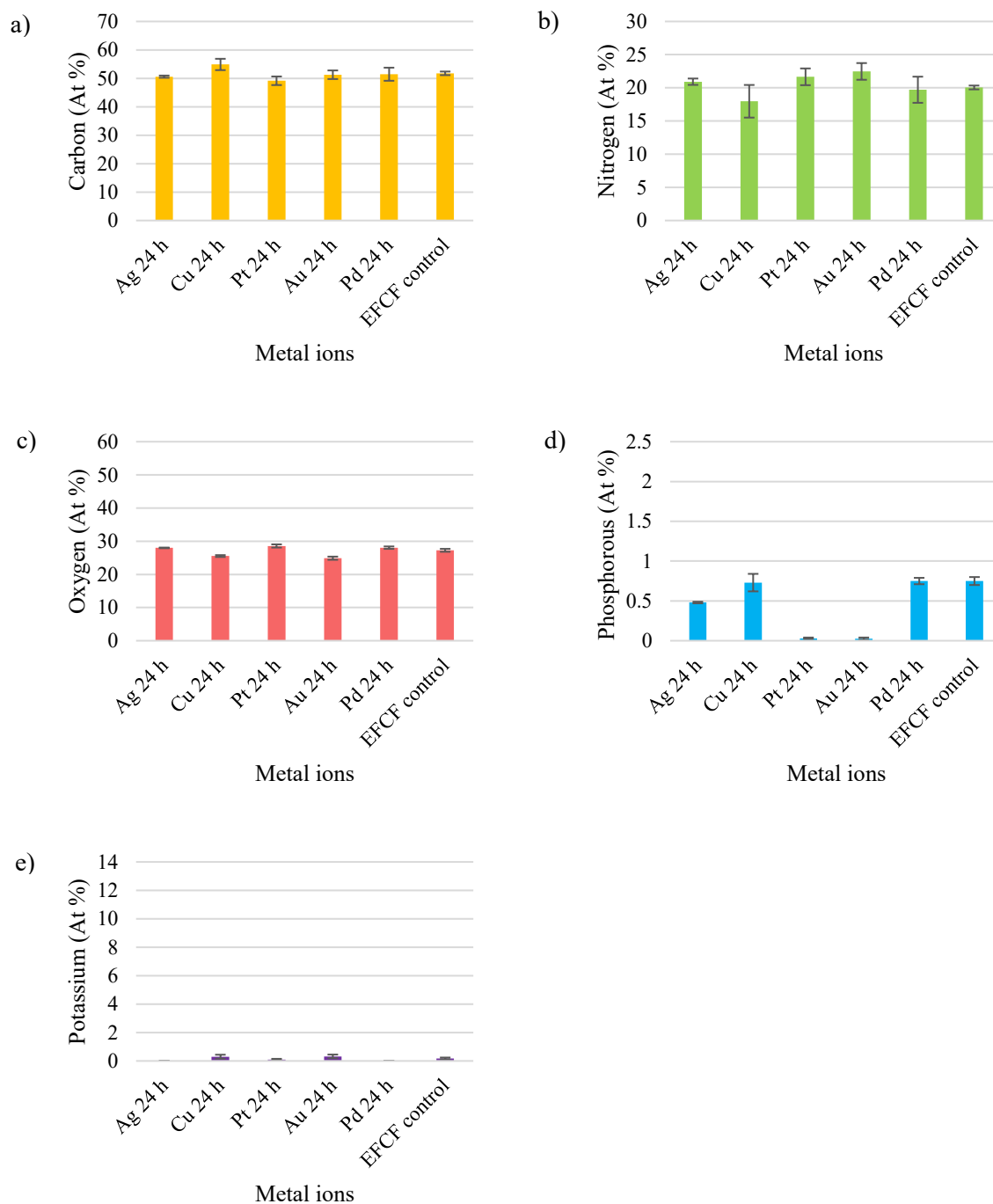
In summary, the Pd ions against *K. pneumoniae* and *A. baumannii* and Cu ions against *E. faecium* demonstrated the most changes in the elemental composition of the bacterial. The least At % effects were noted for Cu ions against *K. pneumoniae*, Cu and Au ions against *A. baumannii* and Pd ions against *E. faecium*. Moreover, some of the metal ions showed variance in the elemental effects in the presence of plasma CF.



**Figure 3.12.** The EDAX results against *K. pneumoniae* in the presence of 10 % plasma conditioning film conditioning films signifying elemental changes after silver, copper, platinum, gold and palladium ions treatment at 24 h. a) At % of carbon, b) At % of nitrogen, c) At % of oxygen, d) At % of phosphorous; e) At % of potassium. Ag = silver, Cu = copper, Pt = platinum, Au = gold and Pd = palladium (n = 3).



**Figure 3.13.** The EDAX results against *A. baumannii* in the presence of 10 % plasma conditioning film signifying elemental changes after silver, copper, platinum, gold and palladium ions treatment at 24 h. a) At % of carbon, b) At % of nitrogen, c) At % of oxygen, d) At % of phosphorous; e) At % of potassium. Ag = silver, Cu = copper, Pt = platinum, Au = gold and Pd = palladium (n = 3).



**Figure 3.14.** The EDAX results against *E. faecium* in the presence of 10 % plasma conditioning film signifying elemental changes after silver, copper, platinum, gold and palladium ions treatment at 24 h. a) At % of carbon, b) At % of nitrogen, c) At % of oxygen, d) At % of phosphorous; e) At % of potassium. Ag = silver, Cu = copper, Pt = platinum, Au = gold and Pd = palladium (n = 3).

### 3.3. Discussion

#### *Elemental changes in the absence of conditioning films*

The elements such as carbon, nitrogen, oxygen, phosphorous and potassium are vital for bacterial cell vital process and growth. Insufficient or deprived of one of the elemental components might hinder the vital processes required to maintain bacterial cell integrity and growth. According to this study results, compared to control Pd ions showed significant changes in all the elements against *K. pneumoniae* in the absence and presence of plasma CF. Moreover, against *A. baumannii* Ag ions on carbon, phosphorous and oxygen At % and Pt ions on carbon, nitrogen and phosphorous At % demonstrated major elemental changes. Against *E. faecium* Ag ions on carbon, nitrogen, phosphorous and potassium At % and Au ions on carbon, nitrogen, oxygen and phosphorous At % also demonstrated major elemental changes. Studies related to analysis of bacteria elemental At % changes after antimicrobial treatment have not previously been investigated, thus it was difficult to compared the results. However, following antimicrobials treatment of the bacteria, it may be that the changes in elemental composition have induced cell stress through the competition of nutrients. One study found that bacterial cell volume decreased as did the size following bacterial growth in phosphorous and protein deprived nutrient conditions. This study explained that bacterial damage could be due to effect on nucleic acids losses (Vrede et al., 2002). Another study demonstrated that carbon and oxygen content reduction might affect the glycogen, fat, nucleic acids and sulphate in amino acids, thus damaging the vital process required for cell survival (Fagerbakke et al., 1996). Heldel et al. (1996) stated that nitrogen forms a base for several amino acids such as glutamine, proline, thus is a vital nutrient for various enzymes and protein of bacteria. It may be that as was demonstrated in this study, the depletion of nitrogen, through competition with another molecule may have led to cell death. The growth of *Bacillus subtilis* has been shown to be affected in potassium limited conditions, which was suggested to be because potassium is



required for ribosomal unit function, pH maintenance of cells and the electron transport chain to maintain ATP function. Alteration of any of these elements and hence cellular function might led to cell damage (Gundlach et al., 2017). It has also been demonstrated that limited nitrogen and phosphorous content affected the sulfolipid and phospholipid composition of the cellular membrane and hence bacterial cell integrity; this was clearly visible in the SEM results after Ag ions and Pt ions treatment in our study (Cotner et al., 2010). Further, the SEM results in this thesis demonstrated shrinkage and shorter cell length after metal ion treatment. Changes in the biochemical composition of the cellular membrane were confirmed by the Raman results following antimicrobial treatments. Thus, it can be assumed that metal ions damage the bacteria at a molecular level.

### 3.4. Chemical changes observed using Raman microscopy

#### 3.4.1. Chemical changes for *K. pneumoniae*, *A. baumannii* and *E. faecium* after metal ions (Ag, Cu, Pt, Au and Pd) treatment at 24 h in the absence of 10 % bovine plasma conditioning film

The Raman spectral profile attributed to cell biomolecules were CH stretch ( $2920\text{ cm}^{-1}$  -  $2960\text{ cm}^{-1}$ ), proteins (C-N stretch:  $760\text{ cm}^{-1}$  –  $810\text{ cm}^{-1}$ ), lipids ( $\text{CH}_2$  and  $\text{CH}_3$  bending:  $1440\text{ cm}^{-1}$  –  $1470\text{ cm}^{-1}$ ) and amides ( $1620\text{ cm}^{-1}$  -  $1680\text{ cm}^{-1}$ ). The chemical effects on bacteria for metal ions were analysed by comparing with bacterial control.

##### *K. pneumoniae*

Against *K. pneumoniae* in the absence of plasma CF, the band shifts noted for control were  $2952\text{ cm}^{-1}$  for CH bond,  $1671\text{ cm}^{-1}$  for amide,  $1442\text{ cm}^{-1}$  for  $\text{CH}_2 / \text{CH}_3$  bending,  $1085\text{ cm}^{-1}$  for C-O stretch and  $784\text{ cm}^{-1}$  for C-N stretch. The maximum band shifts variation in the CH bond ( $2934\text{ cm}^{-1}$ ),  $\text{CH}_2$  and  $\text{CH}_3$  bending ( $1459\text{ cm}^{-1}$ ) and C-O stretch ( $1095\text{ cm}^{-1}$ ) was demonstrated with Cu ions treated bacteria. A strong chemical effect was also demonstrated with Pt and Pd ions for CH bond ( $2935\text{ cm}^{-1}$ ) and amide ( $1661\text{ cm}^{-1}$ ). Moreover, Pt and Pd ions demonstrated a strong effect on C-N stretch ( $792\text{ cm}^{-1}$ ) and C-O stretch ( $1101\text{ cm}^{-1}$ ) respectively. The Cu and Pd ions demonstrated no effect on C-N stretch ( $784\text{ cm}^{-1}$ ). Silver ions demonstrated the greatest effect on amide content ( $1652\text{ cm}^{-1}$ ) (Figure 3.15, a-e).

##### *A. baumannii*

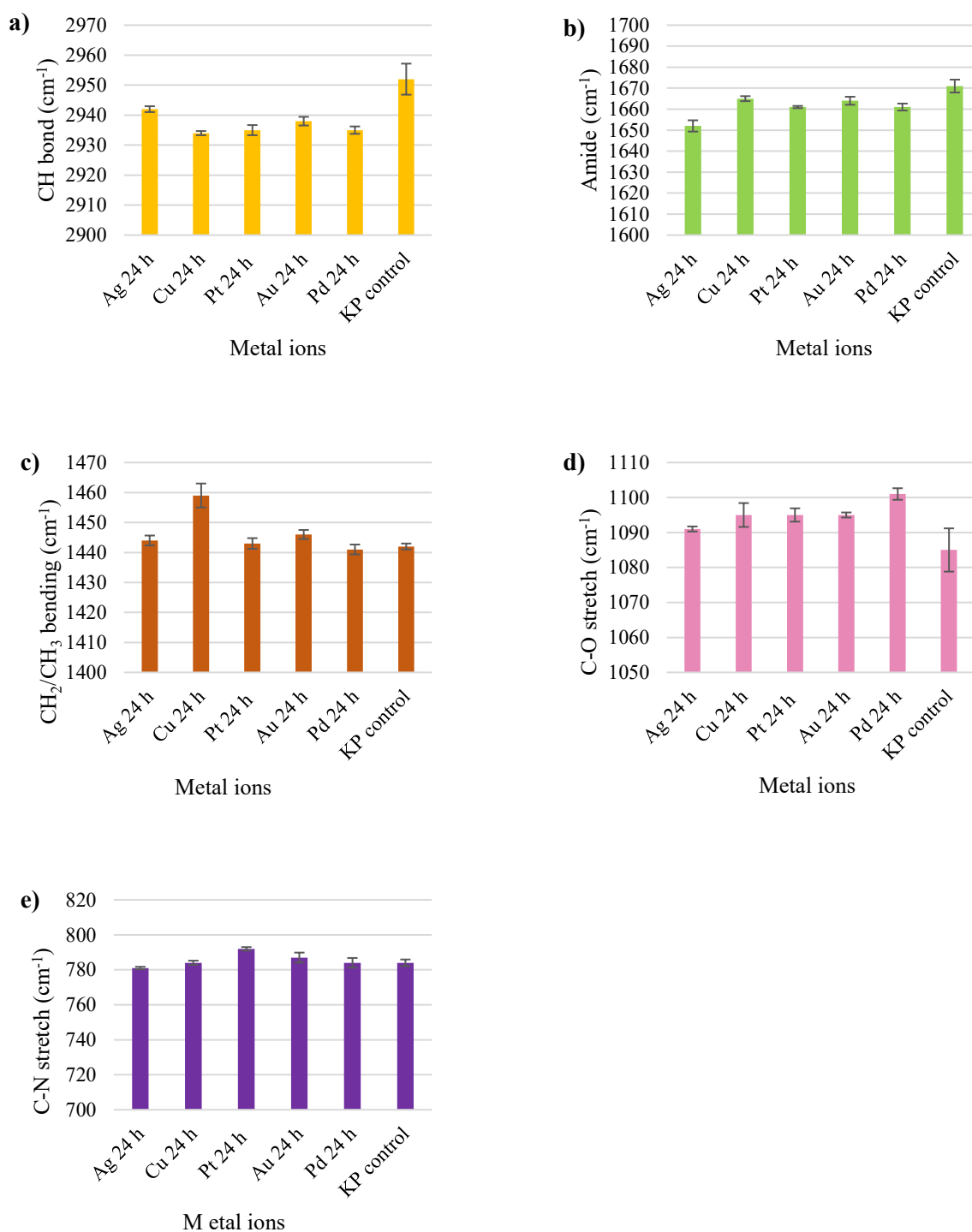
Against *A. baumannii* in the absence of plasma CF, the band shift noted for control were  $2937\text{ cm}^{-1}$  for CH bond,  $1664\text{ cm}^{-1}$  for amide,  $1446\text{ cm}^{-1}$  for  $\text{CH}_2 / \text{CH}_3$  bending,  $1096\text{ cm}^{-1}$  for C-O stretch and  $792\text{ cm}^{-1}$  for C-N stretch. A strong chemical effect was demonstrated for Ag ions with band shift of  $2941\text{ cm}^{-1}$  for CH bond,  $1674\text{ cm}^{-1}$  for amide,  $1452\text{ cm}^{-1}$  for  $\text{CH}_2 / \text{CH}_3$  bending,  $1100\text{ cm}^{-1}$  for C-O stretch and  $784\text{ cm}^{-1}$  for C-N stretch compared with the control. Moreover, an effective chemical band shifts was demonstrated for  $\text{CH}_2/\text{CH}_3$  bending ( $1454\text{ cm}^{-1}$

<sup>1</sup>) with Cu and Pt ions, for C-O stretch (1101 cm<sup>-1</sup>) with Pd ions and for C-N stretch (763 cm<sup>-1</sup>) with Pt ions. A weak chemical shift was demonstrated for CH bond (2932 cm<sup>-1</sup>), amide (1663 cm<sup>-1</sup>) and C-O stretch (1093 cm<sup>-1</sup>) with Cu ions treated bacteria. Moreover, with Pt ions and Au ions demonstrated a weak band shift for amide 1663 cm<sup>-1</sup> and 1448 cm<sup>-1</sup> respectively (Figure 3.16, a-e)

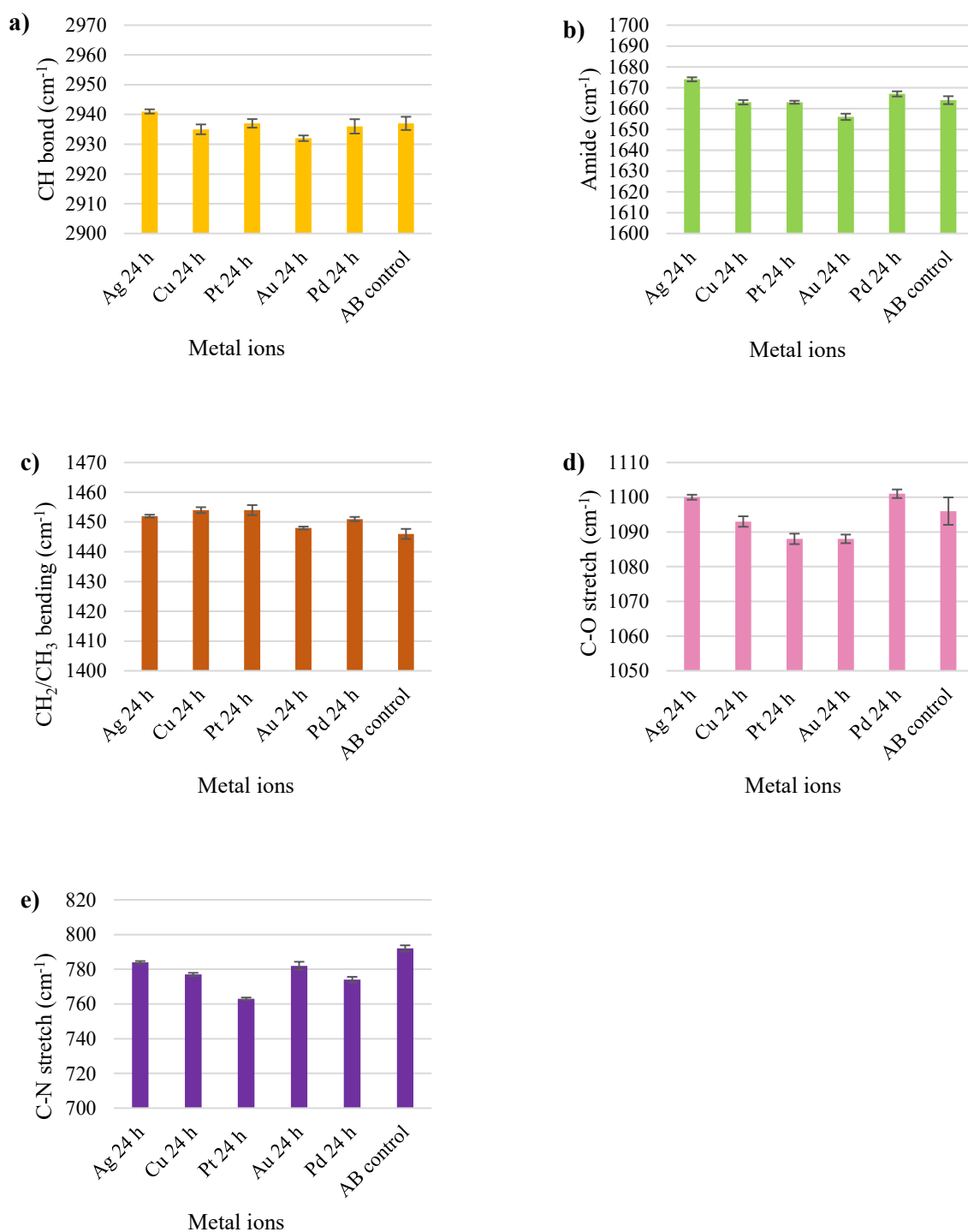
#### *E. faecium*

Against *E. faecium* in the absence of plasma CF, the band shift noted for control were 2936 cm<sup>-1</sup> for CH bond, 1658 cm<sup>-1</sup> for amide, 1450 cm<sup>-1</sup> for CH<sub>2</sub> / CH<sub>3</sub> bending, 1097 cm<sup>-1</sup> for C-O stretch and 787 cm<sup>-1</sup> for C-N stretch. A good chemical effect was demonstrated with Ag ions treated bacterial cells compared to control (amide = 1663 cm<sup>-1</sup>, CH<sub>2</sub> / CH<sub>3</sub> bending = 1454 cm<sup>-1</sup>, and C-N stretch = 798 cm<sup>-1</sup>). The minimal band shift effect was demonstrated on the CH bond (2936 cm<sup>-1</sup>) and amide (1659 cm<sup>-1</sup>) with Cu ions and on the CH<sub>2</sub>/CH<sub>3</sub> bending (1450 cm<sup>-1</sup>) with Au and Pd ions and on the C-N stretch (785 cm<sup>-1</sup>) with Au ions (Figure 3.17, a-e).

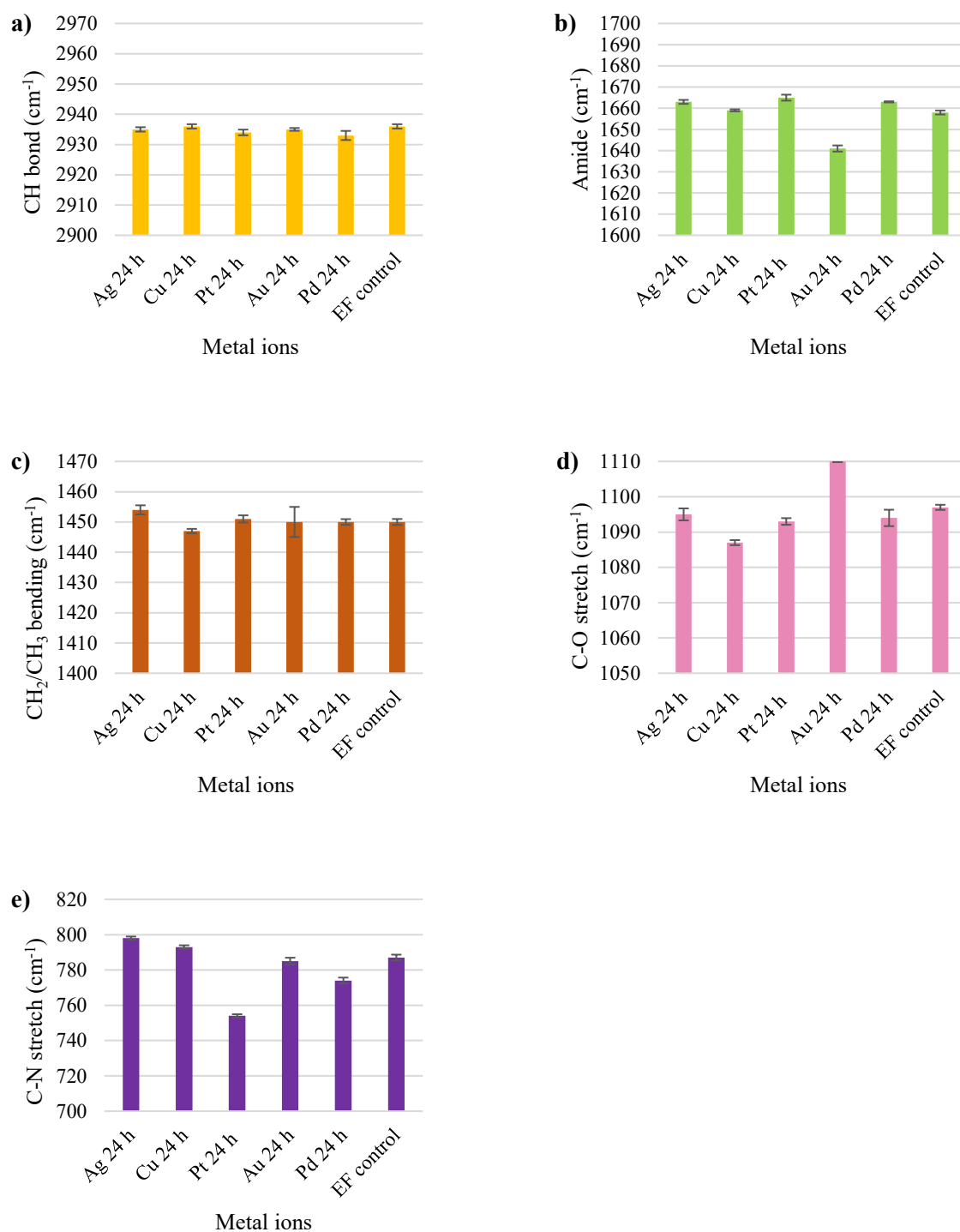
In summary, Raman spectroscopy demonstrated that the metal ions that most affected the molecular vibrations of the bacterial cell wall were Pt ions against *K. pneumoniae* and Ag ions against *A. baumannii* and *E. faecium*, with a weak effect demonstrated following Cu ions incubation against all the tested bacteria.



**Figure 3.15.** Raman spectral bands shifts (cm<sup>-1</sup>) and their tentative band shift assignments for *K. pneumoniae* control and after treatment with Ag, Cu, Pt, Au and Pd ions at 24 h in the absence of 10 % plasma conditioning film; a) CH bond shift, b) Amides shift, c) CH<sub>2</sub> / CH<sub>3</sub> bending shift, d) C-O stretch; e) C-N stretch shift. Ag = silver, Cu = copper, Pt = platinum, Au = gold and Pd = palladium (n = 3).



**Figure 3.16.** Raman spectral bands shifts (cm<sup>-1</sup>) and their band shift tentative assignments for *A. baumannii* control and after treatment with Ag, Cu, Pt, Au and Pd ions at 24 h in the absence of 10 % plasma conditioning film; a) CH bond shift, b) Amides shift, c) CH<sub>2</sub> / CH<sub>3</sub> bending shift, d) C-O stretch; e) C-N stretch shift. Ag = silver, Cu = copper, Pt = platinum, Au = gold and Pd = palladium (n = 3).



**Figure 3.17.** Raman spectral bands shifts (cm<sup>-1</sup>) and their tentative band shift assignments for *E. faecium* control and after Ag, Cu, Pt, Au and Pd ions treatment at 24 h in the absence of 10 % plasma conditioning film; a) CH bond shift, b) Amides shift, c) CH<sub>2</sub> / CH<sub>3</sub> bending shift, d) C-O stretch; e) C-N stretch shift. Ag = silver, Cu = copper, Pt = platinum, Au = gold and Pd = palladium (n = 3).

### **3.4.2. Chemical changes for *Klebsiella pneumoniae*, *A. baumannii* and *E. faecium* after metal ions (Ag, Cu, Pt, Au and Pd) 24 h treatment in the presence of 10 % bovine plasma conditioning film**

The Raman spectral profile attributed to cell biomolecules were CH stretch ( $2920\text{ cm}^{-1}$  -  $2960\text{ cm}^{-1}$ ), proteins (C-N stretch:  $760\text{ cm}^{-1}$  –  $810\text{ cm}^{-1}$ ), lipids ( $\text{CH}_2$  and  $\text{CH}_3$  bending:  $1440\text{ cm}^{-1}$  –  $1470\text{ cm}^{-1}$ ) and amides ( $1620\text{ cm}^{-1}$  -  $1680\text{ cm}^{-1}$ ). The chemical effects on bacteria for metal ions were analysed by comparing with bacterial control.

#### *K. pneumoniae*

Against *K. pneumoniae* in the presence of plasma CF, the band shifts noted for control were  $2943\text{ cm}^{-1}$  for CH bond,  $1677\text{ cm}^{-1}$  for amide,  $1446\text{ cm}^{-1}$  for  $\text{CH}_2 / \text{CH}_3$  bending,  $1095\text{ cm}^{-1}$  for C-O stretch and  $785\text{ cm}^{-1}$  for C-N stretch. The maximum band shifts were demonstrated on the CH bond ( $2932\text{ cm}^{-1}$ ),  $\text{CH}_2$  and  $\text{CH}_3$  bending ( $1454\text{ cm}^{-1}$ ) and C-N stretch ( $776\text{ cm}^{-1}$ ) for bacteria treated with Pd ions. Whilst, Cu ions showed the maximum amide shift ( $1646\text{ cm}^{-1}$ ). Moreover, Pt ions demonstrated a good effect on the CH bond ( $2936\text{ cm}^{-1}$ ), amide ( $1663\text{ cm}^{-1}$ ) and C-N stretch ( $776\text{ cm}^{-1}$ ) band shifts. No change was demonstrated with Cu ions on C-O stretch and with Au ions on C-N stretch band shifts (Figure 3.18, a-e).

#### *A. baumannii*

Against *A. baumannii* in the presence of plasma CF, the band shift noted for control were  $2937\text{ cm}^{-1}$  for CH bond,  $1664\text{ cm}^{-1}$  for amide,  $1446\text{ cm}^{-1}$  for  $\text{CH}_2 / \text{CH}_3$  bending,  $1096\text{ cm}^{-1}$  for C-O stretch and  $792\text{ cm}^{-1}$  for C-N stretch. A strong chemical effect was demonstrated for the Pt ions with band shift of  $2942\text{ cm}^{-1}$  for CH bond,  $1642\text{ cm}^{-1}$  for amide,  $1454\text{ cm}^{-1}$  for  $\text{CH}_2 / \text{CH}_3$  bending,  $1096\text{ cm}^{-1}$  for C-O stretch and  $774\text{ cm}^{-1}$  for C-N stretch compared with the control. A weak effect was demonstrated with Cu ions on the CH bond ( $2931\text{ cm}^{-1}$ ), amide ( $1661\text{ cm}^{-1}$ ) and C-N stretch ( $782\text{ cm}^{-1}$ ), with Pd ions on the  $\text{CH}_2 / \text{CH}_3$  bending ( $1447\text{ cm}^{-1}$ ) and C-O stretch

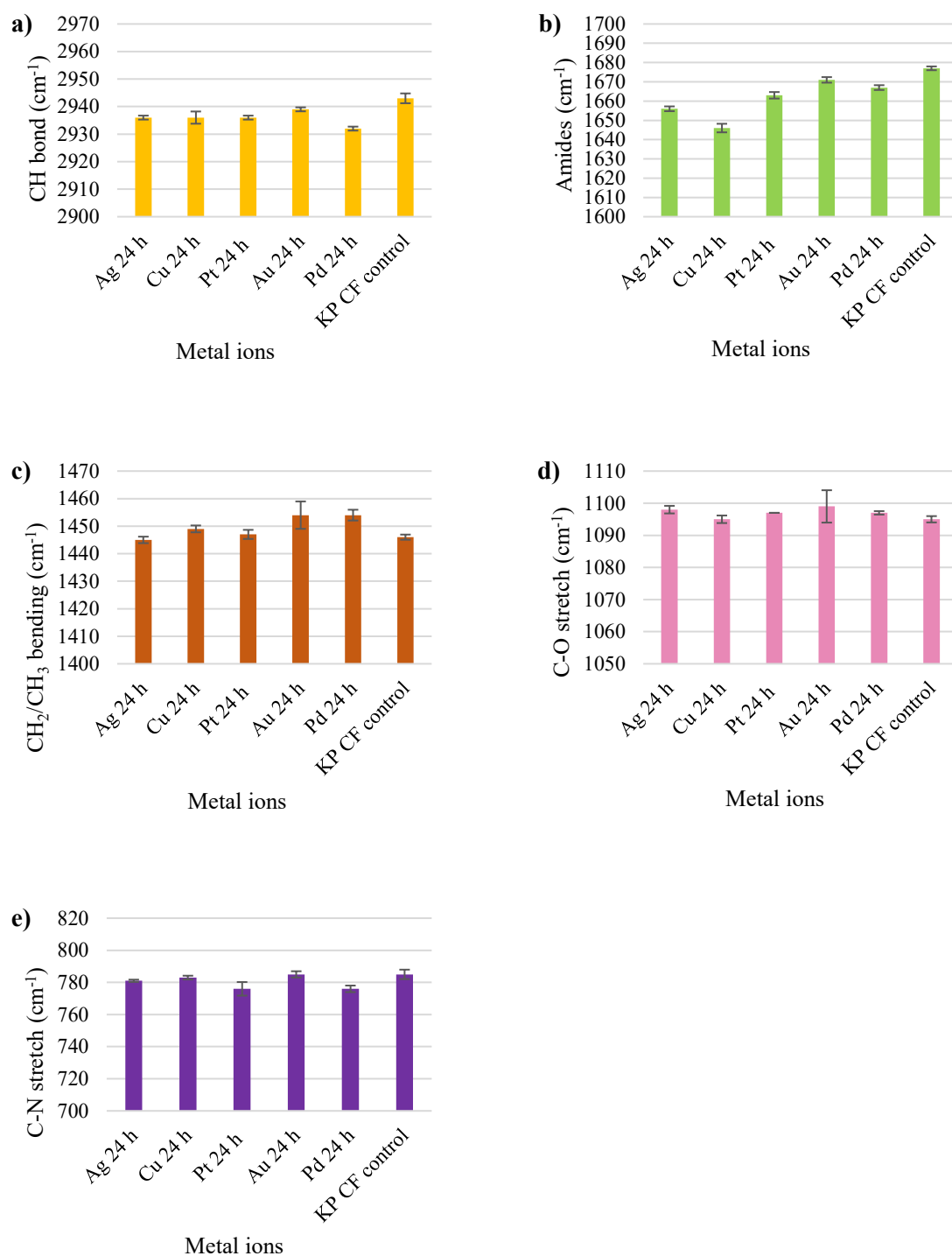
(1098  $\text{cm}^{-1}$ ) and with Ag ions on the C-O stretch (1098  $\text{cm}^{-1}$ ) and C-N stretch (782  $\text{cm}^{-1}$ ) band shift (Figure 3.19, a-e).

#### *E. faecium*

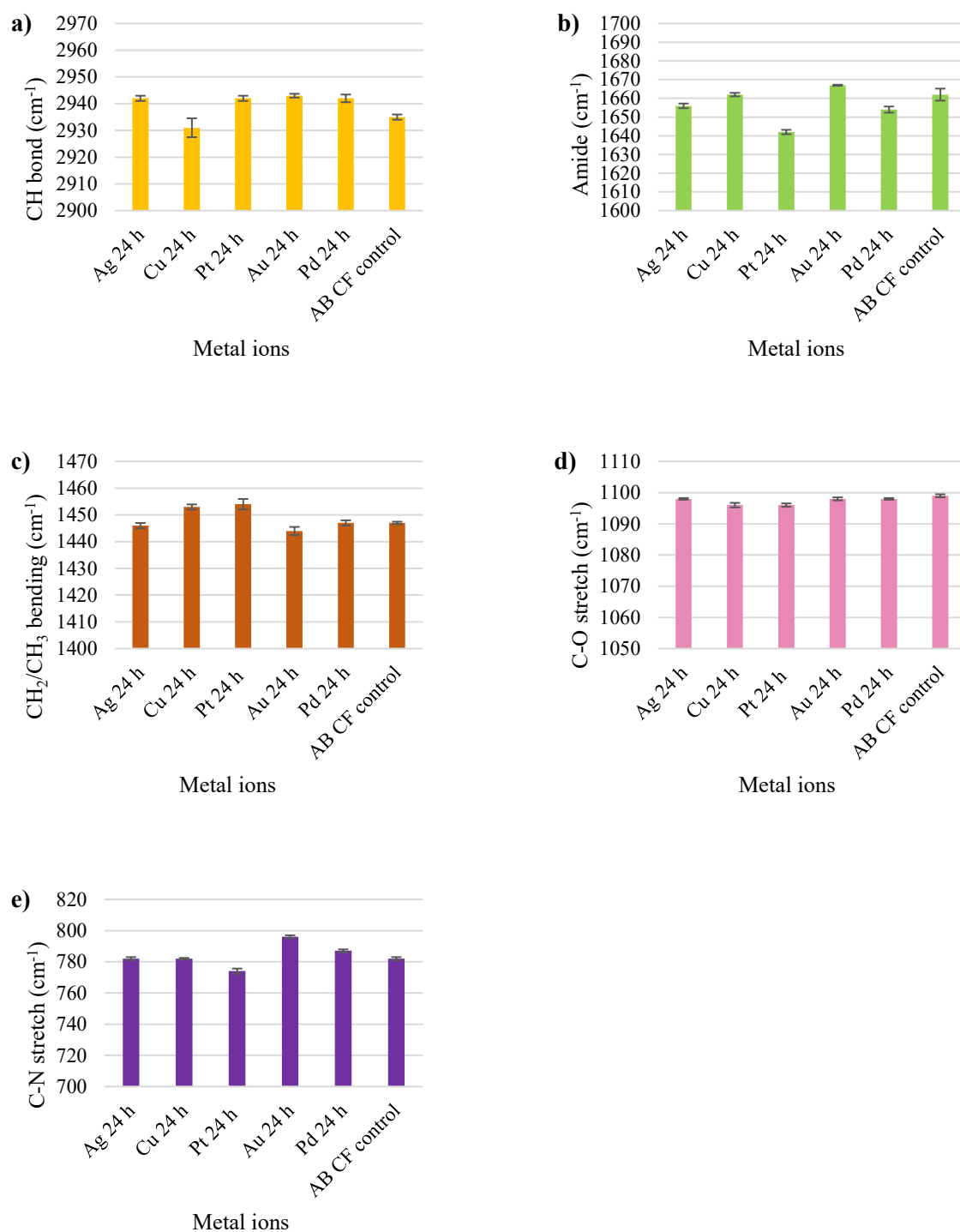
Against *E. faecium* in the presence of plasma CF, the band shift noted for control were 2933  $\text{cm}^{-1}$  for CH bond, 1653  $\text{cm}^{-1}$  for amide, 1452  $\text{cm}^{-1}$  for  $\text{CH}_2 / \text{CH}_3$  bending, 1097  $\text{cm}^{-1}$  for C-O stretch and 783  $\text{cm}^{-1}$  for C-N stretch. The maximum shift on the CH bond (2935  $\text{cm}^{-1}$ ), amide (1614  $\text{cm}^{-1}$ ), C-N stretch (773  $\text{cm}^{-1}$ ) and  $\text{CH}_2 / \text{CH}_3$  bending (1444  $\text{cm}^{-1}$ ) was demonstrated for bacteria treated with Au, Pt, Pd and Ag ions respectively. Whilst, Pd ions on the amide and Cu ions on the  $\text{CH}_2/\text{CH}_3$  bending demonstrated the minimal effects (Figure 3.20, a-e).

In summary, Raman spectroscopy demonstrated that the metal ions that most affected the molecular vibrations of the bacterial cell wall were demonstrated with Pt and Pd ions against *K. pneumoniae* and Pt ions against *A. baumannii* and *E. faecium*. A weak effect was demonstrated with Cu and Au ions against *K. pneumoniae* and Cu ions against *A. baumannii* and *E. faecium*.

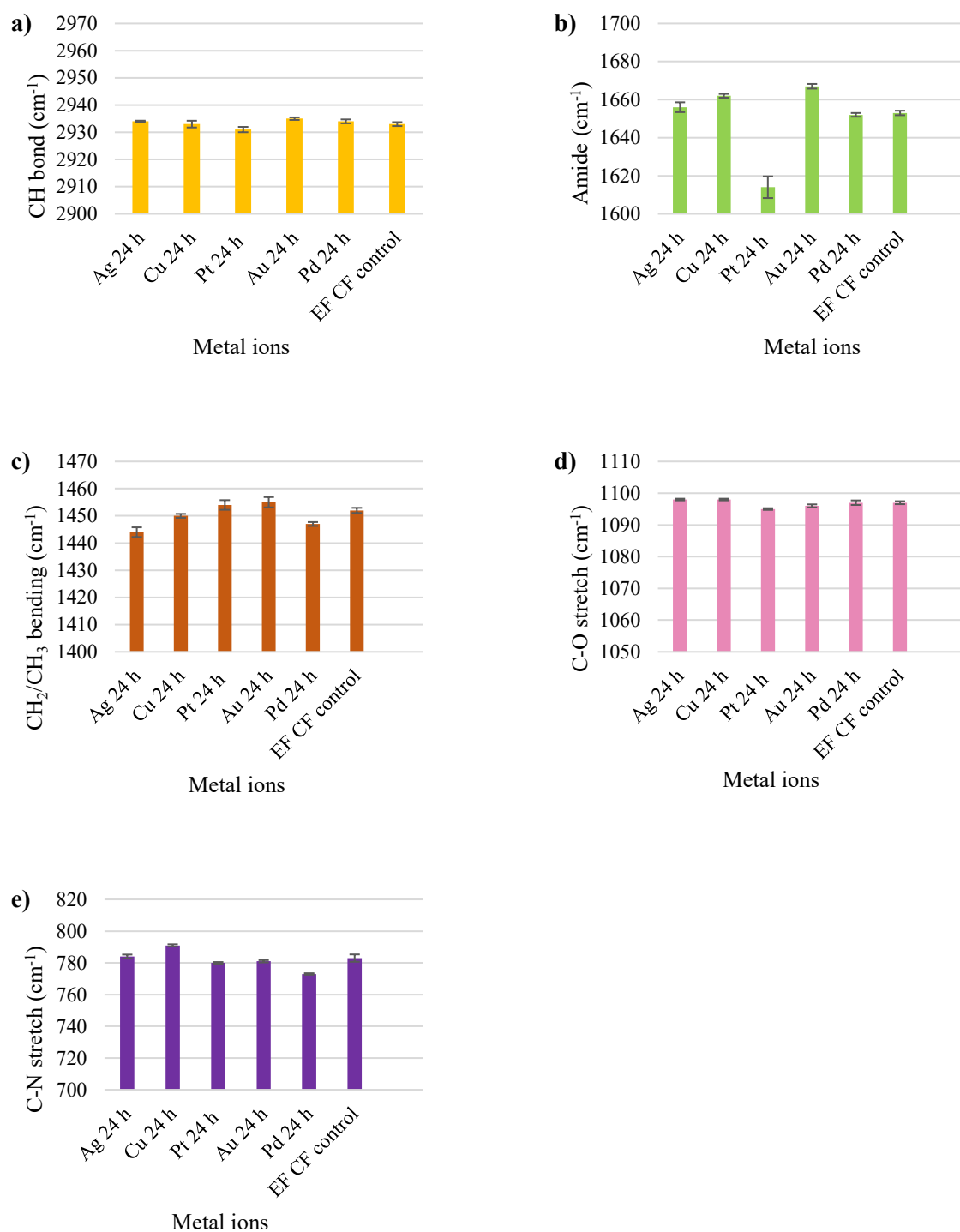




**Figure 3.18.** Raman spectral bands shifts (cm<sup>-1</sup>) and their tentative assignments for *K. pneumoniae* control and after Ag, Cu, Pt, Au and Pd ions treatment at 24 h in the presence of 10 % plasma conditioning film; a) CH bond shift, b) Amides shift, c) CH<sub>2</sub> / CH<sub>3</sub> bending shift, d) C-O stretch; e) C-N stretch shift. Ag = silver, Cu = copper, Pt = platinum, Au = gold and Pd = palladium (n = 3).



**Figure 3.19.** Raman spectral bands shifts (cm<sup>-1</sup>) and their tentative assignments for *A. baumannii* control and after Ag, Cu, Pt, Au and Pd ions treatment at 24 h in the presence of 10 % plasma conditioning film; a) CH bond shift, b) Amides shift, c) CH<sub>2</sub> / CH<sub>3</sub> bending shift, d) C-O stretch; e) C-N stretch shift. Ag = silver, Cu = copper, Pt = platinum, Au = gold and Pd = palladium (n = 3).



**Figure 3.20.** Raman spectral bands shifts (cm<sup>-1</sup>) and their tentative assignments for *E. faecium* control and after Ag, Cu, Pt, Au and Pd ions treatment at 24 h in the presence of 10 % bovine conditioning film; a) CH bond shift, b) Amides shift, c) CH<sub>2</sub> / CH<sub>3</sub> bending shift, d) C-O stretch; e) C-N stretch shift (n = 3). Ag = silver, Cu = copper, Pt = platinum, Au = gold and Pd = palladium (n = 3).

### 3.4. Discussion

#### *Chemical changes in absence of conditioning films*

Following treatment, there were clearly changes in the bacterial cell wall, membrane and cytoplasm observed in the SEM images. The chemical changes that led to these differences in cell morphology was investigated using Raman spectroscopy which measured the vibrational changes of the chemical bonds within the biochemical composition (such as lipids, polysaccharides, nucleic acids and proteins) of the bacterial cells (Armentano et al., 2014). When compared to control, all the tested metal ions demonstrated a reduced shift in the CH stretch and amide against *K. pneumoniae*. Following treatment of the bacteria with either Cu ions and Au ions against *A. baumannii* and Au ions against *E. faecium* a decrease in the CH stretch and amide shifts was demonstrated. Similar to our results, a decrease in the vibrational magnitude was observed in the amide shift corresponding at  $1658\text{ cm}^{-1}$  after ceftazidime, patulin and epigallocatechin gallate 1-3 days bacteria treatment at  $400\text{-}500\text{ }\mu\text{g mL}^{-1}$  (Jung et al., 2014). It has been suggested that the decrease in the amide content corresponded to the denaturation / inhibition of the proteins whilst the decrease in the CH stretch corresponded to the conformational changes in the lipids / polysaccharide / proteins content of the cell wall (Owen et al., 2006; Jung et al., 2014). Both of these induced changes might lead to the destruction of the bacteria. In this thesis, the results found that all the tested metal ions not demonstrate strong vibrational changes in the CH stretch except against *K. pneumoniae*. The reason why this result occurred is unclear as metal ions are known to damage cell wall / membrane and the CH stretch corresponds to aliphatic rings and form a lipid and polysaccharide constitute of bacterial cell wall / membrane. Similar results were obtained were weak to no changes were demonstrated in a signal at  $2932\text{ cm}^{-1}$  vibration after tetracycline treatment against *L. lactis* (Wang et al., 2016).

Other studies that have investigated the effect of antimicrobials on the bacterial cell wall using Raman spectroscopy showed that spectra in the region of  $1100\text{ cm}^{-1} - 900\text{ cm}^{-1}$  corresponded to changes in the bacterial membrane glycosidic linkage (C-O) (Lu et al., 2012). The results in this thesis demonstrated an increase in the C-O band vibration from  $1085\text{ cm}^{-1}$  to  $1110\text{ cm}^{-1}$  after metal ions treatment. Similar results were obtained after gramicidin treatment at  $50\text{ }\mu\text{g mL}^{-1}$  against *S. aureus* (Liou et al., 2015). This suggests that the C-O vibrational change might be due to destruction of bacterial membrane lipid and carbon linkage. Another study proposed that vibrational changes at  $1093\text{ cm}^{-1}$  after diallyl sulphide treatment against *Campylobacter jejuni* might be owing to destruction of phosphodiester bond in the backbone of DNA (Lu et al., 2012). Two studies confirmed vibrational changed peaks at  $1440\text{ cm}^{-1} - 1450\text{ cm}^{-1}$  confirming  $\text{CH}_2$  bend in the lipid and protein based alterations leading to bacteria damage after range of antibiotics treatment including gentamycin, ciprofloxacin and tetracycline against *K. pneumoniae* and *E. coli* (Wang et al., 2016; Premasire et al., 2017). Some of the metal ions treatment resulted in our study with increased vibrational spectral profiles such as Pt ions against *K. pneumoniae* and Ag and Cu ions against *E. faecium* on C-N stretch, Ag ions and Pd ions against *A. baumannii* and Ag ions, Pd ions and Pt ions against *E. faecium* on amide stretch. Likewise, after tetracycline and arsenic treatment the band vibration magnitude were increased at  $1235\text{ cm}^{-1} - 1243\text{ cm}^{-1}$  and  $1680\text{ cm}^{-1}$  respectively against *E. coli* (Cui et al., 2016). The suggested mechanism can be aggregation, accumulation or misfolding of the biomolecules. Such results may be due to the depletion or overlapping of individual monomers of the vital biomolecules after antimicrobial treatment leading to bacterial damage (Tamás et al., 2014). Jung et al. (2014) found that bacterial death could be due to changes in the cellular biomolecules after antimicrobial treatment. This can be observed in the work presented in this thesis from the SEM and Raman results, whereby following incubation of the bacteria by the metal ions demonstrated cell wall / membrane damage and cellular leakage, which corresponds

to the cell death results that were demonstrated in the MIC, MBC and time kill assays. It should be noted that no changes were observed after AuGO treatment on CH<sub>2</sub> / CH<sub>3</sub> bending against *A. baumannii*, Cu ions and Pd ions treatment on C-N stretch against *K. pneumoniae* and Pt ions and Cu ions treatment on CH stretch against *A. baumannii* and *E. faecium* respectively. Thus, further analysis might enhance the understanding of the mechanism of chemical action responsible for bacterial cell death.

### ***Chemical and elemental changes in presence of conditioning films***

The Raman and EDAX results demonstrated that following incubation of the metal ions and GBCs with the bacteria in the presence of plasma conditioning films, chemical and elemental changes were again demonstrated in the cellular structure. In agreement with these results, a study found that the CH stretch shifted to a lower frequency of 2955 cm<sup>-1</sup> to 2835 cm<sup>-1</sup> from 2995 cm<sup>-1</sup> to 2863 cm<sup>-1</sup> after tetracycline treatment on bacterial samples extracted from humans (Trivedi et al., 2015). However, as studies related to testing antimicrobial agents inducing chemical and elemental changes in the presence of organic load by others has not been conducted, it is difficult to compare the data.

### 3.5. Antimicrobial efficacies for ten metal ions in combination against *K. pneumoniae*, *A. baumannii* and *E. faecium*

#### 3.5.1 Zone of inhibition for metal ions combinations in the absence and presence of 10 % bovine plasma conditioning film

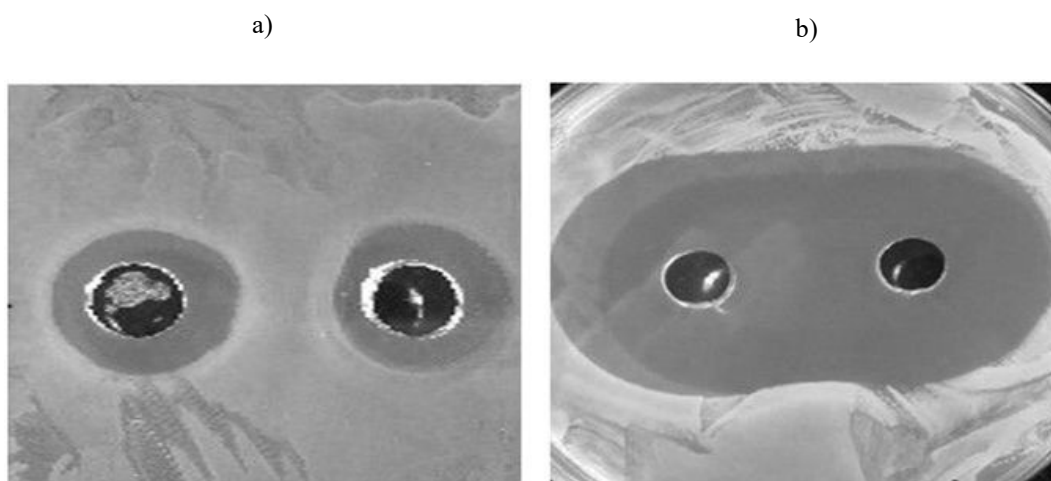
To determine the synergies of the combined metal ions in the presence and absence of 10 % bovine plasma CF, AgCu, AgPt, AgAu, AgPd, CuPt, CuAu, CuPd, AuPt, AuPd and PtPd were tested using the ZoI assay in combination. Gold/platinum, AuPd and PtPd combined ions demonstrated synergy at the 0.5 mgmL<sup>-1</sup> and 1 mgmL<sup>-1</sup> against all the tested bacteria and AgPd, CuAu and CuPd against *K. pneumoniae* showed synergy at 1 mgmL<sup>-1</sup>. The remaining combinations of ions at 1 mgmL<sup>-1</sup> showed additive interactions against *A. baumannii* and *E. faecium*. No inhibition was observed at 0.05 mgmL<sup>-1</sup> of concentration against *E. faecium*. Silver/copper combination demonstrated indifference effects at all the tested concentrations against all the bacteria (Table 3.11). None of the combined ions demonstrated antagonistic interactions.

Overall, the best antimicrobial efficacies of the combined metal ions which displayed synergistic interaction were demonstrated for AuPt, AuPd and PtPd and AgCu. The presence of plasma CF did not demonstrate any effect on the combined metal ions efficacies. *Enterococcus faecium* was found to be the most resistant bacteria.

**Table 3.11.** The ZoI combination assay for interactions type and inhibition grade of combined metal ions against *K. pneumoniae*, *A. baumannii* and *E. faecium* in the absence and presence of 10 % plasma conditioning film. The inhibition zones were graded from 0 to 4, which measured as, 0–4 mm = grade 0, 4–8 mm = grade 1, 8–12 mm = grade 2, 12–16 mm = grade 3 and 16–20 mm = grade 4 (n = 24). To highlight additivity and synergism infections purple and red colour were used respectively.

Combine d ions	Concentr ations (mgmL <sup>-1</sup> )	Type of combination and grade of inhibition		
		<i>K. pneumoniae</i>	<i>A. baumannii</i>	<i>E. faecium</i>
AgCu	0.05	Indifference Grade Cu(0) Ag(1)	Indifference Grade Cu(0) Ag(1)	No inhibition
AgPt	0.05	Indifference Grade Ag(1) Pt(1)	Indifference Grade Ag(1) Pt(1)	No inhibition
AgAu	0.05	Indifference Grade Ag(1) Au(1)	Indifference Grade Ag(1) Au(1)	No inhibition
AgPd	0.05	Indifference Grade Ag(1) Pd(1)	Indifference Grade Ag(1) Pd(1)	No inhibition
CuPt	0.05	Indifference Grade Cu(0) Pt(1)	Indifference Grade Cu(0) Pt(1)	No inhibition
CuAu	0.05	Indifference Grade Cu(0) Au(1)	Indifference Grade Cu(0) Au(1)	No inhibition
CuPd	0.05	Indifference Grade Cu(0) Pd(1)	Indifference Grade Cu(0) Pd(1)	No inhibition
AuPt	0.05	Indifference Grade Au(1) Pt(1)	Indifference Grade Au(1) Pt(1)	No inhibition
AuPd	0.05	Indifference Grade Au(1) Pd(1)	Indifference Grade Au(1) Pd(1)	No inhibition
PtPd	0.05	Indifference Grade Pt(1) Pd(1)	Indifference Grade Pt(1) Pd(1)	No inhibition
AgCu	0.1	Indifference Grade Cu(0) Ag(1)	Indifference Grade Cu(0) Ag(1)	Indifference Grade Cu(0) Ag(1)
AgPt	0.1	Indifference Grade Ag (1) Pt(1)	Indifference Grade Ag (1) Pt(1)	Indifference Grade Ag (1) Pt(1)
AgAu	0.1	Indifference Grade Ag (1) Au(1)	Indifference Grade Ag (1) Au(1)	Indifference Grade Ag (1) Au(1)
AgPd	0.1	Indifference Grade Ag (1) Pd(1)	Indifference Grade Ag (1) Pd(1)	Indifference Grade Ag (1) Pd(1)
CuPt	0.1	Indifference Grade Cu(0) Pt(1)	Indifference Grade Cu(0) Pt(1)	Indifference Grade Cu(0) Pt(1)
CuAu	0.1	Indifference Grade Cu(0) Au(1)	Indifference Grade Cu(0) Au(1)	Indifference Grade Cu(0) Au(1)
CuPd	0.1	Indifference Grade Cu(0) Pd(1)	Indifference Grade Cu(0) Pd(1)	Indifference Grade Cu(0) Pd(1)
AuPt	0.1	Indifference Grade Au(2) Pt(2)	Indifference Grade Au(2) Pt(2)	Indifference Grade Au(1) Pt(1)
AuPd	0.1	Indifference Grade Au(2) Pd(2)	Indifference Grade Au(2) Pd(2)	Indifference Grade Au(1) Pd(1)
PtPd	0.1	Indifference Grade Pt(2) Pd(2)	Indifference Grade Pt(2) Pd(2)	Indifference Grade Pt(1) Pd(1)
AgCu	0.5	Indifference Grade Ag(2) Cu(2)	Indifference Grade Ag(2) Cu(2)	Indifference Grade Ag(1) Cu(1)
AgPt	0.5	Additivity Grade Ag(2) Pt(3)	Indifference Grade Ag(2) Pt(3)	Indifference Grade Ag(1) Pt(2)
AgAu	0.5	Additivity Grade Ag(2) Au(3)	Additivity Grade Ag(2) Au(3)	Indifference Grade Ag(1) Au(2)
AgPd	0.5	Additivity Grade Ag(2) Pd(3)	Additivity Grade Ag(2) Pd(3)	Indifference Grade Ag(1) Pd(2)
CuPt	0.5	Additivity Grade Cu(1) Pt(3)	Additivity Grade Cu(1) Pt(3)	Indifference Grade Cu(1) Pt(2)
CuAu	0.5	Additivity Grade Cu(1) Au(3)	Additivity Grade Cu(1) Au(3)	Indifference Grade Cu(1) Au(2)
CuPd	0.5	Additivity Grade Cu(1) Pd(3)	Additivity Grade Cu(1) Pd(3)	Indifference Grade Cu(1) Pd(2)
AuPt	0.5	Synergy Grade Au(3) Pt(3)	Synergy Grade Au(3) Pt(3)	Additivity Grade Au (2) Pt(2)
AuPd	0.5	Synergy Grade Au(3) Pd(3)	Synergy Grade Au(3) Pd(3)	Additivity Grade Au (2) Au(2)
PtPd	0.5	Synergy Grade Pt(3) Pd(3)	Synergy Grade Pt(3) Pd(3)	Additivity Grade Au (2) Pd(2)
AgCu	1	Indifference Grade Ag(2) Cu(2)	Indifference Grade Ag(2) Cu(2)	Indifference Grade Ag(2) Cu(2)
AgPt	1	Additivity Grade Ag(2) Pt(4)	Additivity Grade Ag(2) Pt(4)	Additivity Grade Ag(2) Pt(3)
AgAu	1	Additivity Grade Ag(2) Au(4)	Additivity Grade Ag(2) Au(4)	Additivity Grade Ag(2) Au(3)
AgPd	1	Synergy Grade Ag(2) Pd(4)	Additivity Grade Ag(2) Pd(4)	Additivity Grade Ag(2) Pd(3)
CuPt	1	Additivity Grade Cu(2) Pt(4)	Additivity Grade Cu(2) Pt(4)	Additivity Grade Cu(1) Pt(3)
CuAu	1	Synergy Grade Cu(2) Au(4)	Additivity Grade Cu(2) Au(4)	Additivity Grade Cu(1) Au(3)
CuPd	1	Synergy Grade Cu(2) Pd(4)	Additivity Grade Cu(2) Pd(4)	Additivity Grade Cu(1) Pd(3)
AuPt	1	Synergy Grade Au(4) Pt(4)	Synergy Grade Au(4) Pt(4)	Synergy Grade Au(3) Pt(3)
AuPd	1	Synergy Grade Au(4) Pd(4)	Synergy Grade Au(4) Pd(4)	Synergy Grade Au(3) Pd(3)
PtPd	1	Synergy Grade Pt(4) Pd(4)	Synergy Grade Pt(4) Pd(4)	Synergy Grade Pt(3) Pd(3)





**Figure 3.21.** Examples of combined metals used in ZoI to demonstrate the interactions. a) Palladium/platinum ions against Gram negative bacteria (indifference interaction) and b) gold/palladium ions against *E. faecium* (synergy interaction).

### **3.5.2 Fractional inhibitory concentration (FIC) for combined metal ions in 2:1, 1:1 and 1:2 ratios**

The FIC was used to determine the synergistic antimicrobial efficacy of the AgCu, AgPt, AgAu, AgPd, CuPt, CuAu, CuPd, AuPt, AuPd and PtPd in the presence and absence of 10 % bovine plasma. The FIC was performed in 2:1, 1:1 and 1:2 ratios of metal ion combinations.

#### **3.5.2.1. FIC against *K. pneumoniae*, *A. baumannii* and *E. faecium* for combined metal ions in the absence of 10 % bovine plasma conditioning film**

##### *K. pneumoniae*

Against *K. pneumoniae* in the absence of CF, AgCu and CuPd combined ions in 1:2 ratio demonstrated an indifferent effect ( $FIC > 1.0 \leq 4.0$ ). The remaining metal ion combinations in the different ratios were found to demonstrate additive effects ( $FIC \text{ index} > 0.5 \text{ and } \leq 1.0$ ) (Table 3.12).

##### *A. baumannii*

Against *A. baumannii*, in the absence of CF, AgCu in all the tested ratios and CuAu in 2:1 produced synergistic antimicrobial effect ( $FIC = \leq 0.5$ ). Copper/platinum were found to demonstrate indifferent antimicrobial effects in all the ratios. The remaining combinations demonstrated additive antimicrobial effects with  $FIC \text{ index} > 0.5 \text{ and } \leq 1.0$  (Table 3.13).

##### *E. faecium*

Against *E. faecium*, in the absence of 10 % CF, AgPd in all the tested ratios, AgAu in 2:1 ratio and Ag in combination with Cu and Pt in 1:2 ratio showed a synergistic effect ( $FIC = \leq 0.5$ ). Gold/palladium in all the three ratios, AgPt in 2:1 and 1:1 ratio, CuPd and AuPt in 1:1 and 1:2 ratios and CuPt in 2:1 ratio showed indifferent antimicrobial effects ( $FIC \text{ index}$

= > 1.0 and  $\leq$  4.0). The remaining combinations demonstrated an additive effect with FIC index > 0.5 and  $\leq$  1.0) (Table 3.14).

### **3.5.2.2. The FIC against *K. pneumoniae*, *A. baumannii* and *E. faecium* for combined metal ions in the presence of 10 % bovine plasma conditioning film**

#### *K. pneumoniae*

Against *K. pneumoniae*, all the combinations were found to demonstrate synergistic antimicrobial efficacy except for CuPd in all the three tested ratios, CuPt in 2:1 and CuAu in a 1:2 ratio. The Cu ions in combination with Pt, Au and Pd ions demonstrated additive effects with FIC index > 0.5 and  $\leq$  1.0 (Table 3.12).

#### *A. baumannii*

Against *A. baumannii*, CuPt in all the tested ratios, Cu in combination with Au and Pd in 2:1 and 1:1 ratio and Pd in combination with Au and Pt in 1:1 ratio demonstrated additivity (FIC index = > 0.5 and  $\leq$  1.0). The remaining tested metal ions combinations demonstrated synergism ( $\leq$  0.5) (Table 3.13).

#### *E. faecium*

Against *E. faecium*, only AgCu in 1:2 ratio demonstrated synergy. Silver/copper, CuPt and CuPd in 1:1 ratio and AgPt, AuPt, AuPd and PtPd in 1:2 ratio demonstrated an additive effect with FIC index > 0.5 and  $\leq$  1.0. The rest of the combinations were found to have indifferent antimicrobial efficacies with FIC index of > 1.0 and  $\leq$  4.0 (Table 3.14).

In summary, in the absence of the plasma CF, the least antimicrobially active combined metal ions against *K. pneumoniae* were AgCu and CuPd, against *A. baumannii* was CuPt and against *E. faecium* was AuPd. The least active combined ions in presence of plasma were CuPd, CuPt and CuAu against *K. pneumoniae* and AgPd, AgAu and CuAu against *E. faecium*. The best efficacies were demonstrated for AgCu (without CF) and Ag combinations

(with CF) against *A. baumannii*, AgPd (without CF) and AgCu (with CF) against *E. faecium* and Ag combinations and AuPt, AuPd and PtPd against *K. pneumoniae*.

Overall, Gram-negative pathogens in the presence of 10 % CF were found to be more sensitive to the metal ions. The different ratios of metal ion combinations affected the antimicrobial interactions/efficacies. No combinations demonstrated an antagonist interaction.

**Table 3.12.** Fractional inhibitory concentration in 2:1, 1:1 and 1:2 ratios in the absence and presence of 10 % plasma conditioning film against *K. pneumoniae* (n = 4).

Synergy = < 0.5, additivity  $0.5 \leq 1.0$ ,  $1.0 \leq 4.0$  indifference and  $> 4.0$  = antagonism > 4.0 (Sueke et al., 2010). Au = gold, Cu = copper, Pt = platinum, Pd = palladium and Ag = silver. Synergistic interaction was highlighted using red colour.

Zol combinations	2:1		1:1		1:2	
	Without CF	With CF	Without CF	With CF	Without CF	With CF
AgCu	0.60 ± 0	0.31 ± 0	0.58 ± 0	0.28 ± 0	1.10 ± 0	0.45 ± 0.04
AgPt	0.83 ± 0.13	0.41 ± 0	0.66 ± 0	0.32 ± 0.05	0.77 ± 0	0.27 ± 0.04
AgAu	0.88 ± 0	0.37 ± 0	0.74 ± 0.12	0.37 ± 0	0.55 ± 0	0.37 ± 0
AgPd	0.66 ± 0.11	0.41 ± 0	0.74 ± 0.12	0.43 ± 0	0.55 ± 0	0.45 ± 0
CuPt	0.99 ± 0	0.58 ± 0	0.93 ± 0.15	0.34 ± 0	0.74 ± 0	0.49 ± 0.08
CuAu	0.77 ± 0	0.49 ± 0	0.68 ± 0.11	0.49 ± 0.12	0.52 ± 0	0.62 ± 0
CuPd	0.77 ± 0	0.58 ± 0	0.91 ± 0	0.60 ± 0.14	1.05 ± 0	0.79 ± 0
AuPt	0.77 ± 0	0.41 ± 0	0.83 ± 0	0.21 ± 0	0.88 ± 0	0.45 ± 0
AuPd	0.66 ± 0	0.41 ± 0	0.66 ± 0	0.43 ± 0	0.66 ± 0	0.45 ± 0
PtPd	0.88 ± 0	0.49 ± 0	0.83 ± 0	0.49 ± 0	0.77 ± 0	0.43 ± 0.05

**Table 3.13.** Fractional inhibitory concentration in 2:1, 1:1 and 1:2 ratios in the absence and presence of 10 % plasma conditioning film against *A. baumannii* (n = 4).

Synergy = < 0.5, additivity  $0.5 \leq 1.0$ ,  $1.0 \leq 4.0$  indifference and  $> 4.0$  = antagonism > 4.0 (Sueke et al., 2010). Au = gold, Cu = copper, Pt = platinum, Pd = palladium and Ag = silver. Synergistic interaction was highlighted using red colour.

ZnI combinations	2:1		1:1		1:2	
	Without CF	With CF	Without CF	With CF	Without CF	With CF
AgCu	0.37 ± 0	0.24 ± 0	0.46 ± 0	0.15 ± 0.02	0.49 ± 0	0.12 ± 0
AgPt	0.66 ± 0.13	0.24 ± 0.04	0.62 ± 0.11	0.37 ± 0	0.58 ± 0.09	0.41 ± 0
AgAu	0.99 ± 0	0.24 ± 0.04	0.74 ± 0	0.37 ± 0	0.99 ± 0	0.41 ± 0
AgPd	0.83 ± 0.11	0.24 ± 0.04	0.74 ± 0	0.37 ± 0	0.66 ± 0	0.41 ± 0
CuPt	1.16 ± 0	0.66 ± 0	1.37 ± 0.19	0.93 ± 0.16	1.58 ± 0.26	0.62 ± 0.10
CuAu	0.49 ± 0	0.66 ± 0	0.62 ± 0	0.93 ± 0.16	0.74 ± 0	0.41 ± 0
CuPd	0.66 ± 0	0.66 ± 0	0.74 ± 0	0.93 ± 0.16	0.83 ± 0	0.41 ± 0
AuPt	0.88 ± 0	0.49 ± 0	0.83 ± 0	0.49 ± 0	0.77 ± 0	0.49 ± 0
AuPd	0.83 ± 0	0.49 ± 0	0.74 ± 0	0.62 ± 0.10	0.66 ± 0	0.49 ± 0
PtPd	0.60 ± 0	0.37 ± 0.06	0.58 ± 0	1.00 ± 0	0.55 ± 0	0.49 ± 0

**Table 3.14.** Fractional inhibitory concentration in 2:1, 1:1 and 1:2 ratios in the absence and presence of 10 % plasma conditioning film against *E. faecium* (n = 4).

Synergy = < 0.5, additivity  $0.5 \leq 1.0$ ,  $1.0 \leq 4.0$  indifference and  $> 4.0$  = antagonism > 4.0 (Sueke et al., 2010). Au = gold, Cu = copper, Pt = platinum, Pd = palladium and Ag = silver. Synergistic interaction was highlighted using red colour.

ZnI combinations	2:1		1:1		1:2	
	Without CF	With CF	Without CF	With CF	Without CF	With CF
AgCu	$0.74 \pm 0$	$1.03 \pm 0.18$	$0.62 \pm 0$	$0.74 \pm 0$	$0.37 \pm 0.06$	$0.49 \pm 0.08$
AgPt	$1.10 \pm 0$	$1.16 \pm 0$	$1.16 \pm 0$	$1.24 \pm 0$	$0.45 \pm 0.07$	$0.99 \pm 0.16$
AgAu	$0.41 \pm 0.06$	$1.32 \pm 0$	$0.58 \pm 0$	$1.49 \pm 0$	$0.60 \pm 0$	$1.24 \pm 0.20$
AgPd	$0.24 \pm 0$	$1.16 \pm 0$	$0.37 \pm 0.06$	$1.24 \pm 0$	$0.49 \pm 0$	$1.33 \pm 0$
CuPt	$1.13 \pm 0.04$	$1.03 \pm 0.17$	$0.79 \pm 0$	$0.99 \pm 0$	$0.97 \pm 0$	$1.16 \pm 0$
CuAu	$0.60 \pm 0$	$1.24 \pm 0.21$	$0.79 \pm 0$	$1.24 \pm 0$	$0.97 \pm 0$	$1.49 \pm 0$
CuPd	$0.99 \pm 0$	$1.03 \pm 0.17$	$1.24 \pm 0$	$0.99 \pm 0$	$1.49 \pm 0$	$1.16 \pm 0$
AuPt	$0.66 \pm 0$	$1.83 \pm 0$	$1.33 \pm 0$	$1.74 \pm 0$	$1.33 \pm 0$	$0.83 \pm 0$
AuPd	$1.21 \pm 0$	$1.83 \pm 0$	$1.16 \pm 0$	$1.74 \pm 0$	$1.10 \pm 0$	$0.83 \pm 0$
PtPd	$0.60 \pm 0$	$1.49 \pm 0$	$0.58 \pm 0$	$1.49 \pm 0$	$0.55 \pm 0$	$0.74 \pm 0$

### **3.5.3. The fractional bactericidal concentration (FBC) for combined metal ions in 2:1, 1:1 and 1:2 ratios**

#### **3.5.3.1. The FBC against *K. pneumoniae*, *A. baumannii* and *E. faecium* for combined metal ions in the absence of 10 % bovine plasma conditioning film**

The FBC was used to determine the synergistic antimicrobial efficacy of the metal ions in combination in the presence and absence of 10 % bovine plasma CF. The FBC was performed in 2:1, 1:1 and 1:2 ratios of metal ion combinations.

##### *K. pneumoniae*

Against *K. pneumoniae* in the absence of CF, all the metal ion combinations demonstrated indifferent effects except CuAu in 2:1 ratio. Only CuAu in 2:1 ratio demonstrated an additive effect with FBC index = 0.99 (Table 3.15).

##### *A. baumannii*

Against *A. baumannii* in the absence of CF, AgCu in 2:1 and 1:2 ratios and AgPd in 1:1 and AgPt in 1:2 ratio produced synergistic antimicrobial effect (FBC =  $\leq 0.5$ ). Copper/platinum in 2:1 and 1:1 ratio, CuAu and CuPd in 2:1 and AgCu in 1:2 ratio was found to demonstrate indifference antimicrobial effects (FBC =  $\geq 1.0$  and  $< 4.0$ ). The remaining combinations demonstrated additive antimicrobial effects with FBC index  $> 0.5$  and  $\leq 1.0$  (Table 3.16).

##### *E. faecium*

Against *E. faecium*, in the absence of 10 % CF, AgCu in all the ratios and AgPt in 1:1 ratio demonstrated a synergistic effect with FBC index =  $\leq 0.5$ . Gold in combination with Pt and Pd in all ratios, PtPd in 2:1 and 1:2 ratio and AgPt and Cu in combination with Pt, Au and Pd in 2:1 ratio demonstrated additive antimicrobial interactions FBC =  $> 0.5$  and  $\leq 1.0$ . The remaining combinations were found with indifferent antimicrobial effects FBC =  $> 1.0$  and  $\leq 4.0$  (Table 3.17).



### **3.5.3.1. The FBC against *K. pneumoniae*, *A. baumannii* and *E. faecium* for combined metal ions in the presence of 10 % bovine plasma conditioning film**

#### *K. pneumoniae*

Against *K. pneumoniae*, AgCu, AuPt, AuPd and PtPd in all the three tested ratio and Ag in combination with Pt, Au and Pd in 2:1 and 1:2 ratio demonstrated a synergistic effect. The remaining metal ion combinations demonstrated an additive antimicrobial effect (FBC =  $> 0.5$  and  $\leq 1.0$ ) (Table 3.15).

#### *A. baumannii*

Against *A. baumannii*, all the silver combinations in the tested three ratios except AgPd in the 1:2 ratio demonstrated synergistic antimicrobial efficacies (FBC index =  $\leq 0.5$ ). The remaining combinations except CuPd in 1:2 ratio demonstrated an additive antimicrobial effect with FBC index =  $> 0.5$  and  $\leq 1.0$  (Table 3.16).

#### *E. faecium*

Against *E. faecium*, only AgCu in 1:2 ratio demonstrated a synergistic antimicrobial efficacy with  $\leq 0.5$  FBC index. Silver/copper in 2:1 and 1:1, AuPt, AuPd and PtPd in 1:1 and 1:2, Ag in combination with Pt, Au and Pd demonstrated an additive antimicrobial effect with FBC index =  $> 0.5$  and  $\leq 1.0$ . The remaining combinations were found to produce an indifferent antimicrobial interaction FBC index  $> 1.0$  and  $\leq 4.0$  (Table 3.17).

Overall, in the absence of 10 % plasma CF, CuAu against *K. pneumoniae* and AgCu against *A. baumannii* and *E. faecium* demonstrated the best efficacies. Whilst in the presence of 10 % plasma CF, AgCu against all the tested pathogens and AuPt, AuPd and PtPd against *K. pneumoniae* and AgPt and AgAu against *A. baumannii* demonstrated the best antimicrobial efficacies.

Overall, *Enterococcus faecium* was found to be a resistant species out of the three tested microbes. The different ratios of metal combinations demonstrated that metal ions in combination affected the antimicrobial interactions/efficacies. No combinations demonstrated an antagonist interaction.

**Table 3.15.** Fractional bactericidal concentration in 2:1, 1:1 and 1:2 ratios in the absence and presence of 10 % plasma conditioning film against *K. pneumoniae* (n = 4).

Synergy =  $< 0.5$ , additivity  $> 0.5 \leq 1.0$ ,  $> 1.0 \leq 4.0$  indifference and  $> 4.0$  = antagonism  $> 4.0$  (Sueke et al., 2010). Au = gold, Cu = copper, Pt = platinum, Pd = palladium and Ag = silver. Synergistic interaction was highlighted using red colour.

ZoI combinations	2:1		1:1		1:2	
	Without CF	With CF	Without CF	With CF	Without CF	With CF
AgCu	$1.12 \pm 0$	$0.33 \pm 0$	$1.16 \pm 0$	$0.53 \pm 0.04$	$1.10 \pm 0$	$0.29 \pm 0$
AgPt	$1.10 \pm 0$	$0.41 \pm 0$	$2.00 \pm 0.33$	$0.78 \pm 0.04$	$1.55 \pm 0$	$0.45 \pm 0$
AgAu	$1.10 \pm 0$	$0.41 \pm 0$	$1.33 \pm 0$	$0.78 \pm 0.04$	$1.55 \pm 0$	$0.45 \pm 0$
AgPd	$1.10 \pm 0$	$0.41 \pm 0$	$1.33 \pm 0$	$0.78 \pm 0.04$	$2.33 \pm 0.38$	$0.45 \pm 0$
CuPt	$1.99 \pm 0$	$0.66 \pm 0$	$1.87 \pm 0.31$	$0.74 \pm 0$	$1.49 \pm 0$	$0.83 \pm 0$
CuAu	$0.99 \pm 0$	$0.66 \pm 0$	$1.24 \pm 0$	$0.74 \pm 0$	$2.24 \pm 0.37$	$0.83 \pm 0$
CuPd	$1.99 \pm 0$	$0.66 \pm 0$	$2.50 \pm 0$	$0.74 \pm 0$	$2.99 \pm 0$	$0.83 \pm 0$
AuPt	$1.99 \pm 0$	$0.49 \pm 0$	$2.00 \pm 0$	$0.49 \pm 0$	$1.99 \pm 0$	$0.49 \pm 0$
AuPd	$1.99 \pm 0$	$0.49 \pm 0$	$2.00 \pm 0$	$0.49 \pm 0$	$1.99 \pm 0$	$0.49 \pm 0$
PtPd	$2.99 \pm 0.49$	$0.49 \pm 0$	$3.00 \pm 0.50$	$0.49 \pm 0$	$2.99 \pm 0.49$	$0.49 \pm 0$

**Table 3.16.** Fractional bactericidal concentration in 2:1, 1:1 and 1:2 ratios in the absence and presence of 10 % plasma conditioning film against *A. baumannii* (n = 4).

Synergy = < 0.5, additivity  $0.5 \leq 1.0$ ,  $1.0 \leq 4.0$  indifference and  $> 4.0$  = antagonism  $> 4.0$  (Sueke et al., 2010). Au = gold, Cu = copper, Pt = platinum, Pd = palladium and Ag = silver. Synergistic interaction was highlighted using red colour.

ZoI combinations	2:1		1:1		1:2	
	Without CF	With CF	Without CF	With CF	Without CF	With CF
AgCu	0.31 ± 0.05	0.21 ± 0.02	1.20 ± 0	0.21 ± 0.02	0.33 ± 0	0.15 ± 0.02
AgPt	0.74 ± 0.12	0.36 ± 0	0.99 ± 0	0.42 ± 0	0.49 ± 0	0.48 ± 0
AgAu	0.55 ± 0	0.33 ± 0	0.58 ± 0	0.37 ± 0	0.60 ± 0	0.41 ± 0
AgPd	0.99 ± 0	0.41 ± 0	0.49 ± 0	0.49 ± 0	0.99 ± 0	0.58 ± 0
CuPt	1.32 ± 0	0.63 ± 0.07	1.50 ± 0	0.74 ± 0.09	1.66 ± 0	0.96 ± 0
CuAu	1.16 ± 0.19	0.58 ± 0.07	0.91 ± 0	0.65 ± 0.08	1.05 ± 0	0.83 ± 0
CuPd	1.32 ± 0	0.72 ± 0.09	0.74 ± 0	0.87 ± 0.1	0.83 ± 0	1.16 ± 0
AuPt	0.99 ± 0	0.53 ± 0	0.99 ± 0	0.54 ± 0	0.99 ± 0	0.56 ± 0
AuPd	0.99 ± 0	0.58 ± 0	0.99 ± 0	0.62 ± 0	0.74 ± 0.12	0.66 ± 0
PtPd	0.74 ± 0.12	0.64 ± 0	0.74 ± 0.24	0.67 ± 0	0.99 ± 0	0.69 ± 0

**Table 3.17.** Fractional bactericidal concentration in 2:1, 1:1 and 1:2 ratios in the absence and presence of 10 % plasma conditioning film against *E. faecium* (n = 4).

Synergy =  $< 0.5$ , additivity  $> 0.5 \leq 1.0$ ,  $> 1.0 \leq 4.0$  indifference and  $> 4.0$  = antagonism  $> 4.0$  (Sueke et al., 2010). Au = gold, Cu = copper, Pt = platinum, Pd = palladium and Ag = silver. Synergistic interaction was highlighted using red colour.

ZoI combinations	2:1		1:1		1:2	
	Without CF	With CF	Without CF	With CF	Without CF	With CF
AgCu	0.20 ± 0	0.99 ± 0	0.09 ± 0	0.78 ± 0.09	0.08 ± 0	0.49 ± 0
AgPt	0.66 ± 0	1.46 ± 0	0.37 ± 0	1.39 ± 0.17	1.66 ± 0	0.73 ± 0
AgAu	1.99 ± 0.33	1.46 ± 0	1.50 ± 0	1.39 ± 0.17	1.66 ± 0	0.73 ± 0
AgPd	1.32 ± 0	1.46 ± 0	1.50 ± 0	1.39 ± 0.17	1.66 ± 0	0.73 ± 0
CuPt	0.99 ± 0	1.06 ± 0	1.25 ± 0	1.13 ± 0.14	2.24 ± 0.37	1.06 ± 0
CuAu	0.99 ± 0	1.06 ± 0	1.25 ± 0	1.13 ± 0.14	1.49 ± 0	1.06 ± 0
CuPd	0.75 ± 0.12	1.06 ± 0	1.25 ± 0	1.13 ± 0.14	1.49 ± 0	1.06 ± 0
AuPt	1.00 ± 0	1.99 ± 0	0.99 ± 0	0.99 ± 0	0.99 ± 0	0.99 ± 0
AuPd	1.00 ± 0	1.99 ± 0	0.99 ± 0	0.99 ± 0	0.74 ± 0.12	0.99 ± 0
PtPd	1.00 ± 0	1.99 ± 0	1.49 ± 0.25	0.99 ± 0	0.74 ± 0.12	0.99 ± 0

### 3.5. Discussion

#### *Combined metal ions antimicrobial efficacies*

Following this study, the ZoI combination, FIC and FBC results demonstrated that none of the combinations of metal ions showed antagonistic interactions. Though Cu ions were found to be a weak antimicrobial when tested individually, AgCu combined ions were found to display synergism in most of the tested ratios in the FIC and FBC test against *A. baumannii* and *E. faecium*. Moreover, CuAu against *A. baumannii* demonstrated synergism in the FIC test. In agreement with our results, a synergistic effect was demonstrated for Ag and Cu combined ions that inactivated (99.99 %) water contaminated with pathogens including *A. baumannii* within 6 hours in a batch disinfection test (Huang et al., 2008). In agreement with our work, it has been shown that when Cu and Ag transition metals were combined, the MIC were reduced to 0.5 and 0.25 respectively with demonstration of > 80 % of *E. coli* and *B. subtilis* inhibition for AgCu combination (Garza-Cervantes et al., 2017). This combined mode of action may be due to Cu acting as iron (Fe) homolog and replacing essential micronutrient Fe uptake (Lemire et al., 2013; Zenzen et al., 2018). Thus, this might increase diffusion of the combined antimicrobial into the bacterial cell membrane through efflux pumps (Lemire et al., 2013). Inside the bacteria Ag, Cu and Au ions attack vital cellular activities leading to cell lysis (Hoiby et al., 2010; Lemire et al., 2013). According to a study by Ahmad et al. (2014), Ag ions significantly enhanced the antimicrobial action of *Mentha piperita* essential oil by producing a synergistic interaction. The mean ZoI for *Mentha piperita* against *E. coli* (12 mm) and *S. aureus* (17 mm) was demonstrated, which increased to 21 mm for the Ag and *Mentha piperita* combination. Another study has shown that the addition of Au ions in combination with Ag nanoparticles decreased their overall negative charge. This might explain a mechanism of action that would lead to a greater adherence of metal cation particles to the bacterial surface

through the electrostatic interactions, thus increasing their antimicrobial effects (Wang et al., 2016).

### ***Conditioning film effect on combined metal ions antimicrobial activity***

Interestingly, in the presence of 10 % bovine plasma, the combined ions demonstrated an elevated antimicrobial efficacy, whilst the single metal ions did not, suggesting an adjuvant effect.

### ***Chemistry between plasma proteins and metal ions***

The enhanced antimicrobial efficacy demonstrated in presence of plasma proteins may be due to one or a combined mechanism of action categorised as i) the affinity of the metal ions to bind to the plasma proteins, ii) redox reactions, iii) electrostatic reactions, iv) charge of metal and plasma proteins, v) co-ordination complex formation and vi) interaction with bacterial cell (Sotogaku et al., 1999; Corbin et al., 2008; Zeitlinger et al., 2011). A two-way redox reaction might occur, where positively charged metal ions show strong affinity towards negatively charged proteins present in the plasma (Zeitlinger et al., 2011). This affinity between metal ion and protein can make them bind reversibly or irreversibly (Jackson and Byrne, 1996). The exchange of ions occurring through redox reaction is dependent on oxidation state of both the components (Zanzen et al., 2013; Dudev and Lim, 2014). According to a study by Dudev and Lim, (2014), the net charge of protein plays a vital role in the electrostatic reactions with metal ions. Proteins with a high negative charge surface potentially attract more cations and thus increases binding (Sotogaku et al., 1999). However, the formation of co-ordination protein metal complexes is a multifaceted process where only a metal ion with specific oxidation charge can show binding properties to precise plasma proteins surface site (Sotogaku et al., 1999; Dudev and Lim, 2014). For example, metal ions such as  $\text{Cu}^{+2}$ ,  $\text{Mn}^{+2}$  and  $\text{Ni}^{+2}$  bind to N-terminal site of albumin through peptide bond and forms a stable planner co-ordinate complex,

whilst, metals  $\text{Zn}^{+1}$  or  $\text{Zn}^{+2}$  cannot displace the amide group of albumin and hence cannot form complexes (Bal et al., 2013; Slavin et al., 2017).

*Metal-plasma protein complex antimicrobial efficacies on bacteria*

Once metal ions form a complex with proteins, different modes of action may occur. For example, before metal ions attach to the oppositely charge bacterial membrane components, bacteria might absorb the proteins components (Hulander et al., 2009). This bacterial and metal-plasma protein complex attachment might generate electrochemical potential difference between metal ions in the complex (Hulander et al., 2009; Garza-Cervantes, 2017), thus resulting in an enhanced antimicrobial effect. It has also been suggested that the electrochemical potential difference between Ag ions and aluminium oxide salts generate reactive oxygen ions (Slavin et al., 2017). Another study suggested that the presence of reactive oxygen reacts with water (in our case present in proteins of bovine plasma), which releases additional free oxygen radicals into the milieu (Kittler et al., 2010; Yang et al., 2017). This free oxygen radical ultimately lead to ROS generation (Slavin et al., 2017). Thus, the damage cause to the bacterial has been proposed to originate with ROS release and oxidative damage, owing to bacteria attachment to the protein-metal complex. This may occur before the metal ions target the bacteria (Graza-Cervantes, 2017; Yang et al., 2017). Metals ions then later act on the bacterial cell-membrane and internalise within the bacteria, disrupting one or another vital cellular process (Lemire et al., 2013). This binding process between the metal-plasma protein complex and the bacterial surfaces may increase the combined ions antimicrobial efficacies. Contrasting data was reported in a study by Gnanadhas et al. (2013) where the best efficacy for PVP-AgNPs was found following the least interaction with BSA proteins. However, other molecules that bound to a BSA conditioning film, for example cit-AgNPs and uncapped AgNPs were found to be less antimicrobially active (Gnanadhas et al., 2013). Another mechanism might be that the plasma proteins undergo conformational changes whilst forming a complex



with the metal (Dudev and Lim, 2014). This might alter the protein present in plasma surfaces epitopes, which could alter (and may enhance or decrease) bacterial attachment with the bounded metal ions (Hulander et al., 2009).

The binding affinity and electrostatic bond between metals and plasma proteins is influenced by other parameters such as pH, ionic radius of metal, temperature and competition between the metal valence ions (Sotogaku et al., 1999; Dudev and Lim., 2014). Thus, further investigations might aid in better understanding of the antimicrobial mechanistic activity. However, as most of the metal ions demonstrated synergistic in the presence of plasma proteins, such combinations may possess the potential to be used as biocides also *in vivo* like conditions.

Thus, the action of these different metal ions against a range of different bacterial species requires further in-depth elucidation to determine their exact modes of action (Lemire et al., 2013). Moreover, as metal form and antimicrobial efficacies are co-related, testing individual metal in different forms against range of bacteria might give in-depth knowledge about efficacies.

### **3.6. Crystal violet biofilm assay to test antimicrobial efficacies for five single metal ions and ten combined metal ions against *K. pneumoniae*, *A. baumannii* and *E. faecium* in the presence and absence of 10 % plasma conditioning film**

#### **3.6.1. Antibiofilm assay for five single metal ions against *K. pneumoniae*, *A. baumannii* and *E. faecium* in the presence and absence of 10 % bovine plasma conditioning film**

The antibiofilm efficacy of five metal ions was evaluated by comparing the growth by measuring the absorbance of treated bacterial biofilms with the respective negative controls after 24 h.

##### *K. pneumoniae*

Against *K. pneumoniae* in the absence of plasma CF, Au and Pd ions at 0.5 mgmL<sup>-1</sup> demonstrated no viable bacterial biofilm density (OD = 0). In the presence of plasma CF, Pt, Au and Pd ions demonstrated no viable bacterial biofilm growth (OD = 0). Interestingly, Pt and Au ions demonstrated a slightly greater viable bacterial biofilm growth at 0.25 mgmL<sup>-1</sup> (0.03 and 0.05 respectively) than at 0.1 mgmL<sup>-1</sup> (0.02 and 0.04 respectively). Silver (0.02, 0.03, 0.04, 0.07) and Cu (0.01, 0.02, 0.05, 0.06) ions demonstrated an increase in antibiofilm efficacy with an increase in ion concentration in the presence or absence of plasma.

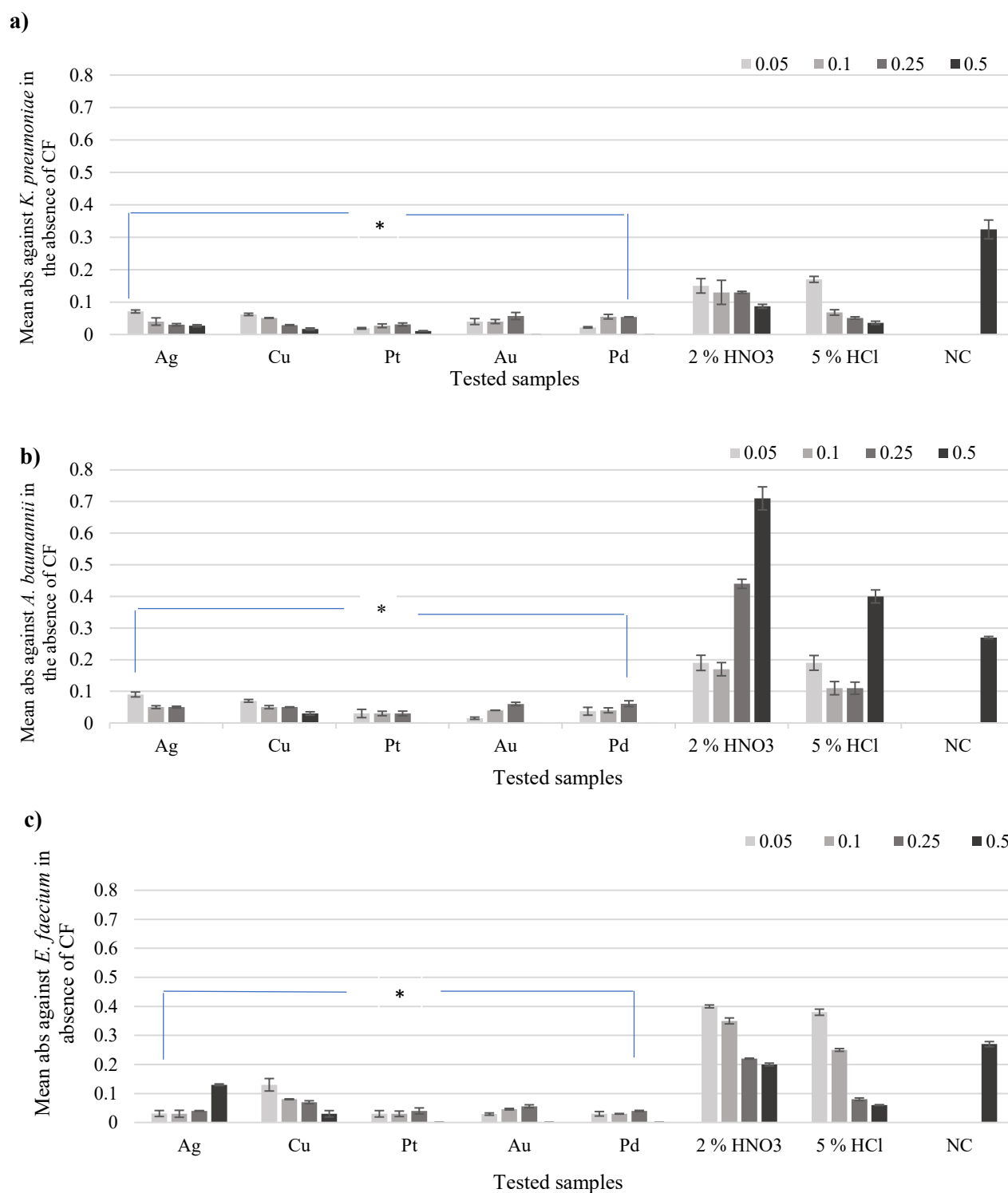
##### *A. baumannii*

Against *A. baumannii* in the absence or presence of plasma, Ag, Pt, Au and Pd ions demonstrated 100 % bacterial biofilm inhibition (OD = 0) at 0.5 mgmL<sup>-1</sup>. In the absence of CF, Au and Pd ions demonstrated a slightly greater viable bacterial biofilm growth at 0.25 mgmL<sup>-1</sup> (0.06 and 0.06 respectively) than at 0.1 mgmL<sup>-1</sup> (0.04). Silver (0, 0.05, 0.05, 0.09), Cu (0.03, 0.05, 0.05, 0.07) and Pt (0, 0.03, 0.03, 0.03) ions in absence of plasma CF and all tested metal ions in presence of plasma CF demonstrated an increase in antibiofilm efficacy with concentrations increase.

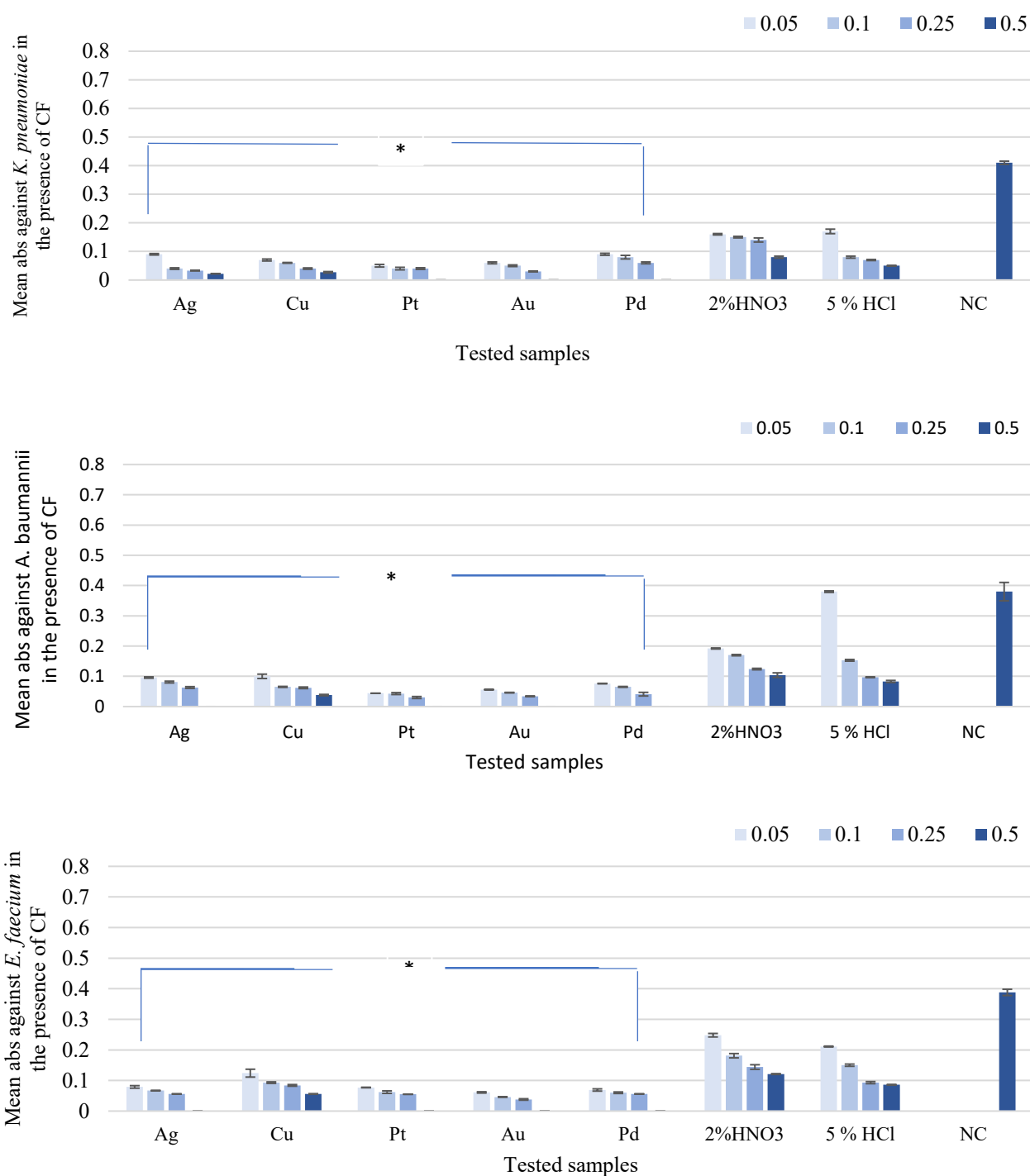
### *E. faecium*

Against *E. faecium*, in the absence or presence of plasma, Pt, Au and Pd ions demonstrated 100 % bacterial biofilm inhibition ( $OD = 0$ ) at  $0.5 \text{ mgmL}^{-1}$ . It should be noted that Ag ions demonstrated a higher viable biofilm growth ( $OD = > 0.1$ ) in absence of CF, however demonstrated 100 % biofilm inhibition in the presence of plasma CF. In absence of plasma, the Pt (0.04), Au (0.05) and Pd (0.04) ions tested at  $0.25 \text{ mgmL}^{-1}$  demonstrated a greater biofilm growth than when tested at lower concentrations ( $0.05 \text{ mgmL}^{-1}$  (0.03, 0.04, 0.03 respectively) and  $0.1 \text{ mgmL}^{-1}$  (0.03, 0.02, 0.03 respectively)).

Overall, against *K. pneumoniae* Au and Pd ions (without plasma CF) and Pt, Au and Pd ions (with plasma CF), against *A. baumannii* Ag, Pt, Au and Pd ions in both the conditions and against *E. faecium* Pt, Au and Pd ions (without plasma) and Ag, Pt, Au and Pd ions (with plasma) demonstrated the best antibiofilm efficacies. Copper ions demonstrated the least antibiofilm efficacies in all the tested conditions.



**Figure 3.22.** Biofilm absorbance after Ag, Cu, Pt, Au and Pd ions treatment against a) *K. pneumoniae*, b) *A. baumannii* and c) *E. faecium* in the absence of 10 % plasma conditioning film. All the metal ions demonstrated a statistical significance compared to negative control ( $p < 0.001$ ). Ag = silver, Cu = copper, Pt = platinum, Au = gold and Pd = palladium ( $n = 3$ ).



**Figure 3.23.** Biofilm absorbance after Ag, Cu, Pt, Au and Pd ions treatment against a) *K. pneumoniae*, b) *A. baumannii* and c) *E. faecium* in the presence of 10 % plasma conditioning film. All the metal ions demonstrated a statistical significance compared to negative control ( $p < 0.001$ ). Ag = silver, Cu = copper, Pt = platinum, Au = gold and Pd = palladium (n = 3).

### **3.6.2. Antibiofilm assay for ten combined ions against *K. pneumoniae*, *A. baumannii* and *E. faecium* in the absence of 10 % bovine plasma conditioning films**

The antibiofilm efficacy of AgCu, AgPt, AgAu, AgPd, CuPt, CuAu, CuPd, AuPt, AuPd and PtPd (2:1, 1:1 and 1:2 ratios) were evaluated using CVBA. The efficacies were analysed by comparing the growth absorbance of treated bacterial biofilms with respective negative controls after 24 h. It should be noted that all the tested metal ions demonstrated a lower absorbance than the respective acid controls.

#### *K. pneumoniae*

Against *K. pneumoniae*, AuPt, AuPd and PtPd combined ions demonstrated no biofilm growth at 0.5 mgmL<sup>-1</sup> at all the tested ratios ( $p < 0.001$ ). Copper/platinum in all the three ratios at 0.05 mgmL<sup>-1</sup> (0.29) and 0.1 mgmL<sup>-1</sup> (0.24) demonstrated the highest bacterial biofilm growth. (Figure 3.24, a-c).

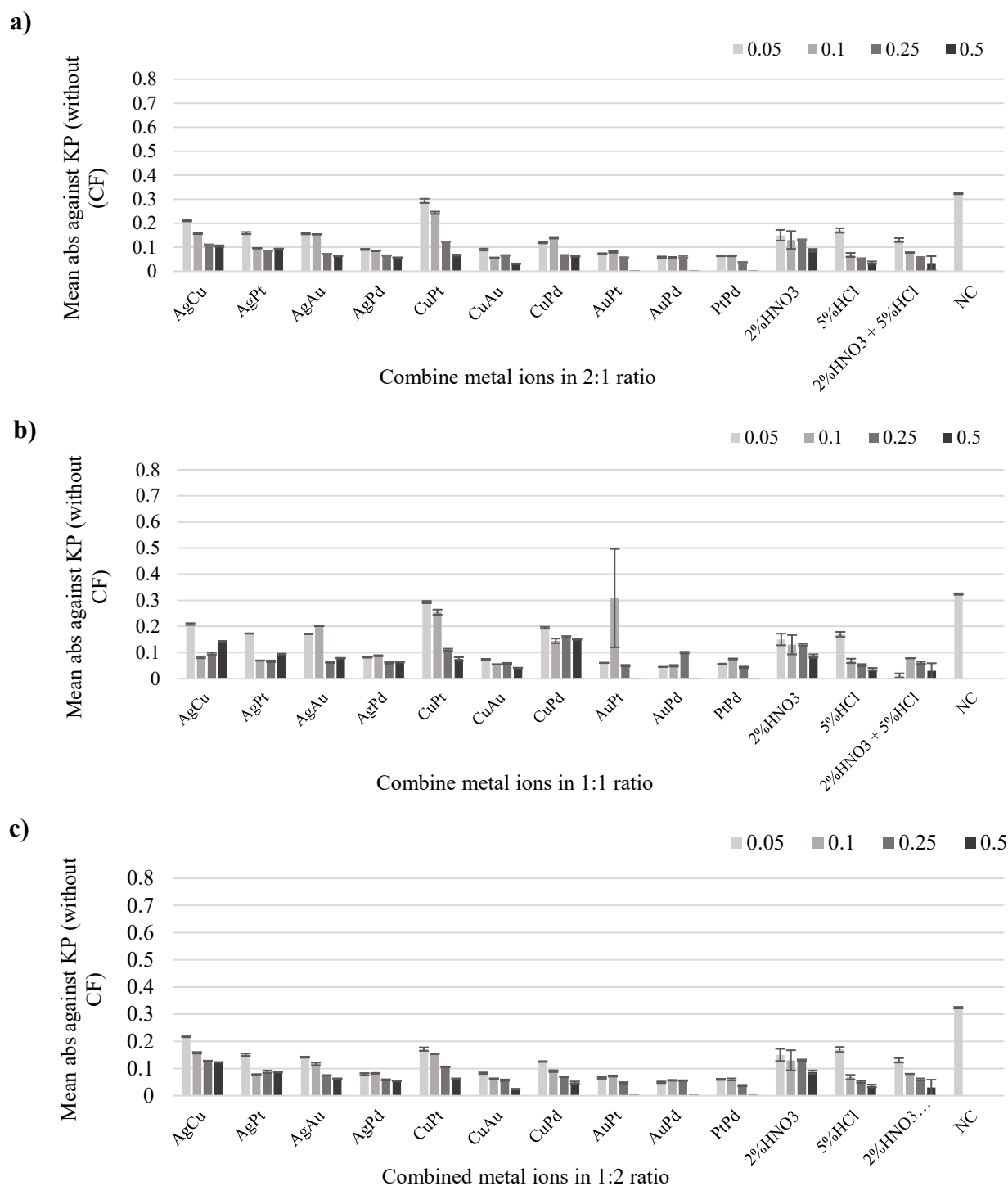
#### *A. baumannii*

Against *A. baumannii*, AuPt, AuPd and PtPd combined ions showed 100 % inhibition with OD = 0 ( $p < 0.001$ ). Combined ions of AgPt, CuPt and CuPd demonstrated the lowest antibiofilm activity (OD = 0.1 – 0.5). Silver/platinum ions (0.05) displayed a greater viable bacterial biofilm grow that 0.05 mgmL<sup>-1</sup> than negative control (0.4). The combined ions were the least effective overall in controlling biofilm growth in a 1:1 ratio compared to the 2:1 and 1:2 ratios (Figure 3.25, a-c).

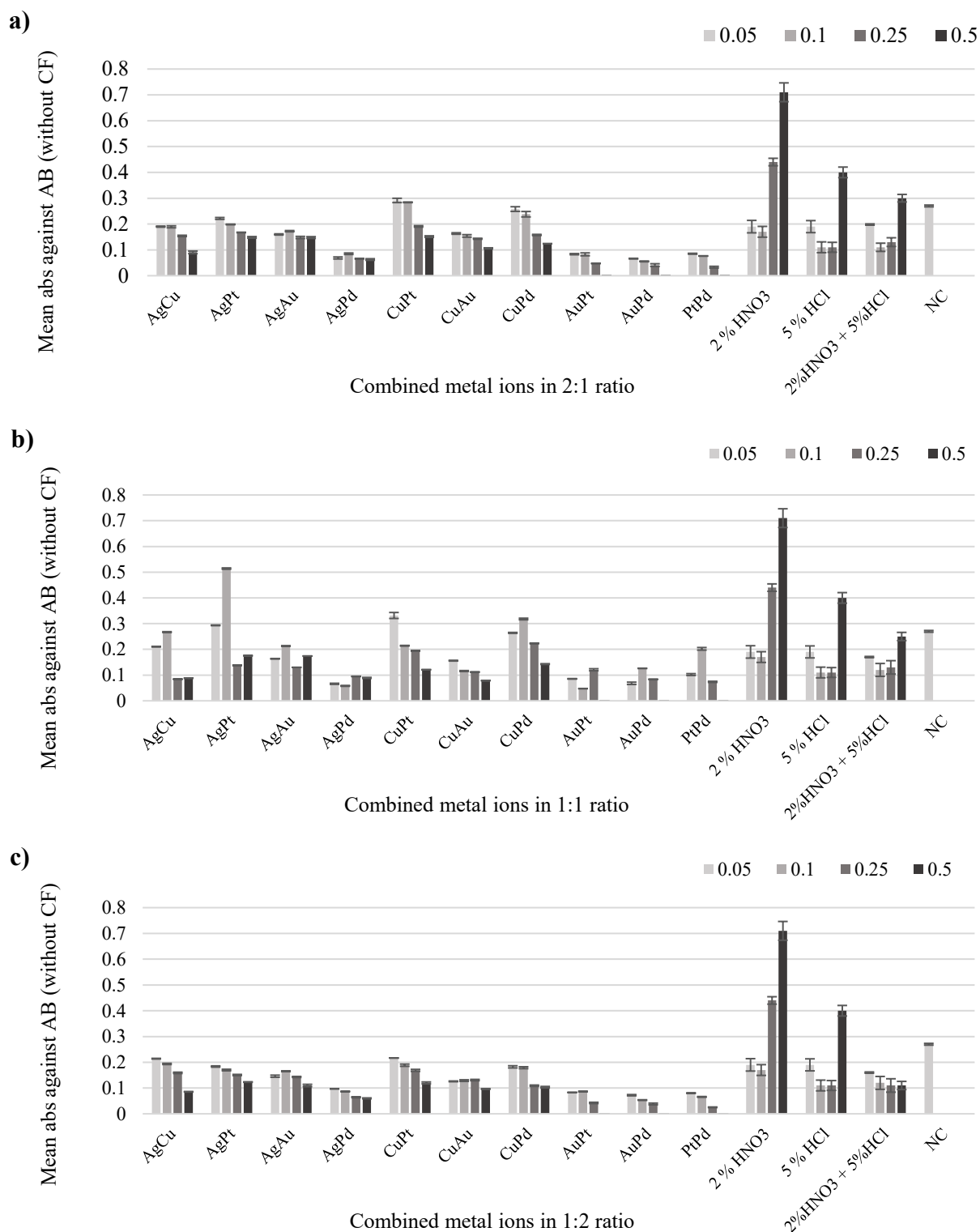
#### *E. faecium*

Against *E. faecium*, AuPt, AuPd and PtPd ion combinations showed 100 % growth inhibition with OD = 0 ( $p < 0.001$ ). The copper ions combination with Ag, Pt and Pd ions demonstrated a lower antibiofilm efficacy in all the tested ratios (0.1- 0.3) (Figure 3.26, a-c).

In summary combined ions of AuPt, AuPd and PtPd demonstrated the best combinations to deter biofilm growth, while CuPt demonstrated the least antibiofilm efficacy.

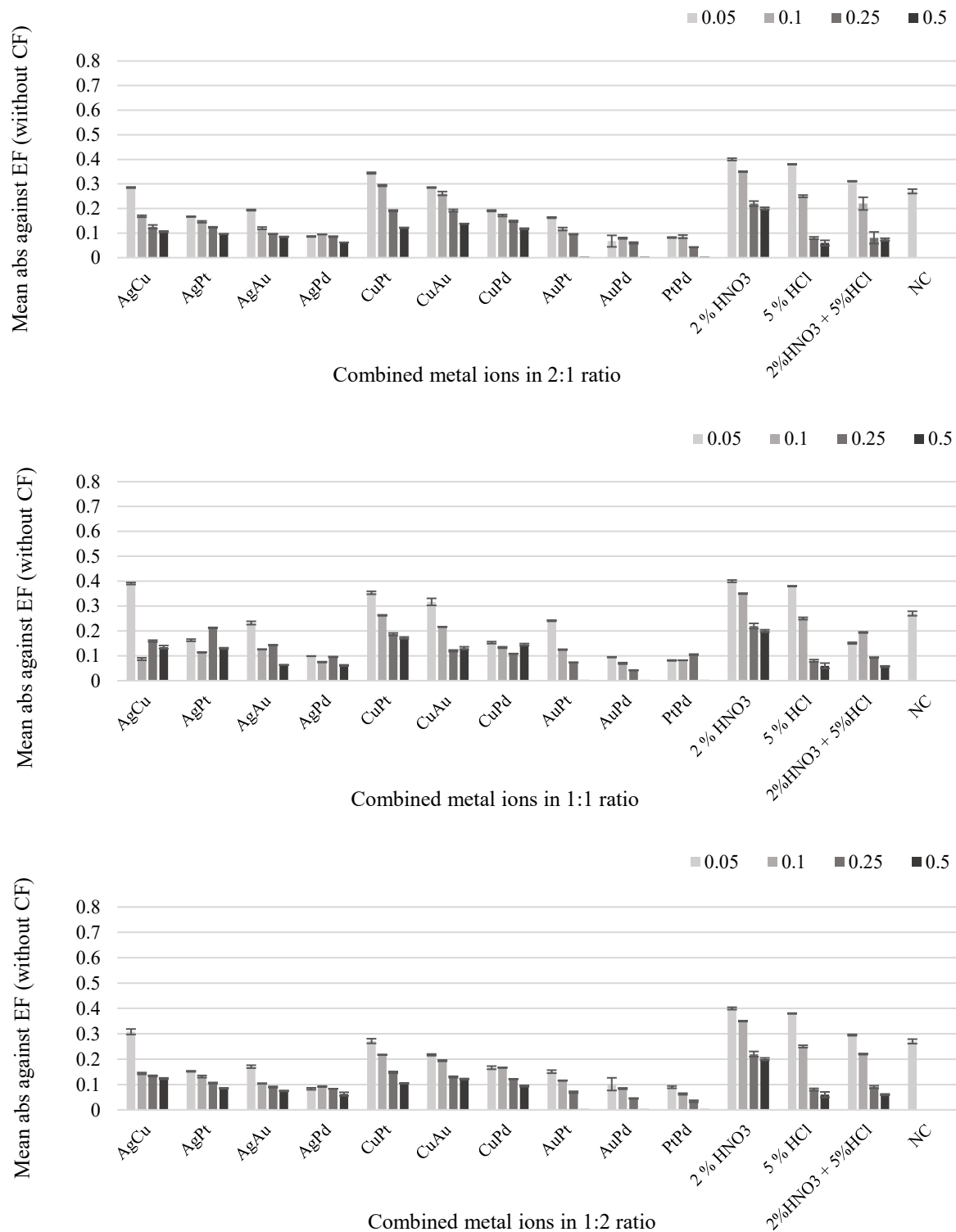


**Figure 3.24.** The CVBA results for metal ions and controls in the absence of 10 % plasma conditioning film against *K. pneumoniae* a) 2:1 ratio, b) 1:1 ratio and c) 1:2 ratio. Ag = silver, Cu = copper, Pt = platinum, Au = gold and Pd = palladium (n = 3).



**Figure 3.25.** The CVBA results for metal ions and controls in the absence of 10 % plasma conditioning film against *A. baumannii* a) 2:1 ratio, b) 1:1 ratio and c) 1:2 ratio. Ag = silver, Cu = copper, Pt = platinum, Au = gold and Pd = palladium (n = 3).





**Figure 3.26.** The CVBA results for metal ions and controls in the absence of 10 % plasma conditioning film against *E. faecium* a) 2:1 ratio, b) 1:1 ratio and c) 1:2 ratio. Ag = silver, Cu = copper, Pt = platinum, Au = gold and Pd = palladium (n=3).

### **3.6.3. Antibiofilm assay for ten combined ions against *K. pneumoniae*, *A. baumannii* and *E. faecium* in the presence of 10 % bovine plasma conditioning film**

The antibiofilm efficacy of AgCu, AgPt, AgAu, AgPd, CuPt, CuAu, CuPd, AuPt, AuPd and PtPd (2:1, 1:1 and 1:2 ratios) were evaluated using CVBA. The efficacies were analysed by comparing the absorbance to determine the growth of the treated bacterial biofilms with respective negative controls grown in presence of 10 % bovine plasma after 24 h. It was found that all the tested ions demonstrated a lower absorbance than the respective acid controls.

#### *K. pneumoniae*

Against *K. pneumoniae*, AuPt, AuPt and PtPd combined ions demonstrated no viable biofilm growth at 0.5 mgmL<sup>-1</sup> in all the tested ratios ( $p < 0.001$ ). Silver/copper, AgPt and AgPd combined ions in all the three ratios at 0.05 mgmL<sup>-1</sup> and 0.1 mgmL<sup>-1</sup> demonstrated the least antibiofilm efficacies (OD = up to 0.22). Copper combinations with Au, Pt and Pd ions demonstrated a moderate antibiofilm efficacy (OD = 0.13) (Figure 3.27, a-c).

#### *A. baumannii*

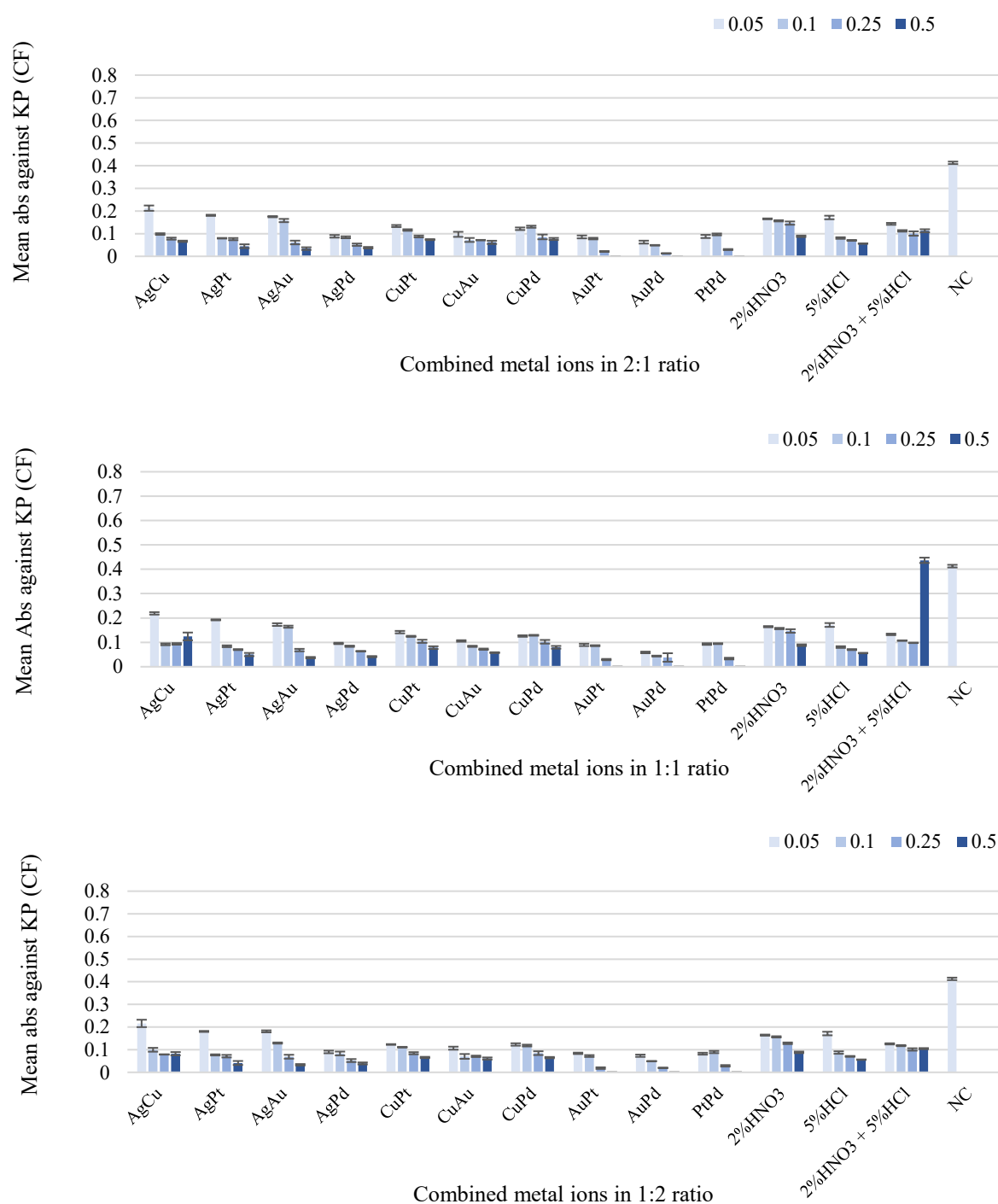
Against *A. baumannii*, AuPt, AuPd and PtPd combined ions showed 100 % inhibition with OD = 0 ( $p < 0.001$ ) at 0.5 mgmL<sup>-1</sup>. AuPt, AuPd and PtPd and AgPd combined ions reduced biofilm growth at all tested concentrations and in all ratios (OD 0.002 - 0.1). Combined ions of CuPd demonstrated the lowest antibiofilm activity (OD = 0.1 – 0.22). The remaining combined ions displayed a moderate antibiofilm activity (OD = 0.03 – 0.2) (Figure 3.28, a-c).

#### *E. faecium*

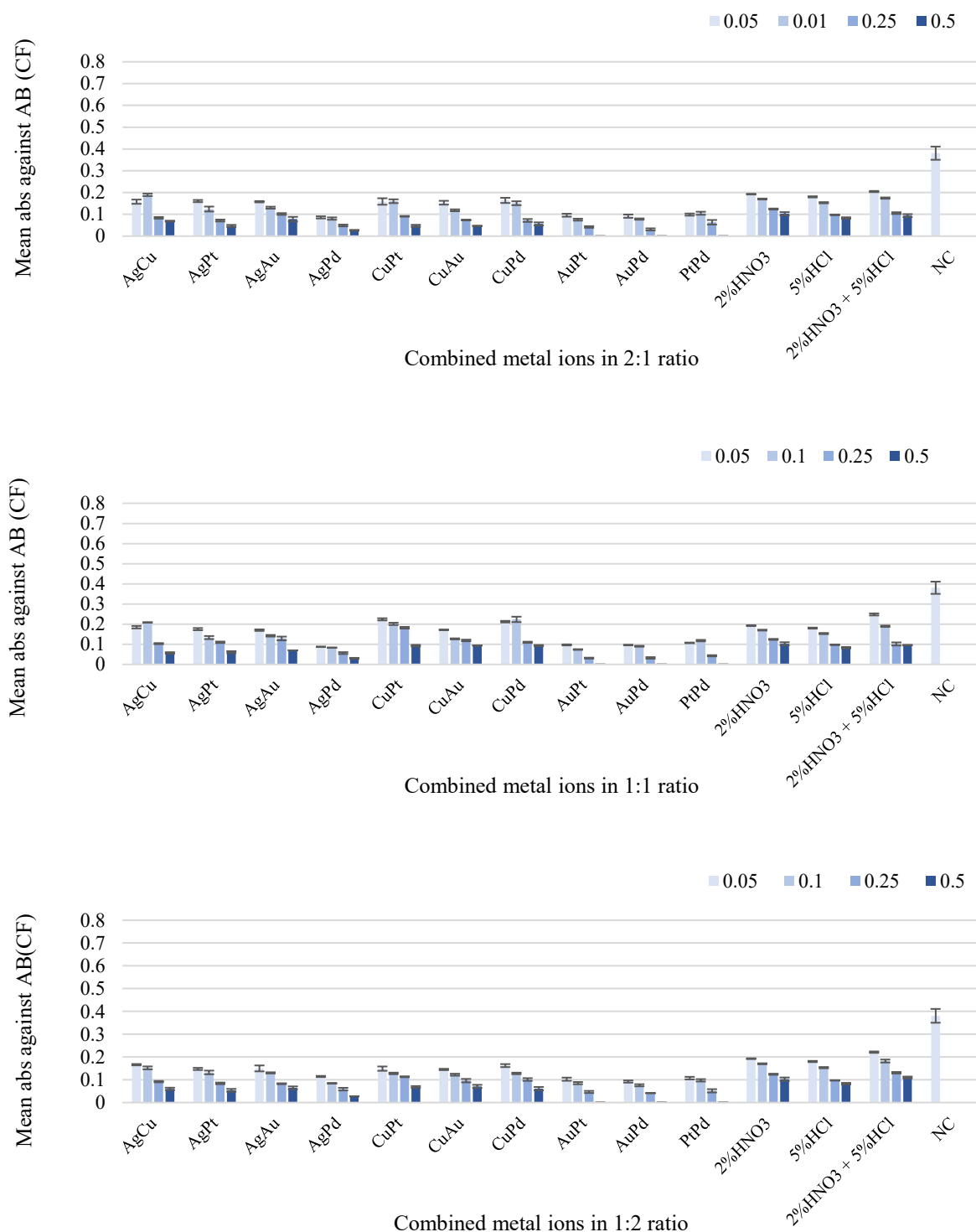
Against *E. faecium*, AuPt, AuPd and PtPd combined ions showed 100 % inhibition with OD = 0 ( $p < 0.001$ ). Moreover, comparatively AuPd and PtPd and AgPd combined ions delivered the greatest antibiofilm efficacies at all tested concentrations and in all ratios (OD 0.002 - 0.1). Combined ions of AgCu at 0.05 mgmL<sup>-1</sup> and CuPt and CuAu at all tested concentrations

demonstrated the lowest antibiofilm efficacy in all the tested ratios (OD = 0.1 – 0.3) (Figure 3.27, a-c).

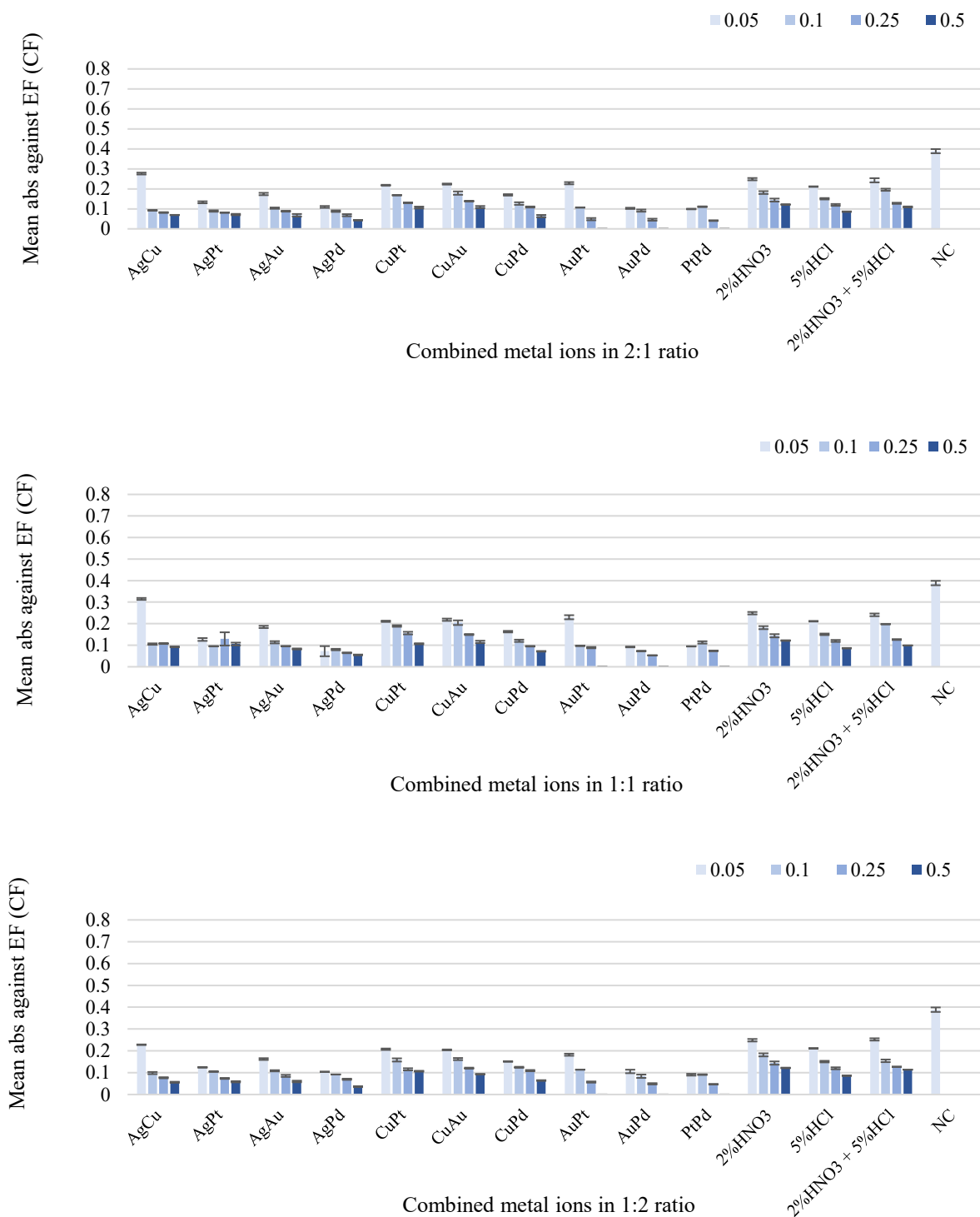
In summary, combined ions of AuPt, AuPd and PtPd against Gram-negative bacteria and AuPd and PtPd against *E. faecium* demonstrated the best antibiofilm efficacies, while copper ions combinations demonstrated the least antibiofilm efficacies. Interestingly, all the tested combined ions demonstrated a greater antibiofilm efficacy (OD = 0 – 0.33) in presence of plasma compared to the absence of plasma (OD = 0 – 0.5).



**Figure 3.27.** The CVBA results for metal ions and controls in the presence of 10 % plasma conditioning film against *K. pneumoniae* a) 2:1 ratio, b) 1:1 ratio and c) 1:2 ratio. Ag = silver, Cu = copper, Pt = platinum, Au = gold and Pd = palladium (n = 3).



**Figure 3.28.** The CVBA results for metal ions and controls in the presence of 10 % plasma conditioning film against *A. baumannii* a) 2:1 ratio, b) 1:1 ratio and c) 1:2 ratio. Ag = silver, Cu = copper, Pt = platinum, Au = gold and Pd = palladium (n = 3).



**Figure 3.29.** The CVBA results for metal ions and controls in the presence of 10 % plasma conditioning film against *E. faecium* a) 2:1 ratio, b) 1:1 ratio and c) 1:2 ratio. Ag = silver, Cu = copper, Pt = platinum, Au = gold and Pd = palladium (n = 3).

### 3.6. Discussion

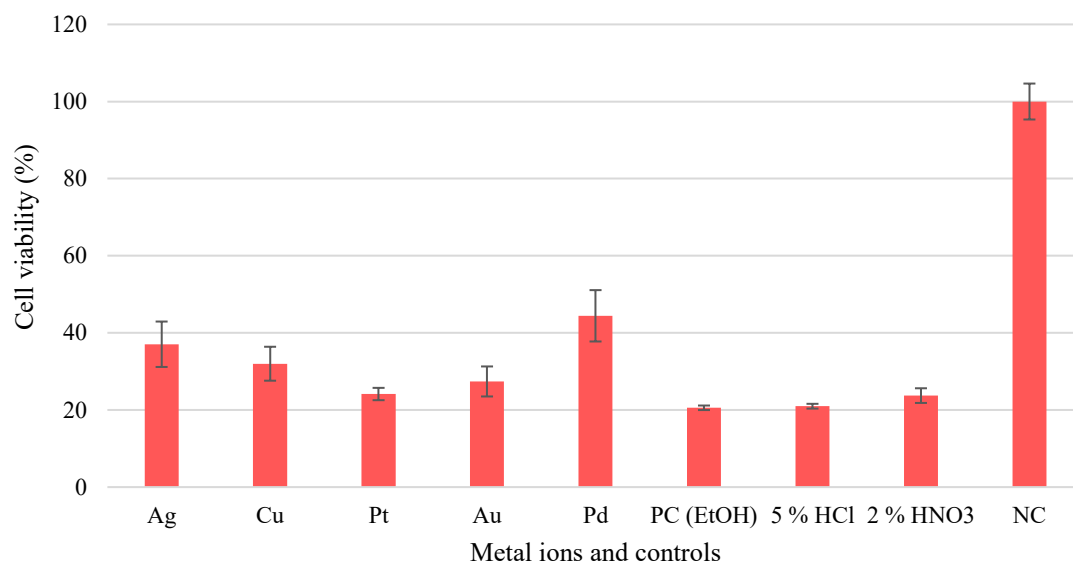
#### *Antibiofilm efficacies in the absence and presence of plasma conditioning film*

The difference in metal ion antimicrobial activity on biofilms can be explained based on the extent by which these cations are neutralised or sequestered to the EPS of the bacterial biofilms (Silvestry-Rodriguez et al., 2008). It is thought that the bacterial biofilms demonstrate multifactorial resistance mechanisms and the biosorption of reactive and charged species in the liquid phase is one of the major mechanisms of bacterial protection (Aslam, 2008). The biosorption process, may result in the antimicrobial compound becoming neutralized and /or diluted to sub-lethal concentrations (Massop and Davidson, 2003). This will result in the antimicrobial effect of the metal ions not being effective, once they reach the biofilms. In addition, cation size, charge ratio, oxidation state, bacterial EPS charge and physical conditions such as pH and temperature affect the amount of binding of the antimicrobial agent to the biofilm (Monteiro et al., 2009). This ultimately can influence the diffusion and extent of penetration of the antimicrobial agent. In agreement with our results, it has been shown that Ag demonstrated a reduction in the bacterial biofilm communities of the water distribution system at 14 – 20  $\mu\text{g mL}^{-1}$ , however, it failed to completely eradicate them (Silvestry-Rodriguez et al., 2008). Thus, it can be hypothesised that in our study, the Ag and Cu ions ( $0.5 \text{ mg mL}^{-1}$ ) concentration was not enough to reach the bacteria inside the EPS complex, unlike Pt, Au and Pd ions which demonstrated a complete inhibition of the biofilm. Though presence of plasma CF increased bacterial biofilm growth absorbance, however the antibiofilm metal ions results were consistent in the presence and absence of CF, this suggests that the biofilm is influencing the rate of antimicrobial efficacies.

### **3.7. Cytotoxicity for five metal ions (Ag, Cu, Pt, Au and Pd)**

The skin fibroblast controls demonstrated 100 % viability in the MTT assay. Palladium ions demonstrated the least cell toxicity with 44 % cell viability. In contrast to our results, platinum chloride salts demonstrated the least and palladium chloride demonstrated a moderate biotoxicity for osteoblast and mouse fibroblast cell lines (Egorova and Ananikov, 2016). Silver and Au ions showed 37 % and 32 % cell viability and a moderate cell toxicity. Platinum (24 %) and copper ions (27 %) demonstrated the most toxic cell effects with a comparable cell viability as positive controls (20 % - 24 %) (Figure 3.30). Similar to the results demonstrated in this work, Cu and Au ions were found to demonstrate a toxicity to human oligodendroglial cells and human gingival fibroblasts at concentrations between 9.8  $\mu\text{M}$  and 2083  $\mu\text{M}$  (Issa et al., 2007).





**Figure 3.30.** Cytotoxicity assays for Ag, Cu, Pt, Au and Pd ions against skin fibroblast cells (n = 3). Ag = silver, Cu = copper, Pt = platinum, Au = gold and Pd = palladium.

## Chapter 4

### **Antimicrobial efficacies of graphene-based compounds against *K. pneumoniae*, *A. baumannii* and *E. faecium* with and without presence of 10 % bovine plasma**

#### **3.0. Introduction**

All the tests described in the introduction section of chapter 3 (page; 71 and 72) were repeated on the GBCs.

##### *Objective*

- Evaluate the antimicrobial efficacies of the graphene-based compounds (GBCs) against three selected pathogens in the absence and presence of 10 % bovine plasma.
- Demonstrate the morphological, elemental and chemical changes for GO, AgGO, AuGO and PdGO in the absence and presence of 10 % bovine plasma.
- Determine the antimicrobial efficacies of GO, AgGO, CuGO, AuGO and PdGO against selected bacterial biofilms in the absence and presence of 10 % bovine plasma.
- Determine antimicrobial efficacies of GBCs combinations (GOAgGO, GOCuGO, GOAuGO, GOPdGO, AgGOCuGO, AgGOAuGO, AgGOPdGO, CuGOAuGO, CuGOPdGO and AuGOPdGO) in the absence and presence of 10 % bovine plasma.

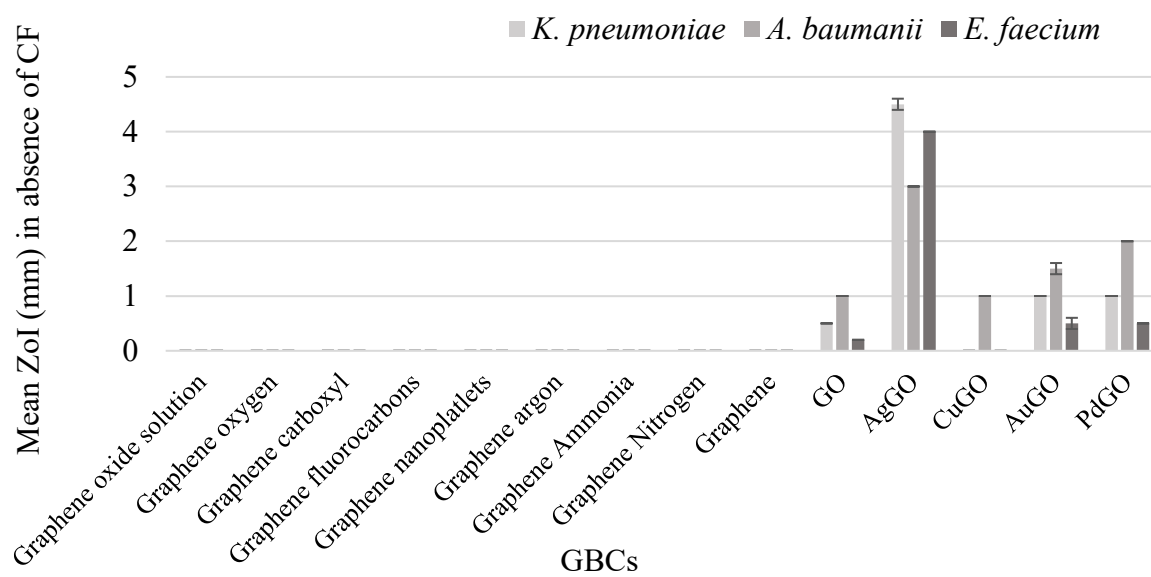
## **4.1. Antimicrobial efficacies for fourteen graphene-based compounds in the absence and presence of 10 % bovine plasma condition film**

### **4.1.1. Zone of inhibition with and without plasma conditioning film**

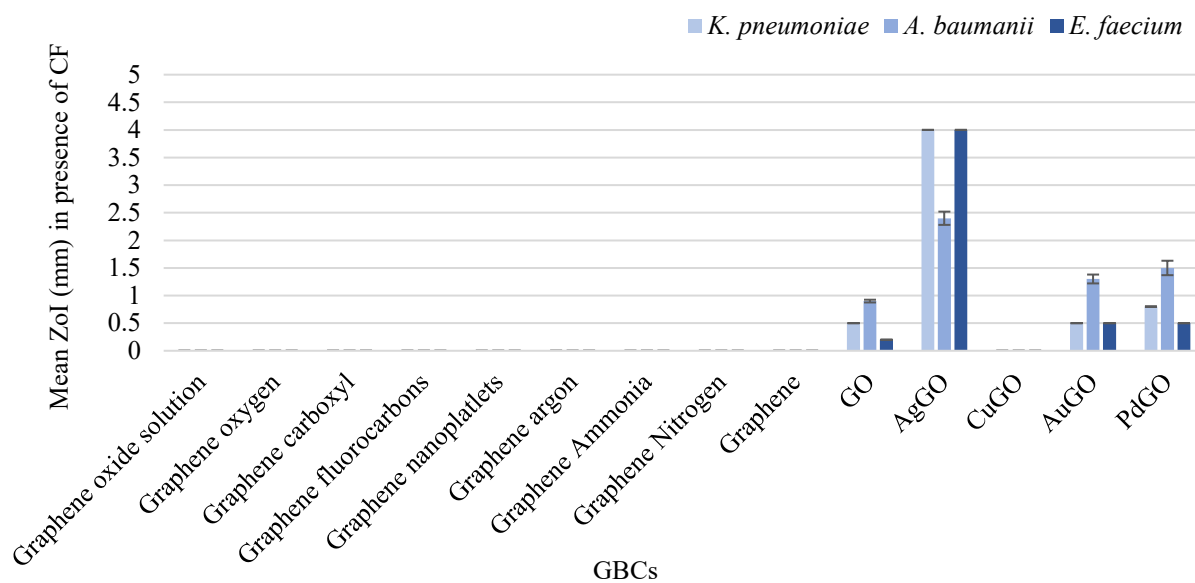
The ZoI test was performed for fourteen graphene-based compounds (GBCs) against the three medical pathogens. Following the tests, AgGO showed the strongest inhibitory effects with 4 - 4.5 mm, 2 - 3 mm and 4 mm of ZoI against *K. pneumoniae*, *A. baumannii* and *E. faecium* respectively in the presence or absence of plasma CF. Gold-graphene oxide and PdGO showed little antibacterial effects with 0.5 mm to 1.5 mm of inhibition. Copper-GO only demonstrated 1 mm of inhibition against *A. baumannii* in absence of plasma conditioning film (CF). The remaining nine tested components GO solution, graphene oxygen, graphene carbonyl, graphene fluorocarbons, graphene nanoplatelets, graphene argon, graphene ammonia, graphene nitrogen and graphene were found to demonstrate no zones of inhibition in the presence or absence of plasma.

*Enterococcus faecium* was found to be the most resistant bacteria. The presence of plasma CF were found to reduce the inhibitory effects (0.5 mm to 1 mm) for AgGO, GO, CuGO, AuGO and PdGO against the three tested bacteria (Figure 4.1 and 4.2).

Overall, AgGO has demonstrated the best inhibitory efficacy and CuGO was the least active compared to GO, AgGO, AuGO and PdGO.



**Figure 4.1.** ZOI (mm) for fourteen GBCs at  $0.01 \text{ mgmL}^{-1}$  in the absence of 10 % plasma conditioning film against *K. pneumoniae*, *A. baumannii* and *E. faecium* ( $n = 24$ ).



**Figure 4.2.** ZoI (mm) for fourteen GBCs at  $0.01 \text{ mgmL}^{-1}$  in the presence of 10 % plasma conditioning film against *K. pneumoniae*, *A. baumannii* and *E. faecium* (n = 24).

#### **4.1.2. Minimum inhibitory concentration (MIC) with and without 10 % plasma conditioning film**

Following the MIC test, AgGO showed the strongest inhibition activity against all the three pathogens ( $0.015 \text{ mgml}^{-1}$  to  $0.031 \text{ mgml}^{-1}$ ) when tested in the absence or presence of plasma CF. The GO solution, graphene oxygen, graphene carbonyl, graphene fluorocarbons, graphene nanoplatelets, graphene argon, graphene ammonia, graphene nitrogen and graphene demonstrated no inhibition in the presence or absence of plasma CF. Apart from AgGO, the inhibitory efficacies were in the order of  $\text{PdGO} > \text{GO} > \text{AuGO} > \text{CuGO}$  in the absence and presence of CF against all bacteria.

The presence of plasma CF found to increase the inhibitory concentration only for GO ( $0.046 \text{ mgml}^{-1}$  without CF and  $0.062 \text{ mgml}^{-1}$  with CF) against *A. baumannii* (Table 4.1 and 4.2).

Overall, AgGO demonstrated the best inhibitory efficacy and CuGO was the least active antimicrobial compared to GO, AgGO, AuGO and PdGO. Except for GO MICs, the presence of plasma did not exhibit any impact on other GBCs MICs.

**Table 4.1.** Minimum inhibitory concentrations result in mgml<sup>-1</sup> for fourteen GBCs in absence of 10 % plasma conditioning film against *K. pneumoniae*, *A. baumannii* and *E. faecium* (n = 4). The highlighted red colour represents the greatest antimicrobial efficacy.

Compounds	<i>Klebsiella pneumoniae</i>	<i>Acinetobacter baumannii</i>	<i>Enterococcus faecium</i>
Graphene oxide solution	> 0.5 ± 0	> 0.5 ± 0	> 0.5 ± 0
Graphene	> 0.5 ± 0	> 0.5 ± 0	> 0.5 ± 0
Graphene carboxyl	> 0.5 ± 0	> 0.5 ± 0	> 0.5 ± 0
Graphene fluorocarbons	> 0.5 ± 0	> 0.5 ± 0	> 0.5 ± 0
Graphene nanoplatelets	> 0.5 ± 0	> 0.5 ± 0	> 0.5 ± 0
Graphene oxygen	> 0.5 ± 0	> 0.5 ± 0	> 0.5 ± 0
Graphene argon	> 0.5 ± 0	> 0.5 ± 0	> 0.5 ± 0
Graphene ammonia	> 0.5 ± 0	> 0.5 ± 0	> 0.5 ± 0
Graphene nitrogen	> 0.5 ± 0	> 0.5 ± 0	> 0.5 ± 0
GO	0.062 ± 0	0.046 ± 0	0.125 ± 0
AgGO	0.031 ± 0	0.015 ± 0	0.031 ± 0
CuGO	0.125 ± 0	0.125 ± 0	0.25 ± 0
AuGO	0.062 ± 0	0.062 ± 0	0.125 ± 0
PdGO	0.062 ± 0	0.062 ± 0	0.062 ± 0

**Table 4.2.** Minimum inhibitory concentrations result in  $\text{mgml}^{-1}$  for fourteen GBCs in the presence of 10 % plasma conditioning film against *K. pneumoniae*, *A. baumannii* and *E. faecium* (n = 4). The highlighted red colour represents the greatest antimicrobial efficacy.

Compounds	<i>Klebsiella pneumoniae</i>	<i>Acinetobacter baumannii</i>	<i>Enterococcus faecium</i>
Graphene oxide solution	$> 0.5 \pm 0$	$> 0.5 \pm 0$	$> 0.5 \pm 0$
Graphene	$> 0.5 \pm 0$	$> 0.5 \pm 0$	$> 0.5 \pm 0$
Graphene carboxyl	$> 0.5 \pm 0$	$> 0.5 \pm 0$	$> 0.5 \pm 0$
Graphene fluorocarbons	$> 0.5 \pm 0$	$> 0.5 \pm 0$	$> 0.5 \pm 0$
Graphene nanoplatelets	$> 0.5 \pm 0$	$> 0.5 \pm 0$	$> 0.5 \pm 0$
Graphene oxygen	$> 0.5 \pm 0$	$> 0.5 \pm 0$	$> 0.5 \pm 0$
Graphene argon	$> 0.5 \pm 0$	$> 0.5 \pm 0$	$> 0.5 \pm 0$
Graphene ammonia	$> 0.5 \pm 0$	$> 0.5 \pm 0$	$> 0.5 \pm 0$
Graphene nitrogen	$> 0.5 \pm 0$	$> 0.5 \pm 0$	$> 0.5 \pm 0$
GO	$0.062 \pm 0$	$0.062 \pm 0$	$0.125 \pm 0$
AgGO	$0.031 \pm 0$	$0.015 \pm 0$	$0.031 \pm 0$
CuGO	$0.125 \pm 0$	$0.125 \pm 0$	$0.25 \pm 0$
AuGO	$0.062 \pm 0$	$0.062 \pm 0$	$0.125 \pm 0$
PdGO	$0.062 \pm 0$	$0.062 \pm 0$	$0.062 \pm 0$



### **4.1.3. Minimum bactericidal concentration (MBC) with and without 10 %**

#### **bovine plasma conditioning film**

Following the MBC test, the AgGO demonstrated the best bactericidal activity against all the three pathogens ( $0.031 \text{ mgml}^{-1}$  to  $0.0.62 \text{ mgml}^{-1}$ ) in the absence or presence of plasma CF. The GO solution, graphene oxygen, graphene carbonyl, graphene fluorocarbons, graphene nanoplatelets, graphene argon, graphene ammonia, graphene nitrogen and graphene were found to present no inhibition in the presence and absence of plasma. Apart from AgGO, the bactericidal efficacies were in the order of  $\text{PdGO} > \text{GO} > \text{AuGO} > \text{CuGO}$  in the absence and presence of CF against all bacteria.

The presence of 10 % bovine plasma CF demonstrated no profound effect on the bactericidal concentrations for any of the tested components (Table 4.3 and 4.4).

Overall, AgGO demonstrated the best bactericidal efficacy and CuGO was the least active antimicrobial compared to GO, AgGO, AuGO and PdGO.

**Table 4.3.** Minimum bactericidal concentrations in mgml<sup>-1</sup> for fourteen GBCs in the absence of 10 % plasma conditioning film against *K. pneumoniae*, *A. baumannii* and *E. faecium* (n = 4). The highlighted red colour represents the greatest antimicrobial efficacy.

Compounds	<i>Klebsiella pneumoniae</i>	<i>Acinetobacter baumannii</i>	<i>Enterococcus faecium</i>
Graphene oxide solution	> 0.5 ± 0	> 0.5 ± 0	> 0.5 ± 0
Graphene	> 0.5 ± 0	> 0.5 ± 0	> 0.5 ± 0
Graphene carboxyl	> 0.5 ± 0	> 0.5 ± 0	> 0.5 ± 0
Graphene fluorocarbons	> 0.5 ± 0	> 0.5 ± 0	> 0.5 ± 0
Graphene nanoplatelets	> 0.5 ± 0	> 0.5 ± 0	> 0.5 ± 0
Graphene oxygen	> 0.5 ± 0	> 0.5 ± 0	> 0.5 ± 0
Graphene argon	> 0.5 ± 0	> 0.5 ± 0	> 0.5 ± 0
Graphene ammonia	> 0.5 ± 0	> 0.5 ± 0	> 0.5 ± 0
Graphene nitrogen	> 0.5 ± 0	> 0.5 ± 0	> 0.5 ± 0
GO	0.125 ± 0	0.062 ± 0	0.25 ± 0
AgGO	0.062 ± 0	0.031 ± 0	0.062 ± 0
CuGO	0.25 ± 0	0.25 ± 0	0.25 ± 0
AuGO	0.125 ± 0	0.125 ± 0	0.187 ± 0
PdGO	0.125 ± 0	0.125 ± 0	0.125 ± 0

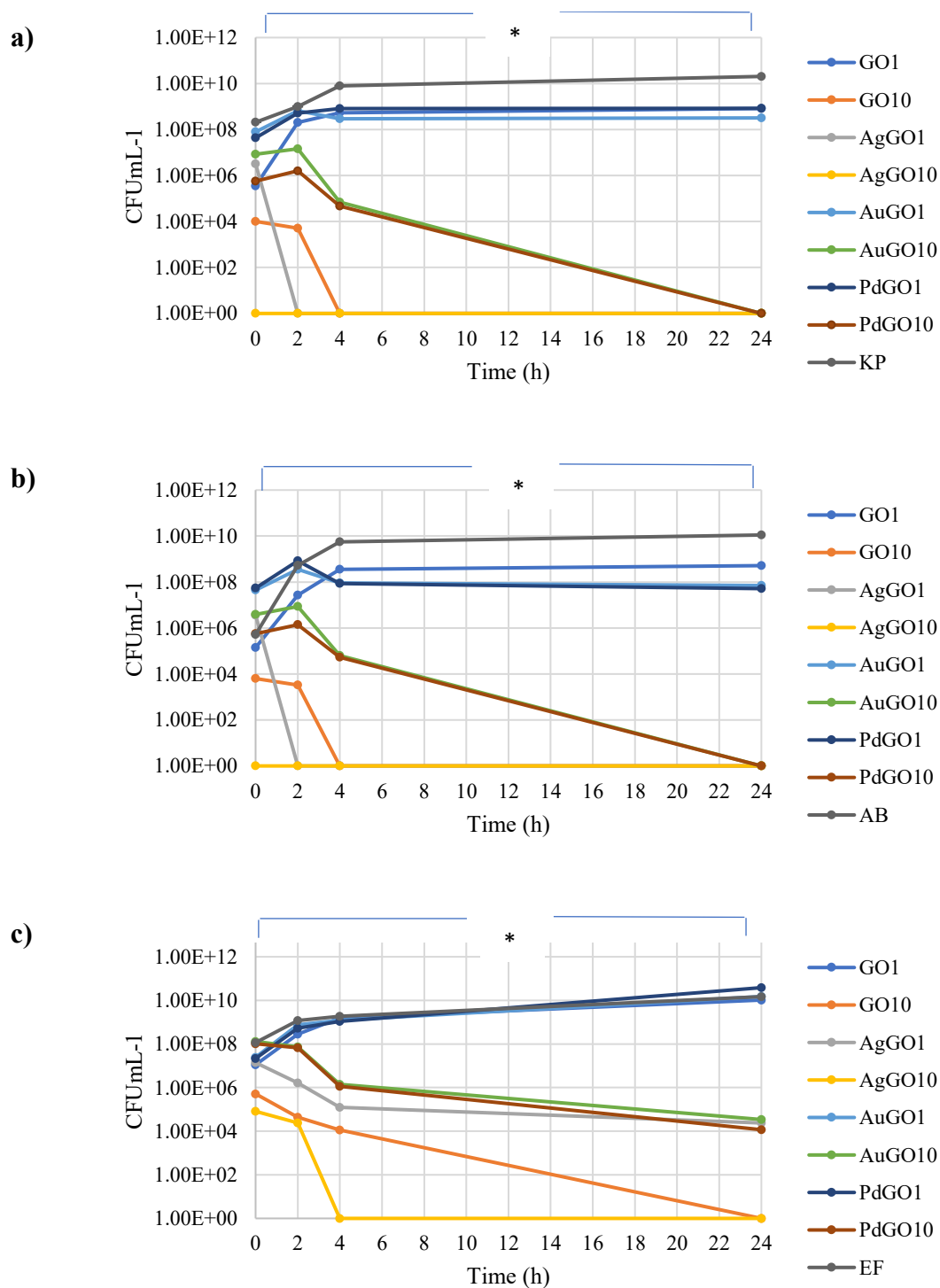
**Table 4.4.** Minimum bactericidal concentrations in mgml<sup>-1</sup> for fourteen GBCs in the presence of 10 % plasma conditioning film against *K. pneumoniae*, *A. baumannii* and *E. faecium* (n = 4). The highlighted red colour represents the greatest antimicrobial efficacy.

Compounds	<i>Klebsiella pneumoniae</i>	<i>Acinetobacter baumannii</i>	<i>Enterococcus faecium</i>
Graphene oxide solution	> 0.5 ± 0	> 0.5 ± 0	> 0.5 ± 0
Graphene	> 0.5 ± 0	> 0.5 ± 0	> 0.5 ± 0
Graphene carboxyl	> 0.5 ± 0	> 0.5 ± 0	> 0.5 ± 0
Graphene fluorocarbons	> 0.5 ± 0	> 0.5 ± 0	> 0.5 ± 0
Graphene nanoplatelets	> 0.5 ± 0	> 0.5 ± 0	> 0.5 ± 0
Graphene oxygen	> 0.5 ± 0	> 0.5 ± 0	> 0.5 ± 0
Graphene argon	> 0.5 ± 0	> 0.5 ± 0	> 0.5 ± 0
Graphene ammonia	> 0.5 ± 0	> 0.5 ± 0	> 0.5 ± 0
Graphene nitrogen	> 0.5 ± 0	> 0.5 ± 0	> 0.5 ± 0
GO	0.125 ± 0	0.062 ± 0	0.25 ± 0
AgGO	0.062 ± 0	0.031 ± 0	0.062 ± 0
CuGO	0.25 ± 0	0.25 ± 0	0.25 ± 0
AuGO	0.125 ± 0	0.125 ± 0	0.187 ± 0
PdGO	0.125 ± 0	0.125 ± 0	0.125 ± 0

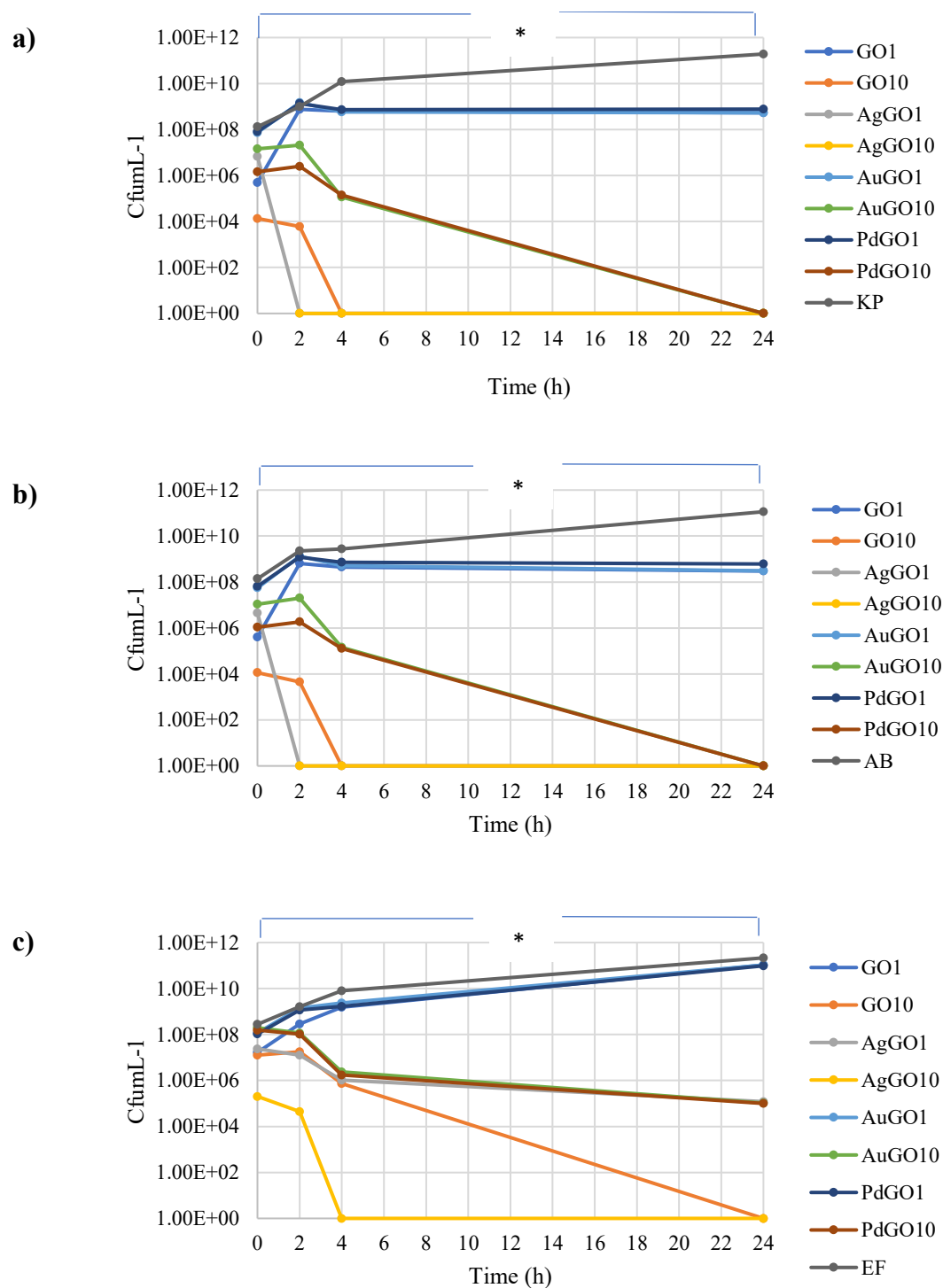
#### **3.1.4. Time kill assay for selected GBCs (graphene oxide (GO) and metal-GO hybrids (AgGO, AuGO and PdGO)) in the absence and presence of 10 % bovine plasma conditioning film**

The time kill assay was performed to investigate the antibacterial efficacies for GO, AgGO, AuGO and PdGO (1 mg and 10 mg) at 0, 2 h, 4 h and 24 h time points against three pathogens in the presence and absence of 10 % serum bovine plasma. Silver-GO at 1 mg showed no viable count after 2 h against both the tested Gram-negative species and 6 logs of bacterial reduction against *E. faecium*. The best antibacterial efficacy was demonstrated for 10 mg of AgGO with no viable count at 0 h against both the tested Gram-negative species and at 4 h against Gram-positive bacteria respectively ( $p < 0.05$ ) (Figure 4.3 and 4.4). Graphene oxide at 4 h of treatment and AuGO and PdGO after 24 h of treatment at 10 mg demonstrated no viable count ( $p < 0.05$ ) against *A. baumannii* and *K. pneumoniae* (Figure 4.3 and 4.4 – a, b). Against *E. faecium* at 10 mg concentration, GO showed no viable bacterial count and AuGO and PdGO demonstrated 6 logs of bacterial reduction after 24 h of treatment (Figure 4.3 and 4.4 – c). Two to three log bacterial viable count reduction was demonstrated for GO, AuGO and PdGO (1 mg) at 24 h treatment against *A. baumannii* and *K. pneumoniae* (Figure 4.3 and 4.4 – a, b). No reduction was found for GO, AuGO and PdGO at 1 mg of concentration against *E. faecium* (Figure 4.3 and 4.4 – c).

Thus, in summary, AgGO demonstrated the best antimicrobial efficacy and AuGO was the least active antimicrobial efficacy.



**Figure 4.3.** Time kill assay for GO, AgGO, AuGO and PdGO at 1 mg and 10 mg concentrations against a) *K. pneumoniae*, b) *A. baumannii* and c) *E. faecium* in the absence of 10 % plasma conditioning film ( $p < 0.05$ ).



**Figure 4.4.** Time kill assay results of GO, AgGO, AuGO and PdGO at 1 mg and 10 mg concentrations against a) *K. pneumoniae*, b) *A. baumannii* and c) *E. faecium* in the presence of 10 % plasma conditioning films ( $p < 0.05$ ).

## 4.1. Discussion

### *Antimicrobial efficacies of the graphene based compounds*

From the results of the ZoI, MIC, MBC and time kill tests, AgGO displayed the best antimicrobial efficacy followed with PdGO and GO. Similarly, amongst the GO, graphite, AgGO and zinc oxide-graphene oxide, AgGO demonstrated the best antimicrobial with MIC of  $0.12 \text{ mg mL}^{-1}$  against *E. coli* / *Enterococcus faecium* and  $0.25 \text{ mg mL}^{-1}$  against *S. aureus* / *K. pneumoniae* (Whitehead et al., 2017). In another study by Xu et al. (2011), AgGO nanocomposites displayed a large inhibitory zone against *S. aureus* and *E. coli* (up to 17 mm).

### *Physical and chemical factors of graphene based compounds*

#### *Antimicrobial efficacies and physical factors of graphene based compounds*

One of the most well described mechanisms for the antimicrobial action of graphene-based metal compounds can be induction of oxidative stress generated by GO. Reactive oxygen species might be produced upon adsorption of oxygen on the edges and pits present on the GO flakes (Zou et al., 2016). Graphene oxide also contains high amounts of oxygen related functional groups such as carboxyl and hydroxyl on the surface (Jin et al., 2017). It is feasible that the oxygen content might be reduced by various cellular enzymes which generates ROS, once in contact with the bacteria (Zou et al., 2016). It has been shown that GO generated higher levels of ROS than graphene owing to the larger number of oxygen functional group present, thus making them better antimicrobials (Santos et al., 2012). This was confirmed for poly(vinylcarbazole)-GO nanocomposites with the highest percentage of thiols present in a glutathione loss test (an antioxidant that nullifies ROS production) at  $1 \text{ mg mL}^{-1}$  compared to a graphene nanocomposite (Musico et al., 2014). Another antibacterial mechanism of GO is described to be wrapping and trapping. It can be assumed that the grooves, defects and distortions that are formed during the production of GO from graphene aids in trapping bacterial cells (Krishnamoorthy et al., 2012). Once trapped, the nano-walls of the GO induce

bacterial damage by wrapping around the bacterial membrane and hindering vital cellular process (Akhavan and Ghaderi, 2010). It is also assumed that this trap and wrap phenomenon will cut off bacterial nutrient supplies and other conditions required for growth (Zou et al., 2016). Supporting results were observed where graphene oxide polymer nanocomposites and carbon nanotube GO compounds altered the bacterial cell shape and integrity and inhibited cell proliferation by wrapping around them (Akhavan and Ghaderi, 2010; Mejias Carpio et al., 2012).

*Antimicrobial efficacies and chemical factors of graphene based compounds*

Several chemical factors influence AgGO antibacterial mechanism. It has been suggested that the chemical properties of GO such as negative zeta potential, partial hydrophobicity and presence of carboxyl groups on the surface enhance its antimicrobial properties (Kurantowicz et al., 2015; Prasad et al., 2016). According to Kurantowicz et al. (2015), GO negative zeta potential (-49.8 mega volt) and partial hydrophobic nature resulted in a greater bacterial attraction / adhesion to the surfaces. Moreover, owing to the presence of carboxyl group in the macromolecule bacterial structures such as fatty acids and amino acids, the GO surface rich in carboxyl group can be speculated to play an attractive role to attach bacteria on their surfaces. (Sanchez et al., 2012; Kurantowicz et al., 2015).

Work by others has been in agreement with the results found in this study, whereby GO was found to show a good antimicrobial efficacy against *E. coli* with MIC of 25  $\mu\text{g mL}^{-1}$  (Veerapandian et al., 2013). Apart from physically damaging bacterial membrane Kurantowicz et al. (2015), other detrimental effects of GO could be induction of oxidative stress and hindrance in adenosine phosphate (ATP) production (He et al., 2010; Liu et al., 2011). Copper-GO nanoparticles have also been demonstrated to show antimicrobial efficacy against *Pseudomonas syringe* producing inhibition of 12.5 mm at 16  $\mu\text{g mL}^{-1}$  (Li et al., 2017). Similarly, another study demonstrated an effective MIC of 40 mM and 20 mM with CuO



nanoparticles against *E. coli* and *S. aureus* respectively (DeAlba-Montero et al., 2017). This was in contrast with our results, where CuGO demonstrated poor antibacterial activity.

that particle size was not found to affect the antimicrobial activity of ZnO.

The GO solution, graphene, graphene oxygen, graphene carboxyl, graphene fluorocarbons, graphene nanoplatelets, graphene argon, graphene nitrogen and graphene ammonia did not demonstrate any bacteriostatic or bactericidal effects. Little has been reported about other tested graphene materials except for the graphene and graphene nanoplatelets. Graphene nano-walls and graphene nanoplatelets have been found to demonstrate effective antibacterial efficacies (Jastrzebska et al., 2012). Similarly, a study by Scaffaro et al. (2017) found an effective inhibitory effect (32 mm) for graphene nanoplatelets against *Micrococcus luteus*. Furthermore, a drop diffusion method demonstrated only 26 % and 41 % *E. coli* and *S. aureus* survival for graphene nano-walls (Jastrzebska et al., 2012).

The reason that the functionalised graphene's tested in this study did not demonstrate any antimicrobial efficacy may be explained as mentioned in the Barbolina et al. (2016) study, regarding a purity of the tested graphene-based derivatives. Accordingly, the commercial purchased GO flakes were found to demonstrate no bacterial potency in the cell viability test against *E. coli* at 1 mgmL<sup>-1</sup> concentration (Barbolina et al., 2016). Since the above-mentioned graphene derivatives were purchased from a commercial supplier, it is unknown as to the exact nature of the graphene shape and size in the solution provided which could invariably hinder their antibacterial activity. Further analysis of the functionalised graphene to characterise them would increase the knowledge of the specification of these purchased compounds.

#### *Conditioning film effect on single graphene based compound antimicrobial efficacies*

The presence of the bovine plasma CF was not shown to have a major influence on the antimicrobial efficacies of the graphene derivatives. Only 0.5 mm to 1 mm of ZoI reduction for the GO, CuGO, AgGO and PdGO was demonstrated. In the MIC assay, only GO inhibitory

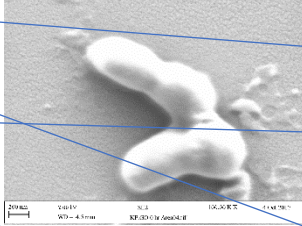
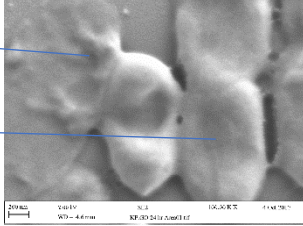
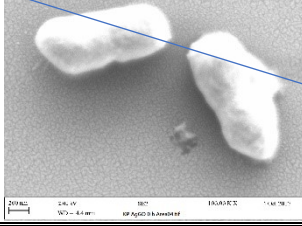
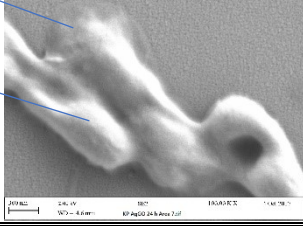
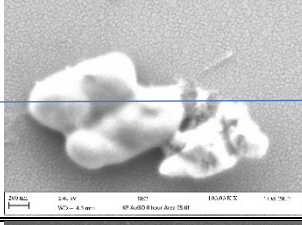
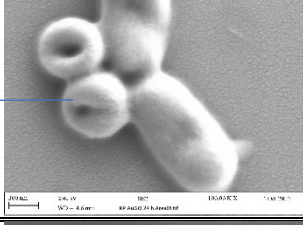
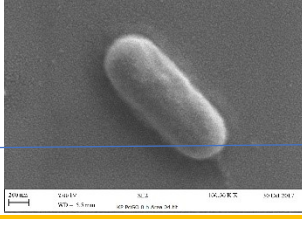
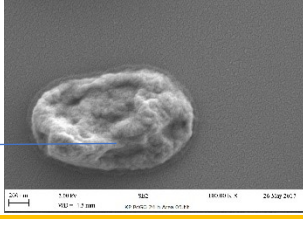
concentration against *A. baumannii* were found to be reduced in the presence of CF. In agreement with our results, the presence of bovine plasma conditioning agent film was shown not to demonstrate any effect on the antimicrobial effects of Ti-nitride and Ag coated surfaces against *S. aureus* (Saubade et al., 2018). However, in contrast to these results, uncapped Ag nanoparticles (AgNps) have been shown to display a lower antimicrobial efficacy in presence of 3 % BSA compared to poly(vinylpyrrolidone) coated AgNps (PVP-AgNps) and citrate coated AgNPs (cit-AgNps) against *Salmonella typhirium* at 3  $\mu\text{gmL}^{-1}$  (Gnanadhas et al., 2013). Since in the work presented in this thesis, the CF did not alter the antibacterial activity when used with the graphene derivatives it may be suggested that the graphene oxide did not compete with the bovine plasma proteins. This suggests that graphene based materials possess the potential to be used as antibacterial material / biocides where organic load is present. However, investigations in presence of other CFs such as blood, serum and other biological fluids would increase this knowledge.

## **4.2. Morphological changes observed using SEM for GO and metal-GO hybrids**

### **4.2.1. Structural changes in the *Klebsiella pneumoniae*, *A. baumannii* and *E. faecium* after GO, AgGO, AuGO and PdGO treatment at 0 h and 24 h in the absence of 10 % bovine plasma conditioning film**

The untreated cells were found to have normal and smooth surface and intact shape (Table 4.5 – 4.7, a). However, after treatment, all the bacterial cells were found morphological changes after 24 h. When compared with the control, the treated bacterial cells were found to demonstrate a ‘rougher’ looking surface. This might be owing to the deposition of the GO and metal-GO hybrids particles. The other prominent damage was a compressed cell surface with large pits and cell seepage (with AgGO ion treatment). The 24 h AuGO treatment left the cell structure deformed and augmented with a ‘spongy’ rounded shape. The bacterial cells shape changed to swollen, round or irregular after the treatment compared with control (Table 4.5 – 4.7, i – iv, b and c). Against *E. faecium* AgGO and AuGO, against *A. baumannii* AgGO and against *K. pneumoniae* GO and AgGO demonstrated cell leakage. Palladium-GO treated *K. pneumoniae* cell showed the greatest changes with surface pits / holes and egg like oval shape after 24 h (Table 4.5).

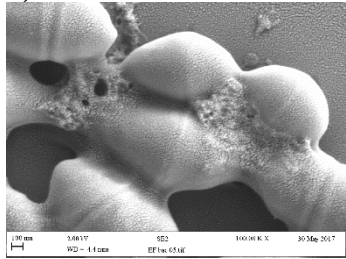
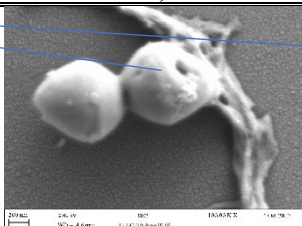
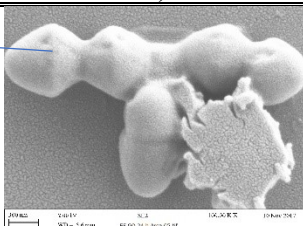
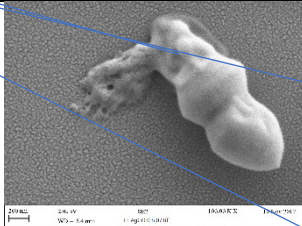
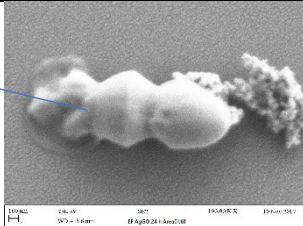
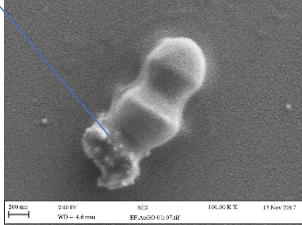
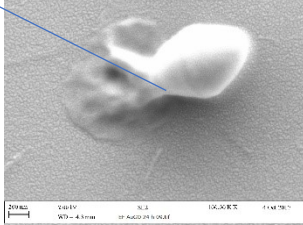
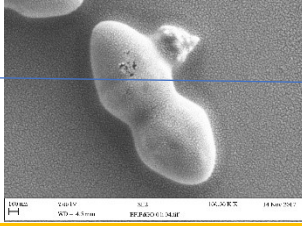
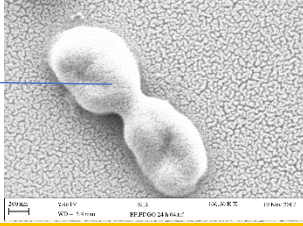
**Table 4.5.** Changes in the *K. pneumoniae* morphology using SEM in the absence of 10 % plasma conditioning film after GO and metal-GO hybrids treatment (0 h and 24 h). GO = graphene oxide, AgGO = silver graphene oxide, AuGO = gold graphene oxide and PdGO = palladium graphene oxide.

Control	Metal-GO hybrids	<i>K. pneumoniae</i> after 0 h Metal-GO hybrids treatment in the absence of CF	<i>K. pneumoniae</i> after 24 h Metal-GO hybrids treatment in the absence of CF
		b)	c)
Cell leakage	GO i)		
Cell elongation	AgGO ii)		
	AuGO iii)		
Spongy and swollen shape	PdGO iv)		
Pits and oval shape			

**Table 4.6.** Changes in the *A. baumannii* morphology using SEM in the absence of 10 % plasma conditioning film after GO and metal-GO hybrids treatment (0 h and 24 h). GO = graphene oxide, AgGO = silver graphene oxide, AuGO = gold graphene oxide and PdGO = palladium graphene oxide.

Control	Metal-GO hybrids	<i>A. baumannii</i> after 0 h Metal-GO hybrids treatment in the absence of CF	<i>A. baumannii</i> after 24 h Metal-GO hybrids treatment in the absence of CF
		b)	c)
Compressed surface	GO	i)	
Cell leakage	AgGO	ii)	
a)	AuGO	iii)	
Swollen cell	PdGO	iv)	
Pits formation			

**Table 4.7.** Changes in the *E. faecium* morphology using SEM in the in the absence of 10 % plasma conditioning films after GO and metal-GO hybrids treatment (0 h and 24 h). GO = graphene oxide, AgGO = silver graphene oxide, AuGO = gold graphene oxide and PdGO = palladium graphene oxide.

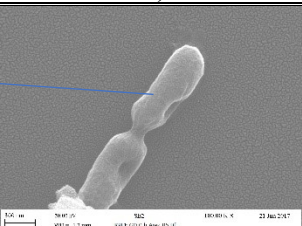
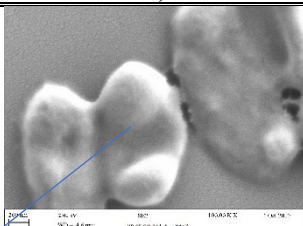
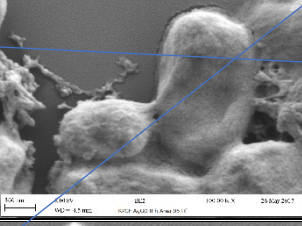
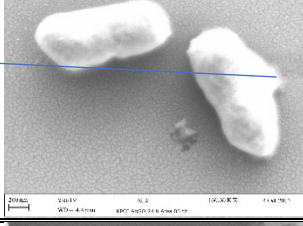
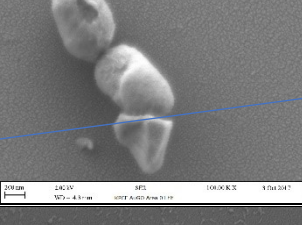
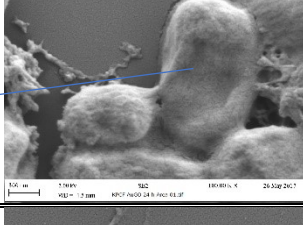
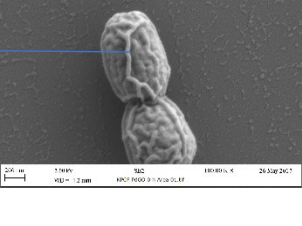
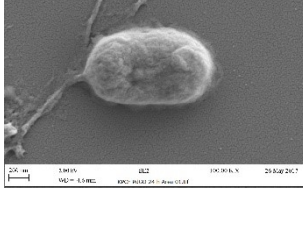
Control	Metal-GO hybrids	<i>E. faecium</i> after 0 h metal treatment in the absence of CF	<i>E. faecium</i> after 24 h metal treatment in the absence of CF
<p>Pit formations ←</p> <p>Cell leakage ←</p> <p><b>a)</b> </p> <p>Compressed surface ←</p>	GO i)	<b>b)</b> 	<b>c)</b> 
	AgGO ii)		
	AuGO iii)		
	PdGO iv)		

#### **4.2.2. *Klebsiella pneumoniae*, *A. baumannii* and *E. faecium* structural changes after GO, AgGO, AuGO and PdGO treatment at 0 h and 24 h in the presence of 10 % bovine plasma conditioning film**

The untreated cells were intact and appeared undamaged before treatment (Table 4.8 – 4.10, a). However, again, all the bacterial cells were to demonstrate changes in morphologies after 24 h treatment compared with 0 h. The Gram–negative pathogens were found with the greatest morphologically damage when compared with the *E. faecium*. *Enterococcus faecium* cells at 0 h treatment was relatively smooth and looked undamaged. The prominent *E. faecium* and *K. pneumoniae* changes was appearance of cellular content leakage following treatment with AgGO after 24 h. Palladium-GO treated *K. pneumoniae* cells showed the appearance of lines on surface with extensive pits. Against *K. pneumoniae* GO and AuGO and against *A. baumannii* PdGO at 24 h treatment demonstrated that the bacteria looked to have a damaged centre and swollen edges. Moreover, cell elongation was demonstrated at 0 h treatment against *A. baumannii* for AuGO and PdGO and for GO against *K. pneumoniae*. Moreover, cell shrinkage and broader width were also demonstrated at 24 h following GO, AuGO and PdGO treatment against *A. baumannii* and *K. pneumoniae* (Table 4.8 – 4.10, i-iv, b and c).

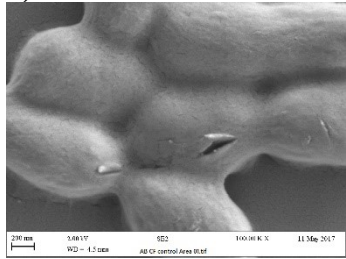
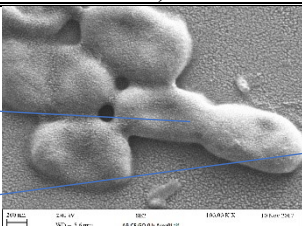
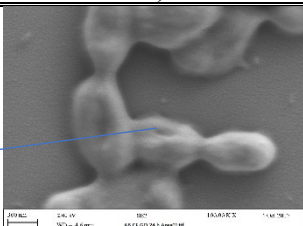
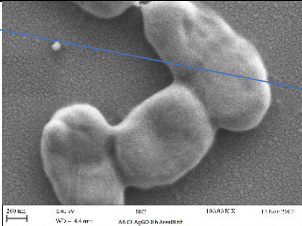
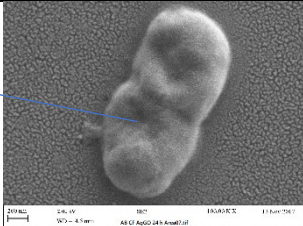
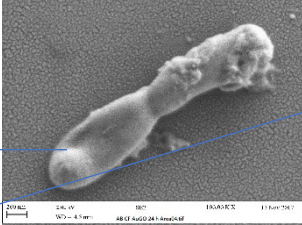
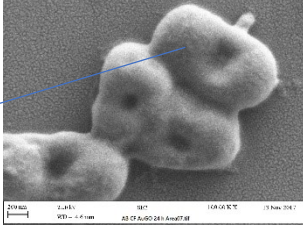
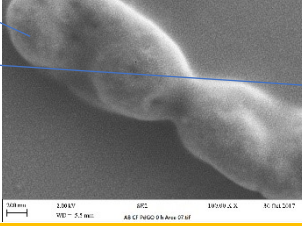
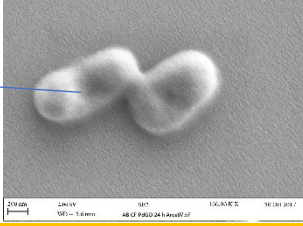


**Table 4.8.** Changes in the *K. pneumoniae* morphology using SEM in the presence of 10 % plasma conditioning film after treatment with GO and mtal-GO hybrids (0 h and 24 h). GO = graphene oxide, AgGO = silver graphene oxide, AuGO = gold graphene oxide and PdGO = palladium graphene oxide.

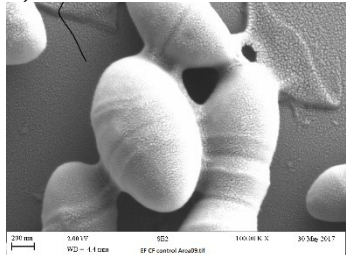
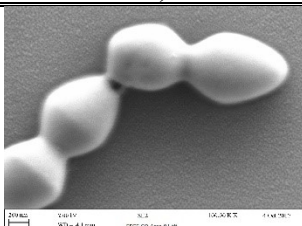
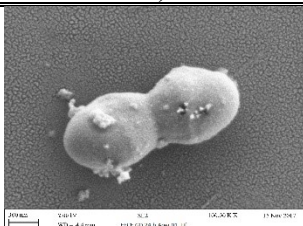
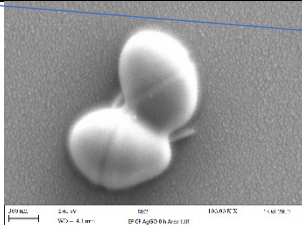
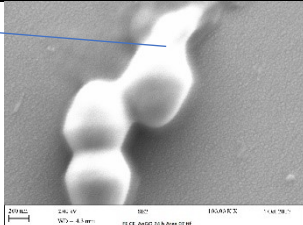
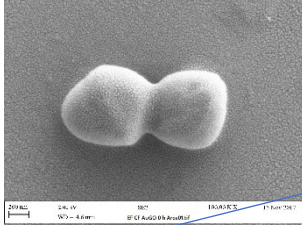
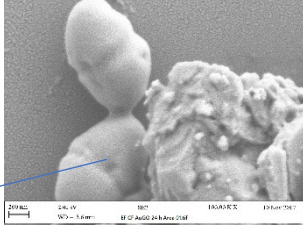
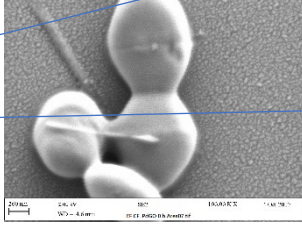
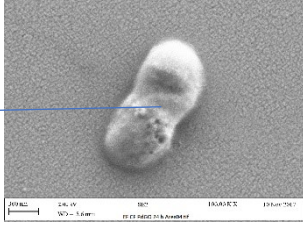
Control	Metal-GO hybrids	<i>K. pneumoniae</i> after 0 h metal treatment in the presence of CF	<i>K. pneumoniae</i> after 24 h metal treatment in the presence of CF
		b)	c)
Cell elongation and centre pits	GO i)		
a) Cell leakage	AgGO ii)		
	AuGO iii)		
Compressed centre and swollen edges	PdGO iv)		
Lines on surface			



**Table 4.9.** Changes in the *A. baumannii* morphology using SEM in the presence of 10 % plasma conditioning film after treatment with GO and metal-GO hybrids (0 h and 24 h). GO = graphene oxide, AgGO = silver graphene oxide, AuGO = gold graphene oxide and PdGO = palladium graphene oxide.

Control	Metal- GO hybrids	<i>A. baumannii</i> after 0 h metal treatment in the presence of CF	<i>A. baumannii</i> after 24 h metal treatment in the presence of CF
		b)	c)
<b>a)</b>  Flattened /elongated cells surface  Compressed surface  Flattened /elongated cells  Shorter cells with centre pits	GO i)		
	AgGO ii)		
	AuGO iii)		
	PdGO iv)		

**Table 4.10.** Changes in the *E. faecium* morphology using SEM in the presence of 10 % plasma conditioning film after treatment with GO and metal-GO hybrids (0 h and 24 h). GO = graphene oxide, AgGO = silver graphene oxide, AuGO = gold graphene oxide and PdGO = palladium graphene oxide.

Control	Metal-GO hybrids	<i>E. faecium</i> after 0 h metal treatment in the presence of CF	<i>E. faecium</i> after 24 h metal treatment in the presence of CF
<b>a)</b>  Cell leakage Pits formation	GO i)	<b>b)</b> 	<b>c)</b> 
	AgGO ii)		
	AuGO iii)		
	PdGO iv)		

## **4.2. Discussion**

All the tested bacterial cells demonstrated physical abnormalities GO and metal-GO hybrids treatment compared to the untreated cells in this study in the absence and presence of plasma CF. It has been suggested that the antimicrobial action of GO and metal-GO hybrids might be attack to the cell membrane affecting cell permeability resulting in cell leakage (K. Gupta et al., 2016; Das et al., 2017). The suggested mechanism is described in the SEM subsection of chapter 3.

### 4.3. Elemental changes observed using EDAX

#### 4.3.1. Elemental changes against *Klebsiella pneumoniae*, *A. baumannii* and *E. faecium* after GO, AgGO, AuGO and PdGO at 24 h treatment in the absence of 10 % bovine plasma conditioning film

The EDAX analysis results were presented for an average of three atomic percentage (At %) for untreated cells and cells treated with GO, AgGO, AuGO and PdGO at 24 h.

##### *K. pneumoniae*

Against *K. pneumoniae* in the absence of plasma CF, the control elemental At % were 51.33 % for carbon, 20 % for nitrogen, 28 % for oxygen, 0.41 % for phosphorous and 0.15 % for potassium. Compared with the control, AgGO demonstrated the greatest effects in the At % of carbon (58 %), oxygen (22 %), phosphorous (0.01 %). Graphene-oxide showed the maximum changes in the At % of potassium (1.02%). The nitrogen At % was the most affected with PdGO treatment. The phosphorous and potassium content disappeared after PdGO and AuGO and PdGO treatment respectively (Figure 4.5, a-e).

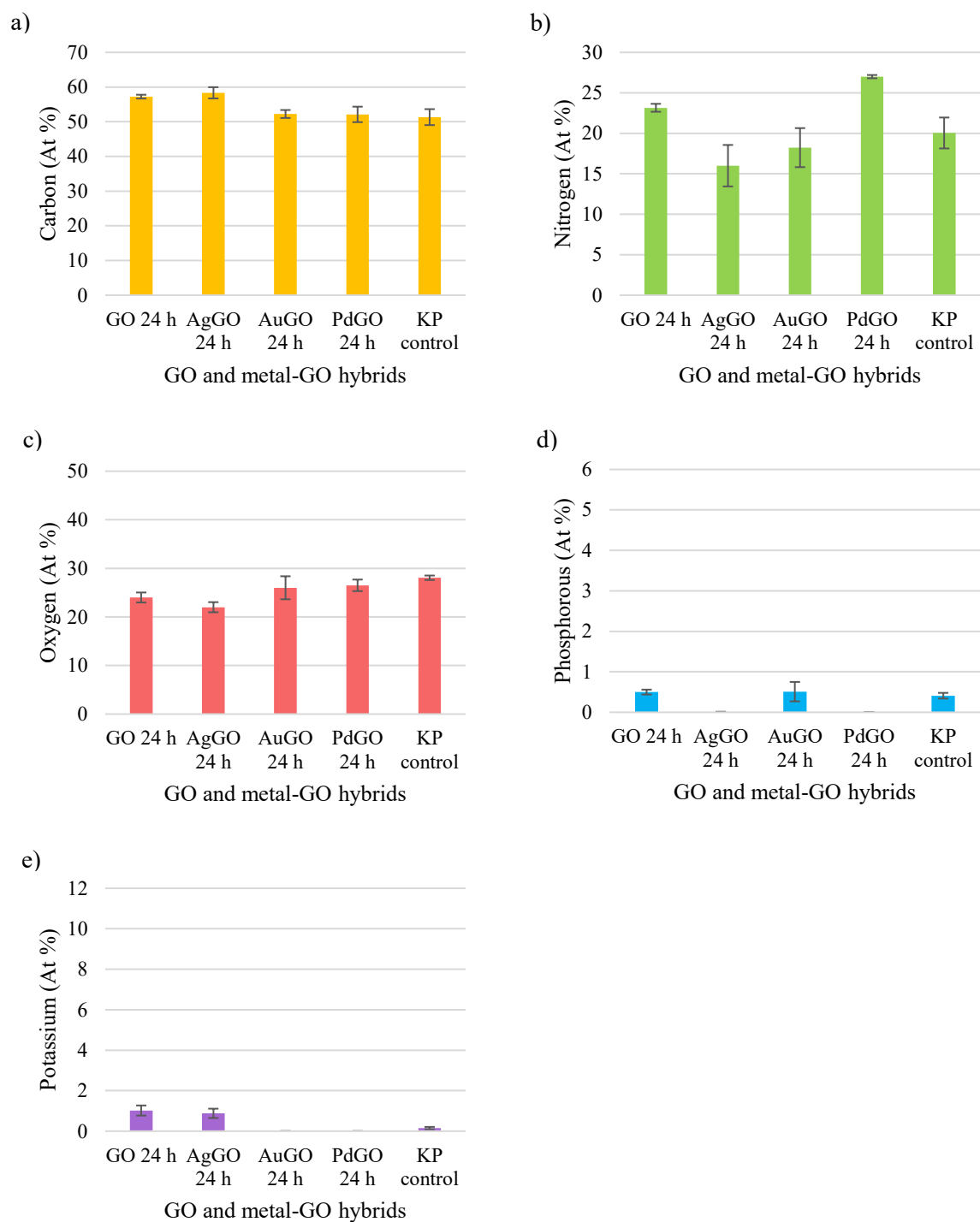
##### *A. baumannii*

Against *A. baumannii* in the absence of plasma CF, the control elemental At % were 49 % for carbon, 23 % for nitrogen, 27 % for oxygen, 0.86 % for phosphorous and 0.51 % for potassium. The greatest elemental changes were demonstrated for PdGO treated bacterial cells with At % for carbon = 66 %, nitrogen = 5 %, oxygen = 43 %, phosphorous = 0.11 % and potassium = 11 % compared with the control. A noteworthy change was demonstrated for GO in At % of oxygen (31 %) and for AuGO in At % nitrogen = 13 %. The potassium and phosphorous content disappeared after AgGO treatment. No change was found in the At % of oxygen (26 %) with AgGO and AuGO treatment (Figure 4.6, a-e).

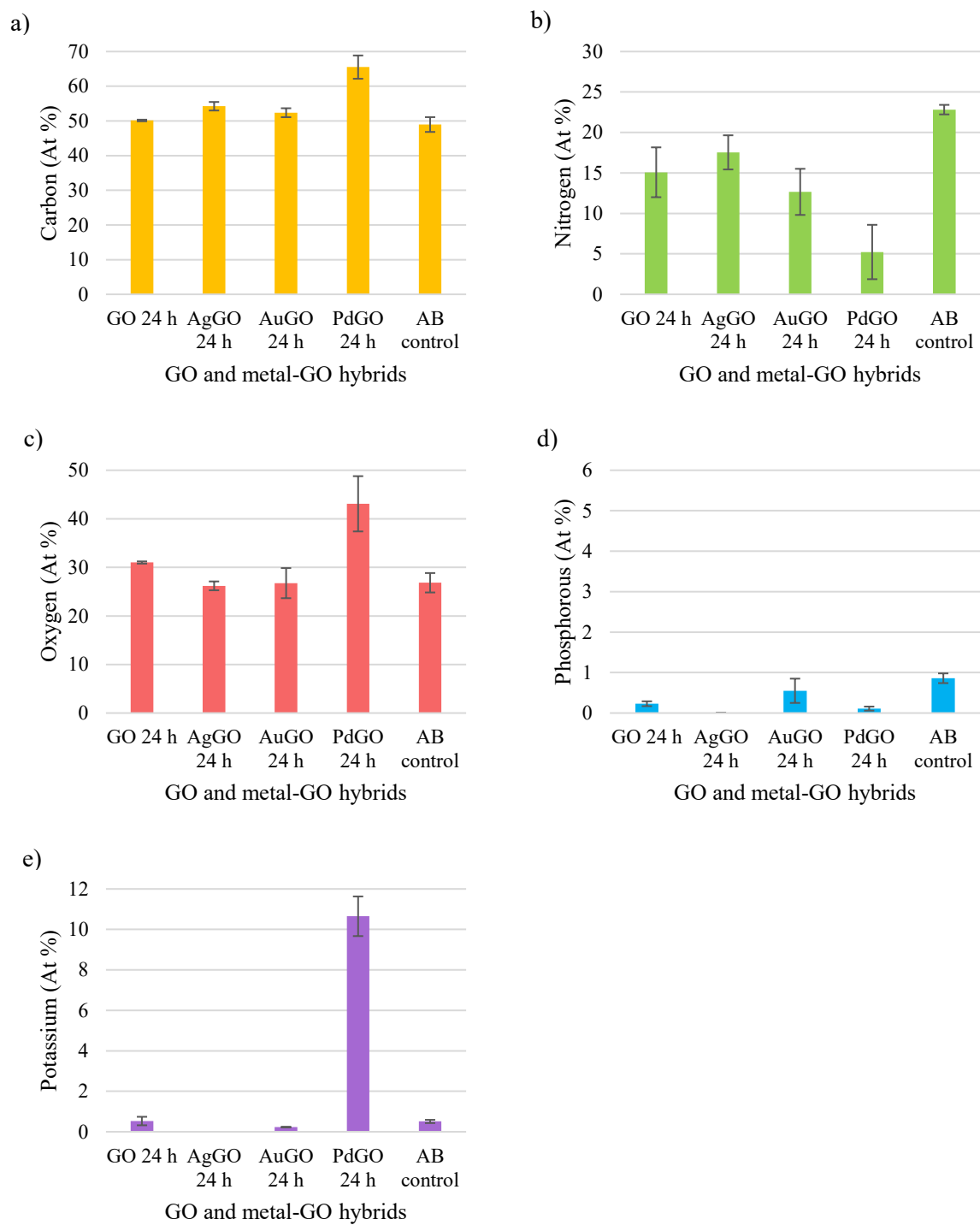
### *E. faecium*

Against *E. faecium* in the absence of plasma CF, the control elemental At % were 46 % for carbon, 24 % for nitrogen, 30 % for oxygen, 0.29 % for phosphorous and 0.4 % for potassium. Changes in carbon (55 %) and nitrogen (16 %) At % were noted for AuGO and AgGO compared to the control. Moreover, AuGO demonstrated the maximum effects on At % of oxygen (25 %) and phosphorous (0.8 %). The potassium content disappeared after AgGO, AuGO and PdGO treatment (Figure 4.7, a-e).

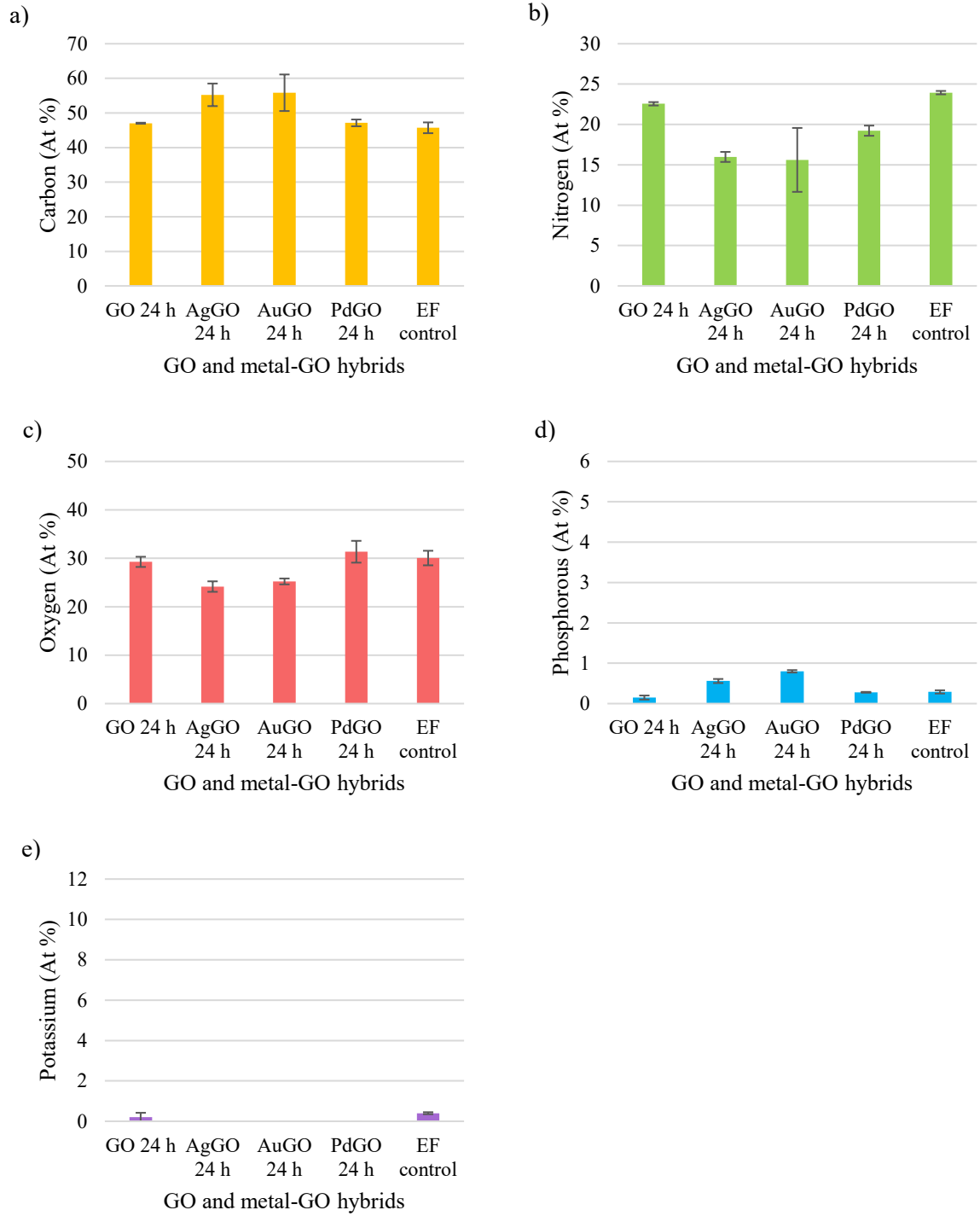
In summary, AgGO against *K. pneumoniae* and *E. faecium* and PdGO against *A. baumannii* demonstrated the greatest elemental changes. The least At % effects were noted for AuGO against *K. pneumoniae*, AgGO against *A. baumannii* and GO against *E. faecium*.



**Figure 4.5.** The EDAX results against *K. pneumoniae* in the absence of 10 % plasma conditioning film signifying elemental changes after GO, AgGO, AuGO and PdGO treatment at 24 h. a) At % of carbon, b) At % of nitrogen, c) At % of oxygen, d) At % of phosphorous; e) At % of potassium (n = 3).



**Figure 4.6.** The EDAX results against *A. baumannii* in the absence of 10 % plasma conditioning film signifying elemental changes after GO, AgGO, AuGO and PdGO treatment at 24 h. a) At % of carbon, b) At % of nitrogen, c) At % of oxygen, d) At % of phosphorous; e) At % of potassium (n = 3).



**Figure 4.7.** The EDAX results against *E. faecium* in the absence of 10 % plasma conditioning film signifying elemental changes GO, AgGO, AuGO and PdGO treatment at 24 h. a) At % of carbon, b) At % of nitrogen, c) At % of oxygen, d) At % of phosphorous; e) At % of potassium (n = 3).



#### **4.3.2. Elemental changes against *Klebsiella pneumoniae*, *A. baumannii* and *E. faecium* after GO, AgGO, AuGO and PdGO 24 h treatment in the presence of 10 % bovine plasma conditioning film**

The EDAX analysis results were presented for an average of three atomic percentage (At %) for untreated cells and treated with GO, AgGO, AuGO and PdGO at 24 h.

##### *K. pneumoniae*

Against *K. pneumoniae* in the presence of CF, the control elemental At % were 55 % for carbon, 16 % for nitrogen, 28 % for oxygen, 0.32 % for phosphorous and 0.85 % for potassium. Compared with the control, AgGO demonstrated the greatest effects in the At % of carbon (59 %), nitrogen (11 %), oxygen (22 %) and phosphorous (0.01 %). The greatest potassium change was demonstrated for GO (1.1 %). Moreover, GO demonstrated an effect on At % of carbon (56 %), nitrogen (20 %) and oxygen (23 %). The phosphorous and potassium content disappeared after PdGO and AuGO and PdGO treatment respectively (Figure 4.8, a-e).

##### *A. baumannii*

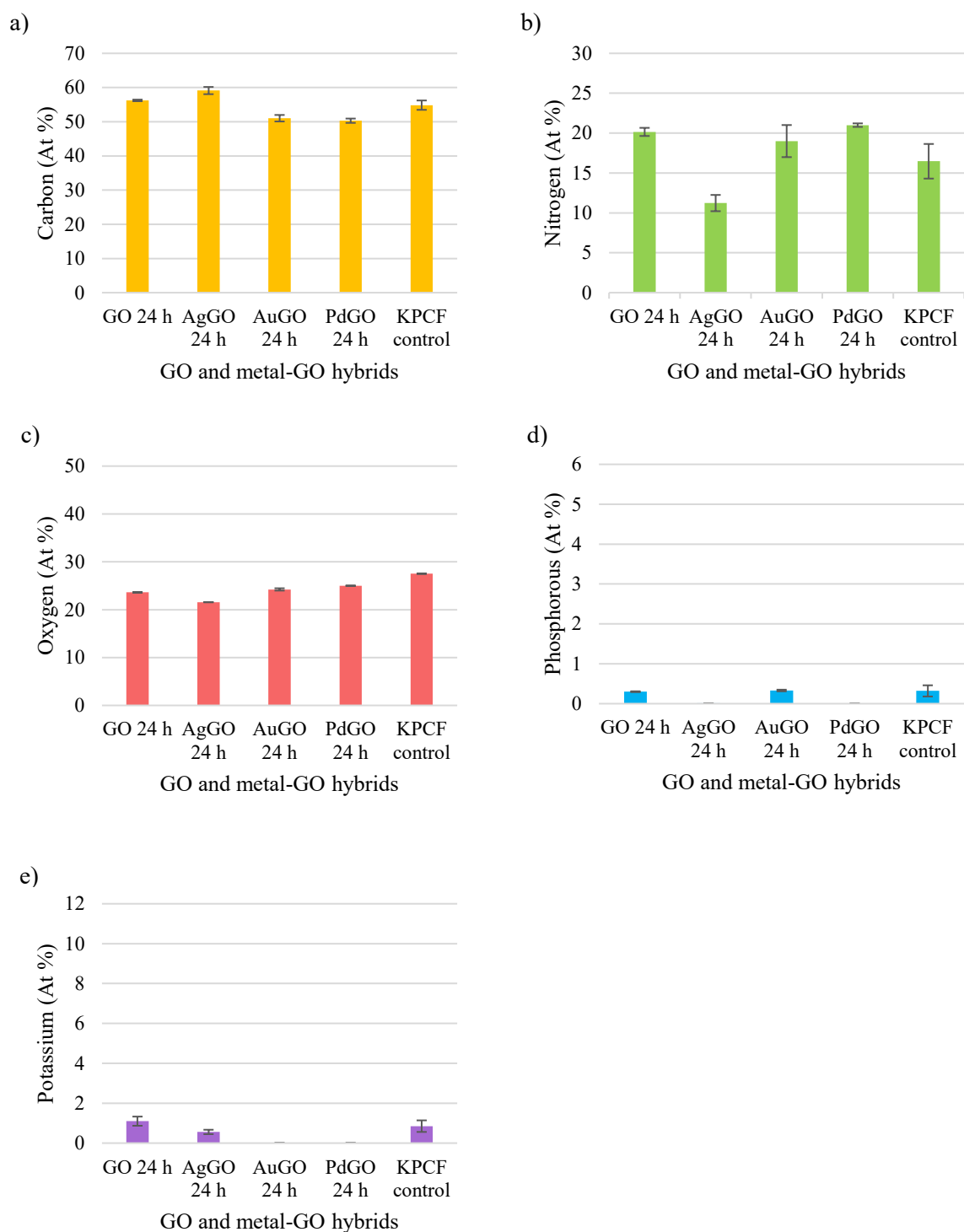
Against *A. baumannii* in the presence of plasma CF, the control elemental At % was 54 % for carbon, 17 % for nitrogen, 28 % for oxygen, 0.09 % for phosphorous and 0.52 % for potassium. Large changes were demonstrated for PdGO treated bacterial cells with At % for carbon = 62 %, nitrogen = 6 %, oxygen = 39 %, phosphorous = 0 % and potassium = 11 % compared with control. A noteworthy change was demonstrated for AuGO in At % of nitrogen (11 %). The potassium and phosphorous content disappeared after AuGO and PdGO treatment respectively. No change was found in the At % of oxygen (26 %) with GO and nitrogen (17 %) for GO and AgGO treatment (Figure 4.9, a-e).

##### *E. faecium*

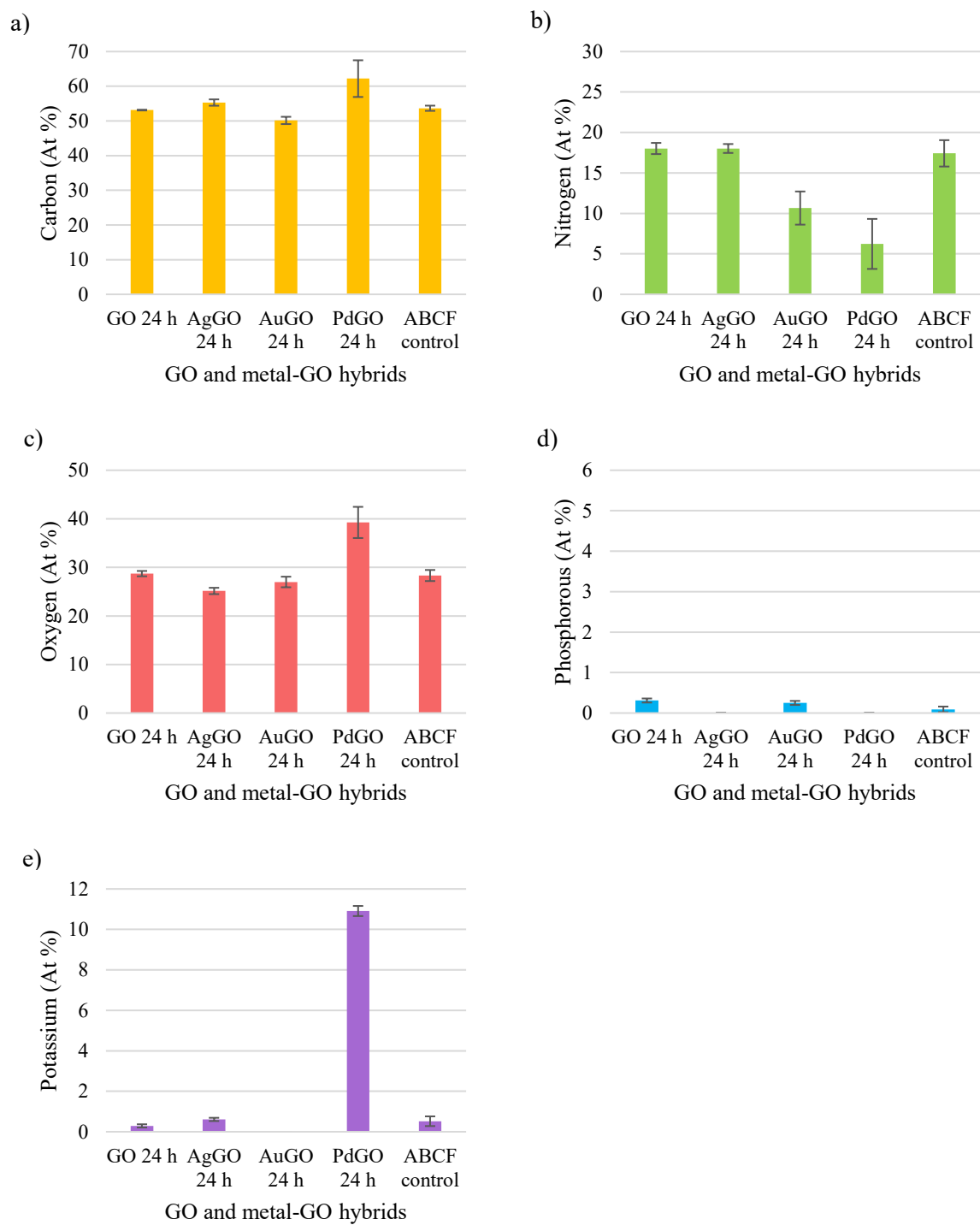
Against *E. faecium* in the presence of plasma CF, the control elemental At % were 52 % for carbon, 20 % for nitrogen, 27 % for oxygen, 0.75 % for phosphorous and 0.17 % for potassium.

Changes in the content of carbon (53 %), nitrogen (14 %) and phosphorous (5 %) At % changes was noted for AgGO compared to control. The maximum oxygen At % effect was noted for PdGO (35 %). Moreover, AuGO demonstrated good elemental effects on At % of N (15 %). The potassium content disappeared after AgGO, AuGO and PdGO treatment (Figure 4.10, a-e).

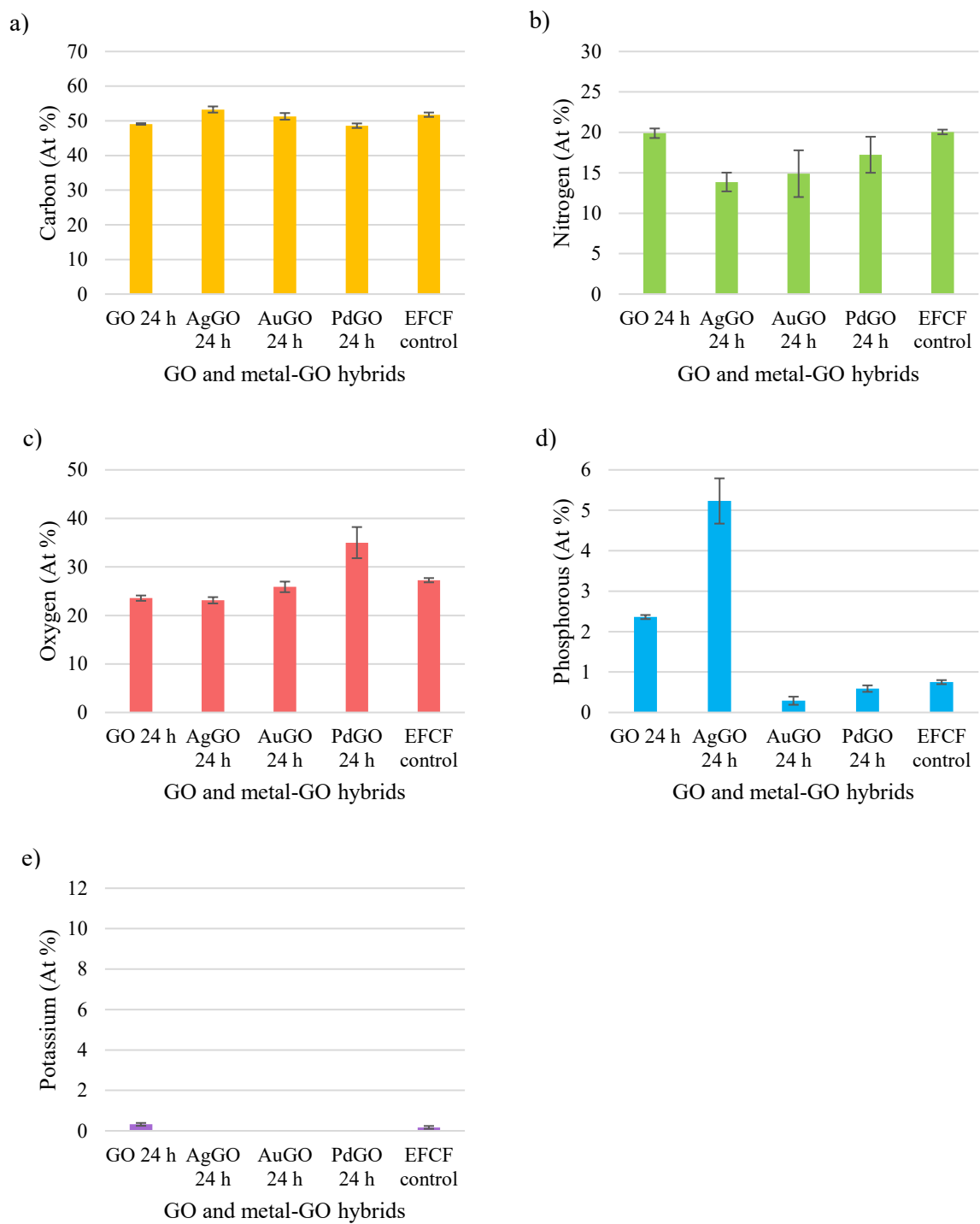
In summary, AgGO against *K. pneumoniae* and *E. faecium* and PdGO against *A. baumannii* demonstrated the best elemental changes. The least At % effects were noted for AuGO against *K. pneumoniae*, GO against *A. baumannii* and *E. faecium*. Moreover, some of the GO and metal-GO showed variance in the elemental effects in the presence of plasma CF compared to absence of CF.



**Figure 4.8.** The EDAX results against *K. pneumoniae* in the presence of 10 % plasma conditioning film signifying elemental changes after GO, AgGO, AuGO and PdGO treatment at 24 h. a) At % of carbon, b) At % of nitrogen, c) At % of oxygen, d) At % of phosphorous; e) At % of potassium (n = 3).



**Figure 4.9.** The EDAX results against *A. baumannii* in the presence of 10 % plasma conditioning film signifying elemental changes after GO, AgGO, AuGO and PdGO treatment at 24 h. a) At % of carbon, b) At % of nitrogen, c) At % of oxygen, d) At % of phosphorous; e) At % of potassium (n = 3).



**Figure 4.10.** The EDAX results against *E. faecium* in the presence of 10 % plasma conditioning film signifying elemental changes after GO, AgGO, AuGO and PdGO treatment at 24 h. a) At % of carbon, b) At % of nitrogen, c) At % of oxygen, d) At % of phosphorous; e) At % of potassium (n = 3).

#### 4.4. Chemical changes observed using Raman Spectroscopy

##### 4.4.1. Chemical changes for *K. pneumoniae*, *A. baumannii* and *E. faecium* after GO, AgGO, AuGO and PdGO at 24 h treatment in the absence of 10 % bovine plasma conditioning film

The spectral profiles attributed to cell biomolecules were CH stretch ( $2920\text{ cm}^{-1}$  -  $2960\text{ cm}^{-1}$ ), proteins (C-N stretch:  $760\text{ cm}^{-1}$  –  $810\text{ cm}^{-1}$ ), lipids ( $\text{CH}_2$  and  $\text{CH}_3$  bending:  $1440\text{ cm}^{-1}$  –  $1470\text{ cm}^{-1}$ ) and amides ( $1620\text{ cm}^{-1}$  -  $1680\text{ cm}^{-1}$ ). The chemical effects on bacteria for GO and metal-GO hybrids were analysed by comparing with bacterial control.

##### *K. pneumoniae*

Against *K. pneumoniae* in the absence of plasma CF, the band shifts noted for control were  $2952\text{ cm}^{-1}$  for CH bond,  $1671\text{ cm}^{-1}$  for amide,  $1442\text{ cm}^{-1}$  for  $\text{CH}_2 / \text{CH}_3$  bending,  $1085\text{ cm}^{-1}$  for C-O stretch and  $784\text{ cm}^{-1}$  for C-N stretch. The maximum band shifts were noted for AgGO treated bacteria ( $2932\text{ cm}^{-1}$  for CH bond,  $1661\text{ cm}^{-1}$  for amide,  $1460\text{ cm}^{-1}$  for  $\text{CH}_2 / \text{CH}_3$  bending,  $1099\text{ cm}^{-1}$  for C-O stretch and  $755\text{ cm}^{-1}$  for C-N stretch). No effect was demonstrated in the  $\text{CH}_2 / \text{CH}_3$  bending for AuGO treated bacteria. A noteworthy shift was demonstrated with PdGO treatment in the CH bond ( $2938\text{ cm}^{-1}$ ), amide ( $1665\text{ cm}^{-1}$ ), C-O ( $1091\text{ cm}^{-1}$ ) and C-N ( $765\text{ cm}^{-1}$ ). The minimal shift was noted for CH bond ( $2940\text{ cm}^{-1}$ ), amide ( $1668\text{ cm}^{-1}$ ), C-O ( $1095\text{ cm}^{-1}$ ) and C-N ( $772\text{ cm}^{-1}$ ) with GO treated bacteria (Figure 4.11, a-e).

##### *A. baumannii*

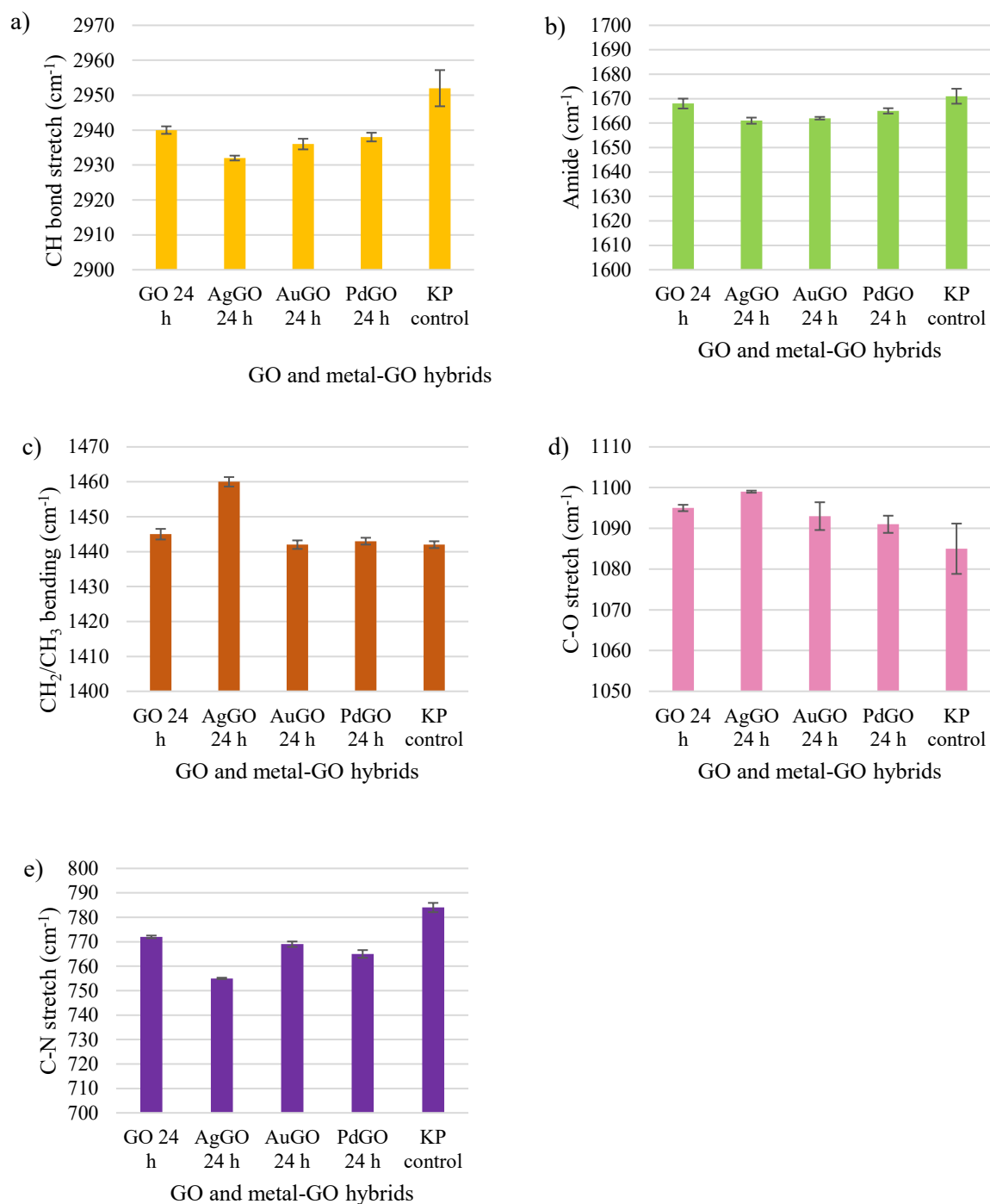
Against *A. baumannii* in the absence of plasma CF, the band shift noted for control were  $2937\text{ cm}^{-1}$  for CH bond,  $1664\text{ cm}^{-1}$  for amide,  $1446\text{ cm}^{-1}$  for  $\text{CH}_2 / \text{CH}_3$  bending,  $1096\text{ cm}^{-1}$  for C-O stretch and  $792\text{ cm}^{-1}$  for C-N stretch. The maximum band shifts were noted for AgGO treated bacteria with  $2930\text{ cm}^{-1}$  for CH bond,  $1658\text{ cm}^{-1}$  for amide,  $1462\text{ cm}^{-1}$  for  $\text{CH}_2 / \text{CH}_3$  bending,  $1081\text{ cm}^{-1}$  for C-O stretch and  $742\text{ cm}^{-1}$  for C-N stretch. A noteworthy shift was demonstrated in the C-N stretch with GO ( $779\text{ cm}^{-1}$ ), AuGO ( $765\text{ cm}^{-1}$ ) and PdGO ( $774\text{ cm}^{-1}$ ) treatment. The

minimal shifts were noted for CH bond ( $2936\text{ cm}^{-1}$ ) and amide ( $1664\text{ cm}^{-1}$ ) with AuGO and for  $\text{CH}_2 / \text{CH}_3$  bending ( $1445\text{ cm}^{-1}$ ), C-O ( $1095\text{ cm}^{-1}$ ) and C-N ( $774\text{ cm}^{-1}$ ) with PdGO treated bacteria (Figure 4.12, a-e).

#### *E. faecium*

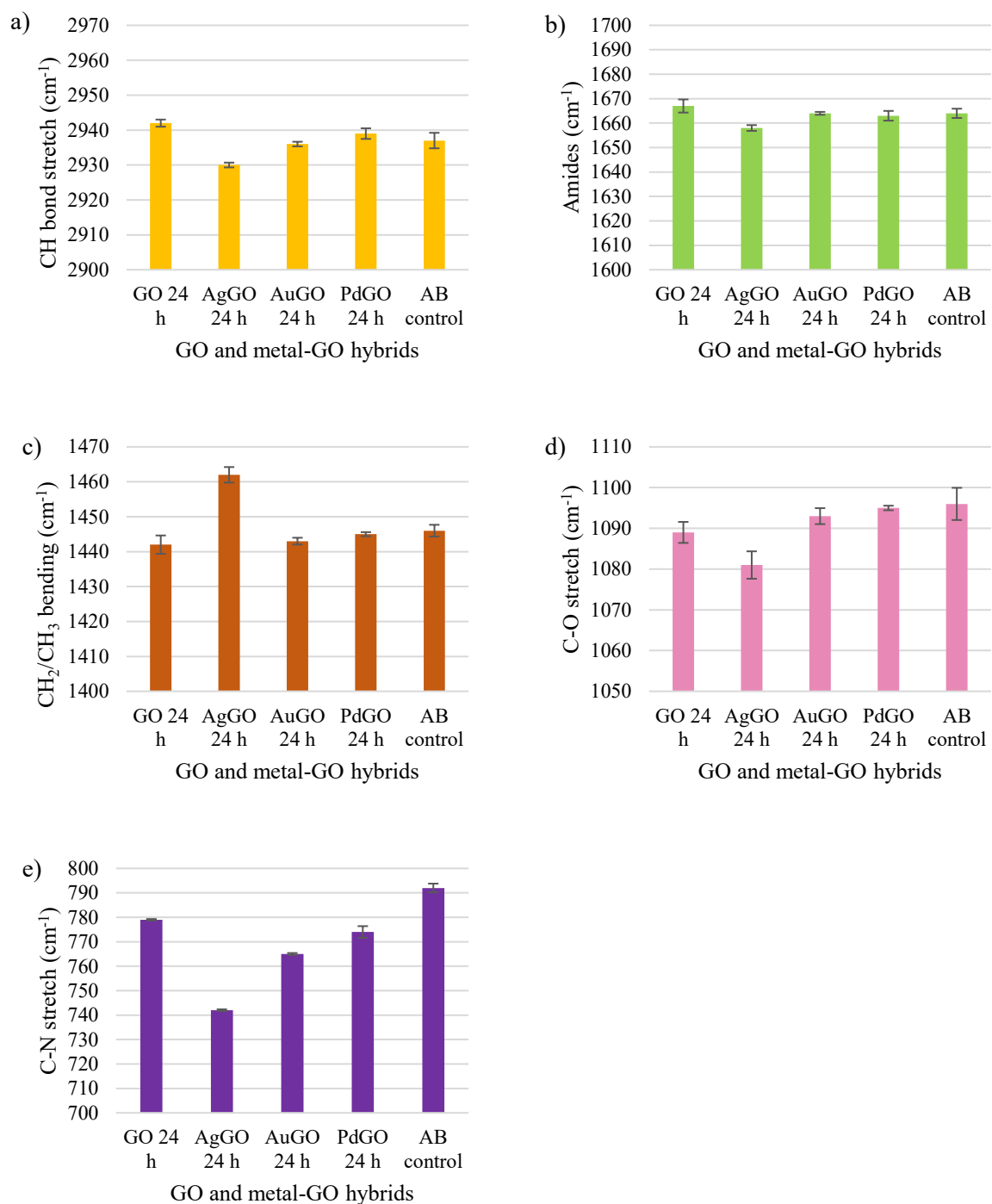
Against *E. faecium* in the absence of CF, the band shift noted for control were  $2936\text{ cm}^{-1}$  for CH bond,  $1658\text{ cm}^{-1}$  for amide,  $1450\text{ cm}^{-1}$  for  $\text{CH}_2 / \text{CH}_3$  bending,  $1097\text{ cm}^{-1}$  for C-O stretch and  $787\text{ cm}^{-1}$  for C-N stretch. The most chemical band shifts were demonstrated with PdGO treated bacterial cells compared to control (CH bond =  $2945\text{ cm}^{-1}$ , amide =  $1640\text{ cm}^{-1}$ ,  $\text{CH}_2/\text{CH}_3$  bending =  $1439\text{ cm}^{-1}$ , C-O stretch =  $1088\text{ cm}^{-1}$  and C-N stretch =  $760\text{ cm}^{-1}$ ). Moreover, AgGO demonstrated strong chemical effects with band shift of  $2945\text{ cm}^{-1}$  for CH bond,  $1642\text{ cm}^{-1}$  for amide,  $1460\text{ cm}^{-1}$  for  $\text{CH}_2/\text{CH}_3$  bending,  $1089\text{ cm}^{-1}$  for C-O stretch and  $762\text{ cm}^{-1}$  for C-N stretch. The least C-N stretch band shift was demonstrated with GO ( $781\text{ cm}^{-1}$ ). Whilst, AuGO was least effective for CH bond ( $2935\text{ cm}^{-1}$ ), amide ( $1660\text{ cm}^{-1}$ ), C-O ( $1095\text{ cm}^{-1}$ ) and  $\text{CH}_2/\text{CH}_3$  bending ( $1445\text{ cm}^{-1}$ ) shifts (Figure 4.13, a-e).

In summary, AgGO against *K. pneumoniae* and *A. baumannii* and PdGO against *E. faecium* showed the maximum chemical changes, whilst, GO against *K. pneumoniae*, AuGO and PdGO against *A. baumannii* and AuGO against *E. faecium* showed the minimal chemical change.

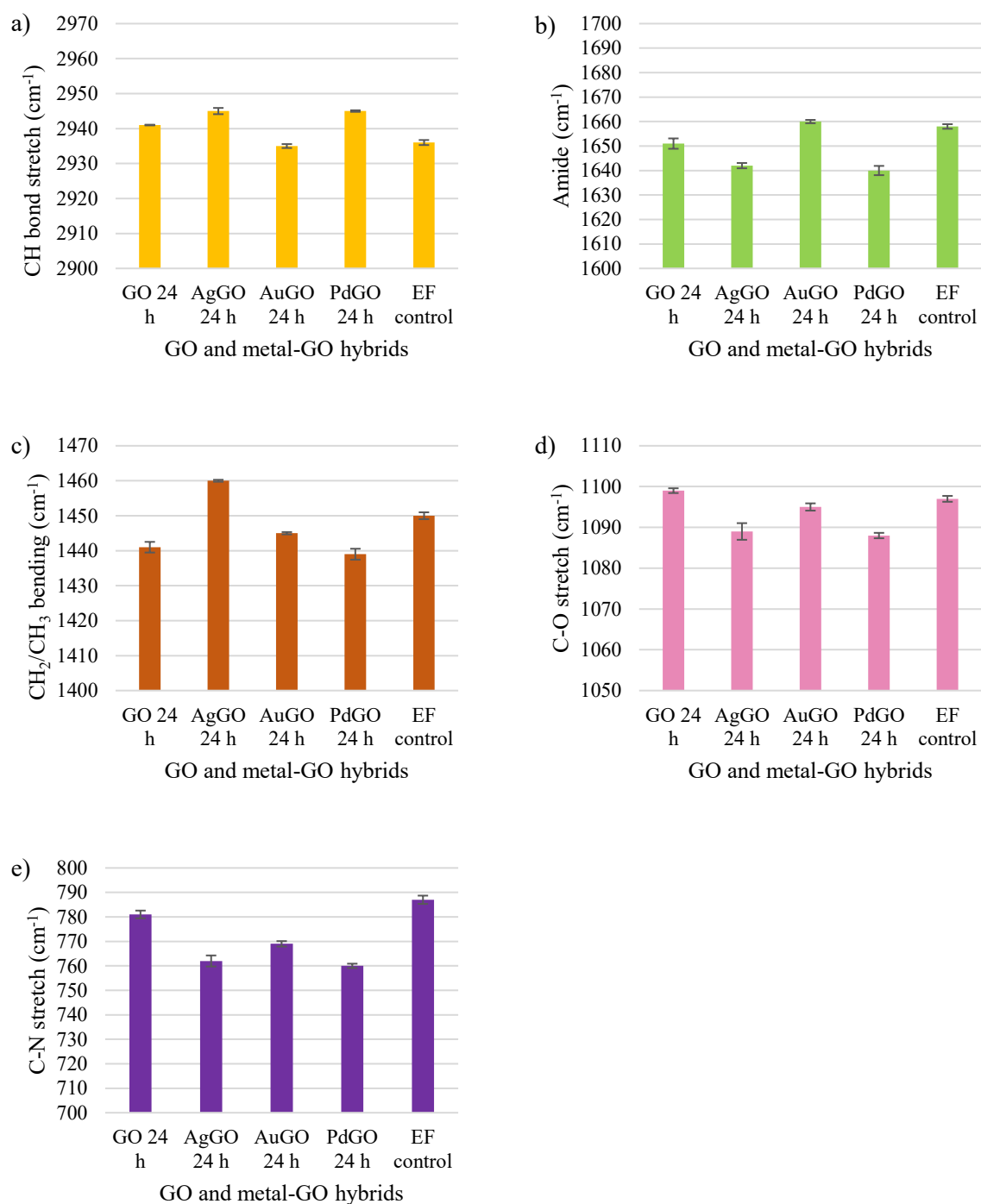


**Figure 4.11.** Raman spectral bands shifts (cm<sup>-1</sup>) and their assignments for *K. pneumoniae* control and after treatment with GO, AgGO, AuGO and PdGO at 24 h in the absence of 10 % plasma conditioning film; a) CH bond shift, b) Amides shift, c) CH<sub>2</sub> / CH<sub>3</sub> bending shift, d) C-O stretch; e) C-N stretch shift (n = 3).





**Figure 4.12.** Raman spectral bands shifts (cm<sup>-1</sup>) and their assignments for *A. baumannii* control and after treatment with GO, AgGO, AuGO and PdGO at 24 h in the absence of 10 % plasma conditioning film; a) CH bond shift, b) Amides shift, c) CH<sub>2</sub> / CH<sub>3</sub> bending shift, d) C-O stretch; e) C-N stretch shift (n = 3).



**Figure 4.13.** Raman spectral bands shifts (cm<sup>-1</sup>) and their assignments for *E. faecium* control and after GO, AgGO, AuGO and PdGO treatment at 24 h in the absence of 10 % plasma conditioning film; a) CH bond shift, b) Amides shift, c) CH<sub>2</sub> / CH<sub>3</sub> bending shift, d) C-O stretch; e) C-N stretch shift (n = 3).

#### **4.4.2. Chemical changes observed using Raman Spectroscopy for *Klebsiella pneumoniae*, *A. baumannii* and *E. faecium* after GO, AgGO, AuGO and PdGO at 24 h treatment in the presence of 10 % bovine plasma conditioning film**

The spectral profile attributed to cell biomolecules were CH stretch ( $2920\text{ cm}^{-1}$  -  $2960\text{ cm}^{-1}$ ), proteins (C-N stretch:  $760\text{ cm}^{-1}$  –  $810\text{ cm}^{-1}$ ), lipids ( $\text{CH}_2$  and  $\text{CH}_3$  bending:  $1440\text{ cm}^{-1}$  –  $1470\text{ cm}^{-1}$ ) and amides ( $1620\text{ cm}^{-1}$  -  $1680\text{ cm}^{-1}$ ). The chemical effects on bacteria for GO and metal-GO were analysed by comparing with bacterial control.

##### *K. pneumoniae*

Against *K. pneumoniae* in the presence of plasma CF, the band shifts noted for control were  $2943\text{ cm}^{-1}$  for CH bond,  $1677\text{ cm}^{-1}$  for amide,  $1446\text{ cm}^{-1}$  for  $\text{CH}_2 / \text{CH}_3$  bending,  $1095\text{ cm}^{-1}$  for C-O stretch and  $785\text{ cm}^{-1}$  for C-N stretch. The maximum band shifts were noted for AgGO treated bacteria ( $2930\text{ cm}^{-1}$  for CH bond,  $1665\text{ cm}^{-1}$  for amide,  $1462\text{ cm}^{-1}$  for  $\text{CH}_2 / \text{CH}_3$  bending,  $1099\text{ cm}^{-1}$  for C-O stretch and  $752\text{ cm}^{-1}$  for C-N stretch). A noteworthy shift was demonstrated with PdGO and AuGO treated bacteria. The minimal shift was noted for CH bond ( $2940\text{ cm}^{-1}$ ), amide ( $1666\text{ cm}^{-1}$ ), C-O ( $1091\text{ cm}^{-1}$ ) and C-N ( $775\text{ cm}^{-1}$ ) with GO treated bacteria (Figure 4.14, a-e).

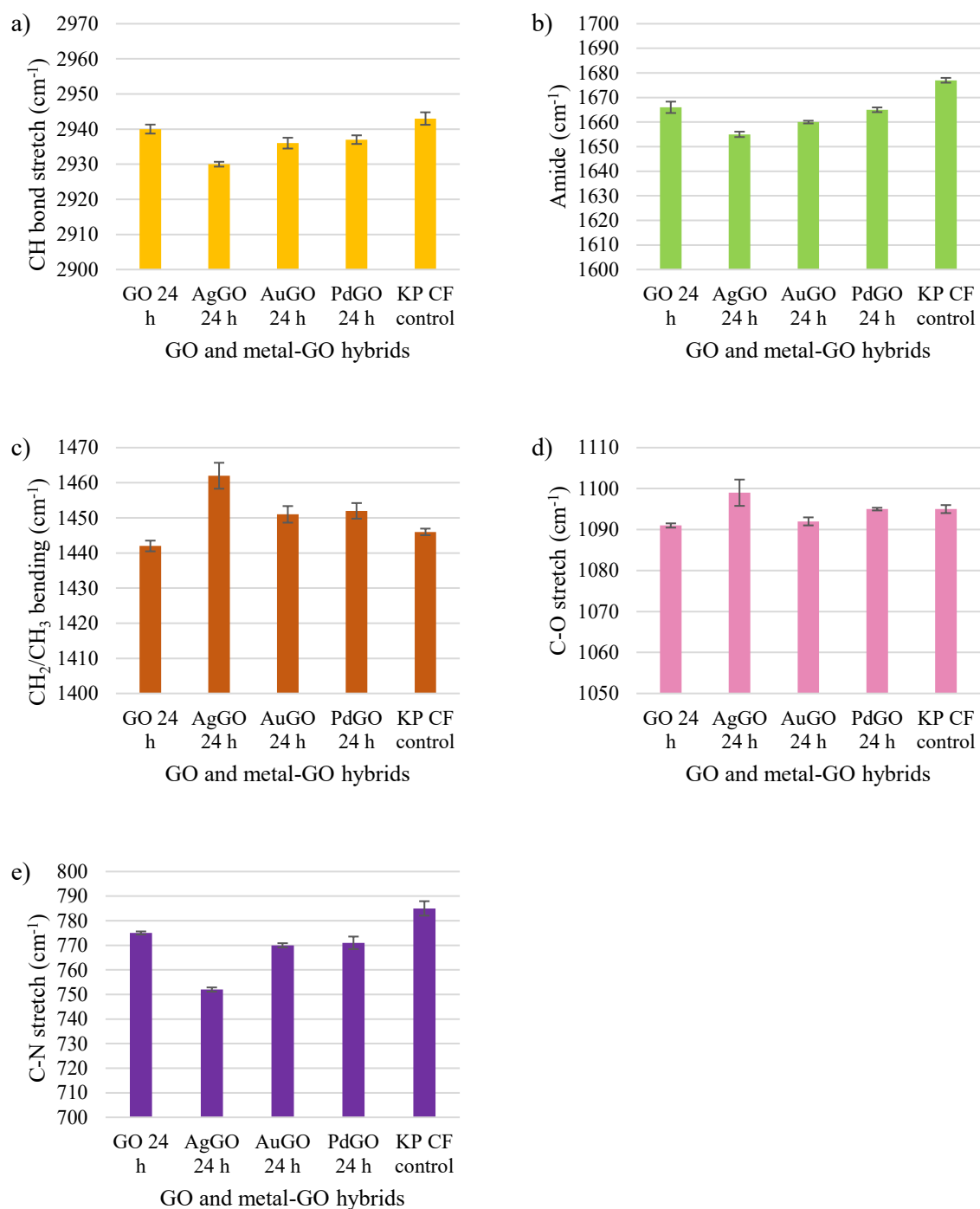
##### *A. baumannii*

Against *A. baumannii* in the presence of plasma CF, the band shift noted for control were  $2935\text{ cm}^{-1}$  for CH bond,  $1662\text{ cm}^{-1}$  for amide,  $1447\text{ cm}^{-1}$  for  $\text{CH}_2 / \text{CH}_3$  bending,  $1099\text{ cm}^{-1}$  for C-O stretch and  $782\text{ cm}^{-1}$  for C-N stretch. The maximum band shifts were noted for AgGO treated bacteria with  $2929\text{ cm}^{-1}$  for CH bond,  $1653\text{ cm}^{-1}$  for amide,  $1465\text{ cm}^{-1}$  for  $\text{CH}_2 / \text{CH}_3$  bending,  $1085\text{ cm}^{-1}$  for C-O stretch and  $748\text{ cm}^{-1}$  for C-N stretch. The minimal shifts were noted for CH bond ( $2934\text{ cm}^{-1}$ ), amide ( $1662\text{ cm}^{-1}$ ),  $\text{CH}_2 / \text{CH}_3$  bending ( $1448\text{ cm}^{-1}$ ), C-O ( $1096\text{ cm}^{-1}$ ) and with PdGO and C-N ( $781\text{ cm}^{-1}$ ) with GO treated bacteria (Figure 4.15, a-e).

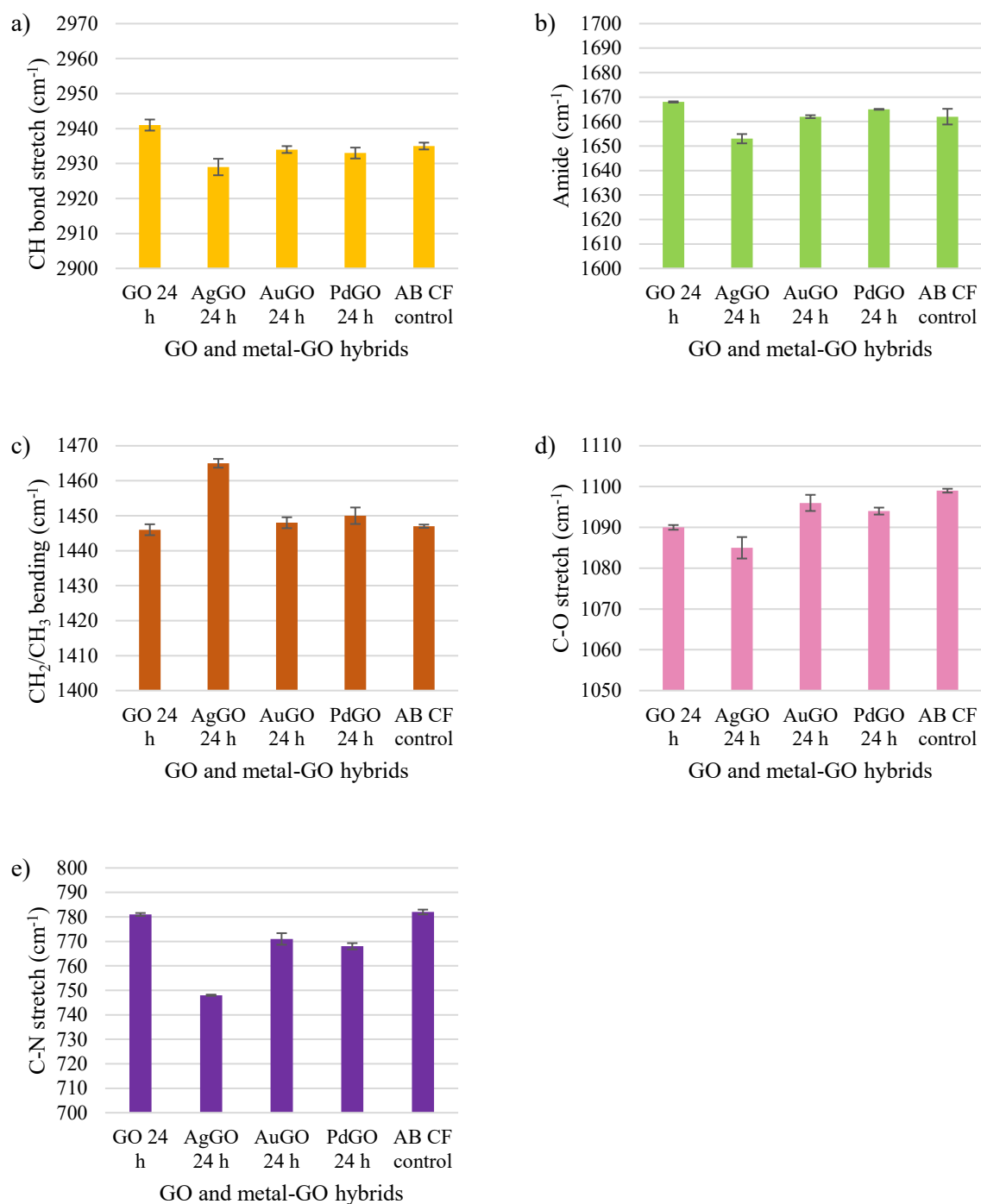
### *E. faecium*

Against *E. faecium* in the presence of plasma CF, the band shift noted for control were 2933  $\text{cm}^{-1}$  for CH bond, 1653  $\text{cm}^{-1}$  for amide, 1452  $\text{cm}^{-1}$  for  $\text{CH}_2 / \text{CH}_3$  bending, 1097  $\text{cm}^{-1}$  for C-O stretch and 783  $\text{cm}^{-1}$  for C-N stretch. The greatest chemical band shifts were demonstrated with PdGO treated bacterial cells compared to control (CH bond = 2948  $\text{cm}^{-1}$ , amide = 1641  $\text{cm}^{-1}$ ,  $\text{CH}_2/\text{CH}_3$  bending = 1438  $\text{cm}^{-1}$ , C-O stretch = 1084  $\text{cm}^{-1}$  and C-N stretch = 761  $\text{cm}^{-1}$ ). Moreover, AgGO demonstrated strong chemical effects with band shift of 2942  $\text{cm}^{-1}$  for CH bond, 1640  $\text{cm}^{-1}$  for amide, 1468  $\text{cm}^{-1}$  for  $\text{CH}_2/\text{CH}_3$  bending, 1089  $\text{cm}^{-1}$  for C-O stretch and 765  $\text{cm}^{-1}$  for C-N stretch. Whilst, AuGO was least effective for CH bond (2934  $\text{cm}^{-1}$ ), C-O (1094  $\text{cm}^{-1}$ ). The minimal band shift change was demonstrated with GO treated bacteria for amide (1656  $\text{cm}^{-1}$ ) and C-N stretch (780  $\text{cm}^{-1}$ ) (Figure 4.16, a-e).

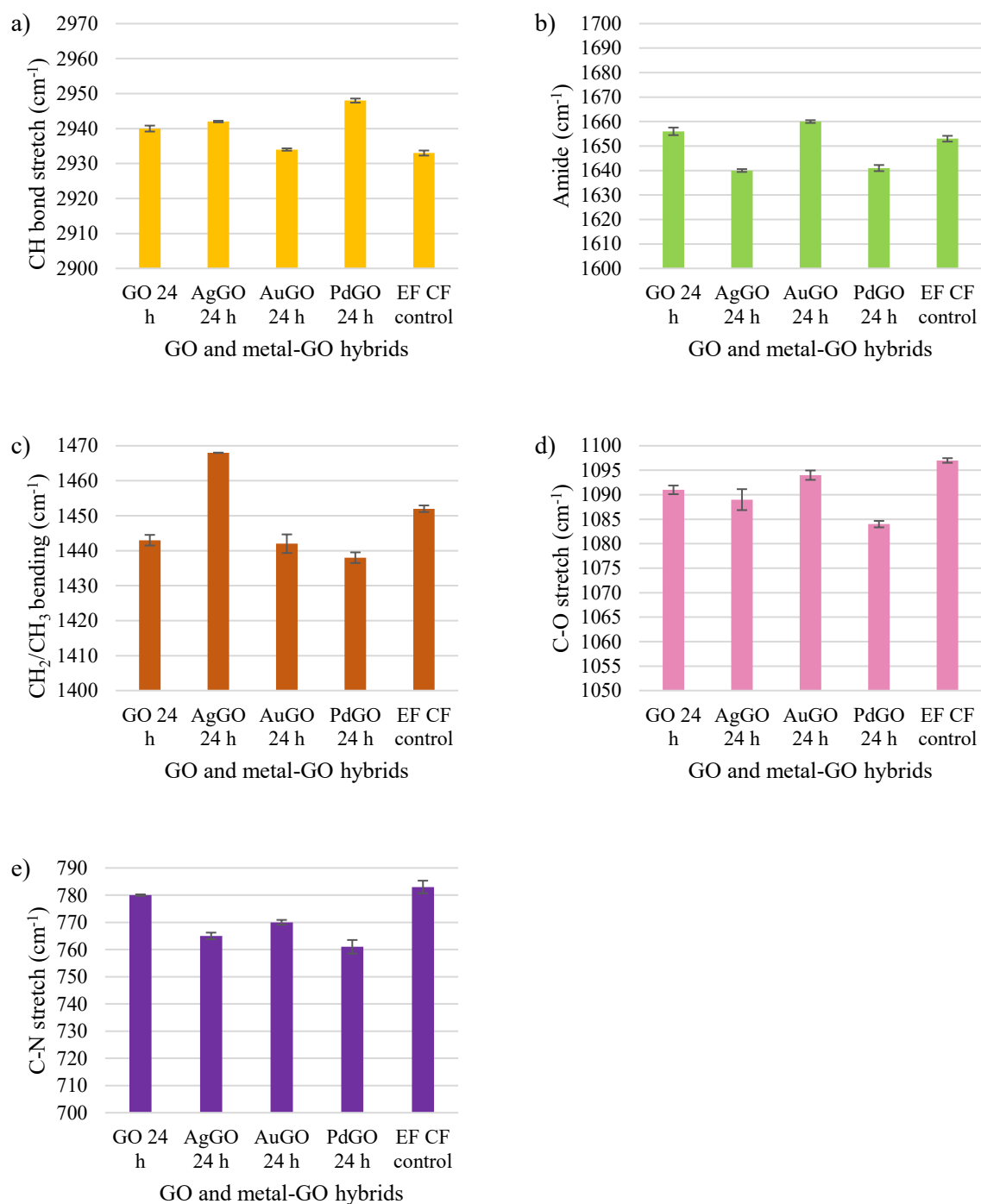
In summary, AgGO against *K. pneumoniae* and *A. baumannii* and PdGO against *E. faecium* showed the maximum chemical change, whilst, GO against *K. pneumoniae*, AuGO against *A. baumannii* and GO against *E. faecium* showed the minimal chemical change. Moreover, some of the GO and metal-GO showed differences in the chemical bondings in the presence of plasma CF compared to absence of CF.



**Figure 4.14.** Raman spectral bands shifts (cm<sup>-1</sup>) and their assignments for *K. pneumoniae* control and after GO, AgGO, AuGO and PdGO treatment at 24 h in the presence of 10 % plasma conditioning film; a) CH bond shift, b) Amides shift, c) CH<sub>2</sub> / CH<sub>3</sub> bending shift, d) C-O stretch; e) C-N stretch shift (n = 3).



**Figure 4.15.** Raman spectral bands shifts (cm<sup>-1</sup>) and their assignments for *A. baumannii* control and after GO, AgGO, AuGO and PdGO treatment at 24 h in the presence of 10 % plasma conditioning film; a) CH bond shift, b) Amides shift, c) CH<sub>2</sub> / CH<sub>3</sub> bending shift, d) C-O stretch; e) C-N stretch shift (n = 3).



**Figure 4.16.** Raman spectral bands shifts ( $\text{cm}^{-1}$ ) and their assignments for *E. faecium* control and after GO, AgGO, AuGO and PdGO treatment at 24 h in the presence of 10 % plasma conditioning film; a) CH bond shift, b) Amides shift, c)  $\text{CH}_2 / \text{CH}_3$  bending shift, d) C-O stretch; e) C-N stretch shift ( $n = 3$ ).

#### **4.4. Discussion**

As described in chapter 3 discussion of elemental and chemical changes, there are significant changes on chemical and At % of elements of bacteria after GBCs treatment. This as described before in sub-section of EDAX and Raman results of chapter 3, can affect the integral cell components of bacteria that might lead to its damage / destruction. Thus, in presence or absence of CFs, GBCs can also damage at molecular level.



#### **4.5. Antimicrobial efficacies for eight combined GO and metal-GO hybrids against *K. pneumoniae*, *A. baumannii* and *E. faecium***

##### **4.5.1 Zone of inhibition for combined GO and metal-GO hybrids with and without 10 % bovine plasma conditioning film**

The combined effects of the GOAgGO, GOCuGO, GOAuGO, GOPdGO, AgGOCuGO, AgGOAuGO, AgGOPdGO, CuGOAuGO, CuGOPdGO and AuGOPdGO was evaluated using the ZoI combination test in the presence and absence of 10 % bovine plasma CF. All the tested combinations demonstrated an indifferent effect with the inhibition grade of 1 (0 – 4 mm). No tested combination showed antagonist, additive or synergistic effects (Table 4.11).

**Table 4.11.** The ZoI combination assay for interactions type and inhibition grade of GO and metal-GO hybrids combination against *K. pneumoniae*, *A. baumannii* and *E. faecium* in the absence and presence of 10 % plasma. The inhibition zones were graded from 0 to 4, which measured as, 0–4 mm = grade 0, 4–8 mm = grade 1, 8–12 mm = grade 2, 12–16 mm = grade 3 and 16–20 mm = grade 4 (n = 24).

Metal combinations	Type of combination and grade of inhibition		
	<i>K. pneumoniae</i>	<i>A. baumannii</i>	<i>E. faecium</i>
<b>GOAgGO</b>	Indifference Grade GO(1) AgGO(1)	Indifference Grade GO(1) AgGO(1)	Indifference Grade GO(1) AgGO(1)
<b>GOCuGO</b>	Indifference Grade GO(1) CuGO(1)	Indifference Grade GO(1) CuGO(1)	Indifference Grade GO(1) CuGO(1)
<b>GOAuGO</b>	Indifference Grade GO(1) AuGO(1)	Indifference Grade GO(1) AuGO(1)	Indifference Grade GO(1) AuGO(1)
<b>GOPdGO</b>	Indifference Grade GO(1) CuGO(1)	Indifference Grade GO(1) CuGO(1)	Indifference Grade GO(1) CuGO(1)
<b>AgGOCuGO</b>	Indifference Grade AgGO(1) CuGO(1)	Indifference Grade AgGO(1) CuGO(1)	Indifference Grade AgGO(1) CuGO(1)
<b>AgGOAuGO</b>	Indifference Grade AgGO(1) AuGO(1)	Indifference Grade AgGO(1) AuGO(1)	Indifference Grade AgGO(1) AuGO(1)
<b>AgGOPdGO</b>	Indifference Grade AgGO(1) PdGO(1)	Indifference Grade AgGO(1) PdGO(1)	Indifference Grade AgGO(1) PdGO(1)
<b>CuGOAuGO</b>	Indifference Grade CuGO(1) AuGO(1)	Indifference Grade CuGO(1) AuGO(1)	Indifference Grade CuGO(1) AuGO(1)
<b>CuGOPdGO</b>	Indifference Grade CuGO(1) PdGO(1)	Indifference Grade CuGO(1) PdGO(1)	Indifference Grade CuGO(1) PdGO(1)
<b>AuGOPdGO</b>	Indifference Grade AuGO(1) PdGO(1)	Indifference Grade AuGO(1) PdGO(1)	Indifference Grade AuGO(1) PdGO(1)

#### **4.5.2. Fractional inhibitory concentration (FIC) for combined GO and metal-GO hybrids in 2:1, 1:1 and 1:2 ratios in the absence and presence of 10 % bovine plasma conditioning film**

The FIC was used to determine the synergistic inhibitory antimicrobial efficacy of the GO and metal-GO hybrids combination in the presence and absence of 10 % bovine plasma CF. The FIC was performed in 2:1, 1:1 and 1:2 ratios.

##### **4.5.2.1. FIC against *K. pneumoniae*, *A. baumannii* and *E. faecium* in the absence of 10 % bovine plasma conditioning film**

###### *K. pneumoniae*

Against *K. pneumoniae*, GOAuGO, GOPdGO and AuGOPdGO combinations demonstrated additive effects ( $FIC = > 0.5$  and  $\leq 1.0$ ) in all the tested ratios. The least active antimicrobial combinations which demonstrated indifferent effects were the AgGO combination with CuGO, AuGO and PdGO (Table 4.12).

###### *A. baumannii*

Against *A. baumannii*, AuGOPdGO in 1:2 and 1:1 and CuGO in combination with GO, AuGO and PdGO in 1:1 ratio demonstrated an additive efficacy ( $FIC = > 0.5$  and  $\leq 1.0$ ). All the remaining combinations demonstrated indifferent efficacy ( $FIC = > 1.0$  and  $\leq 4.0$ ) (Table 4.13).

###### *E. faecium*

Against *E. faecium*, GO in combination with CuGO and AuGO demonstrated a strong antimicrobial efficacy with synergistic interactions in 2:1 and 1:2 ratios ( $FIC \leq 0.5$ ) and an additive antimicrobial effect in 1:1 ratio ( $FIC = > 0.5$  and  $\leq 1.0$ ). The GOAgGO demonstrated antimicrobial efficacy with synergism in 2:1, additivity in 1:2 and indifference

in 1:1 ratio. In all the tested ratios, AgGOPdGO and AuGOPdGO demonstrated indifferent antimicrobial effects in all the tested ratios (Table 4.14).

#### **4.5.2.2. FIC against *K. pneumoniae*, *A. baumannii* and *E. faecium* in the presence of 10 % bovine plasma conditioning film**

##### *K. pneumoniae*

Against *K. pneumoniae*, only AuGOPdGO demonstrated additive antimicrobial effects in presence of plasma CF in all the tested ratios. The least active antimicrobial with indifference effects were AgGO combination with CuGO, AuGO and PdGO (without plasma) and GOCuGO combination (with plasma). The presence of plasma CF reduced the antimicrobial efficacy with a greater number of combinations demonstrating an indifferent antimicrobial effect ( $FIC > 1.0$  and  $\leq 4.0$ ) (Table 4.12).

##### *A. baumannii*

Against *A. baumannii*, AuGOPdGO, GO in combination with AuGO and PdGO demonstrated an additive antimicrobial efficacy in all the tested ratios. GOCuGO showed additive antimicrobial effects in 2:1 and 1:2 ratios. The remaining combinations demonstrated indifferent antimicrobial efficacy (Table 4.13).

##### *E. faecium*

Against *E. faecium*, GOCuGO, GOAuGO and AuGOPdGO demonstrated an additive antimicrobial effect in all the tested ratios ( $FIC = > 0.5$  and  $\leq 1.0$ ). The AuGOPdGO, GOPdGO, AgGOCuGO, AgGOAuGO, AgGOPdGO demonstrated an indifferent antimicrobial activity in all the tested ratios ( $FIC = > 1.0$  and  $\leq 4.0$ ) (Table 4.14).

In summary, in the absence and presence of plasma CF, AuGOPdGO demonstrated the best antimicrobial efficacies against Gram-negative pathogens and GOCuGO and GOAuGO were the most active antimicrobial against *E. faecium*. The least active antimicrobial

combinations were AgGOAuGO, AgGOCuGO and AgGOPdGO in absence of plasma CF and GOCuGO in the presence of CF against *K. pneumoniae*. Most of the tested combinations against *A. baumannii* and *E. faecium* demonstrated an indifferent antimicrobial effect.

**Table 4.12.** Fractional inhibitory concentration in 2:1, 1:1 and 1:2 ratios in the absence and presence of 10 % plasma conditioning film against *K. pneumoniae* (n = 4).

Synergy = < 0.5, additivity  $0.5 \leq 1.0$ ,  $1.0 \leq 4.0$  indifference and  $> 4.0$  = antagonism  $> 4.0$  (Sueke et al., 2010). GO = graphene oxide, AgGO = silver graphene oxide, CuGO = copper graphene oxide, AuGO = gold graphene oxide and PdGO = palladium graphene oxide. Additive interaction was highlighted using purple colour.

GBCs combinations	2:1		1:1		1:2	
	Without CF	With CF	Without CF	With CF	Without CF	With CF
GOAgGO	0.64 ± 0	0.64 ± 0	1.50 ± 0	1.50 ± 0	1.00 ± 0.17	1.64 ± 0
GOCuGO	0.82 ± 0	1.66 ± 0	0.74 ± 0	1.49 ± 0	1.28 ± 0	1.28 ± 0
GOAuGO	0.98 ± 0	2.00 ± 0	1.00 ± 0	2.00 ± 0	0.96 ± 0	0.96 ± 0
GOPdGO	0.98 ± 0	2.00 ± 0	1.00 ± 0	2.00 ± 0	0.96 ± 0	0.96 ± 0
AgGOCuGO	0.72 ± 0	0.72 ± 0	1.24 ± 0	2.49 ± 0	1.93 ± 0	1.93 ± 0
AgGOAuGO	0.80 ± 0	0.80 ± 0	1.50 ± 0	1.50 ± 0	2.58 ± 0	2.58 ± 0
AgGOPdGO	0.80 ± 0	0.80 ± 0	1.50 ± 0	1.50 ± 0	2.58 ± 0	2.58 ± 0
CuGOAuGO	1.32 ± 0	1.32 ± 0	0.74 ± 0	1.49 ± 0	1.01 ± 0.17	0.82 ± 0
CuGOPdGO	1.32 ± 0	1.32 ± 0	0.74 ± 0	1.49 ± 0	0.82 ± 0	0.82 ± 0
AuGOPdGO	0.98 ± 0	0.98 ± 0	1.00 ± 0	1.00 ± 0	0.98 ± 0	0.98 ± 0

**Table 4.13.** Fractional inhibitory concentration in 2:1, 1:1 and 1:2 ratios in the absence and presence of 10 % plasma conditioning film against *A. baumannii* (n = 4).

Synergy = < 0.5, additivity  $0.5 \leq 1.0$ ,  $1.0 \leq 4.0$  indifference and  $> 4.0$  = antagonism > 4.0 (Sueke et al., 2010). GO = graphene oxide, AgGO = silver graphene oxide, CuGO = copper graphene oxide, AuGO = gold graphene oxide and PdGO = palladium graphene oxide. Additive interaction was highlighted using purple colour.

GBCs combinations	2:1		1:1		1:2	
	Without CF	With CF	Without CF	With CF	Without CF	With CF
GOAgGO	$2.22 \pm 0.25$	$1.49 \pm 0$	$1.32 \pm 0$	$2.56 \pm 0$	$1.55 \pm 0.17$	$1.49 \pm 0$
GOCuGO	$1.05 \pm 0$	$0.82 \pm 0$	$0.92 \pm 0$	$1.49 \pm 0$	$1.55 \pm 0$	$0.65 \pm 0$
GOAuGO	$1.21 \pm 0$	$0.98 \pm 0$	$1.17 \pm 0$	$1.00 \pm 0$	$1.09 \pm 0$	$0.98 \pm 0$
GOPdGO	$1.21 \pm 0$	$0.98 \pm 0$	$1.17 \pm 0$	$1.00 \pm 0$	$1.09 \pm 0$	$0.98 \pm 0$
AgGOCuGO	$1.41 \pm 0.37$	$2.15 \pm 0$	$1.71 \pm 0.29$	$2.31 \pm 0$	$1.66 \pm 0$	$1.66 \pm 0$
AgGOAuGO	$1.49 \pm 0$	$1.49 \pm 0$	$1.24 \pm 0$	$1.24 \pm 0$	$1.74 \pm 0.21$	$1.99 \pm 0$
AgGOPdGO	$1.49 \pm 0$	$1.49 \pm 0$	$1.24 \pm 0$	$1.24 \pm 0$	$1.74 \pm 0.21$	$1.99 \pm 0$
CuGOAuGO	$1.32 \pm 0$	$1.32 \pm 0$	$0.74 \pm 0$	$1.49 \pm 0$	$1.66 \pm 0.17$	$1.66 \pm 0$
CuGOPdGO	$1.32 \pm 0$	$1.32 \pm 0$	$0.74 \pm 0$	$1.49 \pm 0$	$1.66 \pm 0$	$1.66 \pm 0$
AuGOPdGO	$0.98 \pm 0$	$0.98 \pm 0$	$1.00 \pm 0$	$1.00 \pm 0$	$2.00 \pm 0$	$0.98 \pm 0$

**Table 4.14.** Fractional inhibitory concentration in 2:1, 1:1 and 1:2 ratios in the absence and presence of 10 % plasma conditioning film against *E. faecium* (n = 4).

Synergy =  $< 0.5$ , additivity  $> 0.5 \leq 1.0$ ,  $> 1.0 \leq 4.0$  indifference and  $> 4.0$  = antagonism  $> 4.0$  (Sueke et al., 2010). GO = graphene oxide, AgGO = silver graphene oxide, CuGO = copper graphene oxide, AuGO = gold graphene oxide and PdGO = palladium graphene oxide. Additive and synergistic interactions were highlighted using purple and red colours respectively.

GBCs combinations	2:1		1:1		1:2	
	Without CF	With CF	Without CF	With CF	Without CF	With CF
GOAgGO	0.48 ± 0	0.97 ± 0	1.24 ± 0	1.24 ± 0	0.72 ± 0	1.48 ± 0
GOCuGO	0.40 ± 0	0.82 ± 0.09	0.74 ± 0	0.74 ± 0	0.49 ± 0.08	0.66 ± 0
GOAuGO	0.48 ± 0	0.99 ± 0.10	0.99 ± 0	0.99 ± 0	0.48 ± 0	0.99 ± 0
GOPdGO	0.65 ± 0	1.32 ± 0.14	1.49 ± 0	1.49 ± 0	0.82 ± 0	1.66 ± 0
AgGOCuGO	1.40 ± 0	1.40 ± 0	2.24 ± 0	2.24 ± 0	0.80 ± 0	1.65 ± 0
AgGOAuGO	1.48 ± 0	1.48 ± 0	1.87 ± 0.31	2.49 ± 0	0.97 ± 0	1.98 ± 0
AgGOPdGO	1.64 ± 0	1.64 ± 0	2.25 ± 0.37	3.00 ± 0	1.30 ± 0	2.66 ± 0
CuGOAuGO	0.66 ± 0	0.66 ± 0	0.74 ± 0	0.74 ± 0	1.24 ± 0.20	0.82 ± 0
CuGOPdGO	0.99 ± 0	0.99 ± 0	1.24 ± 0	1.24 ± 0	2.25 ± 0.37	1.50 ± 0
AuGOPdGO	1.32 ± 0	1.32 ± 0	1.49 ± 0	1.49 ± 0	1.66 ± 0	1.66 ± 0



#### **4.5.3. Fractional bactericidal concentration (FIC) for combined GO and metal-GO hybrids in 2:1, 1:1 and 1:2 ratios in the absence and presence of plasma**

The FBC were used to determine the synergistic bactericidal antimicrobial efficacy of the GO and metal-GO hybrids combination in the presence and absence of 10 % bovine plasma. The FBC were performed in 2:1, 1:1 and 1:2 ratios.

##### **4.5.3.1. FBC against *K. pneumoniae*, *A. baumannii* and *E. faecium* in the absence of 10 % bovine plasma conditioning film**

###### *K. pneumoniae*

Against *K. pneumoniae* in the absence of plasma CF, GO in combination with CuGO, AuGO and PdGO and AuGOPdGO combinations demonstrated additive antimicrobial effects ( $FIC = > 0.5 \leq 1.0$ ) in all the tested ratios. The, GOAgGO demonstrated synergistic antimicrobial effects in 1:2 ratio. The least active antimicrobial with indifferent effects was AgGO combination with CuGO, AuGO and PdGO (Table 4.15).

###### *A. baumannii*

Against *A. baumannii* in the absence of plasma CF, AuGOPdGO in 2:1 and 1:1 ratio and CuGO in combination with AuGO and PdGO in 1:1 ratio demonstrated an additive antimicrobial efficacy ( $FIC = > 0.5$  and  $\leq 1.0$ ). The remaining tested combination were found to demonstrate indifferent antimicrobial efficacies ( $FIC = > 1.0$  and  $\leq 4.0$ ) (Table 4.16).

###### *E. faecium*

Against *E. faecium* in the absence of plasma CF, GOCuGO in 2:1 and 1:2 ratios and GOAgGO in 2:1 ratio demonstrated a strong antimicrobial efficacy with synergistic interactions ( $FIC \leq 0.5$ ). Moreover, GOAuGO and GOPdGO demonstrated good antimicrobial efficacy with additive effects in 2:1 and 1:2 ratios. In all the tested ratios, AgGOPdGO and AuGOPdGO demonstrated indifferent antimicrobial effects (Table 4.17).

#### **4.5.3.1. FBC against *K. pneumoniae*, *A. baumannii* and *E. faecium* in the presence of 10 % bovine plasma CF**

##### *K. pneumoniae*

Against *K. pneumoniae*, only AuGOPdGO demonstrated additive antimicrobial effects in presence of plasma CF in all the tested ratios. The least active antimicrobial with indifference effects were the GOCuGO combination. The presence of plasma CF decreased the antimicrobial efficacy with a greater number of combinations demonstrating indifferent antimicrobial results ( $FIC > 1.0$  and  $\leq 4.0$ ) (Table 4.15).

##### *A. baumannii*

Against *A. baumannii*, AuGOPdGO, GO in combination with AuGO and PdGO demonstrated an additive antimicrobial efficacy in all the tested ratios. The GOCuGO showed antimicrobial additive effects in 2:1 and 1:2 ratios. The remaining combinations demonstrated indifferent antimicrobial efficacy (Table 4.16).

##### *E. faecium*

Against *E. faecium*, GOCuGO showed a strong antimicrobial efficacy with a synergistic interaction in 2:1 ratio and additive antimicrobial effects in 1:1 and 1:2 ratios. The AuGOPdGO, GOPdGO, AgGOCuGO, AgGOAuGO, AgGOPdGO demonstrated an indifferent antimicrobial activity in all the tested ratios ( $FIC = > 1.0$  and  $\leq 4.0$ ) (Table 4.17).

In summary, in the absence and presence of plasma CF, AuGOPdGO demonstrated the best antimicrobial efficacies against Gram-negative pathogens and GOCuGO demonstrated the greatest antimicrobial efficacy against *E. faecium*. The combinations with the least antimicrobial efficacies were AgGOAuGO, AgGOCuGO and AgGOPdGO in absence of plasma CF and GOCuGO in the presence of CF against *K. pneumoniae*. The majority of the

tested combinations demonstrated an indifferent antimicrobial effect against *A. baumannii* and *E. faecium*.

**Table 4.15.** Fractional bactericidal concentration in 2:1, 1:1 and 1:2 ratios in the absence and presence of 10 % plasma conditioning film against *K. pneumoniae* (n = 4).

Synergy = < 0.5, additivity  $0.5 \leq 1.0$ ,  $1.0 \leq 4.0$  indifference and  $> 4.0$  = antagonism > 4.0 (Sueke et al., 2010). GO = graphene oxide, AgGO = silver graphene oxide, CuGO = copper graphene oxide, AuGO = gold graphene oxide and PdGO = palladium graphene oxide. Additive and synergistic interactions were highlighted using purple and red colours respectively.

GBCs combinations	2:1		1:1		1:2	
	Without CF	With CF	Without CF	With CF	Without CF	With CF
GOAgGO	0.56 ± 0.14	0.65 ± 0	1.49 ± 0	1.30 ± 0.16	0.32 ± 0	1.35 ± 0.27
GOCuGO	0.82 ± 0	1.66 ± 0	0.74 ± 0	1.50 ± 0	0.66 ± 0	1.41 ± 0.07
GOAuGO	0.99 ± 0	1.99 ± 0	0.99 ± 0	2.00 ± 0	0.99 ± 0	0.99 ± 0
GOPdGO	0.99 ± 0	1.99 ± 0	0.99 ± 0	2.00 ± 0	0.99 ± 0	0.99 ± 0
AgGOCuGO	0.82 ± 0	0.74 ± 0	1.49 ± 0	2.19 ± 0.27	2.66 ± 0	2.00 ± 0
AgGOAuGO	0.82 ± 0	0.82 ± 0	1.49 ± 0	1.49 ± 0	2.66 ± 0	2.66 ± 0
AgGOPdGO	0.82 ± 0	0.82 ± 0	1.49 ± 0	1.49 ± 0	2.66 ± 0	2.66 ± 0
CuGOAuGO	1.32 ± 0	1.32 ± 0	0.74 ± 0	1.50 ± 0	0.82 ± 0	0.82 ± 0
CuGOPdGO	1.32 ± 0	1.32 ± 0	0.74 ± 0	1.50 ± 0	0.82 ± 0	0.82 ± 0
AuGOPdGO	0.99 ± 0	0.99 ± 0	0.99 ± 0	0.99 ± 0	0.99 ± 0	0.99 ± 0

**Table 4.16.** Fractional bactericidal concentration in 2:1, 1:1 and 1:2 ratios in the absence and presence of 10 % plasma conditioning film against *A. baumannii* (n = 4).

Synergy = < 0.5, additivity  $0.5 \leq 1.0$ ,  $> 1.0 \leq 4.0$  indifference and  $> 4.0$  = antagonism > 4.0 (Sueke et al., 2010). GO = graphene oxide, AgGO = silver graphene oxide, CuGO = copper graphene oxide, AuGO = gold graphene oxide and PdGO = palladium graphene oxide  
Synergistic interaction was highlighted using purple colour.

GBCs combinations	2:1		1:1		1:2	
	Without CF	With CF	Without CF	With CF	Without CF	With CF
GOAgGO	$1.98 \pm 0.33$	$1.49 \pm 0.25$	$1.50 \pm 0$	$2.56 \pm 0$	$1.64 \pm 0$	$1.49 \pm 0$
GOCuGO	$1.50 \pm 0$	$0.82 \pm 0$	$1.24 \pm 0$	$1.49 \pm 0$	$2.00 \pm 0$	$0.65 \pm 0$
GOAuGO	$1.66 \pm 0$	$0.98 \pm 0$	$1.49 \pm 0$	$1.00 \pm 0$	$1.32 \pm 0$	$0.98 \pm 0$
GOPdGO	$1.66 \pm 0$	$0.98 \pm 0$	$1.49 \pm 0$	$1.00 \pm 0$	$1.32 \pm 0$	$0.98 \pm 0$
AgGOCuGO	$1.40 \pm 0$	$2.15 \pm 0.37$	$1.12 \pm 0$	$2.31 \pm 0$	$1.65 \pm 0$	$1.66 \pm 0$
AgGOAuGO	$1.48 \pm 0$	$1.49 \pm 0$	$1.24 \pm 0$	$1.24 \pm 0$	$1.98 \pm 0$	$1.99 \pm 0$
AgGOPdGO	$1.48 \pm 0$	$1.49 \pm 0$	$1.24 \pm 0$	$1.24 \pm 0$	$1.98 \pm 0$	$1.99 \pm 0$
CuGOAuGO	$1.32 \pm 0$	$1.32 \pm 0$	$0.74 \pm 0$	$1.49 \pm 0$	$1.66 \pm 0$	$1.66 \pm 0$
CuGOPdGO	$1.32 \pm 0$	$1.32 \pm 0$	$0.74 \pm 0$	$1.49 \pm 0$	$1.66 \pm 0$	$1.66 \pm 0$
AuGOPdGO	$0.99 \pm 0$	$0.98 \pm 0$	$0.99 \pm 0$	$1.00 \pm 0$	$1.99 \pm 0$	$0.98 \pm 0$

**Table 4.17.** Fractional bactericidal concentration in 2:1, 1:1 and 1:2 ratios in the absence and presence of 10 % plasma conditioning film against *E. faecium* (n = 4).

Synergy = < 0.5, additivity  $0.5 \leq 1.0$ ,  $1.0 \leq 4.0$  indifference and  $> 4.0$  = antagonism > 4.0 (Sueke et al., 2010). GO = graphene oxide, AgGO = silver graphene oxide, CuGO = copper graphene oxide, AuGO = gold graphene oxide and PdGO = palladium graphene oxide. Additive and synergistic interactions were highlighted using purple and red colours respectively.

GBCs combinations	2:1		1:1		1:2	
	Without CF	With CF	Without CF	With CF	Without CF	With CF
GOAgGO	0.48 ± 0	0.99 ± 0	1.09 ± 0.13	1.24 ± 0	0.74 ± 0	1.50 ± 0
GOCuGO	0.49 ± 0	0.49 ± 0	1.00 ± 0	1.00 ± 0	0.49 ± 0	0.99 ± 0
GOAuGO	0.55 ± 0	0.55 ± 0	1.16 ± 0	1.16 ± 0	0.60 ± 0	1.21 ± 0
GOPdGO	0.66 ± 0	0.66 ± 0	1.50 ± 0	1.50 ± 0	0.82 ± 0	1.66 ± 0
AgGOCuGO	1.50 ± 0	1.50 ± 0	2.19 ± 0.27	2.51 ± 0	0.99 ± 0	2.00 ± 0
AgGOAuGO	1.55 ± 0	1.55 ± 0	2.34 ± 0.29	1.68 ± 0	1.10 ± 0	2.22 ± 0
AgGOPdGO	1.66 ± 0	1.66 ± 0	2.63 ± 0.32	3.01 ± 0	1.32 ± 0	2.66 ± 0
CuGOAuGO	1.10 ± 0	1.10 ± 0	1.16 ± 0	1.16 ± 0	1.21 ± 0	1.21 ± 0
CuGOPdGO	1.10 ± 0	1.32 ± 0	1.16 ± 0	1.50 ± 0	1.21 ± 0	1.66 ± 0
AuGOPdGO	1.55 ± 0	1.55 ± 0	1.66 ± 0	1.66 ± 0	1.77 ± 0	1.77 ± 0

## 4.5. Discussion

### *Combined graphene oxide and metal-graphene oxide antimicrobial efficacies in absence of conditioning films*

A combination of the GO mechanism coupled with the presence of metal ions may in some cases result in synergistic antimicrobial effects. In the presence of GO, the metal ion could further induce the production of ROS by interrupting the electron transmembrane chain and interacting with respiratory enzymes of the cells (Holt and Bard, 2005). This dual mechanism would create an imbalance between the ROS generation and the intrinsic ability of the bacteria to readily detoxify the reactive intermediates and repair cellular damage. The surplus ROS formation and their inadequate elimination would result in the production of oxidative stress (Zou et al., 2016; Jin et al., 2017). This proceeds other antimicrobial mechanisms that occur in the cell-membrane such as cross-linking, denaturation and fracture of phospholipids leading to cell death (Jin et al., 2017). It may also be hypothesised that, as the GO weakens the bacterial wall, penetration of the metal ions released from the graphene metal hybrids will gain ‘easier’ access into the damaged bacterial membrane and into the cytoplasm (Musico et al., 2014). Once inside the cell, various vital bacterial intracellular mechanisms can be damaged by the metal ions. Two studies demonstrated 100 % bacterial killing and > 20 mm of inhibition at 50 to 150  $\mu\text{g mL}^{-1}$  for reduced GO against *E. coli*, *S. aureus* and *P. aeruginosa* (Turcheniuk et al., 2015; Saikia et al., 2016). These studies also demonstrated that reduced GO nano-walls demonstrated the trap and wrap mechanism against bacteria, which might lead to bacterial death owing to easier penetration of Au ions and their antimicrobial actions on the bacterial cellular mechanism. A study by Dasari Shareena et al. (2018), demonstrated that Au nanoparticles caused bacterial cell death owing to the leakage of sugars and proteins by binding to the bacterial membrane cross-linkage components. Further, silver ions released from nanoparticles, strongly bind to the thiol groups of bacterial proteins, which has been suggested

to inhibit with cell division causing bacterial death (Shao et al., 2015; Chandraker et al., 2017). Copper ions released from reduced GO based GOCu nanoparticles have been demonstrated to cause lipid and protein oxidation, thus causing cellular damage, resulting in a 99.9 % *E. coli* and *S. aureus* inhibition at 16 mgL<sup>-1</sup> (Ouyang et al., 2013). Similarly, GO-Ag nanocomposites demonstrated 100 % *E. coli* inhibition at 100 µgmL<sup>-1</sup>.

In the work presented in this thesis, AgGO combinations with AuGO, CuGO and PdGO demonstrated the least antimicrobial efficacy with indifferent interactions against *K. pneumoniae*. The decrease seen in the work presented in this thesis can be attributed to chemistry of metal ions that might work against each other. In agreement to our results, a study demonstrated that a Cu (II) and Zn (II) combined peptide complex demonstrated no antimicrobial activity when compared to their individual effects (8 mm – 9 mm) (Porciatti et al., 2010). The study claimed that this result was as a consequence of both the metal ions competing with each other to bind with the bacterial sites (nitrogen, sulphur). Thus, they resulted in a negative antimicrobial effect resulting in a decrease in each other's antimicrobial efficacy (Oboda et al., 2018). These results demonstrate that the complexing of antimicrobials does not always work as expected and thus needs serious considerations.

#### *Conditioning film effect on combined graphene oxide and metal-graphene oxide hybrids antimicrobial efficacies*

Against *A. baumannii* in the presence of plasma CF, GO in combination with CuGO, AuGO and PdGO and AuGOPdGO demonstrated additive effects. Whilst most of the tested combination showed indifference efficacy in the FIC and FBC results. It is difficult to know the exact mechanism for the difference in the antimicrobial mechanism in the presence of the plasma CF. However, a study stated that experimental surrounding such as liquid or solid medium, selected bacterial species, presence of *in vivo* like conditions, oxygen content during experimentation affects the antimicrobial mechanism (Zou et al., 2016). The GO antimicrobial



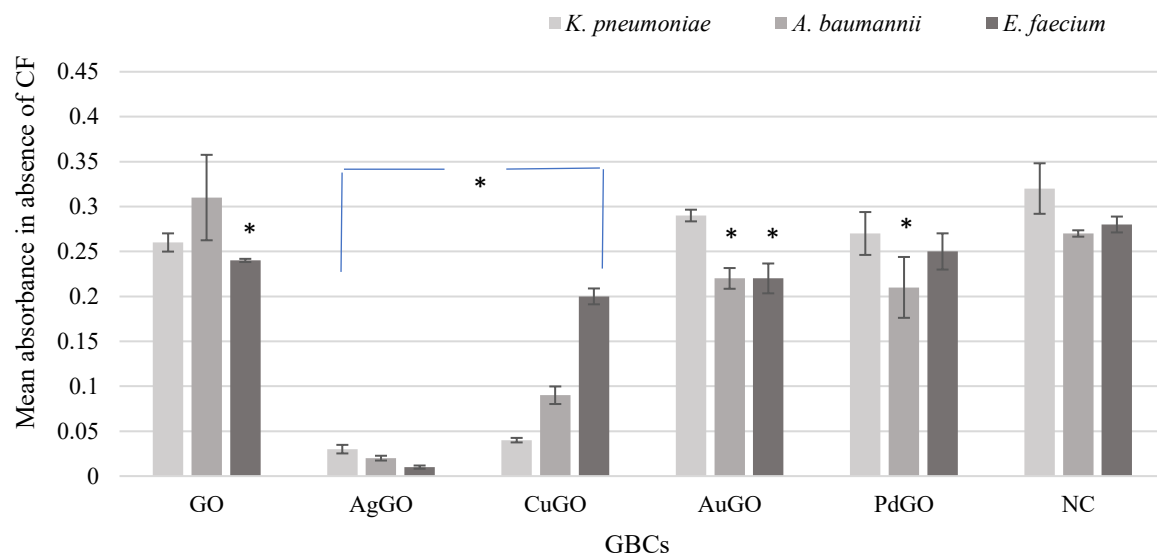
activity was found to be reduce in presence of bovine plasma CF. Accordingly, the plate killing assay in absence of plasma demonstrated 72 % killing which reduced to 60 % in BSA presence against *E. coli* at 200  $\mu\text{g mL}^{-1}$  (Hui et al., 2014). In contrast, GO were found to efficiently expedite *E. coli* growth in all the CFU $\text{mL}^{-1}$  at 25  $\mu\text{g mL}^{-1}$  in presence of Luria–Bertani broth, which contains peptises and peptones as organic load (Ruiz et al., 2011). It is assumed organic content of the conditioning films might bind to the surface of GO through covalent bond. Furthermore, the presence of organic load voids the planner spaces of the GO, thus affecting its antibacterial potency (Hui et al., 2014). However, another study stated that smaller size particles of GO may decrease the percentage of proteins to occupy the void space (Mu et al., 2012). Thus, detailed investigations selecting specific GO size and shape, physiochemical conditions, broad range of pathogens selection and presence of body fluids might increase the understanding regarding varying antimicrobial potency of GO based compounds.

#### **4.6. Crystal violet biofilm assay (CVBA) to test antimicrobial efficacies for single and combined GO and metal-GO hybrids against *K. pneumoniae*, *A. baumannii* and *E. faecium* in the presence and absence of plasma conditioning film**

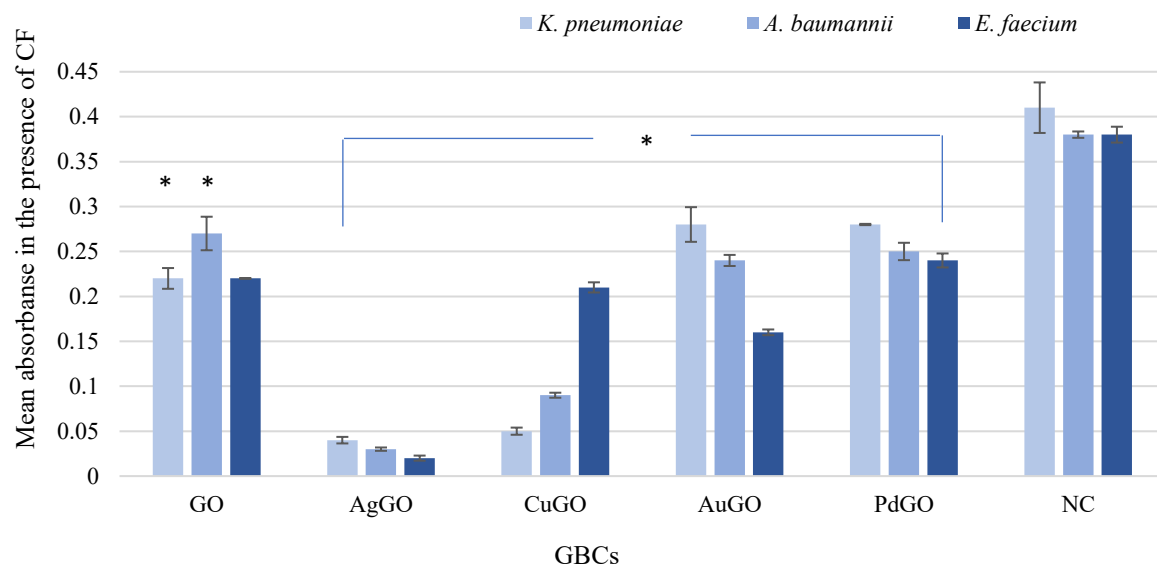
##### **4.6.1. Antibiofilm assay for GO and metal-GO hybrids against *K. pneumoniae*, *A. baumannii* and *E. faecium* in the presence and absence of 10 % bovine plasma conditioning film**

The CVBA was performed to assess the antibacterial activity after 24 h treatment with GO, AgGO, CuGO, AuGO and PdGO against the three bacteria in the form of biofilms. Following the CVBA test in absence of 10 % bovine plasma, AgGO and CuGO against all tested pathogens; GO against *E. faecium*; AuGO against *A. baumannii* and *E. faecium* and PdGO against *A. baumannii* showed a significance antimicrobial efficacy compared negative control bacteria biofilm ( $p < 0.05$ ). In the presence of 10 % bovine plasma all the tested GBCs except GO against *A. baumannii* showed a significant antimicrobial efficacy compared to the negative control bacteria biofilm ( $p < 0.05$ ). The bacterial biofilms were found to be more resistant in absence of plasma CF for AuGO, PdGO and GO (Figure 4.17 and 4.18).

Overall, with the lowest absorbance, AgGO demonstrated the best antibiofilm efficacy followed with CuGO and GO demonstrated the least antibiofilm activity.



**Figure 4.17.** The CVBA results for GO and metal-GO hybrids in the absence of 10 % plasma conditioning film against a) *K. pneumoniae*, b) *A. baumannii* and c) *E. faecium* (n = 3).

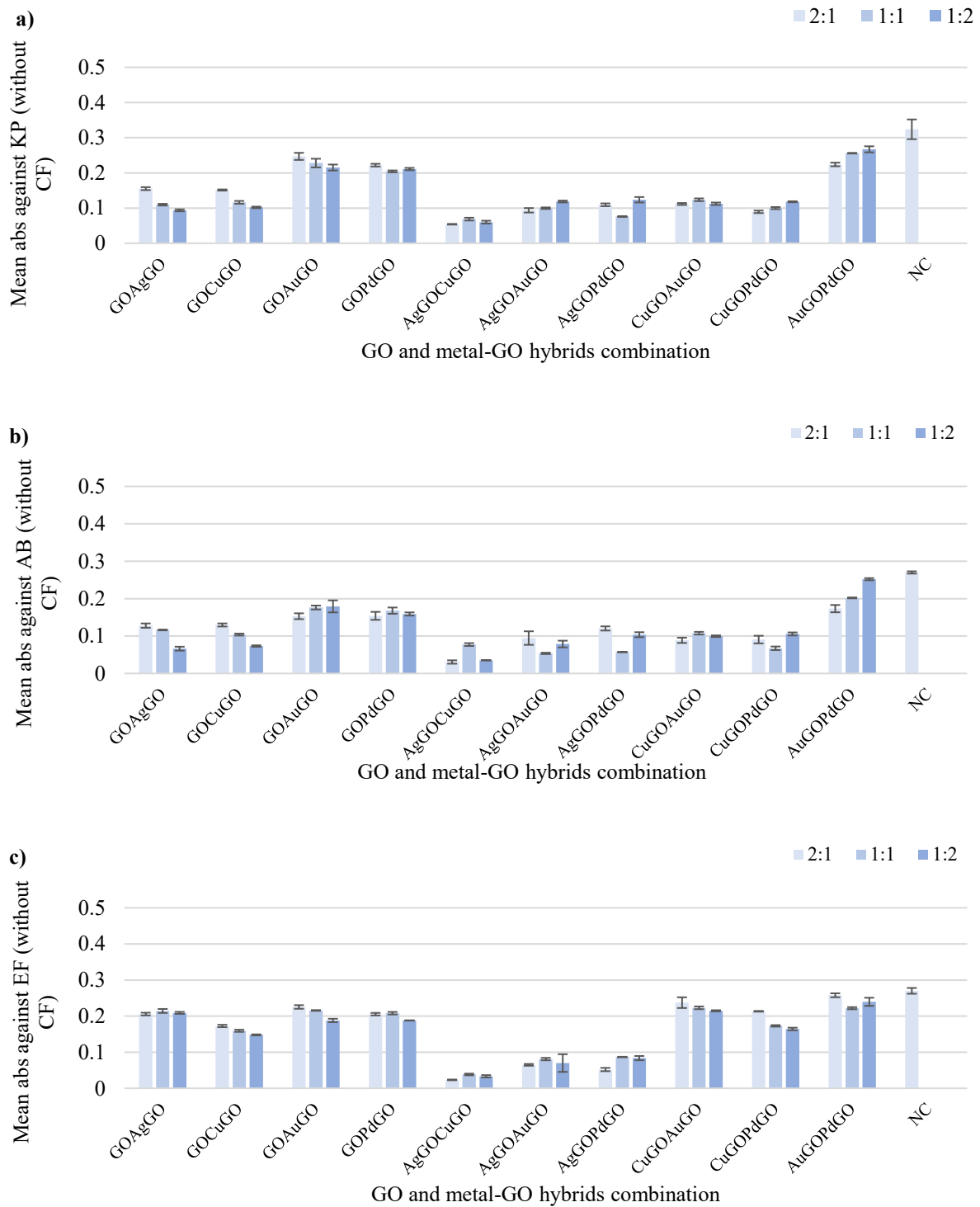


**Figure 4.18.** The CVBA results for five GBCs in the presence of 10 % plasma conditioning film against a) *K. pneumoniae*, b) *A. baumannii* and c) *E. faecium*. (n = 3).

**4.6.2. Antibiofilm assay GO and metal-GO hybrids in combinations against *K. pneumoniae*, *A. baumannii* and *E. faecium* in the absence of 10 % bovine plasma conditioning films**

The combined effects of the GOAgGO, GOCuGO, GOAuGO, GOPdGO, AgGOCuGO, AgGOAuGO, AgGOPdGO,, CuGOAuGO, CuGOPdGO and AuGOPdGO were tested using CVBA. Following the CVBA results in 2:1, 1:1 and 1:2 ratios in the absence of 10 % bovine plasma CF, when compared with the negative control all the GBC combinations showed a statistical significance ( $p < 0.01$ ) except AuGOPdGO in 2:1 and 1:2 ratio (Figure 4.20, a-c).

Overall, AgGOCuGO demonstrated the best antibiofilm efficacy with lowest biofilm absorbance and AuGOPdGO demonstrated the least efficacy with the greatest absorbance compared to control.

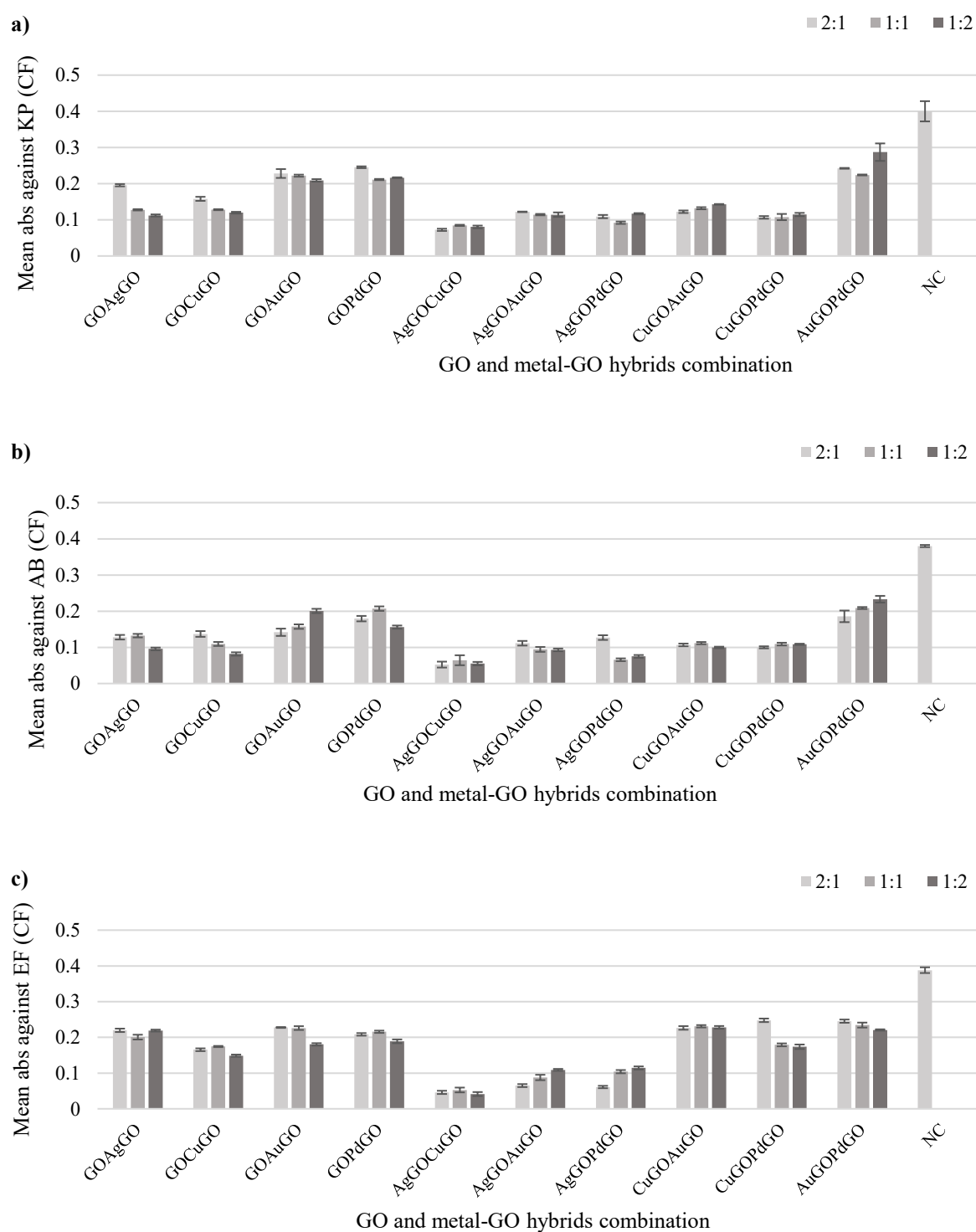


**Figure 4.19.** The CVBA results for GO and metal-GO hybrids combination in 2:1, 1:1 and 1:2 ratios in the absence of 10 % plasma conditioning film against a) *K. pneumoniae*, b) *A. baumannii* and c) *E. faecium* (n = 3).

#### **4.6.3. Biofilm results against *K. pneumoniae*, *A. baumannii* and *E. faecium* in the presence of 10 % bovine plasma conditioning film**

The combined effects of the GOAgGO, GOCuGO, GOAuGO, GOPdGO, AgGOCuGO, AgGOAuGO, AgGOPdGO,, CuGOAuGO, CuGOPdGO and AuGOPdGO were tested using CVBA. Following the CVBA results in 2:1, 1:1 and 1:2 ratios in the presence of 10 % bovine plasma CF, when compared with the negative control all the GBC combinations showed a highly statistical significance ( $p < 0.01$ ) (Figure 4.21, a-c).

Overall, AgGOCuGO demonstrated the best antibiofilm efficacy with lowest biofilm absorbance and AuGOPdGO demonstrated the least efficacy with the greatest absorbance compared to control.



**Figure 4.20.** The CVBA results for GO and metal-GO hybrids combination in 2:1, 1:1 and 1:2 ratios in the presence of 10 % plasma conditioning film against a) *K. pneumoniae*, b) *A. baumannii* and c) *E. faecium* (n = 3).



## 4.6. Discussion

### *Graphene oxide and metal-graphene oxide hybrids antibiofilm efficacies in the absence and presence of plasma conditioning film*

The CVBA assay results for GO-metal hybrids, AgGO and CuGO (without CF) and AgGO, CuGO, AuGO and PdGO (with CF) demonstrated statistically significant antibiofilm activity.

The lowest absorbance compared to bacterial control biofilm was recorded for AgGO. It is interesting to mention that CuGO was the least active antimicrobial against the tested bacteria in the planktonic form, whilst it demonstrated the second best antibiofilm efficacies. AuGO and PdGO combinations with GO, AgGO and each other were found with least antibiofilm efficacy. In agreement to our study results, a study confirmed that AgNPs of 40 nm size coated catheters displayed a complete bacterial biofilm inhibition after 18 h of treatment (Palanisamy et al., 2014). A study confirmed that Au coated nanoparticles at 100  $\mu$ M demonstrated complete eradication of *K. pneumoniae* biofilm in time dependent biofilm assay (Ahmed et al., 2016).

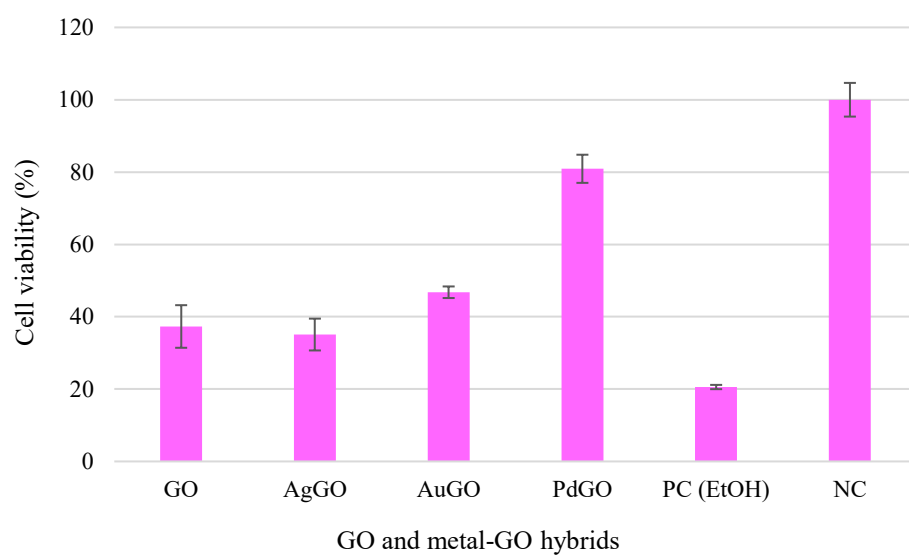
The antibiofilm efficacies of the tested graphene-based derivatives can be explained owing to the cumulative efficacies between GO and metal ions. Several studies have reported irreversible physical damage of the bacterial cell membrane for GO (Hu et al., 2010; Chen et al., 2014; He et al., 2015). To extend this, a study confirmed extraction of phospholipid content with GO treatment from the damaged bacterial membrane (Hegab et al., 2016). Increased or prolonged GO exposure might develop strong van der Waals interactions between membrane lipids and the GO interface. This physical damage can create stress within biofilm matrix and alter (reduce or increase) its other biochemical compositions (Masurkar et al., 2012). Moreover, the bacterial micro colonies inside the biofilm matrix are held in a stack like structures, which are separated through channels composed mainly of water. The reduction of biochemical content alters the passage of nutrients through this channel resulting in an easy diffusion of

antimicrobial agents (in our case metal ions) (Namasivayam et al., 2013). This process overall can lead to bacterial biofilm inhibition.

The results from this study demonstrated an increased in biofilm mass absorbance in the presence of CF compared to when organic load was absent. The elevated growth may be due to the increase in the availability of nutrients. The presence of organic soil can led to different biochemical composition of the biofilms (Aslam, 2008). Thus, the difference in the mechanistic activity of the tested metal ion and GO-metal hybrids in the presence and absence of CF can be attributed to the plasma CF affecting the metabolic and physiology of EPS structure in the biofilm matrix (Massop and Davidson, 2003).

#### **4.7. Cytotoxicity for GO and metal-GO hybrids**

The skin fibroblast controls demonstrated 100 % viability in the MTT assay. Palladium-GO demonstrated the least cell toxicity with 81 % cell viability, followed with AuGO with 47 % cell viability. A moderate cell toxicity was demonstrated for GO and AgGO with 37 % and 35 % cell viability (Figure 4.22). It has been demonstrated that there was a biocompatibility of GO at  $20\ \mu\text{g mL}^{-1}$ , however, cytotoxicity was demonstrated at  $50\ \mu\text{g mL}^{-1}$  (Pang et al., 2017). A study confirmed that reduced-GO-Ag nanocomposite demonstrated a reduction on human liver cells at  $50\ \mu\text{g mL}^{-1}$ . (Ali et al., 2018).



**Figure 4.21.** Cytotoxicity assays for GO, AgGO, AuGO and PdGO against skin fibroblast cells (n = 3).

## Chapter 5

### 5. Discussion

Bacterial infections have become one of the major public health issues. Moreover, bacterial biofilms are estimated to cause nearly 80 % of infections. Antibiotics were widely used to address this issue; however, the misuse of antibiotics has resulted in increased bacterial resistance. Antimicrobial resistance has developed as one of the primary healthcare related problems that threatens the effective prevention and treatment of patients (Boucher et al., 2009). This has led to an increase in the treatment costs, and mortality and morbidity of patients, putting a substantial financial and staffing burden on healthcare (Pham et al., 2015; Al-Jumaili et al., 2017). Bacteria have also been shown to demonstrate resistance to biocides used as antiseptics or disinfectants in hospital settings (Arancibia et al., 2000; Chen and Cooper, 2002). In order to slow down the transmission of potentially infectious microorganisms, there has been investigations into the use of alternative products such as metals and graphene materials as antimicrobial / biocidal agents (Silver et al., 2006; Bregnocchi et al., 2017; Whitehead et al., 2017; Vaidya et al., 2018). Metals in various forms such as surfaces, metal complexes, metal ions and metal nanoparticles have demonstrated an effective antimicrobial efficacy against a broad range of MDR pathogens (Elsome et al., 1999; Tom et al., 2004; Espirito et al., 2011; Chandra et al., 2011; Dizaj et al., 2014; Maleki Diza et al., 2015 and Ji et al., 2016). Currently, graphene-based materials are being proposed as novel effective antibacterial (Chen et al., 2014; Whitehead et al., 2017). In order to try to find novel antimicrobials to tackle the issue of the rise in bacterial infections, the research presented in this thesis investigated the antimicrobial efficacies of range of metal ions, graphene oxide, GO-metal hybrids against three prominent ESKAPE pathogens of healthcare concern, *K. pneumoniae*, *A. baumannii* and *E. faecium*.

## 5.1. Antimicrobial efficacies for metal ions and graphene based compounds

### *Antimicrobial efficacies and metal ions chemistry*

#### *d and p blocks transition metals*

All the tested metals belong to either d and p blocks of the transition metals in a periodic table. This means they possess a range of oxidation states and a strong redox reaction capacity (Livage, 1993). Thus, it can be hypothesised that metals with such properties might demonstrate an effective antimicrobial activity as they can easily bind with the negatively charged bacterial membranes (Lemire et al., 2013). This was in part true for the Ag, Au, Pt, Rh and Pd ions that displayed an effective antimicrobial potency.

#### *Redox reaction*

It can be assumed that the redox reaction between these ions and phosphate /amine /sulfhydryl groups may possibly affect two vital processes inside the bacterial cell (Beloglazkina et al., 2016). Firstly, these five metal ions can bind to the large cavities of the ribosome, such as the peptide-conducting tunnel passing through the ribosomal subunit. Secondly, they might hinder the translation and transcription process required for the RNA and DNA formation (Bien et al., 1999). Thus, this two-way redox reaction leads to protein dysfunction and ultimately destruction of bacteria cell (Bien et al., 1999; Huang et al., 2011; Thomas et al., 2011). Moreover, the antimicrobial efficacy is determined, to some degree, by the inherent physicochemical characteristics of the metal ions (Kolmas et al., 2014). Antimicrobial drugs whose active species is positively charged ions have been demonstrated to display an affinity for the negative sugar residues and phosphate groups on the microbial cell membrane (Dizaj et al., 2014). Metal ions might demonstrate one of the mechanisms such as cell-membrane / cell-wall degradation, protein dysfunction, oxidative stress enzymes disruption or DNA denaturation that might result in bacterial impairment owing (Lemire et al., 2013).

### *Electronegativity*

In this study, which used metal ions in solution, the most electronegative metals produced the best antimicrobial results overall. This may be a result of the hydrated metal ions being highly attracted to polar sites on the bacterial cell surface; these highly attractive forces resulting in increased interactions which resulted in their increased antimicrobial efficacy (Lemire et al., 2013). Supporting results were demonstrate for Rh ions (2.28 electronegativity) which have been shown to demonstrate and increased affinity for phosphate or sulfhydryl groups inside the bacterial cell compared to other tested metal ions (for example Y = 1.22 or In = 1.78) (Bien et al., 1999; Beloglozkina et al., 2016).

### *Outer shell structure*

Although, Pt has similar value of electronegativity as Rh, other co-founding factors such as the metal ions oxidation state, the metal's outer shell structure and milieu inside the bacterial cell influences metal ion antimicrobial efficacy. A study investigated the bacterial toxicity of metal ions based on their outer shell structure and classified them as; class I (ions with filled *p* orbitals; e.g. Ga, Y), class II ions (ions with partly filled or filled *d* orbitals; Pt, Au, Pd, Cu, Ag, Mo) and class III (ions with filled *s* orbitals; Cu, Rh, Ru, Ta). The study results using MIC test against *Cupriavidus metallidurans* demonstrated that the metal ions belonging to the class II were the most antimicrobial (Frankel et al., 2016). Metal ions belonging to the class II are considered as soft acids that demonstrate strong affinities for the electron donating sulphur and nitrogen found in protein of *K. pneumoniae*, *A. baumannii* and *E. faecium*. The exchange of electrons between class II metal cations and accepting anionic protein groups (in this case of bacteria) forms covalent bonds. Moreover, oxidation state determines the metal's activity and classified them as redox active or inactive. Redox active metals possess several oxidation states and can house a variable number of valence electrons (Harrison et al., 2008; Lemire et al., 2013). However, redox inactive metals have one oxidation state and can accommodate a

limited number of electrons. Thus, metal reactivity towards biomolecules is influenced by both tendencies to acquire electrons and the ability for the metals to be reduced (Finney & O'Halloran, 2003; Lemire *et al.*, 2013). Thus, varying chemical factors influenced the metal ions antimicrobial efficacy against the bacterial cells.

Thus, the tested metal ions demonstrated varying level of bacterial toxicity and it can be assumed that various chemical and biological aspects impact their antimicrobial efficacy against bacteria.

#### ***Antimicrobial efficacies and form and size of the graphene based compounds***

It is assumed that the form, size and the active components of the compounds also affects their antibacterial potency (Whitehead *et al.*, 2017). The particle atomic structure might affect its bacterial interaction intensity (Selim *et al.*, 2015). According to the Pal *et al.* (2007), the difference in the particles atomic structure might alter their surface properties and hence, their interaction with the with bacteria, thus producing different degrees of antimicrobial efficacy. Another theory for the differencing antimicrobial efficacies demonstrated with metals can be the particle size of the tested compounds. The particle size of the graphene derivatives tested in this study were relatively large compared to AgGO. It has been suggested that the smaller the size of the compounds, the greater the compounds antibacterial efficacy. However, inconsistent data have been reported in a study by Chen *et al.* (2014), where it was demonstrated that particle size was not found to affect the antimicrobial activity of ZnO.

### **5.2. Methodology and concentration impact on the metal ions, graphene oxide and metal-graphene oxide hybrids antimicrobial efficacies**

#### ***Methodology***

In our study, when tested individually, Rh ions were found to be most active in the ZoI test, followed with Pt and Pd ions. However, Ag, Pt, Au and Pd ions demonstrated the best antimicrobial efficacies in other tests. Moreover, in a combined metal ions tests, AgCu was



the least active in the ZoI test, whilst found to synergism and additive effects in the FIC and FBC test. Following GBCs results, AgGO was found to be the consistent strongest antimicrobial in all the individual GBCs antimicrobial tests. The ZoI results of the combined GBCs antimicrobial efficacy demonstrated indifferent interactions for all tested combinations. Whilst, few combinations demonstrated additive effects and GO in combination with AgGO, CuGO and AuGO against *E. faecium* and GOAgGO against *A. baumannii* (1:2 ratio) demonstrated synergism in the FIC and FBC.

This difference in results may be due to the chemistry of the metal, or that the ZoI is carried out in a semisolid matrix, whereas the other assays used a liquid nutrient. The ZoI was included throughout this work as it is a standard testing procedure.

#### *Effect of concentrations*

It is hypothesized that an effective concentration of bacterial toxicity varies for each antimicrobial agent (Hou et al., 2017). GO and graphene at 50  $\mu\text{g mL}^{-1}$  and 100  $\mu\text{g mL}^{-1}$  concentrations were incubated with *S. aureus* and a dose dependent assay was performed. After 0 h, 8 h and 24 h not only the higher concentration displayed a strong graphene material activity, but also GO displayed a greater efficacy at both tested concentrations (Pang et al., 2017). Similarly, The Pt, Pd, Rh and iridium tetradentate macrocyclic demonstrated an increase in inhibitory zones with increase in the concentration increases (125  $\mu\text{g mL}^{-1}$ , 250  $\mu\text{g mL}^{-1}$  and 500  $\mu\text{g mL}^{-1}$ ) (Chandra et al., 2011).

In this study concentration effect on antimicrobial efficacy were analysed using ZoI and CVBA and CFU $\text{mL}^{-1}$  tests. The ZoI test was performed using agar well diffusion method. Hence, it can be assumed that agar wells allowed leaching of the ionic solution. This solid-liquid phase interaction increased with greater tested metal ions concentrations, thus demonstrating a greater ion leaching through agar and a greater antimicrobial effect (Thomas et al., 2011). Whilst, CFU $\text{mL}^{-1}$  and CVBA were performed in a liquid medium. It can be assumed that metal

interacted with bacteria in liquid phase through electrostatic force (Silvestry-Rodriguez et al., 2008).

#### *Effect of ratios*

The FIC, FBC and CVBA were performed in this study in three ratios 2:1, 1:1 and 1:2. In this study, Cu even at highest tested concentrations was a weak antimicrobial individually in all the assays. However, AgCu displayed synergism in 1:2 FIC ratios against *E. faecium*. The AgCu combination demonstrated a synergistic efficacy in at all tested FIC ratio against *A. baumannii*. In our study, the FIC and FBC results displayed greater metal ions efficacies in presence of plasma CF. The results demonstrate that the antimicrobial efficacy, when used in ratios cannot be assumed.

### **5.3. Difference in antimicrobial efficacies against Gram-positive and Gram-negative bacteria**

In this study the metal ion and graphene-metal hybrids antimicrobial potency were evaluated against two Gram-negative bacteria (*K. pneumoniae* and *A. baumannii*) and one Gram-positive bacteria (*E. faecium*). Overall, the Gram-positive *E. faecium* were found to be the most resistant compared to the Gram-negative species. However, GO in combination with AgGO, CuGO and AuGO and AgCu demonstrated synergism against *E. faecium*. This result is interesting since in the individual metal ion assays and the graphene combinations, *E. faecium* was demonstrated to be the most recalcitrant bacteria.

The difference in the bacterial cell-wall structure and content is considered a major factor for varying bacterial resistant properties towards antimicrobial agents (Martinez de Tejada et al., 2012). Accordingly, the cell-wall of Gram-positive bacteria is composed of thick peptidoglycan layer. Apart from thick peptidoglycan, Gram-positive cell-wall also consists of teichoic acids and proteins (Lambert, 2002). The teichoic acids crosslink the peptidoglycan layer and contribute to its overall anionic nature. In addition, lipoteichoic acid bind to peptidoglycan

layer connecting it to outside milieu (Martinez de Tejada et al., 2012). Proteins are also embedded and bind with peptidoglycan layer through covalent / non-covalent bonds (Weidenmaier and Peschel, 2008; Martinez de Tejada et al., 2012). The simpler Gram-positive cell-wall structure compared to Gram-negative is thought to provide easier entry to a cell of a toxic substance. However, the internal bacterial mechanism such as efflux pumps, degradative or inactivating enzymes (e.g. beta-lactamases) or modification of the antimicrobial target site might increase their antimicrobial resistance (Webber and Piddock, 2003; Poole, 2005). All or one of the mentioned mechanisms could explain the greater inhibitory values for the tested metal ions and GO-metal hybrids in all the assays against *E. faecium* (Lambert, 2002).

The Gram-negative bacterial cell-wall contains a thin peptidoglycan layer sandwich within the outer and inner membrane, which is responsible for bacterial cell strength. The outer layer is a lipid-protein bilayer, with phospholipids in the inner leaflets and lipopolysaccharide in the outer leaflets and embedded transmembrane proteins (Beveridge, 1999; Sperandio et al., 2009). Some of these proteins might act as porins which act as channels for hydrophilic materials diffusion. This composition makes the outer membrane selectively permeable, which might aid in removal of unwanted toxic substances through efflux pumps (Bomberger et al., 2009; Sperandio et al., 2009; Schwechheimer and Kuehn, 2015). The tested metal ions and GO-metal hybrids demonstrated broad spectrum intracellular antimicrobial mechanism against bacteria such as DNA damage to release of ROS (Liu et al., 2011; Lemire et al., 2013). However, it is important that first antimicrobial agents bypass the first line of bacterial cell-wall defence to reach the intracellular bacterial target site (Martinez de Tejada et al., 2012). Several studies reported that metal ions and GO demonstrated a potential activity on the bacterial cell membrane and diffusion through selective permeable Gram-negative outer membrane (Kannan et al., 2008; Liu et al., 2011; Nazari et al., 2012; Chen et al., 2014). This can be in part true for a greater antimicrobial activity demonstrated against *K. pneumoniae* and

*A. baumannii*. Similar results were found with a greater Au antimicrobial potency against Gram negative *P. aeruginosa* and *E. coli* compared to Gram positive *S. aureus* (Nazari et al., 2012). An Ag alginate wound dressing displayed a greater inhibitory potency against Gram-negative species compared to Gram-positive species (Thomas et al., 2011). A ZoI assay for GO-Ag nanocomposite at 100  $\mu$ L demonstrated a greater antibacterial activity against *E. coli* (18 mm) compared to *S. aureus* (17.2 mm) (Chandraker et al., 2017)

#### **5.4. Host cell toxicity**

Toxicity is a consequence of antimicrobial agent exposure and over-accumulation leading to cell damage (Sahmali et al., 1991). Though metal ions and GBCs were found to be active antimicrobials, however, it is well-documented that one of the main limitations in using transition metals and GBCs as antimicrobial agents is their toxicity to eukaryotic cells (Takano et al., 2002; Issa et al., 2007; Lammel et al., 2013). Our study amongst tested metal ions Pd and amongst tested GBCs; PDGO were found to be least toxic. Various other factors such as pH, presence of organic loads, temperature and other environmental conditions might alter the toxicity, thus further investigations would be helpful (Sahmali et al., 1991; Issa et al., 2017).

## Chapter 6

### 6. Conclusion and Future Work

#### 6.1. Conclusion

The focus of the present dissertation was to investigate the antimicrobial efficacies for metal ions and GBCs alone and in combined form in the absence and presence of 10 % bovine plasma against three medical pathogens in planktonic and biofilm phenotypes.

The zone of inhibition results demonstrated that in the presence or absence of CF, Rh and Pt consistently killed all the bacterial types,

The MIC and MBC test confirmed that against *K. pneumoniae* in the presence or absence of CF Pt, Au, Pd ions were the most effective, whilst Ag, Ti and Ta ions were the most effective antimicrobial against *A. baumannii* and Ag, Pt, Au and Pd ions were the most effective against *E. faecium*. Using the time kill assays Pt, Au, Pd against *K. pneumoniae*, Au, Pd against *A. baumannii* and Ag against *E. faecium* were the most effective antimicrobials. This clearly demonstrates that the methodology used affects the results, and that overall, Ag, Pt, Au, Pd were the most effective antimicrobials. In the biofilm assays, Pt, Au, Pd were consistently the most effective antimicrobial metal ions.

Following the combined metal ion assays, in the zone of inhibition and biofilm assays, AuPd, AuPt and PtPd were the most consistently successful combinations against all the bacteria in the presence or absence of CF. For the FIC and FBC, AgCu in a 1:2 ratio in the presence or absence of CF was effective against all the bacteria, with the exception of the FIC for *A. baumannii* in the presence of a conditioning film, and FBC *K. pneumoniae* in the absence of conditioning film. AgGO was consistently effective in the ZoI, MIC, MBC, time kill and biofilm assays in the presence or absence of CF.

The SEM, EDAX and Raman confirmed changed to the bacterial morphology or biochemistry that was in line with the antimicrobial results demonstrated in the other assays.

The cytotoxicity assay on the skin fibroblast cell lines confirmed that Pd ions and PdGO were the least toxic.

This research results demonstrated that overall, Pt, Au, Pd and Au metal ions and AgGO were the most active antimicrobials in the presence or absence of CF. However, their cell host toxicity should be considered. These metal ions and GBCs could be considered to be used in applications such as biocides or antimicrobials to reduce bacterial transmission and infection in a hospital setting.

## **6.2. Future work recommendations**

This study research showed that metal ions, GO and metal-GO hybrids demonstrated antimicrobial efficacies that resulted in chemical and morphological changes in the bacterial cells. Further analysis would improve knowledge regarding the mode of action and the effects on the molecular mechanisms of the tested antimicrobial agents on the different bacteria and may uncover why in the systems tested in this work that *E. faecium* was the most resistant bacteria. Moreover, the combined metal ions showed a greater antimicrobial efficacy in the presence of 10 % plasma CF. This is a noteworthy outcome, as it can be hypothesised that metal ions combinations were an active antimicrobial in presence of *in vivo* like conditions. Additional analysis using range of biological fluids would increase the knowledge and understanding of the adjunctive effect of the biological milieu on the antimicrobial effects of the metals. Copper ions in the single antimicrobial efficacy tests were found to be least active, whilst demonstrated a good to strong antimicrobial efficacy when tested in combinations. Moreover, CuGO also demonstrated a good antibiofilm efficacy, however was least active against bacterial planktonic phenotypes. Thus, antimicrobial testing various metals and GO based compounds in different forms such as surface, coupons, sheets or complex might demonstrate significant co-relation between form of antimicrobial agents and their efficacies. Since copper in a sheet form or coating is known to demonstrate antimicrobial efficacy, this

suggests that much further work is needed to understand the effects of the metals dependent on their chemical species. Furthermore, testing of metal ions and GBCs against broad spectrum of Gram-positive and Gram-negative bacteria might provide an insight about their antimicrobial efficacies and their used as potential antimicrobial agents. This research tested cell toxicity for skin fibroblast cells only for selected metal ions, GO and metal-GO hybrids. Some of the tested metal ions and GBCs demonstrated a lowered cell toxicity. However, testing these antimicrobials for various human cell lines at various concentrations increase knowledge toxicity for host cells and this should include the elucidation of the inflammatory pathways involved. The tested antimicrobials should be further investigated using a wider range of assays, including their efficacy when incorporated into formulations for use as antimicrobial agents.

## Presentations

### Oral presentation

‘Antimicrobial efficacy of metal ions alone and in combinations against *planktonic and biofilm phenotypes*’ presented 20 minutes talk in the 17<sup>th</sup> International Biodeterioration & Biodegradation Symposium (2017), Manchester Metropolitan University, UK.

‘Antimicrobial efficacy of GO and metal-GO compounds against planktonic and biofilm phenotypes’ presented 5 minutes talk in the 42<sup>nd</sup> annual conference of medical microbiologist – Micron (2018), Bengaluru, India.

### Poster Presentation

‘*In vitro* investigation of metal ions alone and in combination against antimicrobial resistant (AMR) medical pathogens’ presented at Biofilms 7 conference (2016), University of Porto, Portugal.

‘Antimicrobial efficacy of metal ions alone and in combinations against medically relevant pathogens’ presented at Sfam microbial resistant meeting (2017), London, UK.

‘Antimicrobial efficacy of metal ions alone and in combinations against medically relevant pathogens’ presented at Science and Engineering Research Symposium (2017), Manchester Metropolitan University, UK.

‘*In vitro* investigation of single and combined metal ions against three medical pathogens’ presented a flash poster presentation on for oral/poster presentation in the Bacterial-Material interactions, USA, 2017

‘Antimicrobial efficacy of metals against pathogenic bacteria’ presented at 5<sup>th</sup> Eurobiofilms conference (2018), Netherlands.

‘Investigation of metal ions against *Enterococcus faecium* in planktonic and biofilm phenotypes’ presented at presented at Sfam microbial resistant meeting (2018), London, UK.



## Publications

MY. Vaidya, AJ. McBain, JA. Butler, CE. Banks, KA. Whitehead (2017). Antimicrobial Efficacy and Synergy of Metal Ions against Enterococcus faecium, Klebsiella pneumoniae and Acinetobacter baumannii in Planktonic and Biofilm Phenotypes. Scientific Reports. 7(1)

KA. Whitehead, M. Vaidya, C. Liauw, D. Brownson, P. Ramalingam, et al. (2017). Antimicrobial activity of graphene oxide-metal hybrids. International Biodeterioration & Biodegradation. 123, pp.182-190.

M. Vaidya, A. McBain, C. Banks, KA. Vagg-Whitehead (2018). Single and combined antimicrobial efficacies for nine metal ion solutions against Klebsiella pneumoniae, Acinetobacter baumannii and Enterococcus faecium. International Biodeterioration and Biodegradation.

## Appendix

**Table 1.** Normal distribution validity using Shapiro-Wilk test onto data of time kill assay in presence of conditioning films.

		<i>Klebsiella pneumoniae</i>	<i>Acinetobacter baumannii</i>	<i>Enterococcus faecium</i>
Samples	Time	Significance		
Ag0.01	0	.915	.537	.780
	2	.344	.174	.862
	4	.806	.826	.672
	24	.696	.600	.637
Ag0.1	0	.702	.503	.363
	2	.817	.206	.747
	4	.463	.780	.878
	24	.157	.851	.183
Ag1	0	.298	.194	.843
	2	.194	.862	.235
	4	.637	.109	.762
	24	.	.	.
Cu0.01	0	.495	.712	.797
	2	.780	.576	.890
	4	.281	.253	.339
	24	.317	.637	.482
Cu0.1	0	.747	.712	.463
	2	.567	.637	.567
	4	.000	.806	.183
	24	.843	.756	.266
Cu1	0	1.000	.702	.637
	2	.593	.637	.817
	4	.679	1.000	.878
	24	.878	.266	.298
Pt0.01	0	.747	.567	.537
	2	.780	.800	.762
	4	.433	.567	.235
	24	.424	.780	.692
Pt0.1	0	.886	.129	.831
	2	.800	.298	.094
	4	1.000	.384	1.000
	24	.915	.510	.843
Pt1	0	1.000	.702	.220
	2	.637	1.000	.890
	4			

	24	.	.	1.000
		.	.	.537
Au0.01	0	.081	.956	.274
	2	.567	1.000	.549
	4	.688	.391	.424
	24	.962	.147	.605
Au0.1	0	.194	.862	.000
	2	.482	.843	.843
	4	.679	.726	.253
	24	.107	.567	.637
Au1	0	.862	.637	.942
	2	1.000	.157	.157
	4	.	.	.377
	24	.	.	.890
Pd0.01	0	.363	.298	.363
	2	.927	.823	.567
	4	.948	.157	.221
	24	.961	.298	.417
Pd0.1	0	.000	1.000	.298
	2	.935	1.000	.878
	4	.583	.726	.800
	24	.324	.637	.094
Pd1	0	.253	.554	1.000
	2	.567	.298	.144
	4	.	.	.726
	24	.	.	.463

**Table 2.** Normal distribution validity using Shapiro-Wilk test onto data of time kill assay in absence of conditioning films.

		<i>Klebsiella pneumoniae</i>	<i>Acinetobacter baumannii</i>	<i>Enterococcus faecium</i>
Samples	Time	Significance		
Ag0.01	0	.084	.497	.583
	2	.281	.348	.384
	4	.927	.339	.073
	24	.605	.956	.708
Ag0.1	0	.637	1.000	.843
	2	.637	.194	.780
	4	.780	.463	.780
	24	.363	.688	.739
Ag1	0	.756	.	.463
	2	.051	.	.194
	4	.	.	.298
	24	.	.	.
Cu0.01	0	.915	.817	.794
	2	.111	.672	.384
	4	.900	1.000	.637
	24	.206	.939	.114
Cu0.1	0	.235	.702	.817
	2	.537	.281	.942
	4	.537	.554	.637
	24	.463	.463	.520
Cu1	0	.797	.726	.780
	2	.463	1.000	.554
	4	.407	.274	.235
	24	.537	.407	.463
Pt0.01	0	.417	.567	.637
	2	.637	.384	.339
	4	.485	.688	.878
	24	.826	.843	.915
Pt0.1	0	.790	.843	.927
	2	.605	.911	.363
	4	.637	.100	.806
	24	1.000	.417	.132
Pt1	0	1.000	.747	.780
	2	.	.	.235
	4	.	.	.520
	24	.	.	.298
Au0.01	0	.339	.391	.956
	2			

	4			
	24	.194	.266	.915
		.298	.298	.739
		.747	.672	.739
Au0.1	0	.510	.702	.274
	2	.593	.726	.780
	4	.637	.122	.583
	24	.927	.637	.826
Au1	0	.	.	.878
	2	.	.	.927
	4	.	.	.537
	24	.	.	.328
Pd0.01	0	.605	.679	.637
	2	.323	.780	.637
	4	.915	.890	.520
	24	.961	.583	.286
Pd0.1	0	.417	.780	.637
	2	.497	.900	.826
	4	1.000	.363	.637
	24	.192	.637	.363
Pd1	0	.	.	1.000
	2	.	.	.702
	4	.	.	1.000
	24	.	.	.780

**Table 3.** Normal distribution validity using Shapiro-Wilk test onto the data of the Crystal violet biofilm assay in the presence of conditioning films.

Samples	<i>Klebsiella pneumonia</i>	<i>Acinetobacter baumannii</i>	<i>Enterococcus faecium</i>
	Significance		
Ag500	.637	.	.
Ag250	.363	.157	.637
Ag100	.174	.000	.637
Ag50	.363	.407	.554
Cu500	.363	.000	1.000
Cu250	.194	.174	.702
Cu100	.363	.000	.567
Cu50	.132	.637	.756
Pt500	.	.	.
Pt250	.637	.424	1.000
Pt100	.206	.583	.339
Pt50	.712	.000	.000
Au500	.	.	.
Au250	1.000	.637	.194
Au100	.157	.463	.637
Au50	.424	.000	.220
Pd500	.	.	.
Pd250	.144	.150	.637
Pd100	.144	.637	.363
Pd50	.132	.000	.637

**Table 4.** Normal distribution validity using Shapiro-Wilk test onto the data of the Crystal violet biofilm assay in the absence of conditioning films

Samples	<i>Klebsiella pneumonia</i>	<i>Acinetobacter baumannii</i>	<i>Enterococcus faecium</i>
	Significance		
Ag500	0.000	-	1.000
Ag250	1.000	.726	.780
Ag100	1.000	.915	.637
Ag50	.5830	1.000	1.000
Cu500	.637	.927	.964
Cu250	1.000	.637	1.000
Cu100	0.000	.628	1.000
Cu50	0.000	1.000	.824
Pt500	0.000	-	-
Pt250	.747	.483	0.000
Pt100	.726	1.000	.637
Pt50	.843	.970	.463
Au500	-	.843	-
Au250	.893	0.000	1.000
Au100	.756	0.000	.637
Au50	.915	1.000	.702
Pd500	-	-	-
Pd250	1.000	1.000	.780
Pd100	1.000	.806	.637
Pd50	.637	.920	1.000

**Table 5.** Normal distribution validity using Shapiro-Wilk test onto the data of the Crystal violet biofilm assay in the presence of conditioning films

Samples	<i>Klebsiella pneumonia</i>	<i>Acinetobacter baumannii</i>	<i>Enterococcus fecium</i>
	Significance		
GO	.537	.000	.107
AgGO	.298	1.000	.000
CuGO	.298	1.000	.747
AuGO	.227	.637	.000
PdGO	.000	.780	.510

**Table 6.** Normal distribution validity using Shapiro-Wilk test onto the data of the Crystal violet biofilm assay in the absence of conditioning films

Samples	<i>Klebsiella pneumonia</i>	<i>Acinetobacter baumannii</i>	<i>Enterococcus fecium</i>
	Significance		
GO	.114	.911	.637
AgGO	.637	.266	.000
CuGO	.780	.712	.637
AuGO	.593	.908	1.000
PdGO	.152	.102	.253



**Table 7.** Normal distribution validity using Shapiro-Wilk test onto data of time kill assay in presence of conditioning films.

		<i>Klebsiella pneumoniae</i>	<i>Acinetobacter baumannii</i>	<i>Enterococcus faecium</i>
Samples	Time	Significance		
GO	0	.220	.672	.911
	2	.554	.878	.417
	4		.843	.463
	24	.	.780	.927
AgGO	0	.	.157	.964
	2	.	.	.317
	4	.	.	.567
	24	.	.	.235
AuGO	0	.281	.328	.407
	2	.817	.537	.391
	4	.806	.391	.921
	24	.	.900	.817
PdGO	0	.344	.000	.927
	2	.900	.668	.878
	4	.826	.567	.637
	24	.	.274	.921

**Table 8.** Normal distribution validity using Shapiro-Wilk test onto data of time kill assay in absence of conditioning films.

		<i>Klebsiella pneumoniae</i>	<i>Acinetobacter baumannii</i>	<i>Enterococcus faecium</i>
Samples	Time	Significance		
GO	0	1.000	.537	.726
	2	.213	.747	.094
	4	.890	.424	.780
	24	.935	.206	.
AgGO	0	.567	.484	.696
	2	.	.	.600
	4	.	.	.
	24	.	.	.
AuGO	0	.702	.915	.348
	2	.716	.600	.298
	4	.935	.000	1.000
	24	.637	.637	.780
PdGO	0	.424	.000	.545
	2	.780	.000	.672
	4	.094	.220	.593
	24	.174	.206	.637



# OPEN Antimicrobial Efficacy and Synergy of Metal Ions against *Enterococcus faecium*, *Klebsiella pneumoniae* and *Acinetobacter baumannii* in

## Planktonic and Biofilm Phenotypes

Misha Y. Vaidya<sup>1</sup>, Andrew J. McBain <sup>2</sup>, Jonathan A. Butler<sup>1</sup>, Craig E. Banks<sup>1</sup> & Kathryn A. Whitehead<sup>1</sup>

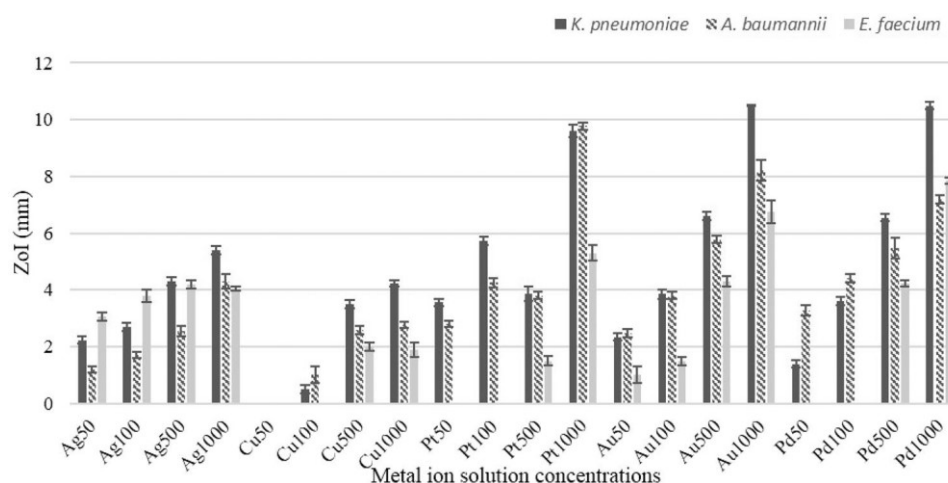
The effects of metal ion solutions (silver, copper, platinum, gold and palladium) were determined individually and in combination against *Enterococcus faecium*, *Acinetobacter baumannii* and *Klebsiella pneumoniae*. Platinum, gold and palladium showed the greatest antimicrobial efficacy in zone of inhibition (Zoi) assays. When tested in combinations using Zoi assays, gold/platinum, gold/palladium and platinum/palladium were indicative of synergy. Microbial inhibitory concentration demonstrated platinum and gold against *Enterococcus faecium*, platinum against *Klebsiella pneumoniae* and platinum and silver against *Acinetobacter baumannii* were optimal. Minimal bactericidal concentrations determined the greatest bactericidal activity was again platinum gold and palladium against all three bacteria. Fractional Inhibitory Concentration (FIC) studies demonstrated that the silver/platinum combination against *Enterococcus faecium*, and silver/copper combination against *Acinetobacter baumannii* demonstrated antimicrobial synergy. Following crystal violet biofilm assays for single metal ion solutions, antimicrobial efficacies were demonstrated for all the metals against all the bacteria. Synergistic assays against biofilms demonstrated gold/palladium, gold/platinum and platinum/palladium resulted in the greatest antimicrobial efficacy. Overall, platinum, palladium and gold metal ion solutions in individual use or combination demonstrated the greatest antimicrobial efficacies against planktonic or biofilm bacteria. This work demonstrates the potential for using a range of metal ions, as biocidal formulations against both planktonic or biofilm bacteria.

The antimicrobial properties of metals have been recognised throughout the history of medicine and healthcare<sup>1</sup>. The application of metals in medicine was common until the discovery of antibiotics. Nevertheless, at the beginning of the twenty-first century, a rapid increase in antimicrobial resistance has been observed, which has corresponded with a lack of new antibiotic drugs. To reduce the transmission of potentially infectious microorganisms, there has been a revival of interest in the utilization of metals as antimicrobial/biocidal agents<sup>2</sup>.

There is now a need for alternative biocidal formulations that may be used as active antimicrobials<sup>3,4</sup>. Biocidal products as outlined in the EU Biocides Directive (98/8/EC), are those that are intended to destroy, render harmless, prevent the action of, or otherwise exert a controlling effect on any harmful organism by chemical or biological means (i.e. disinfectants, antiseptics and preservatives)<sup>2</sup>. Metal surfaces such as silver (Ag) and copper (Cu) have shown antimicrobial efficacies that may control bacterial transmission and infection risks in laboratory settings and hospital environments<sup>5,6</sup>. Palladium (Pd) alloys have also been considered as potential materials for use as temporary implants to prevent cardiovascular disease infections<sup>7</sup>. Platinum (Pt) possesses metallurgic properties that enable it for use as an antimicrobial in medical implants, such as cardiovascular

<sup>1</sup> School of Healthcare Science, Manchester Metropolitan University, Chester St, Manchester, M1 5GD, UK. <sup>2</sup> School of Health Sciences, Faculty of Biology, Medicine and Health, The University of Manchester, Manchester, M13 9PT, UK. Correspondence and requests for materials should be addressed to K.A.W. (email: [K.A.Whitehead@mmu.ac.uk](mailto:K.A.Whitehead@mmu.ac.uk))

defibrillators or hip and knee implants and catheters<sup>8</sup>. Gold (Au) nanoparticles have been previously explored for use as delivery vehicles for thioguanine<sup>9</sup>, and various antibiotics<sup>10–12</sup>. The synergistic effects of metals or their complexes have



**Figure 1.** Zone of inhibition values for five metals at different concentrations against tested three pathogens demonstrating that at higher concentrations platinum, gold and palladium were the most effective antimicrobials whereas at lower concentrations silver demonstrated the greatest antimicrobial activity ( $p < 0.001$ ). Au = gold, Cu = copper, Pt = platinum, Pd = palladium and Ag = silver. 50, 100, 500 and 1000 are at concentrations in  $\text{mgL}^{-1}$  ( $n = 12$ ).

also been demonstrated<sup>13, 14</sup>. For example, phosphogold dithiocarbonate complexes have demonstrated to have comparable antimicrobial potency when compared to various antibiotics such as chloramphenicol against resistant pathogens<sup>13</sup>. An antimicrobial effect has also been demonstrated for  $\text{Au}^{+3}$  whereby an increase in bacterial inhibition was demonstrated when combined with cephalexin, clindamycin or vancomycin against *Escherichia coli* and *Pseudomonas aeruginosa*<sup>14</sup>.

*Enterococcus faecium* is an emergent Gram-positive opportunistic pathogen that is the causative agent of several nosocomial infections including complicated urinary tract infections and surgical wound infections<sup>15–17</sup>. *Enterococcus* is difficult to inactivate due to its high level recalcitrance and tolerance of a wide range of growth conditions. *E. faecium* can survive for long periods of time on environmental surfaces including medical equipment, bedrails and door knobs<sup>15, 18, 19</sup>. *Klebsiella pneumoniae* is a Gram-negative microorganism that has a large polysaccharide capsule surrounding the bacterial cell, which both protects the bacteria and acts as a barrier to antimicrobial agents<sup>20</sup>. This species is an opportunistic pathogen principally related with hospital-acquired infections including those of the respiratory and urinary tract<sup>21</sup>. *A. baumannii* also has a role in hospital-acquired infections particularly in causing bacteremia, pneumonia, urinary tract and wound infections<sup>22</sup>. These bacterial strains also have the ability to form biofilms on abiotic and biotic substrates, which may be problematic on catheters, potentially leading to an increase in transmission and infection risks. This may result in increased patient morbidity and mortality<sup>12–14, 23</sup>. In order to determine the potential of a range of metal ions for their use as biocidal agents, a pilot study was carried out to determine the antimicrobial efficacy of five metals, both individually and in combination against *E. faecium*, *K. pneumoniae* and *A. baumannii* planktonic or biofilm phenotypes. The potential future use of such antimicrobials would be as biocidal agents for use where intensive cleaning solutions were required.

## Results

**Zone of inhibition (ZoI) for single and combined metals.** Zones of inhibition assays were used to determine the antimicrobial efficacies of the metal ions in a semi-solid media. Zone of inhibition assays using the individual or combined metal solutions, demonstrated an increase in antimicrobial activity which correlated with increased metal ion solution concentration ( $p < 0.001$ ) (Fig. 1). When used individually, platinum, gold and palladium demonstrated the greatest ZoIs against all tested microbes ( $>5$  mm and  $<11$  mm) at  $1000 \text{ mgL}^{-1}$  concentration. Copper demonstrated the lowest antimicrobial efficacies, ( $>2$  mm and  $<4$  mm ZoI) at  $1000 \text{ mgL}^{-1}$  concentration. Against *E. faecium*, only silver and gold exhibited antimicrobial activity at lower concentrations ( $50 \text{ mgL}^{-1}$ ) (3 mm and 1 mm respectively).

In order to determine the synergies of the metal ions, they were tested using ZoI assays in combination. It was demonstrated (Table 1), that the metal solutions gold/platinum, gold/palladium and platinum/palladium were most effective antimicrobial combinations and demonstrated synergy at the higher concentrations tested (Fig. 2b). However, most of the metal ion combinations tested using ZoI assays demonstrated an indifferent response (Fig. 2a). Interestingly at the lower concentration of  $100 \text{ mgL}^{-1}$  silver/platinum, silver/gold and silver/palladium demonstrated antimicrobial activities equivalent to gold/platinum, gold/palladium and platinum/palladium (Table 1).

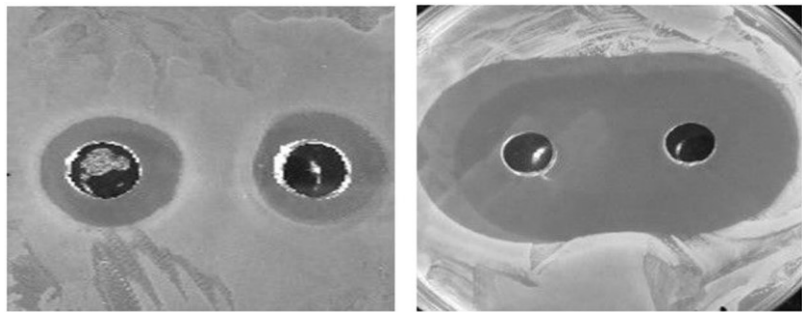
**Minimal inhibitory concentrations (MIC) and minimal bactericidal concentrations (MBC) for single metals.** Following the MIC tests, the most effective antimicrobial metal ion solutions were found to be platinum against *K. pneumoniae* ( $3.90 \text{ mgL}^{-1}$ ), silver and gold ( $3.90 \text{ mgL}^{-1}$ ) against *A. baumannii* and platinum and gold against *E. faecium* ( $11.71 \text{ mgL}^{-1}$ ) (Table 2). A similar pattern was demonstrated for the MBC with the

		AgCu	AgPt	AgAu	AuPd	CuPt	CuAu	CuPd	AuPt	AuPd	PtPd
50 $\text{mgL}^{-1}$	<i>E. faecium</i>	0	0	0	0	0	0	0	0	0	0
	<i>A. baumannii</i>	1	2	2	2	1	1	1	2	2	2
	<i>K. pneumoniae</i>	1	2	2	2	1	1	1	2	2	2
100 $\text{mgL}^{-1}$	<i>E. faecium</i>	1	2	2	2	1	1	1	2	2	2
	<i>A. baumannii</i>	1	2	2	2	1	1	1	4	4	4
	<i>K. pneumoniae</i>	1	2	2	2	1	1	1	4	4	4
500 $\text{mgL}^{-1}$	<i>E. faecium</i>	2	3	3	3	3	3	3	4	4	4
	<i>A. baumannii</i>	4	5	5	5	4	4	4	6	6	6
	<i>K. pneumoniae</i>	4	5	5	5	4	4	4	6	6	6
1000 $\text{mgL}^{-1}$	<i>E. faecium</i>	4	4	4	4	4	4	4	6	6	6
	<i>A. baumannii</i>	4	6	6	6	6	6	6	8	8	8
	<i>K. pneumoniae</i>	4	6	6	6	6	6	6	8	8	8

**Table 1.** Zone of inhibition assays for metal combinations against *E. faecium*, *A. baumannii* and *K. pneumoniae* (mm) demonstrating that platinum/palladium, gold/palladium or gold/platinum demonstrated the greatest antimicrobial activity. Au = gold, Cu = copper, Pt = platinum, Pd = palladium and Ag = silver ( $n = 3$ ). The inhibition zones were graded from 0 to 4, which measured as, 0–4 mm = grade 0, 4–8 mm = grade 1, 8–12 mm = grade 2, 12–16 mm = grade 3 and 16–20 mm = grade 4.

Test samples	<i>K. pneumoniae</i>		<i>A. baumannii</i>		<i>E. faecium</i>	
	MIC	MBC	MIC	MBC	MIC	MBC
Ag	$11.71 \pm 2.76$	$11.71 \pm 2.76$	$3.90 \pm 0$	$7.81 \pm 0$	$15.62 \pm 0$	$62.50 \pm 0$
Cu	$15.62 \pm 0$	$15.62 \pm 0$	$15.62 \pm 0$	$15.62 \pm 0$	$62.50 \pm 0$	$125.00 \pm 0$
Pt	$3.90 \pm 0$	$3.90 \pm 0$	$5.85 \pm 1.38$	$7.81 \pm 0$	$11.71 \pm 2.76$	$31.25 \pm 0$
Au	$5.85 \pm 1.38$	$3.90 \pm 0$	$3.90 \pm 0$	$5.85 \pm 1.38$	$11.71 \pm 2.76$	$31.25 \pm 0$
Pd	$5.85 \pm 1.38$	$3.90 \pm 0$	$7.81 \pm 0$	$7.81 \pm 0$	$15.62 \pm 0$	$31.25 \pm 0$

**Table 2.** Minimal inhibitory concentration and minimal bactericidal concentration (mgL<sup>-1</sup>) values for the metals against tested three bacteria demonstrating that platinum and gold displayed the most inhibitory concentrations and platinum, gold and palladium demonstrated the most potent MBCs. Au = gold, Cu = copper, Pt = platinum, Pd = palladium and Ag = silver (n = 3).



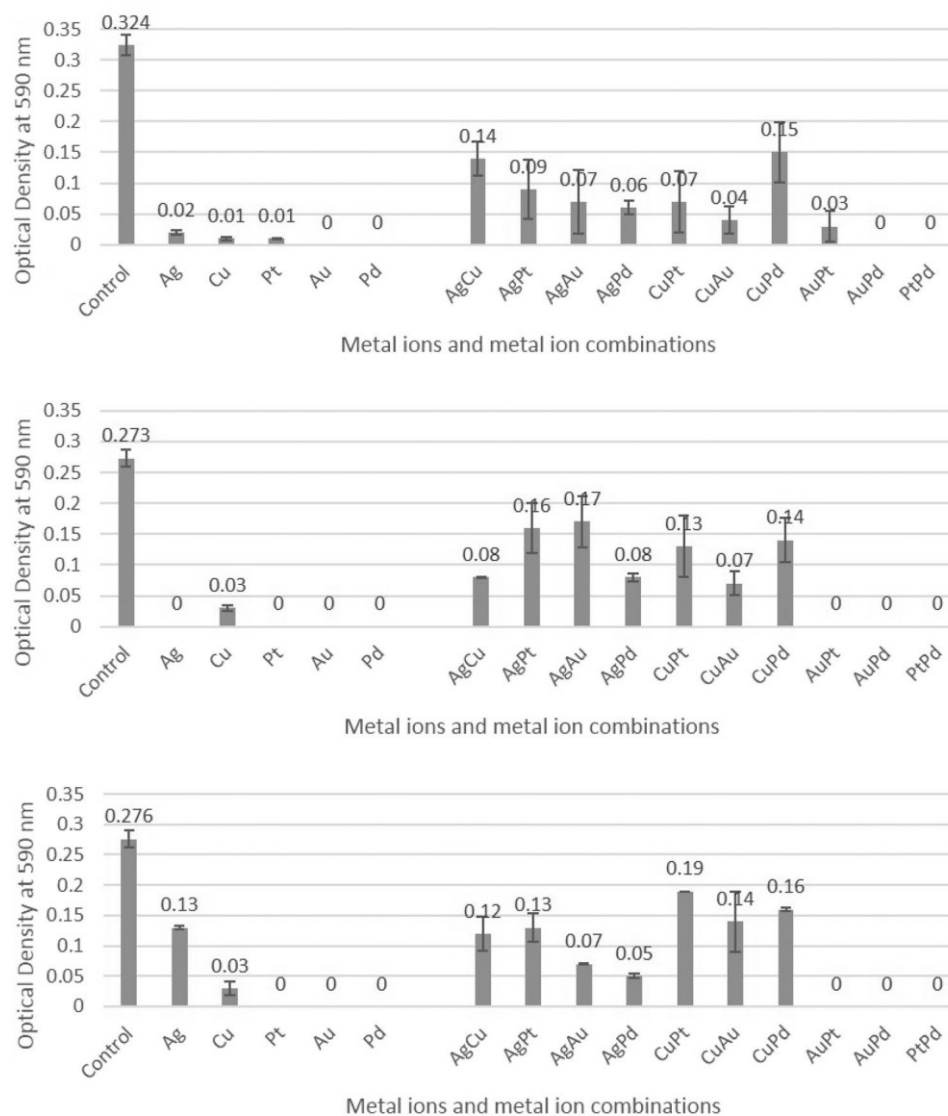
**Figure 2.** Examples of combined metals used in ZoI to demonstrate the interactions. (a) Palladium/platinum against Gram negative bacteria (indifference interaction) and (b) gold/palladium against *E. faecium* (synergy interaction).

greatest bactericidal activity for platinum, gold and palladium at 3.90 mgL<sup>-1</sup> against *K. pneumoniae*, 5.85 mgL<sup>-1</sup> (gold) and 7.81 mgL<sup>-1</sup> (platinum and palladium) against *A. baumannii* and 31.25 mgL<sup>-1</sup> (gold, platinum and palladium) against *E. faecium*. Silver showed equable antimicrobial efficacy as platinum, gold and palladium against *A. baumannii* ( $\leq 7.81$  mgL<sup>-1</sup>) and moderate efficacy against rest two pathogens. Copper was found to be the least active with an antimicrobial efficacy at 15.62 mgL<sup>-1</sup> against the two Gram-negative bacteria and 125.00 mgL<sup>-1</sup> against *E. faecium* (Table 3).

**Fractional inhibitory concentration (FIC) for metal combinations.** The FIC was used to determine the synergistic antimicrobial efficacy of the metals in combination in a solution. The FIC determined that the silver/palladium combination against *E. faecium* and silver/copper combination against *A. baumannii* demonstrated

Metal ion combinations	AgCu	AgPt	AgAu	AgPd	CuPt	CuAu	CuPd	AuPt	AuPd	Ptpd
<i>K. pneumoniae</i>	0.57 ± 0	0.66 ± 0	0.73 ± 0.68	0.73 ± 0.68	0.92 ± 0.68	0.67 ± 0.68	0.90 ± 0	0.83 ± 0	0.66 ± 0	0.83 ± 0
<i>A. baumannii</i>	0.46 ± 0.34	0.61 ± 0.34	0.74 ± 0.34	0.74 ± 0	1.37 ± 1.38	0.62 ± 0	0.73 ± 0	0.83 ± 0	0.74 ± 0	0.57 ± 0
<i>E. faecium</i>	0.62 ± 0	1.16 ± 0	0.58 ± 0	0.37 ± 0.68	0.79 ± 0	0.79 ± 0	1.24 ± 0	1.33 ± 0	2.77 ± 0	1.10 ± 0

**Table 3.** Fractional inhibitory concentration index for metal ion combinations demonstrating a synergistic antimicrobial efficacy for silver/copper against *K. pneumoniae* and silver/palladium against *E. faecium*. Synergy = <0.5, indifference = 0.5–4.0 or antagonism = >4.0. Au = gold, Cu = copper, Pt = platinum, Pd = palladium and Ag = silver (n = 3).



**Figure 3. (a–c)** Biofilm growth in the presence of metal ions tested individually and in combination at 500 mgL<sup>-1</sup> against **(a)** *K. pneumoniae*, **(b)** *A. baumannii* and **(c)** *E. faecium* using crystal violet biofilm assay. The metals were tested in a 1:1 ratio. Au = gold, Cu = copper, Pt = platinum, Pd = palladium and Ag = silver (n = 3).

synergistic antimicrobial efficacy (Table 3) (FIC synergistic value  $\leq 0.5$ ). All other metal combinations demonstrated indifferent FIC activities (FIC  $> 0.5 < 4.0$ ). No metal ion solution combinations were found to demonstrate antagonistic interactions ( $>4.0$ ) against the three tested microbes (Table 3).

**Biofilm accumulation assays for single and combined metals.** The biofilm assays for the individual metal solutions demonstrated excellent antimicrobial efficacies for all the metals at 500 mgL<sup>-1</sup> concentration against all the three bacteria (Fig. 3a–c). The silver against *E. faecium* was the only result that demonstrated partial antimicrobial activity. Synergistic assays against the biofilms demonstrated that at the greatest concentration (500 mgL<sup>-1</sup>) gold/palladium, gold/platinum and platinum/palladium resulted in the greatest antimicrobial efficacy with no detectable biofilm formation against all three tested bacteria along with silver/palladium and copper/gold against *K. pneumoniae* and silver/palladium against *E.*



*faecium*. Most of the other metal combinations demonstrated partial antimicrobial activity, with only a few demonstrating little antimicrobial activity. None of the metal ion combinations demonstrated no antimicrobial activity.

## Discussion

With the increase in hospital-acquired infections and the development of multidrug resistant bacteria, it is imperative that new biocidal and antimicrobial formulations are found. Metal compounds and complexes of palladium, platinum, copper, gold and silver have been shown to demonstrate effective antimicrobial efficacies against a broad range of AMR pathogens<sup>5, 6, 10, 19</sup>. Metals such as silver in wound dressings, copper on touch surfaces of patient equipment and gold and palladium coatings on catheters are considered to possess potential antimicrobial properties to reduce bacterial infection and transmission risks<sup>24–26</sup>. However, few studies have demonstrated the antimicrobial efficacy of platinum, gold and palladium in their ionic forms or in combination, although their complexes (tetradentate macrocyclic, cisplatin, etc.) have been shown to demonstrate inhibition against bacterial pathogens<sup>27–29</sup>.

As expected, concentration played a pivotal role in increasing the antimicrobial activity in the present study. Similar results have been demonstrated by others for complexes containing N-(thiophen-2-ylmethylene)benzo[d] thiazol-2-amine schiff bases with copper, zinc, cobalt and nickel whereby antimicrobial efficacy increased with increasing concentrations (from 5 mgL<sup>-1</sup> to 20 mgL<sup>-1</sup>)<sup>30</sup>. Copper, nickel and cobalt combined with coumarin-8-yl ligands have also showed greater bacterial inhibition at 100 mgL<sup>-1</sup> compared to 25 mgL<sup>-1</sup> or 50 mgL<sup>-1</sup> against *K. pneumoniae*<sup>31</sup>. This is probably due to the greater quantity of metal ions resulting in increased metal-bacterial interactions, leading to increased cell death<sup>14</sup>.

Overall, platinum, gold and palladium demonstrated the greatest antimicrobial efficacies against both planktonic bacteria and biofilms. However, in its ionic form, copper demonstrated little antimicrobial effect against cells or biofilms. In our work, which used metal ions in solution, the most electronegative metals produced the best antimicrobial results overall. This may be a result of the high electronegativity of the metal ions being highly attracted to the negatively charged bacteria. The result of these highly attractive forces may result in increased bacterial-metal ion interactions leading to greater antimicrobial efficacy and thus increased cell death.

Although copper and silver are known antimicrobials these were not the most active metal ion solutions tested. The platinum, gold and palladium being the most effective antimicrobials was determined in all the assays, except in the results from the FIC. The FIC demonstrated that the silver combinations (silver/palladium against *E. faecium* and silver/copper against *A. baumannii*), demonstrated the most antimicrobial synergistic combination. This might be since, in our work the metal ions were in solutions whereas work by others usually involves the investigation of the antimicrobial efficacy of the metals in the form of surfaces, nanoparticles or complexes and it is known that the form of the metal will affect the antimicrobial mechanism of action. Although the MIC, MBC and FIC were carried out in liquid media, it may be that when the metals were combined as in the FIC, the metal ions interacted in a different way, resulting in the silver having a predominant effect. However, the reason for the FIC result with the silver is unclear and requires further investigation but it may be due to the principal oxidation state of the silver. What is clear is that the assay used does influence the results and one assay alone should not be used to determine the overall antimicrobial efficacy of a compound.

Platinum nanoparticles have demonstrated antimicrobial efficacies against *Bacillus subtilis*, *Staphylococcus aureus*, *Pseudomonas aeruginosa* and *Escherichia coli*<sup>32</sup> whereas others have found no effect<sup>33</sup>. A study tested the antibacterial properties of nine different metal surfaces against *S. aureus* and *E. coli* and found that in agreement with our results, palladium demonstrated greater antimicrobial efficacy than the other metals tested<sup>34</sup>. A study by Kawakami *et al.* (2008) also looked at the antimicrobial efficacy of a number of metals including platinum and palladium and it was found that they were effective against *E. coli*. However, in contrast to our results, their study found that gold demonstrated little

effect against *E. coli* or *S. aureus*<sup>35</sup>. However, gold in nanoparticle and ionic form has been suggested to have antimicrobial activity<sup>12</sup>, and gold nanoparticles have also been shown to inhibit biofilm formation<sup>36</sup>. Although not as effective in our study, silver in other forms has demonstrated antimicrobial efficacy. Silver alginate has been shown to have antimicrobial efficacy against bacterial species isolated from burn wounds including *A. baumannii*, *K. pneumoniae* and *E. faecium*<sup>25, 37</sup>. It is also well known that copper surfaces have antimicrobial efficacy against a wide range of microbes<sup>38–40</sup>.

The differing toxic effects of metals and their components on bacteria can be due to various mechanisms such as antioxidant depletion, deoxyribonucleic acid (DNA) damage, impaired membrane function and/or interference with nutrient assimilation<sup>2</sup>. The most common hypothesis for the antimicrobial action of silver involves silver ions binding to the proteins and enzymes in the cell wall, cell membrane and peptidoglycan. This causes structural changes in the cell wall, such as pits. This increases cell permeability, leading to distortion and finally lysis of the cells<sup>40–42</sup>. Another antimicrobial mechanism of silver is its ability to inter-chelate with the phosphorus elements in bacterial DNA, which results in impaired ability to replicate and express ribosomal subunit proteins and other cellular proteins<sup>43–45</sup>. Platinum's primary cisplatin target is DNA but it also has an affinity for the sulphur and selenium donors present in many proteins<sup>46, 47</sup>. A palladium complex with 1,6-bis(benzimidazol-2-yl)-3,4-dithiahexane was thought to exhibit bacterial toxicity mechanisms due to metal protein binding leading to DNA damage, causing cell death. Although the chemistry of palladium is very similar to that of platinum, palladium complexes differ from those of platinum in several respects. Palladium exhibits a greater propensity to exchange ligands, which is about 105 times higher than platinum<sup>48</sup>. The ligand dissociation generates active metal species that can easily interact with other compounds, thus palladium complexes are toxic because of their higher reactivity<sup>48</sup>. The mechanistic action of gold is thought to be due to strong cationic attractions to the negatively charged plasma membrane of microbes which leads to cell membrane disruption, Reactive Oxygen Species (ROS) accumulation and consequent cell death<sup>35, 49</sup>. Copper ions released from copper alloys have been suggested to target bacteria by increasing ROS production and thus inducing DNA damage. However, this concept is controversial as it has further been demonstrated that disruption of the cell envelope is the mode of action of contact killing mediated by dry metallic copper surfaces<sup>38</sup>. In terms of our results, this concept holds true and would in part explain the low antimicrobial results when the copper was in solution. Further, there are significant differences that exist between the exposure of bacteria to copper ions and exposure to metallic copper surfaces, since the cells on dry metallic copper surfaces are not in an environment that promotes growth. Therefore, these cells face challenges that are different from those in an aqueous environment<sup>38</sup>. It has also been suggested that the antibacterial property of copper ions do not act like some other metals ions such as silver<sup>50</sup>. Thus, it may be that when the bacteria are in direct contact with copper surfaces an enhanced antimicrobial effect is achieved.

To the author's knowledge, studies showing the antimicrobial efficacies of individual and combined metal ions has been little researched. A metal's antimicrobial mechanistic activity is dependent on its chemical properties (for example donor atom selectivity, reduction potential), which govern their reactivity in bacterial cells. Thus, using antimicrobial agents in combination may further increase their antimicrobial efficacy by producing a synergistic effect<sup>51–53</sup>. In agreement with our results, work by others has also demonstrated that silver ions showed a lower MBC value for *E. coli* planktonic cells than for biofilms<sup>54</sup>. Since the physiology, gene expression and morphology of planktonic cells differs from those cells in biofilms, the difference in the efficacy of the antimicrobial agents against the bacteria in their different states might not be that unexpected<sup>53–55</sup>.

## Conclusion

In this pilot study, gold, platinum and palladium demonstrated the most effective antimicrobial activity overall for individual metal ion solutions against both planktonic or biofilm phenotypes for three pathogens and could potentially be used in biocidal formulations where intensive cleaning is required. The synergistic combinations of



gold/platinum, gold/palladium and platinum/palladium have the potential to be used in a range of antimicrobial or biocidal combinations, particularly against the medically-relevant pathogens tested in this study. Other metals demonstrated some antimicrobial and synergistic activity under certain conditions and against particular cells. Overall platinum demonstrated the greatest antimicrobial efficacy. The results suggest that when used as potential antimicrobials, the combinations selected must be tested towards bacteria in their relevant physiological states. It should be noted that the results of this preliminary study were only carried out against one strain of each bacterial species and hence future work will investigate the antimicrobial effects of the metal ions against a range of bacterial isolates.

## Methods

**Cultures and Media.** Stock cultures of *K. pneumoniae* strain NCTC9633 and *A. baumannii* strain 12156 were subcultured onto Nutrient agar (NA) and incubated at 37 °C for 24 h. *E. faecium* strain NCTC7171 was subcultured onto columbia blood agar (Oxoid, UK) supplemented with 5% defibrinated horse blood in a 5% CO<sub>2</sub> incubator for 24 h at 37 °C. Brain heart infusion (BHIA) agar (Oxoid, UK) and brain heart infusion broth (BHIB) (Oxoid, UK) were used for all the microbiological tests for *E. faecium*. Nutrient agar and nutrient broth (NB) (Oxoid, UK) were used to perform all the assays for *K. pneumoniae* or *A. baumannii*. Gram-negative microorganisms were incubated at 37 °C overnight in an aerobic atmosphere whilst *E. faecium* was incubated in a 5% CO<sub>2</sub> incubator for 24 h at 37 °C in static conditions for all the other assays in this study. All the assays were repeated at least thrice (n = 3).

**Chemical Preparation.** Single element standard calibration solutions for Ion Coupled Plasma – Atomic Adsorption Spectroscopy (ICP-AAS) of 1000 mgL<sup>-1</sup> of silver, copper, platinum, gold and palladium (Sigma-Aldrich, UK) were used. These were diluted with sterile water to the respective metal ion concentrations.

**Bacterial preparation.** Ten millilitres of appropriate broth was put into a sterile universal for the Zone of inhibition (ZoI) assays. One hundred and fifty millilitres of appropriate broth was put into a conical flask for minimum inhibitory concentrations (MIC), minimum bactericidal concentration (MBC) and fractional inhibitory concentration (FIC) and crystal violet biofilm assays (CVBAs). These were inoculated with a single colony of bacteria and incubated overnight according to the conditions in the culture and media sub-section. Cells were harvested by centrifugation (3500 g for 10 min) and then washed with 10 mL sterile distilled water and vortexed to ensure an even distribution of the cell suspension. The washed cells were again re-harvested. The pellet was re-suspended in 10 mL of broth, vortexed and the resultant cell suspension was adjusted to an optical density at 540 nanometres (nm) (OD<sub>540</sub>) of 1.0 using a spectrophotometer. The cell concentration corresponded to  $3.95 \times 10^8$  colony-forming units per mL (CFU mL<sup>-1</sup>) at an OD<sub>540</sub> of 1.0.

**Zone of inhibition assays.** Respective agar was poured into sterile Petri dishes, which were then cooled and 100 µL of cell suspension was pipetted and spread across the entire area of the agar. Three equal wells (8 mm diameter) were cut out of the each agar plate using a sterile cork borer and stainless steel needle. To each of the wells, 100 µL of the metal ion solution was added. The plates were incubated as mentioned in cultures and media sub-section. The ZoI was measured using the different metal ion solution concentrations, 50 mgL<sup>-1</sup>, 100 mgL<sup>-1</sup>, 500 mgL<sup>-1</sup> and 1000 mgL<sup>-1</sup>. Following incubation, the ZoI was measured in mm from four sides of each well to determine an average mean value (n = 12).

**Zone of inhibition assays (synergy).** For the synergy assays, the same method was carried out as above (zone of inhibition) except that two wells were cut from the agar, 6 mm apart (n = 3). The concentration of the metal ions used in the ZoI synergy assays was 50 mgL<sup>-1</sup>, 100 mgL<sup>-1</sup>, 500 mgL<sup>-1</sup> and 1000 mgL<sup>-1</sup>. Following incubation, the inhibition zones were graded from 0 to 4, which measured as, 0–4 mm – grade 0, 4–8 mm – grade 1,

8–12 mm – grade 2, 12–16 mm – grade 3 and 16–20 mm – grade 4. The grade of inhibition of the metal ion solution combinations were calculated as follows;

$$\Sigma \text{ metal ion solution combination} = \text{first metal grade of inhibition} + \text{second metal grade of inhibition} \quad (1)$$

**Individual metal ion MIC and MBC assays.** One millilitre of Triphenyl tetrazolium chloride (TTC) blue metabolic dye (Sigma-Aldrich, UK), was added into 9 mL of the OD adjusted cell suspension so that the working concentration of the dye was 0.15% w/v. To determine the MIC, 100  $\mu\text{L}$  of the test samples were added to a 96 well flat-bottomed microtiter plate (MTP). One hundred microliters of bacterial suspension with the TTC dye was then added; the first column of cell/metal ion suspension was mixed, then 100  $\mu\text{L}$  of the sample/bacterial mix was transferred to the column 2 wells and repeated until column 10. To column 11, 100  $\mu\text{L}$  of bacterial suspension without a metal (positive control) was added and to column 12 and 100  $\mu\text{L}$  of un-inoculated broth was added (negative control). After incubation, the MIC was taken as lowest concentration that inhibited the visible growth of the bacteria by comparison with the controls. Growth was indicated by a change of colour in the well to dark blue/purple. Twenty-five microliters of culture was taken from the first well that showed no growth and the last well that demonstrated growth and was pipetted onto agar plates using Miles and Misra methodology<sup>56, 57</sup> ( $n = 3$ ). After incubation, the lowest concentration well sample that showed no bacterial growth on the agar plate was determined to be the MBC for that test sample ( $n = 3$ ).

**Fractional inhibitory concentrations assay.** The bacterial suspension and test samples for the FIC test were prepared as described in the sub-section culture and media and MIC method, except that both metal ion solutions were added to the wells in a 1:1 ratio. Following incubation at 37 °C for 24 h, the FIC values were calculated as;

$$\Sigma = \text{FIC of antimicrobial A} + \text{FIC of antimicrobial B}$$

$$\frac{\text{MIC or MBC of antimicrobial A in combination}}{\text{MIC or MBC of antimicrobial A alone}} + \frac{\text{MIC or MBC of antimicrobial B in combination}}{\text{MIC or MBC of antimicrobial B alone}}$$

depending on the FIC values, the antimicrobial interaction was evaluated as synergy = <0.5, indifference = 0.5–4.0 or antagonism = >4.0 ( $n = 3$ ).

**Crystal Violet Biofilm Assay (CVBA).** *Preparation of stainless steel coupons.* Fine polished (FP) 304 grade stainless steel coupons (10 mm  $\times$  10 mm) were used in the assays. Coupons were washed thoroughly by sequentially putting the coupons into beakers each containing either acetone, methanol or ethanol (BDH, UK) for 10 min with a sterile water wash in between each, and for the final step. The washed coupons were air dried and stored in sealed plastic containers at room temperature until used.

*Biofilm formation and CVBA (adapted from Christen et al. 1985).* The cell suspension was prepared in the same manner as described in culture and media sub-section. Twelve well culture plates were used to grow the biofilms. Cleaned coupons were placed in the centre of the well with the fine polished surface facing upward. One millilitre of adjusted OD cell suspension was added to each well and incubated for 7 days at 37 °C to produce a biofilm. Plates were wrapped in Parafilm™ to prevent moisture loss and air contaminants over the long incubation time. After incubation, the stainless-steel coupons were carefully washed with 2 mL of sterile distilled water using a pipette to remove any loose planktonic cells whilst avoiding damaging the biofilms. The coupons were air dried at room temperature for 2 h. One millilitre of metal ion solution at 500  $\text{mgL}^{-1}$  was added into each respective well.

Respective agar broths were also added into one of the wells to serve as a negative control. The plates were incubated for 24 h at 37 °C. Following incubation, the metal ion solutions were removed. The coupons were carefully washed with 1 mL of sterile distilled water and were air dried at room temperature. One millilitre of 0.03% crystal violet solution (Oxoid, UK) was added into each well with a coupon and left for 30 min. The coupons were gently washed with 2 mL sterile distilled water to remove any excess stain. The coupons were placed into new 12 well plates and air dried at room temperature for 1 h. One millilitre of 33% glacial acetic acid (BDH, UK) was added to each well and left for 30 min to solubilise any stained biofilm. The solution was removed and the absorbance measured at OD590 (n = 3). Bacterial biofilms were divided into breakpoint categories; OD < 0.067 antimicrobial; OD ≥ 0.068 but ≤ 0.135 partial antimicrobial activity; ≥OD 0.136–≤0.270 negligible antimicrobial activity; >0.271 no antimicrobial activity. These values were determined using quartiles of the lowest OD value determined from the control.

**Statistical analyses.** Mean values were used to compare the antimicrobial efficacy results of the metal ion solution samples at varying concentrations. Standard deviation or standard error were calculated to analyse the distributions of the data from the mean value, and confidence intervals of 95% were calculated for the ZoI, FIC and MBC synergy tests results to plot error bars.

## References

1. Elsom, A. M. *et al.* Antimicrobial activities *in vitro* and *in vivo* of transition element complexes containing gold(I) and osmium(VI). *J. Antimicrob. Chemother.* **37**, 911, doi:10.1093/jac/37.5.911 (1996).
2. Lemire, J. A. *et al.* Antimicrobial activity of metals: mechanisms, molecular targets and applications. *Nat. Rev. Microbiol.* **11**, 371, doi:10.1038/nrmicro3028 (2013).
3. Arai, T. *et al.* Ecotoxicology of antifouling biocides. (Springer Japan, 2009).
4. Eriksson, J. *et al.* Regulating chemical risks: European and global challenges. (Springer Science & Business Media, Netherlands 2010).
5. Feng, Q. L. *et al.* A mechanistic study of the antibacterial effect of silver ions on *Escherichia coli* and *Staphylococcus aureus*. *J. Biomed. Mater. Res.* **52**, 662, doi:10.1002/1097-4636(20001215)52:4<662::aid-jbm10>3.0.co;2-3 (2000).
6. Christophe Espirito, S. *et al.* Bacterial Killing by Dry Metallic Copper Surfaces. *Appl. Environ. Microbiol.* **77**, 794, doi:10.1128/AEM.01599-10 (2011).
7. Woodward, B. F. Analysis: Palladium in Temporary and Permanently Implantable Medical Devices. *Platin. Met. Rev.* **56**, 213, doi:10.1595/147106712X651748 (2012).
8. Cowley, A. & Woodward, B. A Healthy Future: Platinum in Medical Applications. *Platin. Met. Rev.* **55**, 98, doi:10.1595/147106711X566816 (2011).
9. Selvaraj, V. *et al.* Antimicrobial and anticancer efficacy of antineoplastic agent capped gold nanoparticles. *J. Biomed. Nanotechnol.* **6**, 129, doi:10.1166/jbn.2010.1115 (2010).
10. Tom, R. T. *et al.* Ciprofloxacin-protected gold nanoparticles. *Langmuir*. **20**, 1909, doi:10.1021/la0358567 (2004).
11. Grace, A. N. & Pandian, K. Quinolone Antibiotic-Capped Gold Nanoparticles and Their Antibacterial Efficacy Against Gram Positive and Gram Negative Organisms. *J. Bionanosci.* **1**, 96, doi:10.1166/jbns.2007.018 (2007).
12. Zhang, Y. *et al.* Antimicrobial Activity of Gold Nanoparticles and Ionic Gold. *J. Environ. Sci. Health. C. Environ. Carcino. Ecotoxicol. Rev.* **33**, 286, doi:10.1080/10590501.2015.1055161 (2015).
13. Sim, J. H. *et al.* *In vitro* antibacterial and time-kill evaluation of phosphane-gold(I) dithiocarbamates, R<sub>3</sub>PAu[S<sub>2</sub>CN(iPr)CH<sub>2</sub>CH<sub>2</sub>OH] for R = Ph, Cy and Et, against a broad range of Gram-positive and Gram-negative bacteria. *Gold. Bull.* **47**, 225, doi:10.1007/s13404014-0144-y (2014).
14. Nazari, Z. *et al.* The combination effects of trivalent gold ions and gold nanoparticles with different antibiotics against resistant *Pseudomonas aeruginosa*. *Gold. Bull.* **45**, 53, doi:10.1007/s13404-012-0048-7 (2012).
15. Arias, C. A. & Murray, B. E. The rise of the Enterococcus: beyond vancomycin resistance. *Nat. Rev. Microbiol.* **10**, 266, doi:10.1038/nrmicro2761 (2012).
16. Arias, C. A. & Murray, B. E. Emergence and management of drug-resistant enterococcal infections. *Expert. Rev. Anti. Infect. Ther.* **6**, 637, doi:10.1586/14787210.6.5.637 (2008).
17. Mohamed, J. A. & Huang, D. B. Biofilm formation by enterococci. *J. Med. Microbiol.* **56**, 1581, doi:10.1099/jmm.0.47331-0 (2007).
18. Jia, W. *et al.* Prevalence and antimicrobial resistance of Enterococcus species: A Hospital-Based Study in China. *Int. J. Environ. Res. Public. Health* **11**, 3424, doi:10.3390/ijerph110303424 (2014).
19. Bradley, C. R. & Fraiese, A. P. Heat and chemical resistance of enterococci. *J. Hosp. Infect.* **34**, 191, doi:10.1016/S0195-6701(96)900651 (1996).
20. Highsmith, A. K. & Jarvis, W. R. Klebsiella pneumoniae: selected virulence factors that contribute to pathogenicity. *Infect. Control* **6**, 75, doi:10.1017/S0195941700062640 (1985).
21. Paczosa, M. K. & Meccas, J. Klebsiella pneumoniae: going on the offense with a strong defense. *Microbiol. Mol. Biol. Rev.* **80**, 629, doi:10.1128/MMBR.00078-15 (2016).
22. Gootz, T. D. & Marra, A. Acinetobacter baumannii: an emerging multidrug-resistant threat. *Expert. Rev. Anti. Infect. Ther.* **6**, 309, doi:10.1586/14787210.6.3.309 (2008).
23. Grace, A. N. & Pandian, K. Quinolone Antibiotic-Capped Gold Nanoparticles and Their Antibacterial Efficacy Against Gram Positive and Gram Negative Organisms. *J. Bionanosci.* **1**, 96, doi:10.1166/jbns.2007.018 (2007).
24. Chandra, S. *et al.* Spectral and antimicrobial studies on tetraaza macrocyclic complexes of Pd-II, Pt-II, Rh-III and Ir-III metal ions. *J. Saudi. Chem. Soc.* **15**, 49, doi:10.1016/j.jscs.2010.09.005 (2011).

25. Thomas, J. G. *et al.* *In vitro* antimicrobial efficacy of a silver alginate dressing on burn wound isolates. *J. Wound. Care* **20**, 124, doi:10.12968/jowc.2011.20.3.124 (2011).
26. Huang, H. I. *et al.* *In vitro* efficacy of copper and silver ions in eradicating *Pseudomonas aeruginosa*, *Stenotrophomonas maltophilia* and *Acinetobacter baumannii*: implications for on-site disinfection for hospital infection control. *Water. Res* **42**, 73, doi:10.1016/j.watres.2007.07.003 (2008).
27. Saygun, O. *et al.* Gold and Gold-Palladium Coated Polypropylene Grafts in a S. epidermidis Wound Infection Model. *J. Surg. Res.* **131**, 73, doi:10.1016/j.jss.2005.06.020 (2006).
28. Mishra, A. K. *et al.* Synthesis, characterization, antibacterial and cytotoxic study of platinum (IV) complexes. *Bioorg. Med. Chem.* **14**, 6333, doi:10.1016/j.bmc.2006.05.047 (2006).
29. Adam, A. M. A. *et al.* Synthesis and spectroscopic characterizations of noble metal complexes (gold, silver, platinum) in the presence of selenium, and their biological applications as antibacterial, antifungal, and anticancer. *Res. Chem. Intermediat* **41**, 965, doi:10.1007/s11164-013-1249-2 (2015).
30. Etaïw, S. E. H. *et al.* Synthesis, spectral, antimicrobial and antitumor assessment of Schiff base derived from 2-aminobenzothiazole and its transition metal complexes. *Spectrochim. Acta. A. Mol. Biomol. Spectros* **79**, 1331, doi:10.1016/j.saa.2011.04.064 (2011).
31. Patil, S. A. *et al.* Co(II), Ni(II) and Cu(II) complexes with coumarin-8-yl Schiff-bases: Spectroscopic, *in vitro* antimicrobial, DNA cleavage and fluorescence studies. *Spectrochim. Acta. A. Mol. Biomol. Spectros* **79**, 1128, doi:10.1016/j.saa.2011.04.032 (2011).
32. Ayaz Ahmed, K. B. *et al.* Platinum nanoparticles inhibit bacteria proliferation and rescue zebrafish from bacterial infection. *RSC. Adv.* **6**, 44415, doi:10.1039/c6ra03732a (2016).
33. Cho, K. H. *et al.* The study of antimicrobial activity and preservative effects of nanosilver ingredient. *Electrochim. Acta.* **51**, 956, doi:10.1016/j.electacta.2005.04.071 (2005).
34. Yasuyuki, M. *et al.* Antibacterial properties of nine pure metals: a laboratory study using *Staphylococcus aureus* and *Escherichia coli*. *Biofouling*. **26**, 851, doi:10.1080/08927014.2010.527000 (2010).
35. Kawakami, H. *et al.* Antibacterial properties of metallic elements for alloying evaluated with application of JIS Z 2801:2000. *ISIJ. Int.* **48**, 1299, doi:10.2355/isijinternational.48.1299 (2008).
36. Yu, Q. L. *et al.* Inhibition of gold nanoparticles (AuNPs) on pathogenic biofilm formation and invasion to host cells. *Sci. Rep.* **6**, 26667, doi:10.1038/srep26667 (2016).
37. Castellano, J. J. *et al.* Comparative evaluation of silver-containing antimicrobial dressings and drugs. *Int. Wound. J* **4**, 114, doi:10.1111/j.1742-481X.2007.00316.x (2007).
38. Santo, C. E. *et al.* Bacterial Killing by Dry Metallic Copper Surfaces. *Appl. Environ. Microbiol.* **77**, 794, doi:10.1128/AEM.01599-10 (2011).
39. Noyce, J. O. *et al.* Potential use of copper surfaces to reduce survival of epidemic methicillin-resistant *Staphylococcus aureus* in the healthcare environment. *J. Hosp. Infect.* **63**, 289, doi:10.1016/j.jhin.2005.12.008 (2006).
40. Casey, A. L. *et al.* Role of copper in reducing hospital environment contamination. *J. Hosp. Infect.* **74**, 72, doi:10.1016/j.jhin.2009.08.018 (2010).
41. Sondi, I. & Salopek-Sondi, B. Silver nanoparticles as antimicrobial agent: a case study on *E. coli* as a model for Gram-negative bacteria. *J. Colloid. Interface. Sci.* **275**, 177, doi:10.1016/j.jcis.2004.02.012 (2004).
42. Pal, S. *et al.* Does the Antibacterial Activity of Silver Nanoparticles Depend on the Shape of the Nanoparticle? A Study of the GramNegative Bacterium *Escherichia coli*. *Appl. Environ. Microbiol.* **73**, 1712, doi:10.1128/AEM.02218-06 (2007).
43. Edwards-Jones, V. The benefits of silver in hygiene, personal care and healthcare. *Lett. Appl. Microbiol.* **49**, 147, doi:10.1111/j.1472765X.2009.02648.x. (2009).
44. Schierholz, J. M. & Beuth, J. Implant infections: a haven for opportunistic bacteria. *J. Hosp. Infect.* **49**, 87, doi:10.1053/jhin.2001.1052 (2001).
45. Kim, S. H. *et al.* Antimicrobial effects of silver nanoparticles. *Nanomed. Nanotech. Biol. Med* **3**, 95, doi:10.1016/j.nano.2006.12.001 (2007).
46. Rai, M. *et al.* Silver nanoparticles as a new generation of antimicrobials. *Biotechnol. Adv.* **27**, 76, doi:10.1016/j.biotechadv.2008.09.002 (2009).
47. Lippard, S. J. New chemistry of an old molecule: cis-[Pt(NH<sub>3</sub>)<sub>2</sub>Cl<sub>2</sub>]. *Sci.* **218**, 1075, doi:10.1126/science.6890712 (1982).
48. Roberts, J. J. & Thomson, A. J. The mechanism of action of antitumor platinum compounds. *Prog. Nucleic. Acid. Res. Mol. Biol.* **22**, 71, doi:10.1016/S0079-6603(08)60799-0 (1979).
49. Medici, S. *et al.* Noble metals in medicine: Latest advances. *Coord. Chem. Rev.* **284**, 329, doi:10.1016/j.ccr.2014.08.002 (2015).
50. Huh, A. J. & Kwon, Y. J. Nanoantibiotics: A new paradigm for treating infectious diseases using nanomaterials in the antibiotics resistant era. *J. Control. Release.* **156**, 128, doi:10.1016/j.jconrel.2011.07.002 (2011).
51. Faúndez, G. *et al.* Antimicrobial activity of copper surfaces against suspensions of *Salmonella enterica* and *Campylobacter jejuni*. *BMC Microbiol.* **4**, 19, doi:10.1186/1471-2180-4-19 (2004).
52. Ahmad, A. *et al.* Antimicrobial activity of *Mentha piperita* essential oil in combination with silver ions. *Synergy.* **1**, 92, doi:10.1016/j.synres.2014.11.001 (2014).
53. Aslan, H. G. *et al.* Synthesis, characterization and antimicrobial activity of salicylaldehyde benzenesulfonylhydrazone (Hsalbsmh) and its Nickel(II), Palladium(II), Platinum(II), Copper(II), Cobalt(II) complexes. *Inorg. Chem. Commun.* **14**, 1550, doi:10.1016/j.inoche.2011.05.024 (2011).
54. Choi, O., Yu, C. P., Esteban Fernandez, G. & Hu, Z. Interactions of nanosilver with *Escherichia coli* cells in planktonic and biofilm cultures. *Water Res* **44**, 6095, doi:10.1016/j.watres.2010.06.069 (2010).
55. Landini, P. *et al.* Molecular mechanisms of compounds affecting bacterial biofilm formation and dispersal. *Appl. Microbiol. Biotechnol.* **86**, 813, doi:10.1007/s00253-010-2468-8 (2010).
56. Hedges, A. J. Estimating the precision of serial dilutions and viable bacterial counts. *Int. J. Food. Microbiol.* **76**, 207, doi:10.1016/S0168-1605(02)00022-3 (2002).
57. Christensen, G. D. *et al.* Adherence of Coagulase-Negative Staphylococci to Plastic Tissue Culture Plates: a Quantitative Model for the Adherence of Staphylococci to Medical Devices. *J. Clin. Microbiol.* **22** 996, doi:0095-1137/85/120996-11\$02.00/0 (1985).

## Author Contributions

Misha Vaidya carried out the experimental work. Kathryn A. Whitehead oversaw the project and the manuscript preparation. Andrew J. McBain, Jonathan A. Butler and Craig E. Banks contributed to the project design and writing of the manuscript.

# Additional Information

**Competing Interests:** The authors declare that they have no competing interests.

**Publisher's note:** Springer Nature remains neutral with regard to jurisdictional claims in published maps and institutional affiliations.



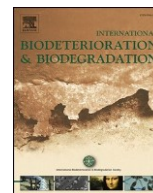
**Open Access** This article is licensed under a Creative Commons Attribution 4.0 International License, which permits use, sharing, adaptation, distribution and reproduction in any medium or format, as long as you give appropriate credit to the original author(s) and the source, provide a link to the Creative Commons license, and indicate if changes were made. The images or other third party material in this article are included in the article's Creative Commons license, unless indicated otherwise in a credit line to the material. If material is not included in the article's Creative Commons license and your intended use is not permitted by statutory regulation or exceeds the permitted use, you will need to obtain permission directly from the copyright holder. To view a copy of this license, visit <http://creativecommons.org/licenses/by/4.0/>.

© The Author(s) 2017



Contents lists available at [ScienceDirect](#)

## International Biodeterioration &amp; Biodegradation

journal homepage: [www.elsevier.com/locate/ibid](http://www.elsevier.com/locate/ibid)

## Antimicrobial activity of graphene oxide-metal hybrids



K.A. Whitehead <sup>a,\*</sup>, M. Vaidya <sup>a</sup>, C.M. Liao <sup>w</sup>, D.A.C. Brownson <sup>b</sup>, P. Ramalingam <sup>b,c</sup>,  
J. Kamieniak <sup>b</sup>, S.J. Rowley-Neale <sup>b</sup>, L.A. Tetlow <sup>a</sup>, J.S.T. Wilson-Nieuwenhuis <sup>a</sup>, D. Brown <sup>a</sup>, A.J.  
McBain <sup>d</sup>, J. Kulandaivel <sup>c</sup>, C.E. Banks <sup>a,b</sup>

<sup>a</sup> School of Healthcare Science, Manchester Metropolitan University, Chester Street, Manchester, M1 5GD, UK <sup>b</sup> Faculty of Science and Engineering, Manchester Metropolitan University, Manchester, Chester Street, M1 5GD, UK <sup>c</sup> Centre for Nanoscience and Nanotechnology, School of Physics, Bharathidasan University, Tamil Nadu, 620024, India <sup>d</sup> Division of Pharmacy and Optometry, School of Health Sciences, Faculty of Biology, Medicine and Health, The University of Manchester, Manchester, M13 9PT, UK

## article info

## Article history:

Received 16 November 2016

Received in revised form

5 May 2017

Accepted 28 June 2017 Available

online 10 July 2017

## Keywords:

Antimicrobials

Graphene oxide

Biocide

ESKAPE

Nano/Micro particles

Pathogens

## abstract

With resistant bacteria on the increase, there is a need for new combinations of antimicrobials/biocidal agents to help control the transmission of such microorganisms. Particulate forms of graphite, graphene oxide (GO) and metal-hybrid compounds (silver-graphene oxide (AgGO) and zinc oxide graphene oxide (ZnOGO)) were fabricated and characterised. X-Ray diffraction and Diffuse Reflectance Infrared Fourier Transform Spectroscopy demonstrated the composition of the compounds. Scanning Electron Microscopy and Energy Dispersive X-Ray Spectroscopy determined the compounds were heterogeneous and irregular in shape and size and that the level of silver in the AgGO sample was 57.9 wt% and the ZnOGO contained 72.65 wt % zinc. The compounds were tested for their antimicrobial activity against four prominent bacteria; *Escherichia coli*, *Staphylococcus aureus*, *Enterococcus faecium* and *Klebsiella pneumoniae*. AgGO was the most effective antimicrobial (Minimum inhibitory concentration *E. coli*/*Enterococcus faecium* 0.125 mg mL<sup>-1</sup>; *S. aureus*/*K. pneumoniae* 0.25 mg mL<sup>-1</sup>). The addition of Ag enhanced the activity of GO against the bacteria tested, including the generally recalcitrant *K. pneumoniae* and *Enterococcus faecium*. These findings demonstrated that GO-metal hybrids have the potential to be utilised as novel antimicrobials or biocides in liquid formulations, biomaterials or coatings for use in the treatment of wounds where medically relevant bacteria are becoming increasingly resistant.

© 2017 Elsevier Ltd. All rights reserved.

## 1. Introduction

Concerns about bacterial resistance from community-acquired and food-borne pathogens has been growing for a number of years at both national and international levels. Several Gram-positive and Gram-negative bacteria including *Escherichia coli*, *Klebsiella pneumoniae*, *Enterococcus faecium* and *Staphylococcus aureus* are currently considered as emergent global pathogens, which pose a huge global health problem (Boucher et al., 2009).

Metals have been used for decades to treat various infectious diseases, and their antimicrobial efficacies are now being reevaluated owing to the emergence of resilient pathogens. A particular interest has emerged particularly in the use of these

compounds for topical/therapeutic use as well as for disinfection to prevent the adhesion and transmission of bacterial species. Silver is one of the most widely investigated metals for antimicrobial applications, and is being used in a number of medical purposes including catheters, biomaterials and wound dressings. Zinc oxide (ZnO) is used in such applications as food packaging (Tayel et al., 2011), textiles (Velmurugan et al., 2016), as antimicrobials (Deokar et al., 2016), and in wound dressings (Chaturvedi et al., 2016). Nanoparticles are interesting in that they can be synthesized with a high surface area to volume ratio and with unusual morphologies that contain sharp edges and corners. Graphite and the graphene derivatives have traditionally been used in electrochemistry, from applications in energy technologies, such as batteries and fuel cells and they have also been used in an array of functional composites (Unwin et al., 2016). Work has recently

suggested that the graphene family of compounds also possess antimicrobial properties (Liu et al., 2011; Wang et al., 2012). By

\* Corresponding author.

E-mail address: [k.a.whitehead@mmu.ac.uk](mailto:k.a.whitehead@mmu.ac.uk) (K.A. Whitehead).

<http://dx.doi.org/10.1016/j.ibiod.2017.06.020> 0964-8305/© 2017

Elsevier Ltd. All rights reserved.

combining the antimicrobial activity of metals together with the physical effect of GO on the bacterial cell walls, it may be hypothesised that the antimicrobial activity of graphene products may be increased.

A number of disinfectants and antiseptics have been reported to be showing signs of becoming less effective so there is a need for the development of novel microbicides due to the current limitations (Russel and Chopra, 1990; Jennings et al., 2015). Transmission and infection problems due to bacterial adhesion to surfaces can be mitigated in part by the development of alternative antimicrobial sources/biocides. The aim of this work was to determine if metalGO hybrid compounds demonstrated increased antimicrobial efficacy compared to graphite and GO, against a range of bacteria. The development of such alternative antimicrobial actives may prove beneficial for use in such formulations such as biocidal, disinfecting or topical antimicrobials or cleaning agents or for incorporation into biomaterial coatings.

## 2. Materials and methods

### 2.1. Synthesis of compounds and characterisation

For the synthesis of the compounds, all chemicals (analytical grade or higher) were used as received from Sigma-Aldrich (UK) without any further purification and all solutions were prepared with deionised water of resistivity not less than 18.2 MU cm. Synthetic graphite powder was commercially obtained from Gwent Group (Pontypool, UK).

Graphene oxide (GO) was synthesized by the Hummers method via the oxidation of synthetic graphite (Hummers Jr. and Offeman, 1958). Graphite flakes (5 g) and NaNO<sub>3</sub> (2.5 g) were combined in 115 mL of H<sub>2</sub>SO<sub>4</sub> (conc.) and stirred for 30 min. Whilst kept in an ice bath (<5 C), KMnO<sub>4</sub> (15.0 g) was gradually added to the suspension and the rate of addition was controlled to keep the reaction temperature below 15 C. The mixture was heated to 35 C for a 30 min period and underwent continuous stirring producing a brown paste. A further dilution was made by adding 250 mL of water to the mixture and the temperature was increased to 70 C for 15 min. The resultant mixture was diluted by adding H<sub>2</sub>O until a final volume of 1 L was obtained. Finally, the solution was treated with 15 mL of H<sub>2</sub>O<sub>2</sub> (30% w/w) to terminate the reaction, at which stage the solution became yellow in appearance. For purification, the mixture was filtrated and the obtained solid was washed thoroughly with Milli Q water several times in order to avoid sulphate contamination. After purification, the powder was dried at 60 C during 48 h.

In the preparation of the AgGO, a sonochemical reduction method was utilised (Anandan and Muthukumar, 2015). Following preparation of the GO, 0.5 g was added to 150 mL of ethylene glycol and sonicated for 30 min. In a separate vesicle, 1.0 g of silver nitrate was added to 20 mL of ethylene glycol and sonicated for 30 min. The silver nitrate dispersion was added dropwise to the GO solution whilst undergoing sonication for 30 min to produce a homogeneous mixture. Finally, 50 mL of 0.1 M NaBH<sub>4</sub> was added to the resultant AgGO mixture and a further 30 min of sonication was performed. The product was purified with repeated steps of H<sub>2</sub>O and ethanol washing, after which the solution was dried at 50 C.

The ZnOGO was fabricated by dissolving 5.0 g GO in 200 mL of N, N-dimethylformamide (DMF), along with 20 mL of 1 M zinc acetate dihydrate (pH of 6.5). The homogeneous solution was heated to 60 C and was stirred continuously for 120 min, after which the solution was heated to 250 C.

Following solvent evaporation, partial ZnO/ZnOHGO was produced. The resulting dried product was collected and ground in an agate mortar prior to being annealed at 450 C for 120 min within atmospheric conditions to obtain the final ZnOGO product (Liu et al., 2012).

#### 2.1.1. Preparation of compounds for testing

For the analysis of the fabricated compounds, 20 mg of each test compound was added to 20 mL of sterile distilled water. The samples were vortexed for 10 s and immediately 10 mL of prepared sample was pipetted onto a 10 mm 10 mm polished silicon wafer (Montco Silicon Technologies, USA) and air dried for 30 min. The samples were stored at room temperature, in desiccators until use.

#### 2.1.2. X-Ray Diffraction (XRD)

In order to identify the crystal phase of the compounds, X-Ray Diffraction (XRD) was performed using a PANalytical X'pert powder diffraction platform. Nickel filtered copper Ka radiation (1 ¼ 1.54 Å) was used, with an anode voltage of 40 kV an anode current of 30 mA. A reflection transmission spinner stage (15 rpm) was implemented to hold the powder samples. The XRD parameters were step size: 0.13; sample: powder; slit (antiscatter) size: 1/4. The 2q range was set between 10 and 100, in correspondence with literature ranges associated with the characterised samples (Li et al., 2007; Zhou et al., 2007; Kumar et al., 2013; Chowdhuri et al., 2015; Liu et al., 2016). Additionally, to ensure well-defined peaks, an exposure of 50 s per 2q step was implemented.

#### 2.1.3. Diffuse Reflectance Infrared Fourier Transform Spectroscopy (DRIFTS)

Diffuse Reflectance Fourier Transform Infrared Spectroscopy (DRIFTS) was carried out using a Spectra-Tech DRIFTS cell fitted in a Thermo e Nicolet Nexus FTIR spectrophotometer. The instrument was thoroughly purged (30 L/min) with CO<sub>2</sub> and water-free air, produced using a Balaston purge gas generator. All samples were diluted to ca. 5 % wt. in finely ground KBr (Sigma, UK). The samples were used as received, with no further grinding. The sample was folded into the pre-ground KBr using a micro-spatula. The microsampling cup was over-filled slightly and the cup dropped from a height of 1 cm onto the bench in order to shake off the excess mixture whilst at the same time, produce a slightly domed and naturally randomised, surface of KBr diluted sample. The same batch of ground KBr was used as the background. The background and sample spectra were made up of 164 scans with resolution set to 4 cm<sup>-1</sup>. As the sample was diluted with KBr there were no specular reflection components so a blocker was not used. Spectra were plotted in absorbance (Liauw, 2003).

#### 2.1.4. Scanning Electron Microscopy (SEM) and Energy Dispersive X-Ray Spectroscopy (EDX)

In order to determine the shape, size and atomic elemental weight of the compounds, the samples were fixed to stubs using carbon tabs (Agar, UK). Scanning Electron Microscopy (Carl Zeiss Ltd.) was carried out using a Supra 40VP SEM with SmartSEM software. Energy Dispersive X-Ray (EDAX Inc.) was carried out using an Apollo 40 SDD system with Genesis software.

### 2.2. Microbiology and antibacterial testing

#### 2.2.1. Stock cultures of bacteria

In preparation for the antimicrobial assays, stock cultures of *S. aureus* NCTC 4137, *K. pneumoniae* NCTC 9633 or *E. coli* NCTC 10418 were inoculated onto nutrient agar (NA) or nutrient broth (NB) and incubated at 37 C for 24 h. Stock

cultures of *Enterococcus faecium* NCTC 7171 were cultured onto Columbia blood agar with horse blood in a 5%, Brain heart infusion agar (BHIA) (Oxoid, UK) or brain heart infusion broth (BIHB) and incubated in 5% CO<sub>2</sub> for 24 h at 37 °C. All medias were obtained from Oxoid (UK).

#### 2.2.2. Preparation of microbiological cultures

Ten millilitres of appropriate broth was inoculated with a single colony of bacteria and incubated overnight according to the above conditions. Following incubation, cells were harvested at 567 g for 10 min and washed once, re-suspended in sterile distilled water, vortexed for 30 s, and then centrifuged again at 567 g for 10 min. The inocula were examined in a spectrophotometer at 540 nm and compared against a blank of sterile distilled water to determine their optical density. They were then diluted accordingly and quantified using serial dilutions. The cell concentrations corresponded to; *E. coli* 4.20 × 10<sup>8</sup>, *S. aureus* 1.30 × 10<sup>8</sup>, *Enterococcus faecium* 3.95 × 10<sup>8</sup> and *K. pneumoniae* 2.82 × 10<sup>8</sup> colony forming units per mL (CFU/mL).

#### 2.2.3. Zones of inhibition

The zones of inhibition assays were performed to test the antimicrobial efficacy of each individual compound (n = 24). One hundred microliters of prepared cell suspension was pipetted and spread across the surface of the agar. Three equal wells (8 mm diameter) were cut out of the each agar plates. To each of the wells, 100 µL of suspended compound was added. The plates were incubated in the appropriate air conditions and temperature for 24 h. Following incubation, the zones of inhibition was measured in mm from four sides of each well to determine an average mean value (n = 24).

#### 2.2.4. Minimum inhibitory concentrations (MIC)

The minimal inhibitory concentration (MIC) is defined as the lowest concentration of antimicrobial to prevent bacterial growth (Russel and Chopra, 1990). One millilitre of triphenyl tetrazolium chloride (TTC) blue metabolic dye (Sigma-Aldrich, UK), was added into 9 mL of the cell suspension so that the working concentration of the dye was 0.15% w/v. To determine the MIC, the samples and bacteria were added to a 96 well flat-bottomed microtiter plate (MTP) and a serial dilution method used across the plate. A bacterial suspension without any compound (positive control) and uninoculated broth (negative control) was included. After incubation, the MIC was taken as lowest concentration that inhibited the visible growth of the bacteria by comparison with the controls. Growth was indicated by a change of colour in the well to dark blue/purple.

#### 2.2.5. Minimum bactericidal concentration (MBC)

The MBC is defined as the lowest concentration required to completely inactivate the inoculum at a given time (Humphreys et al., 2011). To perform the MBC assays, 25 µL was sampled and pipetted onto agar plates from the MIC well that showed no growth and also from the first well that showed growth and incubated overnight in appropriate conditions. After incubation, the lowest concentration well sample that showed no growth on the agar plate was determined to be the MBC for that test sample.

#### 2.2.6. Statistical analysis

Statistical tests were carried out using a two tailed distribution t-test with two sample homoscedastic variance. Results were reported as mean ± standard error or percentage and any observed differences were considered significant at a p < 0.05.

## 3. Results

### 3.1. Particle characterisation

In order to assess the antibacterial activity of four compounds, graphite, GO, AgGO and ZnOGO, the compounds and hybrid molecules were firstly obtained or synthesized, then characterised and then tested using well-established antibacterial assays. The XRD patterns relating to the graphite powder produced the expected characteristic diffraction peaks at 2θ 26.6, 44.7 and 54.6, corresponding to the (002), (101) and (004) diffraction peaks of graphite powder respectively (Fig. 1a and a0). XRD (Fig. 1 a0) plotted over a narrower 2θ range and with a finer counts scale, showed some disordered material as evidenced by the wide peak between ca. 7 and 17 and by a characteristic 'sharp' peak was evident at 2θ 11.8 (Fig. 1b). The composition of the GO sample was confirmed as corresponding to the (002) diffraction peak of disordered GO. Application of the Bragg equation to the reflection peak angles, revealed that the interplanar distance increased from 0.35 nm in graphite to 0.75 nm in graphene oxide. For the latter, EDX gave 54.6 wt% C and 45.3 wt% O (O/C ratio 0.83), whilst the former (graphite) had an oxygen content of only 8.9 wt%, with all of the remainder being carbon (Table 1).

The ZnOGO was confirmed by XRD to have a high concentration of ZnO (Fig. 1c). Diffraction peaks were evident at 2θ 32.2, 34.8, 36.7, 48.0, 57.0, 63.3, 66.8, 69.5 and 72.9 which corresponded to the (100), (002), (101), (102), (110), (103), (112), (201) and (004) crystalline planes of ZnO, respectively (Liu et al., 2012). EDX revealed that the ZnOGO contained C (8.60 wt%), O (18.75 wt%) and Zn (72.65 wt%). Due to the low level of carbon in ZnOGO, the (002) reflection for GO (centred at ca. 10) (Fig. 1c0) was very weak. The ZnOGO was light grey in colour thus confirming the presence of carbon in the sample.

Following analysis of the AgGO, the diffraction peaks occurred at 2θ 38.7, 44.9, 65.0 and 77.9 (Fig. 1d). These peaks corresponded to the (111), (200), (220) and (311) crystallographic planes of face-centred cubic silver. A small amount of Ag<sub>2</sub>O was present as evidenced by the corresponding (110) and (111) reflections at 28.4 and 3332.8 respectively. The (002) reflection of the GO was significantly attenuated (Fig. 1d) and shifted from 11.8 to 10 (d<sub>(002)</sub> 0.86 nm). There was also a broad reflection peak over the range 12 and 18, with two small peaks centred at 15 and 20 (Fig. 1d0) whereby corresponding d values were 0.60 nm and 0.44 nm, respectively, indicating the presence of disordered structures.

Diffuse Reflectance Infrared Fourier Transform Spectroscopy (DRIFTS) was used to further characterise the compounds. Overlaid DRIFTS spectra of the 4000 cm<sup>-1</sup> to 2000 cm<sup>-1</sup> region for the graphite, GO and AgGO demonstrated that the DRIFTS spectrum of graphite (Fig. 2a) was largely featureless as expected, though there was a small and negative hydrogen bonded OH stretching peak which was due to there being slightly more moisture in the background than the sample. The size and position of this band did not hinder interpretation of this spectral region for GO or AgGO. Graphene oxide (Fig. 2b) showed the expected broad envelope of hydrogen bonded OH stretching vibrations from 3700 cm<sup>-1</sup> to 2500 cm<sup>-1</sup>, together with some OH bands at 3650 cm<sup>-1</sup> that appeared to be much less involved in hydrogen bonding. Interaction of the GO with the silver (Fig. 2c) appeared to remove the latter OH stretching band and generally attenuated the hydrogen bonded OH stretching within the region above 3350 cm<sup>-1</sup>. There were some small aliphatic C-H stretching vibrations at 2946 cm<sup>-1</sup> (asymmetric) and 2877 cm<sup>-1</sup> (symmetric). The 2000 cm<sup>-1</sup> to 400 cm<sup>-1</sup> region of the same three samples demonstrated that the graphite spectrum (Fig. 3a) was again featureless apart from a small negative peak at 1650 cm<sup>-1</sup> which could be assigned to an O-H bend of water, indicating again



that there was slightly more moisture in the background than the sample; this peak did not interfere with interpretation. The GO featured all the expected peaks (Fig. 3b); carbonyl stretching ( $1738\text{ cm}^{-1}$ ); skeletal aromatic C=C vibrations ( $1615\text{ cm}^{-1}$ ); C-OH stretching ( $1356\text{ cm}^{-1}$ ); C-O-C stretching ( $1225\text{ cm}^{-1}$ ); C-O stretching ( $1056\text{ cm}^{-1}$ ); aromatic C-H bending

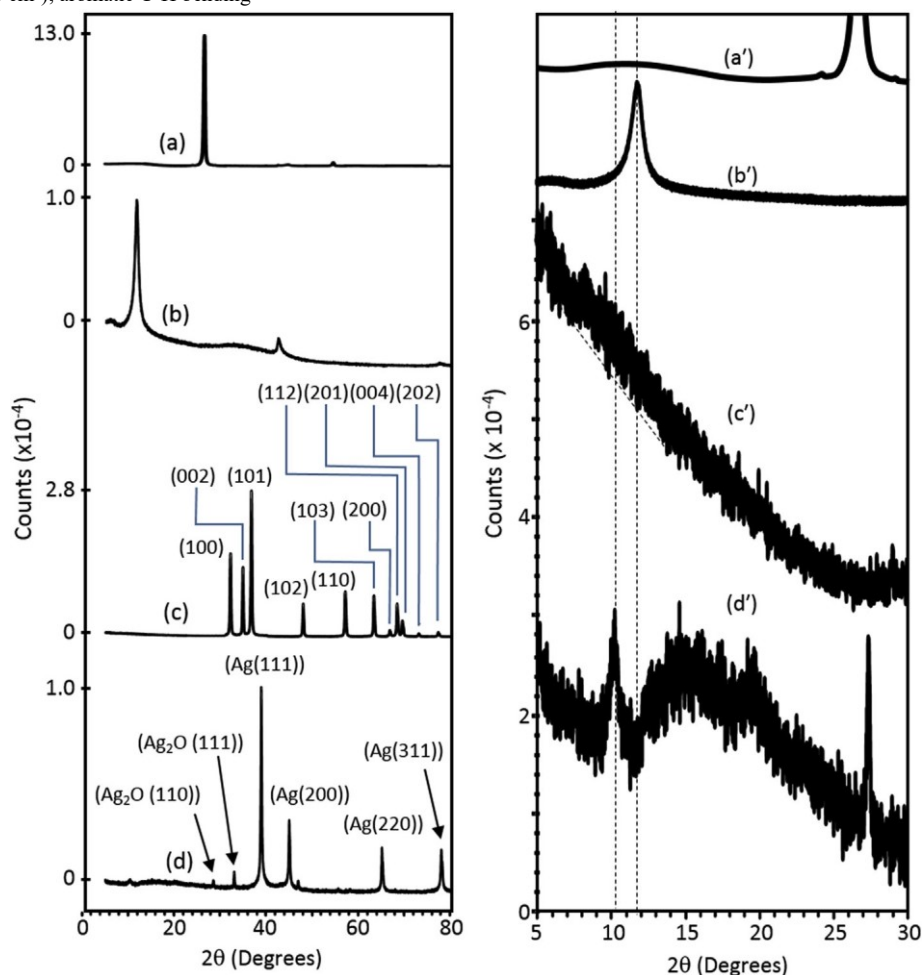


Fig. 1. X-Ray Diffraction patterns for; (a) graphite, (b) graphene oxide (GO), (c) zinc oxide e graphene oxide hybrid (ZnOGO) and (d) silver e graphene oxide hybrid (AgGO). Note the individual peak heights e patterns have been compressed to fit. In the right hand stack, patterns a0 to d0 correspond to those in the left stack but are plotted over a narrower  $2\theta$  range on common counts scale (with Y-shifting for presentation purposes). ZnOGO and AgGO have 50 x boosted counts and are Y-shifted for presentation purposes.

Table 1

EDX analysis demonstrating the elemental percentage weight of the compounds.

	C	O	Ag	Zn
Graphite	$91.12 \pm 0.13$	$8.88 \pm 0.13$	N/A	N/A
GO	$54.15 \pm 0.79$	$45.85 \pm 0.79$	N/A	N/A
ZnOGO	$8.60 \pm 0.04$	$18.75 \pm 0.17$	N/A	$72.65 \pm 0.13$
AgGO	$14.50 \pm 1.50$	$15.74 \pm 1.03$	$69.77 \pm 2.53$	N/A

N/A Not applicable for elemental analysis.

( $849\text{ cm}^{-1}$ ). The AgGO (Fig. 3c) also featured the same absorption bands but with the following significant differences: carbonyl stretching, skeletal aromatic C=C vibrations and C-O-C stretching vibrations were all red-shifted by  $10\text{ cm}^{-1}$ ,  $29\text{ cm}^{-1}$  and  $5\text{ cm}^{-1}$ , respectively. Furthermore, the C-O vibration was split and consisted of a blue shifted component ( $1078\text{ cm}^{-1}$ ) and a red shifted component ( $1037\text{ cm}^{-1}$ ) (Table 2).

Overlaid spectra of the synthesised ZnO and ZnOGO demonstrated in both spectra, carbon dioxide absorption at  $2350\text{ cm}^{-1}$  (Fig. 4) and carbonate absorptions at ca.  $1580\text{ cm}^{-1}$  and  $1380\text{ cm}^{-1}$  (Fig. 5). SEM showed that the compounds were heterogeneous and irregular in size (Table 3) and shape (Fig.

6). Graphite (Fig. 6a) had a flattened, irregular, random orientation, fractured, sheet like morphology with sharp, cleaved edges ( $0.10\text{ mm} \times 25.7\text{ mm}$ ). Graphene oxide (Fig. 6b) was composed of aggregated creased platelets

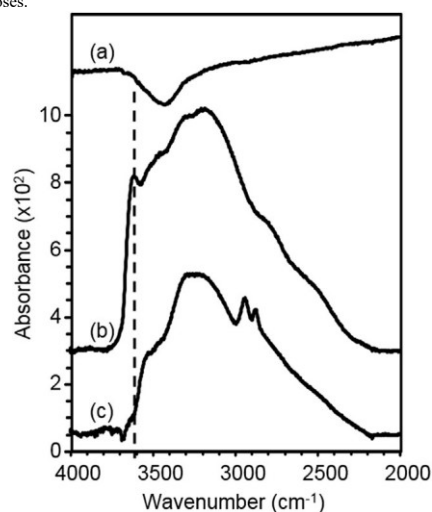


Fig. 2. DRIFTS spectra ( $4000\text{ cm}^{-1}$  to  $2000\text{ cm}^{-1}$ ) of (a) graphite, (b) graphene oxide (GO) and (c) silver e graphene oxide hybrid (AgGO).

(0.20 mme20.0 mm). The ZnOGO (Fig. 6c) consisted of numerous aggregated nanoparticles and/or nanoparticles covering micron-

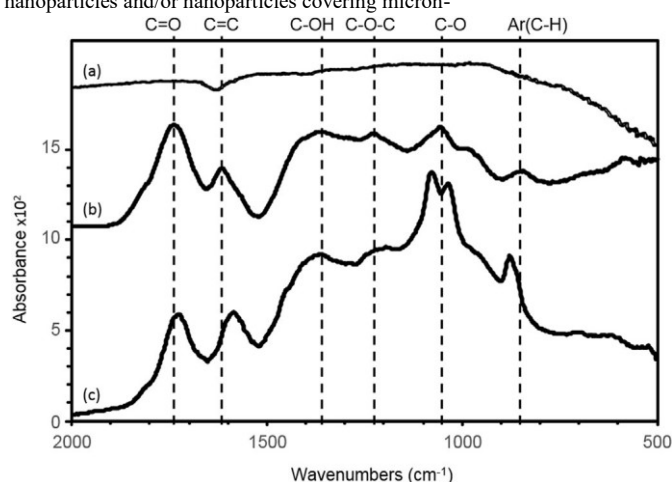


Fig. 3. DRIFTS spectra (2000  $\text{cm}^{-1}$  to 500  $\text{cm}^{-1}$ ) of (a) graphite, (b) graphene oxide (GO) and (c) silver e graphene oxide hybrid (AgGO).

sized particles (0.05 mme30.0 mm). AgGO (Fig. 6d) was similar to GO in appearance; creased aggregated platelets with a random scattering of nanoparticles (possibly silver and/or silver oxide) (0.01 mm- 13.0 mm).

### 3.2. Microbiological analysis

Zones of inhibition assays were carried out against Gramnegative *E. coli* and *K. pneumoniae* and Gram-positive *S. aureus* and *Enterococcus faecium* (Fig. 7). Following the zone of inhibition assays, all the compounds demonstrated antimicrobial activity against *E. coli* and all the GO-containing compounds demonstrated antimicrobial activity against *S. aureus*. Graphite was only effective against *E. coli* and thus demonstrated a significantly greater antimicrobial efficacy than GO or ZnOGO against this bacteria ( $p > 0.05$ ). The most effective antimicrobial overall against the bacteria using zones of inhibition was AgGO which provided the greatest zones of inhibition against *E. coli* (4.48 mm) and *S. aureus* (4.50 mm).

The MIC results demonstrated that against *E. coli* all the compounds were effective at concentrations of 0.125  $\text{mg mL}^{-1}$ . Against *S. aureus*, graphene oxide was the most effective (0.125  $\text{mg mL}^{-1}$ ) whilst AgGO was the most effective against *Enterococcus faecium* (0.125  $\text{mg mL}^{-1}$ ). *K. pneumoniae* was again the most difficult bacteria to inhibit. However, the ZnOGO and AgGO compounds demonstrated statistically significant inhibitory effects compared to the graphite and GO compounds against *K. pneumoniae* at concentrations of 0.25  $\text{mg mL}^{-1}$  ( $p > 0.05$ ). MBCs demonstrated that against *E. coli*, ZnOGO and AgGO were the most effective at 0.125  $\text{mg mL}^{-1}$ . GO, ZnOGO and AgGO were all effective against

C-O	1056	1078	p22
		1037	19
Aromatic C-H	849	879	p30

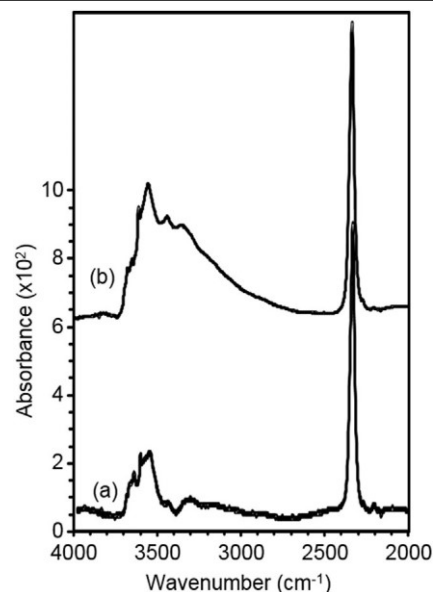


Fig. 4. DRIFTS spectra (4000  $\text{cm}^{-1}$  to 2000  $\text{cm}^{-1}$ ) of (a) synthesised zinc oxide (ZnO), (b) synthesised zinc oxide e graphene oxide hybrid (ZnOGO).

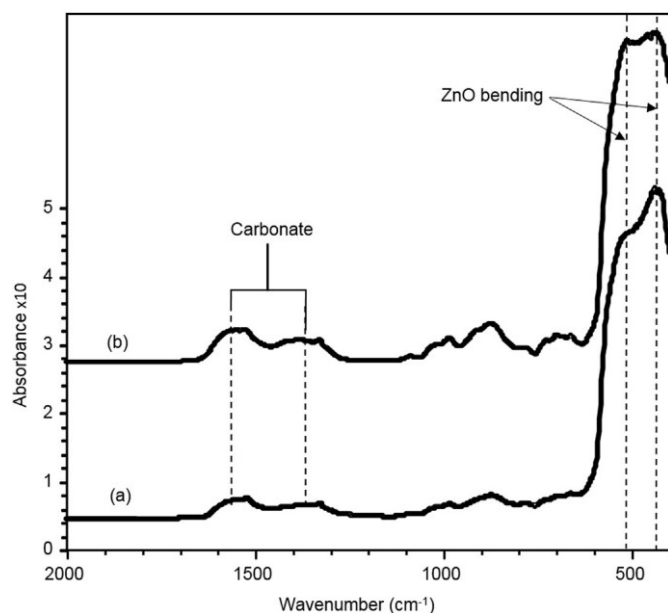


Fig. 5. DRIFTS spectra (2000  $\text{cm}^{-1}$  to 400  $\text{cm}^{-1}$ ) of (a) synthesised zinc oxide (ZnO), (b) synthesised zinc oxide e graphene oxide hybrid (ZnOGO).

Table 2  
Effect of silver addition on infrared absorption frequencies.

Group vibration	Vibration frequency ( $\text{cm}^{-1}$ )		Dn ( $\text{cm}^{-1}$ )
	GO	Ag-GO	
C%O	1738	1728	10
C%C	1615	1586	29
C-OH	1356	1363	p7
C-O-C	1225	1220	5

Table 3  
Minimum to maximum size range of the particles.

	Smallest size (mm)	Greatest size (mm)
Graphite	0.10	25.7
Graphene oxide	0.20	20.0
ZnOGO	0.05	30.0
AgGO	0.01	13.0

*S. aureus* at a concentration of 0.25 mg mL<sup>-1</sup> whilst AgGO was the most effective against *Enterococcus faecium* (0.125 mg mL<sup>-1</sup>) (Fig. 8b). It was demonstrated that as with the other assays, *K. pneumoniae* was the most difficult bacteria to eradicate,

## 4. Discussion

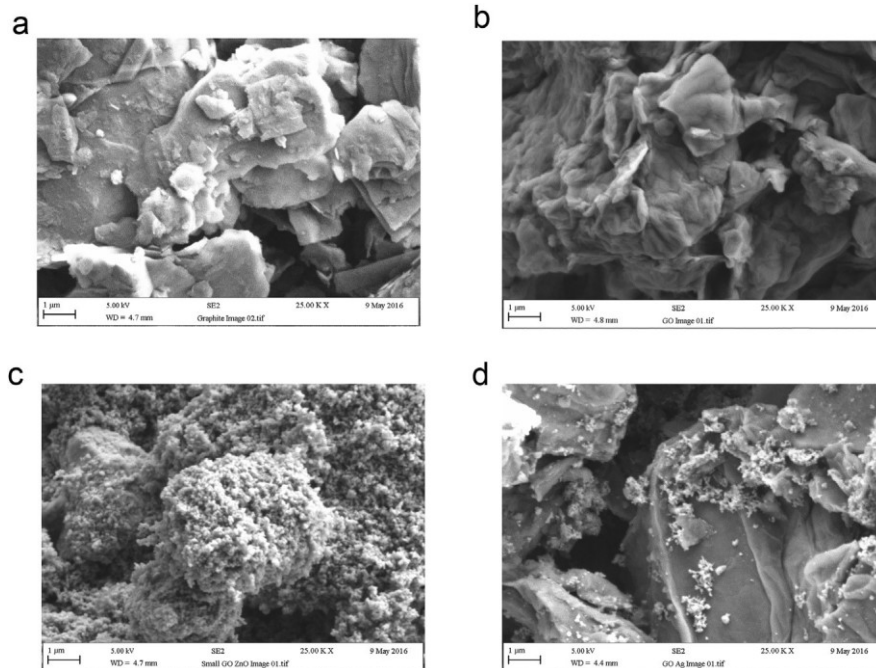


Fig. 6. SEM images demonstrating the morphology and particle sizes of a) graphite, b) graphene oxide (GO), c) zinc oxide e graphene oxide hybrid (ZnOGO) and d) silver e graphene oxide hybrid (AgGO).

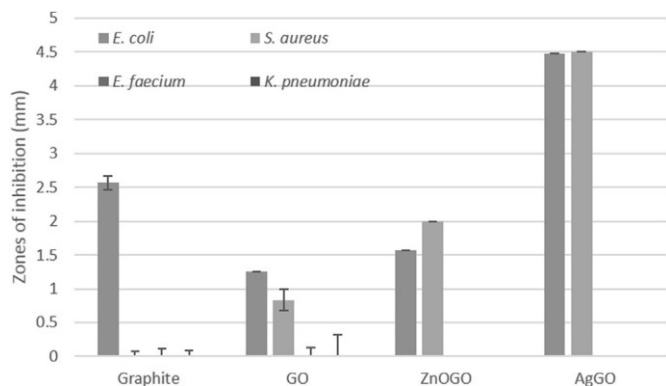


Fig. 7. Zone of inhibition measurements demonstrating the antimicrobial efficacy of the compounds. The silver e graphene oxide hybrid (AgGO) was determined to be the most effective antimicrobial using this method. *K. pneumoniae* and *E. faecium* did not demonstrate inhibition by the compounds using this method.

demonstrating the greatest MBC values. However, AgGO was the most effective antimicrobial against this bacteria at a concentration of 0.25 mg mL<sup>-1</sup>.

### 4.1. Characterisation of compounds

The XRD patterns relating to the graphite powder produced the expected characteristic diffraction peaks (Peng et al., 2013). The composition of the GO sample was confirmed (Chowdhuri et al., 2015) and it was evident that the (002) reflection had shifted to a lower angle and was of much lower intensity, relative to the same reflection in graphite. These observations are well established and indicate the formation of pendent oxygen containing functional groups on the top and bottom surfaces of the basal planes that increase the interplanar distance; this resulted in the shift of the (002) reflection to a lower angle demonstrating significantly decreased stacking uniformity (resulting in reduced reflection intensity). This is consistent with the DRIFTS data that indicated prolific functionalisation. The XRD also demonstrated disruption of the relatively ordered stacking of GO platelets due to non-uniform intercalation by the ZnO nanoparticles and/or coverage of the ZnO particles by GO, which may have contributed to a reduced intensity of the reflection (Chowdhuri et al., 2015). The AgGO peaks corresponded to crystallographic planes of face-centred cubic silver (Zhou et al., 2007). A small amount of Ag<sub>2</sub>O was present but as the atomic radius of silver is 0.17 nm, it is conceivable that individual silver atoms may have intercalated the platelets (Dhoondia and Chakraborty, 2012). The attenuation of the (002) reflection indicated that the otherwise relatively regular stacking of GO had probably been disrupted by non-uniformly sized Ag nanoparticles between the GO platelets. It is also plausible that the GO may form a coating on the Ag nanoparticles (Oo, 2007; Das et al., 2011; Ma et al., 2011). The level of silver (by EDX) in the sample was 57.9 wt%; a mix of GO intercalation by Ag nanoparticles and GO coating of Ag nanoparticles may therefore be likely. The level of carbon (20.3 wt%) can be accommodated by the proposed structures of the hybrid. The oxygen in the Ag<sub>2</sub>O will have contributed to the amount of overall oxygen identified in the sample (21.8 wt %).

The DRIFTS spectrum of graphite was largely featureless as expected. GO showed the expected broad envelope of hydrogen bonded OH stretching

vibrations. AgGO appeared to remove the latter OH stretching band and generally attenuated the hydrogen bonded OH stretching. This may be due to the interaction of the silver with weakly hydrogen bonded OH groups (phenolic OH and other OH) of the GO. The more general attenuation of the hydrogen bonded O-H bands, within the region above  $3350\text{ cm}^{-1}$ , may be related to reduced water content in the AgGO and/or interaction of the silver with the hydrogen bonded OH groups of the GO. There were some small aliphatic C-H stretching vibrations. These may be due to residual ethylene glycol from the compound synthesis and to

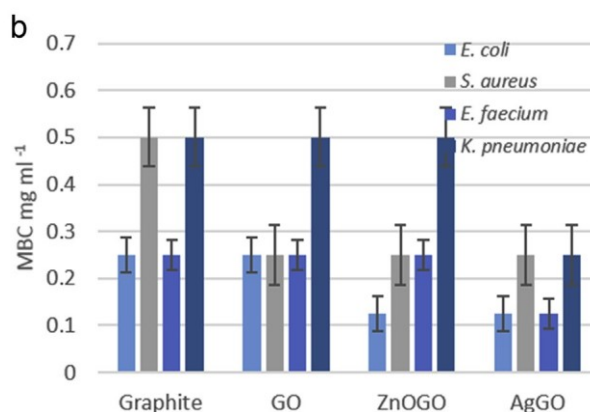
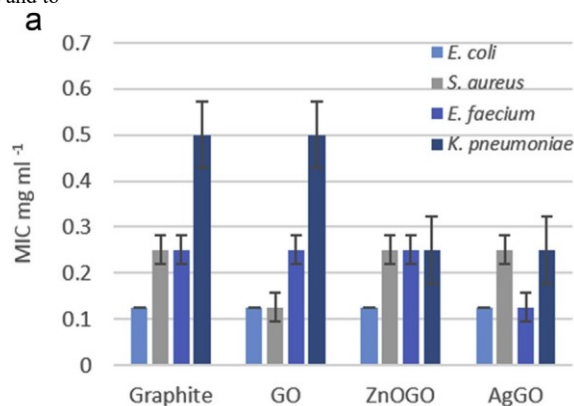


Fig. 8. a) MIC and b) MBC of compounds against the four medically relevant bacteria demonstrating that the silver e graphene oxide hybrid (AgGO) demonstrated the greatest inhibitory and bactericidal effect.

a lesser extent, residual ethanol from washing. The C-O vibration was split and consisted of a blue shifted component ( $1078\text{ cm}^{-1}$ ) and a red shifted component ( $1037\text{ cm}^{-1}$ ). These observations indicated a significant interaction of the GO platelets with the silver. The latter is further supported by a blue shift in the aromatic CH bending and C-OH stretching band. Interaction of the silver with carbonyl species and with the residual p-electrons in the GO would lead to the observed red shifts as the bond vibration was damped by interaction with the electron orbitals of silver atoms. This would also result in shortening of the aromatic C-H bonds and phenolic and carboxylic acid C-OH bonds, hence giving rise to the observed blue shift. The split in the C-O vibration indicated silver interactions having varying effects on the different ether linkages in the GO. It may be speculated that the ether groups at the platelet edges would be blue shifted and those actually pendant from a platelet surface may be red-shifted due to their interaction with the silver atoms. These observations are supported by the XRD data which indicated that the usual relatively ordered structure of the GO had been destroyed by its interaction with the silver. It may be that the silver atoms/particles had intercalated the layers resulting in highly nonuniform stacking. This would lead to the significantly attenuated and broadened GO related reflections in the XRD data for the AgGO.

The features observed using the DRIFTS analysis were expected in the ZnO that had been synthesised via this route since the carbonate and carbon dioxide would be decomposition products of the starting materials (Selim et al., 2015). The carbonate would have been converted to  $\text{CO}_2$  as the annealing temperature increased, resulting in the  $\text{CO}_2$  becoming trapped within the structure. Interestingly, the OH stretching bands were more intense in the ZnOGO, and it may be that these were related to the GO, though the associated carbonyl and C-O bands could not be resolved. This may be explained by the strong association between the GO and ZnO resulting in attenuation of these vibrations. The GO may have coated the surface of the synthesised ZnO particles and/or could have become interleaved within the synthesised ZnO structures. In either case, the relatively ordered stacking of the GO platelets had become disrupted. The XRD data supports the latter proposition. The other area of interest in these spectra was the Zn-O bending vibrations at ca.  $440$  and  $520\text{ cm}^{-1}$ . In the ZnOGO, the ZnO band at  $520\text{ cm}^{-1}$  was stronger than in the synthesised ZnO (Fig. 5b). To the

authors knowledge, such observations have not been reported elsewhere, but it may be related to a difference in the chemical environment and possibly due to the interactions with the GO.

SEM demonstrated that the compounds were heterogeneous and irregular in size and shape. The ZnOGO particles had the greatest size range ( $0.05\text{ mm}$  to  $30\text{ mm}$ ), whereas AgGO and ZnOGO had the smallest sized particles ( $0.01\text{ mm}$  and  $0.05\text{ mm}$  respectively) demonstrating the availability of both nano- and micron sized particles.

#### 4.2. Microbiology

The zone of inhibition assays demonstrated that none of the compounds had any effect against *Enterococcus faecium* or *K. pneumoniae*. This may be due to the zone of inhibition method being carried out using a semi-solid media; this combined with the thick capsule of the *K. pneumoniae* and the insusceptible nature of the *Enterococcus faecium* may have resulted in the reduced antimicrobial effect demonstrated. Further, the bacteria in this method were growing on the agar in colonies. These 'communities' of bacteria may have been more resistant to the antimicrobial effects of the compounds, similar to the effects observed when bacteria form biofilms (Gilbert et al., 2002) rather than what was observed when the bacteria are in planktonic form as in the MIC and MBC.

Work by others has demonstrated the antibacterial activities of graphite and graphite oxide towards *E. coli* and it was found that a GO dispersion demonstrated an 89.7% of loss viability at  $40\text{ mg mL}^{-1}$  (Liu et al., 2007). In our work, we demonstrated an antimicrobial activity of GO at much lower concentrations against the four bacterial strains tested (MIC  $\geq 0.125\text{ mg mL}^{-1}$ ;

MBC  $\geq 0.25\text{ mg mL}^{-1}$  to  $0.5\text{ mg mL}^{-1}$ ). Work by Xie et al. (2011) demonstrated the MIC of ZnO nanoparticles for *Escherichia coli* O157:H7 was found to be  $0.4\text{ mg mL}^{-1}$ . In comparison with our work, ZnOGO was the most antimicrobial compound against *E. coli* with an MIC at the lower concentration of  $0.125\text{ mg mL}^{-1}$ . However, the *E. coli* used in our study was a different strain. The ZnOGO was also inhibitory against *S. aureus*, *Enterococcus faecium* and *K. pneumoniae* at a MIC of  $0.25\text{ mg mL}^{-1}$ . GO and AgGO were also effective against *S. aureus* and *Enterococcus faecium* at concentrations of  $0.125\text{ mg mL}^{-1}$ . Work by others also demonstrated that the MIC for ZnO nanoparticles was  $1.5\text{ mg mL}^{-1}$  and  $3.1\text{ mg mL}^{-1}$  against *S. aureus* and *E. coli* respectively demonstrating that in some cases our ZnOGO compound was more effective than the antimicrobial action of ZnO alone used in other studies (Franklin et al., 2007; Azam et al., 2012). The MIC against *Enterococcus faecium* and *K. pneumoniae* was optimal with the AgGO hybrid compound.

ZnOGO also demonstrated the same MIC as AgGO against *K. pneumoniae*.



Results from the MBC assays demonstrated that *K. pneumonia* was the most difficult bacteria to eradicate. Work by others using MBC assays with 18 nm nanoparticles of ZnO demonstrated that the concentration of particles required against *E. coli* was 0.018 mg mL<sup>-1</sup> and 0.016 mg mL<sup>-1</sup> against *S. aureus* (Xie et al., 2011). However, in contrast with their results, our compounds required greater concentrations in order to obtain the MBC. This may be explained by the particle size of our compounds being generally larger. It has been suggested that the smaller the size of the compounds, the greater the antimicrobial activity of the agent, however contradictory results have been reported where size dependent effects were not found to influence the antimicrobial activity of ZnO (Chen et al., 2014).

The antimicrobial activity of the hybrid compounds may be explained in part by either the shape of the compound particles or by the percent of active facets. The atomic structure of the particle surface will affect its interaction with the bacterial cells (Selim et al., 2015). It is expected that the adsorption of atoms and molecules as a result of the interaction of the particles with the environment will be altered on the different planes, thus the difference in the atomic structure of the particles may result in a difference in their surface properties that could affect their interaction with the bacteria, leading to different antimicrobial efficacies (Pal et al., 2007). It has been suggested that high density facets with (111) faces exhibit greater amounts of antimicrobial activity (Pal et al., 2007). This is in agreement with our work since the AgGO demonstrated the greatest numbers of (111) planes. Combined with the shape of the compounds, these crystal structures can influence their mechanism of bacterial internalisation of the cell wall (Sirelkhatim et al., 2015).

Work by Liu et al. (2011) focused on the interactions of GO and graphite on bacterial membranes against *Escherichia coli*. In agreement with our results, they showed that a GO dispersion had a greater amount on antibacterial activity than graphite. GO and graphite are thought to confer antimicrobial activity due to membrane stress on the bacterial cells induced by the sharp edges of the compounds (Liu et al., 2011; Chen et al., 2014). An interesting fact that was evidenced in this work was that the type of antimicrobial assay used produced a range of results and thus it may be concluded that the use of one antimicrobial assay to determine the efficacy of compounds is not sufficient. Further, the type of antimicrobial assay used should be selected in line with the proposed final application of the antimicrobials.

Following each of the antimicrobial tests, AgGO demonstrated the greatest overall antimicrobial efficacies. *E. coli* was the most susceptible to the compounds followed by *S. aureus*, *Enterococcus faecium* and finally *K. pneumoniae*. This can be explained in part by the nature of the microorganisms physiology. The Gram-negative microorganisms *E. coli* and *K. pneumoniae* are surrounded by an outer and inner cell membrane which have between them a thin layer of peptidoglycan. However, *K. pneumoniae* also has a large polysaccharide capsule surrounding the bacterial cell; in addition, this capsule acts as a barrier to antimicrobial agents (Highsmith and Jarvis, 1985). *S. aureus* and *Enterococcus faecium* are Gram-positive bacteria that have a cell membrane, chiefly composed of thick peptidoglycan. However, *Enterococci* are intrinsically more resistant to many antibiotics since unlike acquired resistance and virulence traits which are usually encoded by plasmids or transposon elements, their intrinsic resistance is based on chromosomal genes (Huycke et al., 1998). Further, a number of antibiotics demonstrate bacteriostatic but not bactericidal activity against *Enterococcus faecium* bacteria (Huycke et al., 1998). Thus, the use of AgGO against these two resilient bacteria may be an important step in maintaining the hygienic status of areas into which the molecule is applied or incorporated.

## 5. Conclusions

ZnOGO and AgGO hybrid compounds were successfully produced and characterised. AgGO was the most effective antimicrobial and enhanced the activity of GO. The effect of the compounds on the bacteria did not relate to the Gram-positive or Gram-negative structures of the bacteria but rather, was due to their microorganisms overall physiology. GO-metal hybrids have the potential to be beneficially utilised as novel antimicrobials or biocides in settings where bacteria are becoming increasingly problematic.

## Acknowledgements

The authors would like to acknowledge that the work was funded by Manchester Metropolitan University. Parameshwari Ramalingam (PR) would like to thank the DST, Govt. of India and British Council, UK for DST-INSPIRE (No: IF110362/DST/INSPIRE Fellowship/2011) fellowship and Newton-Bhabha Internship (No. DST/INSPIRE/NBHF/2014/10) respectively.

## References

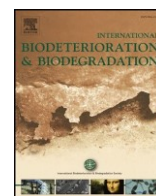
- Anandan, S., Muthukumar, S., 2015. Microstructural, crystallographic and optical characterizations of Cu-doped ZnO nanoparticles co-doped with Ni. *J. Mater. Sci. Mater. Electron.* 26, 4298e4307.
- Azam, A., Ahmed, A.S., Oves, M., Khan, M.S., Habib, S.S., Memic, A., 2012. Antimicrobial activity of metal oxide nanoparticles against Gram-positive and Gram-negative bacteria: a comparative study. *Int. J. Nanomedicine* 7, 6003e6009.
- Boucher, H.W., Talbot, G.H., Bradley, J.S., Edwards, J.E., Gilbert, D., Rice, L.B., Scheld, M., Spellberg, B., Bartlett, J., 2009. Bad bugs, No drugs: No escape! An update from the infectious diseases society of America. *Clin. Infect. Dis.* 48, 1e12.
- Chaturvedi, A., Bajpai, A.K., Bajpai, J., Singh, S.K., 2016. Evaluation of poly (vinyl alcohol) based cryogel-zinc oxide nanocomposites for possible applications as wound dressing materials. *Mater. Sci. Eng. C-Materials Biol. Appl.* 65, 408e418.
- Chen, J., Peng, H., Wang, X., Shao, F., Yuan, Z., Han, H., 2014. Graphene oxide exhibits broad-spectrum antimicrobial activity against bacterial phytopathogens and fungal conidia by intertwining and membrane perturbation. *Nanoscale* 6, 1879e1889.
- Chowdhuri, A.R., Tripathy, S., Chandra, S., Roy, S., Sahu, S.K., 2015. A ZnO decorated chitosan/graphene oxide nanocomposite shows significantly enhanced antimicrobial activity with ROS generation. *RSC Adv.* 5, 49420e49428.
- Das, M.R., Sarma, R.K., Saikia, R., Kale, V.S., Shelke, M.V., Sengupta, P., 2011. Synthesis of silver nanoparticles in an aqueous suspension of graphene oxide sheets and its antimicrobial activity. *Colloids Surfaces B Biointerfaces* 83, 16e22.
- Deokar, A.R., Shalom, Y., Perelshtein, I., Perkash, N., Gedanken, A., Banin, E., 2016. A topical antibacterial ointment made of Zn-doped copper oxide nanocomposite. *J. Nanoparticle Res.* 18, 1e6.
- Dhondia, Z.H., Chakraborty, H., 2012. Lactobacillus mediated synthesis of silver oxide nanoparticles. *Nanomater. Nanotechnol.* 2, 15.
- Franklin, N.M., Rogers, N.J., Apte, S.C., Batley, G.E., Gadd, G.E., Casey, P.S., 2007. Comparative toxicity of nanoparticulate ZnO, bulk ZnO, and ZnCl<sub>2</sub> to a freshwater microalga (*Pseudokirchneriella subcapitata*): the importance of particle solubility. *Environ. Sci. Technol.* 41, 8484e8490.
- Gilbert, P., Allison, D.G., McBain, A.J., 2002. Biofilms in vitro and in vivo: do singular mechanisms imply cross-resistance? *J. Appl. Microbiol.* 92, 98se110s.
- Highsmith, A.K., Jarvis, W.R., 1985. *Klebsiella pneumoniae*: selected virulence factors that contribute to pathogenicity. *Infect. Control* 6, 75e77.
- Hummers Jr., W.S., Offeman, R.E., 1958. Preparation of graphitic oxide. *J. Am. Chem. Soc.* 80, 1339.
- Humphreys, G., Lee, G.L., Percival, S.L., McBain, A.J., 2011. Combinatorial activities of ionic silver and sodium hexametaphosphate against microorganisms associated with chronic wounds. *J. Antimicrob. Chemother.* 66, 2556e2561.
- Huycke, M.M., Sahm, D.F., Gilmore, M.S., 1998. Multiple-drug resistant enterococci: the nature of the problem and an agenda for the future. *Emerg. Infect. Dis.* 4, 239e249.
- Jennings, M.C., Minbiole, K.P., Wuest, W.M., 2015. Quaternary ammonium compounds: an antimicrobial mainstay and platform for innovation to address bacterial resistance. *ACS Infect. Dis.* 1, 288e303.
- Kumar, S.S., Venkateswarlu, P., Rao, V.R., Rao, G.N., 2013. Synthesis, characterization and optical properties of zinc oxide nanoparticles. *Int. Nano Lett.* 3, 30.
- Li, Z.Q., Lu, C.J., Xia, Z.P., Zhou, Y., Luo, Z., 2007. X-ray diffraction patterns of graphite and turbostratic carbon. *Carbon* 45, 1686e1695.
- Liau, C.M., 2003. In: Roth, R.N. (Ed.), *Particulate Filled Composites*, second ed. Smithers RAPRA technology.

- Liu, L.F., Barford, J., Yeung, K.L., Si, G., 2007. Non-UV based germicidal activity of metal-doped TiO<sub>2</sub> coating on solid surfaces. *J. Environ. Sci. (China)* 19, 745e750.
- Liu, S., Zeng, T.H., Hofmann, M., Burcombe, E., Wei, J., Jiang, R., Kong, J., Chen, Y., 2011. Antibacterial activity of graphite, graphite oxide, graphene oxide, and reduced graphene oxide: membrane and oxidative stress. *ACS Nano* 5, 6971e6980.
- Liu, Q., Yao, X., Zhou, X., Qin, Z., Liu, Z., 2012. Varistor effect in Agegraphene/epoxy resin nanocomposites. *Scr. Mater.* 66, 113e116.
- Liu, H., Zhang, Y., Yang, H., Xiao, W., Sun, L., 2016. Filter paper inspired zinc oxide nanomaterials with high photocatalytic activity for degradation of methylene orange. *J. Chem.* 2016, 1e7.
- Ma, J., Zhang, J., Xiong, Z., Yong, Y., Zhao, X.S., 2011. Preparation, characterization and antibacterial properties of silver-modified graphene oxide. *J. Mater. Chem.* 21, 3350e3352.
- Oo, H.W.M., 2007. Infrared Spectroscopy of Zinc Oxide and Magnesium Nanostructures. Ph.D Thesis. Washington State University.
- Pal, S., Tak, Y.K., Song, J.M., 2007. Does the antibacterial activity of silver nanoparticles depend on the shape of the Nanoparticle? A study of the gramnegative bacterium *Escherichia coli*. *Appl. Environ. Microbiol.* 73, 1712e1720.
- Peng, S.G., Fan, X.J., Li, S., Zhang, J., 2013. Green synthesis and characterization of graphite oxide by orthogonal experiment. *J. Chil. Chem. Soc.* 58, 2213e2217.
- Russel, A.D., Chopra, I., 1990. Understanding Antimicrobial Resistance and Action. Ellis Horwood, Chichester.
- Selim, M.S., El-Safty, S.A., El-Sockary, M.A., Hashem, A.I., Abo Elenien, O.M., ElSaeed, A.M., Fatthallah, N.A., 2015. Modeling of spherical silver nanoparticles in silicone-based nanocomposites for marine antifouling. *RSC Adv.* 5, 63175e63185.
- Sirelkhatim, A., Mahmud, S., Seeni, A., Kaus, N.H.M., Ann, L.C., Bakhori, S.K.M., Hasan, H., Mohamad, D., 2015. Review on zinc oxide nanoparticles: antibacterial activity and toxicity mechanism. *Nano-Micro Lett.* 7, 219e242.
- Tayel, A.A., El-Tras, W.F., Moussa, S., El-Baz, A.F., Mahrous, H., Salem, M.F., Brimer, L., 2011. Antibacterial action of zinc oxide nanoparticles against foodborne pathogens. *J. Food Saf.* 31, 211e218.
- Unwin, P.R., Guell, A.G., Zhang, G.H., 2016. Nanoscale electrochemistry of sp(2) carbon materials: from graphite and graphene to carbon nanotubes. *Accounts Chem. Res.* 49, 2041e2048.
- Velmurugan, P., Park, J.H., Lee, S.M., Yi, Y.J., Cho, M., Jang, J.S., Myung, H., Bang, K.S., Oh, B.T., 2016. Eco-friendly approach towards green synthesis of zinc oxide nanocrystals and its potential applications. *Artif. Cells Nanomedicine Biotechnol.* 44, 1537e1543.
- Wang, D., An, J., Luo, Q., Li, X., Yan, L., 2012. *Nano Antimicrobials*. Springer, London New York.
- Xie, Y., He, Y., Irwin, P.L., Jin, T., Shi, X., 2011. Antibacterial activity and mechanism of action of zinc oxide nanoparticles against *Campylobacter jejuni*. *Appl. Environ. Microbiol.* 77, 2325e2331.
- Zhou, J., Zhao, F., Wang, Y., Zhang, Y., Yang, L., 2007. Size-controlled synthesis of ZnO nanoparticles and their photoluminescence properties. *J. Luminescence* 122, 195e197.



Contents lists available at ScienceDirect

## International Biodeterioration &amp; Biodegradation

journal homepage: [www.elsevier.com/locate/ibid](http://www.elsevier.com/locate/ibid)

## Single and combined antimicrobial efficacies for nine metal ion solutions against *Klebsiella pneumoniae*, *Acinetobacter baumannii* and *Enterococcus faecium*

Misha Vaidya<sup>a</sup>, Andrew J. McBain<sup>b</sup>, Craig E. Banks<sup>c</sup>, Kathryn A. Whitehead<sup>a,1</sup><sup>a</sup> Microbiology at Interfaces Group, Faculty of Science and Engineering, Manchester Metropolitan University, Chester St. Manchester M1 5GD, UK <sup>b</sup>School of Health Sciences, Faculty of Biology, Medicine and Health, The University of Manchester, Manchester, M13 9PT, UK <sup>c</sup> Faculty of Science

and Engineering, Manchester Metropolitan University, Chester St. Manchester M1 5GD, UK

## ARTICLE INFO

## Keywords:

Biocides

Metal ions

Bacteria

Antimicrobial

Synergy

Transmission

## ABSTRACT

Infection caused by *Klebsiella pneumoniae*, *Acinetobacter baumannii* and *Enterococcus faecium* can be difficult to treat. New biocidal products are needed in order to reduce the transmission of such bacteria from surfaces to patients. This fundamental study aimed to investigate the antimicrobial efficacy of nine metal ion solutions (yttrium, indium, niobium, titanium, tantalum, rhodium, ruthenium, zinc and gallium) using zone of inhibition (ZOI), minimum inhibitory concentration (MIC) and minimum bactericidal concentrations (MBC). Fractional inhibitory concentration (FIC) and fractional bactericidal concentration (FBC) assays were used to determine antimicrobial activities of various combinations. The rhodium metal ion solution when applied singly demonstrated the best antimicrobial efficacies against all the bacteria tested. FICs indicated that the rhodium/ruthenium combination was either synergistic or additive against all three tested bacteria. This metal ion combination also exhibited synergistic activity against *E. faecium* following in FBCs. Our data presented indicated the potential of the rhodium and/or ruthenium metal ions for antiseptics, disinfection and for incorporation into hygienic surfaces.

<sup>1</sup> Corresponding author.E-mail address: [K.A.Whitehead@mmu.ac.uk](mailto:K.A.Whitehead@mmu.ac.uk) (K.A. Whitehead).

## 1. Introduction

There has been a rise in the number of multidrug resistant (MDR) bacterial infections in hospital settings leading to increased mortality, morbidity, hospitalization and treatment costs (Olar et al., 2010). It is estimated that 9% of in-patients in England and Wales suffer from hospital-acquired infections, which is reported to result in around 5000 deaths and extra care related costs of over £1 billion per year. These infections are caused in part by transmission across the wards (Smith and Hunter, 2008). There are a number of pathogens that are demonstrating increasing resistance from the biocidal action of antimicrobial agents, producing a new mode of pathogenesis (Pendleton et al., 2013). *Klebsiella pneumoniae*, *Acinetobacter baumannii* and *Enterococcus faecium* are three such bacteria out of the six 'ESKAPE' pathogens that are considered to be a leading cause of nosocomial infections (Santajit and Indrawattana, 2016). Such bacteria may persist on hospital and biomaterial surfaces including catheters, stethoscopes and disinfectant soap dispensers (Smith and Hunter, 2008). Ampicillin and vancomycin resistant *E. faecium* has demonstrated a constant threat in the incidence of health-care infections (Pendleton et al., 2013). In recent times, *K. pneumoniae* and *A. baumannii* have acquired the ability to synthesize a variety of beta-lactamase enzymes that can destroy the chemical structure of beta-lactam antibiotics, thus making these bacteria multidrug resistant (Santajit and Indrawattana, 2016).

The lack of potential antimicrobial agents against such bacteria is a major cause for concern. Thus, there is a need to develop novel approaches to prevent the transmission of bacteria that cause such infections (Santos et al., 2014). Metals such as molybdenum, titanium and tantalum have been used as biomaterials coatings on implants to decrease the bacterial adherence (Ribeiro et al., 2016; Chang et al., 2014; Haenle et al., 2011). Rhodium complexes with tetraaza macrocyclic and ruthenium (II) carbonyl thiosemicarbazone complexes have been shown to have effective antimicrobial efficacy against range of bacteria (Bien et al., 1999; Kannan et al., 2008; Jayabalakrishnan and Natarajan, 2002). Gallium and zinc ions co-ordinated with protoporphyrin and mesoporphyrin respectively have showed up to 90% antibacterial efficacy against *Staphylococcus epidermis* and *Pseudomonas aeruginosa* (Ma et al., 2013). Titanium and its alloys have been used in various medical implants such as bone screws, dental restorations and artificial joints owing to their biocompatibility and also reputedly due to their bactericidal properties (He et al., 2017). This fundamental study investigated the antimicrobial efficacy of nine metal ion solutions individually and in combination against *K. pneumoniae*, *A. baumannii* and *E. faecium* to determine if they might provide potential biocidal solutions.

## 2. Materials and methods

### 2.1. Cultures and media

*Enterococcus faecium* NCTC 7171 was cultured onto Columbia blood agar (Oxoid, UK) (supplemented with 20 mL defibrinated horse blood), incubated in 5% CO<sub>2</sub> for 24 h at 37 °C in static conditions. *K. pneumoniae* NCTC 9633 and *A. baumannii* NCTC 12156 were cultured onto Nutrient agar (NA) (Oxoid, UK) and incubated for 24 h at 37 °C. Brain heart infusion (BHIA) agar (Oxoid, UK) and brain heart infusion broth (BHIB) (Oxoid, UK) (*E. faecium*) and nutrient agar and nutrient broth (NB) (Oxoid, UK) (*K. pneumoniae* or *A. baumannii*) were used for all subsequent experiments and were incubated as above (Vaidya et al., 2017).

### 2.2. Preparation of metal ion solutions

Standard solutions of 1000 mg L<sup>-1</sup> of yttrium (Y<sub>2</sub>O<sub>3</sub> + HNO<sub>3</sub>), titanium (Ti metal + HNO<sub>3</sub>), tantalum (Ta metal + HNO<sub>3</sub> (HF traces)), indium (In metal + HNO<sub>3</sub>), niobium (Nb metal + HNO<sub>3</sub> (HF traces)), rhodium (RhCl<sub>3</sub> + HCl), ruthenium (Re metal + HNO<sub>3</sub>), zinc (Zn metal + HNO<sub>3</sub>) and gallium (Ga metal + HNO<sub>3</sub>) (Sigma-Aldrich, UK) were used and diluted with sterile water to obtain 500 mg L<sup>-1</sup>, 100 mg L<sup>-1</sup> and 50 mg L<sup>-1</sup> metal concentrations.

### 2.3. Bacterial preparation

The appropriate broth was inoculated with a single colony of bacteria and incubated overnight according to the aforementioned conditions. Cells were harvested at 567 g for 10 min and washed using sterile distilled water three



times for the ZoI test and double strength broth for cells to be used in the MIC/MBC tests. Cells were re-harvested by centrifugation for 10 min at 567 g and adjusted using sterile distilled water to an optical density (OD)  $1.0 \pm 0.1$ . The colony forming units per mL (CFU mL<sup>-1</sup>) were calculated and cell concentrations corresponded to *K. pneumoniae*  $2.82 \times 10^8$ , *A. baumannii*  $1.85 \times 10^8$  and *E. faecium*  $3.95 \times 10^8$

#### 2.4. Zone of inhibition (ZoI) assays

One hundred microliters of prepared cell suspension was spread across the agar and three wells (8 mm diameter) were cut from the agar. One hundred microliters of the metal ion solution (at different metal ion solution concentrations, 50 mg L<sup>-1</sup>, 100 mg L<sup>-1</sup>, 500 mg L<sup>-1</sup> and 1000 mg L<sup>-1</sup>) was added to the well and the plates were incubated as specified above. The radius of inhibition was measured in mm to determine the average mean value (n=12).

#### 2.5. Minimum inhibitory concentration (MIC) and minimum bactericidal concentration (MBC) assays (adapted from Vaidya et al., 2017)

To 9 mL of cell suspension, one mL of triphenyl tetrazolium chloride (TTC) blue metabolic dye (Sigma-Aldrich, UK), was added. One hundred microliters of bacterial suspension with the TTC dye and the metal ion solutions was added to a 96 well flat-bottomed micro titre plate. The first column of was mixed, and subsequent 100 µL of the sample/ bacterial mix was transferred to sequential wells and repeated until column 10, whereby 100 µL of the mixture was disposed of. A positive control and a negative control was carried out at the same time. The MIC was taken as lowest concentration that inhibited the visible growth of the bacteria, indicated by a change of colour to blue. From the first well that showed no growth and the last well that demonstrated growth, 25 µL of suspension was pipetted onto agar and incubated. The lowest concentration that showed no bacterial growth was determined to be the MBC (n=3).

#### 2.6. Fractional inhibitory concentrations (FIC) and fractional bactericidal concentrations (FBC) index

This method was adapted from Vaidya et al. (2017). In brief, the MIC and MBC metal ion solution synergies were determined using FIC and FBC antimicrobial screening respectively. Both metal ion solutions were added in a 1:1 ratio to the wells. The FIC and FBC values were calculated using the following formula;  $\Sigma FIC$  or  $\Sigma FBC = FIC$  or  $FBC$  of antimicrobial A +  $FIC$  or  $FBC$  of antimicrobial B = [1]

MIC or MBC of antimicrobial A in combination

---

MIC or MBC of antimicrobial A alone

+

MIC or MBC of antimicrobial B in combination

---

MIC or MBC of antimicrobial B alone

The antimicrobial interaction was evaluated as  $\leq 0.5$ =synergy, >

$0.5 \leq 1$ =additivity,  $1 < 4$ =autonomy and  $> 4$ =antagonism (Doern, 2014) (n=3).

#### 2.7. Statistical analysis

The average values were used to compare the results and standard error to determine the distributions of the data. The intervals at 95% confidence were also determined.

### 3. Results

The nine metal ion solutions showed varying levels of toxicity against the bacteria. The metal ions were in an acidic solution and control assays were carried out to determine the effects of the acids on bacterial viability. It was found that the acids did not significantly affect the results (data not shown).

### 3.1. Zone of inhibition

The ZoI results displayed a significant increase in antimicrobial activity with an increase in concentration ( $p < 0.05$ ). At a concentration of  $1000 \text{ mg L}^{-1}$  the rhodium metal ion solution was the most antimicrobial (11.5 mm, 12.5 mm and 7 mm *K. pneumonia*, *A. baumannii* and *E. faecium* respectively) followed by ruthenium for *K. pneumonia* (10.66 mm) and *A. baumannii* (8mm) with antimicrobial efficacy demonstrated for titanium and tantalum against *E. faecium* (both at 5 mm) (Fig. 1). Overall, at low concentrations, the least antimicrobially effective metal ion solutions were yttrium and zinc. With the exception of titanium ion solution, all the metal ion solutions demonstrated no antimicrobial efficacy at lower concentrations ( $50 \text{ mg L}^{-1}$  and  $100 \text{ mg L}^{-1}$ ) against *E. faecium* (Fig. 1) ( $p > 0.05$ ). Thus, *Enterococcus faecium* was found to be the most resistant at all the metal ion solutions tested concentrations.

### 3.2. Minimum inhibitory and bactericidal concentrations

Following the MIC assay, the rhodium and tantalum metal ion solution showed the best antimicrobial efficacy against all the tested bacteria ( $7.81 \text{ mg L}^{-1}$  against the Gram-negative bacteria and  $31.25 \text{ mg L}^{-1}$  against *E. faecium*). The ruthenium metal ion solution was also inhibitory against *A. baumannii* and *E. faecium* ( $7.81 \text{ mg L}^{-1}$  and  $31.25 \text{ mg L}^{-1}$  respectively) and the titanium metal ion solution was also inhibitory against *E. faecium* ( $31.25 \text{ mg L}^{-1}$ ). The zinc ion solution against all three bacteria ( $31.25 \text{ mg L}^{-1}$  *K. pneumoniae* and *A. baumannii*;  $125.00 \text{ mg L}^{-1}$  against *E. faecium*) and the yttrium ion solution ( $31.25 \text{ mg L}^{-1}$  and *A. baumannii*;  $125.00 \text{ mg L}^{-1}$  against *E. faecium*) demonstrated the least antimicrobial inhibition (Table 1).

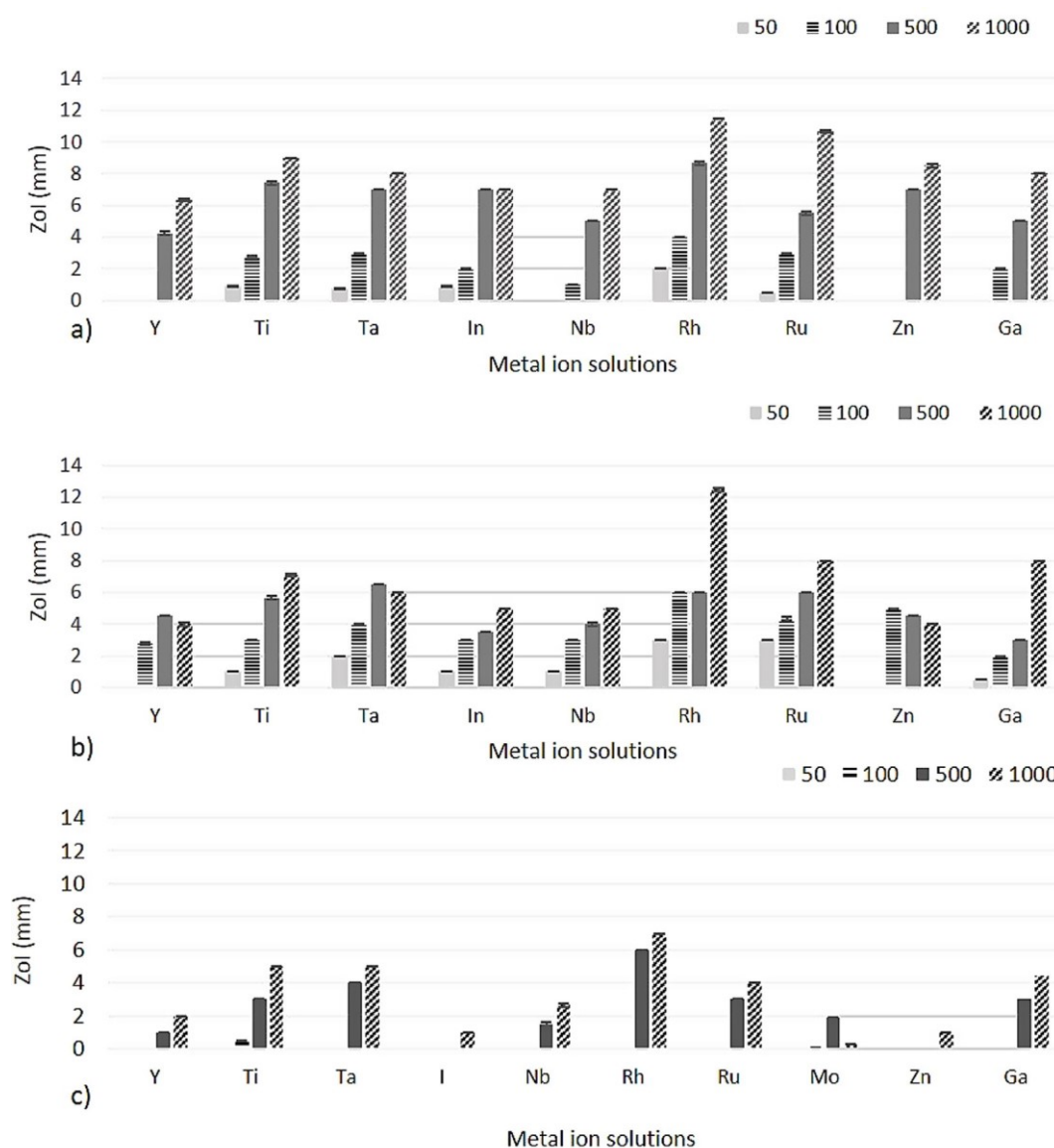


Fig. 1. The ZOI in millimetre for nine metal ion solutions against a) *K. pneumoniae* b) *A. baumannii* and c) *E. faecium* demonstrated the best antimicrobial efficacy for rhodium (n = 12). Y = Yttrium, Ti =titanium, Ta = Tantalum, In = Indium, Nb = Niobium, Rh = Rhodium, Ru = Ruthenium, Zn =Zinc and Ga = Gallium.

Table 1 Minimum inhibitory concentrations in mg/L for nine metal ion solutions against three tested pathogens demonstrating the best antimicrobial efficacy for rhodium and titanium ion solutions (n = 3).

Metal ion solutions	<i>K. pneumoniae</i>	<i>A. baumannii</i>	<i>E. faecium</i>
Zinc	31.25 ± 0	31.25 ± 0	125.00 ± 0
Titanium	15.62 ± 0	15.62 ± 0	31.25 ± 0
Tantalum	7.81 ± 0	7.81 ± 0	31.25 ± 0
Indium	15.62 ± 0	15.62 ± 0	62.50 ± 0
Yttrium	15.62 ± 0	31.25 ± 0	125.00 ± 0
Rhodium	7.81 ± 0	7.81 ± 0	31.25 ± 0
Ruthenium	15.62 ± 0	7.81 ± 0	31.25 ± 0
Gallium	15.62 ± 0	11.75 ± 2.76	62.50 ± 0
Niobium	15.62 ± 0	15.62 ± 0	62.50 ± 0

Following the MBC assays, only the rhodium and the ruthenium demonstrated bactericidal activity against all three bacteria (15.62 mg L<sup>-1</sup>, 7.81 mg L<sup>-1</sup> and 62.50 mg L<sup>-1</sup> against *K. pneumoniae*, *A. baumannii* and *E. faecium* respectively). Against *K. pneumoniae*, titanium, tantalum and gallium demonstrated bactericidal activity (15.62 mg L<sup>-1</sup>), and against *E. faecium* tantalum and gallium also demonstrated bactericidal activity (15.62 mg L<sup>-1</sup> and 62.50 mg L<sup>-1</sup> respectively). The least bactericidal solutions were niobium (*K. pneumoniae* 46.87 mg L<sup>-1</sup>), zinc, indium and yttrium (*A. baumannii* 15.62 mg L<sup>-1</sup>) and zinc (*E. faecium* 250.00 mg L<sup>-1</sup>) (Table 2). In both of the tests, *E. faecium* was found to be the most resistant bacteria.

### 3.3. Fractional inhibitory concentrations and FBC index

The FIC (Table 3) and FBC was used to determine the synergistic antimicrobial efficacy of the metal ion solutions in combination. Following the FIC test, against *K. pneumoniae* only the rhodium/ruthenium combination demonstrated an additive effect (0.74). All the metal ion solution combinations demonstrated additivity effects against *A. baumannii* (0.74–0.99) and *E. faecium* (0.99).

Following the FBC synergy assay (Table 4), only the rhodium/ruthenium combination demonstrated a synergistic antimicrobial efficacy against Gram-positive *E. faecium* (FBC =0.48) (Table 4). The titanium/ tantalum (0.75), titanium/rhodium (0.75) and titanium/ruthenium (0.56) combinations demonstrated an additive antimicrobial effect against *E. faecium*. Overall, *K. pneumoniae* was found to the most resistant bacteria for the dual combinations tested, whilst *E. faecium* was found to the most sensitive bacteria in the FIC and FBC assays.

Table 2 Minimum bactericidal concentrations in mg/L for nine metal ion solutions against three tested pathogens demonstrating the best antimicrobial efficacy for Ru and Rh ion solutions (n =3).

Metal ion solutions	<i>K. pneumoniae</i>	<i>A. baumannii</i>	<i>E. faecium</i>
Zinc	31.25 ± 0	31.25 ± 0	250.00 ± 0
Titanium	15.62 ± 0	15.62 ± 0	125.00 ± 0
Tantalum	15.62 ± 0	15.62 ± 0	62.50 ± 0
Indium	31.25 ± 0	31.25 ± 0	125.00 ± 0
Yttrium	23.43 ± 5.52	31.25 ± 0	125.00 ± 0
Rhodium	15.62 ± 0	7.81 ± 0	62.50 ± 0
Ruthenium	15.62 ± 0	7.81 ± 0	62.50 ± 0
Gallium	15.62 ± 0	15.62 ± 0	62.50 ± 0
Niobium	46.87 ± 11.04	15.62 ± 0	125.00 ± 0

Table 3 Fractional inhibitory concentration index for six tested metal ion solutions combinations demonstrating combined effects for all metal ion solutions against *K. pneumoniae*, *A. baumannii* and *E. faecium*. FIC index = ≤ 0.50 =synergy, >0.50 ≤ 1.00 = additivity, > 1.00 ≤4.00 =autonomy and > 4.00 =antagonism.

	Titanium/Tantalum	Titanium/Rhodium	Titanium/Ruthenium	Tantalum/Rhodium	Tantalum/Ruthenium	Rhodium/Ruthenium
<i>K. pneumoniae</i>	1.50	1.50	1.00	2.00	3.00	0.74
<i>A. baumannii</i>	0.74	0.74	0.74	0.99	0.99	0.99
<i>E. faecium</i>	0.99	0.99	0.99	0.99	0.99	0.99

Table 3 Fractional bactericidal concentration index for six tested metal ion solutions combinations demonstrating combined effects for all metal ion solutions against *K. pneumoniae*, *A. baumannii* and *E. faecium*. FIC index =  $\leq 0.50$  =synergy,  $>0.50 \leq 1.00$  = additivity,  $> 1.00 \leq 4.00$  =autonomy and  $> 4.00$  =antagonism.

	Titanium/Tantalum	Titanium/Rhodium	Titanium/Ruthenium	Tantalum/Rhodium	Tantalum/Ruthenium	Rhodium/Ruthenium
<i>K. pneumoniae</i>	2.00	2.00	2.00	2.00	2.00	1.00
<i>A. baumannii</i>	1.00	1.12	1.50	1.50	1.50	2.00
<i>E. faecium</i>	0.75	0.75	0.56	1.00	1.50	0.48

#### 4. Discussion

The reoccurrence of MDR infections poses a great risk to public health. The development of novel antimicrobial agents and biocides to control and prevent the transmission of bacteria associated with hospital-acquired infections is in need of exploration (Haenle et al., 2011). This study found that the rhodium ion solution showed the best antimicrobial efficacies when tested alone or in combinations. The differences in the antimicrobial efficacies of the metal ions antimicrobial action may be due to their mechanisms of action. The antimicrobial activity of metals may be due to single or combined mechanisms such as enzyme disruption, cell-membrane/cell-wall degradation, deoxyribonucleic acid denaturation, protein dysfunction or oxidative stress (Lemire et al., 2013; Bruins et al., 2000; Varkey, 2010; Mitchell and Kogure, 2006). It has been suggested that physical contact of metal ions with the bacterial cell wall and internalization in the cell might cause oxidization of the cellular components generating reactive oxygen species and interruption of the transmembrane electron transport chain (Dizaj et al., 2014; Kolmas et al., 2014). The antibacterial activity of the rhodium metal ion solution may be due to its liposolubility, electronegativity and initiation of redox reactions (Lemire et al., 2013; Beloglazkina et al., 2016). Rhodium metal possesses liposolubility properties, which is suggested to favour its cell permeability aiding in a greater transport inside a bacterial cell membrane (Bien et al., 1999). Inside the bacterial cell, the higher electronegativity of rhodium (2.28) might demonstrate an increase affinity for amine, phosphate or sulfhydryl groups compared to other tested metal ion solutions (for example Y = 1.22 or In =1.78) (Beloglazkina et al., 2016; Varkey, 2010). Rhodium being a member of d-block transition metals possesses a tendency to lose electrons and be reduced (Greenwood et al., 1998). This redox reaction between rhodium ions and phosphate/amine/sulfhydryl groups may possibly affect two vital processes inside the bacterial cell. Firstly, rhodium can bind to the large cavities of the ribosome, such as the peptide-conducting tunnel passing through the ribosomal subunit. Secondly, it might hinder the translation and transcription process required for the RNA and DNA formation. Thus, this two-way redox reaction leads to protein dysfunction and ultimately destruction of bacteria cell (Beloglazkina et al., 2016; Bien et al., 1999).

It is known that by adding antimicrobial substances together, a synergistic, additive, indifferent or antagonistic result might occur (Doern, 2014). In combination, the most effective metal ion solution was demonstrated to be rhodium/ruthenium. In agreement with our results, rhodium complexes with tetraaza macrocyclic and ruthenium (II) carbonyl thiosemicarbazone complexes have been shown to have effective antimicrobial efficacy against range of bacteria (Bien et al., 1999; Kannan et al., 2008; Jayabalakrishnan and Natarajan, 2002). Further, a rhodium (III) ion complex with tetradentate macrocyclic was shown to demonstrate inhibitory efficacy when compared to platinum (II) and iridium (II) complexes against *E. coli* and *S. aureus* (Chandra et al., 2011). Further studies are needed to understand the mode of action of the antimicrobials when used in combination

This study also demonstrated that tantalum and titanium had some antimicrobial properties. In respect to the other metal ion solutions tested, various values have been previously reported, which seem to be dependent on the formulation of the antimicrobial compounds. In our work, the antimicrobial activity of titanium metal ion solutions was demonstrated. Bis(cyclopentadienyl)titanium (IV) at 1000 ppm has been show to demonstrate greater

antimicrobial efficacy using the ZoI assay (up to 26 mm) than when used without a titanium (IV) complex (up to 16 mm) against *E. coli*, *S. aureus* and *Bacillus subtilis* (Srivastava et al., 2005; Cai et al., 2012). Surfaces coated with 80% titanium have also been shown to have significant antibacterial properties against *E. coli* in a bacterial adhesion test (Seddiki et al., 2014). In work by others, tantalum oxynitride thin films were shown to have little antibacterial efficacy unless combined with silver ions using visible light radiation against *E. coli* (Hsieh et al., 2010). Gallium and zinc ions co-ordinated with protoporphyrin and mesoporphyrin respectively have showed up to 90% antibacterial efficacy against *Staphylococcus epidermis* and *Pseudomonas aeruginosa* (Ma et al., 2013). However, in our work zinc and gallium were not the most antimicrobial metal ion solutions tested. In contrast to our results, indium compounds with curcumin and diacetylcurcumin and yttrium (III) complex with phenanthroline (at 0.05 mg L<sup>-1</sup>) have also been shown to have low MICs (187 µgmL<sup>-1</sup> to 23 µgmL<sup>-1</sup>) against *E. coli*, *S. aureus*, *P. aeruginosa*, *B. subtilis* and *S. epidermidis* (Tajbakhsh et al., 2008). Our study also showed some antimicrobial efficacies for the tantalum metal ion solutions. The addition of niobium to copper (3.8%) has been shown to decrease the bacterial count by up to 99% against *E. coli* using viable bacterial count test (Baena et al., 2006). However, in our study, the antimicrobial efficacy of the niobium metal ion solutions were not significant in the MIC and MBC tests. Overall, *E. faecium* was the most resistant bacteria in the individual ion metal ions, but was the most sensitive bacteria in the FBC assays whereas for *K. pneumonia* and *A. baumannii*, the opposite was found.

## 5. Conclusion

Overall, the rhodium metal ion solution demonstrated the best antimicrobial efficacy against the three tested bacteria. Only the rhodium/ ruthenium combination showed synergism antimicrobial efficacies specifically against *E. faecium*. This fundamental study suggests that specific metal ion combinations used either individually possess the potential to be used as antimicrobials/biocides.

## Funding

This research did not receive any specific grant from funding agencies in the public, commercial, or not-for-profit sectors.

Declaration of interest None.

## Appendix A. Supplementary data

Supplementary data related to this article can be found at <http://dx.doi.org/10.1016/j.ibiod.2018.06.017>.

doi.org/10.1016/j.ibiod.2018.06.017.

## References

- Baena, M.I., Márquez, M.C., Matres, V., Botella, J., Ventosa, A., 2006. Bactericidal activity of copper and niobium–alloyed austenitic stainless steel. *Curr. Microbiol.* 53, 491–495.
- Beloglazkina, E.K., Manzheliy, E.A., Moiseeva, A.A., Maloshitskaya, O.A., Zyk, N.V., Skvortsov, D.A., Osterman, I.A., Sergiev, P.V., Dontsova, O.A., Ivanenkov, Y.A., 2016. Synthesis, characterisation, cytotoxicity and antibacterial activity of ruthenium (II) and rhodium (III) complexes with sulfur-containing terpyridines. *Polyhedron* 107, 27–37.
- Bien, M., Pruchnik, F.P., Seniuk, A., Lachowicz, T.M., Jakimowicz, P., 1999. Studies of antibacterial activity of binuclear rhodium (II) complexes with heterocyclic nitrogen ligands. *J. Inorg. Biochem.* 73, 49–55.
- Bruins, M.R., Kapil, S., Oehme, F.W., 2000. Microbial resistance to metals in the environment. *Ecotoxicol. Environ. Saf.* 45, 198–207.
- Cai, M., Chen, J., Taha, M., 2012. Synthesis, characterization, antibacterial and antifungal activity of yttrium (III) complexes including 1, 10-phenanthroline. *Chin. J. Chem.* 30, 1531–1538.
- Chandra, S., Tyagi, M., Agrawal, S., 2011. Spectral and antimicrobial studies on tetraaza macrocyclic complexes of Pd-II, Pt-II, Rh-III and Ir-III metal ions. *Journal of Saudi Chemical Society* 15, 49–54.
- Chang, Y.Y., Huang, H.L., Chen, H.J., Lai, C.H., Wen, C.Y., 2014. Antibacterial properties and cytocompatibility of tantalum oxide coatings. *Surf. Coating. Technol.* 259, 193–198.
- Dizaj, S.M., Lotfipour, F., Barzegar-Jalali, M., Zarrintan, M.H., Adibkia, K., 2014. Antimicrobial activity of the metals and metal oxide nanoparticles. *Materials Science and Engineering C* 44, 278–284.
- Doern, C.D., 2014. When does 2 plus 2 equal 5? A review of antimicrobial synergy testing. *J. Clin. Microbiol.* 52, 4124–4128.
- Greenwood, N.N., Earnshaw, A., Knovel, 1998. *Chemistry of the Elements*, second ed. Butterworth-Heinemann, Oxford; Boston.
- Haenle, M., Fritsche, A., Zietz, C., Bader, R., Heidenau, F., Mittelmeier, W., Gollwitzer, H., 2011. An extended spectrum bactericidal titanium dioxide (TiO<sub>2</sub>) coating for metallic implants: in vitro effectiveness against MRSA and mechanical properties. *J. Mater.*

- Sci. Mater. Med. 22, 381–387.
- He, X., Zhang, X., Wang, X., Qin, L., 2017. Review of antibacterial activity of titaniumbased implants' surfaces fabricated by micro-arc oxidation. *Coatings* 7, 45–67.
- Hsieh, J.H., Chang, C.C., Chang, Y.K., Cherng, J.S., 2010. Photocatalytic and antibacterial properties of TaON–Ag nanocomposite thin films. *Thin Solid Films* 518, 7263–7266.
- Jayabalakrishnan, C., Natarajan, K., 2002. Ruthenium(II) carbonyl complexes with tridentate Schiff bases and their antibacterial activity. *Transit. Met. Chem.* 27, 75–79.
- Kannan, S., Sivagamasundari, M., Ramesh, R., Liu, Y., 2008. Ruthenium(II) carbonyl complexes of dehydroacetic acid thiosemicarbazone: synthesis, structure, light emission and biological activity. *Journal of Organic Chemistry* 693, 2251–2257.
- Kolmas, J., Groszyk, E., Kwiatkowska-Różycka, D., 2014. Substituted hydroxyapatites with antibacterial properties. *BioMed Res. Int.* 2014, 178123.
- Lemire, J.A., Harrison, J.J., Turner, R.J., 2013. Antimicrobial activity of metals: mechanisms, molecular targets and applications. *Nature Reviews Microbiology* 11, 371–384.
- Ma, H., Darmawan, E.T., Zhang, M., Zhang, L., Bryers, J.D., 2013. Development of a poly (ether urethane) system for the controlled release of two novel anti-biofilm agents based on gallium or zinc and its efficacy to prevent bacterial biofilm formation. *J. Contr. Release* 172, 1035–1044.
- Mitchell, J.G., Kogure, K., 2006. Bacterial motility: links to the environment and a driving force for microbial physics. *FEMS (Fed. Eur. Microbiol. Soc.) Microbiol. Ecol.* 55, 3–16.
- Olar, R., Badea, M., Marinescu, D., Chifiriuc, C.-M., Bleotu, C., Grecu, M.N., Iorgulescu, E.E., Bucur, M., Lazar, V., Finaru, A., 2010. Prospects for new antimicrobials based on N,N-dimethylbiguanide complexes as effective agents on both planktonic and adhered microbial strains. *Eur. J. Med. Chem.* 45, 2868–2875.
- Pendleton, J.N., Gorman, S.P., Gilmore, B.F., 2013. Clinical relevance of the ESKAPE pathogens. *Expert Rev. Anti-infect. Ther.* 11, 297–308.
- Ribeiro, A.M., Flores-Sahagun, T.H.S., Paredes, R.C., 2016. A perspective on molybdenum biocompatibility and antimicrobial activity for applications in implants. *J. Mater. Sci.* 51, 2806–2816.
- Santajit, S., Indrawattana, N., 2016. Mechanisms of antimicrobial resistance in ESKAPE pathogens. *BioMed Res. Int.* <http://dx.doi.org/10.1155/2016/2475067>.
- Santos, A.F., Brotto, D.F., Favarin, L.R.V., Cabeza, N.A., Andrade, G.R., Batistote, M., Cavalheiro, A.A., Neves, A., Rodrigues, D.C.M., Anjos, A. d., 2014. Study of the antimicrobial activity of metal complexes and their ligands through bioassays applied to plant extracts. *Revista Brasileira de Farmacognosia* 24, 309–315.
- Seddiki, O., Harnagea, C., Levesque, L., Mantovani, D., Rosei, F., 2014. Evidence of antibacterial activity on titanium surfaces through nanotextures. *Appl. Surf. Sci.* 308, 275–284.
- Smith, K., Hunter, I.S., 2008. Efficacy of common hospital biocides with biofilms of multidrug resistant clinical isolates. *J. Med. Microbiol.* 57, 966–973.
- Srivastava, A.K., Pandey, O.P., Sengupta, S.K., 2005. Synthesis, spectral and antimicrobial studies of Bis (cyclopentadienyl) titanium (IV) derivatives with schiff bases derived from 2-Amino-5-phenyl-1, 3, 4-thiadiazole. *Bioinorganic Chemistry Applications* 3, 289–297.
- Tajbakhsh, S., Mohammadi, K., Deilami, I., Zandi, K., Fouladvand, M., Ramedani, E., Asayesh, G., 2008. Antibacterial activity of indium curcumin and indium diacetylcurcumin. *Afr. J. Biotechnol.* 7, 3832–3835.
- Varkey, A.J., 2010. Antibacterial properties of some metals and alloys in combating coliforms in contaminated water. *Science Research Essays* 5, 3834–3839.
- Vaidya, M.Y., McBain, A.J., Butler, J.A., Banks, C.E., Whitehead, K.A., 2017. Antimicrobial efficacy and synergy of metal ions against *Enterococcus faecium*, *Klebsiella pneumoniae* and *Acinetobacter baumannii* in planktonic and biofilm phenotypes. *Sci. Rep.* 7.

## References

- Adam, A. M. A., Refat, M. S. and Mohamed, M. A. (2015) 'Synthesis and spectroscopic characterizations of noble metal complexes (gold, silver, platinum) in the presence of selenium, and their biological applications as antibacterial, antifungal, and anticancer.' *Research on Chemical Intermediates*, 41(2) pp. 965-1000.
- Adlhart, C., Verran, J., Azevedo, N. F., Olmez, H., Keinänen-Toivola, M. M., Gouveia, I., Melo, L. F. and Crijns, F. (2018) 'Surface modifications for antimicrobial effects in the healthcare setting: a critical overview.' *Journal of Hospital Infection*, 99(3) pp. 239-249.
- Ahmad, A. and Viljoen, A. (2015) 'The in vitro antimicrobial activity of Cymbopogon essential oil (lemon grass) and its interaction with silver ions.' *Phytomedicine*, 22(6) pp. 657-665.
- Ahmad, A., Khan, A., Samber, N. and Manzoor, N. (2014) 'Antimicrobial activity of Mentha piperita essential oil in combination with silver ions.' *Synergy*, 1(2) pp. 92-98.
- Ahmed, A., Khan, A. K., Anwar, A., Ali, S. A. and Shah, M. R. (2016) 'Biofilm inhibitory effect of chlorhexidine conjugated gold nanoparticles against Klebsiella pneumoniae.' *Microbial Pathogenesis*, 98 pp. 50-56.
- Al-Jumaili, A., Alancherry, S., Bazaka, K. and Jacob, M. V. (2017) 'Review on the Antimicrobial Properties of Carbon Nanostructures.' *Materials*, 10(9) p. 1066.
- Ali, D., Alarifi, S., Alkahtani, S. and Almeer, R. S. (2018) 'Silver-doped graphene oxide nanocomposite triggers cytotoxicity and apoptosis in human hepatic normal and carcinoma cells.' *Int J Nanomedicine*, pp. 5685-5699.
- Almohamad, S., Somarajan, S. R., Singh, K. V., Nallapareddy, S. R. and Murray, B. E. (2014) 'Influence of isolate origin and presence of various genes on biofilm formation by Enterococcus faecium.' *FEMS microbiology letters*, 353(2) pp. 151-156.
- Amachawadi, R. G., Scott, H. M., Aperce, C., Vinasco, J., Drouillard, J. S. and Nagaraja, T. G. (2015) 'Effects of in-feed copper and tylosin supplementations on copper and antimicrobial resistance in faecal enterococci of feedlot cattle.' *Journal of Applied Microbiology*, 118(6) pp. 1287-1297.
- Aminov, R. I. (2010) 'A brief history of the antibiotic era: lessons learned and challenges for the future.' *Frontiers in microbiology*, 1 p. 134.
- Anacona, J., Bastardo, E. and Camus, J. (1999) 'Manganese(II) and palladium(II) complexes containing a new macrocyclic Schiff base ligand: antibacterial properties.' *Transition Metal Chemistry*, 24(4) pp. 478-480.
- Anandan, S. and Muthukumaran, S. (2015) 'Microstructural, crystallographic and optical characterizations of Cu-doped ZnO nanoparticles co-doped with Ni.' *Journal of Materials Science: Materials in Electronics*, 26(6) pp. 4298-4307.
- Ann, L. C., Mahmud, S., Bakhori, S. K. M., Sirelkhatim, A., Mohamad, D., Hasan, H., Seeni, A. and Rahman, R. A. (2014) 'Antibacterial responses of zinc oxide structures against Staphylococcus aureus, Pseudomonas aeruginosa and Streptococcus pyogenes.' *Ceramics International*, 40(2) pp. 2993-3001.
- Arancibia, F., Ewig, S., Martinez, J. A., Ruiz, M., Bauer, T., Marcos, M. A., Mensa, J. and Torres, A. (2000) 'Antimicrobial treatment failures in patients with community-acquired



pneumonia - Causes and prognostic implications.' *American Journal of Respiratory and Critical Care Medicine*, 162(1) pp. 154-160.

Arias, C. A. and Murray, B. E. (2012) 'The rise of the Enterococcus: beyond vancomycin resistance.' *Nat Rev Microbiol*, 10(4) pp. 266-278.

Armentano, I., Arciola, C. R., Fortunati, E., Ferrari, D., Mattioli, S., Amoroso, C. F., Rizzo, J., Kenny, J. M., Imbriani, M. and Visai, L. (2014) 'The interaction of bacteria with engineered nanostructured polymeric materials: a review.' *The Scientific World Journal*, pp. 410423-410418.

Ashurst, J. V. and Dawson, A. (2018) *Pneumonia, Klebsiella*. StatPearls Publishing:Treasure Island (FL).

Aslam, S. M. D. (2008) 'Effect of antibacterials on biofilms.' *AJIC: American Journal of Infection Control*, 36(10) pp. 175.

Aslan, H. G., Özcan, S. and Karacan, N. (2011) 'Synthesis, characterization and antimicrobial activity of salicylaldehyde benzenesulfonylhydrazone (Hsalbsmh) and its Nickel(II), Palladium(II), Platinum(II), Copper(II), Cobalt(II) complexes.' *Inorganic Chemistry Communications*, 14(9) pp. 1550-1553.

Ayaz Ahmed, K. B., Raman, T. and Anbazhagan, V. (2016) 'Platinum nanoparticles inhibit bacteria proliferation and rescue zebrafish from bacterial infection.' *RSC Advances*, 6(50) pp. 44415-44424.

Baena, M. I., Marquez, M. C., Matres, V., Botella, J. and Ventosa, A. (2006) 'Bactericidal activity of copper and niobium-alloyed austenitic stainless steel.' *Curr Microbiol*, 53(6) pp. 491-495.

Bal, W., Sokołowska, M., Kurowska, E. and Faller, P. (2013) 'Binding of transition metal ions to albumin: Sites, affinities and rates.' *BBA - General Subjects*, 1830(12) pp. 5444-5455.

Bao, Q., Zhang, D. and Qi, P. (2011) 'Synthesis and characterization of silver nanoparticle and graphene oxide nanosheet composites as a bactericidal agent for water disinfection.' *Journal of Colloid and Interface Science*, 360(2) pp. 463-470.

Barbolina, I., Woods, C. R., Lozano, N., Kostarelos, K., Novoselov, K. S. and Roberts, I. S. (2016) 'Purity of graphene oxide determines its antibacterial activity.' *2D Materials*, 3(2) p. 025025.

Bartlett, J. G., Gilbert, D. N. and Spellberg, B. (2013) 'Seven ways to preserve the miracle of antibiotics.' *Clinical Infectious Diseases*, 56(10) pp. 1445-1450.

Beloglazkina, E. K., Manzheliy, E. A., Moiseeva, A. A., Maloshitskaya, O. A., Zyk, N. V., Skvortsov, D. A., Osterman, I. A., Sergiev, P. V., Dontsova, O. A. and Ivanenkov, Y. A. (2016) 'Synthesis, characterisation, cytotoxicity and antibacterial activity of ruthenium (II) and rhodium (III) complexes with sulfur-containing terpyridines.' *Polyhedron*, 107 pp. 27-37.

Benedetti, B. T., Peterson, E. J., Kabolizadeh, P., Martínez, A., Kipping, R. and Farrell, N. P. (2011) 'Effects of Noncovalent Platinum Drug-Protein Interactions on Drug Efficacy: Use of Fluorescent Conjugates as Probes for Drug Metabolism.' *Molecular Pharmaceutics*, 8(3) pp. 940-948.

Bennett, J. W. and Chung, K.-T. (2001) 'Alexander Fleming and the discovery of penicillin.' *In Advances in Applied Microbiology*, 49 pp. 163-184.

Berthon, G. (1995) 'Critical evaluation of the stability constants of metal complexes of amino acids with polar side chains (Technical Report).' *Pure and Applied Chemistry*, 67(7) pp. 1117-1240.

Beveridge, T. J. (1999) 'Structures of gram-negative cell walls and their derived membrane vesicles.' *Journal of Bacteriology*, 181(16) pp. 4725-4733.

Bhullar, K., Waglechner, N., Pawlowski, A., Koteva, K., Banks, E. D., Johnston, M. D., Barton, H. A. and Wright, G. D. (2012) 'Antibiotic resistance is prevalent in an isolated cave microbiome.' *PloS one*, 7(4) p. e34953.

Bien, M., Pruchnik, F. P., Seniuk, A., Lachowicz, T. M. and Jakimowicz, P. (1999) 'Studies of antibacterial activity of binuclear rhodium (II) complexes with heterocyclic nitrogen ligands.' *J Inorg Biochem*, 73(1-2) pp. 49-55.

Bomberger, J. M., MacEachran, D. P., Coutermarsh, B. A., Ye, S., O'Toole, G. A. and Stanton, B. A. (2009) 'Long-distance delivery of bacterial virulence factors by *Pseudomonas aeruginosa* outer membrane vesicles.' *PLoS pathogens*, 5(4) p. e1000382.

Boucher, H. W., Talbot, G. H., Bradley, J. S., Edwards, J. E., Gilbert, D., Rice, L. B., Scheld, M., Spellberg, B. and Bartlett, J. (2009) 'Bad Bugs, No Drugs: No ESKAPE! An Update from the Infectious Diseases Society of America.' *Clinical Infectious Diseases*, 48(1) pp. 1-12.

Brahma, U., Kothari, R., Sharma, P. and Bhandari, V. (2018) 'Antimicrobial and anti-biofilm activity of hexadentated macrocyclic complex of copper (II) derived from thiosemicarbazide against *Staphylococcus aureus*.' *Scientific Reports*, 8(1) pp. 8050-8058.

Bregnocchi, A., Zanni, E., Uccelletti, D., Marra, F., Cavallini, D., De Angelis, F., De Bellis, G., Bossù, M., Ierardo, G., Polimeni, A. and Sarto, M. S. (2017) 'Graphene-based dental adhesive with anti-biofilm activity.' *Journal of Nanobiotechnology*, 15(1) pp. 89-13.

Brown-Jaque, M., Calero-Cáceres, W. and Muniesa, M. (2015) 'Transfer of antibiotic-resistance genes via phage-related mobile elements.' *Plasmid*, 79 pp. 1-7.

Brötz-Oesterhelt, H. and Brunner, N. A. (2008) 'How many modes of action should an antibiotic have?' *Current Opinion in Pharmacology*, 8(5) pp. 564-573.

Bush, K. (2013) 'Proliferation and significance of clinically relevant  $\beta$ -lactamases.' *Annals of the New York Academy of Sciences*, 1277(1) pp. 84-90.

Bush, K., Courvalin, P., Dantas, G., Davies, J., Eisenstein, B., Huovinen, P., Jacoby, G. A., Kishony, R., Kreiswirth, B. N., Kutter, E., Lerner, S. A., Levy, S., Lewis, K., Lomovskaya, O., Miller, J. H., Mobashery, S., Piddock, L. J., Projan, S., Thomas, C. M., Tomasz, A., Tulkens, P. M., Walsh, T. R., Watson, J. D., Witkowski, J., Witte, W., Wright, G., Yeh, P. and Zgurskaya, H. I. (2011) 'Tackling antibiotic resistance.' *In Nat Rev Microbiol*, 9 pp. 894-896.

Cai, M., Chen, J. and Taha, M. (2010) 'Synthesis, structures and antibacterial activities of two complexes of yttrium (III) with 2,6-pyridinedicarboxylate.' *Inorganic Chemistry Communications*, 13(1) pp. 199-202.

Cain, A. K., Boinett, C. J., Barquist, L., Dordel, J., Fookes, M., Mayho, M., Ellington, M. J., Goulding, D., Pickard, D., Wick, R. R., Holt, K. E., Parkhill, J. and Thomson, N. R. (2018) 'Morphological, genomic and transcriptomic responses of *Klebsiella pneumoniae* to the last-line antibiotic colistin.' *Sci Rep*, 8(1) p. 9868.

- Campbell, E. A., Korzheva, N., Mustaev, A., Murakami, K., Nair, S., Goldfarb, A. and Darst, S. A. (2001) 'Structural mechanism for rifampicin inhibition of bacterial rna polymerase.' *Cell*, 104(6) pp. 901-912.
- Canduela, M. J., Gallego, L., Sevillano, E., Valderrey, C., Calvo, F. and Perez, J. (2006) 'Evolution of multidrug-resistant *Acinetobacter baumannii* isolates obtained from elderly patients with respiratory tract infections.' *J Antimicrob Chemother*, 57(6) pp. 1220-1222.
- Capeness, M. J., Edmundson, M. C. and Horsfall, L. E. (2015) 'Nickel and platinum group metal nanoparticle production by *Desulfovibrio alaskensis* G20.' *New Biotechnology*, 32(6) pp. 727-731.
- Cardile, A. P., Sanchez, J. C. J., Samberg, M. E., Romano, D. R., Hardy, S. K., Wenke, J. C., Murray, C. K. and Akers, K. S. (2014) 'Human plasma enhances the expression of Staphylococcal microbial surface components recognizing adhesive matrix molecules promoting biofilm formation and increases antimicrobial tolerance In Vitro.' *BMC Research Notes*, 7(1) pp. 457-457.
- Casey, A. L., Adams, D., Karpanen, T. J., Lambert, P. A., Cookson, B. D., Nightingale, P., Miruszenko, L., Shillam, R., Christian, P. and Elliott, T. S. J. (2010) 'Role of copper in reducing hospital environment contamination.' *Journal of Hospital Infection*, 74(1) pp. 72-77.
- Castellano, J. J., Shafii, S. M., Ko, F., Donate, G., Wright, T. E., Mannari, R. J., Payne, W. G., Smith, D. J. and Robson, M. C. (2007) 'Comparative evaluation of silver-containing antimicrobial dressings and drugs.' *International Wound Journal*, 4(2) pp. 114-122.
- Cerqueira, G. M. and Peleg, A. Y. (2011) 'Insights into *Acinetobacter baumannii* pathogenicity.' *IUBMB life*, 63(12) pp. 1055-1060.
- Chandra, S., Tyagi, M. and Agrawal, S. (2011) 'Spectral and antimicrobial studies on tetraaza macrocyclic complexes of Pd-II, Pt-II, Rh-III and Ir-III metal ions.' *JOURNAL OF SAUDI CHEMICAL SOCIETY*, 15(1) pp. 49-54.
- Chandraker, K., Nagwanshi, R., Jadhav, S. K., Ghosh, K. K. and Satnami, M. L. (2017) 'Antibacterial properties of amino acid functionalized silver nanoparticles decorated on graphene oxide sheets.' *Spectrochimica Acta Part A: Molecular and Biomolecular Spectroscopy*, 181 pp. 47-54.
- Chang, Y.-Y., Huang, H.-L., Chen, H.-J., Lai, C.-H. and Wen, C.-Y. (2014) 'Antibacterial properties and cytocompatibility of tantalum oxide coatings.' *Surface and Coatings Technology*, 259 pp. 193-198.
- Chast, F. (2008) 'A history of drug discovery.' *The Practice of Medicinal Chemistry*, 3 pp. 3-62.
- Chen, C. Z. and Cooper, S. L. (2002) 'Interactions between dendrimer biocides and bacterial membranes.' *Biomaterials*, 23(16) pp. 3359-3368.
- Chen, J., Peng, H., Wang, X., Shao, F., Yuan, Z. and Han, H. (2014) 'Graphene oxide exhibits broad-spectrum antimicrobial activity against bacterial phytopathogens and fungal conidia by intertwining and membrane perturbation.' *Nanoscale*, 6(3) pp. 1879-1889.
- Chowdhuri, A. R., Tripathy, S., Chandra, S., Roy, S. and Sahu, S. K. (2015) 'A ZnO decorated chitosan-graphene oxide nanocomposite shows significantly enhanced antimicrobial activity with ROS generation.' *RSC Advances*, 5(61) pp. 49420-49428.

- Christophe Esp rito, S., Ee Wen, L., Christian, G. E., Davide, Q., Dylan, W. D., Christopher, J. C. and Gregor, G. (2011) 'Bacterial Killing by Dry Metallic Copper Surfaces.' *Applied and Environmental Microbiology*, 77(3) pp. 794-802.
- Chung, C. J., Lin, H. I., Tsou, H. K., Shi, Z. Y. and He, J. L. (2008) 'An antimicrobial TiO<sub>2</sub> coating for reducing hospital-acquired infection.' *Journal of Biomedical Materials Research Part B: Applied Biomaterials*, 85(1) pp. 220-224.
- Corbin, B. D., Seeley, E. H., Raab, A., Feldmann, J., Miller, M. R., Torres, V. J., Anderson, K. L., Dattilo, B. M., Dunman, P. M., Gerads, R., Caprioli, R. M., Nacken, W., Chazin, W. J. and Skaar, E. P. (2008) 'Metal Chelation and Inhibition of Bacterial Growth in Tissue Abscesses.' *Science*, 319(5865) pp. 962-965.
- Costerton, J. W., Stewart, P. S. and Greenberg, E. P. (1999) 'Bacterial Biofilms: A Common Cause of Persistent Infections.' *Science*, 284(5418) pp. 1318-1322.
- Cotner, J. B., Hall, E. K., Scott, J. T. and Haldal, M. (2010) 'Freshwater Bacteria are Stoichiometrically Flexible with a Nutrient Composition Similar to Seston.' *Frontiers in Microbiology*, 1 pp. 132.
- Cowan, M. M., Abshire, K. Z., Houk, S. L. and Evans, S. M. (2003) 'Antimicrobial efficacy of a silver-zeolite matrix coating on stainless steel.' *Journal of Industrial Microbiology & Biotechnology*, 30(2) pp. 102-106.
- Cowley, A. and Woodward, B. (2011) 'A Healthy Future: Platinum in Medical Applications.' *Platinum Metals Review*, 55(2) pp. 98-107.
- Cox, G. and Wright, G. D. (2013) 'Intrinsic antibiotic resistance: Mechanisms, origins, challenges and solutions.' *International Journal of Medical Microbiology*, 303(6) pp. 287-292.
- Cui, L., Yang, K., Zhou, G., Huang, W. E. and Zhu, Y.-G. (2017) 'Surface-enhanced Raman spectroscopy combined with stable isotope probing to monitor nitrogen assimilation at both bulk and single-cell level.' *Analytical Chemistry*, 89(11) pp. 5793-5800.
- Cui, L., Chen, P., Chen, S., Yuan, Z., Yu, C., Ren, B. and Zhang, K. (2013) 'In situ study of the antibacterial activity and mechanism of action of silver nanoparticles by surface-enhanced Raman spectroscopy.' *Analytical Chemistry*, 85(11) pp. 5436-5443.
- Dakal, T. C., Kumar, A., Majumdar, R. S. and Yadav, V. (2016) 'Mechanistic Basis of Antimicrobial Actions of Silver Nanoparticles.' *Frontiers in Microbiology*, pp. 1831.
- Das, B., Dash, S. K., Mandal, D., Ghosh, T., Chattopadhyay, S., Tripathy, S., Das, S., Dey, S. K., Das, D. and Roy, S. (2017) 'Green synthesized silver nanoparticles destroy multidrug resistant bacteria via reactive oxygen species mediated membrane damage.' *Arabian Journal of Chemistry*, 10(6) pp. 862-876.
- Dasari Shareena, T. P., McShan, D., Dasmahapatra, A. K. and Tchounwou, P. B. (2018) 'A Review on Graphene-Based Nanomaterials in Biomedical Applications and Risks in Environment and Health.' *Nano-Micro Letters*, 10(3) pp. 1-34.
- Davidson, P. M., Sofos, J. N. and Branen, A. L. (2005) *Antimicrobials in Food*, Third Edition. Food Science and Technology. CRC Press.
- Davies, J. and Davies, D. (2010) 'Origins and Evolution of Antibiotic Resistance.' *Microbiology and Molecular Biology Reviews*, 74(3) pp. 417-433.

- DeAlba-Montero, I., Guajardo-Pacheco, J., Morales-Sánchez, E., Araujo-Martínez, R., Loredó-Becerra, G. M., Martínez-Castañón, G.-A., Ruiz, F. and Compeán Jasso, M. E. (2017) 'Antimicrobial Properties of Copper Nanoparticles and Amino Acid Chelated Copper Nanoparticles Produced by Using a Soya Extract.' *Bioinorganic Chemistry and Applications*, 2017 pp. 1064918-1064916.
- Del Curto, B., Brunella, M. F., Giordano, C., Pedferri, M. P., Valtulina, V., Visai, L. and Cigada, A. (2005) 'Decreased bacterial adhesion to surface-treated titanium.' *The International Journal of Artificial Organs*, 28(7) pp. 718.
- Demain, A. L. (2006) 'From natural products discovery to commercialization: a success story.' *Journal of Industrial Microbiology and Biotechnology*, 33(7) pp. 486-495.
- Di Giulio, M., Zappacosta, R., Di Lodovico, S., Di Campi, E., Siani, G., Fontana, A. and Cellini, L. (2018) 'Antimicrobial and Antibiofilm Efficacy of Graphene Oxide against Chronic Wound Microorganisms.' *Antimicrobial Agents and Chemotherapy*, 62(7) pp. e00547-00518.
- Di Martino, P., Cafferini, N., Joly, B. and Darfeuille-Michaud, A. (2003) 'Klebsiella pneumoniae type 3 pili facilitate adherence and biofilm formation on abiotic surfaces.' *Research in Microbiology*, 154(1) pp. 9-16.
- Dizaj, S. M., Lotfipour, F., Barzegar-Jalali, M., Zarrintan, M. H. and Adibkia, K. (2014) 'Antimicrobial activity of the metals and metal oxide nanoparticles.' *Materials Science and Engineering: C*, 44 pp. 278-284.
- Domingues, S., Harms, K., Fricke, W. F., Johnsen, P. J., Da Silva, G. J. and Nielsen, K. M. (2012) 'Natural transformation facilitates transfer of transposons, integrons and gene cassettes between bacterial species.' *PLoS pathogens*, 8(8) pp. e1002837.
- Doorduyn, D. J., Rooijackers, S. H., van Schaik, W. and Bardoel, B. W. (2016) 'Complement resistance mechanisms of Klebsiella pneumoniae.' *Immunobiology*, 221(10) pp. 1102-1109.
- Dror, N., Mandel, M., Hazan, Z. and Lavie, G. (2009) 'Advances in microbial biofilm prevention on indwelling medical devices with emphasis on usage of acoustic energy.' *Sensors*, 9(4) pp. 2538-2554.
- Dudev, T. and Lim, C. (2014) 'Competition among metal ions for protein binding sites: determinants of metal ion selectivity in proteins.' *Chemical Reviews*, 114(1) pp. 538-556.
- Dufour, D., Leung, V. and Lévesque, C. M. (2010) 'Bacterial biofilm: structure, function, and antimicrobial resistance.' *Endodontic Topics*, 22(1) pp. 2-16.
- Dunne, W. M., Jr. (2002) 'Bacterial adhesion: seen any good biofilms lately?' *Clin Microbiol Rev*, 15(2) pp. 155-166.
- Dunny, G. M., Hancock, L. E. and Shankar, N. (2014) 'Enterococcal biofilm structure and role in colonization and disease.' In *Enterococci: From commensals to leading causes of drug resistant infection* [Internet]. Boston: Massachusetts Eye and Ear Infirmary.
- D'Costa, V. M., King, C. E., Kalan, L., Morar, M., Sung, W. W. L., Schwarz, C., Froese, D., Zazula, G., Calmels, F. and Debruyne, R. (2011) 'Antibiotic resistance is ancient.' *Nature*, 477(7365) p. 457.
- Egorova, K. S. and Ananikov, V. P. (2016) 'Which Metals are Green for Catalysis? Comparison of the Toxicities of Ni, Cu, Fe, Pd, Pt, Rh, and Au Salts.' *Angewandte Chemie International Edition*, 55(40) pp. 12150-12162.

- Elguindi, J., Moffitt, S., Hasman, H., Andrade, C., Raghavan, S. and Rensing, C. (2011) 'Metallic copper corrosion rates, moisture content, and growth medium influence survival of copper ion-resistant bacteria.' *Appl Microbiol Biotechnol*, 89(6) pp. 1963-1970.
- Eliopoulos, G. M., Maragakis, L. L. and Perl, T. M. (2008) 'Acinetobacter baumannii: epidemiology, antimicrobial resistance, and treatment options.' *Clinical Infectious Diseases*, 46(8) pp. 1254-1263.
- Elsome, A. M., HamiltonMiller, J. M. T., Brumfitt, W. and Noble, W. C. (1996) 'Antimicrobial activities in vitro and in vivo of transition element complexes containing gold(I) and osmium(VI).' *Journal of Antimicrobial Chemotherapy*, 37(5), May, pp. 911-918.
- Ernst, R. J., Komor, A. C. and Barton, J. K. (2011) 'Selective cytotoxicity of rhodium metalloinsertors in mismatch repair-deficient cells.' *Biochemistry*, 50(50) pp. 10919-10928.
- Fagerbakke, K. M., Heldal, M. and Norland, S. (1996) 'Content of carbon, nitrogen, oxygen, sulfur and phosphorus in native aquatic and cultured bacteria.' *Aquatic Microbial Ecology*, 10(1) pp. 15-27.
- Farahani, A. (2016) 'State of globe: Enterococci: Virulence factors and biofilm formation.' *Journal of global infectious diseases*, 8(1) pp. 1-2.
- Faron, M. L., Ledebøer, N. A. and Buchan, B. W. (2016) 'Resistance mechanisms, epidemiology, and approaches to screening for vancomycin-resistant enterococcus in the health care setting.' *Journal of Clinical Microbiology*, 54(10) pp. 2436-2447.
- Farrell, D. J., Flamm, R. K., Jones, R. N. and Sader, H. S. (2013) 'Spectrum and potency of ceftaroline tested against leading pathogens causing community-acquired respiratory tract infections in Europe (2010).' *Diagnostic Microbiology and Infectious Disease*, 75(1) pp. 86-88.
- Feng, Q. L., Wu, J., Chen, G. Q., Cui, F. Z., Kim, T. N. and Kim, J. O. (2000) 'A mechanistic study of the antibacterial effect of silver ions on Escherichia coli and Staphylococcus aureus.' *Journal of Biomedical Materials Research*, 52(4) pp. 662-668.
- Ferraris, S. and Spriano, S. (2016) 'Antibacterial titanium surfaces for medical implants.' *Materials Science and Engineering: C*, 61 pp. 965-978.
- Ferris, F. G. and Beveridge, T. J. (1985) 'Functions of bacterial cell surface structures.' *BioScience*, 35(3) pp. 172-177.
- Finney, L. A. and O'Halloran, T. V. (2003) 'Transition metal speciation in the cell: insights from the chemistry of metal ion receptors.' *Science*, 300(5621) pp. 931-936.
- Floss, H. G. and Yu, T.-W. (2005) 'Rifamycin-mode of action, resistance, and biosynthesis.' *Chemical Reviews*, 105(2) pp. 621.
- Fraise, A. P. (2002) 'Biocide abuse and antimicrobial resistance—a cause for concern?' *Journal of Antimicrobial Chemotherapy*, 49(1) pp. 11-12.
- Frankel, M. L., Demeter, M. A., Lemire, J. A. and Turner, R. J. (2016) 'Evaluating the Metal Tolerance Capacity of Microbial Communities Isolated from Alberta Oil Sands Process Water.' *PLoS One*, 11(2) pp. e0148682.
- França, A. and Cerca, N. (2016) 'Plasma is the main regulator of Staphylococcus epidermidis biofilms virulence genes transcription in human blood.' *Pathogens and Disease*, 74(2) pp. 1-5.

- Frère, J.-M., Sauvage, E. and Kerff, F. (2016) 'From "An Enzyme Able to Destroy Penicillin" to Carbapenemases: 70 Years of Beta-lactamase Misbehaviour.' *Current Drug Targets*, 17(9) pp. 974-982.
- Gaballa, A. S. (2010) 'Synthesis, characterization and antimicrobial studies on cis-platinum(II) complexes of 5-nitrosouracil derivatives.' *Spectrochimica Acta Part A: Molecular and Biomolecular Spectroscopy*, 75(1) pp. 146-151.
- Gandon, S. and Vale, P. F. (2014) 'The evolution of resistance against good and bad infections.' *Journal of Evolutionary Biology*, 27(2) pp. 303-312.
- Garza-Cervantes, J. A., Chávez-Reyes, A., Castillo, E. C., García-Rivas, G., Antonio Ortega-Rivera, O., Salinas, E., Ortiz-Martínez, M., Gómez-Flores, S. L., Peña-Martínez, J. A., Pepi-Molina, A., Treviño-González, M. T., Zarate, X., Elena Cantú-Cárdenas, M., Enrique Escarcega-Gonzalez, C. and Morones-Ramírez, J. R. (2017) 'Synergistic Antimicrobial Effects of Silver/Transition-metal Combinatorial Treatments.' *Scientific Reports*, 7(1) pp. 903-916.
- Ghule, K., Ghule, A. V., Chen, B.-J. and Ling, Y.-C. (2006) 'Preparation and characterization of ZnO nanoparticles coated paper and its antibacterial activity study.' *Green Chemistry*, 8(12) pp. 1034.
- Giedraitienė, A., Vitkauskienė, A., Naginienė, R. and Pavilonis, A. (2011) 'Antibiotic resistance mechanisms of clinically important bacteria.' *Medicina*, 47(3) pp. 19.
- Gnanadhas, D. P., Ben Thomas, M., Thomas, R., Raichur, A. M. and Chakravorty, D. (2013) 'Interaction of Silver Nanoparticles with Serum Proteins Affects Their Antimicrobial Activity.' *Antimicrobial Agents and Chemotherapy*, 57(10) pp. 4945.
- Gootz, T. D. and Marra, A. (2008) 'Acinetobacter baumannii: an emerging multidrug-resistant threat.' *Expert Rev Anti Infect Ther*, 6(3) pp. 309-325.
- Gordon, W., Atabakhsh, V. A., Meza, F., Doms, A., Nissan, R., Rizioiu, I. and Stevens, R. H. (2007) 'The antimicrobial efficacy of the erbium, chromium: yttrium-scandium-gallium-garnet laser with radial emitting tips on root canal dentin walls infected with Enterococcus faecalis.' *The Journal of the American Dental Association*, 138(7) pp. 992-1002.
- Gorle, A. K., Feterl, M., Warner, J. M., Wallace, L., Keene, F. R. and Collins, J. G. (2014) 'Tri- and tetra-nuclear polypyridyl ruthenium(II) complexes as antimicrobial agents.' *Dalton Transactions*, 43(44) pp. 16713-16725.
- Gould, I. M. and Bal, A. M. (2013) 'New antibiotic agents in the pipeline and how they can help overcome microbial resistance.' *Virulence*, 4(2) pp. 185-191.
- Grass, G., Rensing, C. and Solioz, M. (2011) 'Metallic Copper as an Antimicrobial Surface.' *Applied and Environmental Microbiology*, 77(5) pp. 1541-1547.
- Gross, M. (2013) 'Antibiotics in crisis.' *Current Biology*, 23(24) pp. R1063-R1065.
- Guilhelmelli, F., Vilela, N., Albuquerque, P., Derengowski, L., Silva-Pereira, I. and Kyaw, C. (2013) 'Antibiotic development challenges: the various mechanisms of action of antimicrobial peptides and of bacterial resistance.' *Frontiers in Microbiology*, 4 pp. 353.
- Gundlach, J., Herzberg, C., Hertel, D., Thürmer, A., Daniel, R., Link, H. and Stülke, J. (2017) 'Adaptation of Bacillus subtilis to Life at Extreme Potassium Limitation.' *mBio*, 8(4) pp. e00861-00817.

- Gupta, K., Barua, S., Hazarika, S. N., Manhar, A. K., Nath, D., Karak, N., Namsa, N. D., Mukhopadhyay, R., Kalia, V. C. and Mandal, M. (2014) 'Green silver nanoparticles: enhanced antimicrobial and antibiofilm activity with effects on DNA replication and cell cytotoxicity.' *RSC Advances*, 4(95) pp. 52845-52855.
- Gupta, P. D. and Birdi, T. J. (2017) 'Development of botanicals to combat antibiotic resistance.' *Journal of Ayurveda and Integrative Medicine*, 8(4) pp. 266-275.
- Habiba, K., Bracho-Rincon, D. P., Gonzalez-Feliciano, J. A., Villalobos-Santos, J. C., Makarov, V. I., Ortiz, D., Avalos, J. A., Gonzalez, C. I., Weiner, B. R. and Morell, G. (2015) 'Synergistic antibacterial activity of PEGylated silver-graphene quantum dots nanocomposites.' *Applied Materials Today*, 1(2) pp. 80-87.
- Haenle, M., Fritsche, A., Zietz, C., Bader, R., Heidenau, F., Mittelmeier, W. and Gollwitzer, H. (2011) 'An extended spectrum bactericidal titanium dioxide (TiO<sub>2</sub>) coating for metallic implants: in vitro effectiveness against MRSA and mechanical properties.' *J Mater Sci Mater Med*, 22(2) pp. 381-387.
- Hancock, R. E. W. and Brinkman, F. S. L. (2002) 'FUNCTION OF PSEUDOMONAS PORINS IN UPTAKE AND EFFLUX.' *Annual Reviews in Microbiology*, 56(1) pp. 17-38.
- Hans, M., Támara, J. C., Mathews, S., Bax, B., Hegetschweiler, A., Kautenburger, R., Solioz, M. and Mücklich, F. (2014) 'Laser cladding of stainless steel with a copper-silver alloy to generate surfaces of high antimicrobial activity.' *Applied Surface Science*, 320 pp. 195-199.
- Harrison, J. J., Turner, R. J., Joo, D. A., Stan, M. A., Chan, C. S., Allan, N. D., Vrionis, H. A., Olson, M. E. and Ceri, H. (2008) 'Copper and quaternary ammonium cations exert synergistic bactericidal and antibiofilm activity against *Pseudomonas aeruginosa*.' *Antimicrob Agents Chemother*, 52(8) pp. 2870-2881.
- He, J., Zhu, X., Qi, Z., Wang, C., Mao, X., Zhu, C., He, Z., Li, M. and Tang, Z. (2015) 'Killing Dental Pathogens Using Antibacterial Graphene Oxide.' *ACS Applied Materials & Interfaces*, 7(9) pp. 5605-5611.
- Hegab, H. M., ElMekawy, A., Zou, L., Mulcahy, D., Saint, C. P. and Ginic-Markovic, M. (2016) 'The controversial antibacterial activity of graphene-based materials.' *Carbon*, 105 pp. 362-376.
- Heidenau, F., Mittelmeier, W., Detsch, R., Haenle, M., Stenzel, F., Ziegler, G. and Gollwitzer, H. (2005) 'A novel antibacterial titania coating: Metal ion toxicity and in vitro surface colonization.' *Journal of Materials Science-Materials in Medicine*, 16(10), Oct, pp. 883-888.
- Heldal, M., Norland, S., Fagerbakke, K. M., Thingstad, F. and Bratbak, G. (1996) 'The elemental composition of bacteria: a signature of growth conditions?' *Marine Pollution Bulletin*, 33(1-6) pp. 3-9.
- Hendrickx, A. P. A., Van Schaik, W. and Willems, R. J. L. (2013) 'The cell wall architecture of *Enterococcus faecium*: from resistance to pathogenesis.' *Future microbiology*, 8(8) pp. 993-1010.
- Hobman, J. L. and Crossman, L. C. (2015) 'Bacterial antimicrobial metal ion resistance.' *Journal of Medical Microbiology*, 64(5) pp. 471-497.
- Hollenbeck, B. L. and Rice, L. B. (2012) 'Intrinsic and acquired resistance mechanisms in enterococcus.' *Virulence*, 3(5) pp. 421-569.



- Holt, K. B. and Bard, A. J. (2005) 'Interaction of silver(I) ions with the respiratory chain of *Escherichia coli*: an electrochemical and scanning electrochemical microscopy study of the antimicrobial mechanism of micromolar Ag<sup>+</sup>.' *Biochemistry*, 44(39) pp. 13214-13223.
- Howard, A., O'Donoghue, M., Feeney, A. and Sleator, R. D. (2012) '*Acinetobacter baumannii*: an emerging opportunistic pathogen.' *Virulence*, 3(3) pp. 243-250.
- Hrenovic, J., Milenkovic, J., Goic-Barisic, I. and Rajic, N. (2013) 'Antibacterial activity of modified natural clinoptilolite against clinical isolates of *Acinetobacter baumannii*.' *Microporous and Mesoporous Materials*, 169 pp. 148-152.
- Hu, W., Peng, C., Luo, W., Lv, M., Li, X., Li, D., Huang, Q. and Fan, C. (2010) 'Graphene-based antibacterial paper.' *ACS Nano*, 4(7) pp. 4317-4323.
- Huang, H.-L., Chang, Y.-Y., Lai, M.-C., Lin, C.-R., Lai, C.-H. and Shieh, T.-M. (2010) 'Antibacterial TaN-Ag coatings on titanium dental implants.' *Surface and Coatings Technology*, 205(5) pp. 1636-1641.
- Huang, H. I., Shih, H. Y., Lee, C. M., Yang, T. C., Lay, J. J. and Lin, Y. E. (2008) 'In vitro efficacy of copper and silver ions in eradicating *Pseudomonas aeruginosa*, *Stenotrophomonas maltophilia* and *Acinetobacter baumannii*: implications for on-site disinfection for hospital infection control.' *Water Res*, 42(1-2) pp. 73-80.
- Huang, K. C., Mukhopadhyay, R., Wen, B., Gitai, Z. and Wingreen, N. S. (2008) 'Cell Shape and Cell-Wall Organization in Gram-Negative Bacteria.' *Proceedings of the National Academy of Sciences of the United States of America*, 105(49) pp. 19282-19287.
- Huang, X., Bao, X., Liu, Y., Wang, Z. and Hu, Q. (2017) 'Catechol-Functional Chitosan/Silver Nanoparticle Composite as a Highly Effective Antibacterial Agent with Species-Specific Mechanisms.' *Scientific Reports*, 7(1) pp. 1860-1810.
- Huddleston, J. R. (2014) 'Horizontal gene transfer in the human gastrointestinal tract: potential spread of antibiotic resistance genes.' *Infection and Drug Resistance*, 7 pp. 167.
- Huh, A. J. and Kwon, Y. J. (2011) '"Nanoantibiotics": A new paradigm for treating infectious diseases using nanomaterials in the antibiotics resistant era.' *Journal of Controlled Release*, 156(2) pp. 128-145.
- Hui, L., Piao, J.-G., Auletta, J., Hu, K., Zhu, Y., Meyer, T., Liu, H. and Yang, L. (2014) 'Availability of the Basal Planes of Graphene Oxide Determines Whether It Is Antibacterial.' *ACS Applied Materials & Interfaces*, 6(15) pp. 13183-13190.
- Hulander, M., Hong, J., Andersson, M., Gervén, F., Ohrlander, M., Tengvall, P. and Elwing, H. (2009) 'Blood interactions with noble metals: coagulation and immune complement activation.' *ACS Applied Materials & Interfaces*, 1(5) pp. 1053-1062.
- Hummers Jr, W. S. and Offeman, R. E. (1958) 'Preparation of graphitic oxide.' *Journal of the American Chemical Society*, 80(6) pp. 1339-1339.
- Humphreys, G., Lee, G. L., Percival, S. L. and McBain, A. J. (2011) 'Combinatorial activities of ionic silver and sodium hexametaphosphate against microorganisms associated with chronic wounds.' *Journal of Antimicrobial Chemotherapy*, 66(11) pp. 2556-2561.
- Høiby, N., Bjarnsholt, T., Givskov, M., Molin, S. and Ciofu, O. (2010) 'Antibiotic resistance of bacterial biofilms.' *International Journal of Antimicrobial Agents*, 35(4) pp. 322-332.

- Ijaz, M. F., Zhukova, Y., Konopatsky, A., Dubinskiy, S., Korobkova, A., Pustov, Y., Brailovski, V. and Prokoshkin, S. (2018) 'Effect of Ta addition on the electrochemical behaviour and functional fatigue life of metastable Ti-Zr-Nb based alloy for indwelling implant applications.' *Journal of Alloys and Compounds*, 748 pp. 51-56.
- Iqbal, M. S., Taqi, S. G., Arif, M., Wasim, M. and Sher, M. (2009) 'In vitro distribution of gold in serum proteins after incubation of sodium aurothiomalate and auranofin with human blood and its pharmacological significance.' *Biological Trace Element Research*, 130(3) pp. 204-209.
- Issa, Y., Brunton, P., Waters, C. M. and Watts, D. C. (2007) 'Cytotoxicity of metal ions to human oligodendroglial cells and human gingival fibroblasts assessed by mitochondrial dehydrogenase activity.' *Dental Materials*, 24(2) pp. 281-287.
- Jackson, G. E. and Byrne, M. J. (1996) 'Metal ion speciation in blood plasma: gallium-67-citrate and MRI contrast agents.' *Journal of nuclear medicine: official publication, Society of Nuclear Medicine*, 37(2) pp. 379.
- Jamal, M., Tasneem, U., Hussain, T. and Andleeb, S. (2015) 'Bacterial biofilm: its composition, formation and role in human infections.' *RRJMB*, 4 pp. 1-14.
- Jarm, V. (2014) 'Terminology for Biorelated Polymers and Applications (IUPAC Recommendations 2012).' *Kemija u Industriji*, 63(11-12) pp. 411-432.
- Jastrzębska, A. M., Kurtycz, P. and Olszyna, A. R. (2012) 'Recent advances in graphene family materials toxicity investigations.' *Journal of Nanoparticle Research*, 14(12) pp. 1-21.
- Jayabalakrishnan, C. and Natarajan, K. (2002) 'Ruthenium (II) carbonyl complexes with tridentate Schiff bases and their antibacterial activity.' *Transition Metal Chemistry*, 27(1) pp. 75-79.
- Ji, H., Sun, H. and Qu, X. (2016) 'Antibacterial applications of graphene-based nanomaterials: Recent achievements and challenges.' *Advanced Drug Delivery Reviews*, 105 pp. 176-189.
- Jin, J., Zhang, L. I., Shi, M., Zhang, Y. and Wang, Q. (2017) 'Ti-GO-Ag nanocomposite: the effect of content level on the antimicrobial activity and cytotoxicity.' *International Journal of Nanomedicine*, 12 pp. 4209.
- Jondle, C. N., Gupta, K., Mishra, B. B. and Sharma, J. (2018) 'Klebsiella pneumoniae infection of murine neutrophils impairs their efferocytic clearance by modulating cell death machinery.' *PLoS pathogens*, 14, pp. e1007338.
- Jones, S. A., Bowler, P. G., Walker, M. and Parsons, D. (2004) 'Controlling wound bioburden with a novel silver-containing Hydrofiber® dressing.' *Wound Repair and Regeneration*, 12(3) pp. 288-294.
- Joyanes, P., Pascual, A., Martinez-Martinez, L., Hevia, A. and Perea, E. J. (2000) 'In vitro adherence of Enterococcus faecalis and Enterococcus faecium to urinary catheters.' *Eur J Clin Microbiol Infect Dis*, 19(2) pp. 124-127.
- Jung, G. B., Nam, S. W., Choi, S., Lee, G.-J. and Park, H.-K. (2014) 'Evaluation of antibiotic effects on Pseudomonas aeruginosa biofilm using Raman spectroscopy and multivariate analysis.' *Biomedical optics express*, 5(9) pp. 3238-3251.
- Jung, W. K., Koo, H. C., Kim, K. W., Shin, S., Kim, S. H. and Park, Y. H. (2008) 'Antibacterial Activity and Mechanism of Action of the Silver Ion in Staphylococcus aureus and Escherichia coli.' *Applied and Environmental Microbiology*, 74(7) pp. 2171-2178.

- Juribašić, M., Molčanov, K., Kojić-Prodić, B., Bellotto, L., Kralj, M., Zani, F. and Tušek-Božić, L. (2011) 'Palladium (II) complexes of quinolinyaminophosphonates: Synthesis, structural characterization, antitumor and antimicrobial activity.' *Journal of Inorganic Biochemistry*, 105(6) pp. 867-879.
- Kahraman, M., Zamaleeva, A. I., Fakhrullin, R. F. and Culha, M. (2009) 'Layer-by-layer coating of bacteria with noble metal nanoparticles for surface-enhanced Raman scattering.' *Analytical and Bioanalytical Chemistry*, 395(8) pp. 2559.
- Kaiser, C. A., Krieger, M., Lodish, H. and Berk, A. (2007) *Molecular cell biology*. WH Freeman.
- Kalan, L. and Wright, G. D. (2011) 'Antibiotic adjuvants: Multicomponent anti-infective strategies.' *Expert Reviews in Molecular Medicine*, 13 pp. e5.
- Kamel, M. S., Khosa, A., Tawse-Smith, A. and Leichter, J. (2014) 'The use of laser therapy for dental implant surface decontamination: a narrative review of in vitro studies.' *Lasers in Medical Science*, 29(6) pp. 1977-1985.
- Kannan, S., Sivagamasundari, M., Ramesh, R. and Liu, Y. (2008) 'Ruthenium(II) carbonyl complexes of dehydroacetic acid thiosemicarbazone: Synthesis, structure, light emission and biological activity.' *Journal of Organometallic Chemistry*, 693(13) pp. 2251-2257.
- Kardos, N. and Demain, A. L. (2011) 'Penicillin: the medicine with the greatest impact on therapeutic outcomes.' *Applied Microbiology and Biotechnology*, 92(4) pp. 677.
- Kashef, N. and Hamblin, M. R. (2017) 'Can microbial cells develop resistance to oxidative stress in antimicrobial photodynamic inactivation?' *Drug Resistance Updates*, 31 pp. 31-42.
- Kaufmann, B. B. and Hung, D. T. (2010) 'The fast track to multidrug resistance.' *Molecular Cell*, 37(3) pp. 297-298.
- Kawakami, H., Yoshida, K., Nishida, Y., Kikuchi, Y. and Sato, Y. (2008) 'Antibacterial properties of metallic elements for alloying evaluated with application of JIS Z 2801:2000.' *ISIJ International*, 48(9) pp. 1299-1304.
- Kaye, K. S. and Pogue, J. M. (2015) 'Infections caused by resistant gram-negative bacteria: epidemiology and management.' *Pharmacotherapy: The Journal of Human Pharmacology and Drug Therapy*, 35(10) pp. 949-962.
- Khan, H. A., Baig, F. K. and Mehboob, R. (2017) 'Nosocomial infections: Epidemiology, prevention, control and surveillance.' *Asian Pacific Journal of Tropical Biomedicine*, 7(5) pp. 478-482.
- Khan, S. A. and Yusuf, M. (2009) 'Synthesis, spectral studies and in vitro antibacterial activity of steroidal thiosemicarbazone and their palladium (Pd (II)) complexes.' *Eur J Med Chem*, 44(5) pp. 2270-2274.
- Kim, J., Jo, A., Chukeatirote, E. and Ahn, J. (2016) 'Assessment of antibiotic resistance in *Klebsiella pneumoniae* exposed to sequential in vitro antibiotic treatments.' *Annals of clinical microbiology and antimicrobials*, 15(1) pp. 60.
- Kim, J., Pitts, B., Stewart, P. S., Camper, A. and Yoon, J. (2008) 'Comparison of the Antimicrobial Effects of Chlorine, Silver Ion, and Tobramycin on Biofilm.' *Antimicrobial Agents and Chemotherapy*, 52(4) pp. 1446-1453.

- Kingston, W. (2004) 'Streptomycin, Schatz v. Waksman, and the balance of credit for discovery.' *Journal of the History of Medicine and Allied Sciences*, 59(3) pp. 441-462.
- Kittler, S., Greulich, C., Diendorf, J., Köller, M. and Epple, M. (2010) 'Toxicity of Silver Nanoparticles Increases during Storage Because of Slow Dissolution under Release of Silver Ions.' *Chemistry of Materials*, 22(16) pp. 4548-4554.
- Klaus-Joerger, T., Joerger, R., Olsson, E. and Granqvist, C.-G. (2001) 'Bacteria as workers in the living factory: metal-accumulating bacteria and their potential for materials science.' *TRENDS in Biotechnology*, 19(1) pp. 15-20.
- Kogan, L. A. (2005) 'How Europe employs disguised regulatory protectionism to weaken American free enterprise.' *International Journal of Economic Development*, 7(2-3) pp. 65.
- Kohanski, M. A., Dwyer, D. J. and Collins, J. J. (2010) 'How antibiotics kill bacteria: from targets to networks.' *Nature Reviews Microbiology*, 8(6) pp. 423.
- Kollef, M. H. and Fraser, V. J. (2001) 'Antibiotic resistance in the intensive care unit.' *Annals of Internal medicine*, 134(4) pp. 298-314.
- Kolmas, J., Groszyk, E. and Kwiatkowska-Różycka, D. (2014) 'Substituted hydroxyapatites with antibacterial properties.' *BioMed research international*, 2014(2) pp. 178123.
- Kondratyeva, K., Navon-Venezia, S. and Carattoli, A. (2017) 'Klebsiella pneumoniae: a major worldwide source and shuttle for antibiotic resistance.' *FEMS Microbiology Reviews*, 41(3) pp. 252-275.
- Kovala-Demertzi, D., Demertzis, M. A., Filiou, E., Pantazaki, A. A., Yadav, P. N., Miller, J. R., Zheng, Y. and Kyriakidis, D. A. (2003) 'Platinum (II) and palladium (II) complexes with 2-acetyl pyridine 4N-ethyl thiosemicarbazone able to overcome the cis-platin resistance. Structure, antibacterial activity and DNA strand breakage.' *Biometals*, 16(3) pp. 411-418.
- Kreisler, M., Kohnen, W., Marinello, C., Schoof, J., Langnau, E., Jansen, B. and d'Hoedt, B. (2003) 'Antimicrobial efficacy of semiconductor laser irradiation on implant surfaces.' *The International Journal of Oral & Maxillofacial Implants*, 18(5) pp. 706.
- Kresge, N., Simoni, R. D. and Hill, R. L. (2004) 'Selman Waksman: the father of antibiotics.' *Journal of Biological Chemistry*, 279(48) pp. e7-e7.
- Krishnamoorthy, K., Veerapandian, M., Yun, K. and Kim, S. J. (2013) 'New function of molybdenum trioxide nanoplates: Toxicity towards pathogenic bacteria through membrane stress.' *Colloids and Surfaces B: Biointerfaces*, 112 pp. 521-524.
- Krishnani, K. K., Zhang, Y., Xiong, L., Yan, Y., Boopathy, R. and Mulchandani, A. (2012) 'Bactericidal and ammonia removal activity of silver ion-exchanged zeolite.' *Bioresource Technology*, 117 pp. 86-91.
- Kumar, S. S., Venkateswarlu, P., Rao, V. R. and Rao, G. N. (2013) 'Synthesis, characterization and optical properties of zinc oxide nanoparticles.' *International Nano Letters*, 3(1) pp. 30.
- Kurantowicz, N., Sawosz, E., Jaworski, S., Kutwin, M., Strojny, B., Wierzbicki, M., Szeliga, J., Hotowy, A., Lipińska, L., Koziński, R., Jagiełło, J. and Chwalibog, A. (2015) 'Interaction of graphene family materials with *Listeria monocytogenes* and *Salmonella enterica*.' *Nanoscale Research Letters*, 10(1) pp. 1-12.

Lambert, P. A. (2002) 'Cellular impermeability and uptake of biocides and antibiotics in Gram-positive bacteria and mycobacteria.' *Journal of Applied Microbiology*, 92 pp. 46S-54S.

Lammel, T., Boisseaux, P., Fernández-Cruz, M.-L. and Navas, J. M. (2013) 'Internalization and cytotoxicity of graphene oxide and carboxyl graphene nanoplatelets in the human hepatocellular carcinoma cell line Hep G2.' *Particle and Fibre Toxicology*, 10(1) pp. 27.

Lee, C.-R., Lee, J. H., Park, K. S., Jeon, J. H., Kim, Y. B., Cha, C.-J., Jeong, B. C. and Lee, S. H. (2017a) 'Antimicrobial resistance of hypervirulent *Klebsiella pneumoniae*: epidemiology, hypervirulence-associated determinants, and resistance mechanisms.' *Frontiers in Cellular and Infection Microbiology*, 7 pp. 483.

Lee, C.-R., Lee, J. H., Park, M., Park, K. S., Bae, I. K., Kim, Y. B., Cha, C.-J., Jeong, B. C. and Lee, S. H. (2017b) 'Biology of *Acinetobacter baumannii*: pathogenesis, antibiotic resistance mechanisms, and prospective treatment options.' *Frontiers in Cellular and Infection Microbiology*, 7 pp. 55.

Lellouche, J., Friedman, A., Gedanken, A. and Banin, E. (2012) 'Antibacterial and antibiofilm properties of yttrium fluoride nanoparticles.' *International Journal of Nanomedicine*, 7 pp. 5611-5624.

Lemire, J. A., Harrison, J. J. and Turner, R. J. (2013) 'Antimicrobial activity of metals: mechanisms, molecular targets and applications.' *Nature Reviews Microbiology*, 11(6) pp. 371-384.

Lenntech. (2015) Chemical elements listed by atomic number and electronic configuration. [Online] [Assessed on 15 March 2017]

<http://www.lenntech.com/periodic/number/atomic-number.htm>

<http://www.lenntech.com/periodic-chart-elements/electronegativity.htm>

Li, B., Yao, J., Niu, J., Liu, J., Wang, L., Feng, M. and Sun, Y. (2018) 'Effects of Graphene Oxide on the Structure and Properties of Regenerated Wool Keratin Films.' *Polymers*, 10(12), 1318.

Li, F., Collins, J. G. and Keene, F. R. (2015) 'Ruthenium complexes as antimicrobial agents.' *Chemical Society Reviews*, 44(8) pp. 2529-2542.

Li, F., Mulyana, Y., Feterl, M., Warner, J. M., Collins, J. G. and Keene, F. R. (2011) 'The antimicrobial activity of inert oligonuclear polypyridylruthenium (II) complexes against pathogenic bacteria, including MRSA.' *Dalton transactions*, 40(18) pp. 5032.

Li, J., Xie, S., Ahmed, S., Wang, F., Gu, Y., Zhang, C., Chai, X., Wu, Y., Cai, J. and Cheng, G. (2017) 'Antimicrobial Activity and Resistance: Influencing Factors.' *Frontiers in Pharmacology*, 8 pp. 364.

Ligon, B. L. (2004) 'Penicillin: its discovery and early development.' *Seminars in Pediatric Infectious Diseases*, 15(1) pp. 52-57.

Lin, M. F. and Lan, C. Y. (2014) 'Antimicrobial resistance in *Acinetobacter baumannii*: From bench to bedside.' *World J Clin Cases*, 2(12) pp. 787-814.

Liou, J.-W., Hung, Y.-J., Yang, C.-H. and Chen, Y.-C. (2015) 'The antimicrobial activity of gramicidin A is associated with hydroxyl radical formation.' *PloS one*, 10(1) pp. e0117065.

- Lippard, S. J. (1982) 'New chemistry of an old molecule: cis-[Pt(NH<sub>3</sub>)<sub>2</sub>Cl<sub>2</sub>].' *Science*, 218(4577) pp. 1075-1082.
- Liu, A., Tran, L., Becket, E., Lee, K., Chinn, L., Park, E., Tran, K. and Miller, J. H. (2010) 'Antibiotic sensitivity profiles determined with an Escherichia coli gene knockout collection: generating an antibiotic bar code.' *Antimicrobial Agents and Chemotherapy*, 54(4) pp. 1393-1403.
- Liu, Q., Yao, X., Zhou, X., Qin, Z. and Liu, Z. (2012) 'Varistor effect in Ag-graphene/epoxy resin nanocomposites.' *Scripta Materialia*, 66(2) pp. 113-116.
- Liu, S., Zeng, T. H., Hofmann, M., Burcombe, E., Wei, J., Jiang, R., Kong, J. and Chen, Y. (2011) 'Antibacterial activity of graphite, graphite oxide, graphene oxide, and reduced graphene oxide: membrane and oxidative stress.' *ACS Nano*, 5(9) pp. 6971-6980.
- Livage, J. (1993) 'Redox reactions in transition metal oxide gels.' *Journal of Sol-Gel Science and Technology*, 1(1) pp. 21-33.
- Livermore, D. M. (2012) 'Current epidemiology and growing resistance of gram-negative pathogens.' *The Korean Journal of Internal Medicine*, 27(2) pp. 128.
- Llor, C. and Bjerrum, L. (2014) 'Antimicrobial resistance: risk associated with antibiotic overuse and initiatives to reduce the problem.' *Therapeutic Advances in Drug Safety*, 5(6) pp. 229-241.
- Longo, F., Vuotto, C. and Donelli, G. (2014) 'Biofilm formation in Acinetobacter baumannii.' *New Microbiol*, 37(2) pp. 119-127.
- Lorite, G. S., Rodrigues, C. M., de Souza, A. A., Kranz, C., Mizaikoff, B. and Cotta, M. A. (2011) 'The role of conditioning film formation and surface chemical changes on Xylella fastidiosa adhesion and biofilm evolution.' *J Colloid Interface Sci*, 359(1) pp. 289-295.
- Lourenço, C., Macdonald, T. J., Gavriilidis, A., Allan, E., MacRobert, A. J. and Parkin, I. P. (2018) 'Effects of bovine serum albumin on light activated antimicrobial surfaces.' *RSC Advances*, 8(60) pp. 34252-34258.
- Lu, P.-J., Huang, S.-C., Chen, Y.-P., Chiueh, L.-C. and Shih, D. Y.-C. (2015) 'Analysis of titanium dioxide and zinc oxide nanoparticles in cosmetics.' *Journal of Food and Drug Analysis*, 23(3) pp. 587-594.
- Lu, X., Samuelson, D. R., Rasco, B. A. and Konkel, M. E. (2012) 'Antimicrobial effect of diallyl sulphide on Campylobacter jejuni biofilms.' *Journal of Antimicrobial Chemotherapy*, 67(8) pp. 1915-1926.
- Luyt, C.-E., Bréchet, N., Trouillet, J.-L. and Chastre, J. (2014) 'Antibiotic stewardship in the intensive care unit.' *Critical care*, 18(5) pp. 480.
- Ma, H., Darmawan, E. T., Zhang, M., Zhang, L. and Bryers, J. D. (2013) 'Development of a poly(ether urethane) system for the controlled release of two novel anti-biofilm agents based on gallium or zinc and its efficacy to prevent bacterial biofilm formation.' *Journal of Controlled Release*, 172(3) pp. 1035-1044.
- Ma, J., Zhang, J., Xiong, Z., Yong, Y. and Zhao, X. S. (2011) 'Preparation, characterization and antibacterial properties of silver-modified graphene oxide.' *Journal of Materials Chemistry*, 21(10) pp. 3350-3352.

Madigan, M. T. (2015) Brock biology of microorganisms. Fourteenth; Global; ed., Harlow, Essex: Pearson Education Limited.

Magiorakos, A. P., Srinivasan, A., Carey, R. B., Carmeli, Y., Falagas, M. E., Giske, C. G., Harbarth, S., Hindler, J. F., Kahlmeter, G. and Olsson-Liljequist, B. (2012) 'Multidrug-resistant, extensively drug-resistant and pandrug-resistant bacteria: an international expert proposal for interim standard definitions for acquired resistance.' *Clinical Microbiology and Infection*, 18(3) pp. 268-281.

Mah, T.-F. C. and O'Toole, G. A. (2001) 'Mechanisms of biofilm resistance to antimicrobial agents.' *Trends in Microbiology*, 9(1) pp. 34-39.

Maleki Dizaj, S., Mennati, A., Jafari, S., Khezri, K. and Adibkia, K. (2015) 'Antimicrobial Activity of Carbon-Based Nanoparticles.' *Advanced Pharmaceutical Bulletin*, 5(1), pp. 19-23.

Malloy, A. M. W. and Campos, J. M. (2011) 'Extended-spectrum beta-lactamases: a brief clinical update.' *The Pediatric Infectious Disease Journal*, 30(12) pp. 1092-1093.

Manchanda, V., Sanchaita, S. and Singh, N. (2010) 'Multidrug resistant acinetobacter.' *J Glob Infect Dis*, 2(3) pp. 291-304.

Manson, J. M., Hancock, L. E. and Gilmore, M. S. (2010) 'Mechanism of chromosomal transfer of *Enterococcus faecalis* pathogenicity island, capsule, antimicrobial resistance, and other traits.' *Proceedings of the National Academy of Sciences*, 107(27) pp. 12269-12274.

Mardare, C. C. and Hassel, A. W. (2014) 'Investigations on bactericidal properties of molybdenum-tungsten oxides combinatorial thin film material libraries.' *ACS Combinatorial Science*, 16(11) pp. 631-639.

Martin, R. M., Cao, J., Brisse, S., Passet, V., Wu, W., Zhao, L., Malani, P. N., Rao, K. and Bachman, M. A. (2016) 'Molecular epidemiology of colonizing and infecting isolates of *Klebsiella pneumoniae*.' *mSphere*, 1(5) pp. e00261-00216.

Martinez de Tejada, G., Sánchez-Gómez, S., Rázquin-Olazarán, I., Kowalski, I., Kaonis, Y., Heinbockel, L., Andrä, J., Schürholz, T., Hornef, M., Dupont, A., Garidel, P., Lohner, K., Gutschmann, T., David, S. A. and Brandenburg, K. (2012) 'Bacterial cell wall compounds as promising targets of antimicrobial agents I. Antimicrobial peptides and lipopolyamines.' *Current Drug Targets*, 13(9) p. 1121.

Masurkar, S. A., Chaudhari, P. R., Shidore, V. B. and Kamble, S. P. (2012) 'Effect of biologically synthesised silver nanoparticles on *Staphylococcus aureus* biofilm quenching and prevention of biofilm formation.' *IET Nanobiotechnology*, 6(3) pp. 110-114.

McConoughey, S. J., Howlin, R., Granger, J. F., Manring, M. M., Calhoun, J. H., Shirtliff, M., Kathju, S. and Stoodley, P. (2014) 'Biofilms in periprosthetic orthopedic infections.' *Future Microbiology*, 9(8) pp. 987-1007.

McCord, C. and Chowdhury, Q. (2003) 'A cost effective small hospital in Bangladesh: what it can mean for emergency obstetric care.' *International Journal of Gynecology & Obstetrics*, 81(1) pp. 83-92.

McMurry, L., Petrucci, R. E. and Levy, S. B. (1980) 'Active Efflux of Tetracycline Encoded by Four Genetically Different Tetracycline Resistance Determinants in *Escherichia coli*.' *Proceedings of the National Academy of Sciences of the United States of America*, 77(7) pp. 3974-3977.

- Michael, C. A., Dominey-Howes, D. and Labbate, M. (2014) 'The antimicrobial resistance crisis: causes, consequences, and management.' *Frontiers in Public Health*, 2 pp. 145.
- Miller, W. R., Munita, J. M. and Arias, C. A. (2014) 'Mechanisms of antibiotic resistance in enterococci.' *Expert Review of Anti-infective Therapy*, 12(10) pp. 1221-1236.
- Mishra, A. K., Mishra, S. B., Manav, N., Saluja, D., Chandra, R. and Kaushik, N. K. (2006) 'Synthesis, characterization, antibacterial and cytotoxic study of platinum (IV) complexes.' *Bioorg Med Chem*, 14(18) pp. 6333-6340.
- Mitosch, K. and Bollenbach, T. (2014) 'Bacterial responses to antibiotics and their combinations.' *Environmental Microbiology Reports*, 6(6) pp. 545-557.
- Montefour, K., Frieden, J., Hurst, S., Helmich, C., Headley, D., Martin, M. and Boyle, D. A. (2008) 'Acinetobacter baumannii: an emerging multidrug-resistant pathogen in critical care.' *Crit Care Nurse*, 28(1) pp. 15-25; quiz 26.
- Monteiro, D. R., Gorup, L. F., Takamiya, A. S., Ruvollo-Filho, A. C., Camargo, E. R. d. and Barbosa, D. B. (2009) 'The growing importance of materials that prevent microbial adhesion: antimicrobial effect of medical devices containing silver.' *International Journal of Antimicrobial Agents*, 34(2) pp. 103-110.
- Mossop, K. F. and Davidson, C. M. (2003) 'Comparison of original and modified BCR sequential extraction procedures for the fractionation of copper, iron, lead, manganese and zinc in soils and sediments.' *Analytica Chimica Acta*, 478(1) pp. 111-118.
- Mukherjee, T., Sen, B., Patra, A., Banerjee, S., Hundal, G. and Chattopadhyay, P. (2014) 'Cyclometalated rhodium (III) complexes bearing dithiocarbamate derivative: Synthesis, characterization, interaction with DNA and biological study.' *Polyhedron*, 69 pp. 127-134.
- Munita, J. M. and Arias, C. A. (2016) 'Mechanisms of Antibiotic Resistance.' *Microbiology spectrum*, 4(2) pp 0016.
- Musico, Y. L. F., Santos, C. M., Dalida, M. L. P. and Rodrigues, D. F. (2014) 'Surface Modification of Membrane Filters Using Graphene and Graphene Oxide-Based Nanomaterials for Bacterial Inactivation and Removal.' *ACS Sustainable Chemistry & Engineering*, 2(7) pp. 1559-1565.
- Muñiz, C. C., Zelaya, T. E. C., Esquivel, G. R. and Fernández, F. J. (2007) 'Penicillin and cephalosporin production: A historical perspective.' *Revista Latinoamericana de Microbiología*, 49(3-4) pp. 88-98.
- Namasivayam, S. K. R., Christo, B. B., Arasu, S. M. K., Kumar, K. A. M. and Deepak, K. (2013) 'Anti biofilm effect of biogenic silver nanoparticles coated medical devices against biofilm of clinical isolate of Staphylococcus aureus.' *Global Journal of Medical Research*, 3(3) pp. 25-29.
- Nanda, S. S., Yi, D. K. and Kim, K. (2016) 'Study of antibacterial mechanism of graphene oxide using Raman spectroscopy.' *Scientific Reports*, 6 pp. 28443.
- Nation, R. L., Velkov, T. and Li, J. (2014) 'Colistin and polymyxin B: peas in a pod, or chalk and cheese?' *Clin Infect Dis*, 59(1) pp. 88-94.
- Nazari, Z., Banoee, M., Sepahi, A., Rafii, F. and Shahverdi, A. (2012) 'The combination effects of trivalent gold ions and gold nanoparticles with different antibiotics against resistant Pseudomonas aeruginosa.' *Gold Bulletin*, 45(2) pp. 53-59.



- Nicolle, L. E. (2014) 'Catheter associated urinary tract infections.' *Antimicrobial Resistance and Infection Control*, 3(1) pp. 23.
- Nielsen, K. M., Bøhn, T. and Townsend, J. P. (2014) 'Detecting rare gene transfer events in bacterial populations.' *Frontiers in Microbiology*, 4 pp. 415.
- Nies, D. H. (1999) 'Microbial heavy-metal resistance.' *Appl Microbiol Biotechnol*, 51(6) pp 730-750.
- Niveditha, S., Pramodhini, S., Umadevi, S., Kumar, S. and Stephen, S. (2012) 'The isolation and the biofilm formation of uropathogens in the patients with catheter associated urinary tract infections (UTIs).' *Journal of clinical and diagnostic research: JCDR*, 6(9) pp. 1478.
- Oboda, D., Kozowski, H. and Rowińska-Yrek, M. (2018) 'Antimicrobial peptide-metal ion interactions - a potential way of activity enhancement.' *New Journal of Chemistry*, 42(1) pp. 756-7568.
- Okeke, I. N., Laxminarayan, R., Bhutta, Z. A., Duse, A. G., Jenkins, P., O'Brien, T. F., Pablos-Mendez, A. and Klugman, K. P. (2005) 'Antimicrobial resistance in developing countries. Part I: recent trends and current status.' *The Lancet Infectious Diseases*, 5(8) pp. 481-493.
- Olakanmi, O., Gunn, J. S., Su, S., Soni, S., Hassett, D. J. and Britigan, B. E. (2010) 'Gallium disrupts iron uptake by intracellular and extracellular *Francisella* strains and exhibits therapeutic efficacy in a murine pulmonary infection model.' *Antimicrob Agents Chemother*, 54(1) pp. 244-253.
- Ouyang, Y., Ouyang, Y., Cai, X., Shi, Q., Liu, L., Wan, D. and Tan, S. (2013) 'Poly-L-lysine-modified reduced graphene oxide stabilizes the copper nanoparticles with higher water-solubility and long-term additively antibacterial activity.' *Colloids and Surfaces B: Biointerfaces*, 107 pp. 107-114.
- Owen, C. A., Selvakumaran, J., Nottingher, I., Jell, G., Hench, L. L. and Stevens, M. M. (2006) 'In vitro toxicology evaluation of pharmaceuticals using Raman micro-spectroscopy.' *J Cell Biochem*, 99(1) pp. 178-186.
- Oxford, J. and Kozlov, R. (2013) 'Antibiotic resistance-a call to arms for primary healthcare providers.' *Int J Clin Pract Suppl*, (180) pp. 1-3.
- Paczosa, M. K. and Mecsas, J. (2016) '*Klebsiella pneumoniae*: Going on the Offense with a Strong Defense.' *Microbiology and Molecular Biology Reviews*, 80(3) pp. 629.
- Paganelli, F. L., Willems, R. J. L., Jansen, P., Hendrickx, A., Zhang, X., Bonten, M. J. M. and Leavis, H. L. (2013) 'Enterococcus faecium biofilm formation: identification of major autolysin AtlAEfm, associated Acm surface localization, and AtlAEfm-independent extracellular DNA Release.' *MBio*, 4(2) pp. e00154-00113.
- Page`s, J.-M., Masi, M. and Barbe, J. (2005) 'Inhibitors of efflux pumps in Gram-negative bacteria.' *Trends in Molecular Medicine*, 11(8) pp. 382-389.
- Page`s, J.-M., James, C. E. and Winterhalter, M. (2008) 'The porin and the permeating antibiotic: a selective diffusion barrier in Gram-negative bacteria.' *Nature Reviews Microbiology*, 6(12) pp. 893-903.
- Pal, S., Tak, Y. K. and Song, J. M. (2007) 'Does the Antibacterial Activity of Silver Nanoparticles Depend on the Shape of the Nanoparticle? A Study of the Gram-Negative Bacterium *Escherichia coli*.' *Applied and Environmental Microbiology*, 73(6) pp. 1712-1720.

- Palanisamy, N. K., Ferina, N., Amirulhusni, A. N., Mohd-Zain, Z., Hussaini, J., Ping, L. J. and Durairaj, R. (2014) 'Antibiofilm properties of chemically synthesized silver nanoparticles found against *Pseudomonas aeruginosa*.' *Journal of Nanobiotechnology*, 12(1) pp. 2.
- Palmer, K. L., Daniel, A., Hardy, C., Silverman, J. and Gilmore, M. S. (2011) 'Genetic basis for daptomycin resistance in enterococci.' *Antimicrobial Agents and Chemotherapy*, 55(7) pp. 3345-3356.
- Pandey, A. and Shrivastava, N. (2013) 'Research Article Effect of Metal Ions on Antibacterial Activity of Aloe Barbadensis Mill. & Coriandrum Sativum Against Various Pathogens.' *Scholars Academic Journal of Biosciences*, 1(4) pp. 119-130.
- Pang, L., Dai, C., Bi, L., Guo, Z. and Fan, J. (2017) 'Biosafety and antibacterial ability of graphene and graphene oxide in vitro and in vivo.' *Nanoscale research letters*, 12(1) pp. 564.
- Paterson, D. L. (2006) 'Resistance in gram-negative bacteria: Enterobacteriaceae.' *American Journal of Infection Control*, 34(5) pp. S20-S28.
- Pendleton, J. N., Gorman, S. P. and Gilmore, B. F. (2013) 'Clinical relevance of the ESKAPE pathogens.' *Expert Rev Anti Infect Ther*, 11(3) pp. 297-308.
- Percival, S. L., Suleman, L., Vuotto, C. and Donelli, G. (2015) 'Healthcare-associated infections, medical devices and biofilms: risk, tolerance and control.' *Journal of Medical Microbiology*, 64(Pt 4) pp. 323-334.
- Perez, F., Hujer, A. M., Hujer, K. M., Decker, B. K., Rather, P. N. and Bonomo, R. A. (2007) 'Global challenge of multidrug-resistant *Acinetobacter baumannii*.' *Antimicrob Agents Chemother*, 51(10) pp. 3471-3484.
- Perreault, F., de Faria, A. F., Nejati, S. and Elimelech, M. (2015) 'Antimicrobial Properties of Graphene Oxide Nanosheets: Why Size Matters.' *ACS Nano*, 9(7) pp. 7226-7236.
- Pham, V. T. H., Truong, V. K., Quinn, M. D. J., Notley, S. M., Guo, Y., Baulin, V. A., Al Kobaisi, M., Crawford, R. J. and Ivanova, E. P. (2015) 'Graphene Induces Formation of Pores That Kill Spherical and Rod-Shaped Bacteria.' *ACS Nano*, 9(8) pp. 8458-8467.
- Piddock, L. J. V. (2012) 'The crisis of no new antibiotics—what is the way forward?' *The Lancet Infectious Diseases*, 12(3) pp. 249-253.
- Pletz, M. W., Hagel, S. and Forstner, C. (2017) 'Who benefits from antimicrobial combination therapy?' *Lancet Infectious Diseases*, 17(7) pp. 677-678.
- Poole, K. (2005) 'Efflux-mediated antimicrobial resistance.' *The Journal of Antimicrobial Chemotherapy*, 56(1) pp. 20.
- Poon, V. K. M. and Burd, A. (2004) 'In vitro cytotoxicity of silver: implication for clinical wound care.' *Burns*, 30(2) pp. 140-147.
- Porciatti, E., Milenković, M., Gaggelli, E., Valensin, G., Kozłowski, H., Kamysz, W. and Valensin, D. (2010) 'Structural Characterization and Antimicrobial Activity of the Zn(II) Complex with P113 (Demegen), a Derivative of Histatin 5.' *Inorganic Chemistry*, 49(19) pp. 8690-8698.
- Pradeev Raj, K., Sadaiyandi, K., Kennedy, A. and Sagadevan, S. (2017) 'Photocatalytic and antibacterial studies of indium-doped ZnO nanoparticles synthesized by co-precipitation technique.' *Journal of Materials Science: Materials in Electronics*, 28(24) pp. 19025-19037.

Prasad, K., Lekshmi, G. S., Ostrikov, K., Lussini, V., Blinco, J., Mohandas, M., Vasilev, K., Bottle, S., Bazaka, K. and Ostrikov, K. (2017) 'Synergic bactericidal effects of reduced graphene oxide and silver nanoparticles against Gram-positive and Gram-negative bacteria.' *Scientific Reports*, 7 pp. 1591.

Prestinaci, F., Pezzotti, P. and Pantosti, A. (2015) 'Antimicrobial resistance: a global multifaceted phenomenon.' *Pathogens and Global Health*, 109(7) pp. 309-318.

Quintana, R. M., Jardine, A. P., Montagner, F., Fatturi Parolo, C. C., Morgental, R. D. and Poli Kopper, P. M. (2017) 'Effect of human, dentin, albumin and lipopolysaccharide on the antibacterial activity of endodontic activity of endodontic irrigants.' *J Conserv Dent*, 20(5) pp. 341-345.

Qureshi, N., Patil, R., Shinde, M., Umarji, G., Causin, V., Gade, W., Mulik, U., Bhalerao, A. and Amalnerkar, D. P. (2015) 'Innovative biofilm inhibition and anti-microbial behavior of molybdenum sulfide nanostructures generated by microwave-assisted solvothermal route.' *Applied Nanoscience*, 5(3) pp. 331-341.

Rago, I., Bregnocchi, A., Zanni, E., D'Aloia, A. G., De Angelis, F., Bossu, M., De Bellis, G., Polimeni, A., Uccelletti, D. and Sarto, M. S. (2015) 'Antimicrobial activity of graphene nanoplatelets against *Streptococcus mutans*.' *15<sup>th</sup> International Conference on Nanotechnology. Rome, Italy* [Online] [Assessed on 15<sup>th</sup> December 2018]. <https://libguides.mmu.ac.uk/refguide/mmuharvard>

Raman, N., Selvan, A. and Sudharsan, S. (2011) 'Metallation of ethylenediamine based Schiff base with biologically active Cu(II), Ni(II) and Zn(II) ions: Synthesis, spectroscopic characterization, electrochemical behaviour, DNA binding, photonuclease activity and in vitro antimicrobial efficacy.' *Spectrochimica Acta Part A: Molecular and Biomolecular Spectroscopy*, 79(5) pp. 873-883.

Ramirez, M. S. and Tolmasky, M. E. (2010) 'Aminoglycoside modifying enzymes.' *Drug Resistance Updates*, 13(6) pp. 151-171.

Randall, C. P., Mariner, K. R., Chopra, I. and O'Neill, A. J. (2013) 'The target of daptomycin is absent from *Escherichia coli* and other gram-negative pathogens.' *Antimicrobial Agents and Chemotherapy*, 57(1) pp. 637-639.

Ravichandran, K., Chidhambaram, N. and Gobalakrishnan, S. (2016) 'Copper and Graphene activated ZnO nanopowders for enhanced photocatalytic and antibacterial activities.' *Journal of Physics and Chemistry of Solids*, 93 pp. 82-90.

Reddy, P., Chadaga, S. and Noskin, G. A. (2009) 'Antibiotic considerations in the treatment of multidrug-resistant (MDR) pathogens: A case-based review.' *Journal of Hospital Medicine: An Official Publication of the Society of Hospital Medicine*, 4(6) pp. E8-E15.

Revanasiddappa, H. D., Vijaya, B., Shivakumar, L. and Shiva Prasad, K. (2012) 'Synthesis, Structural Characterization, and Antimicrobial Activity Evaluation of New Binuclear Niobium (V) Tartrate Complexes with Biologically Important Drugs.' *ISRN Inorganic Chemistry*, 2013.

Rhodes, A., Evans, L. E., Alhazzani, W., Levy, M. M., Antonelli, M., Ferrer, R., Kumar, A., Sevransky, J. E., Sprung, C. L., Nunnally, M. E., Rochwerf, B., Rubenfeld, G. D., Angus, D. C., Annane, D., Beale, R. J., Bellingham, G. J., Bernard, G. R., Chiche, J.-D., Coopersmith, C., de Backer, D. P., French, C. J., Fujishima, S., Gerlach, H., Hidalgo, J. L., Hollenberg, S. M., Jones, A. E., Karnad, D. R., Kleinpell, R. M., Koh, Y., Lisboa, T. C., Machado, F. R., Marini, J. J., Marshall, J. C., Mazuski, J. E., McIntyre, L. A., McLean, A. S., Mehta, S., Moreno, R. P.,

- Myburgh, J., Navalesi, P., Nishida, O., Osborn, T. M., Perner, A., Plunkett, C. M., Ranieri, M., Schorr, C. A., Seckel, M. A., Seymour, C. W., Shieh, L., Shukri, K. A., Simpson, S. Q., Singer, M., Thompson, B. T., Townsend, S. R., van der Poll, T., Vincent, J.-L., Wiersinga, W. J., Zimmerman, J. L. and Dellinger, R. P. (2017) 'Surviving Sepsis Campaign: International Guidelines for Management of Sepsis and Septic Shock: 2016.' *Intensive Care Medicine*, 43(3) pp. 304-377.
- Rigo, A., Corazza, A., di Paolo, M. L., Rossetto, M., Ugolini, R. and Scarpa, M. (2004) 'Interaction of copper with cysteine: stability of cuprous complexes and catalytic role of cupric ions in anaerobic thiol oxidation.' *Journal of Inorganic Biochemistry*, 98(9) pp. 1495-1501.
- Roberts, J. J. and Thomson, A. J. (1979) 'The mechanism of action of antitumor platinum compounds.' *Prog Nucleic Acid Res Mol Biol*, 22 pp. 71-133.
- Rogers, H. J., Woods, V. E. and Synge, C. (1982) 'Antibacterial effect of the scandium and indium complexes of enterochelin on *Escherichia coli*.' *J Gen Microbiol*, 128(10) pp. 2389-2394.
- Rosu, T., Pasculescu, S., Lazar, V., Chifiriuc, C. and Cernat, R. (2006) 'Copper(II) complexes with ligands derived from 4-amino-2,3-dimethyl-1-phenyl-3-pyrazolin-5-one: synthesis and biological activity.' *Molecules*, 11(11) pp. 904-914.
- Rosa, R. G., Schwarzbald, A. V., Dos Santos, R. P., Turra, E. E., Machado, D. P. and Goldani, L. Z. (2014) 'Vancomycin-resistant *Enterococcus faecium* Bacteremia in a tertiary care hospital: epidemiology, antimicrobial susceptibility, and outcome.' *Biomed Res Int*, pp. 958469.
- Russel, A. D., Chopra, I., (1990). 'Understanding antimicrobial resistance and action'. Ellis Horwood:Chichester.
- Russell, A. D. (2003) 'Biocide use and antibiotic resistance: the relevance of laboratory findings to clinical and environmental situations.' *The Lancet infectious diseases*, 3(12) pp. 794-803.
- Römling, U., Kjelleberg, S., Normark, S., Nyman, L., Uhlin, B. E., Åkerlund, B., Medicinska, f., Institutionen för, m., Molekylär Infektionsmedicin, S., Umeå Centre for Microbial, R. and Umeå, u. (2014) 'Microbial biofilm formation: a need to act.' *Journal of Internal Medicine*, 276(2) pp. 98-110.
- Sadekuzzaman, M., Yang, S., Mizan, M. F. R. and Ha, S. D. (2015) 'Current and Recent Advanced Strategies for Combating Biofilms.' *Comprehensive Reviews in Food Science and Food Safety*, 14(4) pp. 491-509.
- Şahmali, S. M., Kural, O. and Kiliç, Z. (1991) 'Systemic effects of nickel-containing dental alloys: analysis of nickel levels in serum, liver, kidney, and oral mucosa of guinea pigs.' *Quintessence International*, 22(12).
- Saikia, I., Sonowal, S., Pal, M., Boruah, P. K., Das, M. R. and Tamuly, C. (2016) 'Biosynthesis of gold decorated reduced graphene oxide and its biological activities.' *Materials Letters*, 178 pp. 239-242.
- Samani, S., Hossainipour, S. M., Tamizifar, M. and Rezaie, H. R. (2013) 'In vitro antibacterial evaluation of sol-gel-derived Zn-, Ag-, and (Zn + Ag)-doped hydroxyapatite coatings against methicillin-resistant *Staphylococcus aureus*.' *J Biomed Mater Res A*, 101(1) pp. 222-230.

- Sanchez, V. C., Jachak, A., Hurt, R. H. and Kane, A. B. (2012) 'Biological interactions of graphene-family nanomaterials: an interdisciplinary review.' *Chemical Research in Toxicology*, 25(1) pp. 15-34.
- Santajit, S. and Indrawattana, N. (2016) 'Mechanisms of antimicrobial resistance in ESKAPE pathogens.' *BioMed Research International*, 2016(2016) pp. 2475067.
- Santo, C. E., Lam, E. W., Elowsky, C. G., Quaranta, D., Domaille, D. W., Chang, C. J. and Grass, G. (2011) 'Bacterial Killing by Dry Metallic Copper Surfaces.' *Applied and Environmental Microbiology*, 77(3) pp. 794-802.
- Santos, A. F., Brotto, D. F., Favarin, L. R. V., Cabeza, N. A., Andrade, G. R., Batistote, M., Cavaleiro, A. A., Neves, A., Rodrigues, D. C. M. and Anjos, A. d. (2014) 'Study of the antimicrobial activity of metal complexes and their ligands through bioassays applied to plant extracts.' *Revista Brasileira de Farmacognosia*, 24(3) pp.309-315.
- Santos, C. M., Mangadlao, J., Ahmed, F., Leon, A., Advincula, R. C. and Rodrigues, D. F. (2012) 'Graphene nanocomposite for biomedical applications: fabrication, antimicrobial and cytotoxic investigations.' *Nanotechnology*, 23(39) pp. 395101.
- Saravanapavan, P., Gough, J. E., Jones, J. R. and Hench, L. L. (2004) 'Antimicrobial macroporous gel-glasses: dissolution and cytotoxicity.' *Trans Tech Publ*, 254.
- Sasso, R. C. and Garrido, B. J. (2008) 'Postoperative spinal wound infections.' *JAAOS-Journal of the American Academy of Orthopaedic Surgeons*, 16(6) pp. 330-337.
- Saubade, F. J., Hughes, S., Wickens, D. J., Wilson-Nieuwenhuis, J., Dempsey-Hibbert, N., Crowther, G. S., West, G., Kelly, P., Banks, C. E. and Whitehead, K. A. (2018) 'Effectiveness of titanium nitride silver coatings against Staphylococcus spp. in the presence of BSA and whole blood conditioning agents.' *International Biodeterioration & Biodegradation*.
- Saygun, O., Agalar, C., Aydinuraz, K., Agalar, F., Daphan, C., Saygun, M., Ceken, S., Akkus, A. and Baki Denkbaz, E. (2006) 'Gold and Gold-Palladium Coated Polypropylene Grafts in a S. epidermidis Wound Infection Model.' *Journal of Surgical Research*, 131(1) pp. 73-79.
- Scaffaro, R., Botta, L., Maio, A. and Gallo, G. (2017) 'PLA graphene nanoplatelets nanocomposites: Physical properties and release kinetics of an antimicrobial agent.' *Composites Part B*, 109 pp. 138-146.
- Scarpa, M., Momo, F., Viglino, P., Vianello, F. and Rigo, A. (1996) 'Activated oxygen species in the oxidation of glutathione A kinetic study.' *Biophysical Chemistry*, 60(1-2) pp. 53-61.
- Schembri, M. A., Blom, J., Krogfelt, K. A. and Klemm, P. (2005) 'Capsule and fimbria interaction in Klebsiella pneumoniae.' *Infection and Immunity*, 73(8) pp. 4626-4633.
- Schroll, C., Barken, K. B., Krogfelt, K. A. and Struve, C. (2010) 'Role of type 1 and type 3 fimbriae in Klebsiella pneumoniae biofilm formation.' *BMC Microbiology*, 10(1) pp. 179.
- Schwechheimer, C. and Kuehn, M. J. (2015) 'Outer-membrane vesicles from Gram-negative bacteria: biogenesis and functions.' *Nature reviews. Microbiology*, 13(10) pp. 605-619.
- Schäffer, C. and Messner, P. (2005) 'The structure of secondary cell wall polymers: how Gram-positive bacteria stick their cell walls together.' *Microbiology*, 151(3) pp. 643-651.

- Seddiki, O., Harnagea, C., Levesque, L., Mantovani, D. and Rosei, F. (2014) 'Evidence of antibacterial activity on titanium surfaces through nanotextures.' *Applied Surface Science*, 308 pp. 275-284.
- Selim, M. S., El-Safty, S. A., El-Sockary, M. A., Hashem, A. I., Abo Elenien, O. M., El-Saeed, A. M. and Fatthallah, N. A. (2015) 'Modeling of spherical silver nanoparticles in silicone-based nanocomposites for marine antifouling.' *RSC Advances*, 5(78) pp. 63175-63185.
- Shahid, M., Sobia, F., Singh, A., Malik, A., Khan, H. M., Jonas, D. and Hawkey, P. M. (2009) 'Beta-lactams and beta-lactamase-inhibitors in current-or potential-clinical practice: a comprehensive update.' *Critical Reviews in Microbiology*, 35(2) pp. 81-108.
- Shakil, S., Khan, R., Zarrilli, R. and Khan, A. U. (2008) 'Aminoglycosides versus bacteria—a description of the action, resistance mechanism, and nosocomial battleground.' *Journal of Biomedical Science*, 15(1) pp. 5-14.
- Shao, W., Liu, X., Min, H., Dong, G., Feng, Q. and Zuo, S. (2015) 'Preparation, Characterization, and Antibacterial Activity of Silver Nanoparticle-Decorated Graphene Oxide Nanocomposite.' *ACS Applied Materials & Interfaces*, 7(12) pp. 6966-6973.
- Sharma, K., Singh, R. V. and Fahmi, N. (2011) 'Palladium(II) and platinum(II) derivatives of benzothiazoline ligands: Synthesis, characterization, antimicrobial and antispermato-genic activity.' *Spectrochimica Acta Part A: Molecular and Biomolecular Spectroscopy*, 78(1) pp. 80-87.
- Sharma, V. K., Johnson, N., Cizmas, L., McDonald, T. J. and Kim, H. (2016) 'A review of the influence of treatment strategies on antibiotic resistant bacteria and antibiotic resistance genes.' *Chemosphere*, 150 pp. 702-714.
- Science notes. (2015) List of electronic configurations of elements. [Online] [Assessed on 16th March, 2018]. <http://sciencenotes.org/list-of-electronic-configurations-of-elements/>
- Shorr, A. F. (2009) 'Review of studies of the impact on Gram-negative bacterial resistance on outcomes in the intensive care unit.' *Critical Care Medicine*, 37(4) pp. 1463-1469.
- Silva, R. A., Walls, M., Rondot, B., Da Cunha Belo, M. and Guidoin, R. (2002) 'Electrochemical and microstructural studies of tantalum and its oxide films for biomedical applications in endovascular surgery.' *Journal of Materials Science: Materials in Medicine*, 13(5) pp. 495-500.
- Silver, S., Phung, L. T. and Silver, G. (2006) 'Silver as biocides in burn and wound dressings and bacterial resistance to silver compounds.' *Journal of Industrial Microbiology and Biotechnology*, 33(7) pp. 627-634.
- Silvestry-Rodriguez, N., Bright, K. R., Slack, D. C., Uhlmann, D. R. and Gerba, C. P. (2008) 'Silver as a Residual Disinfectant To Prevent Biofilm Formation in Water Distribution Systems.' *Applied and Environmental Microbiology*, 74(5) pp. 1639-1641.
- Sim, J.-H., Jamaludin, N., Khoo, C.-H., Cheah, Y.-K., Halim, S., Seng, H.-L. and Tiekink, E. T. (2014) 'In vitro antibacterial and time-kill evaluation of phosphanegold(I) dithiocarbamates, R<sub>3</sub>PAu[S<sub>2</sub>CN(iPr)CH<sub>2</sub>CH<sub>2</sub>OH] for R = Ph, Cy and Et, against a broad range of Gram-positive and Gram-negative bacteria.' *Gold Bulletin*, 47(4) pp. 225-236.
- Singh, K. V., Weinstock, G. M. and Murray, B. E. (2002) 'An Enterococcus faecalis ABC Homologue (Lsa) Is Required for the Resistance of This Species to Clindamycin and Quinupristin-Dalfopristin.' *Antimicrobial Agents and Chemotherapy*, 46(6) pp. 1845-1850.

- Sirelkhatim, A., Mahmud, S., Seeni, A., Kaus, N. H. M., Ann, L. C., Bakhori, S. K. M., Hasan, H. and Mohamad, D. (2015) 'Review on Zinc Oxide Nanoparticles: Antibacterial Activity and Toxicity Mechanism.' *Nano-Micro Letters*, 7(3) pp. 219-242.
- Slate, A. J., Wickens, D., Wilson-Nieuwenhuis, J., Dempsey-Hibbert, N., West, G., Kelly, P., Verran, J., Banks, C. E. and Whitehead, K. A. (2019) 'The effects of blood conditioning films on the antimicrobial and retention properties of zirconium-nitride silver surfaces.' *Colloids and Surfaces B: Biointerfaces*, 173 pp. 303-311.
- Slavin, Y. N., Asnis, J., Häfeli, U. O. and Bach, H. (2017) 'Metal nanoparticles: understanding the mechanisms behind antibacterial activity.' *Journal of Nanobiotechnology*, 15(1) pp. 65-20.
- Smith, K. and Hunter, I. S. (2008) 'Efficacy of common hospital biocides with biofilms of multi-drug resistant clinical isolates.' *J Med Microbiol*, 57(Pt 8) pp. 966-973.
- Sommer, M. O. and Dantas, G. (2011) 'Antibiotics and the resistant microbiome.' *Curr Opin Microbiol*, 14(5) pp. 556-563.
- Sondi, I. and Salopek-Sondi, B. (2004) 'Silver nanoparticles as antimicrobial agent: a case study on *E. coli* as a model for Gram-negative bacteria.' *Journal of Colloid and Interface science*, 275(1) pp. 177-182.
- Song, F., Koo, H. and Ren, D. (2015) 'Effects of Material Properties on Bacterial Adhesion and Biofilm Formation.' *Journal of Dental Research*, 94(8) pp. 1027.
- Sotogaku, N., Endo, K., Hirunuma, R., Enomoto, S., Ambe, S. and Ambe, F. (1999) 'Binding Properties of Various Metals to Blood Components and Serum Proteins: A Multitracer Study.' *Journal of Trace Elements in Medicine and Biology*, 13(1) pp. 1-6.
- Spellberg, B. and Gilbert, D. N. (2014) 'The future of antibiotics and resistance: a tribute to a career of leadership by John Bartlett.' *Clinical Infectious Diseases*, 59(2) pp. S71-S75.
- Sperandeo, P., Dehò, G. and Polissi, A. (2009) 'The lipopolysaccharide transport system of Gram-negative bacteria.' *Biochimica et Biophysica Acta (BBA)-Molecular and Cell Biology of Lipids*, 1791(7) pp. 594-602.
- Stefanović, O., Radojević, I., Vasić, S. and Čomic, L. (2012) 'Antibacterial activity of naturally occurring compounds from selected plants.' In *Antimicrobial Agents*. IntechOpen.
- Steindl, G., Heuberger, S. and Springer, B. (2012) 'Antimicrobial effect of copper on multidrug-resistant bacteria.' *Wiener Tierärztliche Monatsschrift*, 99 pp. 38-43.
- Stevenson, J., Barwinska-Sendra, A., Tarrant, E. and Waldron, K. J. (2013) 'Mechanism of action and application of the antimicrobial properties of copper.' *Microbial pathogens and strategies for combating them: Science, Technology and Education*, pp. 468-479.
- Stobie, N., Duffy, B., McCormack, D. E., Colreavy, J., Hidalgo, M., McHale, P. and Hinder, S. J. (2008) 'Prevention of *Staphylococcus epidermidis* biofilm formation using a low-temperature processed silver-doped phenyltriethoxysilane sol-gel coating.' *Biomaterials*, 29(8) pp. 963-969.
- Sutterlin, S., Tano, E., Bergsten, A., Tallberg, A. B. and Melhus, A. (2012) 'Effects of silver-based wound dressings on the bacterial flora in chronic leg ulcers and its susceptibility in vitro to silver.' *Acta Derm Venereol*, 92(1) pp. 34-39.

Szunerits, S. and Boukherroub, R. (2016) 'Antibacterial activity of graphene-based materials.' *J. Mater. Chem. B*, 4(43) pp. 6892-6912.

Szymański, P., Frączek, T., Markowicz, M. and Mikiciuk-Olasik, E. (2012) 'Development of copper based drugs, radiopharmaceuticals and medical materials.' *Biometals*, 25(6), pp. 1089-1112.

Takano, Y., Taguchi, T., Suzuki, I., Balis, J. U. and Yuri, K. (2002) 'Cytotoxicity of heavy metals on primary cultured alveolar type II cells.' *Environmental Research*, 89(2) pp. 138-145.

Tamayo, L. A., Zapata, P. A., Vejar, N. D., Azocar, M. I., Gulppi, M. A., Zhou, X., Thompson, G. E., Rabagliati, F. M. and Paez, M. A. (2014) 'Release of silver and copper nanoparticles from polyethylene nanocomposites and their penetration into *Listeria monocytogenes*.' *Mater Sci Eng C Mater Biol Appl*, 40 pp. 24-31.

Tamás, M. J., Sharma, S. K., Ibstedt, S., Jacobson, T., Christen, P., Institutionen för kemi och m., Naturvetenskapliga, f., Faculty of, S., Göteborgs, u., Gothenburg, U. and Department of Chemistry and Molecular, B. (2014) 'Heavy metals and metalloids as a cause for protein misfolding and aggregation.' *Biomolecules*, 4(1) pp. 252-267.

Tedjo, C., Neoh, K. G., Kang, E. T., Fang, N. and Chan, V. (2007) 'Bacteria-surface interaction in the presence of proteins and surface attached poly(ethylene glycol) methacrylate chains.' *J Biomed Mater Res A*, 82(2) pp. 479-491.

The Catalyst. (no year) Periodic table with oxidation numbers [Online] [Assessed on 16th March, 2017].

<http://www.thecatalyst.org/oxnotabl.html>

Thomas, J. G., Slone, W., Linton, S., Okel, T., Corum, L. and Percival. (2011) 'In vitro antimicrobial efficacy of a silver alginate dressing on burn wound isolates.' *Journal of Wound Care*, 20(3) pp. 124-128.

Thomson, J. M. and Bonomo, R. A. (2005) 'The threat of antibiotic resistance in Gram-negative pathogenic bacteria: beta-lactams in peril!' *Curr Opin Microbiol*, 8(5) pp. 518-524.

Tom, R. T., Suryanarayanan, V., Reddy, P. G., Baskaran, S. and Pradeep, T. (2004) 'Ciprofloxacin-protected gold nanoparticles.' *Langmuir*, 20(5) pp. 1909-1914.

Trivedi, M., Patil, S., Shettigar, H., Bairwa, K. and Jana, S. (2015) 'Spectroscopic characterization of chloramphenicol and tetracycline: an impact of biofield treatment.' *Pharmaceutical Analytical Acta*, 6(7).

Turcheniuk, K., Hage, C.-H., Spadavecchia, J., Serrano, A. Y., Larroulet, I., Pesquera, A., Zurutuza, A., Pisfil, M. G., Héliot, L., Boukaert, J., Boukherroub, R. and Szunerits, S. (2015) 'Plasmonic photothermal destruction of uropathogenic *E. coli* with reduced graphene oxide and core/shell nanocomposites of gold nanorods/reduced graphene oxide.' *Journal of Materials Chemistry B*, 3(3) pp. 375-386.

Tuson, H. H. and Weibel, D. B. (2013) 'Bacteria-surface interactions.' *Soft Matter*, 9(17) pp. 4368-4438.

Unemo, M. and Shafer, W. M. (2014) 'Antimicrobial resistance in *Neisseria gonorrhoeae* in the 21st century: past, evolution, and future.' *Clinical Microbiology Reviews*, 27(3) pp. 587-613.



- Vaidya, M., McBain, A. J., Banks, C. E. and Whitehead, K. A. (2018) 'Single and combined antimicrobial efficacies for nine metal ion solutions against *Klebsiella pneumoniae*, *Acinetobacter baumannii* and *Enterococcus faecium*.' *International Biodeterioration & Biodegradation*.
- Van Bambeke, F., Balzi, E. and Tulkens, P. M. (2000) 'Antibiotic efflux pumps.' *Biochemical Pharmacology*, 60(4) pp. 457-470.
- Van Tyne, D. and Gilmore, M. S. (2014) 'Friend turned foe: evolution of enterococcal virulence and antibiotic resistance.' *Annual Review of Microbiology*, 68 pp. 337-356.
- Van Tyne, D., Martin, M. and Gilmore, M. (2013) 'Structure, function, and biology of the *Enterococcus faecalis* cytolysin.' *Toxins*, 5(5) pp. 895-911.
- Veerapandian, M., Zhang, L., Krishnamoorthy, K. and Yun, K. (2013) 'Surface activation of graphene oxide nanosheets by ultraviolet irradiation for highly efficient anti-bacterials.' *Nanotechnology*, 24(39) pp. 395706.
- Velkov, T., Roberts, K. D., Nation, R. L., Wang, J., Thompson, P. E. and Li, J. (2014) 'Teaching 'old' polymyxins new tricks: new-generation lipopeptides targeting gram-negative 'superbugs'.' *ACS Chemical Biology*, 9(5) pp. 1172-1177.
- Ventola, C. L. (2015) 'The antibiotic resistance crisis: part 1: causes and threats.' *Pharmacy and therapeutics*, 40(4) pp. 277.
- Villers, D., Espaze, E., Coste-Burel, M., Giauffret, F., Ninin, E., Nicolas, F. and Richet, H. (1998) 'Nosocomial *Acinetobacter baumannii* infections: microbiological and clinical epidemiology.' *Ann Intern Med*, 129(3) pp. 182-189.
- von Wintersdorff, C. J. H., Penders, J., van Niekerk, J. M., Mills, N. D., Majumder, S., van Alphen, L. B., Savelkoul, P. H. M. and Wolffs, P. F. G. (2016) 'Dissemination of antimicrobial resistance in microbial ecosystems through horizontal gene transfer.' *Frontiers in Microbiology*, 7 pp. 173.
- Vos, d. W. M. (2015) 'Microbial biofilms and the human intestinal microbiome.' *npj Biofilms and Microbiomes*, 1(1) pp. 15005.
- Vrede, K., Heldal, M., Norland, S. and Bratbak, G. (2002) 'Elemental Composition (C, N, P) and Cell Volume of Exponentially Growing and Nutrient-Limited Bacterioplankton.' *Applied and Environmental Microbiology*, 68(6) pp. 2965-2971.
- Vuotto, C., Longo, F., Balice, M., Donelli, G. and Varaldo, P. (2014) 'Antibiotic resistance related to biofilm formation in *Klebsiella pneumoniae*.' *Pathogens*, 3(3) pp. 743-758.
- Wang, H., Wilksch, J. J., Chen, L., Tan, J. W. H., Strugnell, R. A. and Gee, M. L. (2016) 'Influence of fimbriae on bacterial adhesion and viscoelasticity and correlations of the two properties with biofilm formation.' *Langmuir*, 33(1) pp. 100-106.
- Wang, P., Pang, S., Zhang, H., Fan, M. and He, L. (2016) 'Characterization of *Lactococcus lactis* response to ampicillin and ciprofloxacin using surface-enhanced Raman spectroscopy.' *Analytical and Bioanalytical Chemistry*, 408(3) pp. 933-941.
- Wang, Y., Wu, Y., Yang, H., Xue, X. and Liu, Z. (2016) 'Co-doping TiO<sub>2</sub> with boron and/or yttrium elements: Effects on antimicrobial activity.' *Materials Science and Engineering: B*, 211 pp. 149-155.

- Wang, Y.-T., Fang, Y., Zhao, M., Li, M.-X., Ji, Y.-M. and Han, Q.-X. (2017) 'Cu(ii), Ga(iii) and In(iii) complexes of 2-acetylpyridine N (4)-phenylthiosemicarbazone: synthesis, spectral characterization and biological activities.' *Med Chem Comm*, 8(11) pp. 2125-2132.
- Webber, M. A. and Piddock, L. J. V. (2003) 'The importance of efflux pumps in bacterial antibiotic resistance.' *Journal of Antimicrobial Chemotherapy*, 51(1) pp. 9-11.
- Weber, B. S., Harding, C. M. and Feldman, M. F. (2016) 'Pathogenic Acinetobacter: from the cell surface to infinity and beyond.' *Journal of Bacteriology*, 198(6) pp. 880-887.
- Weidenmaier, C. and Peschel, A. (2008) 'Teichoic acids and related cell-wall glycopolymers in Gram-positive physiology and host interactions.' *Nature Reviews Microbiology*, 6(4) pp. 276.
- Wernicki, A., Puchalski, A., Urban-Chmiel, R., Dec, M., Stegierska, D., Dudzic, A. and Wojcik, A. (2014) 'Antimicrobial properties of gold, silver, copper and platinum nanoparticles against selected microorganisms isolated from cases of mastitis in cattle.' *MEDYCYNÁ WETERYNARYJNA-VETERINARY MEDICINE-SCIENCE AND PRACTICE*, 70(9) pp. 564-567.
- Whang, D. W., Miller, L. G., Partain, N. M. and McKinnell, J. A. (2013) 'Systematic review and meta-analysis of linezolid and daptomycin for treatment of vancomycin-resistant enterococcal bloodstream infections.' *Antimicrobial Agents and Chemotherapy*, 57(10) pp. 5013-5018.
- Whitehead, K. A., Vaidya, M., Liauw, C. M., Brownson, D. A. C., Ramalingam, P., Kamieniak, J., Rowley-Neale, S. J., Tetlow, L. A., Wilson-Nieuwenhuis, J. S. T., Brown, D., McBain, A. J., Kulandaivel, J. and Banks, C. E. (2017) 'Antimicrobial activity of graphene oxide-metal hybrids.' *International Biodeterioration & Biodegradation*, 123 pp. 182-190.
- Wilson, D. N. (2014) 'Ribosome-targeting antibiotics and mechanisms of bacterial resistance.' *Nature Reviews Microbiology*, 12(1) pp. 35.
- Woodward, B. (2012) 'Final Analysis: Palladium in Temporary and Permanently Implantable Medical Devices.' *Platinum Metals Review*, 56(3) pp. 213-217.
- Wu, C.-M., Peng, P.-W., Chou, H.-H., Ou, K.-L., Sugiatno, E., Liu, C.-M. and Huang, C.-F. (2018) 'Microstructural, mechanical and biological characterizations of the promising titanium-tantalum alloy for biomedical applications.' *Journal of Alloys and Compounds*, 735 pp. 2604-2610.
- Xia, Y., Jiang, X., Zhang, J., Lin, M., Tang, X., Zhang, J. and Liu, H. (2017) 'Synthesis and characterization of antimicrobial nanosilver/diatomite nanocomposites and its water treatment application.' *Applied Surface Science*, 396 pp. 1760-1764.
- Xu, K. D., McFeters, G. A. and Stewart, P. S. (2000) 'Biofilm resistance to antimicrobial agents.' *Microbiology*, 146(3) pp. 547-549.
- Xu, W.-P., Zhang, L.-C., Li, J.-P., Lu, Y., Li, H.-H., Ma, Y.-N., Wang, W.-D. and Yu, S.-H. (2011) 'Facile synthesis of silver@graphene oxide nanocomposites and their enhanced antibacterial properties.' *Journal of Materials Chemistry*, 21(12) pp. 4593.
- Yang, L., Kuang, H., Zhang, W., Aguilar, Z. P., Wei, H. and Xu, H. (2017) 'Comparisons of the biodistribution and toxicological examinations after repeated intravenous administration of silver and gold nanoparticles in mice.' *Scientific Reports*, 7(1) pp. 3303-3312.

- Yang, L., Liu, Y., Wu, H., Song, Z., Høiby, N., Molin, S. and Givskov, M. (2012) 'Combating biofilms.' *FEMS Immunology and Medical Microbiology*, 65(2) p. 146.
- Yang, M.-Q. and Xu, Y.-J. (2013) 'Selective photoredox using graphene-based composite photocatalysts.' *Physical Chemistry Chemical Physics: PCCP*, 15(44) pp. 1912-19118.
- Yasuyuki, M., Kunihiro, K., Kurissery, S., Kanavillil, N., Sato, Y. and Kikuchi, Y. (2010) 'Antibacterial properties of nine pure metals: a laboratory study using Staphylococcus aureus and Escherichia coli.' *Biofouling*, 26(7) pp. 851-858.
- Yılmaz, Ç. and Özcengiz, G. (2017) 'Antibiotics: Pharmacokinetics, toxicity, resistance and multidrug efflux pumps.' *Biochemical Pharmacology*, 133 pp. 43-62.
- Zaman, S. B., Hussain, M. A., Nye, R., Mehta, V., Mamun, K. T. and Hossain, N. (2017) 'A Review on Antibiotic Resistance: Alarm Bells are Ringing.' *Cureus*, 9(6) pp. e1403.
- Zanzen, U., Bovenkamp, G. L., Krishna, K. S., Hormes, J. and Prange, A. (2013) 'Antibacterial action of copper ions on food-contaminating bacteria.' *Acta Biologica Szegediensis*, 57(2) pp. 149-151.
- Zanzen, U., Bovenkamp-Langlois, L., Klysubun, W., Hormes, J. and Prange, A. (2018) 'The interaction of copper ions with Staphylococcus aureus, Pseudomonas aeruginosa, and Escherichia coli: an X-ray absorption near-edge structure (XANES) spectroscopy study.' *Archives of Microbiology*, 200(3) pp. 401-412.
- Zeitlinger, M. A., Derendorf, H., Mouton, J. W., Cars, O., Craig, W. A., Andes, D., Theuretzbacher, U., Medicinska, f., Medicinska och farmaceutiska, v., Infektionssjukdomar, Uppsala, u. and Institutionen för medicinska, v. (2011) 'Protein Binding: Do We Ever Learn?' *Antimicrobial Agents and Chemotherapy*, 55(7) pp. 3067-3074.
- Zhang, L. J., Zhang, J. A., Zou, X. Z., Liu, Y. J., Li, N., Zhang, Z. J. and Li, Y. (2015) 'Studies on antimicrobial effects of four ligands and their transition metal complexes with 8-mercaptoquinoline and pyridine terminal groups.' *Bioorg Med Chem Lett*, 25(8) pp. 1778-1781.
- Zhang, Y., Zheng, Y., Li, Y., Wang, L., Bai, Y., Zhao, Q., Xiong, X., Cheng, Y., Tang, Z., Deng, Y. and Wei, S. (2015) 'Tantalum Nitride-Decorated Titanium with Enhanced Resistance to Microbiologically Induced Corrosion and Mechanical Property for Dental Application.' *PloS one*, 10(6) pp. e0130774.
- Zhao, L., Chu, P. K., Zhang, Y. and Wu, Z. (2009) 'Antibacterial coatings on titanium implants.' *Journal of biomedical materials research. Part B, Applied Biomaterials*, 91(1) pp. 470-480.
- Zhao, Y., Tian, Y., Cui, Y., Liu, W., Ma, W. and Jiang, X. (2010) 'Small molecule-capped gold nanoparticles as potent antibacterial agents that target gram-negative bacteria.' *Journal of the American Chemical Society*, 132(35) pp. 12349-12356.
- Zhou, J., Zhao, F., Wang, Y., Zhang, Y. and Yang, L. (2007) 'Size-controlled synthesis of ZnO nanoparticles and their photoluminescence properties.' *Journal of Luminescence*, 122 pp. 195-197.
- Zhu, Y., Qiu, Y., Chen, R. and Liao, L. (2015) 'The Inhibition of Escherichia coli Biofilm Formation by Gallium Nitrate-Modified Titanium.' *Journal of Nanoscience and Nanotechnology*, 15(8) pp. 5605.

Zollfrank, C., Gutbrod, K., Wechsler, P. and Guggenbichler, J. P. (2012) 'Antimicrobial activity of transition metal acid MoO<sub>3</sub> prevents microbial growth on material surfaces.' *Materials Science and Engineering: C*, 32(1) pp. 47-54.

Zou, X., Zhang, L., Wang, Z. and Luo, Y. (2016) 'Mechanisms of the antimicrobial activities of graphene materials.' *Journal of the American Chemical Society*, 138(7) pp. 2064-2077.